Design and Synthesis of A$_{2B}$- and Dual-Acting A$_{2A}$/A$_{2B}$ Adenosine Receptor Antagonists

Dissertation

zur

Erlangung des Doktorgrades (Dr. rer. nat.)

der

Mathematisch-Naturwissenschaftlichen Fakultät

der

Rheinischen Friedrich-Wilhelms-Universität Bonn

vorgelegt von

Ahmed Mohamed Abbas Temirak

aus

Kairo, Ägypten

Bonn 2020

Angefertigt mit Genehmigung der Mathematisch-Naturwissenschaftlichen

Fakultät der Rheinischen Friedrich-Wilhelms-Universität Bonn

1. Gutachter: Prof. Dr. Christa E. Müller

2. Gutachter: Prof. Dr. Finn Hansen

Tag der Promotion: 13.10.2020

Erscheinungsjahr: 2020

To my dear parents, my wife Noha
and my son Adam

Table of contents

1. Introduction

1.1. G protein-coupled receptors

G protein-coupled receptors (GPCRs) represent one of the most important classes of transmembrane proteins. They were named based on the coupling with heterotrimeric guanine nucleotide-binding proteins (G proteins).[1,2] GPCRs are the largest gene superfamily of the human genome with more than 800 members.[3] Pharmaceutical companies and researchers have extensively focused their research on GPCRs, and about 34% of the drugs on the market target around 100 GPCRs.[3,4] The advances in protein engineering and crystallization techniques in the last years provided us with a surge of GPCR crystal and cryo-EM structures.[5,6]

1.1.1. GPCR structures

GPCRs are also called seven-transmembrane (7TM) receptors as they consist of seven hydrophobic transmembrane α-helices. These domains are connected by three intracellular loops (ICL1-3) and three extracellular loops (ECL1-3), and contain an extracellular *N*-terminus and an intracellular C-terminus. One of the common features in class A GPCRs are two conserved extracellular cysteine residues that form a disulfide bond (Figure 1). One of these cysteine residues is located in TM3/ECL1 and the other one in ECL2. This disulfide bond is expected to induce and stabilize restricted conformations of GPCR domains.[7] The binding domains of the natural GPCR ligands of GPCRs are quite different, organic agonists bind mainly to the TM region, while peptides bind to the amino terminus or the ECLs.[8]

GPCRs have crucial roles in signal transduction inside the body and are activated by various ligands, for instance hormones, neurotransmitters and photons.[10] When GPCRs are activated, conformational changes occur in the receptors followed by interaction with the intracellular G protein that induces important signaling pathways inside the cell. The greatest homology between GPCRs was observed in the TM domains, while larger differences were found in the extracellular amino terminus which varies from comparatively short sequences in

peptide and neurotransmitter receptors (10-50 amino acids) to 350-600 amino acids in glycoprotein hormone receptors.[11]
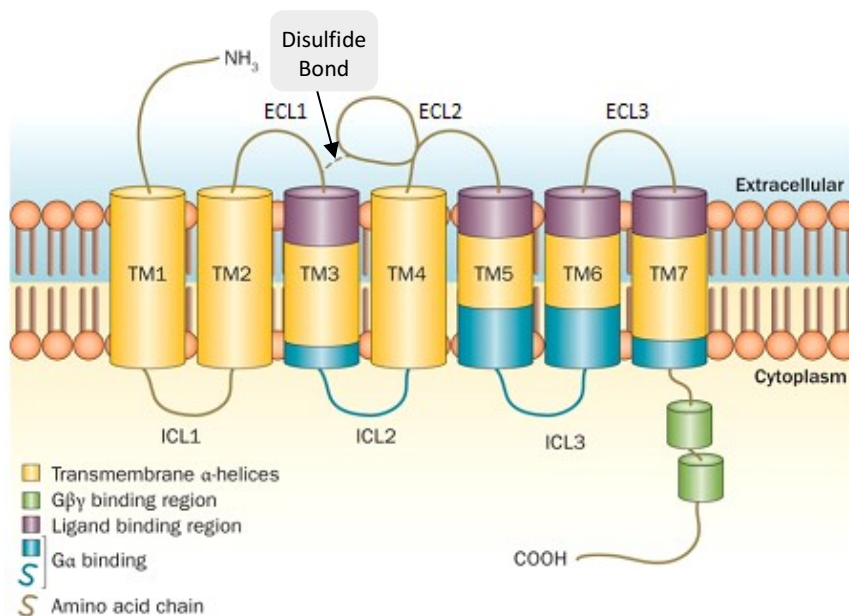
Figure 1. Schematic illustration of the GPCR structure.[9]

1.1.2. Classification of GPCRs

There are two common classification systems for GPCRs. Attwood, Findlay and Kolakowski introduced a classification system for GPCRs in vertebrates and invertebrates in 1994.[12,13] This system categorizes the GPCRs into six classes (class A-F) (Figure 2). Class A is the largest and most studied class to which about 90% of GPCRs belong. These are the rhodopsin-like receptors that are activated by many ligands. Class B comprises the secretin-like receptors, to which larger proteins such as secretin and glucagon bind, while the metabotropic glutamate receptors that bind glutamate represent class C. The other classes do not exist in human, such as class D (fungal pheromone), class E (cAMP receptors), and class F (frizzled/smoothened receptors).

Another classification system that was introduced by Fredriksson *et al*. in 2003 is the GRAFS system.[14] This system classifies GPCRs into five classes: glutamate, rhodopsin,

adhesion, frizzled/taste 2 and secretin receptors. The GRAFS system is classifying only human

GPCRs and is based on their phylogenetic comparison (Table 1).[14]

Table 1. GPCR classification systems.

A-F classification	GRAFS system
Class **A** (Rhodopsin like receptors) **B** (secretin-like receptors) **C** (metabotropic glutamate receptors) **D** (fungal pheromone) **E** (cAMP receptors) **F** (frizzled/smoothened receptors	**G**lutamate receptors **R**hodopsin receptors **A**dhesion receptors **F**rizzled/Taste 2 receptors **S**ecretin receptors

1.1.3. Signal transduction by GPCRs

Receptors are described as cellular macromolecules that transduce chemical signaling

within the cell and are present in an active and inactive conformation.[15,16] Binding of an agonist

to the active conformation of a GPCR, stabilizes this conformation and activates the signal

transduction cascade inside the cell. On the other hand, antagonists can bind to active and

inactive GPCR conformations resulting in the stabilization of the inactive state or to receptor

inactivation, thus inhibiting signal transduction.[15,16] In a balanced unbiased system, GPCR

signaling is mediated through the activation of G proteins; moreover GPCRs bind to adapter

proteins, the so-called β-arrestins, which are controlling receptor desensitization and

internalization (Figure 2).[17,18] Some ligands can stimulate or inhibit various GPCR signaling

pathways differentially and are called 'biased ligands'. These ligands can help us to better

understand the molecular targets and the cellular responses associated with GPCRs and could

be used as novel therapeutics with favorable pharmacology. β-Arrestin-biased ligands can

specifically induce β-arrestin-mediated effects, while G protein-biased ligands activate the G

protein signaling pathway avoiding β-arrestin-mediated desensitization of GPCRs (Figure

2).[17,19]
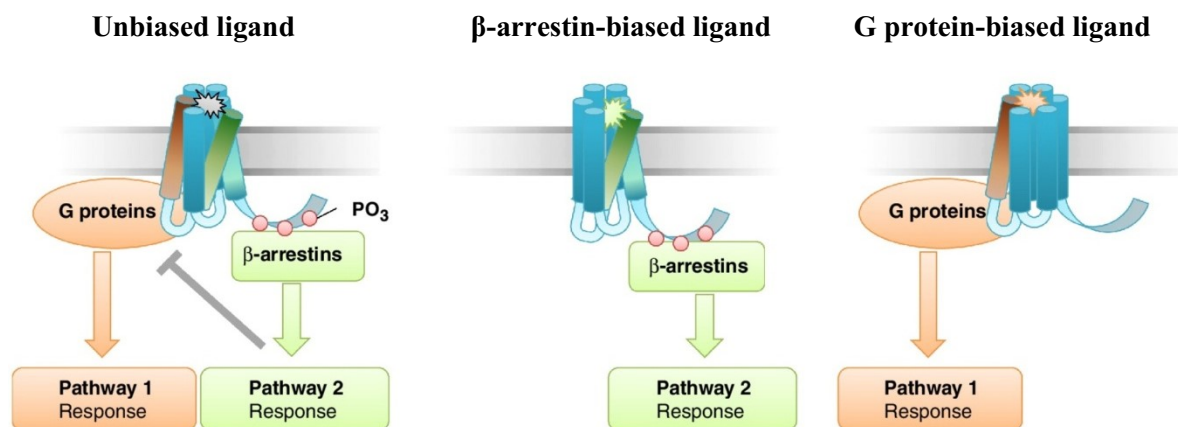
Figure 2. Unbiased and biased GPCR ligands.[17]

G proteins are heterotrimeric guanine nucleotide-binding proteins that bind to the intracellular side of the receptor. They consist of an α-subunit (Gα) and a βγ dimeric subunit (Gβγ). Upon binding of an agonist to the GPCR, an exchange of GDP for GTP occurs in the α-subunit. The activated G protein then dissociates into the activated α subunit (α*) and the βγ subunit.[20] These subunits play an important role in transmitting the extracellular signal from GPCRs to the intracellular secondary messengers systems, which can catalyze the formation of inositol phosphates (IPs), diacylglycerol (DAG), cAMP, and cGMP (Figure 3). The activation or deactivation of these effector proteins depends on the Gα subunit to which the GPCR couples.[21]

Seventeen different Gα subunits exist which are classified into four families (Gα$_s$, Gα$_{i/o}$, Gα$_{q/11}$ and Gα$_{12/13}$).[22] Coupling to Gα$_s$ stimulates adenylate cyclase (AC) that converts ATP to cAMP while Gα$_{i/o}$ suppresses AC thus decreasing cAMP levels (Figure 3).[23] Gα$_{q/11}$ activates phospholipase Cβ (PLCβ), which hydrolyzes phosphatidylinositol 4,5-bisphosphate (PIP$_2$) to 1,4,5-inositol trisphosphate (IP$_3$) and DAG. DAG activates protein kinase C (PKC), whereas IP$_3$ binds to its receptors resulting in massive release of calcium ions into the cytosol.[24] Additionally, Gα$_{12/13}$ signaling involves the activation of RhoGTPase nucleotide exchange factors (RhoGEFs).[25] Many GPCRs can couple to more than one Gα protein,[26] Gα subunits

regulate effector proteins such as AC and phospholipase C (PLC) which produce second messengers such as IP_3 and cAMP. These second messengers control transcription factors inside the cell such as cAMP-responsive element (CRE), nuclear factor of activated T-cells (NFAT) and serum response factor (SRF) (Figure 3).[27]
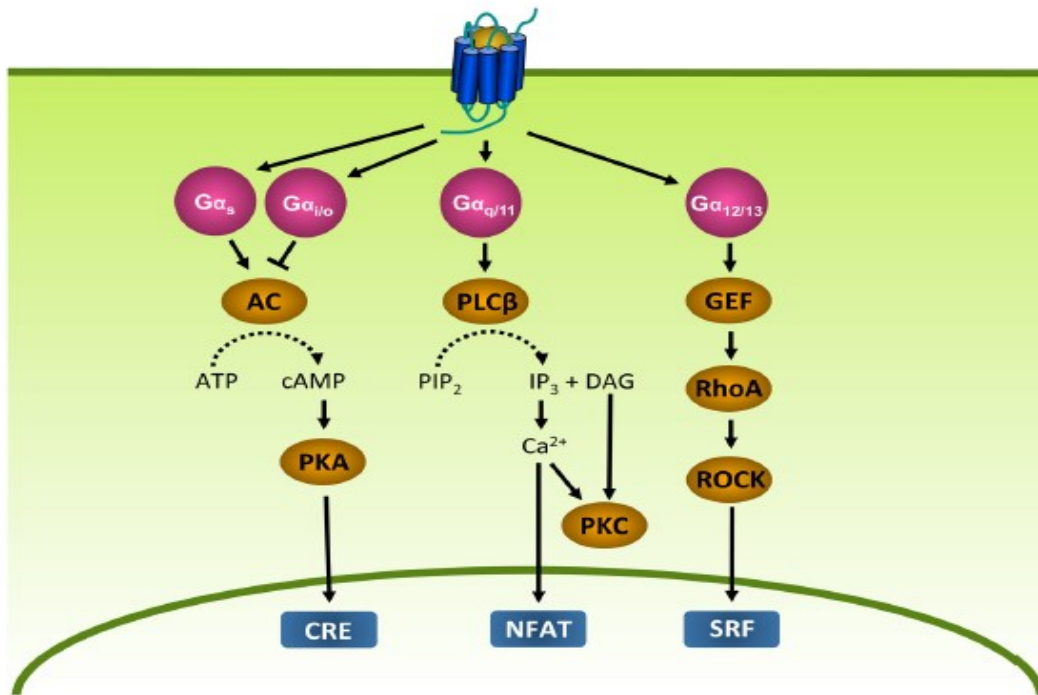
Figure 3. Signal transduction in GPCRs. Gα subunits regulate secondary messengers and transcription factors inside the cell.[27]

1.2. Classification of purinergic receptors

Purinergic receptors belong to the rhodopsin class of receptors, the largest family of GPCRs. They are classified into P1 receptors that are activated by adenosine and P2 receptors that are activated by various nucleotides including ATP, ADP, UTP, UDP and others (Figure 4).[28,29] Moreover, purinergic receptors activated by adenine were discovered and designated P0 receptors. Adenosine receptors (P1) are subdivided into four subtypes (A_1, A_{2A}, A_{2B} and A_3ARs) according to their tendency to activate or suppress adenylyl cyclase (AC) (Figure 4).[30,31] A_1- and $A_{2A}ARs$ show higher affinity for adenosine than A_{2B}- and A_3ARs. A_{2A}- and

$A_{2B}ARs$ activate AC thus increasing cAMP levels, whereas A_1- and A_3ARs inhibit AC thereby decreasing cAMP levels.

Nucleotide receptors (P2) are subdivided into P2X and P2Y receptors according to their structure.[32] There are seven subtypes of the ionotropic P2X receptors (P2X1-7) which are all activated by ATP, while the eight metabotropic P2Y receptors ($P2Y_{1, 2, 4, 6, 11-14}$) are responsive to ATP, ADP, UTP, UDP or UDP-glucose depending on the subtype. The subscript in P2 receptors is based on the chronological order of their cloning.[33] Adenine receptors (P0) have been cloned and characterized in rat, mouse and hamster, but not in humans. The first cloned adenine receptors in rat and hamster were named rAdeR1 and cAdeR1 respectively, while in mouse there are (at least) two adenine receptors, designated mAdeR1 and mAdeR2.[34,35]
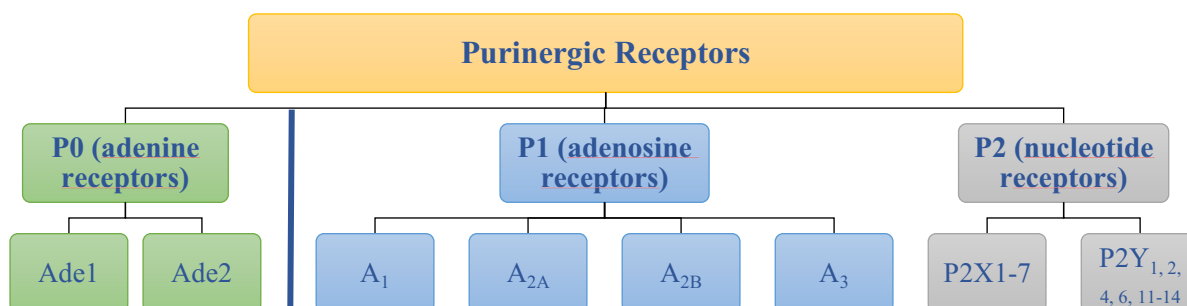
Figure 4. Classification of the purinergic receptors.

1.3. Adenosine receptors

Adenosine receptors (ARs) were cloned in the early 1990s and since then they been extensively characterized. They comprise four subtypes: A_1, A_{2A}, A_{2B} and A_3ARs and are activated by their natural ligand adenosine. ARs are membrane-bound G protein-coupled receptors that are widely distributed throughout the body, in the central nervous system (brain and spinal cord), and also in other organs including heart, lung, colon, liver.[36] ARs are of great interest as drug targets for different therapeutic areas, e.g. ischemia, pain, inflammatory diseases, cancer, epilepsy, and neurodegenerative diseases.[37,38]

1.3.1. Adenosine

Adenosine is an important metabolite which is the building block of nucleic acids and ATP, the molecular currency of energy transfer in mammalian cells.[39] It modulates many biological processes through the activation of the four subtypes of adenosine receptors.[36] The activation of ARs is driven by the availability of adenosine in the extracellular compartment which has two main sources. Firstly, the intracellular adenosine is transported to the extracellular compartment through equilibrative nucleoside transporters (NT) (Figure 5).[40]

Additionally, extracellular adenosine can be produced by breakdown of ATP by the ecto-nucleotidases NTPDase1 (CD39) and ecto-5'-nucleotidase (CD73).[41] Intracellular adenosine is produced either by the hydrolysis of adenosine monophosphate (AMP) by 5'-nucleotidases or through hydrolysis of S-adenosylhomocysteine (Hcy) by hydrolases (SAH-hydrolases) (Figure 5).[40,42] The intracellular pathway of adenosine production is the main source of adenosine under normal conditions, while the extracellular production is mainly activated under pathological conditions for example after tissue injury or hypoxia.[43]

The basal adenosine level under normal physiological conditions is 30-200 nM which is not sufficient to activate the A_{2B}ARs, the AR subtype with the lowest affinity (adenosine EC_{50} at A_{2B} ~ 24 μM).[44] However, under pathological conditions such as hypoxia, inflammation and tissue injury, the adenosine level increases by up to 100-fold, and consequently the A_{2B}ARs are activated.[44]
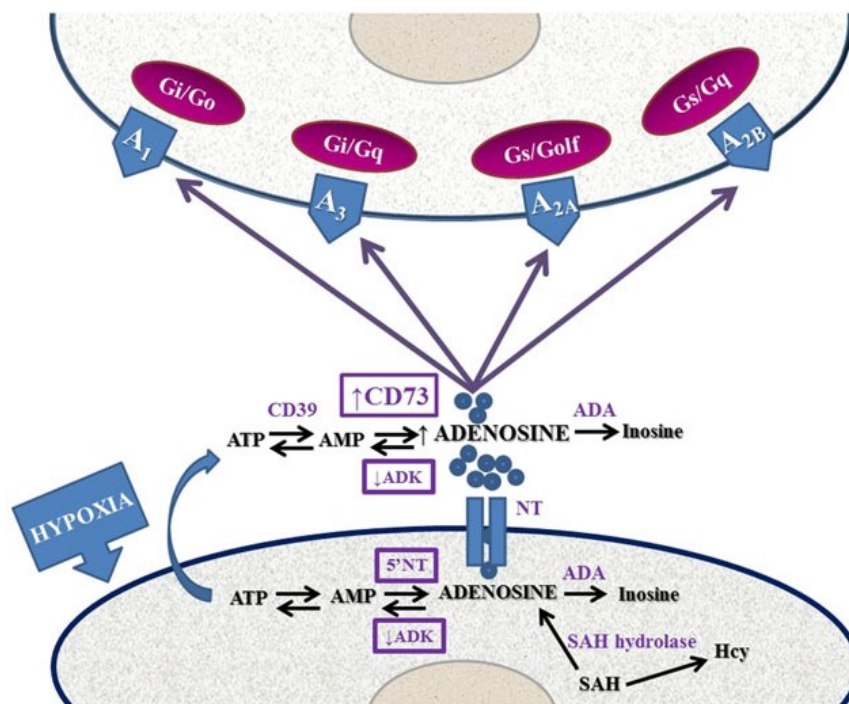
Figure 5. Schematic representation of adenosine interconversion in the intra- and extracellular space.[45]

Adenosine plays an important role as a neurotransmitter and neuromodulator, also regarded as a 'guardian angel' for regulating tissue functions within stress conditions.[46,47] The cardioprotective effects of adenosine were discovered by Drury and Szent-Györgyi in 1929,[48] it promotes vasodilatation, angiogenesis, decreases inflammation and counteracts prolonged ischemia.[49] Adenosine is clinically approved as Adenocard® for the treatment of paroxysmal supraventricular tachycardia.[50] Contrarily, in acute pathological conditions, the overproduction of adenosine results in chronic inflammation and dramatic organ damage.[45] These effects were reported for neurodegenerative diseases, ischemia, diabetes, asthma and cancer. For instance, adenosine disables the anti-tumor immune response in the tumor microenvironment and enhances proliferation and angiogenesis (neovascularization) in tumors.[51] Therefore, targeting the adenosinergic pathways by AR antagonists may be an effective novel therapy for cancer.[45]

1.3.2. X-ray structures

Currently, there are more than 200 X-ray crystal structures for GPCRs deposited in the protein data bank.[52] Studying these crystal structures helps us to understand the binding mode of the ligands to the orthostatic or the allosteric binding pockets of the receptor. GPCR crystal structures display the alpha-helices forming the transmembrane domains, extracellular and the intracellular loops. These new advancements in X-ray crystallographic technologies gave us more knowledge about the structure and function of GPCRs and aided us to rationally design new ligands.[53] Although, crystal structures of the A_1- and the A_{2A}ARs were resolved, structures for A_{2B}- and A_3ARs have not been obtained yet.[52,54,55] Several X-ray structures of the human A_{2A}ARs were described either in agonist-bound active receptor states or in antagonist-bound inactive receptor states. For example, the crystal structure of the A_{2A}AR in complex with its antagonist ZM241385 was reported (PDB id: 5NLX) (Figure 6).[55]
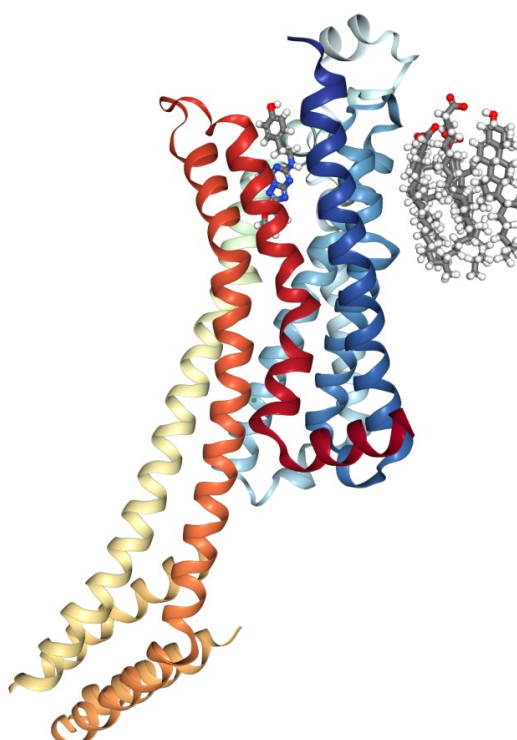
Figure 6. X-ray crystal structure of the adenosine A_{2A}AR in complex with ZM241385 (A_{2A}AR antagonist) (PDB id: 5NLX).[55]

1.4. A₂ᵦ adenosine receptor (A₂ᵦAR)

1.4.1. Molecular characterization of the A₂ᵦ adenosine receptor

A_2 adenosine receptors are subdivided into two subtypes as reported by Daly *et al*. in 1983 based on the findings that one subtype in the rat striatum had higher affinity for adenosine (named $A_{2A}AR$), while the other subtype found throughout the brain showed low affinity for adenosine and was named $A_{2B}AR$.[56] The low affinity $A_{2B}AR$ was firstly cloned by Rivkees and Reppert from rat hypothalamus, and by Pierce from human hippocampus in 1992.[57–59] The gene encoding for the $A_{2B}AR$ is located on chromosome number 17 (17p12-p11.2) spanning 30830
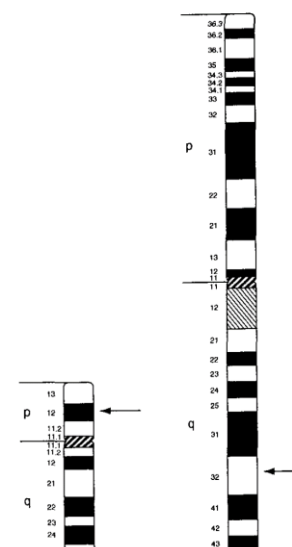
Figure 7. Gene coding for A₂ᵦ receptor.[57]

base pairs (Figure 7). Also, a nonfunctional pseudogene for the $A_{2B}AR$ was described on chromosome 1 (1q32) that exhibits 79% identity to the $A_{2B}AR$ gene. The $A_{2B}AR$ has two transcripts with three exons on the forward strand.[59]

1.4.2. Homology model of the A₂ᵦ adenosine receptor

The X-ray crystal structure of $A_{2B}AR$ has not yet been resolved. In order to know more about the structure and functions of the $A_{2B}AR$, several homology models were built based on the templates of the crystal structures of the $A_{2A}AR$, the most closely related AR paralogue to the $A_{2B}AR$.[60–62] The two ARs share an overall sequence identity of 58% and a similarity of 73%.[63] A_{2A}- and $A_{2B}ARs$ share almost the same binding site for adenosine as shown in the homology model of $A_{2B}AR$, based on the X-ray structure of the $A_{2A}AR$ (PDB code: 2YDO) (Figure 8).[64] Although there is only a single amino acid exchange (leucine L249 in the $A_{2A}AR$ for valine V250 in the $A_{2B}AR$), there is a large difference in the affinity of adenosine for both receptors.[64] Therefore, it is expected that other parts of the $A_{2B}AR$ are involved in

conformational changes leading to the large difference in adenosine affinity, adenosine showed high affinity for the $A_{2A}AR$ and low affinity for the $A_{2B}AR$.
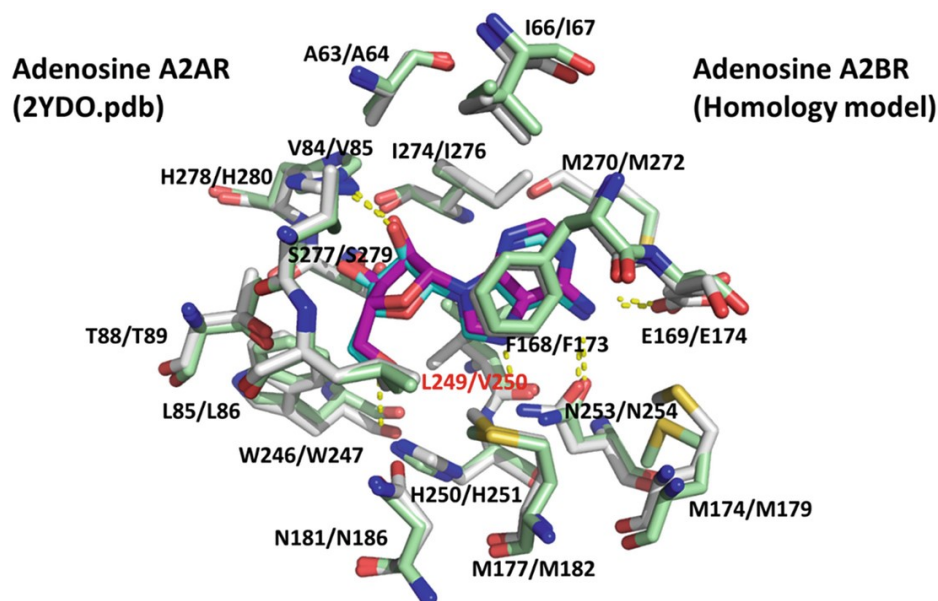
Figure 8. Comparison of the adenosine binding sites of the $A_{2A}AR$ (PDB code: 2YDO) and the $A_{2B}AR$ homology model. The overlay shows that the binding sites differ only in a single amino acid.[64]

Moreover, the $A_{2B}AR$ has a longer extracellular domain (EL2) with two *N*-glycosylation sites, and the EL2 was predicted to play an important role as a gate-keeper for ligand binding, receptor activation and subtype selectivity (Figure 9).[65] Recently, a new study predicted the presence of a meta-binding site for adenosine in the ECL2 using supervised molecular dynamics simulation studies.[66] Additionally, in the $A_{2B}AR$, only one disulfide bond is formed which is essential for ligand binding and receptor activation, whereas in the $A_{2A}AR$, four essential disulfide bonds are formed in the extracellular domains, and the $A_{2A}AR$ is therefore much more rigid.[67,68]
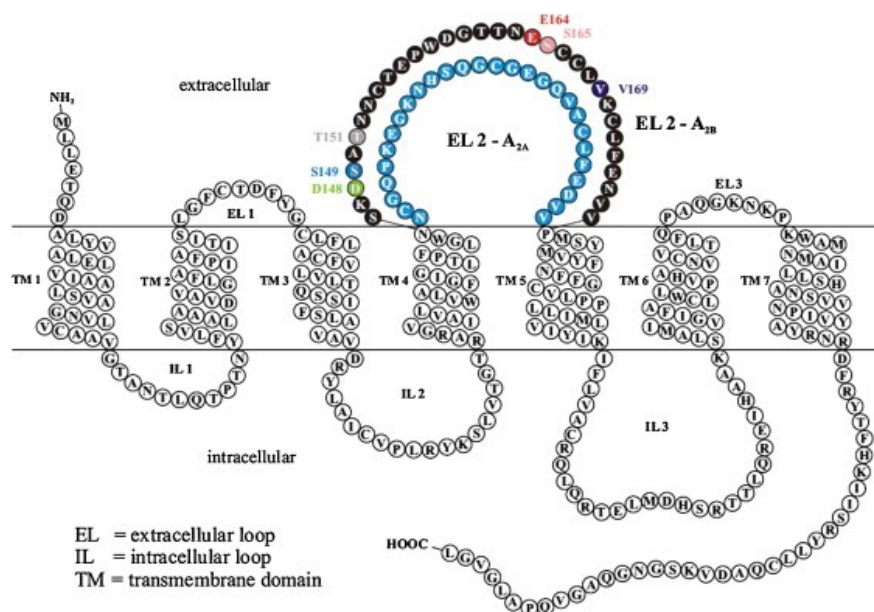
Figure 9. Snakelike plot of the human A_{2B} receptor. EL2-A_{2B} (black), EL2-A_{2A} (blue).[65]

1.4.3. Physiologic and pathologic functions of the A_{2B} adenosine receptor

A_{2B}ARs play an important role in diverse physiological body functions. Under normal conditions, the basal extracellular level of adenosine is not high, thus the A_{2B}AR, the low affinity AR subtype, is not activated.[69] Under pathological conditions such as inflammation and hypoxia, extracellular adenosine levels are highly elevated, and significant upregulation of A_{2B}AR expression was reported indicating an important role of A_{2B}ARs in disease.[44,70] A_{2B}ARs are, for example, expressed in vasculature, brain, large intestine and urinary bladder.[71] Moreover, A_{2B}ARs are found in neuronal cells, alveolar cells, astrocytes and many immune cells including mast cells, macrophages and lymphocytes.[72] Adenosine has been linked to diabetes mellitus, since it affects glucose homeostasis, and to insulin secretion through the activation of A_{2B}ARs. Besides, it prevents insulin resistance under standard nutritional conditions by controlling the activity of alternative macrophages.[73]

In myocardial ischemia, $A_{2B}ARs$ are selectively induced to decrease infarction through vasodilatory effects, decreasing platelet aggregation and adjusting effective metabolism of carbohydrates. Also, the $A_{2B}AR$ promotes tissue adaptation to hypoxia and counteracts hypoxia-induced inflammation.[72] This cardioprotective process involves transcription factor hypoxia-inducible factor (HIF1α) and specificity protein 1 (SP1) (Figure 10).[74] Other studies indicated the important role of $A_{2B}ARs$ in the progression of diabetic nephropathy, renal dysfunction and fibrosis. The inhibition of $A_{2B}ARs$ suppresses the production of VEGF in renal glomeruli. Furthermore, studies showed that the inflammatory cytokine (IL-6) mediated adenosine-activated renal fibrosis downstream of $A_{2B}AR$. Therefore, $A_{2B}AR$ antagonists would play a protective role in VEGF-induced nephropathy and attenuate renal dysfunction and fibrosis.[75,76]
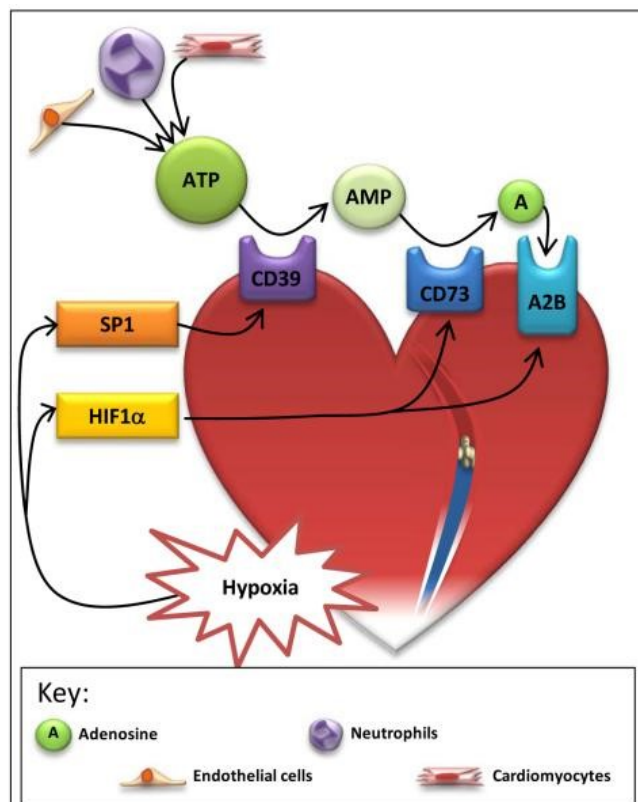
Figure 10. Hypoxia induces $A_{2B}AR$ expression and adenosine production, e.g. in myocardial ischemia, through HIF1 and SP1 respectively.[74]

Introduction

High adenosine levels in tumor tissues generate an immune-tolerant microenvironment and increase tumor growth.[77] $A_{2B}ARs$ were found highly expressed in many cancer cells in comparison to nearby normal tissues, which suggests their vital role in tumor proliferation, metastasis, angiogenesis and immune suppression (Figure 11).[78] Interestingly, the signaling pathways related to $A_{2B}AR$-mediated proliferation in cancer cells are quite diverse in different cancer types. The $A_{2B}AR$ can lead to activation of mitogen-activated protein kinase (MAPK), the cAMP-EPAC pathway, extracellular signal-regulated kinases (ERK1/2) and others.[79]
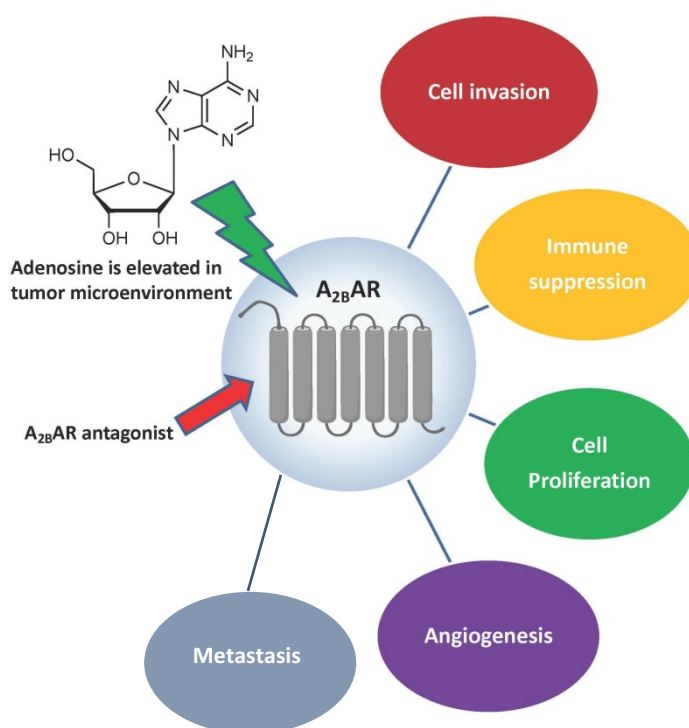
Figure 11. Schematic representation showing the role of $A_{2B}ARs$ and its antagonists in cancer.[78]

It was found that the activation of $A_{2B}ARs$ on tumor cells increased metastasis.[80] The mechanism may involve $A_{2B}AR$-mediated expression of one of the main metastasis transcription factors, Fos-related antigen-1 (Fra-1).[81] Moreover, tumor growth is dependent on angiogenesis, the formation of new blood vessels, that supply cells with oxygen and nutrients (Figure 11).[82] The activation of $A_{2B}ARs$ stimulates the production of angiogenic cytokines by mast cells, and the potent angiogenic factor, vascular endothelial growth factor (VEGF).[83] $A_{2B}AR$ signaling is involved in cancer growth and proliferation, thus $A_{2B}AR$ antagonists are

novel and potential anti-cancer drugs that limits tumor growth, and metastasis and enhance anti-tumor immune response. Currently, several $A_{2B}AR$ antagonists are in clinical trials for treating cancer.[78]

1.4.4. A₂B adenosine receptor selective ligands

1.4.4.1. A₂B adenosine receptor agonists

1.4.4.1.1. Nonselective A₂B adenosine receptor agonists

Although studies of animal models suggest the therapeutic advantage of $A_{2B}AR$ activation in several diseases including lung injury, vascular leakage and ischemia, the development of a potent and selective fully efficacious $A_{2B}AR$ agonist has not yet been achieved.[84] The development of a selective $A_{2B}AR$ agonist would be very important to fully understand the role of the receptor in health and disease. Various agonists for the other AR subtypes (A_1, A_{2A} and A_3ARs) have reached preclinical and clinical evaluation stages, and an $A_{2A}AR$-selective agonist, Regadenoson, is marketed as a diagnostic drug for myocardial perfusion imaging.[85,86] Up till now, some adenosine-derived non-selective $A_{2B}AR$ agonists (Figure 12) and the partial $A_{2B}AR$ agonist, BAY60-6583 (**4a**, Figure 13) have been developed.[64]

Adenosine (**1**) is the natural agonist of ARs, however due to its short half-life, more stable synthetic adenosine derivatives are often used.[87] $A_{2B}AR$ agonists include adenosine-like and non-adenosine-like compounds. 5′-(*N*-ethylcarboxamido)adenosine (NECA, **2**), a non-selective AR agonist, is considered one of the most potent $A_{2B}AR$ agonists with an EC_{50} value in the nanomolar range depending on the expression level.[88] [³H]NECA is used as a radioligand to determine the affinity of agonists for $A_{2B}AR$ in its active conformation.[89] An N^6-substituted NECA derivative (**3**) with a furancarboxamide moiety (Figure 12) appeared to display some $A_{2B}AR$ selectivity, however, this is difficult to assess since the reported functional data (EC_{50})

cannot be directly compared with the affinities obtained in binding studies for **3** at the other

AR subtypes.[90]
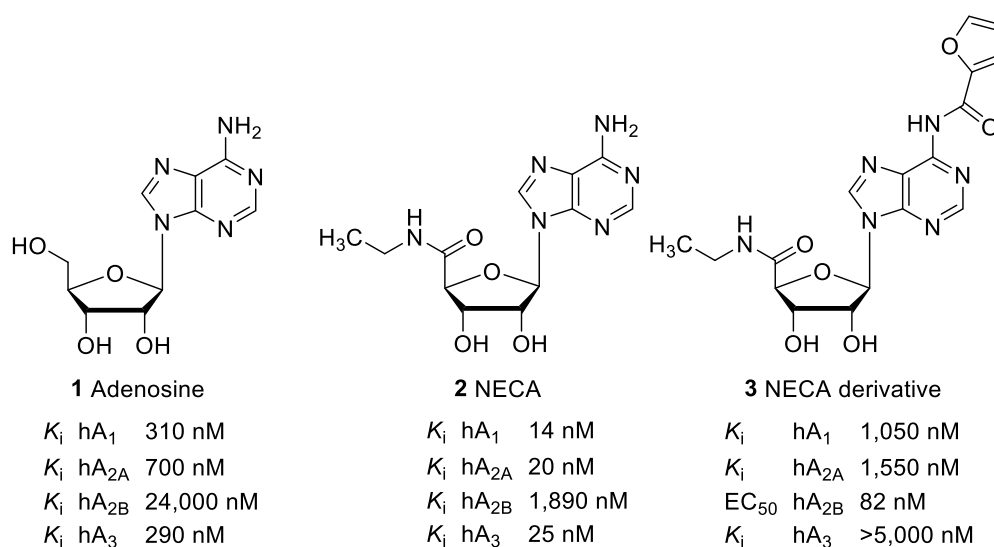
Figure 12. Chemical structures of non-selective A_{2B}AR agonists and their potency and selectivity; (h = human).[87,88,90]

1.4.4.1.2.   Partial A2B adenosine receptor agonists

BAY60-6583 **(4a)** was reported as the most potent and selective A_{2B}AR agonist (Figure

13) and has been extensively used in in vitro and in vivo pharmacological studies.[91] The

activation of A_{2B}ARs is thought to maintain the endothelial cell barrier and to have a

cardioprotective effects.[92] In a model of myocardial reperfusion injury, compound **4a** showed

protective cardiovascular effects.[93] Moreover, compound **4a** induced apoptosis and cell cycle

arrest in breast cancer stem cells.[94] However, recent studies showed that based on the receptor

expression level and local adenosine concentration, compound **4a** would act as a partial agonist

or even as a functional antagonist.[95,96] Thus compound **4a** should be used with caution in

pharmacological studies as it displayed varied efficacies ranging from full to partial A_{2B}AR

agonists and can even act as A_{2B}AR antagonist.[64] Also, it displayed higher affinity for A_{2B}ARs

and lower affinity for the other AR subtypes as compared to NECA (**2**) in binding assays.
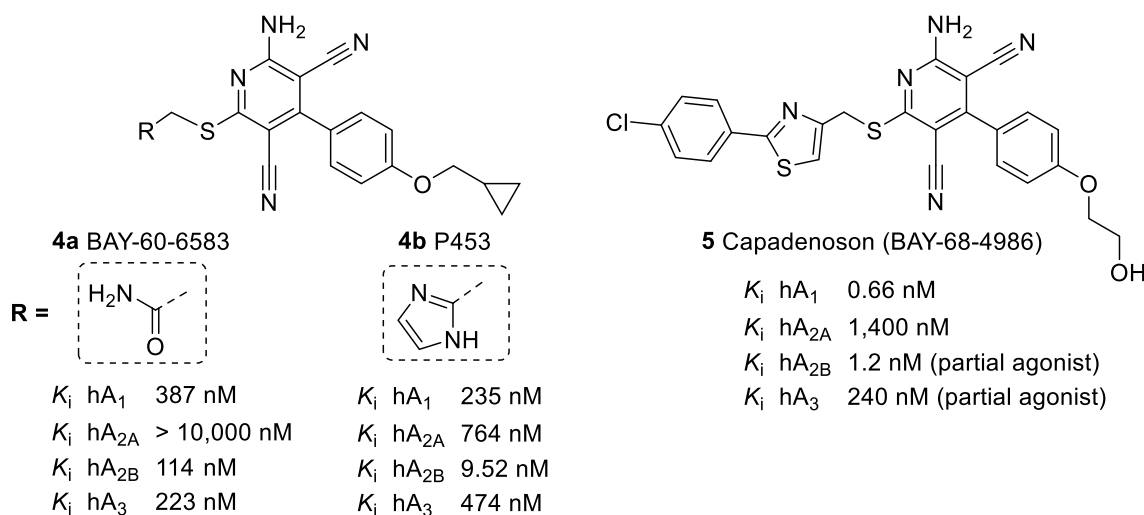
Figure 13. Chemical structures of partial A_{2B}AR agonists; (h = human).[91,97,98]

Recently, compound P453 (**4b**), was reported as a potent partial A_{2B}AR agonist. It shares with **4a** the same amino-3,5-dicyanopyridines scaffold and appeared to show higher potency (Figure 13).[97] Compound **4b** activated A_{2B}ARs causing increased glutamate release at presynaptic terminals thus decreasing paired pulse facilitation (PPF).[99] PPF is expected to be involved in many neuronal tasks such as information processing and simple learning.[100] Furthermore, Capadenoson (BAY-68-4986, **5**), a structural analogue of compound **4a** (Figure 13), was initially classified as a partial A_1AR agonist and underwent phase IIa clinical trials in patients with atrial fibrillation and further in patients with stable angina. Later on, compound **5** was withdrawn from clinical trials.[98,101] Recently, researchers showed the ability of **5** to stimulate also A_{2B}ARs, thus **5** is suggested to act as a dual A_1/A_{2B}AR agonist.[102]

Recent studies have shown that dual agonism of A_1- and A_{2B} ARs can be beneficial in the treatment of heart failure through modulating myocardial fibrosis (A_{2B}AR-mediated) and hypertrophy (A_1AR mediated).[103] Compound VCP746 (**6**) is a dual agonist for A_1- and A_{2B}-ARs that consists of an adenosine moiety and an A_1AR positive allosteric modulator (PAM) moiety connected by an alkyl chain. Compound **6** promoted cardio protection through the activation of the A_1AR and was proposed to display antifibrotic effects through A_{2B}AR

stimulation (Figure 14).[104] Binding affinity of compound **6** at human ARs was determined in Müller group, showing that **6** not only exhibited high binding affinity for A_1- and A_{2B}ARs, but also significant affinity for the A_{2A}AR subtype (unpublished data).
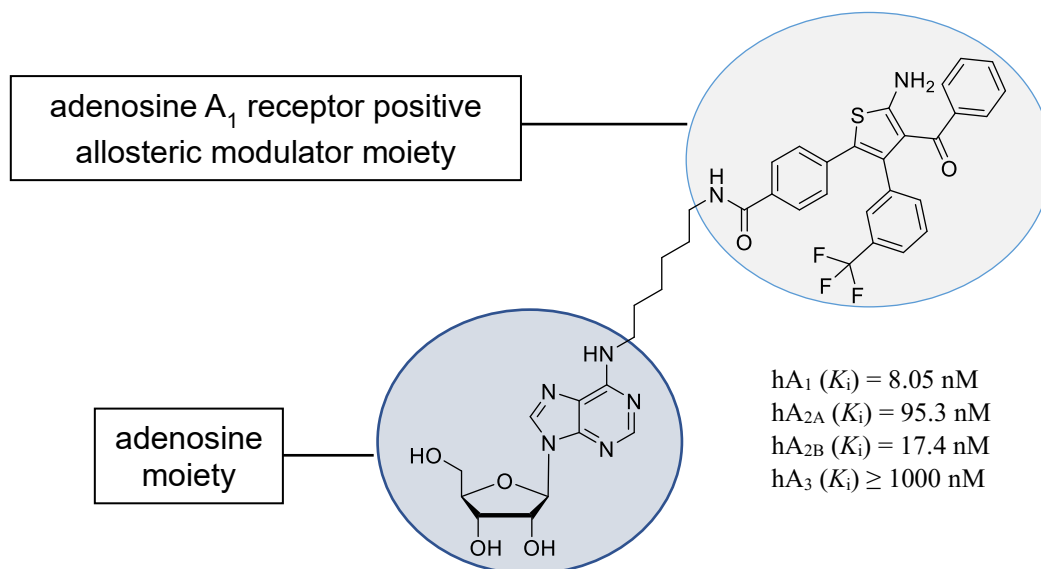
Figure 14. Chemical structure of compound VCP746 (**6**), a dual A_1/A_{2B}AR agonist; (h = human).[104]

1.4.4.1.3. Selective A_1, A_{2A} and A_3 adenosine receptor agonists

Several adenosine-like compounds were reported as selective AR agonists.[85,105] The N^6-substituted adenosine derivative CCPA (**7**), was reported as a highly selective A_1AR agonist. It showed selectivity for the A_1AR in rat and mouse studies, however it is less selective for the A_1AR in humans versus the A_1AR subtype (Figure 15).[106,107]
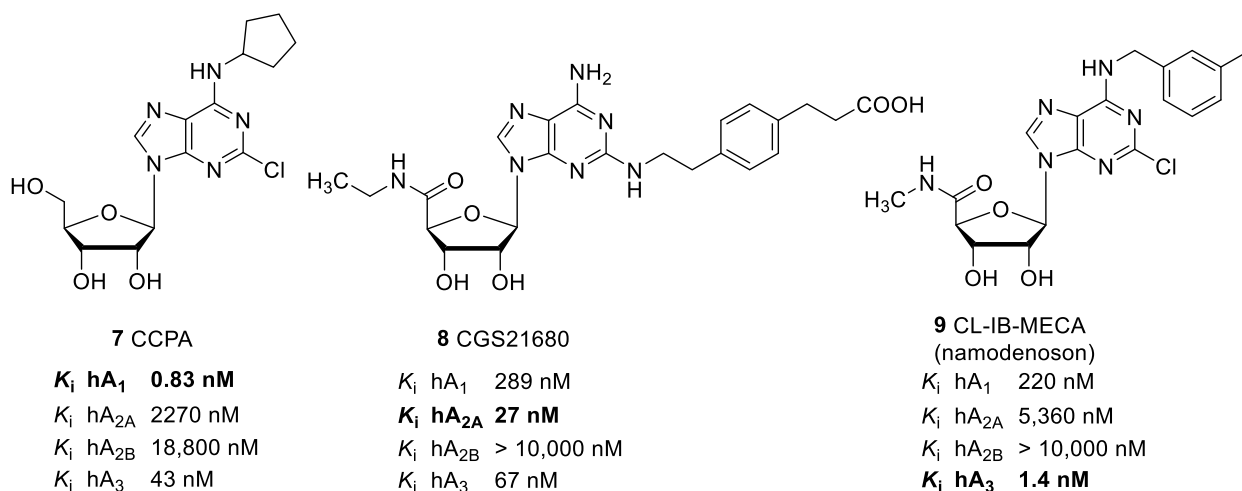
Figure 15. Chemical structure of selective A_1, A_{2A} and A_3AR agonists (**7-9**); (h = human).[106–109]

For the $A_{2A}AR$, CGS21680 (**8**), having a bulky substituent in position 2 of the adenosine scaffold, was reported as a potent and selective $A_{2A}AR$ agonist in rats, expressing moderate selectivity in humans versus the A_1- and A_3AR subtypes.[108] C1-IB-MECA (namodenoson, **9**) was reported as a very potent and selective A_3AR agonist; it is a novel drug candidate which is currently in phase II clinical trials for the treatment of nonalcoholic fatty liver disease (NAFLD) and nonalcoholic steatohepatitis (NASH) (Figure 15).[109]

1.4.4.2. A2B adenosine receptor antagonists

1.4.4.2.1. Nonselective adenosine receptor antagonists

The naturally occurring alkaloids theophylline and caffeine were the first reported non-selective AR antagonists (Figure 16).[63] Caffeine (**10**) is found in common beverages such as coffee and tea, it increases alertness, arousal and energy.[110] Furthermore, some studies suggested the usage of **10**, also in combination with selective $A_{2A}AR$ antagonists, for the treatment of effort-related motivational dysfunction in depression.[111] Theophylline (**11**) is a well-known treatment for asthma, however it interacts with various drugs and it has a narrow therapeutic window, thus its usage has to be closely monitored to avoid toxicity.[112] The antagonist XAC (**12**) exhibits high affinity for all human AR subtypes (Figure 16), an can be regarded as a potent pan-AR antagonist.[64] An X-ray structure of the thermostabilized $A_{2A}AR$ in the inactive conformation in complex with **12** was reported (PDB id: 3REY).[113]

10 Caffeine	**11** Theophylline	**12** XAC
K_i hA_1 10,700 nM	K_i hA_1 6,700 nM	K_i hA_1 6.8 nM
K_i hA_{2A} 9,560 nM	K_i hA_{2A} 1,710 nM	K_i hA_{2A} 18 nM
K_i hA_{2B} 10,400 nM	K_i hA_{2B} 9,070 nM	K_i hA_{2B} 7.8 nM
K_i hA_3 13,300 nM	K_i hA_3 22,300 nM	K_i hA_3 91.9 nM
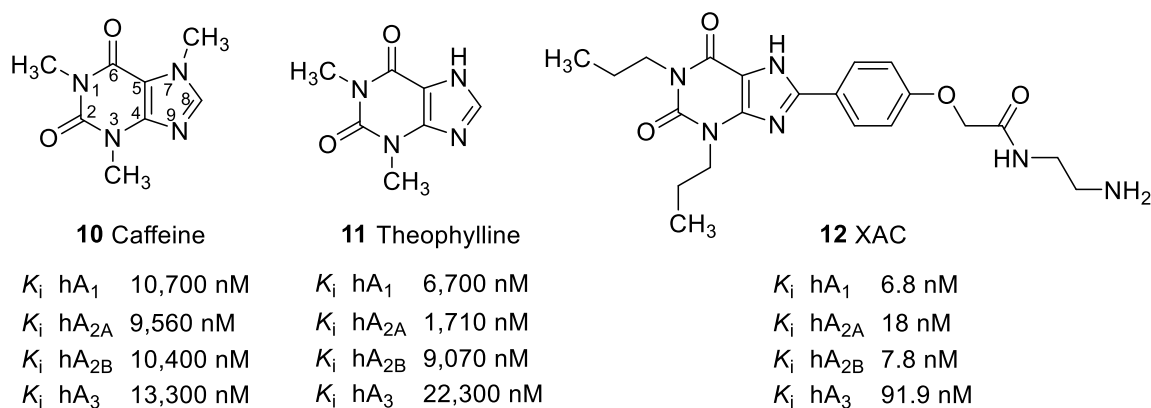
Figure 16. Chemical structures of nonselective AR antagonists; (h = human).[63,113]

1.4.4.2.2. Selective A$_{2B}$ adenosine receptor antagonists

1.4.4.2.2.1. Xanthines

PSB-1115 (**13**) is one of the early reported potent and selective A$_{2B}$AR antagonists that has a sulfonamide group and showing a high water-solubility, therefore it has been frequently used in in vivo studies (Figure 17).[114] It enhanced the intestinal barrier function in colon inflammation in ischemic conditions and reperfusion injury.[115] However, **13** shows selectivity only in humans, not in other species, and it cannot penetrate the central nervous system (CNS) as it is deprotonated under physiological conditions.[114] Direct substitution on the C8 of the xanthine scaffold by different heteroaromatic residues was explored by several research groups.[116] CVT-6883 (**14**), developed by CV Therapeutics (now Gilead), showed good A$_{2B}$AR antagonistic activity and selectivity. Although it inhibited pulmonary inflammation and injury in the lungs of adenosine deaminase (AD) deficient mice, it was discontinued from clinical trials for lung remodeling and pulmonary hypertension.[117]

MRS-1754 (**15**) was reported as a potent and selective A$_{2B}$AR antagonist in humans (Figure 17), however it showed poor oral bioavailability and is nonselective in rats and mice, moreover, it is metabolically unstable.[118,119] Compound **15** inhibited the growth of colon carcinoma cells and induced antiangiogenesis in microvascular endothelial cell lines.[115,120] To overcome the drawbacks of sulfonates, the sulfonamide group was introduced in compound PSB-603 (**16a**, Figure 17), one of the most potent and selective A$_{2B}$AR antagonists. Compound **16a** developed in Müller's research group showed excellent affinity for the human A$_{2B}$AR with a K_i value of 0.553 nM.[121] Subsequently, a high affinity radioligand was prepared ([^{3}H]PSB-603) which is frequently used today in radioligand binding assays.[121] Compound **16a** changed the cellular metabolism in colorectal cancer cells and enhanced their responsiveness to chemotherapy.[122] Moreover, it attenuated the proliferation of multiple prostate cancer cell

lines.[123] Compound **16a** showed high metabolic stability in human, mouse and rat, however it has poor water solubility.[105]

13 PSB-1115

K_i	hA$_1$	> 10,000 nM
K_i	hA$_{2A}$	> 24,000 nM
K_i	hA$_{2B}$	53.4 nM
K_i	hA$_3$	> 10,000 nM

14 GS 6201 (CVT-6883)

K_i	hA$_1$	1,940 nM
K_i	hA$_{2A}$	3,280 nM
K_i	hA$_{2B}$	22 nM
K_i	hA$_3$	1,070 nM

15 MRS-1754

K_i	hA$_1$	403 nM
K_i	hA$_{2A}$	503 nM
K_i	hA$_{2B}$	1.97 nM
K_i	hA$_3$	570 nM

16a PSB-603 16b PSB-1901
X = Cl   X = Br

K_i	hA$_1$	> 10,000 nM	> 1,000 nM
K_i	hA$_{2A}$	> 10,000 nM	> 1,000 nM
K_i	hA$_{2B}$	0.553 nM	0.0835 nM
K_i	hA$_3$	> 10,000 nM	> 1,000 nM
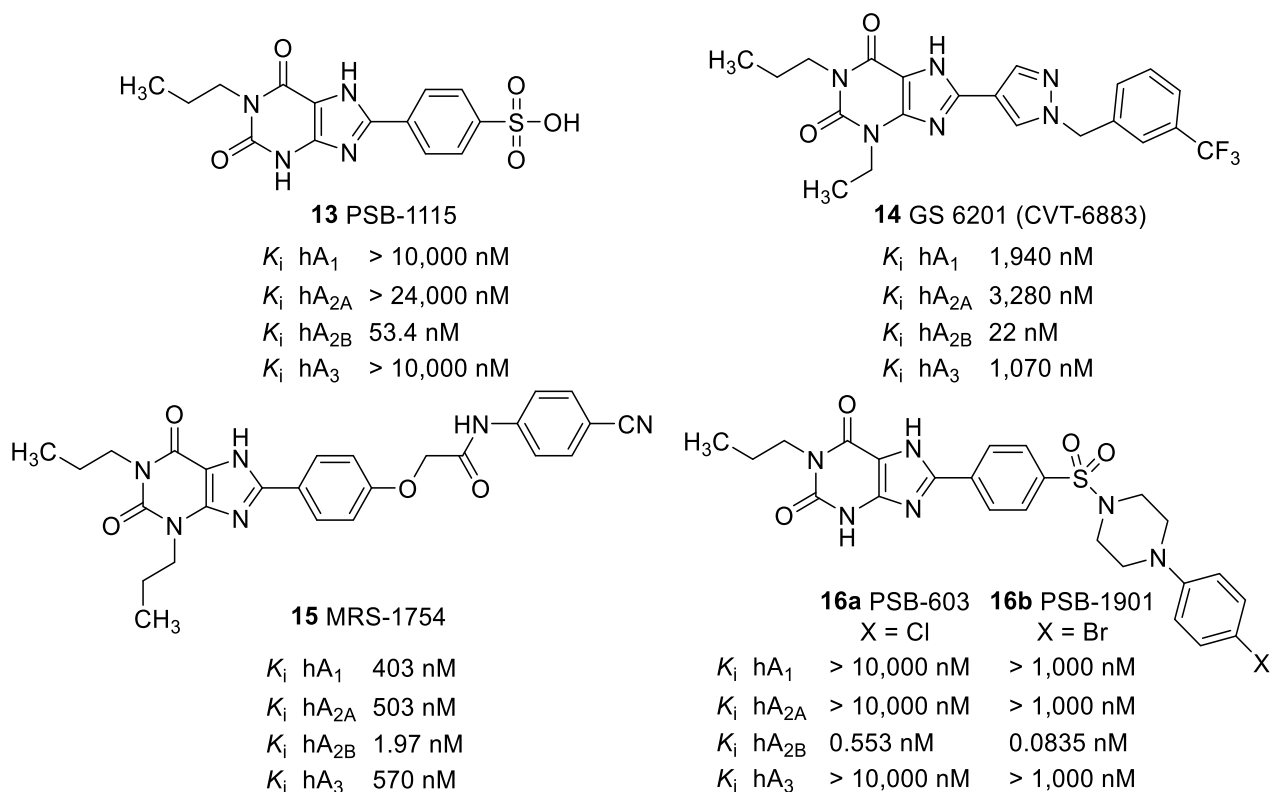
Figure 17. Chemical structures of selective A$_{2B}$AR antagonists with xanthine-core structure; (h = human).[62,114,117,118,121]

Recently, structural modifications in **16a** revealed more potent and selective A$_{2B}$AR antagonists, such as compound PSB-1901 (**16b**, Figure 17).[62] Replacement of the terminal *p*-chlorophenyl substituent in **16a** by a *p*-bromo residue increased the binding affinity of the compound for the human A$_{2B}$AR. Compound **16b** is the most potent and selective A$_{2B}$AR antagonist up to date (human A$_{2B}$ K_i = 0.0835 nM).[62]

1.4.4.2.2.2. Non-xanthines

Several non-xanthine-based A$_{2B}$AR selective antagonists with different heterocyclic scaffolds have been developed. LAS101057 (**17**), a pyrazine derivative (Figure 18) showed promising potency in cell-based assays and in an in vivo OVA-sensitized mouse model of

asthma. After passing preclinical safety studies, it was further selected for phase I clinical trials for asthma treatment.[124] Compound ISAM140 (**18**) was identified as a new potent and selective $A_{2B}AR$ antagonist with a new scaffold resulted from structural modification of the 3,4-dihydropyrimidin-2(1*H*)-one chemotype (Figure 18). The potency of **18** was studied in radioligand binding assays ($K_i = 3.49$ nM) and functional cAMP experiments ($K_B = 27.0$ nM).[125]

17 LAS101057	**18** ISAM140	**19** BAY-545
K_i hA$_1$ > 10,000 nM	K_i hA$_1$ > 10,000 nM	IC$_{50}$ hA$_1$ 1,300 nM
K_i hA$_{2A}$ > 2,500 nM	K_i hA$_{2A}$ > 10,000 nM	IC$_{50}$ hA$_{2A}$ 820 nM
K_i hA$_{2B}$ 24 nM	K_i hA$_{2B}$ 3.49 nM	IC$_{50}$ hA$_{2B}$ 66 nM
K_i hA$_3$ > 10,000 nM	K_i hA$_3$ > 10,000 nM	K_i hA$_{2B}$ 97 nM
		IC$_{50}$ hA$_3$ 6,600 nM
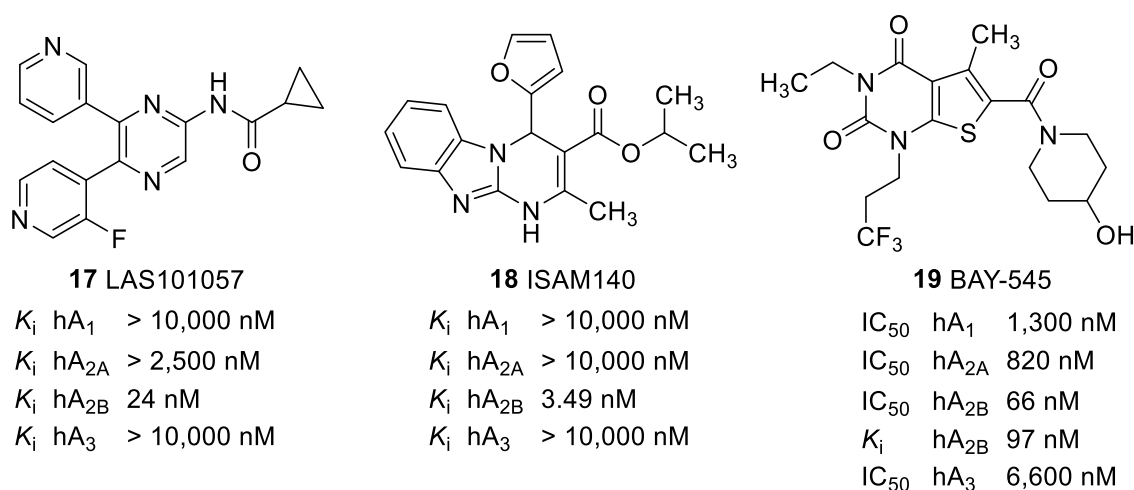
Figure 18. Chemical structures of selective non-xanthine $A_{2B}AR$ antagonists; (h = human).[124–126]

Furthermore, high-throughput screening was carried out by Bayer in 2018 using their corporate substance library (~ 2.8 million compounds were screened), where they reported thienouracil core to be a promising scaffold for selective $A_{2B}AR$ antagonists. BAY-545 (**19**, Figure 18) was selected as a lead structure for subsequent in vivo testing.[126] It was tested in animal models of pulmonary fibrosis, and caused a decrease of pro-fibrotic and pro-inflammatory mediators in the lungs of animals pretreated with a lung fibrosis induction stimulus (fluorescein isothiocyanate (FITC) and silica). Although compound **19** has high exposure after oral administration to mice, yet it is still a moderately potent $A_{2B}AR$ antagonist that needs further optimization.[126] One of the main obstacles facing the in vitro studies of many $A_{2B}AR$ antagonists is their low solubility in body fluids. Selective $A_{2B}AR$ antagonists with improved physicochemical properties are required.

1.4.4.2.3. Selective A$_1$, A$_{2A}$ and A$_3$ adenosine receptor antagonists.

PSB-36 (**20**, Figure 19) is a selective and potent xanthine-based A$_1$AR antagonist that induced inhibition of human T lymphocytes proliferation and cell death.[63] Preladenant (**21**) is considered one of the most potent and selective A$_{2A}$AR antagonists across different species, also it was evaluated in clinical investigations for early Parkinson's disease (PD), however the results did not support its usage as a monotherapy for PD treatment although it was well tolerated.[129] For the A$_3$AR, MRS1523 (**22**), was reported as a potent A$_3$AR antagonist in rodents, yet it showed large species difference in terms of potency and selectivity.[129]

20 PSB-36
K_i **hA$_1$**   **0.7 nM**
K_i hA$_{2A}$ 980 nM
K_i hA$_{2B}$ 187 nM
K_i hA$_3$ 2300 nM

21 Preladenant
K_i hA$_1$ > 1,000 nM
K_i **hA$_{2A}$ 0.9 nM**
K_i hA$_{2B}$ > 1,000 nM
K_i hA$_3$ > 1,000 nM

22 MRS1523
K_i hA$_1$ > 10,000 nM
K_i hA$_{2A}$ 3660
K_i hA$_{2B}$ > 10,000 nM
K_i **hA$_3$ 18.9 nM**
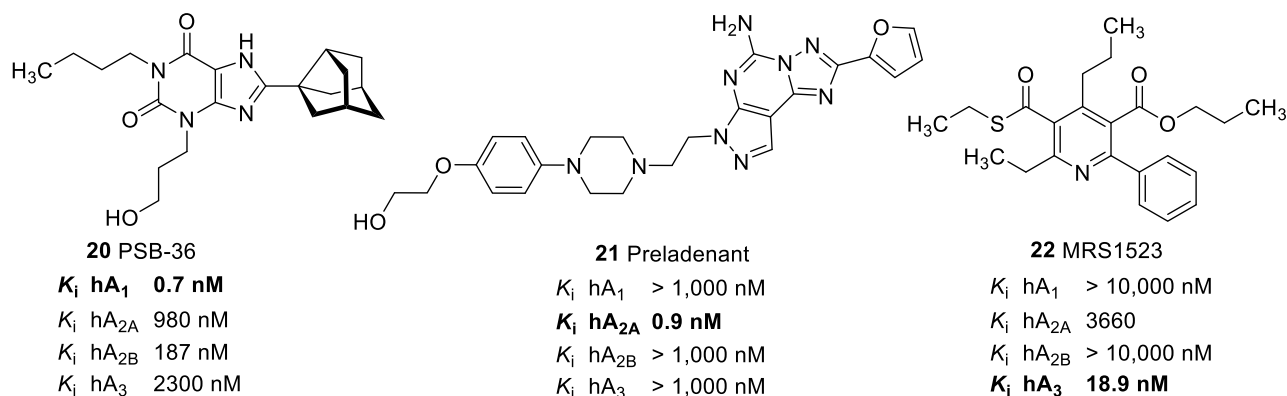
Figure 19. Chemical structure of selective A$_1$, A$_{2A}$ and A$_3$AR antagonists (**20-22**); (h = human).[127–129]

1.4.4.3. Dual A$_{2A}$/A$_{2B}$ adenosine receptor antagonists

Multitargeting is a new concept in drug development where one drug molecule can simultaneously interact with two or more drug targets. This approach can be powerful, in particular in diseases like cancer where the pharmacological cascade is very complex.[130] Additionally, multi-targeting compounds show less side effects and improved compliance in patients as compared to combination therapies.[130] Adenosine blocks the effects of T-lymphocytes to attack cancer tissues through activation of the A$_{2A}$AR. Moreover, A$_{2B}$AR are highly expressed in many cancer cells having a vital role in tumor proliferation, and metastasis.[73] Therefore, developing dual inhibitors that block both receptors A$_{2A}$- and A$_{2B}$ AR, simultaneously could exhibit synergistic effects in cancer (immuno)therapy.[64]

Several dual $A_{2A}/A_{2B}AR$ antagonists were recently reported (Figure 20). AB928 (**23**) was reported as a peripherally restricted potent antagonist of A_{2A}- and $A_{2B}ARs$. A phase I clinical trial was conducted to study safety, tolerability, pharmacokinetics (PK) and pharmacodynamics (PD) of orally applied **23**. The PK profile of compound **23** was dose-proportional and linear which supports its further clinical development as oral anti-cancer therapy.[131] Moreover, a dose escalation phase I study of compound **23** in combination with **AB122** – a fully human monoclonal antibody targeting programmed cell death receptor-1 (PD-1) - will be assessed in participants with advanced malignancies.[132] However, **23** shows only 30-40-fold selectivity versus the A_1AR, which is considered as anti-target for this indication. Furthermore, 2-alkynyl-8-aryl-9-methyladenine derivative E-3210 (**24**) developed by Eisai (Japan) was reported as a dual $A_{2A}/A_{2B}AR$ antagonist (Figure 20), however the affinity data for **24** have not been yet published.[133] Further clinical investigation of this compound for the treatment of irritable bowel syndrome (IBS) was announced.[126,134]

23 AB928

K_B hA_1 64 nM
K_B hA_{2A} 1.5 nM
K_B hA_{2B} 2 nM
K_B hA_3 489 nM

24 E-3210
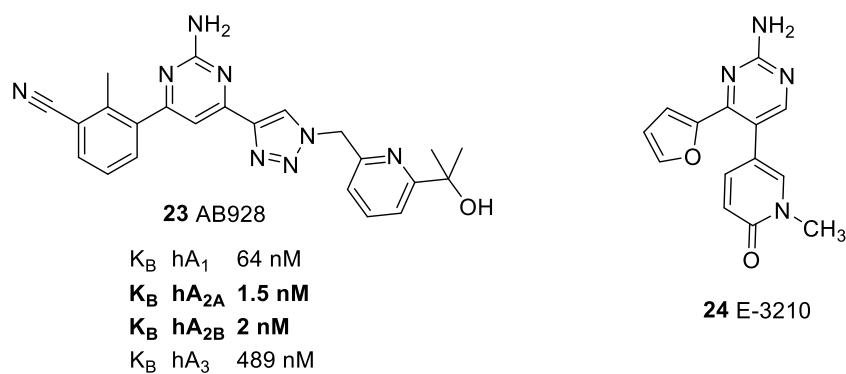
Figure 20. Chemical structures of dual $A_{2A}/A_{2B}AR$ antagonists; (h = human).[133,135]

Studies carried out by X-Chem (USA) showed that dual $A_{2A}/A_{2B}AR$ antagonists exhibited improved anticancer activity over selective A_{2A} antagonists as they can inhibit adenosine signaling in more cell types.[136] After several lead optimizations, they developed the dual $A_{2A}/A_{2B}AR$ antagonists X6350 with good activity and PK properties; however, the chemical structure is not yet available. The reported binding affinities towards human A_{2A}- and $A_{2B}ARs$

were 21.0 nM and 4.4 nM respectively. In addition, X6350 follows all Lipinski's rules of five for drug-likeness, thus it was selected as a clinical candidate.[136] Furthermore, a newly discovered series of dual $A_{2A}/A_{2B}AR$ antagonists was reported by Selvita (Poland). Compounds SEL330-584 and SEL330-639 exhibited high in vitro activity not only at low adenosine levels, but also at high adenosine concentrations (tumor-like adenosine-rich environment), however the compound's structures are not yet accessible.[135,137] Both compounds restored the adenosine agonist-impaired functional activity of molybdate-transporting ATPase (moDC) in cytokine release assays through their inhibition of the $A_{2B}AR$.[138]

1.4.4.4. Allosteric modulators

In addition to the previously described $A_{2B}AR$ agonists and antagonists, some allosteric modulators, namely 1-benzyl-3-ketoindole derivatives **25-28**, were reported (Figure 21).[139,140] These compounds were identified using binding assays, functional assays (cAMP accumulation assay) and [^{35}S]GTPγS binding assays in CHO cells expressing A_1, A_{2A}, A_{2B} and A_3ARs. Compounds **25-26** were reported to act as positive allosteric modulators (PAMs), they increased the efficacy of the AR agonist NECA (**2**) at $A_{2B}ARs$ but they had no effect on their own. Compound **26** increased cAMP production induced by **2** with an EC_{50} 250 nM and a maximal increase from 100% to 237%.[139]
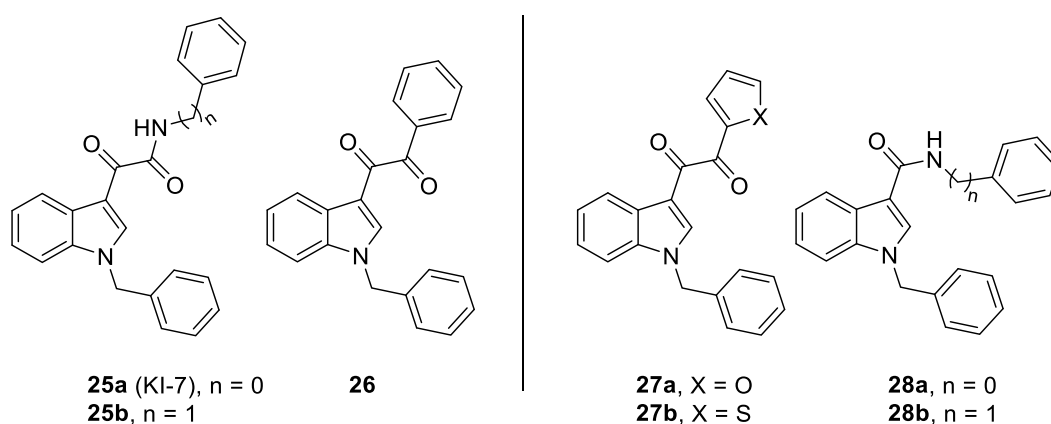

25a (KI-7), n = 0
25b, n = 1

26

27a, X = O
27b, X = S

28a, n = 0
28b, n = 1

Figure 21. Chemical structures of allosteric $A_{2B}AR$ modulators.[139,140]

On the other hand, performing slight alterations in the side chain of the same scaffold resulted in other compounds **27-28** reported as A$_{2B}$AR negative allosteric modulators (NAMs) (Figure 21). Compound **28b** increased the dissociation of the radioligand [^{3}H]NECA from the A$_{2B}$AR and blocked NECA-induced cAMP in CHO cells expressing the A$_{2B}$AR.[140] The inventors of the allosteric A$_{2B}$AR modulators **25-28** had designed these compounds taking into consideration the structural similarity between AR antagonists and GABA$_A$ receptor ligands.

1.4.4.5. Radio- and fluorescent ligands

Radioligand binding assays are important methods for the screening of new potential ligands. Several selective agonist and antagonist radioligands for the different adenosine receptor subtypes were reported.[110] Agonist radioligands label the high-affinity binding site of an active receptor, while antagonist radioligands bind to both the active and inactive conformations of the receptor with similar affinity. However, antagonists with inverse agonistic activity bind with higher affinity to an inactive receptor conformation. Although several selective antagonist radioligands for the A$_{2B}$ARs were reported, such as [^{3}H]MRS-1754 and [^{3}H]PSB-603 **29** (Figure 22), still, a selective agonist radioligand for the A$_{2B}$AR has not yet been developed.[121,141]

Despite extensive trials performed in the Müller group to establish a radioligand binding assay using [^{3}H]BAY 60-6583 (Figure 13), they were successful due to the compound's moderate affinity and high non-specific binding.[89] Alternatively, the tritium-labeled NECA ([^{3}H]NECA, **30**), a non-selective AR agonist can be used in radioligand binding assays to determine the affinity of ligands for the active conformation of the A$_{2B}$AR (Figure 22).[89] However, it can only be used in cell lines not expressing the other AR subtypes.
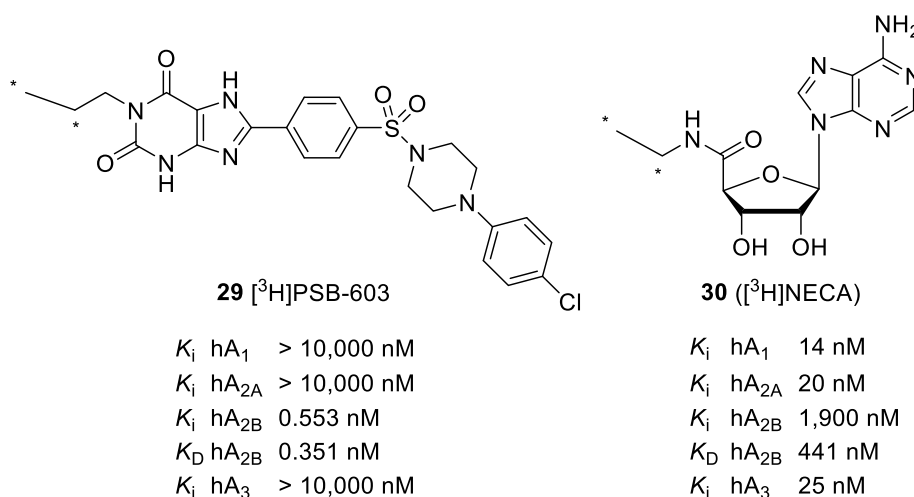
Figure 22. Chemical structures of radioligands for labeling of A$_{2B}$AR; (h = human).[89,121]

Fluorescent ligands represent an important alternative to radioligands to reduce costs and to avoid the risks of handling radioactive waste.[142] Recently, the first potent and selective fluorescent A$_{2B}$AR ligand was reported by the Müller group (PSB-12105, **31**, Figure 23).[61] It selectively labeled A$_{2B}$ARs and was used to establish a homogeneous receptor-ligand binding assay using flow cytometry, as well as a NanoBret^{TM} assay.[61,143] Moreover, a novel radiofluorinated A$_{2B}$AR antagonist was developed as potential ligand for positron emission tomography (PET) imaging. Compound **32** showed high affinity and selectivity for A$_{2B}$ARs (Figure 23). This ligand would help us to quantify the A$_{2B}$ARs in pathological conditions, identifying variations in receptor density in inflammation or cancer models and for monitoring cancer therapies.[144]
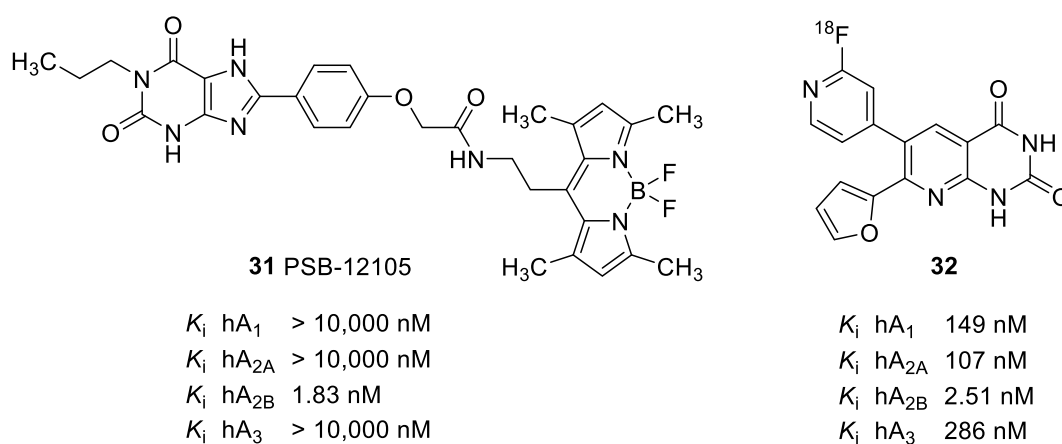
Figure 23. Chemical structures of the fluorescent ligand PSB-12105 (**31**) and the radiofluorinated A$_{2B}$AR antagonist **32**; (h = human).[61,144]

1.4.5. Therapeutic applications of A2B adenosine receptor-selective ligands

Several studies reported the important roles of A_{2B}ARs in many pathological conditions where adenosine levels are elevated, and consequently A_{2B}ARs are activated. For example, A_{2B}AR agonists were reported to have cardioprotective effects in ischemic conditions,[145] while A_{2B}AR antagonists are potential agents for cancer (immune)therapy.[64]

1.4.5.1. A2B adenosine receptor agonists

Although several non-selective AR agonists were reported, such as adenosine and NECA, up to now no fully efficacious A_{2B}AR-selective agonist has been developed. Several potential therapeutic applications were described for BAY-60-6583 (**4a**), the partial A_{2B}AR agonist (Figure 13), for example in obesity-induced diabetes, ischemic stroke and heart infarction.[146,147] Activation of A_{2B}ARs by compound **4a** promoted the proliferation of various cancer cells including human breast cancer cell line, MDA-MB-231 cells, and melanoma cells in a mouse model.[148,149] Because compound **4a** is reported as a partial A_{2B}AR agonist, it should be used with caution if investigated in in vivo studies or in clinical trials to validate that these pharmacological effects are *via* A_{2B}AR activation.[96,150]

1.4.5.2. A2B adenosine receptor antagonists

The inhibition of A_{2B}ARs holds great promise in cancer (immuno)therapy. A_{2B}AR antagonists not only prevent inhibition of immune cells by adenosine in the cancer micro-environment similarly to A_{2A}AR antagonists, but they also inhibit tumor proliferation, metastasis and angiogenesis.[64] The A_{2B}AR antagonist PSB-1115 (**13**, Figure 17) decreased metastasis of $CD73^+$ melanoma cells, and it also increased the anti-tumor activity of dacarbazine, a chemotherapeutic alkylating drug used in the treatment of melanoma and Hodgkin's lymphoma.[149,151]

Theophylline (**11**, Figure 16), a well-known asthma drug, is a non-selective AR antagonist which demonstrated some anti-tumor effects. Although it inhibits all four AR subtypes, its anticancer effect is thought to occur through $A_{2B}AR$ rather than $A_{2A}AR$ based on blockade of A_{2A}- and $A_{2B}AR$ knockout mice study.[152] Moreover, theophylline was tested for its anticancer effects in a chronic lymphocytic leukemia phase II clinical study.[153] $A_{2B}AR$-selective antagonists including PSB-603 (**16a**), GS 6201 (**14**, Figure 17) and ATL-801 inhibited the proliferation of prostate, colon, melanoma and other cancer cells,[123,152,154,155] suggesting a potential role of $A_{2B}AR$-selective antagonists as anticancer agents. Compound **14** developed by CV Therapeutics was the first selective $A_{2B}AR$ antagonist to be clinically evaluated.[153] In Phase I clinical trials, it showed a good safety and pharmacokinetic profile and was found to be suitable for once daily chronic dosing.[156]

Additionally, compound PBF-1129 (structure not disclosed), a reported potent and selective $A_{2B}AR$ antagonist, is clinically investigated as oral treatment for idiopathic pulmonary fibrosis (IPF) and advanced non-small cell lung cancer (NSCLC).[157,158] ATL-844, an $A_{2B}AR$-selective antagonist developed by PGxHealth company, was clinically evaluated in phase II trials for the treatment of asthma and type-2 diabetes mellitus, however both trials were discontinued.[159] Moreover, compound AB928 (**23**, Figure 20), a dual $A_{2A}/A_{2B}AR$ antagonist, is clinically investigated as oral anti-cancer therapy,[131] since it is hypothesized that simultaneous inhibition of both AR subtypes (A_{2A} and A_{2B}) has synergistic effects against some tumors.[78] Oral **23** showed a dose-proportional PK profile and will be investigated in combination with AB122, human monoclonal antibody targeting programmed cell death-1 receptor for the treatment of various cancers.[132]

1.5. Approaches to improve aqueous solubility of target compounds

Currently there are many reported potent and selective $A_{2B}AR$ antagonists that can inhibit $A_{2B}ARs$ with (sub)-nanomolar binding affinity values (Figures 17, 18).[62,121] However, most of these compounds are lacking adequate aqueous solubility required for in vivo studies and subsequent clinical development.[62] Compounds having inadequate physicochemical properties create major challenges for their delivery to the desired biological target.[160] Therefore, several approaches have been explored to overcome these challenges with sparingly soluble drugs including prodrug approaches, structural modifications and various formulation strategies, such as pH adjustment and inclusion of solubilizers.[161]

1.5.1. Prodrugs

Prodrugs are molecules that are biologically inactive and are converted to the active parent drug in vivo through chemical or enzymatic reactions.[162] The US Food and Drug Administration (FDA) has approved more than 30 prodrugs in the past 10 years, they represent 12% of all approved small molecule drugs.[160] Prodrug approaches can increase water solubility, improve oral absorption, enhance chemical stability, and reduce toxicity of the parent drug.[163] There are many approaches to develop prodrugs, such as phosphates, phosphonates, esters and carbamates, however selecting the appropriate one depends on the desired outcome. Here, we will focus on phosphate prodrugs used to improve the solubility of the parent molecule.

The concept behind the phosphate prodrug approach is to convert a polar and/or ionized functional group 'synthetic handle', for example a hydroxyl group, to its respective phosphate prodrug. There are several reported phosphate prodrugs, some of them are already approved drugs on the market, such as the hypnotic agent Fospropofol (Lusedra®, **33**), the orally administered antiretroviral protease inhibitor Fosamprenavir (Lexiva®, **34**) and the antiemetic drug Fosaprepitant (Ivemend®, **35**).[160-162] Moreover, MSX-3 (**36**), the water-soluble prodrug of

the A$_{2A}$AR antagonist MSX-2 (**37**), is directly injectable and widely used as a pharmacological tool in various in vivo studies.[163–165]
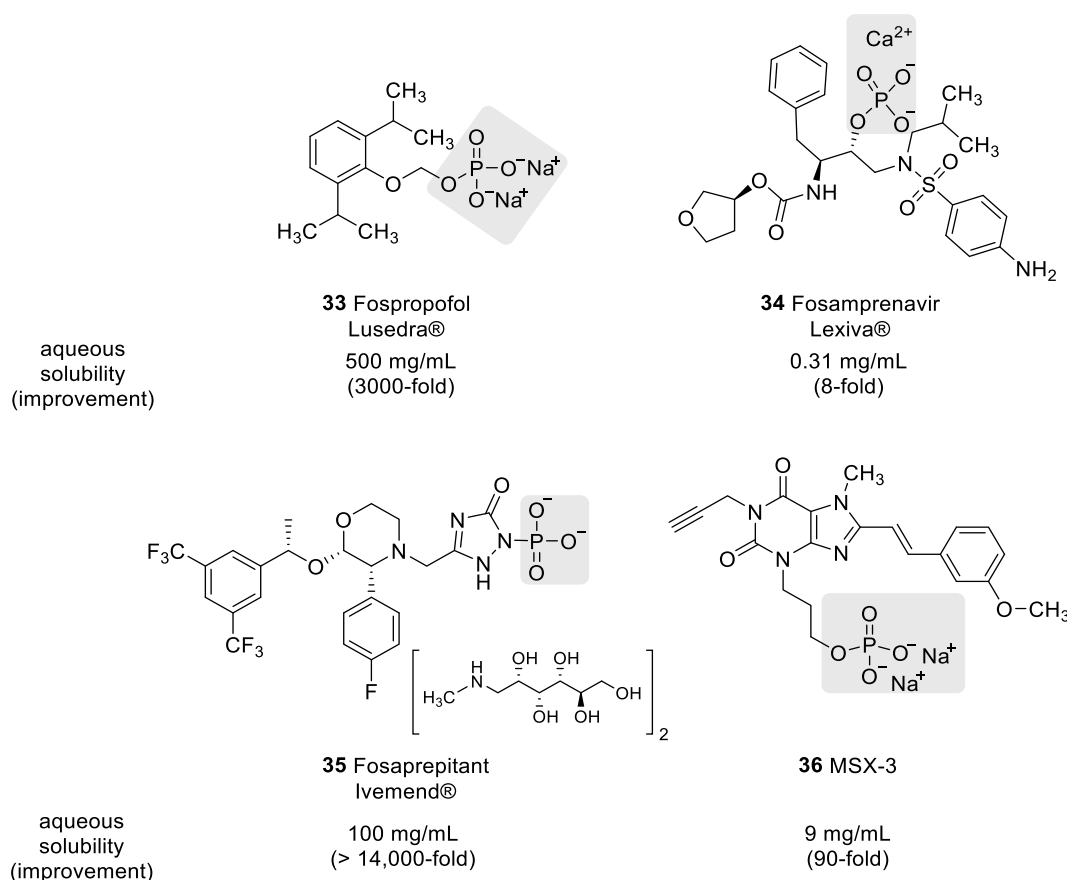
Figure 24. Chemical structures of some phosphate prodrugs.

Phosphate prodrugs display higher aqueous solubility than the parent molecule. The thermodynamic solubility of prodrugs can be modified by the cations.[166] Compound **33** has enhanced aqueous solubility, from 150 µg/mL for propofol to ~ 500 mg/mL for the prodrug. Phosphate prodrug **36** showed an about 100-fold increase in solubility in comparison to its parent compound **37** with a free hydroxy group. After injection, **36** undergoes fast and quantitative bio-conversion by alkaline phosphatase producing the potent A$_{2A}$AR antagonist **37** (Figure 25).[163]
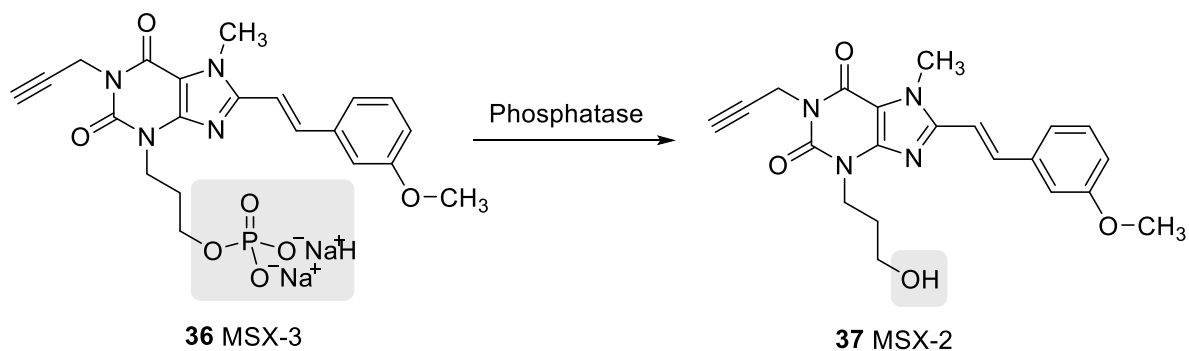
Figure 25. *In-vivo* bioconversion of MSX-3 (**36**) to MSX-2 (**37**).[163,164]

1.5.2. Structural modifications

Optimization of physiochemical properties alongside with biological activity is an important element of successful drug discovery. The high demand in producing potent and selective ligands for specific targets resulted in many cases in increasing the size and hydrophobicity of the lead structure.[167] Improving the solubility of the target compound can be achieved by reducing its hydrophobicity and crystalline stability, while at the same time considering the structure-activity-relationships (SARs) responsible for the biological activity.[168]

Firstly, introducing a polar group, a 'solubilizing appendage', to the target compound is one of the approaches to increase its solubility. Such polar groups should be directed away from the binding site as they can make H-bonding with the target residues and interfere with the binding of the ligand's key pharmacophore features to its target.[160] For example, the replacement of various alkyl groups attached to isothiazole by polar groups such as a hydroxyl group in compound **38d** and an ethoxy group in compound **38c** dramatically increased water solubility from ~100 to > 5000 µg/mL (Figure 26).[168]
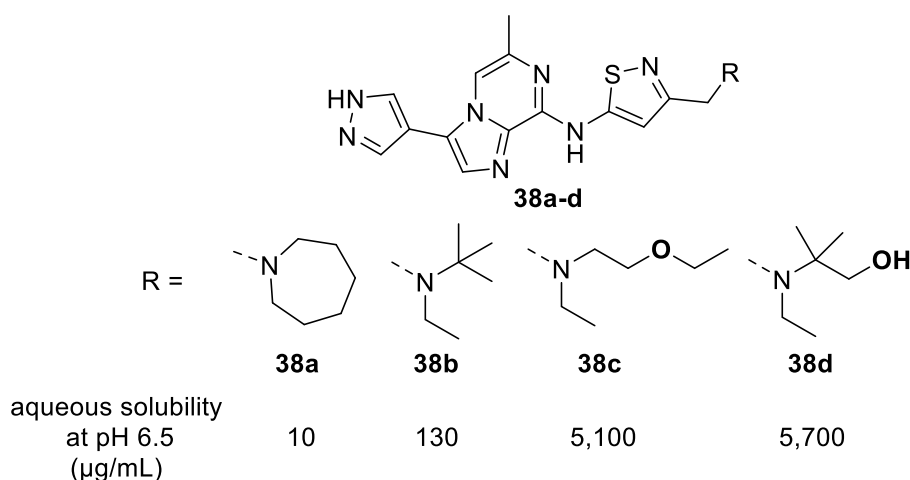
Figure 26. The effect of introducing polar groups on the aqueous solubility of compound **38**.[168]

Moreover, replacing an aromatic phenyl ring by a polar heterocycle, such as pyridine, is one of the common approaches to reduce hydrophobicity. This replacement will not interfere with the final shape of the compound and is often tolerated. Interestingly, we can observe the effect of just changing a single CH group in compound **39** to a nitrogen (pyridyl analogue) in compound **40** resulting in increased solubility by 100-fold at in pH 6.8 (Figure 27).[169]
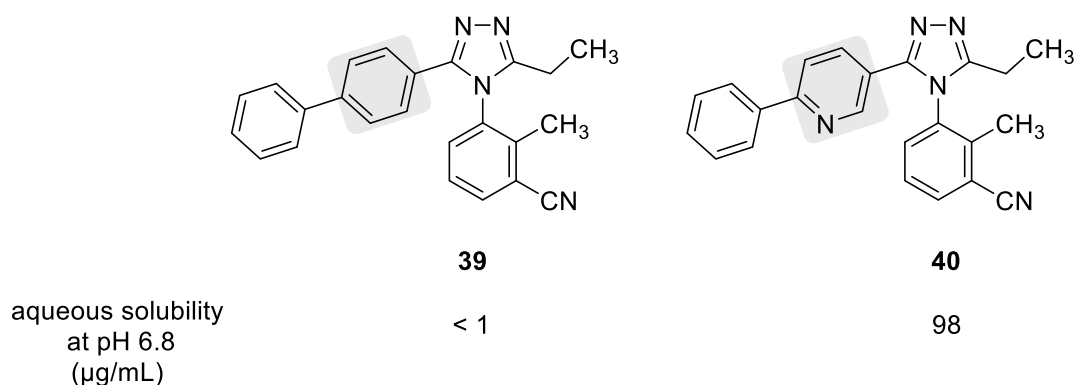
Figure 27. The effect of ring replacements on the aqueous solubility.[169]

Another example shows the effect of heteroatom rearrangements in one heterocyclic ring on the overall solubility of the compound. Compound **41a** having a 1,3,4-oxadiazole ring was found to be much better soluble than compound **41b** having a 1,2,4-oxadiazole and compound **41c** having a 1,2,4-oxadiazole (Figure 28).[170,171] This effect is expected to be related to the higher overall basicity of the 1,3,4-oxadiazoles.[172]

R =			
	41a	**41b**	**41c**
aqueous solubility at pH 7.4 (μg/mL)	118	3.1	4.8
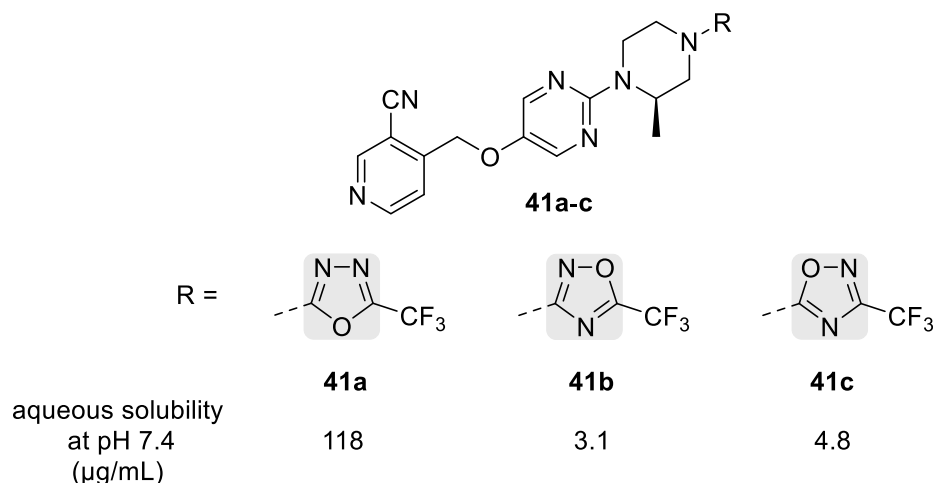
Figure 28. The effect of heteroatom rearrangements on the aqueous solubility.[170,171]

Furthermore, compound AMG 517 (**42**), a vanilloid receptor 1 (TRPV1) antagonist, showed low thermodynamic aqueous solubility that limited its further clinical development as a potential second-generation treatment for chronic pain.[173] Introducing saturation (removing aromaticity) to the 4-(trifluoromethyl)phenyl ring improved greatly the solubility of the compound (**43**, Figure 29).[173] Compound **43** is less hydrophobic (lower cLogP value), this could be anticipated due to the reduction in structural planarity and the disruption of the crystal-stacking capabilities. Moreover, compound **43** showed a lower melting point which supports the interpretation that disruption of planarity accounts in part to the enhanced solubility.[174,175]

	42 (AMG 517)	**43**
aqueous solubility (0.01 M HCl) (μg/mL)	<1	13
cLogP	4.6	3.7
Melting point (°C)	219-221	130-131
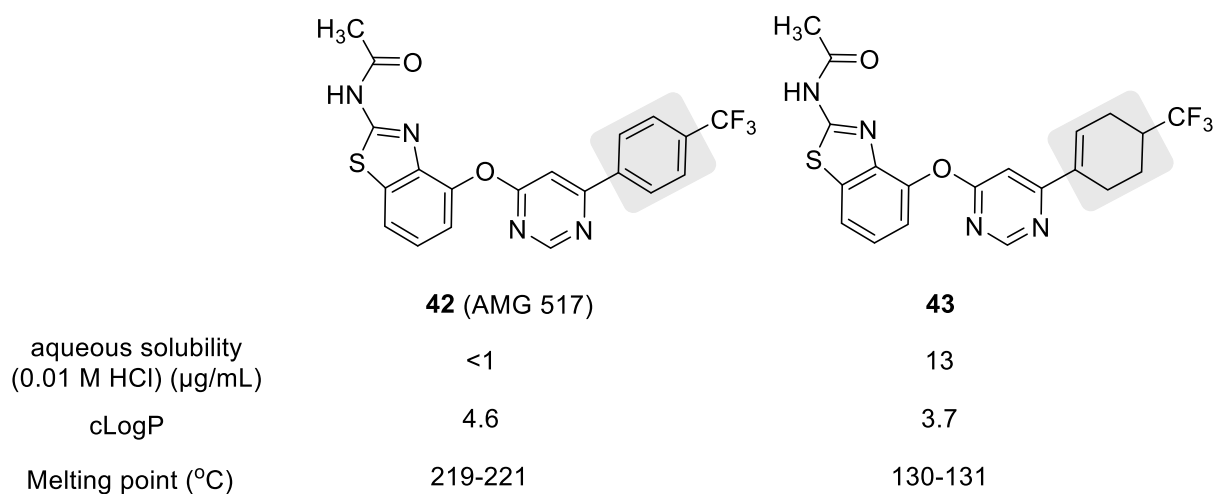
Figure 29. The effect of removing aromaticity on the aqueous solubility of AMG 517 (**42**).

2. Aims of the study

2.1. **Water-soluble prodrugs of A$_{2B}$ adenosine receptor antagonists**

Although several potent and selective A$_{2B}$AR antagonists have been discovered, they are poorly water-soluble, which limits their usage as pharmacological tools. The objective of this project is to structurally optimize the potent A$_{2B}$AR antagonist PSB-1901 (**16b**) to develop water-soluble A$_{2B}$AR antagonist phosphate prodrugs, that can be hydrolyzed by endogenous phosphatases yielding the active drug.[176] The target compounds will bear hydroxy groups attached either at substituent on the *N*3 position of the xanthine moiety or to the large *C*8-xanthine substituent (target structures A-C, Figure 30).
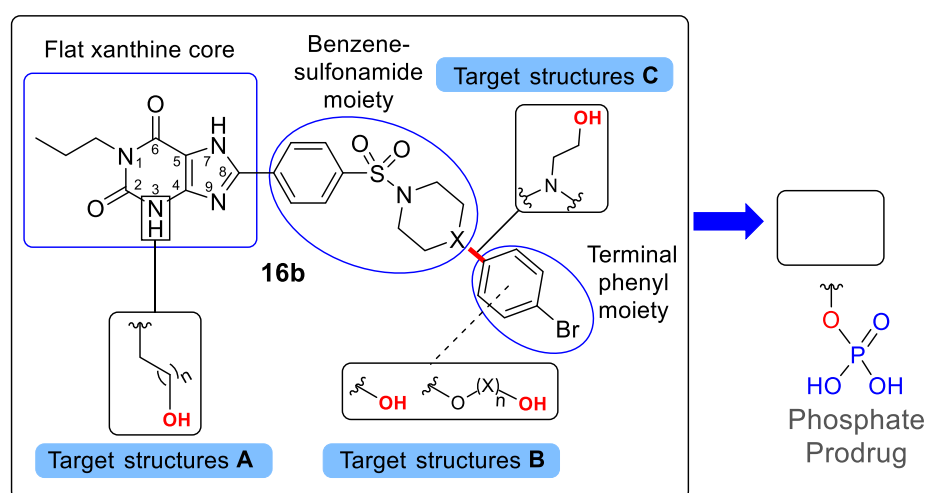
Figure 30. Schematic representation showing the three main partial structures of A$_{2B}$AR antagonist **16b** and the proposed structural modification to obtain three series of hydroxylated target structures **A**, **B** and **C** followed by the preparation of their respective phosphate prodrugs.

The designed compounds share the main pharmacophoric features essential for A$_{2B}$AR activity, including a xanthine scaffold that represents a flat core offering a hydrogen-bond donor group (NH at *N*7 of xanthine) and a hydrogen-bond acceptor group (carbonyl function at *C*6 of xanthine), a propyl substitution at the *N*1 position of xanthine, a benzenesulfonamide moiety and a *p*-bromophenyl substituent at *C*8 of the xanthine core. Compounds showing high affinity and selectivity for the A$_{2B}$AR will be further phosphorylated to yield their respective water-soluble phosphate prodrugs (Figure 30).

2.2. Development of dual A$_{2A}$/A$_{2B}$ adenosine receptor antagonists

Recent studies indicated a beneficial role of synergistically inhibiting A$_{2A}$ and A$_{2B}$ARs for cancer (immuno)therapy.[177,178] Starting from lead compound PSB-1901 (**16b**), we will make several modifications on this scaffold with substituents that are well tolerated by both A$_{2A}$ and A$_{2B}$ARs (Figure 31). Starting with substitution on the xanthine scaffold, we will replace the *N*1-propyl group with an ethyl or methyl residues, and substitute in the *N*3 position with methyl, ethyl, or cyclopropyl substituents. Also, the terminal phenyl ring will be replaced with various heterocyclic rings including pyridine, pyrimidine, thiophene, etc. Different linkers connecting the terminal aromatic ring with the piperazine or piperidine moieties will also be investigated (Figure 31). These various structural modifications will be implemented and evaluated with the aim to develop potent dual A$_{2A}$/A$_{2B}$ adenosine receptors antagonists.
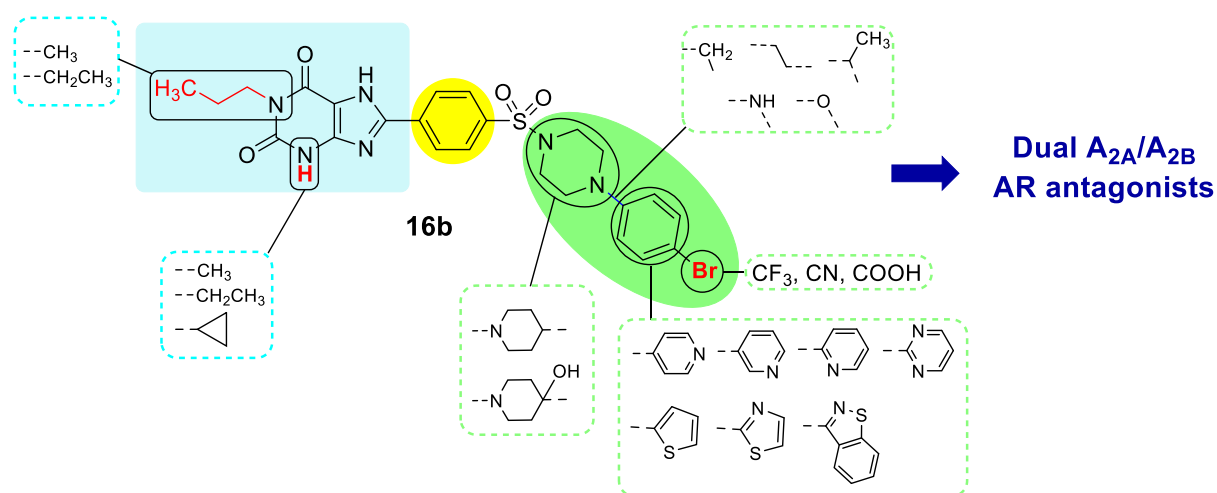
Figure 31. Schematic representation of the proposed structural modification of **16b** to develop potent dual adenosine A$_{2A}$/A$_{2B}$AR antagonists.

3. References

(1)   Jacoby, E.; Bouhelal, R.; Gerspacher, M.; Seuwen, K. The 7 TM G-protein-coupled receptor target family. *ChemMedChem* **2006**, *1*, 760–782.

(2)   Katritch, V.; Cherezov, V.; Stevens, R. C. Structure-function of the G protein–coupled receptor superfamily. *Annu. Rev. Pharmacol. Toxicol.* **2013**, *53*, 531–556.

(3)   Hauser, A. S.; Attwood, M. M.; Rask-Andersen, M.; Schiöth, H. B.; Gloriam, D. E. Trends in GPCR drug discovery: new agents, targets and indications. *Nat. Rev. Drug Discov.* **2017**, *16*, 829–842.

(4)   Overington, J. P.; Al-Lazikani, B.; Hopkins, A. L. How many drug targets are there? *Nat. Rev. Drug Discov.* **2006**, *5*, 993–996.

(5)   Berman, H. M. The protein data bank. *Nucleic Acids Res.* **2000**, *28*, 235–242.

(6)   Munk, C.; Mutt, E.; Isberg, V.; Nikolajsen, L. F.; Bibbe, J. M.; Flock, T.; Hanson, M. A.; Stevens, R. C.; Deupi, X.; Gloriam, D. E. An online resource for GPCR structure determination and analysis. *Nat. Methods* **2019**, *16*, 151–162.

(7)   Ballesteros, J. A.; Weinstein, H. Integrated methods for the construction of three-dimensional models and computational probing of structure-function relations in G protein-coupled receptors. *Methods Neurosci.* **1995**, *25*, 366–428.

(8)   Pin, J. P.; Galvez, T.; Prézeau, L. Evolution, structure, and activation mechanism of family 3/C G-protein-coupled receptors. *Pharmacol. Ther.* **2003**, *98*, 325–354.

(9)   Neumann, E.; Khawaja, K.; Müller-Ladner, U. G protein-coupled receptors in rheumatology. *Nat. Rev. Rheumatol.* **2014**, *10*, 429–436.

(10)   Svoboda, P.; Teisinger, J.; Novotný, J.; Bouřová, L.; Drmota, T.; Hejnová, L.; Moravcová, Z.; Lisý, V.; Rudajev, V.; Stöhr, J.; et al. Biochemistry of transmembrane signaling mediated by trimeric G proteins. *Physiol. Res.* **2004**, *53*, 141–152.

(11)   Kobilka, B. K. G protein coupled receptor structure and activation. *Biochim. Biophys. Acta - Biomembr.* **2007**, *1768*, 794–807.

References

(12) Attwood, T. K.; Findlay, J. B. Fingerprinting G-protein-coupled receptors. *Protein Eng.* **1994**, *7*, 195–203.

(13) Kolakowski, L. F. GCRDb: a G-protein-coupled receptor database. *Receptors Channels* **1994**, *2*, 1–7.

(14) Fredriksson, R.; Lagerström, M. C.; Lundin, L.-G.; Schiöth, H. B. The G-protein-coupled receptors in the human genome form five main families. phylogenetic analysis, paralogon groups, and fingerprints. *Mol. Pharmacol.* **2003**, *63*, 1256–1272.

(15) Neubig, R. R.; Spedding, M.; Kenakin, T.; Christopoulos, A. International Union of Pharmacology Committee on Receptor Nomenclature and Drug Classification. XXXVIII. Update on terms and symbols in quantitative pharmacology. *Pharmacol. Rev.* **2003**, *55*, 597–606.

(16) Ruffolo, R. R. Important concepts of receptor theory. *J. Auton. Pharmacol.* **1982**, *2*, 277–295.

(17) Rominger, D. H.; Cowan, C. L.; Gowen-Macdonald, W.; Violin, J. D. Biased ligands: pathway validation for novel GPCR therapeutics. *Curr. Opin. Pharmacol.* **2014**, *16*, 108–115.

(18) Wang, W.; Qiao, Y.; Li, Z. New insights into modes of GPCR activation. *Trends Pharmacol. Sci.* **2018**, *39*, 367–386.

(19) Rajagopal, S.; Kim, J.; Ahn, S.; Craig, S.; Lam, C. M.; Gerard, N. P.; Gerard, C.; Lefkowitz, R. J. β-Arrestin- but not G protein-mediated signaling by the "decoy" receptor CXCR7. *Proc. Natl. Acad. Sci. U. S. A.* **2010**, *107*, 628–632.

(20) Wettschureck, N.; Offermanns, S. Mammalian G proteins and their cell type specific functions. *Physiol. Rev.* **2005**, *85*, 1159–1204.

(21) Lefkowitz, R. J. A brief history of G-protein coupled receptors (Nobel Lecture). *Angew. Chem. Int.* **2013**, *52*, 6366–6378.

(22) Steinhilber, D.; Schubert-Zsilavecz, M.; Roth, H. *Medizinische chemie targets, arzneistoffe, chemische biologie*; 2010.

(23) Fredholm, B. B.; Abbracchio, M. P.; Burnstock, G.; Dubyak, G. R.; Harden, T. K.; Jacobson, K. A.; Schwabe, U.; Williams, M. Towards a revised nomenclature for P1 and P2 receptors. *Trends Pharmacol. Sci.* **1997**, *18*, 79–82.

(24) Kamato, D.; Thach, L.; Bernard, R.; Chan, V.; Zheng, W.; Kaur, H.; Brimble, M.; Osman, N.; Little, P. J. Structure, function, pharmacology, and therapeutic potential of the G protein, Gα/q,11. *Front. Cardiovasc. Med.* **2015**, *2*, 14.

(25) Li, Q.; Han, X.; Lan, X.; Hong, X.; Li, Q.; Gao, Y.; Luo, T.; Yang, Q.; Koehler, R. C.; Zhai, Y.; et al. Inhibition of tPA-induced hemorrhagic transformation involves adenosine A2B receptor activation after cerebral ischemia. *Neurobiol. Dis.* **2017**, *108*, 173–182.

(26) Suzuki, N.; Hajicek, N.; Kozasa, T. Regulation and physiological functions of G12/13-mediated signaling pathways. *Neurosignals* **2009**, *17*, 55–70.

(27) de Munnik, S. M.; Smit, M. J.; Leurs, R.; Vischer, H. F. Modulation of cellular signaling by herpesvirus-encoded G protein-coupled receptors. *Front. Pharmacol.* **2015**, *6*, 40.

(28) Burnstock, G. A basis for distinguishing two types of purinergic receptor. In *Cell membrane receptors for drugs and hormones: a multidisciplinary approach*; New York: Raven Press, 1987; pp 107–118.

(29) Yan, L.; Burbiel, J. C.; Maass, A.; Müller, C. E. Adenosine receptor agonists: from basic medicinal chemistry to clinical development. *Expert Opin. Emerg. Drugs* **2003**, *8*, 537–576.

(30) Zhou, Q. Y.; Li, C.; Olah, M. E.; Johnson, R. A.; Stiles, G. L.; Civelli, O. Molecular cloning and characterization of an adenosine receptor: the A3 adenosine receptor. *Proc. Natl. Acad. Sci. U. S. A.* **1992**, *89*, 7432–7436.

References

(31) Müller, Christa E.; Stein, B. Adenosine receptor antagonists: Structures and potential therapeutic applications. *Curr. Pharm. Des.* **1996**, *2*, 501–530.

(32) Burnstock, G.; Kennedy, C. Is there a basis for distinguishing two types of P2-purinoceptor? *Gen. Pharmacol.* **1985**, *16*, 433–440.

(33) Abbracchio, M. P.; Burnstock, G.; Boeynaems, J.-M.; Barnard, E. A.; Boyer, J. L.; Kennedy, C.; Knight, G. E.; Fumagalli, M.; Gachet, C.; Jacobson, K. A.; et al. International Union of Pharmacology LVIII: update on the P2Y G protein-coupled nucleotide receptors: from molecular mechanisms and pathophysiology to therapy. *Pharmacol. Rev.* **2006**, *58*, 281–341.

(34) Bender, E.; Buist, A.; Jurzak, M.; Langlois, X.; Baggerman, G.; Verhasselt, P.; Ercken, M.; Guo, H.-Q.; Wintmolders, C.; Van den Wyngaert, I.; et al. Characterization of an orphan G protein-coupled receptor localized in the dorsal root ganglia reveals adenine as a signaling molecule. *Proc. Natl. Acad. Sci. U. S. A.* **2002**, *99*, 8573–8578.

(35) Brunschweiger, A.; Müller, C. E. P2 receptors activated by uracil nucleotides--an update. *Curr. Med. Chem.* **2006**, *13*, 289–312.

(36) Fredholm, B. B.; IJzerman, A. P.; Jacobson, K. A.; Klotz, K.-N. N.; Linden, J. International Union of Pharmacology. XXV. Nomenclature and classification of adenosine receptors. *Pharmacol. Rev.* **2001**, *53*, 527–552.

(37) Ralevic, V.; Burnstock, G. Receptors for purines and pyrimidines. *Pharmacol. Rev.* **1998**, *50*, 413–492.

(38) Chen, J. F.; Eltzschig, H. K.; Fredholm, B. B. Adenosine receptors as drug targets-what are the challenges? *Nat. Rev. Drug Discov.* **2013**, *12*, 265–286.

(39) Fredholm, B. B.; Arslan, G.; Halldner, L.; Kull, B.; Schulte, G.; Wasserman, W. Structure and function of adenosine receptors and their genes. *Naunyn. Schmiedebergs. Arch. Pharmacol.* **2000**, *362*, 364–374.

(40)   Antonioli, L.; Blandizzi, C.; Csóka, B.; Pacher, P.; Haskó, G. Adenosine signalling in diabetes mellitus—pathophysiology and therapeutic considerations. *Nat. Rev. Endocrinol.* **2015**, *11*, 228–241.

(41)   Dal Ben, D.; Lambertucci, C.; Vittori, S.; Volpini, R.; Cristalli, G. GPCRs as therapeutic targets: a view on adenosine receptors structure and functions, and molecular modeling support. *J. Iran. Chem. Soc.* **2005**, *2*, 176–188.

(42)   Liu, Y.-J.; Chen, J.; Li, X.; Zhou, X.; Hu, Y.-M.; Chu, S.-F.; Peng, Y.; Chen, N.-H. Research progress on adenosine in central nervous system diseases. *CNS Neurosci. Ther.* **2019**, *25*, 899–910.

(43)   Sperlagh, B.; Sylvester Vizi, E. The role of extracellular adenosine in chemical neurotransmission in the hippocampus and basal ganglia: pharmacological and clinical aspects. *Curr. Top. Med. Chem.* **2011**, *11*, 1034–1046.

(44)   Beukers, M. W.; den Dulk, H.; van Tilburg, E. W.; Brouwer, J.; Ijzerman, A. P. Why are A2B receptors low-affinity adenosine receptors? mutation of Asn273 to Tyr increases affinity of human A2B Receptor for 2-(1-Hexynyl)adenosine. *Mol. Pharmacol.* **2000**, *58*, 1349–1356.

(45)   Borea, P. A.; Gessi, S.; Merighi, S.; Vincenzi, F.; Varani, K. Pathological overproduction: the bad side of adenosine. *Br. J. Pharmacol.* **2017**, *174*, 1945–1960.

(46)   Ciccarelli, R.; Ballerini, P.; Sabatino, G.; Rathbone, M. P.; D'Onofrio, M.; Caciagli, F.; Di Iorio, P. Involvement of astrocytes in purine-mediated reparative processes in the brain. *Int. J. Dev. Neurosci.* **2001**, *19*, 395–414.

(47)   Borea, P. A.; Gessi, S.; Merighi, S.; Varani, K. Adenosine as a multi-signalling guardian angel in human diseases: when, where and how does it exert its protective effects? *Trends Pharmacol. Sci.* **2016**, *37*, 419–434.

(48)   Drury, A. N.; Szent-Györgyi, A. The physiological activity of adenine compounds with

References

especial reference to their action upon the mammalian heart. *J. Physiol.* **1929**, *68*, 213–237.

(49)   Forman, M. B.; Stone, G. W.; Jackson, E. K. Role of adenosine as adjunctive therapy in acute myocardial infarction. *Cardiovasc. Drug Rev.* **2006**, *24*, 116–147.

(50)   Gessi, S.; Merighi, S.; Varani, K. *The adenosine receptors*; The Receptors; Springer International Publishing: Cham, 2018; Vol. 34.

(51)   Young, A.; Mittal, D.; Stagg, J.; Smyth, M. J. Targeting cancer-derived adenosine: new therapeutic approaches. *Cancer Discov.* **2014**, *4*, 879–888.

(52)   RCSB PDB: Homepage https://www.rcsb.org/ (accessed Nov 11, 2019).

(53)   Ciancetta, A.; Jacobson, K. A. Breakthrough in GPCR crystallography and its impact on computer-aided drug design. In *Methods in Molecular Biology*; Humana Press Inc., 2018; Vol. 1705, pp 45–72.

(54)   Glukhova, A.; Thal, D. M.; Nguyen, A. T.; Vecchio, E. A.; Jörg, M.; Scammells, P. J.; May, L. T.; Sexton, P. M.; Christopoulos, A. Structure of the adenosine A1 receptor reveals the basis for subtype selectivity. *Cell* **2017**, *168*, 867–877.

(55)   Weinert, T.; Olieric, N.; Cheng, R.; Brünle, S.; James, D.; Ozerov, D.; Gashi, D.; Vera, L.; Marsh, M.; Jaeger, K.; et al. Serial millisecond crystallography for routine room-temperature structure determination at synchrotrons. *Nat. Commun.* **2017**, *8*, 542.

(56)   Daly, J. W.; Butts-Lamb, P.; Padgett, W. Subclasses of adenosine receptors in the central nervous system: interaction with caffeine and related methylxanthines. *Cell. Mol. Neurobiol.* **1983**, *3*, 69–80.

(57)   Rivkees, S. A.; Reppert, S. M. RFL9 encodes an A2B-adenosine receptor. *Mol. Endocrinol.* **1992**, *6*, 1598–1604.

(58)   Pierce, K. D.; Furlong, T. J.; Selbie, L. A.; Shine, J. Molecular cloning and expression of an adenosine A2B receptor from human brain. *Biochem. Biophys. Res. Commun.*

1992, *187*, 86–93.

(59) Jacobson, M. A.; Johnson, R. G.; Luneau, C. J.; Salvatore, C. A. Cloning and chromosomal localization of the human A2B adenosine receptor gene (ADORA2B) and its pseudogene. *Genomics* **1995**, *27*, 374–376.

(60) Sherbiny, F. F.; Schiedel, A. C.; Maaß, A.; Müller, C. E. Homology modelling of the human adenosine A2B receptor based on X-ray structures of bovine rhodopsin, the β2-adrenergic receptor and the human adenosine A2A receptor. *J. Comput. Aided. Mol. Des.* **2009**, *23*, 807–828.

(61) Köse, M.; Gollos, S.; Karcz, T.; Fiene, A.; Heisig, F.; Behrenswerth, A.; Kieć-Kononowicz, K.; Namasivayam, V.; Müller, C. E. Fluorescent-labeled selective adenosine A2B receptor antagonist enables competition binding assay by flow cytometry. *J. Med. Chem.* **2018**, *61*, 4301–4316.

(62) Jiang, J.; Seel, C. J.; Temirak, A.; Namasivayam, V.; Arridu, A.; Schabikowski, J.; Baqi, Y.; Hinz, S.; Hockemeyer, J.; Müller, C. E. A2B adenosine receptor antagonists with picomolar potency. *J. Med. Chem.* **2019**, *62*, 4032–4055.

(63) Müller, C. E.; Jacobson, K. A. Recent developments in adenosine receptor ligands and their potential as novel drugs. *Biochim. Biophys. Acta - Biomembr.* **2011**, *1808*, 1290–1308.

(64) Müller, C. E.; Baqi, Y.; Hinz, S.; Namasivayam, V. Medicinal chemistry of A2B adenosine receptors. In *The Adenosine Receptors*; Springer International Publishing: Cham, 2018; pp 137–168.

(65) Seibt, B. F.; Schiedel, A. C.; Thimm, D.; Hinz, S.; Sherbiny, F. F.; Müller, C. E. The second extracellular loop of GPCRs determines subtype-selectivity and controls efficacy as evidenced by loop exchange study at A2 adenosine receptors. *Biochem. Pharmacol.* **2013**, *85*, 1317–1329.

References

(66)   De Filippo, E.; Hinz, S.; Pellizzari, V.; Deganutti, G.; El-Tayeb, A.; Navarro, G.; Franco, R.; Moro, S.; Schiedel, A. C.; Müller, C. E. A2A and A2B adenosine receptors: the extracellular loop 2 determines high (A$_{2A}$) or low affinity (A$_{2B}$) for adenosine. *Biochem. Pharmacol.* **2019**, 113718.

(67)   De Filippo, E.; Namasivayam, V.; Zappe, L.; El-Tayeb, A.; Schiedel, A. C.; Müller, C. E. Role of extracellular cysteine residues in the adenosine A2A receptor. *Purinergic Signal.* **2016**, *12*, 313–329.

(68)   Schiedel, A. C.; Hinz, S.; Thimm, D.; Sherbiny, F.; Borrmann, T.; Maaß, A.; Müller, C. E. The four cysteine residues in the second extracellular loop of the human adenosine A2B receptor: Role in ligand binding and receptor function. *Biochem. Pharmacol.* **2011**, *82*, 389–399.

(69)   Fredholm, B. B. Adenosine, an endogenous distress signal, modulates tissue damage and repair. *Cell Death Differ.* **2007**, *14*, 1315–1323.

(70)   Borea, P. A.; Gessi, S.; Merighi, S.; Vincenzi, F.; Varani, K. Pharmacology of adenosine receptors: the state of the art. *Physiol. Rev.* **2018**, *98*, 1591–1625.

(71)   Yaar, R.; Jones, M. R.; Chen, J.-F.; Ravid, K. Animal models for the study of adenosine receptor function. *J. Cell. Physiol.* **2005**, *202*, 9–20.

(72)   Aherne, C. M.; Kewley, E. M.; Eltzschig, H. K. The resurgence of A2B adenosine receptor signaling. *Biochim. Biophys. Acta - Biomembr.* **2011**, *1808*, 1329–1339.

(73)   Sun, Y.; Huang, P. Adenosine A2B receptor: from cell biology to human diseases. *Front. Chem.* **2016**, *4*, 37.

(74)   Eltzschig, H. K.; Bonney, S. K.; Eckle, T. Attenuating myocardial ischemia by targeting A2B adenosine receptors. *Trends Mol. Med.* **2013**, *19*, 345–354.

(75)   Valladares, D.; Quezada, C.; Montecinos, P.; Concha; Yañez, A. J.; Sobrevia, L.; Martín, R. S. Adenosine A2B receptor mediates an increase on VEGF-A production in

rat kidney glomeruli. *Biochem. Biophys. Res. Commun.* **2008**, *366*, 180–185.

(76) Dai, Y.; Zhang, W.; Wen, J.; Zhang, Y.; Kellems, R. E.; Xia, Y. A2B adenosine receptor–mediated induction of IL-6 promotes CKD. *J. Am. Soc. Nephrol.* **2011**, *22*, 890–901.

(77) Antonioli, L.; Blandizzi, C.; Pacher, P.; Haskó, G. Immunity, inflammation and cancer: a leading role for adenosine. *Nat. Rev. Cancer* **2013**, *13*, 842–857.

(78) Gao, Z.-G.; Jacobson, K. A. A2B adenosine receptor and cancer. *Int. J. Mol. Sci.* **2019**, *20*, 5139.

(79) Schulte, G.; Fredholm, B. B. The Gs-coupled adenosine A2B receptor recruits divergent pathways to regulate ERK1/2 and p38. *Exp. Cell Res.* **2003**, *290*, 168–176.

(80) Ntantie, E.; Gonyo, P.; Lorimer, E. L.; Hauser, A. D.; Schuld, N.; McAllister, D.; Kalyanaraman, B.; Dwinell, M. B.; Auchampach, J. A.; Williams, C. L. An adenosine-mediated signaling pathway suppresses prenylation of the GTPase Rap1B and promotes cell scattering. *Sci. Signal.* **2013**, *6*, ra39–ra39.

(81) Belguise, K.; Kersual, N.; Galtier, F.; Chalbos, D. FRA-1 expression level regulates proliferation and invasiveness of breast cancer cells. *Oncogene* **2005**, *24*, 1434–1444.

(82) Ryzhov, S.; Novitskiy, S. V.; Zaynagetdinov, R.; Goldstein, A. E.; Carbone, D. P.; Biaggioni, I.; Dikov, M. M.; Feoktistov, I. Host A2B receptors promote carcinoma growth. *Neoplasia* **2008**, *10*, 987–995.

(83) Feoktistov, I.; Goldstein, A. E.; Ryzhov, S.; Zeng, D.; Belardinelli, L.; Voyno-Yasenetskaya, T.; Biaggioni, I. Differential expression of adenosine receptors in human endothelial cells: Role of A2B receptors in angiogenic factor regulation. *Circ. Res.* **2002**, *90*, 531–538.

(84) Eltzschig, H. K. Adenosine: an old drug newly discovered. *Anesthesiology* **2009**, *111*, 904–915.

References

(85) Jacobson, K. A.; Tosh, D. K.; Jain, S.; Gao, Z.-G. Historical and current adenosine receptor agonists in preclinical and clinical development. *Front. Cell. Neurosci.* **2019**, *13*, 124.

(86) Eisenstein, A.; Patterson, S.; Ravid, K. The many faces of the A2B adenosine receptor in cardiovascular and metabolic diseases. *J. Cell. Physiol.* **2015**, *230*, 2891–2897.

(87) Knight, B. P.; Zivin, A.; Souza, J.; Goyal, R.; Man, K. C.; Strickberger, A.; Morady, F. Use of adenosine in patients hospitalized in a university medical center. *Am. J. Med.* **1998**, *105*, 275–280.

(88) Gao, Z.-G.; Mamedova, L. K.; Chen, P.; Jacobson, K. A. 2-Substituted adenosine derivatives: affinity and efficacy at four subtypes of human adenosine receptors. *Biochem. Pharmacol.* **2004**, *68*, 1985–1993.

(89) Hinz, S.; Alnouri, W. M.; Pleiss, U.; Müller, C. E. Tritium-labeled agonists as tools for studying adenosine A2B receptors. *Purinergic Signal.* **2018**, *14*, 223–233.

(90) Baraldi, P. G.; Preti, D.; Tabrizi, M. A.; Fruttarolo, F.; Romagnoli, R.; Carrion, M. D.; Cara, L. C. L.; Moorman, A. R.; Varani, K.; Borea, P. A. Synthesis and biological evaluation of novel 1-deoxy-1-[6-[((hetero)arylcarbonyl)hydrazino]- 9H-purin-9-yl]-N-ethyl-beta-D-ribofuran-uronamide derivatives as useful templates for the development of A2B adenosine receptor agonists. *J. Med. Chem.* **2007**, *50*, 374–380.

(91) Eckle, T.; Krahn, T.; Grenz, A.; Köhler, D.; Mittelbronn, M.; Ledent, C.; Jacobson, M. A.; Osswald, H.; Thompson, L. F.; Unertl, K.; et al. Cardioprotection by ecto-5'-nucleotidase (CD73) and A2B adenosine receptors. *Circulation* **2007**, *115*, 1581–1590.

(92) Eltzschig, H. K.; Ibla, J. C.; Furuta, G. T.; Leonard, M. O.; Jacobson, K. A.; Enjyoji, K.; Robson, S. C.; Colgan, S. P. Coordinated adenine nucleotide phosphohydrolysis and nucleoside signaling in posthypoxic endothelium. *J. Exp. Med.* **2003**, *198*, 783–796.

(93) Tian, Y.; Piras, B. A.; Kron, I. L.; French, B. A.; Yang, Z. Adenosine 2B receptor

activation reduces myocardial reperfusion injury by promoting anti-inflammatory macrophages differentiation via PI3K/AKT pathway. *Oxid. Med. Cell. Longev.* **2015**, *2015*, 1–8.

(94) Jafari, S. M.; Joshaghani, H. R.; Panjehpour, M.; Aghaei, M. A2B adenosine receptor agonist induces cell cycle arrest and apoptosis in breast cancer stem cells via ERK1/2 phosphorylation. *Cell. Oncol.* **2018**, *41*, 61–72.

(95) Albrecht, B.; Krahn, T.; Philipp, S.; Rosentreter, U.; Cohen, M. V; Downey, J. M. Abstract 217: Selective adenosine A2B receptor activation mimics postconditioning in a rabbit infarct model. *Circulation* **2006**, *114*, II_14-II_15.

(96) Hinz, S.; Lacher, S. K.; Seibt, B. F.; Müller, C. E. BAY60-6583 acts as a partial agonist at adenosine A2B receptors. *J. Pharmacol. Exp. Ther.* **2014**, *349*, 427–436.

(97) Catarzi, D.; Varano, F.; Varani, K.; Vincenzi, F.; Pasquini, S.; Dal Ben, D.; Volpini, R.; Colotta, V. Amino-3,5-dicyanopyridines targeting the adenosine receptors. ranging from pan ligands to combined A1/A2B partial agonists. *Pharmaceuticals* **2019**, *12*, 159.

(98) Elzein, E.; Zablocki, J. A1 adenosine receptor agonists and their potential therapeutic applications. *Expert Opin. Investig. Drugs* **2008**, *17*, 1901–1910.

(99) Fusco, I.; Cherchi, F.; Catarzi, D.; Colotta, V.; Varano, F.; Pedata, F.; Pugliese, A. M.; Coppi, E. Functional characterization of a novel adenosine A2B receptor agonist on short-term plasticity and synaptic inhibition during oxygen and glucose deprivation in the rat CA1 hippocampus. *Brain Res. Bull.* **2019**, *151*, 174–180.

(100) Fortune, E. S.; Rose, G. J. Short-term synaptic plasticity as a temporal filter. *Trends Neurosci.* **2001**, *24*, 381–385.

(101) Bhatt, K. N.; Butler, J. Myocardial energetics and heart failure: a review of recent therapeutic trials. *Curr. Heart Fail. Rep.* **2018**, *15*, 191–197.

(102) Baltos, J. A.; Vecchio, E. A.; Harris, M. A.; Qin, C. X.; Ritchie, R. H.; Christopoulos,

References

A.; White, P. J.; May, L. T. Capadenoson, a clinically trialed partial adenosine A1 receptor agonist, can stimulate adenosine A2B receptor biased agonism. *Biochem. Pharmacol.* **2017**, *135*, 79–89.

(103) Wakeno, M.; Minamino, T.; Seguchi, O.; Okazaki, H.; Tsukamoto, O.; Okada, K.; Hirata, A.; Fujita, M.; Asanuma, H.; Kim, J.; et al. Long-term stimulation of adenosine A2B receptors begun after myocardial infarction prevents cardiac remodeling in rats. *Circulation* **2006**, *114*, 1923–1932.

(104) Vecchio, E. A.; Chuo, C. H.; Baltos, J.-A.; Ford, L.; Scammells, P. J.; Wang, B. H.; Christopoulos, A.; White, P. J.; May, L. T. The hybrid molecule, VCP746, is a potent adenosine A2B receptor agonist that stimulates anti-fibrotic signalling. *Biochem. Pharmacol.* **2016**, *117*, 46–56.

(105) Müller, C. E.; Baqi, Y.; Namasivayam, V. Agonists and antagonists for purinergic receptors. In *Methods in molecular biology (Clifton, N.J.)*; NLM (Medline), 2020; Vol. 2041, pp 45–64.

(106) Klotz, K.-N. Adenosine receptors and their ligands. *Naunyn. Schmiedebergs. Arch. Pharmacol.* **2000**, *362*, 382–391.

(107) Lohse, M. J.; Klotz, K. N.; Schwabe, U.; Cristalli, G.; Vittori, S.; Grifantini, M. 2-Chloro-N6-cyclopentyladenosine: a highly selective agonist at A1 adenosine receptors. *Naunyn. Schmiedebergs. Arch. Pharmacol.* **1988**, *337*, 687–689.

(108) Nekooeian, A. A.; Tabrizchi, R. Effects of CGS 21680, a selective A2A adenosine receptor agonist, on cardiac output and vascular resistance in acute heart failure in the anaesthetized rat. *Br. J. Pharmacol.* **1998**, *123*, 1666–1672.

(109) Fishman, P.; Salhab, A.; Cohen, S.; Amer, J.; Itzhak, I.; Barer, F.; Safadi, R. The anti-inflammatory and anto-fibrogenic effects of namodenoson in NAFLD/NASH animal models. *J. Hepatol.* **2018**, *68*, S349–S350.

(110) Cappelletti, S.; Daria, P.; Sani, G.; Aromatario, M. Caffeine: cognitive and physical performance enhancer or psychoactive drug? *Curr. Neuropharmacol.* **2015**, *13*, 71–88.

(111) López-Cruz, L.; Salamone, J. D.; Correa, M. Caffeine and selective adenosine receptor antagonists as new therapeutic tools for the motivational symptoms of depression. *Front. Pharmacol.* **2018**, *9*.

(112) Westcott, F. H.; Gillson, R. E. The treatment of bronchial asthma by inhalation therapy with vital capacity studies. *J. Allergy* **1943**, *14*, 420–427.

(113) Doré, A. S.; Robertson, N.; Errey, J. C.; Ng, I.; Hollenstein, K.; Tehan, B.; Hurrell, E.; Bennett, K.; Congreve, M.; Magnani, F.; et al. Structure of the adenosine A2A receptor in complex with ZM241385 and the xanthines XAC and caffeine. *Structure* **2011**, *19*, 1283–1293.

(114) Hayallah, A. M.; Sandoval-Ramírez, J.; Reith, U.; Schobert, U.; Preiss, B.; Schumacher, B.; Daly, J. W.; Müller, C. E. 1,8-Disubstituted xanthine derivatives: synthesis of potent A2B-selective adenosine receptor antagonists. *J. Med. Chem.* **2002**, *45*, 1500–1510.

(115) Du, X.; Ou, X.; Song, T.; Zhang, W.; Cong, F.; Zhang, S.; Xiong, Y. Adenosine A2B receptor stimulates angiogenesis by inducing VEGF and eNOS in human microvascular endothelial cells. *Exp. Biol. Med.* **2015**, *240*, 1472–1479.

(116) Basu, S.; Barawkar, D. A.; Ramdas, V.; Waman, Y.; Patel, M.; Panmand, A.; Kumar, S.; Thorat, S.; Bonagiri, R.; Jadhav, D.; et al. A2B adenosine receptor antagonists: Design, synthesis and biological evaluation of novel xanthine derivatives. *Eur. J. Med. Chem.* **2017**, *127*, 986–996.

(117) Sun, C.-X. Role of A2B adenosine receptor signaling in adenosine-dependent pulmonary inflammation and injury. *J. Clin. Invest.* **2006**, *116*, 2173–2182.

(118) Kim, Y.-C.; Ji, X.; Melman, N.; Linden, J.; Jacobson, K. A. Anilide derivatives of an 8-phenylxanthine carboxylic congener are highly potent and selective antagonists at

References

human A2B adenosine receptors. *J. Med. Chem.* **2000**, *43*, 1165–1172.

(119) Zablocki, J.; Kalla, R.; Perry, T.; Palle, V.; Varkhedkar, V.; Xiao, D.; Piscopio, A.; Maa, T.; Gimbel, A.; Hao, J.; et al. The discovery of a selective, high affinity A(2B) adenosine receptor antagonist for the potential treatment of asthma. *Bioorg. Med. Chem. Lett.* **2005**, *15*, 609–612.

(120) Ma, D.-F. F.; Kondo, T.; Nakazawa, T.; Niu, D.-F. F.; Mochizuki, K.; Kawasaki, T.; Yamane, T.; Katoh, R. Hypoxia-inducible adenosine A2B receptor modulates proliferation of colon carcinoma cells. *Hum. Pathol.* **2010**, *41*, 1550–1557.

(121) Borrmann, T.; Hinz, S.; Bertarelli, D. C. G.; Li, W.; Florin, N. C.; Scheiff, A. B.; Müller, C. E. 1-Alkyl-8-(piperazine-1-sulfonyl)phenylxanthines: development and characterization of adenosine A2B receptor antagonists and a new radioligand with subnanomolar affinity and subtype specificity. *J. Med. Chem.* **2009**, *52*, 3994–4006.

(122) Mølck, C.; Ryall, J.; Failla, L. M.; Coates, J. L.; Pascussi, J.-M. M.; Heath, J. K.; Stewart, G.; Hollande, F. The A2B adenosine receptor antagonist PSB-603 promotes oxidative phosphorylation and ROS production in colorectal cancer cells via adenosine receptor-independent mechanism. *Cancer Lett.* **2016**, *383*, 135–143.

(123) Vecchio, E. A.; Tan, C. Y. R. R.; Gregory, K. J.; Christopoulos, A.; White, P. J.; May, L. T. Ligand-independent adenosine A2B receptor constitutive activity as a promoter of prostate cancer cell proliferation. *J. Pharmacol. Exp. Ther.* **2016**, *357*, 36–44.

(124) Eastwood, P.; Esteve, C.; González, J.; Fonquerna, S.; Aiguadé, J.; Carranco, I.; Doménech, T.; Aparici, M.; Miralpeix, M.; Albertí, J.; et al. Discovery of LAS101057: a potent, selective, and orally efficacious A2B adenosine receptor antagonist. *ACS Med. Chem. Lett.* **2011**, *2*, 213–218.

(125) El Maatougui, A.; Azuaje, J.; González-Gómez, M.; Miguez, G.; Crespo, A.; Carbajales, C.; Escalante, L.; García-Mera, X.; Gutiérrez-de-Terán, H.; Sotelo, E. Discovery of

potent and highly selective A2B adenosine receptor antagonist chemotypes. *J. Med. Chem.* **2016**, *59*, 1967–1983.

(126) Härter, M.; Kalthof, B.; Delbeck, M.; Lustig, K.; Gerisch, M.; Schulz, S.; Kast, R.; Meibom, D.; Lindner, N. Novel non-xanthine antagonist of the A2B adenosine receptor: from HTS hit to lead structure. *Eur. J. Med. Chem.* **2019**, *163*, 763–778.

(127) Kalk, P.; Eggert, B.; Relle, K.; Godes, M.; Heiden, S.; Sharkovska, Y.; Fischer, Y.; Ziegler, D.; Bielenberg, G. W.; Hocher, B. The adenosine A1 receptor antagonist SLV320 reduces myocardial fibrosis in rats with 5/6 nephrectomy without affecting blood pressure. *Br. J. Pharmacol.* **2007**, *151*, 1025–1032.

(128) Mitrovic, V.; Seferovic, P.; Dodic, S.; Krotin, M.; Neskovic, A.; Dickstein, K.; de Voogd, H.; Böcker, C.; Ziegler, D.; Godes, M.; et al. Cardio-renal effects of the A1 adenosine receptor antagonist SLV320 in patients with heart failure. *Circ. Heart Fail.* **2009**, *2*, 523–531.

(129) Stocchi, F.; Rascol, O.; Hauser, R. A.; Huyck, S.; Tzontcheva, A.; Capece, R.; Ho, T. W.; Sklar, P.; Lines, C.; Michelson, D.; et al. Randomized trial of preladenant, given as monotherapy, in patients with early Parkinson disease. *Neurology* **2017**, *88*, 2198–2206.

(130) Ramsay, R. R.; Popovic-Nikolic, M. R.; Nikolic, K.; Uliassi, E.; Bolognesi, M. L. A perspective on multi-target drug discovery and design for complex diseases. *Clin. Transl. Med.* **2018**, *7*, 3.

(131) Seitz, L.; Jin, L.; Leleti, M.; Ashok, D.; Jeffrey, J.; Rieger, A.; Tiessen, R. G.; Arold, G.; Tan, J. B. L.; Powers, J. P.; et al. Safety, tolerability, and pharmacology of AB928, a novel dual adenosine receptor antagonist, in a randomized, phase 1 study in healthy volunteers. *Invest. New Drugs* **2019**, *37*, 711–721.

(132) A study to evaluate the safety and tolerability of immunotherapy combinations in participants with advanced malignancies - full text view - clinicaltrials.gov

References

https://clinicaltrials.gov/ct2/show/NCT03629756 (accessed Oct 9, 2019).

(133) Harada, H.; Asano, O.; Hoshino, Y.; Yoshikawa, S.; Matsukura, M.; Kabasawa, Y.; Niijima, J.; Kotake, Y.; Watanabe, N.; Kawata, T.; et al. 2-Alkynyl-8-aryl-9-methyladenines as novel adenosine receptor antagonists: their synthesis and structure−activity relationships toward hepatic glucose production induced via agonism of the A2B receptor. *J. Med. Chem.* **2001**, *44*, 170–179.

(134) Eisai Co., Ltd. https://www.eisai.com/index.html (accessed Nov 19, 2019).

(135) Galezowski, M.; Wegrzyn, P.; Bobowska, A.; Commandeur, C.; Dziedzic, K.; Nowogrodzki, M.; Obara, A.; Szeremeta-Spisak, J.; Dzielak, A.; Lozinska, I.; et al. Abstract 3770: Characterization of novel dual A2A/A2B adenosine receptor antagonists for cancer immunotherapy. In *Immunology*; American Association for Cancer Research, 2018; pp 3770–3770.

(136) Mcriner, A. J. GPCR hit identification via DNA-encoded libraries and optimization towards therapeutic libraries and optimization towards therapeutic agents for inflammation and oncology. In *7th RSC/SCI symposium on GPCRs in Medicinal Chemistry*; Verona, Italy, 2018.

(137) Galezowski, M.; Węgrzyn, P.; Bobowska, A.; Dziedzic, K.; Szeremeta-Spisak, J.; Nowogrodzki, M.; Satala, G.; Obara, A.; Lozinska-Raj, I.; Dudek, M.; et al. Abstract 4135: Novel dual A2A/A2B adenosine receptor antagonists for cancer immunotherapy: in vitro and in vivo characterization. In *Immunology*; American Association for Cancer Research, 2019; pp 4135–4135.

(138) 33rd Annual meeting & pre-conference programs of the society for immunotherapy of cancer (SITC 2018). *J. Immunother. Cancer* **2018**, *6*, 114.

(139) Trincavelli, M. L.; Giacomelli, C.; Daniele, S.; Taliani, S.; Cosimelli, B.; Laneri, S.; Severi, E.; Barresi, E.; Pugliesi, I.; Greco, G.; et al. Allosteric modulators of human A2B

adenosine receptor. *Biochim. Biophys. Acta - Gen. Subj.* **2014**, *1840*, 1194–1203.

(140) Taliani, S.; Trincavelli, M. L.; Cosimelli, B.; Laneri, S.; Severi, E.; Barresi, E.; Pugliesi, I.; Daniele, S.; Giacomelli, C.; Greco, G.; et al. Modulation of A2B adenosine receptor by 1-Benzyl-3-ketoindole derivatives. *Eur. J. Med. Chem.* **2013**, *69*, 331–337.

(141) Ji, X.; Kim, Y.-C.; Ahern, D. G.; Linden, J.; Jacobson, K. A. [3H]MRS 1754, a selective antagonist radioligand for A2B adenosine receptors. *Biochem. Pharmacol.* **2001**, *61*, 657–663.

(142) Dong, C.; Liu, Z.; Wang, F. Radioligand saturation binding for quantitative analysis of ligand-receptor interactions. *Biophys. Reports* **2015**, *1*, 148–155.

(143) Hinz, S.; Bonasera, D.; Harms, T.; Vielmuth, C.; Heisig, F.; Behrenswerth, A.; Hockemeyer, J.; Müller, C. E. Development of a live cell NanoBret binding assay for adenosine A2B receptors. In *Abstracts from First European Purine Meeting*; 2019; p 12.

(144) Lindemann, M.; Moldovan, R.-P.; Hinz, S.; Deuther-Conrad, W.; Gündel, D.; Dukic-Stefanovic, S.; Toussaint, M.; Teodoro, R.; Juhl, C.; Steinbach, J.; et al. Development of a radiofluorinated adenosine A2B receptor antagonist as potential ligand for PET imaging. *Int. J. Mol. Sci.* **2020**, *21*, 3197.

(145) Ke, J.; Yao, B.; Li, T.; Cui, S.; Ding, H. A2 adenosine receptor-mediated cardioprotection against reperfusion injury in rat hearts is associated with autophagy downregulation. *J. Cardiovasc. Pharmacol.* **2015**, *66*, 25–34.

(146) Phosri, S.; Arieyawong, A.; Bunrukchai, K.; Parichatikanond, W.; Nishimura, A.; Nishida, M.; Mangmool, S. Stimulation of adenosine A2B receptor inhibits endothelin-1-induced cardiac fibroblast proliferation and α-smooth muscle actin synthesis through the cAMP/Epac/PI3K/Akt-signaling pathway. *Front. Pharmacol.* **2017**, *8*.

(147) Patel, L.; Thaker, A. The effects of A2B receptor modulators on vascular endothelial

growth factor and nitric oxide axis in chronic cyclosporine nephropathy. *J. Pharmacol. Pharmacother.* **2015**, *6*, 147.

(148) Fernandez-Gallardo, M.; González-Ramírez, R.; Sandoval, A.; Felix, R.; Monjaraz, E. Adenosine stimulate proliferation and migration in triple negative breast cancer cells. *PLoS One* **2016**, *11*, e0167445.

(149) Iannone, R.; Miele, L.; Maiolino, P.; Pinto, A.; Morello, S. Blockade of A2B adenosine receptor reduces tumor growth and immune suppression mediated by myeloid-derived suppressor cells in a mouse model of melanoma. *Neoplasia* **2013**, *15*, 1400-IN10.

(150) Beukers, M. W.; Chang, L. C. W.; von Frijtag Drabbe Künzel, J. K.; Mulder-Krieger, T.; Spanjersberg, R. F.; Brussee, J.; IJzerman, A. P. New, non-adenosine, high-potency agonists for the human adenosine A2B receptor with an improved selectivity profile compared to the reference agonist N-ethylcarboxamidoadenosine. *J. Med. Chem.* **2004**, *47*, 3707–3709.

(151) Mittal, D.; Sinha, D.; Barkauskas, D.; Young, A.; Kalimutho, M.; Stannard, K.; Caramia, F.; Haibe-Kains, B.; Stagg, J.; Khanna, K. K.; et al. Adenosine 2B receptor expression on cancer cells promotes metastasis. *Cancer Res.* **2016**, *76*, 4372–4382.

(152) Cekic, C.; Sag, D.; Li, Y.; Theodorescu, D.; Strieter, R. M.; Linden, J. Adenosine A2B receptor blockade slows growth of bladder and breast tumors. *J. Immunol.* **2012**, *188*, 198–205.

(153) Wiernik, P. H.; Paietta, E.; Goloubeva, O.; Lee, S. J.; Makower, D.; Bennett, J. M.; Wade, J. L.; Ghosh, C.; Kaminer, L. S.; Pizzolo, J.; et al. Phase II study of theophylline in chronic lymphocytic leukemia: A study of the Eastern Cooperative Oncology Group (E4998). *Leukemia* **2004**, *18*, 1605–1610.

(154) Wei, Q.; Costanzi, S.; Balasubramanian, R.; Gao, Z.-G. G.; Jacobson, K. A. A2B adenosine receptor blockade inhibits growth of prostate cancer cells. *Purinergic Signal.*

2013, *9*, 271–280.

(155) Wei, Q.; Costanzi, S.; Liu, Q.-Z.; Gao, Z.-G.; Jacobson, K. A. Activation of the P2Y1 receptor induces apoptosis and inhibits proliferation of prostate cancer cells. *Biochem. Pharmacol.* **2011**, *82*, 418–425.

(156) Kalla, R. V.; Zablocki, J. Progress in the discovery of selective, high affinity A2B adenosine receptor antagonists as clinical candidates. *Purinergic Signal.* **2009**, *5*, 21–29.

(157) Pipeline - Palobiofarma https://www.palobiofarma.com/pipeline-2/ (accessed Nov 25, 2019).

(158) PBF-1129 in patients with NSCLC - Full Text View - ClinicalTrials.gov https://clinicaltrials.gov/ct2/show/NCT03274479 (accessed Nov 25, 2019).

(159) ATL 844 - AdisInsight https://adisinsight.springer.com/drugs/800028734 (accessed Nov 25, 2019).

(160) Rautio, J.; Meanwell, N. A.; Di, L.; Hageman, M. J. The expanding role of prodrugs in contemporary drug design and development. *Nat. Rev. Drug Discov.* **2018**, *17*, 559–587.

(161) Williams, H. D.; Trevaskis, N. L.; Charman, S. A.; Shanker, R. M.; Charman, W. N.; Pouton, C. W.; Porter, C. J. H. Strategies to address low drug solubility in discovery and development. *Pharmacol. Rev.* **2013**, *65*, 315–499.

(162) Ettmayer, P.; Amidon, G. L.; Clement, B.; Testa, B. Lessons learned from marketed and investigational prodrugs. *J. Med. Chem.* **2004**, *47*, 2393–2404.

(163) Müller, C. E. Prodrug approaches for enhancing the bioavailability of drugs with low solubility. *Chem. Biodivers.* **2009**, *6*, 2071–2083.

(164) Sauer, R.; Maurinsh, J.; Reith, U.; Fülle, F.; Klotz, K. N.; Müller, C. E. Water-soluble phosphate prodrugs of 1-propargyl-8-styrylxanthine derivatives, A2(A)-selective adenosine receptor antagonists. *J. Med. Chem.* **2000**, *43*, 440–448.

References

(165) Hockemeyer, J.; Burbiel, J. C.; Müller, C. E. Multigram-scale syntheses, stability, and photoreactions of A2A adenosine receptor antagonists with 8-styrylxanthine structure: potential drugs for Parkinson's disease. *J. Org. Chem.* **2004**, *69*, 3308–3318.

(166) Boyd, B. J.; Bergström, C. A. S.; Vinarov, Z.; Kuentz, M.; Brouwers, J.; Augustijns, P.; Brandl, M.; Bernkop-Schnürch, A.; Shrestha, N.; Préat, V.; et al. Successful oral delivery of poorly water-soluble drugs both depends on the intraluminal behavior of drugs and of appropriate advanced drug delivery systems. *Eur. J. Pharm. Sci.* **2019**, *137*, 104967.

(167) Walker, M. A. Improving solubility via structural modification. In *Topics in Medicinal Chemistry*; Springer Verlag, 2013; Vol. 9, pp 69–106.

(168) Walker, M. A. Novel tactics for designing water-soluble molecules in drug discovery. *Expert Opin. Drug Discov.* **2014**, *9*, 1421–1433.

(169) Sugane, T.; Tobe, T.; Hamaguchi, W.; Shimada, I.; Maeno, K.; Miyata, J.; Suzuki, T.; Kimizuka, T.; Sakamoto, S.; Tsukamoto, S. Atropisomeric 4-phenyl-4*H*-1,2,4-triazoles as selective glycine transporter 1 inhibitors. *J. Med. Chem.* **2013**, *56*, 5744–5756.

(170) Goldberg, K.; Groombridge, S.; Hudson, J.; Leach, A. G.; MacFaul, P. A.; Pickup, A.; Poultney, R.; Scott, J. S.; Svensson, P. H.; Sweeney, J. Oxadiazole isomers: all bioisosteres are not created equal. *Medchemcomm* **2012**, *3*, 600.

(171) Ritchie, T. J.; Macdonald, S. J. F.; Peace, S.; Pickett, S. D.; Luscombe, C. N. The developability of heteroaromatic and heteroaliphatic rings – do some have a better pedigree as potential drug molecules than others? *Medchemcomm* **2012**, *3*, 1062.

(172) Toulmin, A.; Wood, J. M.; Kenny, P. W. Toward prediction of alkane/water partition coefficients. *J. Med. Chem.* **2008**, *51*, 3720–3730.

(173) Wang, H.-L.; Katon, J.; Balan, C.; Bannon, A. W.; Bernard, C.; Doherty, E. M.; Dominguez, C.; Gavva, N. R.; Gore, V.; Ma, V.; et al. Novel vanilloid receptor-1

antagonists: 3. the identification of a second-generation clinical candidate with improved physicochemical and pharmacokinetic properties. *J. Med. Chem.* **2007**, *50*, 3528–3539.

(174) Doherty, E. M.; Fotsch, C.; Bannon, A. W.; Bo, Y.; Chen, N.; Dominguez, C.; Falsey, J.; Gavva, N. R.; Katon, J.; Nixey, T.; et al. Novel vanilloid receptor-1 antagonists: 2. structure−activity relationships of 4-oxopyrimidines leading to the selection of a clinical candidate. *J. Med. Chem.* **2007**, *50*, 3515–3527.

(175) Brown, A.; Brown, L.; Brown, T. B.; Calabrese, A.; Ellis, D.; Puhalo, N.; Smith, C. R.; Wallace, O.; Watson, L. Triazole oxytocin antagonists: Identification of aryl ether replacements for a biaryl substituent. *Bioorg. Med. Chem. Lett.* **2008**, *18*, 5242–5244.

(176) Sanches, B. M. A.; Ferreira, E. I. Is prodrug design an approach to increase water solubility? *Int. J. Pharm.* **2019**, *568*, 118498.

(177) Allard, B.; Beavis, P. A.; Darcy, P. K.; Stagg, J. Immunosuppressive activities of adenosine in cancer. *Curr. Opin. Pharmacol.* **2016**, *29*, 7–16.

(178) Allard, D.; Turcotte, M.; Stagg, J. Targeting A2 adenosine receptors in cancer. *Immunol. Cell Biol.* **2017**, *95*, 333–339.

4. Results and discussion

4.1. Part I: Water-soluble prodrugs of A$_{2B}$ adenosine receptor antagonists

Water-soluble prodrugs of A_{2B} adenosine receptor antagonists

Ahmed Temirak, Jörg Hockemeyer, Christin Vielmuth, Sonja Hinz, and Christa E. Müller*

PharmaCenter Bonn, Pharmaceutical Institute, Department of Pharmaceutical & Medicinal Chemistry, University of Bonn, An der Immenburg 4, D-53121 Bonn, Germany.

4.1.1. Keywords

Adenosine, A_{2B} adenosine receptor, cancer, immunotherapy, phosphate prodrugs, solubility, structure-activity relationships, xanthine

4.1.2. Abstract

A_{2B} adenosine receptors (A_{2B}ARs) are in the focus of interest as drug targets in (immuno)-oncology since antagonists show antiproliferative, anti-angiogenic, anti-metastatic, immuno-stimulatory and analgesic effects. Potent and selective A_{2B}AR antagonists have been developed, however, antagonists with high water-solubility are lacking but would be required, e.g., for parenteral applications and for enhancing peroral bioavailability. Here, we present the development of water-soluble phosphate prodrugs of potent and selective A_{2B}AR antagonists. We developed three series of xanthine-derived A_{2B}AR antagonists bearing a hydroxy group attached to different positions of the scaffold. The most potent and selective A_{2B}AR antagonists (**30b**, **42**, **50**) were subsequently phosphorylated to obtain the desired phosphate prodrugs **52**-**54**, which display greatly improved water-solubility. These compounds are anticipated to become useful pharmacological tools for *in vivo* studies, e.g. in animal models of cancer and infections, and have potential as future drugs.

4.1.3. Introduction

Adenosine receptors (ARs) are activated by the nucleoside adenosine and belongs to the family of class A (rhodopsin-like) G-protein coupled receptors (GPCRs). They are subdivided into four subtypes, A_1, A_{2A}, A_{2B} and A_3.[1,2] The $A_{2B}AR$ is hardly activated under normal physiological conditions where extracellular adenosine levels are in the nanomolar range and $A_{2B}AR$ expression levels are low. However under pathological conditions, such as hypoxia, inflammation and cancer, $A_{2B}AR$ expression is increased and extracellular adenosine levels rise by about 100-fold.[3] Under these conditions, $A_{2B}ARs$ are activated, indicating the important role of $A_{2B}ARs$ in pathology.[1,4]

$A_{2B}ARs$ are ubiquitously expressed, e.g. in vasculature, neuronal cells, alveolar cells and immune cells including mast cells, macrophages, lymphocytes and astrocytes.[5,6] The roles of $A_{2B}ARs$ are diverse depending on the cell type and timing of receptor activation or inhibition.[7] $A_{2B}AR$ was reported to display a cardioprotective role by promoting tissue adaptation to hypoxia and counteracting hypoxia-induced inflammation; thus $A_{2B}AR$ agonists might be useful for the treatment of coronary heart diseases.[6,8] Recently, the $A_{2B}AR$ has been proposed as a novel target in immuno(oncology), where the high level of extracellular adenosine in tumor tissues and the upregulation of $A_{2B}ARs$ generates an immune-tolerant microenvironment and increases tumor proliferation.[9–11] Therefore, $A_{2B}AR$ antagonists are considered as potential anti-cancer drugs with antiproliferative, antimetastatic, antiangiogenic and immunostimulatory properties, in addition analgesic.[12,13]

Several classes of $A_{2B}AR$ antagonists have been developed, which can be subdivided into xanthine and non-xanthine-derived compounds.[11] The naturally occurring alkaloids caffeine (**1a**) and theophylline (**1b**) are weak, non-selective AR antagonists.[14] Caffeine is found in many beverages and acts as a central nervous system (CNS) stimulant that enhances cognitive and physical performance.[15] It is also used in combination with analgesics and

enhances their effects.[16] Recent study showed that the caffeine in combination with the anti-cancer drug fluorouracil (5-FU) acting as anti-metabolite of nucleotide synthesis, inhibited the progression of hepatocellular carcinoma (HCC) cells in vivo and in vitro and induced cellular apoptosis more efficiently than caffeine or 5-FU monotherapy.[17] Theophylline (**1b**) has been used for the treatment of asthma, however it has a narrow therapeutic window, and therefore its application is now very limited.[18]

Potent and selective xanthine-based $A_{2B}AR$ antagonists include MRS-1754 (**2**), PSB-1115 (**3**), PSB-603 (**4a**), PSB-1901 (**4b**), ATL-801 (**5**) and CVT-6883 (**6**) (Figure 1).[19–22] Compound **2** induced antiangiogenic effects in microvascular endothelial cell lines and inhibited the proliferation of colon carcinoma cells.[19,23,24] Compound **3**, having a sulfonic acid group, showed high water-solubility. However, it has moderate $A_{2B}AR$ affinity and lacks selectivity in rodents. It improved the intestinal barrier functions in colon inflammation in reperfusion injury and ischemic conditions.[24] However, it is deprotonated under physiological conditions, therefore it cannot penetrate the central nervous system (CNS).[20]

To overcome the drawbacks of sulfonates, compound **4a** with a sulfonamide group was developed in our group.[21] It is one of the most potent and selective human $A_{2B}AR$ antagonists with a binding affinity of 0.553 nM.[21] It is used in its tritium-labeled form ([^{3}H]PSB-603) as a radioligand for $A_{2B}AR$ binding assays.[21] Compound **4a** altered the metabolism in colorectal cancer cells and improved their response to chemotherapy.[25] It also decreased the growth of multiple prostate cancer cell lines.[26] Although **4a** displayed high metabolic stability in human, rat and mouse, it is poorly water-soluble which limits its applications.[27] Structural modification of **4a** led to the most potent and selective $A_{2B}AR$ antagonists reported to date, compound **4b** which displays picomolar $A_{2B}AR$ affinity in human (K_i = 83.5 pM) (Figure 1), but again, showing low water-solubility.[22] Furthermore, compound ATL-801 (**5**) significantly decreased the severity of murine colitis and would be an effective treatment for inflammatory bowel

disease.[28] It also blocks the immunosuppressive effects of adenosine thus decreasing the growth of breast and bladder tumors.[29] GS-6201 (**6**) (Figure 1) administered after the onset of ischemia was reported to block cardiac remodeling in mouse after acute myocardial infarction (AMI).[30] It also lowered ventricular arrhythmias and left ventricular dysfunction after AMI in the rat model, therefore it was further clinically evaluated for pulmonary hypertension related with interstitial lung diseases.[31,32]
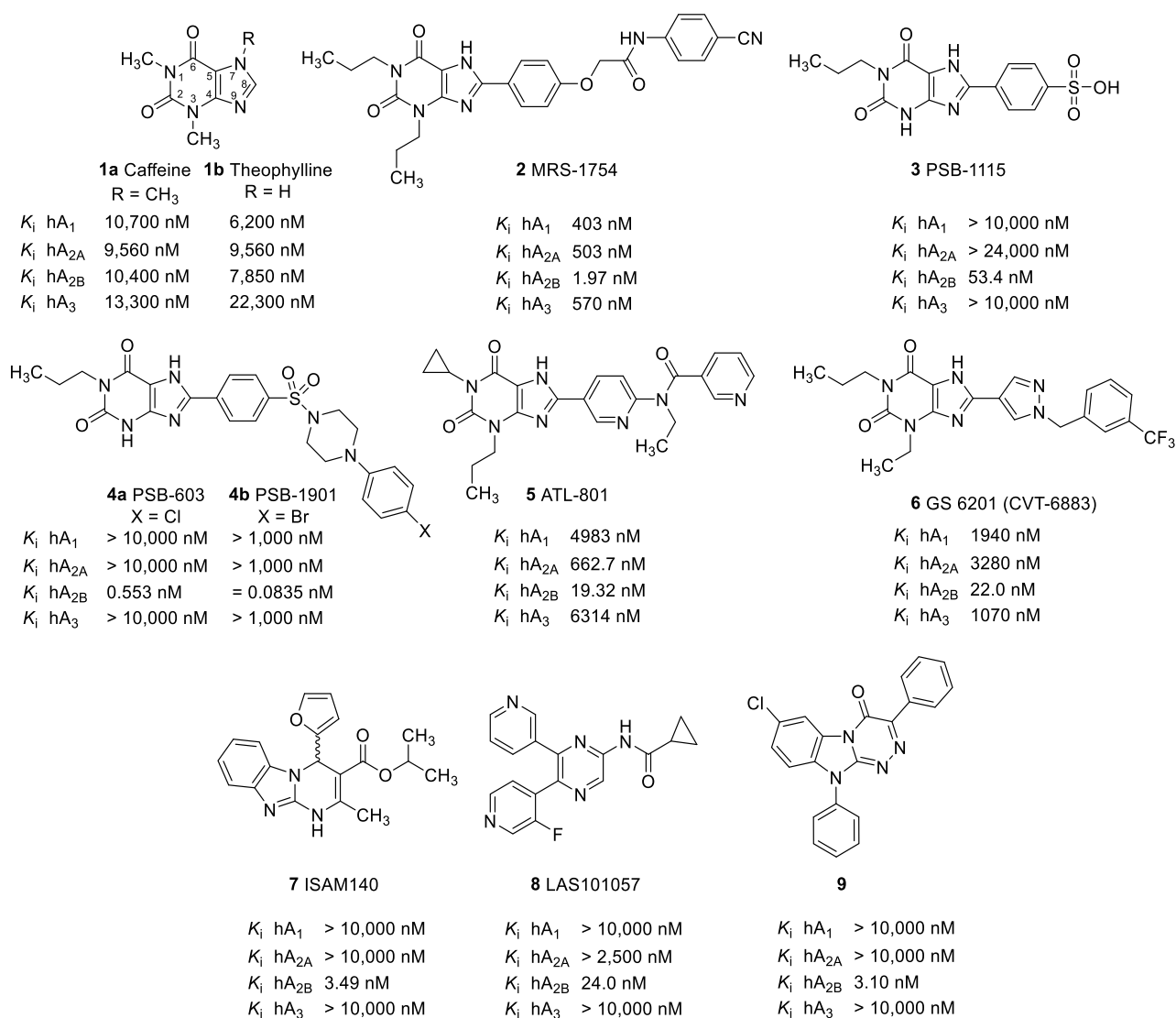

1a Caffeine **1b** Theophylline
R = CH$_3$ R = H

K_i hA$_1$	10,700 nM	6,200 nM
K_i hA$_{2A}$	9,560 nM	9,560 nM
K_i hA$_{2B}$	10,400 nM	7,850 nM
K_i hA$_3$	13,300 nM	22,300 nM

2 MRS-1754

K_i hA$_1$ 403 nM
K_i hA$_{2A}$ 503 nM
K_i hA$_{2B}$ 1.97 nM
K_i hA$_3$ 570 nM

3 PSB-1115

K_i hA$_1$ > 10,000 nM
K_i hA$_{2A}$ > 24,000 nM
K_i hA$_{2B}$ 53.4 nM
K_i hA$_3$ > 10,000 nM

4a PSB-603 **4b** PSB-1901
X = Cl   X = Br

K_i hA$_1$	> 10,000 nM	> 1,000 nM
K_i hA$_{2A}$	> 10,000 nM	> 1,000 nM
K_i hA$_{2B}$	0.553 nM	= 0.0835 nM
K_i hA$_3$	> 10,000 nM	> 1,000 nM

5 ATL-801

K_i hA$_1$ 4983 nM
K_i hA$_{2A}$ 662.7 nM
K_i hA$_{2B}$ 19.32 nM
K_i hA$_3$ 6314 nM

6 GS 6201 (CVT-6883)

K_i hA$_1$ 1940 nM
K_i hA$_{2A}$ 3280 nM
K_i hA$_{2B}$ 22.0 nM
K_i hA$_3$ 1070 nM

7 ISAM140

K_i hA$_1$ > 10,000 nM
K_i hA$_{2A}$ > 10,000 nM
K_i hA$_{2B}$ 3.49 nM
K_i hA$_3$ > 10,000 nM

8 LAS101057

K_i hA$_1$ > 10,000 nM
K_i hA$_{2A}$ > 2,500 nM
K_i hA$_{2B}$ 24.0 nM
K_i hA$_3$ > 10,000 nM

9

K_i hA$_1$ > 10,000 nM
K_i hA$_{2A}$ > 10,000 nM
K_i hA$_{2B}$ 3.10 nM
K_i hA$_3$ > 10,000 nM

Figure 1. Selected A$_{2B}$AR antagonists and their affinities at human AR subtypes.[18–22,28,33–37]

Several classes of A$_{2B}$AR-selective non-xanthine-based antagonists have been described in literature.[11,27] ISAM140 (**7**) a 3,4-dihydropyrimidin-2(1H)-one derivative showed high A$_{2B}$AR antagonistic affinity (K_i = 3.49 nM).[36] Bioisosteric replacements for furan moiety

in **7** with different pentagonal heterocyclic rings, such as oxazole produced potent and selective A$_{2B}$AR antagonists.[38] LAS101057 (**8**), a pyrazine derivative, showed promising potency in cell-based assays and in vivo in an ovalbumin OVA-sensitized mouse model of asthma.[37] It was selected for phase I clinical trials for asthma treatment after optimistic preclinical safety studies results, however further development was discontinued.[37,39] Also, compound **9** having the triazino-benzimidazolone moiety displayed high affinity and selectivity at A$_{2B}$ARs.[33] PBF-1129 (structure not published), a reported potent A$_{2B}$AR antagonist that demonstrated high anti-tumor efficacy, is clinically investigated as treatment for advanced non-small cell lung cancer (NSCLC) and idiopathic pulmonary fibrosis (IPF).[40–42] Although there are many reported potent and selective A$_{2B}$AR antagonists (Figure 1), most of these compounds display limitations with regard to their physicochemical properties. In particular for water-solubility has been a major problem with potent AR antagonists in general and with xanthine derivatives in particular.[21,22,43]

Prodrugs are biologically inactive molecules that undergoes in vivo bio-conversion to the active parent drug through chemical or enzymatic reactions.[44] The preparation of water-soluble prodrugs may overcome the limitations of poorly soluble drugs, allowing parental, including local applications and also improving peroral bioavailability.[45] The development of water-soluble phosphate prodrugs is particularly promising.[45,46] They can be obtained by the phosphorylation of hydroxy (or amino) groups present in the drug molecules and converted to the corresponding salts. Examples for successful phosphate prodrugs are depicted in Figure 2, namely the approved hypnotic drug, Fospropofol (**10**, Lusedra®), the orally administered antiretroviral protease inhibitor, Fosamprenavir (**11**, Lexiva®) and the intravenously administered antiemetic drug Fosaprepitant (Ivemend®, **12**).[46–48] Moreover, MSX-3 (**13**), a water-soluble prodrug of the A$_{2A}$AR antagonist MSX-2, which is directly injectable, has been widely used as a pharmacological tool in vivo studies.[45,49–58] These phosphate prodrugs show

significant improvement in aqueous solubility in comparison to their parent drugs (Figure 2), and their thermodynamic solubility can be modulated by their counterion(s).[59]
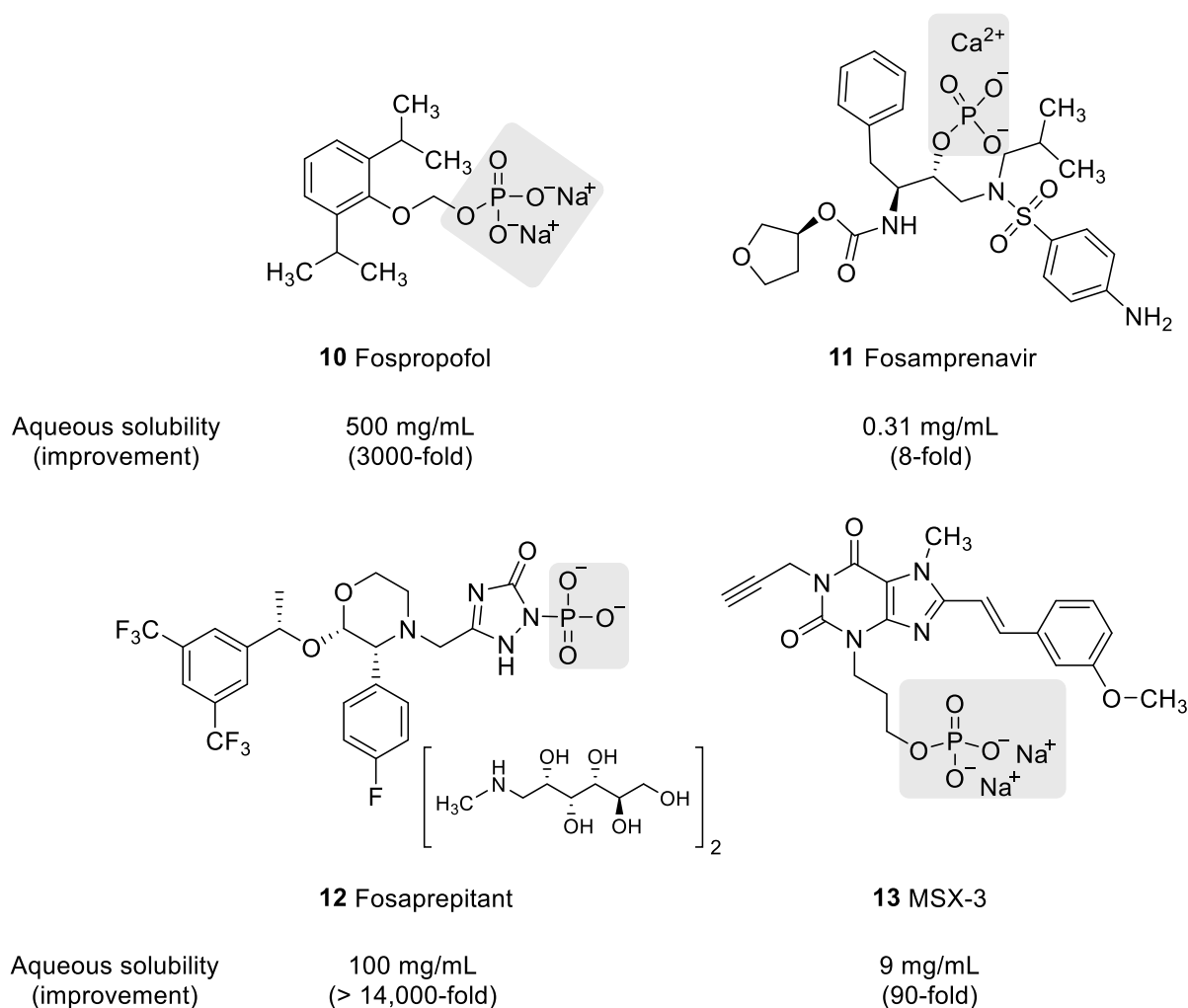

	10 Fospropofol	**11** Fosamprenavir
Aqueous solubility (improvement)	500 mg/mL (3000-fold)	0.31 mg/mL (8-fold)

	12 Fosaprepitant	**13** MSX-3
Aqueous solubility (improvement)	100 mg/mL (> 14,000-fold)	9 mg/mL (90-fold)

Figure 2. Selected phosphate prodrugs, their aqueous solubility and improvement in water-solubility compared to their parent drugs.[45,46,48]

In a previous publication, we presented the development of the outstanding potent and selective A$_{2B}$AR antagonist **4b** (Figure 1). However this compound and its analogue **4a**, display poor aqueous solubility, which limits their applicability, especially for injection.[22] Therefore, starting from a structure-based approach, we designed derivatives into which hydroxy groups were introduced. Since the X-ray crystal structure of the A$_{2B}$AR has not yet been resolved, we used a homology model of the A$_{2B}$AR that was built based on the crystal structure of the

$A_{2A}AR$, the most closely related AR paralogue.[22,60,61] This model helped us to better understand the molecular interactions of **4b** with its receptor binding pocket and to identify possible positions for substitution with polar hydroxy groups.[22] We subsequently synthesized three different series of potent and selective $A_{2B}AR$ antagonists (Figure 3). Selected compounds were subsequently phosphorylated to obtain the desired water-soluble phosphate prodrugs.

4.1.4. Results and discussion

4.1.4.1. Design

The target compounds bear different hydroxy groups either attached at the *N*3 position of xanthine moiety or to the large *C*8 xanthine substituent (Figure 3). In addition, they are sharing the main pharmacophore features essential for $A_{2B}AR$ binding, including xanthine scaffold that represents a flat core offering a hydrogen-bond donor group (NH at *N*7 of xanthine) and a hydrogen-bond acceptor group (carbonyl function at *C*6 of xanthine), propyl substitution at *N*1-position of xanthine, benzenesulfonamide moiety and the *p*-bromo substituent on the terminal phenyl moiety, which increases $A_{2B}AR$ affinity.
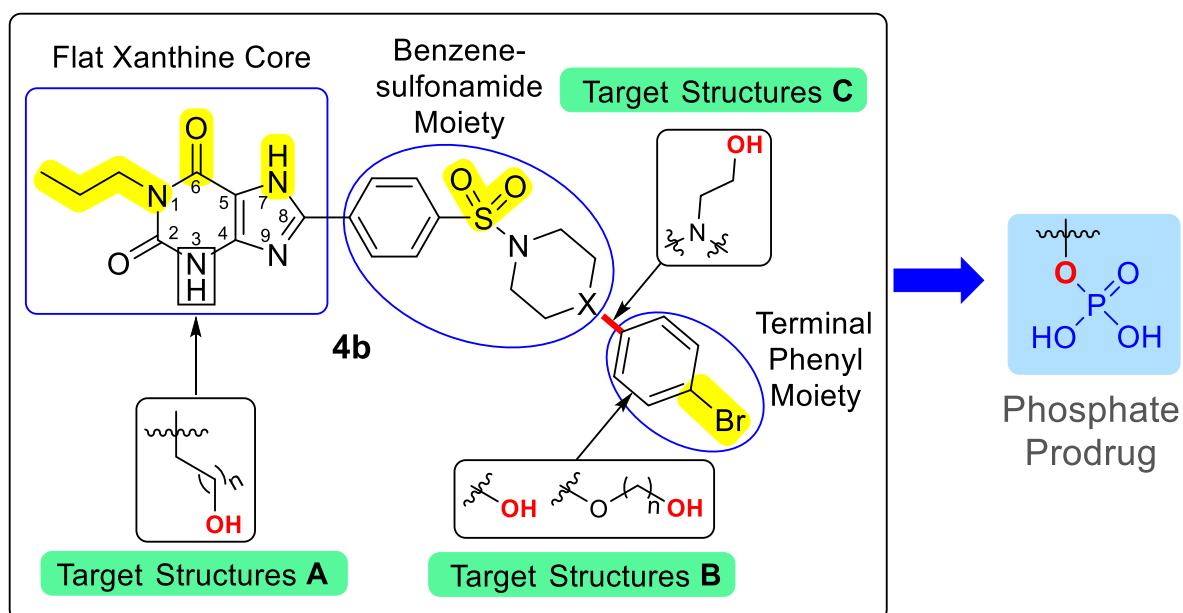

Figure 3. Schematic representation showing the key pharmacophore features of the potent and selective $A_{2B}AR$ antagonist **4b** used as a lead structure and the proposed structural

modifications to obtain the three series of hydroxylated target structures **A**, **B** and **C** followed by the preparation of their respective phosphate prodrugs.

Substitution of the xanthine *N*3-position with hydroxyalkyl chains will yield target structures A (Figure 3). Different substitutions will be implemented on the terminal phenyl ring with phenolic hydroxy or hydroxyalkyl substitution to obtain target structures B. A third strategy was to introduce a hydroxyethyl residue attached to an amino linker connecting the piperidinyl moiety with the terminal phenyl ring resulting in target compounds C. Hydroxy-substituted products that show high affinity and selectivity for $A_{2B}ARs$ will be phosphorylated to their respective water-soluble phosphate prodrugs (Figure 3).

4.1.4.2. Chemistry

The synthetic routes for the target compounds are depicted in Schemes 1-7.

Substitution at N3-xanthine position (target structures A). Different synthetic strategies including protecting group techniques were employed to obtain xanthine derivatives **24** and **30a-d** bearing hydroxyalkyl substituents at the *N*3-position of the xanthine core with various chain length (Schemes 1 and 2). The 3-hydroxypropyl-substituted derivative **24** was prepared as depicted in Scheme 1. The benzoic acid derivatives **16a-c** were prepared by reaction of 4-(chlorosulfonyl)benzoic acid **14** with piperazines **15a-c** in the presence of *N,N*-diisopropylethylamine (DIPEA). Protection of the 6-amino group of **17** was performed using *N,N*-dimethylformamide dimethyl acetal (DMF-DMA)[62] yielding **18**. Subsequent alkylation with 3-iodopropyl acetate led to the intermediate **19**. Treatment of **19** with a solution of methylamine in ethanol cleaved the ester bond as well as the formamidine group yielding **20**. Nitrosation and subsequent reduction of **20** were performed as previously described for uracil derivatives[63] yielding compound **22**. Amide coupling of **22** with the benzoic acid derivative **16a** in the presence of the coupling reagent *N*-ethyl-*N'*-(3-dimethylaminopropyl)-carbodiimide
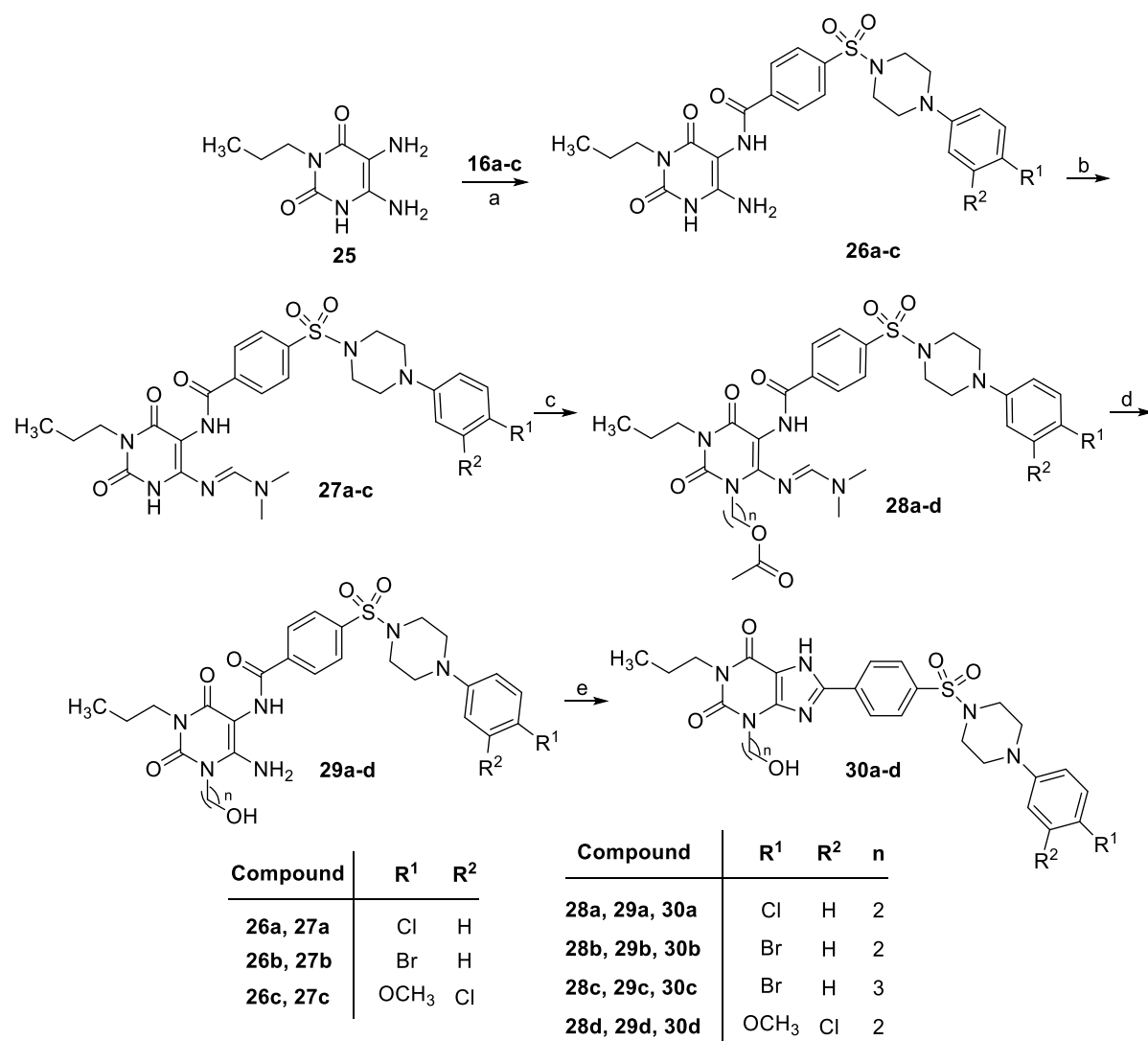
hydrochloride (EDC)[21] led to uracilcarboxamide **23**. Final ring closure reaction of **23** with hexamethyldisilazane (HMDS)[64] at 120 °C afforded the hydroxyl-substituted target compound **24**.

Scheme 1. Preparation of benzoic acid derivatives (**16a-c**) and 3-(3-hydroxypropyl)-substituted xanthine derivative **24**.
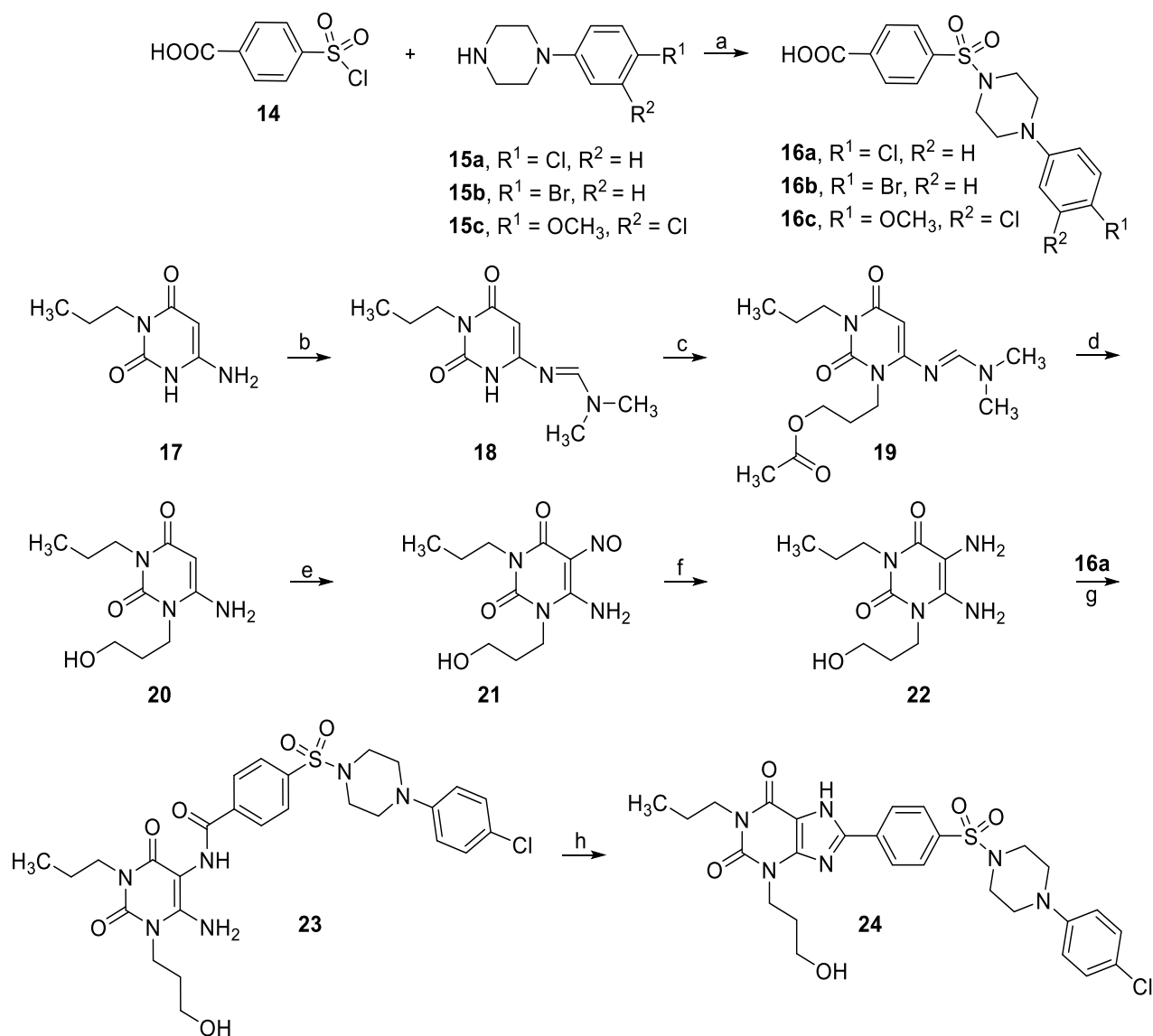
Reagents and conditions: (a) DIPEA, DCM, rt, 48-72 h, 61-75%; (b) DMF-DMA, DMF, 40 °C, 2 h, 44%; (c) 3-iodopropyl acetate, K_2CO_3, acetonitrile, rt, 24 h, 36%; (d) $MeNH_2$ (33% in EtOH), 40 °C, 4 h, 77%; (e) $NaNO_2$, AcOH, H_2O, 65 °C, 2 min, 63%; (f) $Na_2S_2O_4$, NH_3 (12.5% aq), 65 °C, 3 min, 45%; (g) EDC, DMF, rt, 3 h, 36%; (h) (1) HMDS, 120°C, 4 h, (2) 4 M HCl in dioxane, rt, 1 h, 88%.

Scheme 2. Preparation of 3-(3-hydroxypropyl)-substituted xanthine derivatives **30a-d**.

Compound	R^1	R^2
26a, 27a	Cl	H
26b, 27b	Br	H
26c, 27c	OCH$_3$	Cl

Compound	R^1	R^2	n
28a, 29a, 30a	Cl	H	2
28b, 29b, 30b	Br	H	2
28c, 29c, 30c	Br	H	3
28d, 29d, 30d	OCH$_3$	Cl	2

Reagents and conditions: (a) EDC, DMF, rt, 4-8 h, 45-60%; (b) DMF-DMA, DMF, 40 °C, 2-4 h, 61-90%; (c) CH$_3$COO(CH$_2$)$_n$I, K$_2$CO$_3$, DMF, 90 °C, 2-4 h, 45-74%; (d) MeNH$_2$ (33% in EtOH), 40 °C, 4-8 h, 66-93%; (e) (1) HMDS, 120°C, 4 h, (2) 4 M HCl in dioxane, rt, 1 h, 43-63%.

An alternative sequence to obtain 1,3,8-substitued xanthine derivatives bearing different hydroxyalkyl groups at *N3*-positions was explored for the preparation of compounds **30a-d** (Scheme 2). The coupling of 5,6-diamino-3-propyluracil (**25**)[63] with sulfonamido-substituted benzoic acid derivatives **16a-c** in the presence of EDC[20] in DMF at rt yielded intermediates **26a-c**. The 6-aminouracil group of **26a-c** was subsequently protected using DMF-DMA leading to **27a-c**. Alkylation of the uracil *N1*-position with the appropriate alkyl halide

and subsequent simultaneous deprotection resulted in derivatives **29a-d**. The final target compounds **30a-d** were obtained by ring-closure reaction using HMDS[64] at 120 °C. The reaction sequence described in Scheme 2 turned out to be superior to that described in Scheme 1 due to the higher reproducibility with different substituents.

Hydroxy(alkyl)-substitution at the terminal phenyl ring (target structures B). Previously, we have reported A$_{2B}$AR antagonists **31a-e** (Figure 4) possessing high potency and selectivity.[22] These compounds represent derivatives and analogues of lead compound **4a** featuring fluoro, chloro, methoxy or hydroxyl residues in the *meta-* and/or *para*-position of the terminal phenyl ring. In the present study, we synthesized related derivatives bearing a *p*-bromophenyl group, which is known to display high affinity for A$_{2B}$ARs, but with an additional phenolic group (**35**) or a hydroxyalkyl residue (**41b**, **42**) (Scheme 3 and 4).
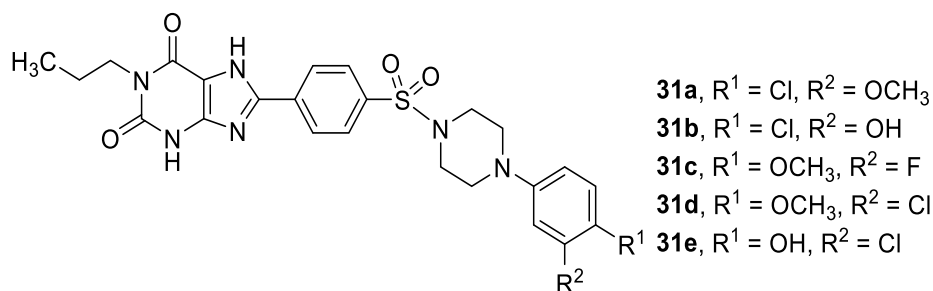

31a, R^1 = Cl, R^2 = OCH$_3$
31b, R^1 = Cl, R^2 = OH
31c, R^1 = OCH$_3$, R^2 = F
31d, R^1 = OCH$_3$, R^2 = Cl
31e, R^1 = OH, R^2 = Cl

Figure 4. Chemical structures of previously reported xanthines **31a-e**.[22]

Bromination of commercially available 2- or 3-methoxyphenylpiperazine led to the desired 4-bromophenylpiperazines **33a,b**.[65] Subsequent aminolysis of the nitrophenyl-sulfonic acid ester **32**[66] with piperazines **33a** or **33b** respectively was performed according to a previously reported procedure[21,22,66,67] under reflux conditions in DMSO under an argon atmosphere producing compounds **34a,b** (Scheme 3). *O*-Demethylation of **34a** using boron tribromide (BBr$_3$) yielded the final product **35** bearing a phenolic group. The *O*-demethylation reaction of compound **34b** using the same conditions was not successful and a dibrominated compound was produced instead, which is highly lipophilic and poorly water-soluble.

Scheme 3. Preparation of compounds **34a,b** and **35**.
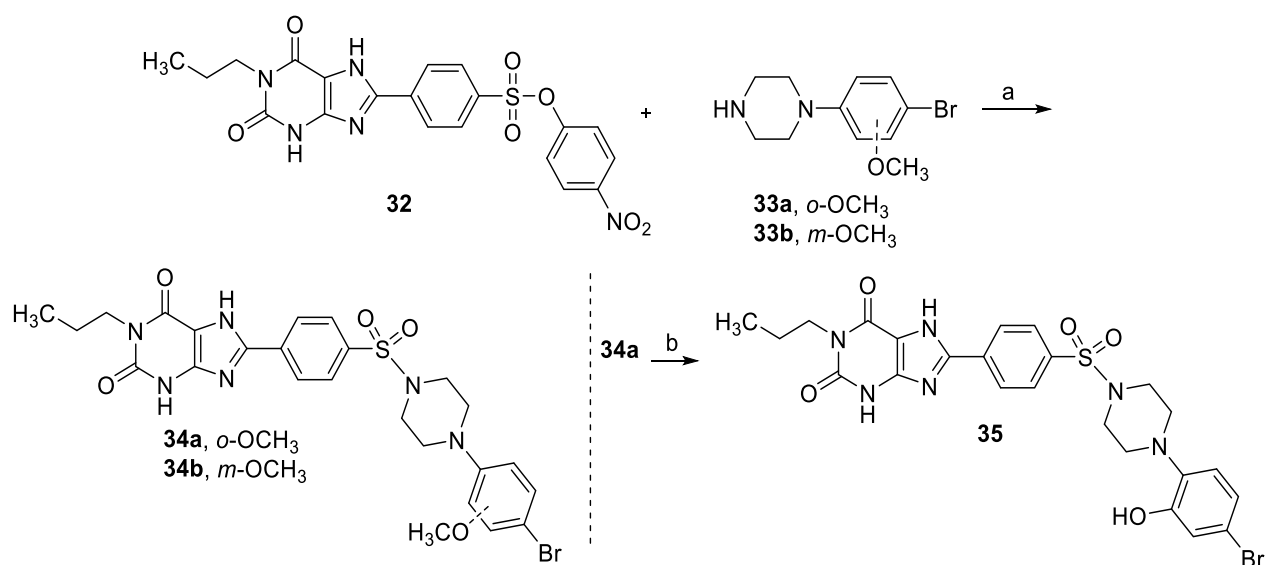
Reagents and conditions: (a) DMSO, Ar, 150 °C, 15-18 h, 25-40%.; (b) 1M BBr$_3$, DCM, 0 °C - rt, 24 h, 26%.

Unfortunately, xanthine derivative **35** featuring an *ortho*-phenolic group, was not suitable for further phosphorylation due to steric hindrance. Therefore, we prepared compounds **41b** and **42** with extended hydroxyalkyl chains (Scheme 4). The commercially available *N*-(*o*-hydroxyphenyl)piperazine (**36**) was boc-protected following standard protocols.[65] The resulting *tert*-butyl 4-(2-hydroxy phenyl)piperazine-1-carboxylate (**37**) was subsequently alkylated with different alkyl halides yielding **38a,b**, which were brominated in the following step yielding the desired *p*-bromophenylpiperazines **39a,b**. Subsequent deprotection under acidic conditions led to the building blocks **40a** and **40b**, which were then coupled with the xanthine-nitrophenyl-sulfonic acid ester **32** in DMSO as described in Scheme 3 affording derivatives **41a** and **41b**. Reduction of **41a** using lithium borohydride yielded the final product **42** bearing a 2-hydroxyethoxy substituent at the *ortho*-position of the terminal phenyl ring (Scheme 4).

**Scheme 4.** Preparation of compounds **41a,b** and **42**.
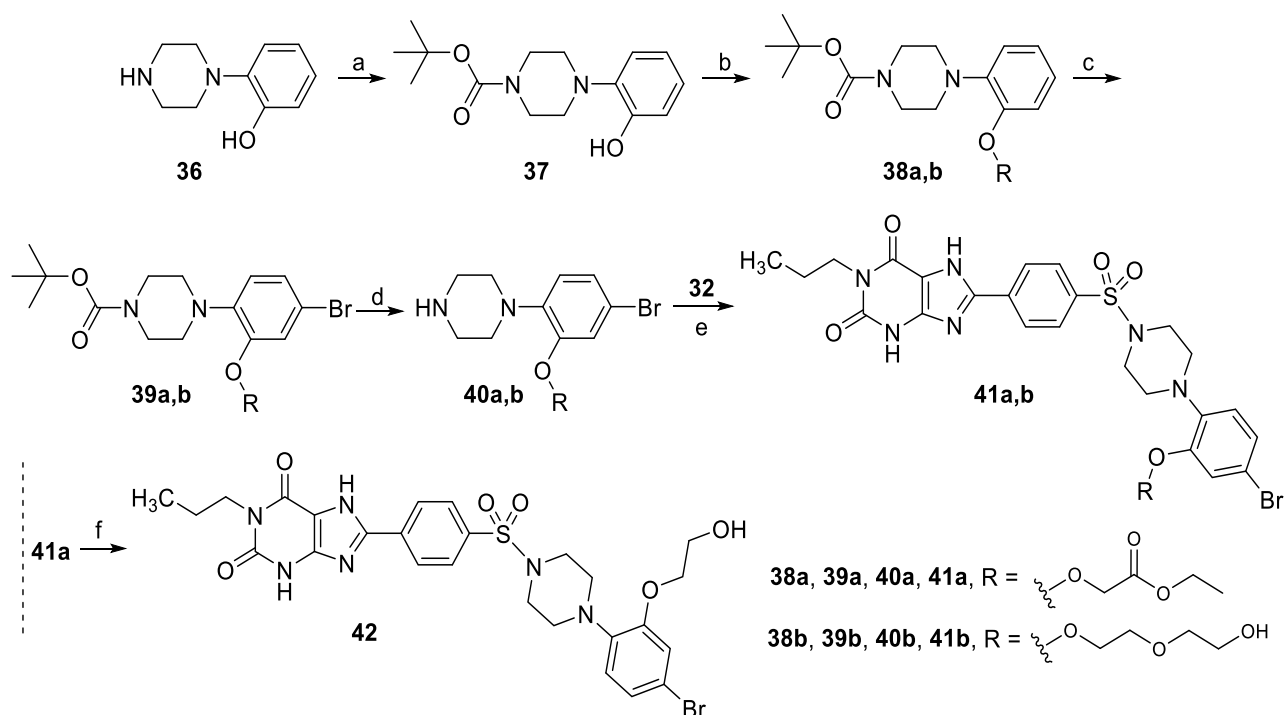
Reagents and conditions: (a) (Boc)$_2$O, NaHCO$_3$, THF/H$_2$O/dioxane (1:1:1), rt, 12 h, 99%; (b) (for **41a**) BrCH$_2$COOCH$_2$CH$_3$, K$_2$CO$_3$, DMF, 40 °C, 4 h, 69%, (for **41b**) Cl(CH$_2$)$_2$O(CH$_2$)$_2$OH, K$_2$CO$_3$, DMF, 100 °C, 24 h, 60%; (c) Br$_2$, DCM, 0 °C - rt, 1 h, 84-90%; (d) TFA, DCM, 0 °C - rt, 20 h, 40-73%; (e) DMSO, 150 °C, 16-18 h, 20-28%; (f) LiBH$_4$, THF, 0 °C - rt, 90 h, 25%.

Substitution at the amino-linker (target structures C). As another novel target, we introduced a hydroxyalkyl chain attached to a nitrogen atom connecting a piperidinyl linker with the terminal phenyl ring. The formation of appropriate building blocks started from *N*-boc-piperidone (**43**) and 4-bromoaniline (**44**). Reductive amination using sodium triacetoxyborohydride in the presence of acetic acid yielded **45**, which was subsequently alkylated with ethyl- or methyl bromoacetate.[68,69] The products were directly *N*-deprotected under acidic conditions leading to **46a,b**. Subsequent reaction of **46a** with 4-(chlorosulfonyl)benzoic acid (**14**) in the presence of DIPEA as a base yielded intermediate **47**. Amide coupling of 5,6-diamino-1-propyluracil (**25**) with **47** in the presence of EDC, followed by ring closure with phosphorus pentoxide[22] in DMF at 120 °C yielded xanthine derivative **49**.

Reduction of the methyl ester of **49** with lithium borohydride (LiBH₄) afforded the final *N*-

hydroxyethyl-substituted xanthine derivative **50** (Scheme 5).

**Scheme 5**. Preparation of compound **50** (Method A).
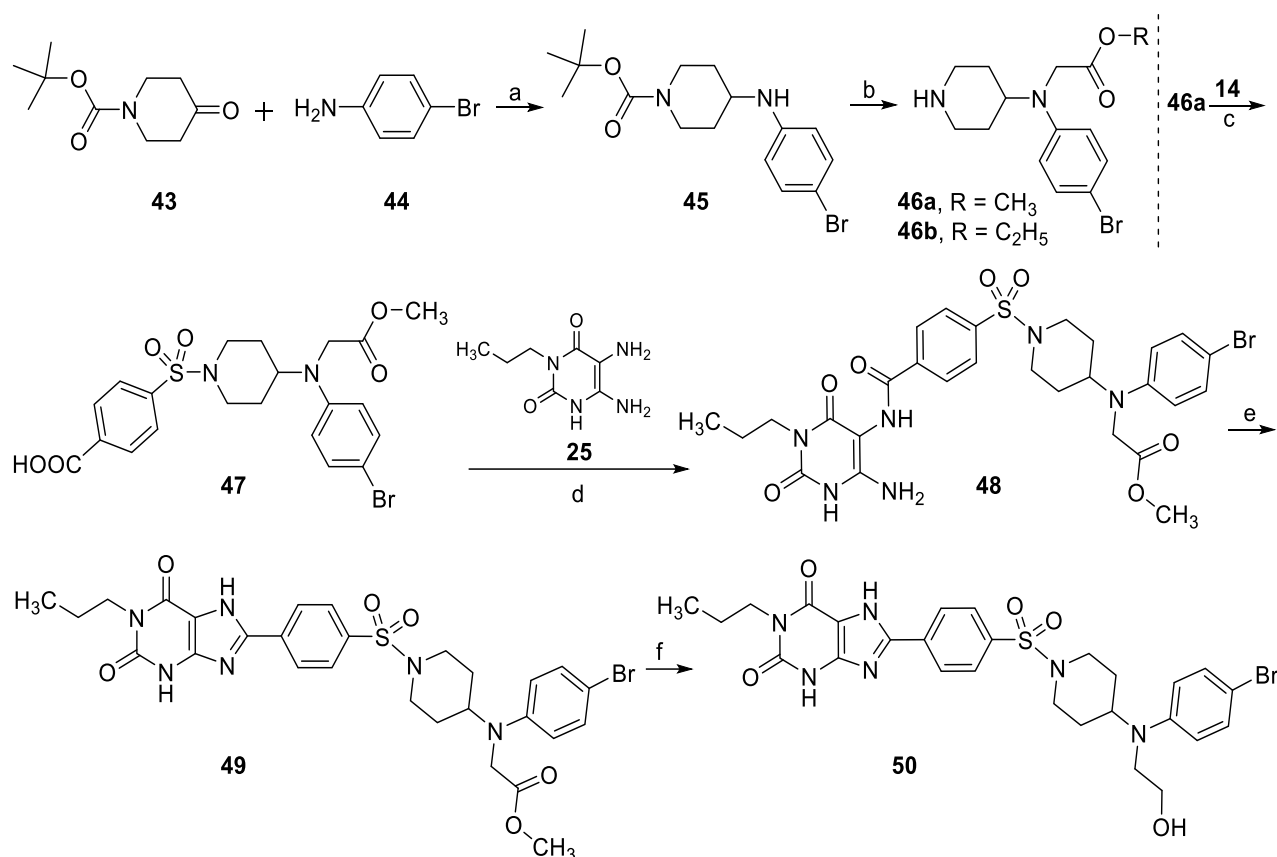
Reagents and conditions: (a) NaBH(OAc)₃, AcOH, DCE, 0 °C - rt, 6 h, 40%; (b) (1)

BrCH₂COOR, DIPEA, 90 °C, 24 h, (2) 4M HCl in dioxane, 0 °C - rt, 12 h, 55-60%; (c) DIPEA,

DCM, rt, 72 h, 53%; (d) EDC, DMF, rt, 8 h, 78%; (e) P₂O₅, DMF, 120 °C, 10 min, 56%; (f)

LiBH₄, THF, 0 °C - rt, 90 h, 40%.

As an alternative approach to synthesize target compound **50** (Method B), we applied the

aminolysis method in analogy to the procedure described in Schemes 3 and 4. Reaction of sulfonic acid

ester **32** with piperazine **46b** yielded compound **51** bearing an ethyl ester which was reduced using

lithium borohydride producing compound **50** (Scheme 6). This method involves fewer steps to obtain

the final product **50** in comparison to method A (Scheme 5) and provides a higher overall yield (Method B: 3.78 %, Method A: 2.04 %).

Scheme 6. Preparation of compound **50** (Method B).
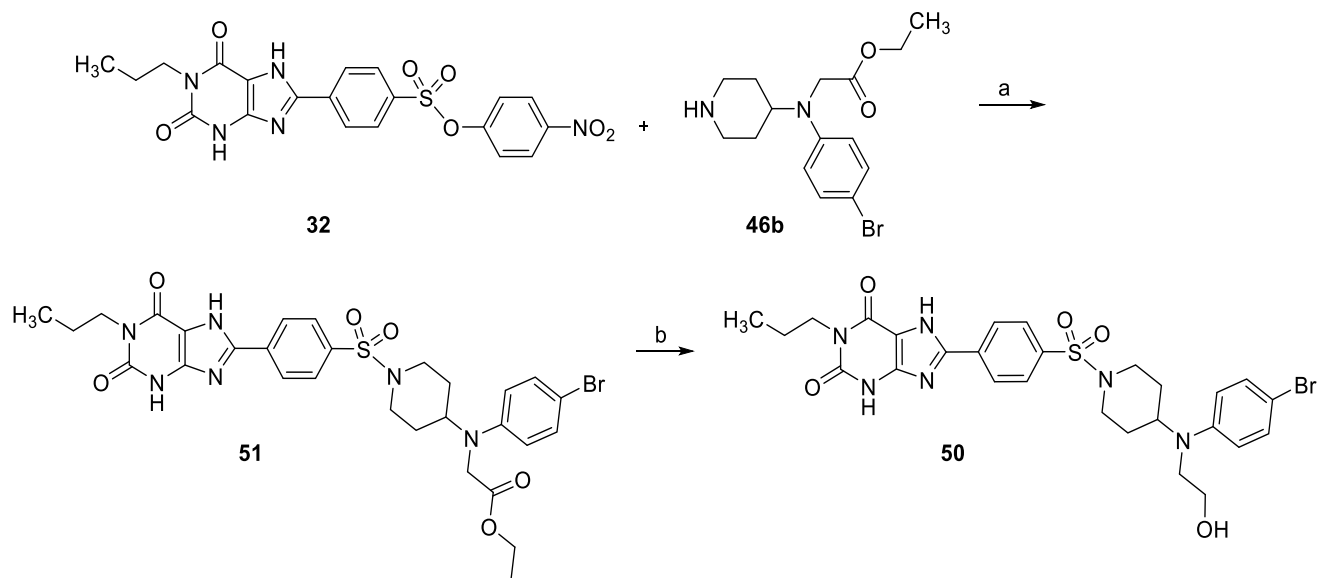
Reagents and conditions: (a) DMSO, 150 °C, 15 h, 45%; (b) LiBH₄,THF, 0 °C - rt, 90 h, 35%.

The synthesized A$_{2B}$AR antagonists were purified using flash chromatography on silica gel (for details see Experimental). Structures, molecular weight, purity, and calculated log P values (cLog P) of the synthesized xanthine derivatives are listed in Table 1.

Table 1. Synthesized A₂BAR antagonists, molecular weights, purities, and calculated Log P values.

	Compd.	R¹	R²	R³	R⁴	M.W.[a]	Purity (%)[b]	cLog P[c]
Target Structures A	**24**	(propyl-OH)	H	H	Cl	587.1	96.7	2.90
	30a	(ethyl-OH)	H	H	Cl	573.1	96.2	2.84
	30b	(ethyl-OH)	H	H	Br	617.5	95.2	3.01
	30c	(propyl-OH)	H	H	Br	631.6	99.0	3.07
	30d	(ethyl-OH)	H	Cl	OCH₃	603.1	97.6	2.68
Target Structures B	**34a**	H	OCH₃	H	Br	603.5	95.0	4.32
	34b	H	H	OCH₃	Br	603.5	95.9	4.32
	35	H	OH	H	Br	589.5	99.0	4.18
	41a	H	(O-CH₂-C(=O)-O-ethyl)	H	Br	675.6	97.4	4.30
	41b	H	(O-CH₂CH₂-O-CH₂CH₂-OH)	H	Br	677.6	96.1	3.59
	42	H	(O-CH₂CH₂-OH)	H	Br	633.5	97.4	3.63
Target Structures C	**49**	R⁵ = (CH₂CH₂-C(=O)-O-CH₃)				659.6	95.4	4.28
	50	R⁵ = (CH₂CH₂CH₂-OH)				631.6	96.2	3.97
	51	R⁵ = (CH₂CH₂-C(=O)-O-ethyl)				673.6	95.4	4.64

[a] Molecular weight was calculated by the Chemdraw software; [b] Purity was determined by HPLC-UV-MS at 254 nm; [c] logarithm of the partition coefficient values (cLog*P)* were calculated by Instant JChem software.[70]

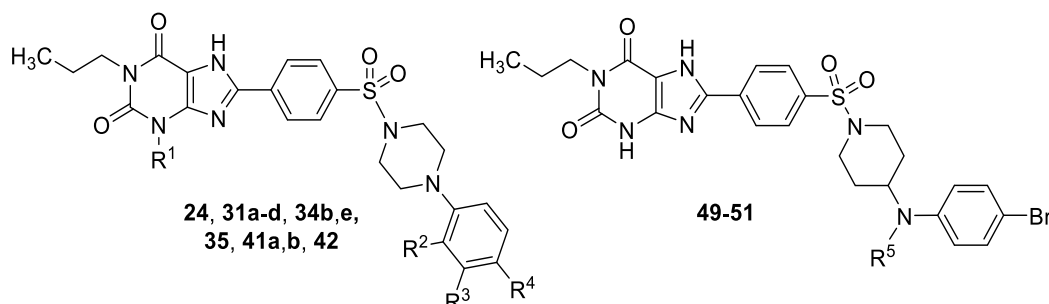### 4.1.4.3. Adenosine receptor affinities

They were carried out to measure the affinity of the synthesized compounds towards at four human AR subtypes, A_1, A_{2A}, A_{2B} and A_3 (Table 2). The A_1AR-selective radioligand [^{3}H]CCPA,[71] the A_{2A}AR-selective radioligand [^{3}H]MSX-2,[72] the A_{2B}AR-selective radioligand [^{3}H]PSB-603,[21] and the A_3AR-selective radioligand [^{3}H]PSB-11[73] were employed.
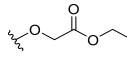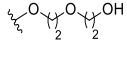
Substitution at N3-xanthine position (target structures A). The first group of xanthine derivatives was substituted at the 3-position of the xanthine core with hydroxyalkyl residues of different linker lengths (Table 2). Previous studies demonstrated that a propyl substituent in the 1-position of xanthine is optimal for high affinity and selectivity for the A_{2B}AR. Also, lipophilic substituents, such as bromo at the *p*-position of the terminal phenyl ring are beneficial probably due to halogen bonding interaction in the aromatic binding pocket of the A_{2B}AR.[21,22] Therefore, we considered these important features in the design of the new molecules. As expected, compounds with a *p*-bromophenyl substituent (**30b** and **30c**) showed 2-6-fold higher A_{2B}AR affinity than analogues with a *p*-chlorophenyl residue (**24** and **30a**).

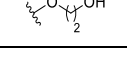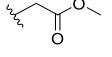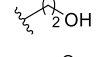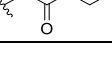Compounds having the longer hydroxyalkyl chains at the *N3*-position (**24** and **30c**) showed similar A_{2B}AR affinity but with increased affinity for several AR subtypes and thus lower A_{2B}AR selectivity than compounds having the shorter alkyl chain (**30a**, **30b** and **30d**). Therefore, hydroxyethyl was superior to a hydroxypropyl residue. Compound **30b** showed high A_{2B}AR affinity ($K_i = 1.34$ nM). In addition, it was about 700-fold selective for A_{2B} over A_1 and A_{2A} ARs and about 35-fold selective over the A_3AR. This A_{2B}AR antagonist was therefore selected for phosphorylation to develop the water-soluble phosphate prodrug **52** (Scheme 7). Although compound **30d** showed more than 100-fold selectivity for the A_{2B}AR over the other AR subtypes, it was less potent at A_{2B}AR than **30b** and therefore not prioritized.

Table 2. Adenosine receptors affinities of synthesized $A_{2B}AR$ antagonists.

Compd.	R^1	R^2	R^3	R^4	$K_i \pm$ SEM (nM) (% inhibition of radioligand binding at indicated concentration)				SI^e
					$A_{2B}AR^a$	A_1AR^b	$A_{2A}AR^c$	A_3AR^d	
24	(CH₂)₃OH	H	H	Cl	2.72 ± 0.35	20.1 ± 11.2	385 ± 99	28.4 ± 10.2	8
30a	(CH₂)₂OH	H	H	Cl	3.09 ± 1.10	≥ 1000 (38%)	264 ± 95	68.7 ± 14.1	23
30b	(CH₂)₂OH	H	H	Br	1.34 ± 0.13	> 1000 (33%)	900 ± 283	45.7 ± 6.9	35
30c	(CH₂)₃OH	H	H	Br	0.492 ± 0.058	≥ 1000 (41%)	23.4 ± 6.8	78.5 ± 22.8	48
30d	(CH₂)₂OH	H	Cl	OCH₃	8.23 ± 3.21	>1000 (32%)	844 ± 139	≈ 1000 (52%)	103
31b^f	H	H	OH	Cl	0.421 ± 0.041	113 ± 39	40.7 ± 10.4	>1000 (31%)	97
31e^f	H	H	Cl	OH	3.55 ± 0.77	≥ 1000 (37%)	93.8 ± 17.7	≥ 1000 (41%)	27
34a	H	OCH₃	H	Br	1.03 ± 0.23	≥ 1000 (43%)	175 ± 32	>1000 (23%)	170
34b	H	H	OCH₃	Br	0.764 ± 0.158	>1000 (31%)	123 ± 27	285 ± 99	161
35	H	OH	H	Br	0.443 ± 0.154	302 ± 65	87.8 ± 5.8	>1000 (32%)	199
41a	H	OCH₂C(O)OEt	H	Br	3.76 ± 1.11	>1000 (28%)	≥ 1000 (41%)	≥ 1000 (42%)	266
41b	H	O(CH₂)₂O(CH₂)₂OH	H	Br	6.27 ± 0.92	≥ 1000 (37%)	446 ± 80	>1000 (33%)	72
42	H	O(CH₂)₂OH	H	Br	0.718 ± 0.038	240 ± 1400	157 ± 53	>1000 (34%)	219
49	R^5 = CH₂C(O)OCH₃				0.318 ± 0.084	>1000 (29%)	971 ± 397	>1000 (19%)	3053
50	R^5 = (CH₂)₂OH				0.473 ± 0.132	237 ± 113	121 ± 44	≈ 1000 (45%)	246
51	R^5 = CH₂C(O)OEt				0.266 ± 0.105	≈ 1000 (17%)	1000 (47%)	>1000 (17%)	3759

(Left margin labels: *Target Structures A* for rows 24–42; *Target* for rows 49–51)

^{a} vs. [³H]PSB-603 (n = 3); ^{b} vs. [³H]CCPA (n = 3); ^{c} vs. [³H]MSX-2 (n = 3); ^{d} vs. [³H]PSB-11 (n = 3); ^{e} selectivity index was calculated by dividing the second lowest K_i value by the $A_{2B}AR$ K_i value; ^{f} previously reported $A_{2B}AR$ antagonists.[22]

Substitution at the terminal phenyl ring (target structures B). The second group of compounds includes those substituted on the terminal phenyl ring with a hydroxy group or hydroxyalkyl residues and concurrently with halides, such as chloro or bromo, that are known to increase $A_{2B}AR$ affinity (Table 2).[22] In our previous study, we found out that compounds having polar hydroxy substituents in the *p*-phenyl position, such as **31e**, are showing moderate affinity and selectivity towards the $A_{2B}AR$.[22] Therefore, in this study, we introduced a bromo-substituent in the *p*-phenyl position for optimal halogen bonding in the $A_{2B}AR$ binding site, while having the phenolic hydroxy group in the *o*-position. Compound **35** displayed the highest selectivity (~200-fold) for the $A_{2B}AR$ over the other AR subtypes in comparison to compounds **31b** (~100-fold) and **31e** (27-fold).

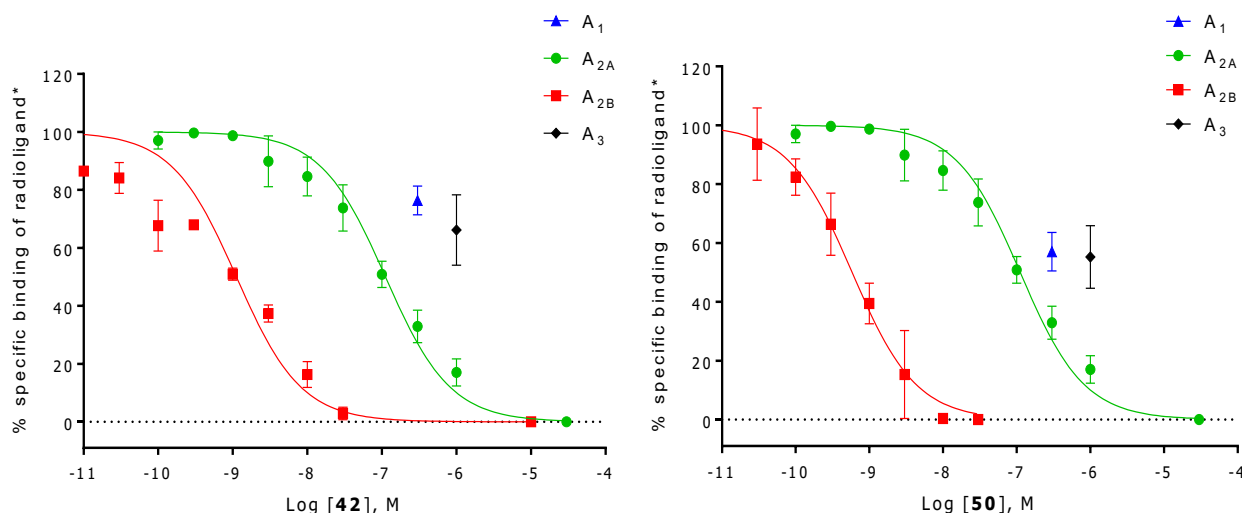**Figure 5.** Concentration-dependent inhibition of radioligand binding by compounds **42** and **50** to the human AR subtypes. Data points are means (SEM of three experiments performed in duplicates. *A_1AR-selective radioligand [^{3}H]CCPA[71], A_{2A}AR- selective radioligand [^{3}H]MSX-2[72], the A_{2B}AR-selective radioligand [^{3}H]PSB-603[21], *A_3AR-selective radioligand [^{3}H]CCPA.[73]

Compound **42** with a hydroxyethyl chain attached to the *ortho*-position of the terminal phenyl ring displayed similar excellent affinity (K_i = 0.718 nM) and A$_{2B}$AR-selectivity (219-fold) (Figures 5 and 6). Thus, we prepared its water-soluble phosphate prodrug **53** (Scheme 7). Compound **41b** having a longer hydroxyalkyl chain (diethylene glycol) displayed 9-fold lower potency and decreased selectivity compared to **42** (Table 2).

Substitution at the amino linker (target structure C). The third group of compounds includes those having hydroxyalkyl chain attached to an amino linker (Table 2). In this novel series of compounds, we have the essential pharmacophoric features that are essential for the A$_{2B}$AR affinity, the free *N*3-position of the xanthine core and the terminal *p*-brormophenyl moiety. Methyl and ethyl acetate derivatives **49** and **51** displayed high affinity (K_i < 0.5 nM) for the A$_{2B}$AR and outstanding selectivity (>3000-fold). indicating that *N*-substitution of 4-(phenylamino)piperidine-substituted sulfophenylxanthines is well tolerated. This modification is new and has not been tried before; it opens up new possibilities for modulating the properties of this class of A$_{2B}$AR antagonists and for attaching functional groups and reporter moieties such as e.g. fluorophores. Target compound **50** bearing a hydroxyethyl group on the nitrogen atom combined with a terminal *para*-bromophenyl ring displayed subnanomolar potency and was highly selective (246-fold, see Figures 5 and 6). We subsequently developed its phosphate prodrug **54** (Scheme 7).

Affinities and selectivities of the best hydroxy-substituted A$_{2B}$AR antagonists are depicted and compared in a column diagram (Figure 6). Three potent and selective A$_{2B}$AR antagonists, **30b**, **42** and **50**, the best one from each target structure A, B and C with respect to high A$_{2B}$AR affinity and AR subtype selectivity were further phosphorylated to yield the respective phosphate prodrugs **52**-**54** (Scheme 7).

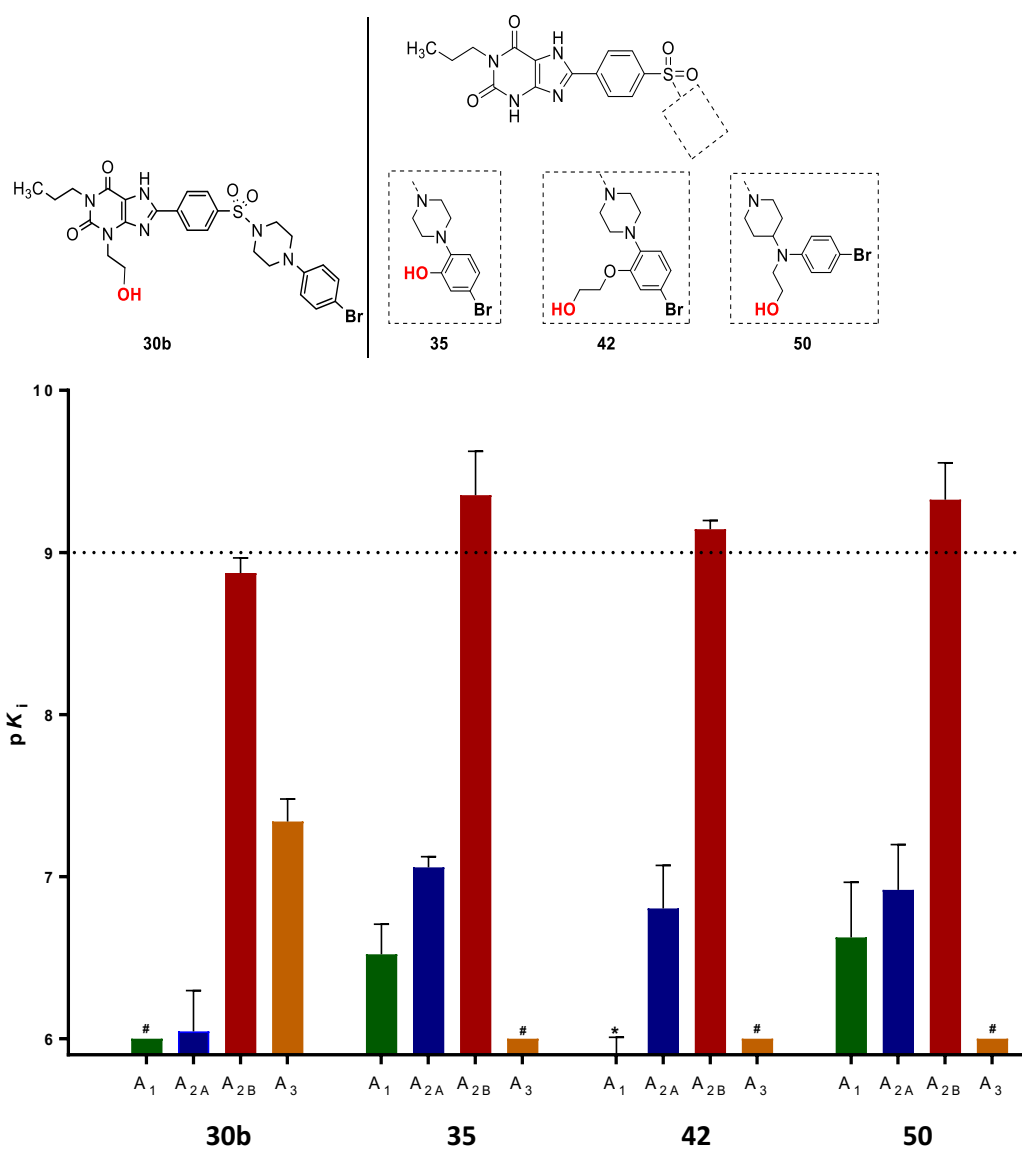**Figure 6.** Affinities of compounds **30b**, **35**, **42** and **50** at the four human AR subtypes (A$_1$, A$_{2A}$, A$_{2B}$ and A$_3$) determined in radioligand binding assays are given as pK_i values; * tested, pK_i < 5.5; # tested, pK$_i$ < 6.

4.1.4.4.   Preparation of phosphate prodrugs

One-pot phosphorylation reaction[45,66,74,75] of hydroxyalkyl groups in **30b**, **42** and **50** was performed in a mixture of phosphoryl chloride and trimethyl phosphate. Hydrolysis of the reaction mixtures with triethylammonium hydrogen carbonate buffer (TEAC) yielded the desired phosphate prodrugs **52-54**. Compound **35** having the phenolic hydroxyl group was not phosphorylated due to the expected steric hindrance.

Scheme 7. Preparation of phosphate prodrugs **52-54**.
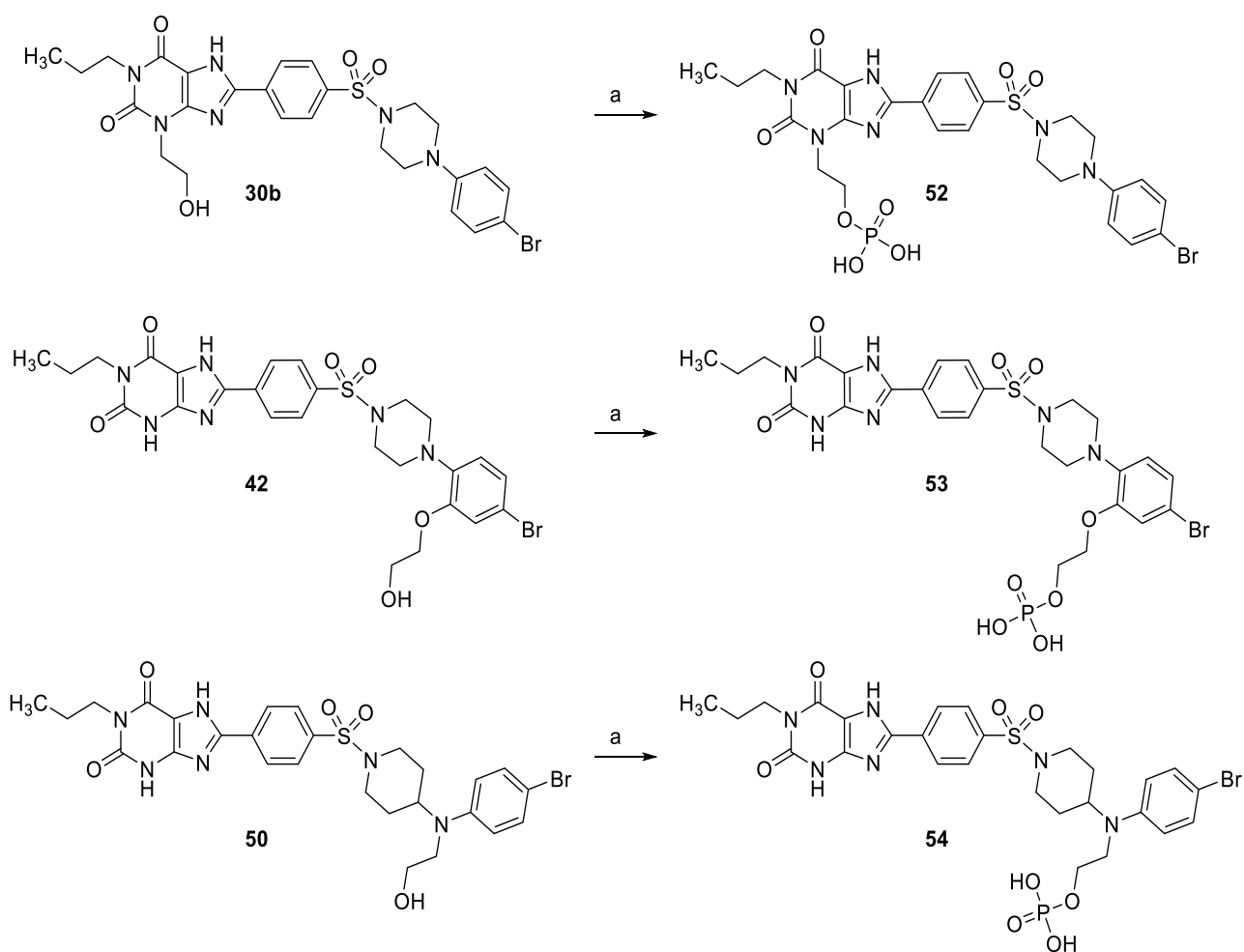
Reagents and conditions: (a) (1) POCl$_3$, PO(OCH$_3$)$_3$, Ar, 0 °C, 6-8 h, (2) TEAC buffer pH 7.4−7.6, 0 °C - rt, 1 h, 45-60%.
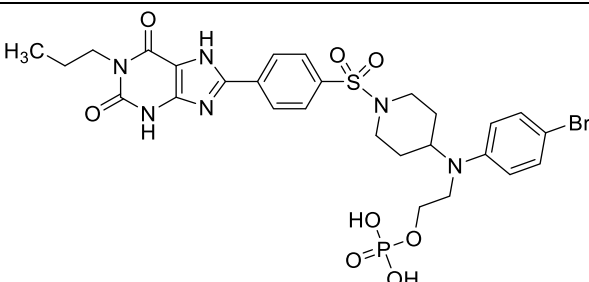
4.1.4.5. **Physicochemical and Pharmacokinetic Properties**
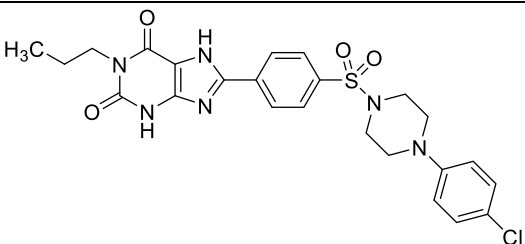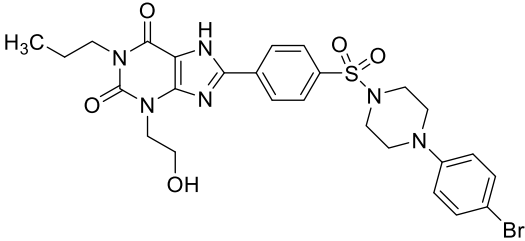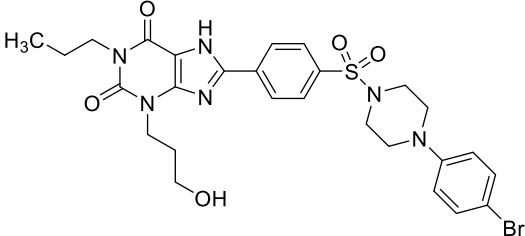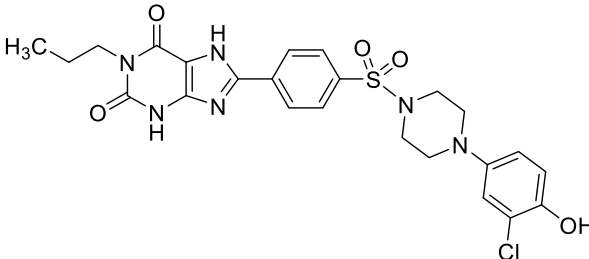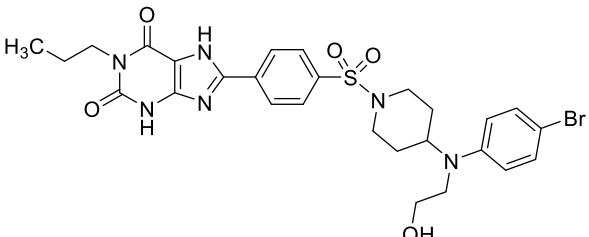
Water solubility is an important pharmacokinetic parameter affecting oral bioavailability. Moreover, it is a prerequisite e.g. for application as injectables, for inhalation, and in eye drops.[48] The water solubility of selected $A_{2B}AR$ antagonists and the phosphate prodrug **54** was measured using semi-thermodynamic approach in PBS buffer (pH 7.4) (Table 3).[76] The water solubility of most of the investigated 8-substituted xanthine derivatives including standard compound **4a** (PSB-603) is very low, only 1 µM or below. The introduction of a hydroxyalkyl group (**30b**, **30c**, **50**) or a phenolic OH group (**31e**) did not improve or only slightly increased solubility. Compound **30c** containing a hydroxypropyl substituent in the *N*3-position of the xanthine core displayed particularly low aqueous solubility, possibly due to the formation of a stable intramolecular hydrogen bond with N9. These results emphasize the importance of pursuing a prodrug approach which is expected to significantly enhance water solubility. We tested this assumption for one example, phosphate prodrug **54**. Compared to the $A_{2B}AR$ antagonist **50** (solubility: 0.2 µM) its prodrug **54** (solubility: 166 µM) displayed an 830-fold increase in solubility. While the solubility of the parent drug **50** is 420-fold of its A_{2B} K_i value, the solubility of the prodrug is 350,000 times higher than the K_i value of the drug.

Table 3. *In-vitro* ADME studies data of selected compounds in comparison to PSB-603 (**4a**); n.d. (not determined)

Compound	Structure	Solubility[a] (µM)	Microsomal stability[b] (µl/min/mg protein)
4a (PSB-603)		0.2 ± 0.1	-3.8

30b (PSB-18007)		0.5 ± 0.3	8.2
30c (PSB-18010)		0.04 ± 0.03	-4.2
31e (PSB-18054)		1.0 ± 0.8	109.4
50 (PSB-18066)		0.2 ± 0.1	51.4
54 (PSB-18150)		166 ± 17	n.d.
Verapamil			217.3

[a] Compounds are dissolved in DMSO to obtain a 20 nM stock solution then diluted with PBS buffer (pH 7.4), followed by vigorous shaking (24 h) and centrifugation (30 min). [b] performed using human liver microsomes at 0.5 mg/ml.

Next, we investigated the compounds' metabolic stability in vitro, in human liver microsomes. The standard $A_{2B}AR$ antagonist **4a** is metabolically very stable, and no degradation was observed within the incubation time of (0, 15, 30, 45 and 60 minutes). The hydroxyalkyl-substituted derivatives (**30b**, **30c**) were similarly stable towards liver

metabolism. In contrast, phenol **31** showed fast metabolic conversion. The hydroxyethyl derivative **50** (structure C) was also metabolized, although more slowly than phenol **31**. Both compounds had a longer half-live than the drug verapamil which was tested for comparison as a drug with low metabolic stability. The $A_{2B}AR$ antagonists (**4a**, **30b**, **30c** and **50**) showed high plasma protein binding (99.2, 99.98, 100.02 and 99.99 % respectively). This may protect them from degradation and increase their half-lives in vivo.[78,79]

4.1.5. Conclusion

In the present study, we modified the structure of the potent and selective $A_{2B}AR$ antagonists PSB-603 (**4a**) and its analog PSB-1901 (**4b**) with the aim to develop water-soluble phosphate prodrugs. These prodrugs can be expected to be readily hydrolyzed by endogenous phosphatases producing the active compound.[45,46] Three different positions were selected for introduction of the hydroxy groups for subsequent phosphorylation. Antagonist **30b** belonging to target structure A, substituted in the *N*3-position of the xanthine core with a hydroxyethyl residue, exhibited high antagonistic affinity for the $A_{2B}AR$, however it also showed moderate affinity for the A_3AR. On the other hand, target structures B and C, substituted on the substituent in the *C*8-position of the xanthine core with a phenolic group or hydroxyalkyl chains and keeping the unsubstituted *N*3-H, also displayed high potency and were additionally highly selective for the $A_{2B}AR$. We successfully phosphorylated three potent $A_{2B}AR$ antagonists representing the three target structures (**30b**, **42** and **50**) and obtained the desired water-soluble phosphate prodrugs **52-54**. For the example of prodrug **54** we could indeed measure a huge (830-fold) increase in water-solubility (166 µM vs. 0.2 µM for the $A_{2B}AR$ antagonist **50**). The developed $A_{2B}AR$ antagonist prodrugs will be valuable tool compounds for in vitro and in vivo studies, and may guide a way for novel drugs in immunooncology, inflammation and pain, as well as further pathologic conditions that are associated with an upregulation of $A_{2B}ARs$.

4.1.6. Experimental section

4.1.6.1. Chemistry

General. All reagents used in this study were commercially obtained from various vendors (Sigma, Aldrich, Merck, Enamine and Acros) and used without further purification. Solvents were used without additional purification or drying, except dichloromethane which was freshly distilled. Reactions were monitored by thin-layer chromatography (TLC) using aluminum sheets coated with silica gel 60 F_{254} (Merck). Column chromatography for the products was performed with a CombiFlash R_f Companion System (Teledyne ISCO, USA) using RediSep packed columns. Preparative HPLC was carried out on a Knauer HPLC system with a Wellchrome K-1800 pump, a WellChrome K-2600 spectrophotometer with a Eurospher 100 C18 column (250 mm × 20 mm, particle size 10 μm). A gradient of methanol or acetonitrile in water was used as indicated below with a flow rate of 15 mL/min. Lyophilization was performed with a CHRIST ALPHA 1-4 LSC freeze dryer.

The purity of all biologically evaluated compounds was determined by HPLC-UV using an LC-MS instrument (Applied Biosystems API 2000 LC-MS/MS, HPLC Agilent 1100) according to the following procedure: compounds were dissolved at a concentration of 0.5 mg/mL in methanol/H_2O (1:1). Then, 10 μL of the sample were injected into a Phenomenex Luna C18 HPLC column (50 mm × 2.00 mm, particle size 3 μm) and chromatographed using a gradient of water/methanol (containing 2 mM ammonium acetate) from 90:10 to 0:100 for 20 min at a flow rate of 250 μL/min. UV absorption was detected from 200 to 950 nm using a diode array detector. Mass spectra were recorded on an API 2000 mass spectrometer (electron spray ion source, Applied Biosystems, Darmstadt, Germany) coupled with an Agilent 1100 HPLC system. For all other intermediate compounds, the same method was employed, but the compounds were dissolved in methanol. High-resolution mass spectra (HRMS) were recorded on a micrOTOF-Q mass spectrometer (Bruker) with an ESI-source coupled with an HPLC

Dionex Ultimate 3000 (Thermo Scientific) using an EC50/2 Nucleodur C18 Gravity 3 μm column (Macherey-Nagel). The column temperature was 25 °C. Ca. 1 μL of a 1 mg/mL solution of the sample in acetonitrile was injected and a flow rate of 0.3 mL/min was applied. HPLC was started with a solution of acetonitrile in water (10:90) containing 2 mM ammonium acetate. The gradient was started after 1 min reaching 100% acetonitrile within 9 min and then it was flushed at this concentration for another 5 min. ^{1}H- and ^{13}C-NMR data were collected on a Bruker Avance 500 MHz NMR spectrometer at 500 MHz (^{1}H), and 126 MHz (^{13}C), or on a 600 MHz NMR spectrometer at 600 MHz (^{1}H), and 151 MHz (^{13}C). DMSO-d_6 or deuterium oxide (D_2O) were used as solvents. Chemical shifts are reported in parts per million (ppm) relative to the deuterated solvent, i.e. DMSO, ^{1}H: 2.50 ppm; ^{13}C: 39.5 ppm; D_2O, δ ^{1}H: 4.80 ppm. Coupling constants J values were reported in Hertz and spin multiplicities are given as s (singlet), d (doublet), t (triplet), m (multiplet) and br (broad).

General procedure A. This procedure has been applied to the preparation of **16a-c** and **47**. To a mixture of 4-(chlorosulfonyl)benzoic acid (**14**, 1 eq) and the appropriate amine (**15a-c** or **46a**, 1eq) dissolved in 20-30 mL of DCM, DIPEA (1.7 eq) was added dropwise and the reaction mixture was stirred at rt for 48-72 h. Upon completion of the reaction, the solvents were evaporated and the obtained residue was washed with water and neutralized with few drops of 1 N HCl and the formed precipitate was collected by filtration. The obtained benzoic acid derivatives **16a-c** and **47** were used in the next step without further purification.

General procedure B. This procedure has been applied to the preparation of **18** and **27a-c**. To a solution of the appropriate uracil derivative (**17** or **26a-c**, 1 eq) in 3-15 mL of DMF, DMF-DMA (2 eq) was added dropwise and the reaction mixture was stirred at 40 ºC for 2-4 h. Upon completion of the reaction, the excess solvents were evaporated and the obtained residue was purified by column chromatography using the eluent system DCM/methanol (9.5:0.5).

General procedure C. This procedure has been applied to the preparation of **28a-d**. To a solution of the appropriate uracil derivative (**27a-c**, 1 eq) in 10-15 mL of anhydrous DMF, K_2CO_3 (2 eq) was added followed by dropwise addition of the appropriate alkyl halide (1.5-2 eq) and the reaction mixture was stirred at 90 °C for 2-4 h. Upon completion of the reaction, the excess DMF was evaporated and the obtained residue was purified by column chromatography using the eluent system DCM/ethanol (9.7:0.3).

General procedure D. This procedure has been applied to the preparation of **20** and **29a-d**. To a flask containing the appropriate uracil derivative (**19** or **28a-d**, 1 eq), methylamine solution (33% in ethanol, 10-15 mL) was added at rt and the reaction mixture was stirred at 40 °C for 4-8 h. Upon completion of the reaction, excess solvents were evaporated and the obtained residue was washed with water and filtered. The obtained precipitate was purified by column chromatography using the eluent system DCM/methanol (9.5:0.5).

General procedure E. This procedure has been applied to the preparation of **23**, **26a-c** and **48**. To a flask containing the appropriate uracil derivative (**22** or **25**, 1 eq), and the appropriate benzoic acid derivative (**16a-c** or **47**, 1 eq) dissolved in 10-20 mL of DMF, the coupling reagent EDC (1.5 eq) was added and the reaction mixture was stirred at rt for 3-8 h. Upon completion of the reaction, 10 mL of water was added and the formed precipitate was collected by filtration. The obtained precipitate was purified by column chromatography using the eluent system DCM/methanol (9.5:0.5).

General procedure F. This procedure has been applied to the preparation of **24** and **30a-d**. To a flask containing the appropriate uracil derivative (**23** or **29a-d**, 1 eq), 5-15 mL of HMDS was added and the reaction mixture was stirred at 120 °C for 4 h. Upon completion of the reaction, the solvents were evaporated and the formed residue was dissolved in HCl (4 M in dioxane, 2-5 mL) and stirred at rt for 1 h. A mixture of ice and aqueous $NaHCO_3$ solution (20 mL) was

added and the mixture was subsequently extracted with ethyl acetate (3 x 10 mL). The organic layers were dried using anhydrous Mg_2SO_4 and evaporated obtaining a residue that was further purified using column chromatography using the eluent system DCM/methanol (9.5:0.5).

General procedure G. This procedure has been applied to the preparation of **34a,b**, **41a,b**, and **51**. To a solution of *p*-nitrophenylsulfonate derivative **32** (1 eq) dissolved in 3-5 mL of anhydrous DMSO, the appropriate amine (**33a,b**, **40a,b** or **46b**, 2-4 eq) was added and the reaction mixture was stirred at 150 °C for 15-20 h under an argon atmosphere. Upon completion of the reaction, the reaction mixture was then poured into 30 mL of water and a precipitate was formed. The solid was filtered off and washed with water (3 × 10 mL) and methanol (3 × 5 mL). Samples were further purified using column chromatography using eluent system DCM/methanol (9.5:0.5).

General procedure H for the synthesis of phosphate prodrugs. This procedure has been applied to the preparation of **52-54**. To a flask containing the appropriate xanthine derivatives (**30b**, **42** or **50**, 1 eq) dissolved in 2-3 mL of trimethyl phosphate and stirred under an argon atmosphere at 0 °C, $POCl_3$ (5 eq) was added dropwise and then the reaction was kept stirring at 0 °C for 6-8 h. Upon completion of the reaction, triethylammonium hydrogen carbonate buffer pH 7.4 – 7.6 (TEAC, 0.2 M, 10 mL) was added at 0 °C followed by stirring at rt for 1 h. The formed solution was freeze-dried and the obtained solid was then purified by reverse-phase high performance liquid chromatography (RP-HPLC) using a gradient of double-distilled water/acetonitrile from 100:0 to 40:60 in 25 min and a flow rate of 20 ml/min, then suitable fractions were collected and lyophilized to obtain the desired products.

4-[4-(4-Chlorophenyl)piperazin-1-yl]sulfonylbenzoic acid (16a). This compound was synthesized according to the general procedure A using **14** (600 mg, 2.72 mmol) and **15a** (535 mg, 2.72 mmol) dissolved in 20 mL DCM, DIPEA (0.8 mL) was added and the reaction mixture

was stirred at rt for 48 h. A white precipitate was obtained in a yield of 65% (670 mg). R_f in DCM/methanol (9:1) = 0.33. HPLC-UV (254 nm) ^{1}H NMR (500 MHz, DMSO-d_6) δ 8.39 (d, J = 8.4 Hz, 2H, CH$_{phenyl}$), 7.92 (d, J = 8.4 Hz, 2H, CH$_{phenyl}$), 7.22 (d, J = 9.2 Hz, 2H, CH$_{phenyl}$), 6.87 (d, J = 9.2 Hz, 2H, CH$_{phenyl}$), 3.38 – 3.29 (m, 4H, CH$_{piperazine}$), 3.24 – 3.17 (m, 4H, CH$_{piperazine}$). ESI-MS, purity: 95.9%. LC-MS positive mode (m/z): 380.9 [M + H]$^+$.

4-[4-(4-Bromophenyl)piperazin-1-yl]sulfonylbenzoic acid (16b). This compound was synthesized according to the general procedure A using **14** (920 mg, 4.16 mmol) and **15b** (1.0 g, 4.16 mmol) dissolved in 30 mL DCM, DIPEA (1.3 mL) was added and the reaction mixture was stirred at rt for 48 h. A white precipitate was obtained in a yield of 61% (1.07 g). R_f in DCM/methanol (9:1) = 0.14. ^{1}H NMR (500 MHz, DMSO-d_6) δ 8.37 (d, J = 8.6 Hz, 2H, CH$_{phenyl}$), 7.89 (d, J = 8.6 Hz, 2H, CH$_{phenyl}$), 7.19 (d, J = 9.0 Hz, 2H, CH$_{phenyl}$), 6.94 (d, J = 9.0 Hz, 2H, CH$_{phenyl}$), 3.36 – 3.30 (m, 4H, CH$_{piperazine}$), 3.25 – 3.17 (m, 4H, CH$_{piperazine}$). ^{13}C NMR (126 MHz, DMSO-d_6) δ 167, 149.3, 131.8, 130.7, 129.1, 126.7, 125.8, 118.1, 111.4, 45.4, 42.7. LC-MS positive mode (m/z): 425.0 [M + H]$^+$.

4-[4-(3-Chloro-4-methoxy-phenyl)piperazin-1-yl]sulfonyl-benzoic acid (13c). This compound was synthesized according to the general procedure A using **14** (391 mg, 1.77 mmol) and **15c** (400 mg, 1.77 mmol) dissolved in 20 mL DCM, DIPEA (0.4 mL) was added and the reaction mixture was stirred at rt for 72 h. A light brown precipitate was obtained in a yield of 75% (550 mg). ^{1}H NMR (500 MHz, DMSO-d_6) δ 8.19 – 8.15 (d, J = 8.3 Hz, 2H, CH$_{phenyl}$), 7.90 – 7.86 (d, J = 8.4 Hz, 2H, CH$_{phenyl}$), 7.00 (d, J = 9.0 Hz, 2H, CH$_{phenyl}$), 6.87 (d, J = 9.0 Hz, 1H, CH$_{phenyl}$), 3.74 (s, 3H, OCH$_3$), 3.20 – 3.10 (m, 4H, CH$_{piperazine}$), 3.08 – 3.02 (m, 4H, CH$_{piperazine}$). ^{13}C NMR (126 MHz, DMSO-d_6) δ 166.2, 148.9, 144.9, 138.6, 135.1, 130.41, 128, 121.6, 118.8, 116.7, 113.7, 56.4, 49, 45.8. LC-MS positive mode (m/z): 411.3 [M + H]$^+$.

6-Amino-3-propyl-1*H*-pyrimidine-2,4-dione (17).[63] To a flask containing 6-aminouracil (10.0 g, 79 mmol) dissolved in 27.5 mL of HMDS, a catalytic amount of ammonium sulfate (0.25 g) was added. The reaction mixture was refluxed with stirring at 190 °C for 1 h until a clear solution was formed. The reaction was cooled to 65 °C, 1-iodopropane (9.75 mL, 100 mmol) was added dropwise and then the reaction mixture was heated for at 120 °C for 2 h. The reaction was monitored using TLC with the eluent system DCM/methanol (9:1). Then, the reaction mixture was cooled to rt and on an ice bath, 50 mL of saturated $NaHCO_3$ solution was added dropwise with stirring until effervescence ceased. The desired product was obtained in a yield of 79% (10.6 g) as an off-white product. R_f in DCM/methanol (9:1) = 0.41. LC-MS (m/z): 170.0 $[M + H]^+$.

N'-(2,4-Dioxo-3-propyl-1*H*-pyrimidin-6-yl)-N,N-dimethyl-formamidine (18). This compound was synthesized according to general procedure B using **17** (2.62 g, 15.5 mmol) dissolved in 15 mL DMF and DMF-DMA (4.11 mL, 31 mmol) was added and the reaction mixture was stirred at 40 °C for 2 h. An off-white precipitate was obtained in a yield of 44% (1.53 g). R_f in DCM/methanol (9:1) = 0.63. ^{1}H NMR (500 MHz, DMSO-d_6) δ 10.60 (s, 1H, NH$_{uracil}$), 8.08 (s, 1H, N=CH), 5.02 (s, 1H, CH$_{uracil}$), 3.64 (m, 2H, CH$_{2(propyl)}$), 3.07 (s, 3H, NCH$_3$), 2.94 (s, 3H, NCH$_3$), 1.48 (m, 2H, CH$_{2(propyl)}$), 0.81 (t, J = 7.5 Hz, 3H, CH$_{3(propyl)}$).^{13}C NMR (126 MHz, CDCl$_3$) δ 163.8 (C4$_{uracil}$), 158.7 (C6$_{uracil}$), 156.8 (C2$_{uracil}$), 151.7 (N=CH), 81.5 (C5$_{uracil}$), 40.6 (NCH$_3$), 40.3 (NCH$_3$), 34.4 (NCH$_2$), 20.9 (CH$_{2(propyl)}$), 11.3 (CH$_{3(propyl)}$). LC-MS positive mode (m/z): 225.2 $[M + H]^+$.

3-[6-[(E)-Dimethylaminomethyleneamino]-2,4-dioxo-3-propyl-pyrimidin-1-yl]propyl acetate (19). To a flask containing **18** (1.0 g, 4.5 mmol) dissolved in 8 mL DMF, K$_2$CO$_3$ (0.93 g, 6.7 mmol) was added followed by dropwise addition of 3-iodopropyl acetate (1.22 g 5.4 mmol). The reaction mixture was stirred at rt for 24 h. Excess solvents were removed by

vaporization followed by the addition of 10 mL water and a white precipitate was formed. The desired product was obtained in a yield of 36% (0.53 g) as white product. R_f in DCM/methanol (9.5:0.5) = 0.33. ^{1}H NMR (500 MHz, DMSO-d_6) δ 8.06 (s, 1H, N=CH), 5.12 (s, 1H, CH$_{uracil}$), 4.03 – 3.98 (m, 4H, 2 CH$_2$), 3.72 – 3.67 (m, 2H, CH$_{2(propyl)}$), 3.10 (s, 3H, NCH$_3$), 2.99 (s, 3H, NCH$_3$), 1.94 (s, 3H, COCH$_3$), 1.89 – 1.83 (m, 2H, CH$_2$), 1.53 – 1.46 (m, 2H, CH$_{2(propyl)}$), 0.82 (t, J = 7.5 Hz, 3H, CH$_{3(propyl)}$). ^{13}C NMR (126 MHz, DMSO-d_6) δ 170.2, 161.9 (C4$_{uracil}$), 158.5 (C6$_{uracil}$), 156.1 (C2$_{uracil}$), 151.7 (N=CH), 82 (C5$_{uracil}$), 62 (OCH$_2$), 41.5 (N1-CH$_2$), 40.4 (NCH$_3$), 40.2 (NCH$_3$), 34.5 (CH$_2$), 27.7 (CH$_2$), 20.9 (CH$_{2(propyl)}$), 20.7 (CH$_{3(acetyl)}$), 11.5 (CH$_{3(propyl)}$). LC-MS positive mode (m/z): 324.1 [M + H]$^+$.

6-Amino-1-(3-hydroxypropyl)-3-propyl-pyrimidine-2,4-dione (20). This compound was synthesized according to general procedure D using **19** (0.26 g, 0.8 mmol) dissolved in 15 mL methylamine solution (33% in ethanol) and the reaction mixture was stirred at 40 °C for 4 h. A white precipitate was obtained in a yield of 77% (170 mg). R_f in DCM/methanol (9:1) = 0.31. ^{1}H NMR (500 MHz, DMSO-d_6) δ 6.71 (s, 2H, NH$_{2(uracil)}$), 4.65 (t, J = 10.8 Hz, 2H, CH$_2$), 3.81 (t, J = 7.1 Hz, 2H, CH$_2$), 3.65 (t, J = 7.1 Hz, 2H, CH$_{2(propyl)}$), 3.41 (d, J = 4.0 Hz, 1H, OH), 1.71 – 1.64 (m, 2H, CH$_2$), 1.50 – 1.42 (m, 2H, CH$_{2(propyl)}$), 0.79 (t, J = 7.4 Hz, 3H, CH$_{3(propyl)}$). ^{13}C NMR (151 MHz, DMSO-d_6) δ 161.3 (C4$_{uracil}$), 154.6 (C6$_{uracil}$), 151.5 (C2$_{uracil}$), 75.5 (C5$_{uracil}$), 58.3 (HOCH$_2$), 58.1 (N1-CH$_2$), 41.3 (N3-CH$_2$), 30.9 (CH$_2$), 20.9 (CH$_{2(propyl)}$), 11.2 (CH$_{3(propyl)}$). LC-MS positive mode (m/z): 227.1 [M + H]$^+$.

6-Amino-1-(3-hydroxypropyl)-5-nitroso-3-propyl-pyrimidine-2,4-dione (21). To a flask containing **20** (0.16 g, 0.6 mmol, 1 eq.) dissolved in acidic solution (2 mL glacial acetic acid and 2 mL water), NaNO$_2$ (0.13 g, 1.8 mmol, 3 eq.) was added and the mixture was stirred at 60 °C for 2 min. Evaporation of the excess acetic acid yielded the desired product **21** in a yield of 63% (94 mg) as a violet solid. R_f in DCM/methanol (9:1) = 0.57. ^{1}H NMR (500 MHz,

DMSO-d_6) δ 13.15 (s, 1H, OH), 3.86 (m, 4H, 2 CH$_2$), 3.45 (t, J = 6.2 Hz, 2H, CH$_{2(propyl)}$), 1.69 (m, 2H, CH$_2$), 1.64 – 1.55 (m, 2H, CH$_{2(propyl)}$), 0.89 (t, J = 7.5 Hz, 3H, CH$_{3(propyl)}$). ^{13}C NMR (126 MHz, DMSO-d_6) δ 160.1 (C4$_{uracil}$), 149.2 (C6$_{uracil}$), 145.8 (C2$_{uracil}$), 139.2, 94.7 (C5$_{uracil}$), 58.2 (N1-CH$_2$), 42.5 (N3-CH$_2$), 29.5 (CH$_2$), 20.8 (CH$_{2(propyl)}$), 11.3 (CH$_{3(propyl)}$). LC-MS positive mode (m/z): 257.2 [M + H]$^+$.

5,6-Diamino-1-(3-hydroxypropyl)-3-propyl-pyrimidine-2,4-dione (22). To a flask containing **21** (200 mg, 0.79 mmol, aqueous ammonia solution (12.5%, 12 mL) was added. The reaction was refluxed at 65 °C for 3 min until the solid was completely dissolved and then Na$_2$S$_2$O$_4$ (275 mg, 1.58 mmol) was added portionwise until the red color disappeared forming a light-yellow solution. The excess solvents were evaporated, and the residue formed was washed with 3 mL of water yielding compound **22**. The desired product was obtained in a yield of 45% (86 mg) as a white product. R_f in DCM/methanol (9:1) = 0.24. ^{1}H NMR (500 MHz, DMSO-d_6) δ 6.09 (s, 2H, NH$_2$), 4.65 (t, J = 5.1 Hz, 1H, OH), 3.87 (t, J = 7.1 Hz, 2H, N1-CH$_2$), 3.75 – 3.69 (m, 2H, CH$_2$), 3.45 – 3.39 (m, 2H, N3-CH$_2$), 2.90 (s, 2H, NH$_2$), 1.74 – 1.66 (m, 2H, CH$_2$), 1.54 – 1.44 (m, 2H, CH$_{2(propyl)}$), 0.81 (t, J = 7.4 Hz, 3H, CH$_{3(propyl)}$). ^{13}C NMR (126 MHz, DMSO-d_6) δ 159.0 (C4$_{uracil}$), 149.6 (C6$_{uracil}$), 144.5 (C2$_{uracil}$), 96.3 (C5$_{uracil}$), 58.0 (N1-CH$_2$), 42.0 (N3-CH$_2$), 31.0 (CH$_2$), 20.9 (CH$_{2(propyl)}$), 11.3 (CH$_{3(propyl)}$). LC-MS positive mode (m/z): 243.3 [M + H]$^+$.

***N*-[6-Amino-1-(3-hydroxypropyl)-2,4-dioxo-3-propyl-pyrimidin-5-yl]-4-[4-(4-chloro phenyl)piperazin-1-yl]sulfonylbenzamide (23).** This compound was synthesized according to general procedure E using **22** (95 mg, 0.39 mmol) and **16a** (150 mg, 0.39 mmol) dissolved in 10 mL DMF, EDC (113 mg, 0.59 mmol) was added and the reaction mixture was stirred at rt for 3 h. A pale-yellow precipitate was obtained in a yield of 36% (75 mg). R_f in DCM/methanol (9:1) = 0.78. ^{1}H NMR (600 MHz, DMSO-d_6) δ 9.18 (s, 1H, NH), 8.20 (d, J =

8.1 Hz, 2H, CH$_{phenyl}$), 7.87 (d, $J = 8.1$ Hz, 2H, CH$_{phenyl}$), 7.20 (d, $J = 9.1$ Hz, 2H, CH$_{phenyl}$), 6.90 (d, $J = 9.1$ Hz, 2H, CH$_{phenyl}$), 6.74 (s, 2H, NH$_2$), 4.70 (s, 1H, NH), 3.93 (t, $J = 7.2$ Hz, 2H, N1 – CH$_2$), 3.71 (t, $J = 6.2$, 8.5 Hz, 2H, CH$_2$), 3.45 (t, $J = 6.4$ Hz, 2H, N3-CH$_2$), 3.21 (m, 4H, CH$_{piperazine}$), 3.03 (m, 4H, CH$_{piperazine}$), 1.77 – 1.70 (m, 2H, CH$_2$), 1.54 – 1.47 (m, 2H, CH$_{2(propyl)}$), 0.82 (t, $J = 7.5$ Hz, 3H, CH$_{3(propyl)}$). ^{13}C NMR (151 MHz, DMSO-d_6) δ 165.5, 159.2 (C4$_{uracil}$), 159.2, 152.1, 150.5, 149.2 (C6$_{uracil}$), 144.5 (C2$_{uracil}$), 139.0, 136.9, 129.2, 128.9, 127.5, 123.4, 117.8, 87.3 (C5$_{uracil}$), 58.1 (N1-CH$_2$), 56.0, 47.9, 45.8, 42.0 (N3-CH$_2$), 32.2, 31.0 (CH$_2$), 29.8, 21.0 (CH$_{2(propyl)}$), 11.3 (CH$_{3(propyl)}$). LC-MS positive mode (m/z): 605.2 [M + H]$^+$.

8-[4-[4-(4-Chlorophenyl)piperazin-1-yl]sulfonylphenyl]-3-(3-hydroxypropyl)-1-propyl-7*H*-purine-2,6-dione (24). This compound was synthesized according to the general procedure F through refluxing **23** (75 mg, 0.12 mmol) in 10 mL HMDS, followed by stirring in HCl (4 M in dioxane, 5 mL). A white precipitate was obtained in a yield of 88% (64 mg). M.p.: 335-339 °C. R_f in DCM/methanol (9:1) = 0.84. ^{1}H NMR (600 MHz, DMSO-d_6) δ 14.19 (s, 1H, OH), 8.37 (d, $J = 8.2$ Hz, 2H, CH$_{phenyl}$), 7.90 (d, $J = 8.2$ Hz, 2H, CH$_{phenyl}$), 7.20 (d, $J = 9.3$ Hz, 2H, CH$_{phenyl}$), 6.90 (d, $J = 9.0$ Hz, 2H, CH$_{phenyl}$), 4.50 (s, 1H, NH), 4.11 (t, $J = 7.0$ Hz, 2H, N1 – CH$_2$), 3.86 (t, $J = 7.5$ Hz, 2H, CH$_2$), 3.48 (t, $J = 6.4$ Hz, 2H, N3-CH$_2$), 3.24 – 3.15 (m, 4H, CH$_{piperazine}$), 3.10 – 3.03 (m, 4H, CH$_{piperazine}$), 1.93 – 1.80 (m, 2H, CH$_2$), 1.65 – 1.50 (m, 2H, CH$_{2(propyl)}$), 0.87 (t, $J = 7.4$ Hz, 3H, CH$_{3(propyl)}$). ^{13}C NMR (151 MHz, DMSO-d_6) δ 154.3 (C4$_{xanthine}$), 150.7, 149.3 (C6$_{xanthine}$), 148.3, 148.0 (C2$_{xanthine}$), 135.8, 133.1, 128.8, 128.5, 127.3, 123.4, 117.8, 108.9 (HOCH$_2$), 58.7 (N1-CH$_2$), 47.9, 45.8, 42.4 (N3-CH$_2$), 41.0, 31.1 (CH$_2$), 21.0 (CH$_{2(propyl)}$), 11.3 (CH$_{3(propyl)}$). HPLC-UV (254 nm) ESI-MS, purity: 96.7%. LC-MS (m/z): 587.3 [M + H]$^+$. HRMS (ESI-TOF) m/z: [M - H]$^-$ calcd. for C$_{27}$H$_{31}$ClN$_6$O$_5$S 586.0920, found 586.0887.

5,6-Diamino-3-propyl-1*H*-pyrimidine-2,4-dione (25).[63] To a flask containing 6-amino-5-nitroso-3-propylpyrimidine-2,4(1*H*,3*H*)-dione (1.0 g, 5.00 mmol), aqueous ammonia solution (12.5%, 14 mL) was added. The reaction was refluxed at 65 °C for 3 min until the solid is completely soluble and then we add $Na_2S_2O_4$ (1.74 g, 10.00 mmol) portionwise till the yellow color disappears forming a colorless solution. The excess solvents were vaporized and the residue formed was washed with 3 mL water yielding the desired product **25**. The desired product was obtained in a yield of 24% (223 mg) and as the product is chemically unstable, it was used directly without further purification. LC-MS positive mode (m/z): 185.2 $[M + H]^+$.

***N*-(6-Amino-2,4-dioxo-3-propyl-1*H*-pyrimidin-5-yl)-4-[4-(4-chlorophenyl)piperazin-1-yl]sulfonylbenzamide (26a).** This compound was synthesized according to general procedure E using **25** (200 mg, 1.10 mmol) and **16a** (419 mg, 1.10 mmol) dissolved in 10 mL DMF, EDC (317 mg, 1.65 mmol) was added and the reaction mixture was stirred at rt for 4 h. A yellow precipitate was obtained in a yield of 48% (300 mg). ^{1}H NMR (600 MHz, DMSO-*d₆*) δ 10.48 (s, 1H, NH), 9.12 (s, 1H, NH), 8.18 (d, *J* = 8.1 Hz, 2H, CH$_{phenyl}$), 7.86 (d, *J* = 8.1 Hz, 2H, CH$_{phenyl}$), 7.20 (d, *J* = 9.1 Hz, 2H, CH$_{phenyl}$), 6.90 (d, *J* = 9.1 Hz, 2H, CH$_{phenyl}$), 6.15 (s, 2H, NH$_2$), 3.61 (t, *J* = 6.4 Hz, 2H, N3-CH$_2$), 3.24 – 3.18 (m, 4H, CH$_{piperazine}$), 3.06 – 3.00 (m, 4H, CH$_{piperazine}$), 1.54 – 1.45 (m, 2H, CH$_{2(propyl)}$), 0.82 (t, *J* = 7.5 Hz, 3H, CH$_{3(propyl)}$). ^{13}C NMR (126 MHz, DMSO-*d₆*) δ 165.3, 160.7 (C4$_{uracil}$), 150.6 (C6$_{uracil}$), 150.1 (C2$_{uracil}$), 149.2, 139.0, 137.0, 129.1, 128.8, 127.5, 123.3, 117.8, 86.7 (C5$_{uracil}$), 47.9 (CH$_{piperazine}$), 45.8 (CH$_{piperazine}$), 41.1 (N3-CH$_2$), 21.1 (CH$_{2(propyl)}$), 11.3 (CH$_{3(propyl)}$). LC-MS positive mode (m/z): 547.3 $[M + H]^+$.

***N*-(6-Amino-2,4-dioxo-3-propyl-1*H*-pyrimidin-5-yl)-4-[4-(4-bromophenyl)piperazin-1-yl]sulfonylbenzamide (26b).** This compound was synthesized according to general procedure E using **25** (434 mg, 2.36 mmol) and **16b** (1.0 g, 2.36 mmol) dissolved in 15 mL DMF, EDC (680 mg, 3.54 mmol) was added and the reaction mixture was stirred at rt for 5 h. A yellow

precipitate was obtained in a yield of 45% (630 mg). R_f in DCM/methanol (9:1) = 0.43. ^{1}H NMR (600 MHz, DMSO-d_6) δ 10.53 (s, 1H, NH), 9.12 (s, 1H, NH), 8.18 (d, J = 8.2 Hz, 2H, CH$_{phenyl}$), 7.86 (d, J = 8.4 Hz, 2H, CH$_{phenyl}$), 7.32 (d, J = 9.1 Hz, 2H, CH$_{phenyl}$), 6.85 (d, J = 9.0 Hz, 2H, CH$_{phenyl}$), 6.18 (s, 2H, NH$_2$), 3.61 (t, J = 7.4 Hz, 2H, N3-CH$_2$), 3.25 – 3.16 (m, 4H, CH$_{piperazine}$), 3.08 – 2.99 (m, 4H, CH$_{piperazine}$), 1.55 – 1.43 (m, 2H, CH$_{2(propyl)}$), 0.83 (t, J = 7.4 Hz, 3H, CH$_{3(propyl)}$). ^{13}C NMR (126 MHz, DMSO-d_6) δ 165.3, 160.7 (C4$_{uracil}$), 150.8 (C6$_{uracil}$), 150.2 (C2$_{uracil}$), 149.5, 139, 137, 131.7, 129.1, 127.5, 118.17, 111, 86.7 (C5$_{uracil}$), 47.7 (CH$_{piperazine}$), 45.7 (CH$_{piperazine}$), 41 (N3-CH$_2$), 21.1 (CH$_{2(propyl)}$), 11.3 (CH$_{3(propyl)}$). LC-MS positive mode (m/z): 593.1 [M + H]$^+$.

N-(6-Amino-2,4-dioxo-3-propyl-1*H*-pyrimidin-5-yl)-4-[4-(3-chloro-4-methoxy-phenyl) piperazin-1-yl]sulfonylbenzamide (26c). This compound was synthesized according to general procedure E using **25** (450 mg, 0.95 mmol) and **16c** (500 mg, 0.95 mmol) dissolved in 15 mL DMF, EDC (350 mg, 1.43 mmol) was added and the reaction mixture was stirred at rt for 8 h. A yellow precipitate was obtained in a yield of 60% (430 mg). ^{1}H NMR (500 MHz, DMSO-d_6) δ 10.51 (s, 1H, NH), 9.14 (s, 1H, NH), 8.19 (d, J = 8.2 Hz, 2H, CH$_{phenyl}$), 7.89 – 7.84 (d, J = 8.2 Hz, 2H, CH$_{phenyl}$), 7.21 – 6.94 (d, J = 8.8 Hz, 2H, CH$_{phenyl}$), 6.62 (d, 1H, CH$_{phenyl}$), 6.19 (s, 2H, NH$_2$), 3.74 (s, 3H, OCH$_3$), 3.70 – 3.62 (t, J = 7.4 Hz, 2H, N3-CH$_2$), 3.22 – 3.09 (m, 4H, CH$_{piperazine}$), 2.98 – 3.07 (m, 4H, CH$_{piperazine}$), 1.43 – 1.62 (m, 2H, CH$_{2(propyl)}$), 0.83 (t, J = 7.4 Hz, 3H, CH$_{3(propyl)}$). ^{13}C NMR (126 MHz, DMSO-d_6) δ 165.3, 162.4, 160.7 (C4$_{uracil}$), 150.7 (C6$_{uracil}$), 150 (C2$_{uracil}$), 148.7, 145.2, 139, 137, 129, 128, 127.5, 121.7, 121.6, 118.62, 116.5, 113.7, 86.7 (C5$_{uracil}$), 56.4, 48.9 (CH$_{piperazine}$), 46 (CH$_{piperazine}$), 41 (N3-CH$_2$), 35.9, 21.1 (CH$_{2(propyl)}$), 11.3 (CH$_{3\,(propyl)}$). LC-MS positive mode (m/z): 577.0 [M + H]$^+$.

(E)-4-((4-(4-chlorophenyl)piperazin-1-yl)sulfonyl)-*N*-(6(((dimethylamino)methylene)amino) 2,4-dioxo-3-propyl-1,2,3,4-tetrahydropyrimidin-5-yl)benzamide (27a). This compound was

synthesized according to the general procedure B using **26a** (300 mg, 0.55 mmol) dissolved in 5 mL DMF, DMF-DMA (130 mg, 1.10 mmol) was added and the reaction mixture was stirred at 40 °C for 3 h. A pale-yellow precipitate was obtained in a yield of 61% (200 mg). R_f in DCM/methanol (9.5:0.5) = 0.26. ^{1}H NMR (500 MHz, DMSO-d_6) δ 10.76 (s, 1H, NH), 9.26 (s, 1H, NH), 8.06 (d, J = 12.9 Hz, 2H, CH$_{phenyl}$), 7.96 (s, 1H, N=CH), 7.87 (d, J = 8.3 Hz, 2H, CH$_{phenyl}$), 7.20 (d, J = 9.1 Hz, 2H, CH$_{phenyl}$), 6.90 (d, J = 9.1 Hz, 2H, CH$_{phenyl}$), 3.70 (t, J = 6.4 Hz, 2H, N3-CH$_2$), 3.23 – 3.16 (m, 4H, CH$_{piperazine}$), 3.09 – 3.00 (m, 4H, CH$_{piperazine}$), 2.94 (s, 3H, N-CH$_3$), 2.83 (s, 3H, N-CH$_3$), 1.57 – 1.47 (m, 2H, CH$_{2(propyl)}$), 0.84 (t, J = 7.4 Hz, 3H, CH$_{3(propyl)}$). ^{13}C NMR (126 MHz, DMSO-d_6) δ 165.9, 161.8 (C4$_{uracil}$), 156.5 (C6$_{uracil}$), 154.7 (N=CH), 150.7 (C2$_{uracil}$), 149.3, 139.0, 137.3, 128.8, 128.6, 127.9, 123.4, 117.8, 96.0 (C5$_{uracil}$), 47.9 (CH$_{piperazine}$), 45.8 (CH$_{piperazine}$), 41.4 (CH$_{2(propyl)}$), 33.9 (N-CH$_3$), 20.9 (CH$_{2(propyl)}$), 11.3 (CH$_{3(propyl)}$). LC-MS positive mode (m/z): 602.3 [M + H]$^+$.

4-[4-(4-Bromophenyl)piperazin-1-yl]sulfonyl-*N*-[6-[(E)-dimethylamino-methyleneamino]-2,4-dioxo-3-propyl-1*H*-pyrimidin-5-yl]benzamide (27b). This compound was synthesized according to the general procedure B using **26b** (100 mg, 0.17 mmol) dissolved in 3 mL DMF and DMF-DMA (41 mg, 0.34 mmol) was added and the reaction mixture was stirred at 40 °C for 4 h. A white precipitate was obtained in a yield of 87% (95 mg). R_f in DCM/methanol (9:1) = 0.49. ^{1}H NMR (500 MHz, DMSO-d_6) δ 10.81 (s, 1H, NH), 9.27 (s, 1H, NH), 8.07 (d, J = 12.9 Hz, 2H, CH$_{phenyl}$), 7.95 (s, 1H, N=CH), 7.87 (d, J = 8.1 Hz, 2H, CH$_{phenyl}$), 7.33 (d, J = 9.1 Hz, 2H, CH$_{phenyl}$), 6.85 (d, J = 9.1 Hz, 2H, CH$_{phenyl}$), 3.72 (t, J = 7.4 Hz, 2H, N3-CH$_2$), 3.23 – 3.16 (m, 4H, CH$_{piperazine}$), 3.09 – 3.00 (m, 4H, CH$_{piperazine}$), 2.94 (s, 3H, NCH$_3$), 2.83 (s, 3H, NCH$_3$), 1.45 – 1.60 (m, 2H, CH$_{2(propyl)}$), 0.84 (t, J = 4.1 Hz, 3H, CH$_{3(propyl)}$). ^{13}C NMR (126 MHz, DMSO-d_6) δ 165.9, 161.7 (C4$_{uracil}$), 156.5 (C6$_{uracil}$), 154.6 (N=CH), 150.5 (C2$_{uracil}$), 149.6, 139.0, 137.3, 131.68, 128.6, 127.8, 118.2, 111, 96 (C5$_{uracil}$), 47.8 (CH$_{piperazine}$), 45.7

(CH$_{piperazine}$), 41.4 (CH$_{2(propyl)}$), 33.9 (*N*-CH$_3$), 20.9 (CH$_{2(propyl)}$), 11.3 (CH$_{3(propyl)}$). LC-MS positive mode (m/z): 646.2 [M + H]$^+$.

[5-(4-{[4-(3-Chloro-4-methoxyphenyl)piperazin-1-yl]sulfonyl}fcytof-*N*-{6-[(E)-[(dimethyl-amino)methylidene]amino]-2,4-dioxo-3-propyl-1,2,3,4-tetrahydropyrimidin-5-yl}benzamide (27c). This compound was synthesized according to the general procedure B using **26c** (760 mg, 1.30 mmol) dissolved in 10 mL anhydrous DMF and DMF-DMA (0.35 mL, 2.6 mmol) was added and the reaction mixture was stirred at 40 ºC for 2 h. A white precipitate was obtained in a yield of 90% (831 mg). LC-MS positive mode (m/z): 632.4 [M + H]$^+$.

2-[5-(4-{[4-(4-chlorophenyl)piperazin-1-yl]sulfonyl}benzamido)-6-[(E)-[(dimethylamino)-methylidene]-amino]-2,4-dioxo-3-propyl-1,2,3,4-tetrahydropyrimidin-1-yl]ethylacetate (28a). This compound was synthesized according to the general procedure C using **27a** (200 mg, 0.33 mmol) dissolved in 10 mL of anhydrous DMF, K$_2$CO$_3$ (150 mg, 0.66 mmol) and 3-iodoethylacetate (106 mg, 0.50 mmol) were added and the reaction mixture was stirred at 90 ºC for 2 h. A pale yellowish precipitate was obtained in a yield of 50% (120 mg). R_f in DCM/methanol (9.5:0.5) = 0.49. ^{1}H NMR (500 MHz, DMSO-*d$_6$*) δ 9.37 (s, 1H, NH), 8.04 (d, *J* = 12.9 Hz, 2H, CH$_{phenyl}$), 7.90 (s, 1H, N=CH), 7.84 (d, *J* = 8.3 Hz, 2H, CH$_{phenyl}$), 7.23 – 7.18 (d, *J* = 9.1 Hz, 2H, CH$_{phenyl}$), 6.93 – 6.87 (d, *J* = 9.1 Hz, 2H, CH$_{phenyl}$), 4.21 (t, *J* = 4.6 Hz, 2H, CH$_2$), 4.19 (t, *J* = 4.4 Hz, 2H, CH$_2$), 3.76 (t, *J* = 6.4 Hz, 2H, N3-CH$_2$), 3.18 – 3.23 (m, 4H, CH$_{piperazine}$), 3.00 – 3.09 (m, 4H, CH$_{piperazine}$), 2.89 (s, 3H, N-CH$_3$), 2.84 (s, 3H, N-CH$_3$), 1.94 (s, 3H, CH$_3$), 1.58 – 1.49 (m, 2H, CH$_{2(propyl)}$), 0.84 (t, *J* = 7.4 Hz, 3H, CH$_{3(propyl)}$). ^{13}C NMR (126 MHz, DMSO-*d$_6$*) δ 170.3, 166.8, 160.6 (C4$_{uracil}$), 156.8 (C6$_{uracil}$), 156.3 (N=CH), 150.8 (C2$_{uracil}$), 149.3 (C5$_{uracil}$), 138.7, 137.6, 128.8, 128.6, 128.0, 123.4, 117.8, 95.7, 61.4 (OCH$_2$), 47.9 (CH$_{piperazine}$), 45.8 (CH$_{piperazine}$), 42.3 (N1-CH$_2$), 42.0 (CH$_{2(propyl)}$), 33.9 (*N*-CH$_3$), 20.8 (CH$_{2(propyl)}$), 20.7 (CH$_3$), 11.3 (CH$_{3(propyl)}$). LC-MS positive mode (m/z): 688.3 [M + H]$^+$.

2-[5-(4-{[4-(4-Bromophenyl)piperazin-1-yl]sulfonyl}benzamido)-6-[(E)-[(dimethylamino)methylidene]amino]-2,4-dioxo-3-propyl-1,2,3,4-tetrahydropyrimidin-1-yl]ethylacetate (28b). This compound was synthesized according to the general procedure C using **27b** (90 mg, 0.14 mmol) dissolved in 10 mL of DMF, K_2CO_3 (40 mg, 0.28 mmol) and 3-iodoethylacetate (60 mg, 0.28 mmol) and the reaction mixture was stirred for at 90 ºC for 2 h. A yellowish precipitate was obtained in a yield of 45% (45 mg). R_f in DCM/methanol (9.5:0.5) = 0.15. ^{1}H NMR (500 MHz, DMSO-d_6) δ 9.37 (s, 1H, NH), 8.04 (d, J = 8.4 Hz, 2H, CH$_{phenyl}$), 7.89 (d, J = 8.4 Hz, 2H, CH$_{phenyl}$), 7.84 (s, 1H, N=CH), 7.33 – 7.28 (d, J = 9.0 Hz, 2H, CH$_{phenyl}$), 6.87 – 6.83 (d, J = 9.0 Hz, 2H, CH$_{phenyl}$), 4.22 (t, J = 3.6 Hz, 2H, CH$_2$), 4.19 (t, J = 4.8 Hz, 2H, CH$_2$), 3.76 (t, J = 6.2 Hz, 2H, N3-CH$_2$), 3.23 – 3.18 (m, 4H, CH$_{piperazine}$), 3.12 – 3.00 (m, 4H, CH$_{piperazine}$), 2.89 (s, 3H, N-CH$_3$), 2.87 (s, 3H, NCH$_3$), 1.94 (s, 3H, CH$_3$), 1.58 – 1.49 (m, 2H, CH$_{2(propyl)}$), 0.84 (t, J = 7.5 Hz, 3H, CH$_{3(propyl)}$). ^{13}C NMR (126 MHz, DMSO-d_6) δ 170.3 , 166.8 , 160.6 (C4$_{uracil}$), 156.7 (C6$_{uracil}$), 156.3 (N=CH), 150.7 (C2$_{uracil}$), 149.6 (C5$_{uracil}$), 138.7, 137.6, 131.7, 128.5, 128.0, 118.2, 111, 95.7, 61.4 (OCH$_2$), 55.97, 47.8 (CH$_{piperazine}$), 45.7 (CH$_{piperazine}$), 42.3 (N1-CH$_2$), 42.0 (CH$_{2(propyl)}$), 33.9 (*N*-CH$_3$), 29.7, 20.8 (CH$_{2(propyl)}$), 20.7(CH$_3$), 11.3 (CH$_{3(propyl)}$). LC-MS positive mode (m/z): 732.2 [M + H]$^+$.

2-[5-[[4-[4-(4-Bromophenyl)piperazin-1-yl]sulfonyl-benzoyl]amino]-6-[(E)dimethylamino-methyleneamino]-2,4-dioxo-3-propyl-pyrimidin-1-yl]propylacetate (28c). This compound was synthesized according to the general procedure C using **27b** (100 mg, 0.16 mmol) dissolved in 10 mL DMF, K_2CO_3 (43 mg, 0.32 mmol) and 3-iodopropyl acetate (72 mg, 0.32 mmol) and the reaction mixture was stirred for at 90 ºC 3 h. A yellowish precipitate was obtained in a yield of 64% (74 mg). R_f in DCM/methanol (9.5:0.5) = 0.42. ^{1}H NMR (500 MHz, DMSO-d_6) δ 9.37 (s, 1H, NH), 8.04 (d, J = 8.4 Hz, 2H, CH$_{phenyl}$), 7.89 (d, J = 8.5 Hz, 2H, CH$_{phenyl}$), 7.82 (s, 1H, N=CH), 7.36 – 7.30 (d, J = 9.0 Hz, 2H, CH$_{phenyl}$), 6.87 – 6.83 (d, J = 9.0 Hz, 2H, CH$_{phenyl}$), 4.00 (t, J = 5.1, 7.0 Hz, 4H, 2 CH$_2$), 3.80 – 3.72 (t, J = 6.2 Hz, 2H, N3-CH$_2$),

3.23 – 3.18 (m, 4H, CH$_{piperazine}$), 3.00 – 3.12 (m, 4H, CH$_{piperazine}$), 2.84 – 2.92 (d, 6H, 2NCH$_3$), 1.97 (s, 3H, CH$_3$), 1.89 (t, J = 6.9 Hz, 2H, CH$_2$), 1.57 – 1.48 (m, 2H, CH$_{2(propyl)}$), 0.84 (t, J = 7.45 Hz, 3H, CH$_{3(propyl)}$). ^{13}C NMR (126 MHz, DMSO-d_6) δ 170.4, 166.9, 160.6 (C4$_{uracil}$), 156.7 (C6$_{uracil}$), 156.3, 150.7 (C2$_{uracil}$), 149.6 (C5$_{uracil}$), 138.7, 137.6, 131.7, 128.5, 127.9, 118.2, 111, 95.6, 62.1 (OCH$_2$), 47.7 (CH$_{piperazine}$), 45.7 (CH$_{piperazine}$), 42.3 (N1-CH$_2$), 40.7 (CH$_{2(propyl)}$), 33.9 (*N*-CH$_3$), 27.4, 20.8 (CH$_{2(propyl)}$), 20.7 (CH$_3$), 11.3 (CH$_{3(propyl)}$). LC-MS positive mode (m/z): 746.2 [M + H]$^+$.

[5-(4-{[4-(3-Chloro-4-methoxyphenyl)piperazin-1-yl]sulfonyl}benzamido)-6-[(E)-[(dimethyl-amino)methylidene]amino]-2,4-dioxo-3-propyl-1,2,3,4-tetrahydropyrimidin-1-yl]methylacetate (28d). This compound was synthesized according to the general procedure C using **27c** (908 mg, 1.44 mmol) dissolved in 15 mL anhydrous DMF, K$_2$CO$_3$ (400 mg, 2.88 mmol) and 3-iodoethylacetate (462 mg, 2.16 mmol) were added and the reaction mixture was stirred for at 90 °C 4 h. A white precipitate was obtained in a yield of 55% (550 mg). LC-MS positive mode (m/z): 704.3 [M + H]$^+$.

***N*-[6-Amino-1-(2-hydroxyethyl)-2,4-dioxo-3-propyl-pyrimidin-5-yl]-4-[4-(4-chlorophenyl) piperazin-1-yl]sulfonylbenzamide (29a).** This compound was synthesized according to the general procedure D using **28a** (106 mg, 0.15 mmol) dissolved in methylamine solution (33% in ethanol, 10 mL) and the reaction mixture was stirred at 40 °C for 8 h. A white precipitate was obtained in a yield of 79% (72 mg). R_f in DCM/methanol (9.5:0.5) = 0.25. ^{1}H NMR (500 MHz, DMSO-d_6) δ 9.17 (s, 1H, NH), 8.20 (d, J = 12.9 Hz, 2H, CH$_{phenyl}$), 7.87 (d, J = 8.4 Hz, 2H, CH$_{phenyl}$), 7.21 (d, J = 9.0 Hz, 2H, CH$_{phenyl}$), 6.90 (d, J = 9.1 Hz, 2H, CH$_{phenyl}$), 6.60 (s, 2H, NH$_2$), 3.98 (t, J = 5.5 Hz, 2H, CH$_2$), 3.72 (t, J = 6.5 Hz, 2H, CH$_2$), 3.62 (t, J = 5.4 Hz, 2H, N3-CH$_2$), 3.23 – 3.21 (m, 4H, CH$_{piperazine}$), 3.09 – 2.98 (m, 4H, CH$_{piperazine}$), 1.58 – 1.50 (m, 2H, CH$_{2(propyl)}$), 0.83 (t, J = 7.5 Hz, 3H, CH$_{3(propyl)}$). ^{13}C NMR (126 MHz, DMSO-d_6) δ 165.5, 159.2

(C4$_{\text{uracil}}$), 152.7 (C6$_{\text{uracil}}$), 150.7 (C2$_{\text{uracil}}$), 149.2 (C5$_{\text{uracil}}$), 139, 137, 129.1, 128.8, 127.5, 123.3, 117.8, 87.8, 59, 47.9 (CH$_{\text{piperazine}}$), 45.8 (CH$_{\text{piperazine}}$), 26.5 (CH$_{2(\text{propyl})}$), 21 (CH$_{2(\text{propyl})}$), 11.4 (CH$_{3(\text{propyl})}$). LC-MS positive mode (m/z): 591.2 [M + H]$^+$.

***N*-[6-amino-1-(2-hydroxyethyl)-2,4-dioxo-3-propyl-pyrimidin-5-yl]-4-[4-(4-bromophenyl) piperazin-1-yl]sulfonylbenzamide (29b).** This compound was synthesized according to the general procedure D using **28b** (78 mg, 0.11 mmol) dissolved in 10 mL methylamine solution (33% in ethanol) and the reaction mixture was stirred at 40 $^{\circ}$C for 8 h. A white precipitate was obtained in a yield of 74% (50 mg). R_f in DCM/methanol (9.5:0.5) = 0.22. ^{1}H NMR (500 MHz, DMSO-d_6) δ 9.17 (s, 1H, NH), 8.20 (d, J = 8.5 Hz, 2H, CH$_{\text{phenyl}}$), 7.87 (d, J = 8.4 Hz, 2H, CH$_{\text{phenyl}}$), 7.32 (d, J = 9.0 Hz, 2H, CH$_{\text{phenyl}}$), 6.85 (d, J = 9.0 Hz, 2H, CH$_{\text{phenyl}}$), 6.60 (s, 2H, NH$_2$), 3.99 (t, J = 5.6 Hz, 2H, CH$_2$), 3.72 (t, J = 6.5 Hz, 2H, CH$_2$), 3.62 (t, J = 5.5 Hz, 2H, N3-CH$_2$), 3.23 – 3.21 (m, 4H, CH$_{\text{piperazine}}$), 3.10 – 2.98 (m, 4H, CH$_{\text{piperazine}}$), 1.53 – 1.50 (m, 2H, CH$_{2(\text{propyl})}$), 0.83 (t, J = 7.5 Hz, 3H, CH$_{3(\text{propyl})}$). ^{13}C NMR (126 MHz, DMSO-d_6) δ 165.5, 159.2 (C4$_{\text{uracil}}$), 152.7 (C6$_{\text{uracil}}$), 150.7 (C2$_{\text{uracil}}$), 149.5 (C5$_{\text{uracil}}$), 139, 137, 131.7, 129.1, 127.5, 123.3, 118.2, 111, 87.8, 59, 47.8 (CH$_{\text{piperazine}}$), 45.7 (CH$_{\text{piperazine}}$), 42 (CH$_{2(\text{propyl})}$), 21 (CH$_{2(\text{propyl})}$), 11.4 (CH$_{3(\text{propyl})}$). LC-MS positive mode (m/z): 637.2 [M + H]$^+$.

***N*-[6-Amino-1-(2-hydroxypropyl)-2,4-dioxo-3-propyl-pyrimidin-5-yl]-4-[4-(4-bromophenyl)-piperazin-1-yl]sulfonylbenzamide (29c).** This compound was synthesized according to the general procedure D using **28c** (68 mg, 0.09 mmol) dissolved in methylamine solution (33% in ethanol, 10 mL) and the reaction mixture was stirred at 40 $^{\circ}$C for 4 h. A white precipitate was obtained in a yield of 93% (55 mg). R_f in DCM/methanol (9.5:0.5) = 0.19. ^{1}H NMR (500 MHz, DMSO-d_6) δ 9.16 (s, 1H, NH), 8.20 (d, J = 8.4 Hz, 2H, CH$_{\text{phenyl}}$), 7.86 (d, J = 8.4 Hz, 2H, CH$_{\text{phenyl}}$), 7.32 (d, J = 9.0 Hz, 2H, CH$_{\text{phenyl}}$), 6.85 (d, J = 9.1 Hz, 2H, CH$_{\text{phenyl}}$), 6.72 (s, 2H, NH$_2$), 4.69 (s, 1H), 3.93 (t, J = 7.2 Hz, 2H, CH$_2$), 3.76 – 3.67 (t, J = 6.5 Hz, 2H, CH$_2$), 3.48 –

3.41 (t, J = 5.5 Hz, 2H, N3-CH$_2$), 3.25 – 3.17 (m, 4H, CH$_{piperazine}$), 2.98 – 3.5 (m, 4H, CH$_{piperazine}$), 1.78 – 1.68 (t, J = 6.5 Hz, 2H, CH$_2$), 1.57 – 1.47 (m, 2H, CH$_{2(propyl)}$), 0.82 (t, J = 7.4 Hz, 3H, CH$_{3(propyl)}$). ^{13}C NMR (126 MHz, DMSO-d_6) δ 165.5, 159.1 (C4$_{uracil}$), 152 (C6$_{uracil}$), 150.5 (C2$_{uracil}$), 149.5 (C5$_{uracil}$), 139, 137, 131.7, 129.1, 127.8, 127.5, 118.2, 111, 87.3, 58.1, 47.8 (CH$_{piperazine}$), 45.7 (CH$_{piperazine}$), 42 (CH$_{2(propyl)}$), 31, 26.5, 21 (CH$_{2(propyl)}$), 11.4 (CH$_{3(propyl)}$). LC-MS positive mode (m/z): 649.2 [M + H]$^+$.

N-[6-Amino-1-(2-hydroxyethyl)-2,4-dioxo-3-propyl-1,2,3,4-tetrahydropyrimidin-5-yl]-4-{[4-(3-chloro-4-methoxyphe-nyl)piperazin-1-yl]sulfonyl}benzamide (29d). This compound was synthesized according to the general procedure D using **28d** (68 mg, 0.09 mmol) dissolved in methylamine solution (33% in ethanol, 10 mL) and the reaction mixture was stirred at 40 ºC for 6 h. A white precipitate was obtained in a yield of 66% (30 mg). LC-MS positive mode (m/z): 621.2 [M + H]$^+$.

8-[4-[4-(4-Chlorophenyl)piperazin-1-yl]sulf-onylphenyl]-3-(2-hydroxyethyl)-1-propyl-7H-purine-2,6-dione (30a). This compound was synthesized according to the general procedure F through refluxing **29a** (70 mg, 0.12 mmol) in 10 mL HMDS, followed by stirring in HCl (4 M in dioxane, 5 mL). A yellow precipitate for **30a** was obtained in a yield of 43% (29 mg). M.p.: 332-337 °C. R_f in DCM/methanol (9.5:0.5) = 0.26. ^{1}H NMR (600 MHz, DMSO-d_6) δ 14.17 (s, 1H, OH), 8.37 (d, J = 10.8 Hz, 2H, CH$_{phenyl}$), 7.90 (d, J = 8.5 Hz, 2H, CH$_{phenyl}$), 7.20 (d, J = 6.2 Hz, 2H, CH$_{phenyl}$), 6.91 (d, J = 9.0 Hz, 2H, CH$_{phenyl}$), 4.13 (m, 2H, N1-CH$_2$), 3.86 (m, 2H, CH$_{2(propyl)}$), 3.70 (t, J = 6.3 Hz, 2H, N3-CH$_2$), 3.23 – 3.16 (m, 4H, CH$_{piperazine}$), 3.08 – 3.02 (m, 4H, CH$_{piperazine}$), 1.93 – 1.80 (m, 2H, CH$_2$), 1.62 – 1.53 (m, 2H, CH$_{2(propyl)}$), 0.88 (t, J = 7.5 Hz, 3H, CH$_{3(propyl)}$). ^{13}C NMR (151 MHz, DMSO-d_6) δ 154.4 (C6$_{xanthine}$), 150.9 (C2$_{xanthine}$), 149.3 (C8$_{xanthine}$), 148.6 (C4$_{xanthine}$), 147.9, 135.9, 133.1, 128.8, 128.5, 127.3, 123.4, 117.8, 108.8 (C5$_{xanthine}$), 57.8 (N1-CH$_2$), 45.8 (CH$_{piperazine}$), 45.4 (CH$_{piperazine}$), 42.4 (CH$_{2(propyl)}$),

21.0 (CH$_{2(propyl)}$), 11.3 (CH$_{3(propyl)}$). HPLC-UV (254 nm) ESI-MS, purity: 96.2%. LC-MS (m/z): 573.1 [M + H]$^+$. HRMS (ESI-TOF) m/z: [M - H]$^-$ calcd. for C$_{25}$H$_{27}$N$_6$O$_4$S 571.1814, found 571.1833.

8-[4-[4-(4-Bromophenyl)piperazin-1-yl]sulfonylphenyl]-3-(2-hydroxyethyl)-1-propyl-7*H*-purine-2,6-dione (30b). This compound was synthesized according to the general procedure F through refluxing **29b** (44 mg, 0.07 mmol) in 5 mL HMDS, followed by stirring in HCl (4 M in dioxane, 2 mL). A white precipitate was obtained in a yield of 63% (27 mg). M.p.: 348-352 °C. *R$_f$* in DCM/methanol (9:1) = 0.55. ^{1}H NMR (500 MHz, DMSO-*d$_6$*) δ 14.4 (s (br), 1H, OH), 8.36 (d, *J* = 10.8 Hz, 2H, CH$_{phenyl}$), 7.89 (d, *J* = 8.5 Hz, 2H, CH$_{phenyl}$), 7.32 (d, *J* = 6.2 Hz, 2H, CH$_{phenyl}$), 6.85 (d, *J* = 9.0 Hz, 2H, CH$_{phenyl}$), 4.13 (m, 2H, N1-CH$_2$), 3.90 – 3.84 (m, 2H, CH$_2$), 3.71 (t, *J* = 6.3 Hz, 2H, N3-CH$_2$), 3.23 – 3.18 (m, 4H, CH$_{piperazine}$), 3.07 – 3.04 (m, 4H, CH$_{piperazine}$), 1.54 – 1.65 (m, 2H, CH$_{2(propyl)}$), 0.88 (t, *J* = 7.5 Hz, 3H, CH$_{3(propyl)}$). ^{13}C NMR (126 MHz, DMSO-*d$_6$*) δ 154.5 (C6$_{xanthine}$), 150.9 (C2$_{xanthine}$), 149.6 (C8$_{xanthine}$), 148.6 (C4$_{xanthine}$), 147.9, 135.7, 133.3, 131.7, 128.4, 127.2, 118.1, 111 (C5$_{xanthine}$), 57.8 (N1-CH$_2$), 47.8 (CH$_{piperazine}$), 45.4 (CH$_{piperazine}$), 42.4 (CH$_{2(propyl)}$), 29.12, 21(CH$_{2(propyl)}$), 11.3 (CH$_{3(propyl)}$). HPLC-UV (254 nm) ESI-MS, purity: 95.2%. LC-MS (m/z): 617.3 [M + H]$^+$. HRMS (ESI-TOF) m/z: [M + H]$^+$ calcd. for C$_{26}$H$_{29}$BrN$_6$O$_5$S 617.1104, found 617.0996.

8-[4-[4-(4-Bromophenyl)piperazin-1-yl]sulfonylphenyl]-3-(2-hydroxyprop-yl)-1-propyl-7*H*-purine-2,6-dione (30c). This compound was synthesized according to the general procedure F through refluxing **29c** (33 mg, 0.05 mmol) in 5 mL HMDS, followed by stirring in HCl (4 M in dioxane, 2 mL). A white precipitate was obtained in a yield of 60% (50 mg). M.p.: 352-357 °C. *R$_f$* in DCM/methanol (9.5:0.5) = 0.59. ^{1}H NMR (500 MHz, DMSO-*d$_6$*) δ 14.17 (s (br), 1H, OH), 8.37 (d, *J* = 8.9 Hz, 2H, CH$_{phenyl}$), 7.90 (d, *J* = 8.6 Hz, 2H, CH$_{phenyl}$), 7.32 (d, *J* = 9.0 Hz, 2H, CH$_{phenyl}$), 6.85 (d, *J* = 9.0 Hz, 2H, CH$_{phenyl}$), 4.12 (m, 2H, N1 – CH$_2$),

3.90 – 3.82 (m, 2H, CH$_2$), 3.48 (t, J = 6.3 Hz, 2H, N3-CH$_2$), 3.23 – 3.15 (m, 4H, CH$_{piperazine}$), 3.09 – 3.03 (m, 4H, CH$_{piperazine}$), 1.87 (m, 2H, CH$_2$), 1.66 – 1.58 (m, 2H, CH$_{2(propyl)}$), 0.87 (t, J = 7.5 Hz, 3H, CH$_{3(propyl)}$). ^{13}C NMR (126 MHz, DMSO-d_6) δ 154.4 (C6$_{xanthine}$), 150.8 (C2$_{xanthine}$), 149.6 (C8$_{xanthine}$), 148 (C4$_{xanthine}$), 135.8, 133.2, 131.7, 128.5, 127.3, 118.2, 111 (C5$_{xanthine}$), 58.7 (N1-CH$_2$), 47.8 (CH$_{piperazine}$), 45.8 (CH$_{piperazine}$), 42.4 (CH$_{2(propyl)}$), 41, 31.1, 21 (CH$_{2(propyl)}$), 11.3 (CH$_{3(propyl)}$). HPLC-UV (254 nm) ESI-MS, purity: 99.1%. LC-MS (m/z): 631.3 [M + H]$^+$. HRMS (ESI-TOF) m/z: [M + H]$^+$ calcd. for C$_{27}$H$_{31}$BrN$_6$O$_5$S 631.1260, found 631,1162.

8-(4-{[4-(3-Chloro-4-methoxyphenyl)piperazin-1-yl]sulfonyl}phenyl)-3-(2-hydroxyethyl)-1-propyl-2,3,6,7-tetrahydro-1*H*-purine-2,6-dione (30d). This compound was synthesized according to the general procedure F through refluxing **29d** (100 mg, 0.16 mmol) in 15 mL HMDS, followed by stirring in HCl (4 M in dioxane, 5 mL). A white precipitate was obtained in a yield of 40% (38 mg). M.p.: 355-360 °C. ^{1}H NMR (500 MHz, DMSO-d_6) δ 14 (s, 1H, NH$_{xanthine}$), 8.36 (d, J = 8.1 Hz, 2H, CH$_{phenyl}$), 7.89 (d, J = 6.8 Hz, 2H, CH$_{phenyl}$), 6.98 (d, J = 6.0 Hz, 2H, CH$_{phenyl}$), 6.84 (dd, J = 9.1 Hz, 1H, CH$_{phenyl}$), 4.17 – 4.11 (m, 2H, CH$_2$), 3.91 – 3.83 (m, 2H, CH$_2$), 3.86 – 3.79 (t, J = 8.9 Hz, 2H, N3-CH$_2$), 3.70 (s, 3H, OCH$_3$), 3.14 – 3.08 (m, 4H, CH$_{piperazine}$), 3.08 – 3.04 (m, 4H, CH$_{piperazine}$), 1.62 – 1.54 (m, 2H, CH$_{2(propyl)}$), 1.23 (s, 1H, OH), 0.88 (t, J = 7.4 Hz, 3H, CH$_{3(propyl)}$). ^{13}C NMR (126 MHz, DMSO-d_6) δ 172.1, 161.7 (C6$_{xanthine}$), 150.9 (C2$_{xanthine}$), 146.3 (C8$_{xanthine}$), 145.3 (C4$_{xanthine}$), 140.1, 133.3, 128.4, 127.1, 121.6, 118.6, 116.5, 113.7 (C5$_{xanthine}$), 56.4, 49 (CH$_{piperazine}$), 46 (CH$_{piperazine}$), 41.4 (N3-CH$_2$), 21.0 (CH$_{2(propyl)}$), 11.3 (CH$_{3(propyl)}$). LC-MS positive mode (m/z): 603.5 [M + H]$^+$. HPLC-UV (254 nm) ESI-MS, purity: 97.6%. LC-MS (m/z): 603.5 [M + H]$^+$. HRMS (ESI-TOF) m/z: [M + H]$^+$ calcd. for C$_{27}$H$_{31}$ClN$_6$O$_6$S 603.1714, found 603.1605.

1-(4-Bromo-2-methoxy-phenyl)piperazine (33a).[65] This compound was synthesized using 1-(2-methoxyphenyl)piperazine (2.62 g, 15.5 mmol) dissolved in 40 mL DCM and cooled to 0 ºC, bromine (0.9 mL, 17 mmol) was added dropwise and the reaction mixture was stirred for at rt for 4 h. Upon completion of the reaction, the reaction mixture was further treated with 20 mL sat. $NaHCO_3$ solution and portioned between water and DCM. The organic layers were dried using anhydrous Mg_2SO_4 and evaporated obtaining an oily residue that was further purified using column chromatography using the eluent system DCM/methanol (9:1). A brownish oil was obtained in a yield of 99% (4.2 g). LC-MS positive mode (m/z): 270.6 [M + H]$^+$.

1-(4-Bromo-3-methoxy-phenyl)piperazine (33b).[65] This compound was synthesized using 1-(3-methoxyphenyl)piperazine (1.0 g, 5.2 mmol) dissolved in 30 mL DCM and cooled to 0 ºC, bromine (0.9 mL, 17 mmol) was added dropwise and the reaction mixture was stirred for at rt for 1 h. Upon completion of the reaction, the reaction mixture was further treated with 20 mL $NaHCO_3$ and portioned between water and DCM. The organic layers were dried using anhydrous Mg_2SO_4 and evaporated obtaining an oily residue that was further purified using column chromatography using the eluent system DCM/methanol (9:1). A white solid was obtained in a yield of 32% (440 mg). LC-MS positive mode (m/z): 270.8 [M + H]$^+$.

8-(4-{[4-(4-Bromo-2-methoxyphenyl)-piperazin-1-yl]sulfonyl}phenyl)-1-propyl-2,3,6,7-tetra-hydro-1*H*-purine-2,6-dione (34a). This compound was synthesized according to the general procedure G using **32** (300 mg, 0.636 mmol) and **33a** (400 mg, 1.48 mmol) dissolved in 5 mL of anhydrous DMSO and the reaction mixture was stirred at 150 ºC for 15 h. A white precipitate was obtained in a yield of 40% (150 mg). M.p.: 344-346 °C. ^{1}H NMR (500 MHz, DMSO-*d₆*) δ 14.03 (s, 1H, NH$_{xanthine}$), 11.95 (s, 1H, NH$_{xanthine}$), 8.35 (d, J = 8.5 Hz, 2H, CH$_{phenyl}$), 7.88 (d, J = 8.5 Hz, 2H, CH$_{phenyl}$), 7.04 (d, J = 2.2 Hz, 1H, CH$_{phenyl}$), 7.02 (d, J = 2.2

Hz, 1H, CH$_{phenyl}$), 6.80 (dd, J = 8.5 Hz, 1H, CH$_{phenyl}$), 3.73 – 3.70 (m, 2H, N3-CH$_2$), 3.82 (s, 3H, OCH$_3$), 3.06 – 3.01 (m, 4H, CH$_{piperazine}$), 3.01 – 2.97 (m, 4H, CH$_{piperazine}$), 1.61 – 1.58 (m, 2H, CH$_{2(propyl)}$), 0.87 (t, J = 7.4 Hz, 3H, CH$_{3(propyl)}$). ^{13}C NMR (126 MHz, DMSO-d_6) δ 155.1 (C6$_{xanthine}$), 153, 151.1 (C2$_{xanthine}$), 148.2 (C8$_{xanthine}$), 147.8 (C4$_{xanthine}$), 139.8, 135.6, 133.3, 128.5, 127.1, 123.4, 120.2, 114.9, 108.8 (C5$_{xanthine}$), 68.7, 56, 55.9, 49.3 (CH$_{piperazine}$), 46.3 (CH$_{piperazine}$), 41.7 (N3-CH$_2$), 32.2, 30.8, 29.8, 21 (CH$_{2(propyl)}$), 11.4 (CH$_{3(propyl)}$). HPLC-UV (254 nm) ESI-MS, purity: 95%. LC-MS (m/z): 603.3 [M + H]$^+$. HRMS (ESI-TOF) m/z: [M + H]$^+$calcd. for C$_{25}$H$_{27}$BrN$_6$O$_5$S 603.0947, found 603.0659.

8-(4-{[4-(4-Bromo-3-methoxyphenyl)piperazin-1-yl]sulfonyl}phenyl)-1-propyl-2,3,6,7-tetra-hydro-1H-purine-2,6-dione (34b). This compound was synthesized according to the general procedure G using **32** (150 mg, 0.32 mmol) and **33b** (200 mg, 0.74 mmol) dissolved in 3 mL of anhydrous DMSO and the reaction mixture was stirred at 150 °C for 18 h. A white precipitate was obtained in a yield of 25% (30 mg). M.p.: 339-342 °C. ^{1}H NMR (500 MHz, DMSO-d_6) δ 11.93 (s, 1H, NH$_{xanthine}$), 8.33 (d, J = 8.3 Hz, 2H, CH$_{phenyl}$), 7.88 (d, J = 8.3 Hz, 2H, CH$_{phenyl}$), 7.28 (d, J = 8.7 Hz, 1H, CH$_{phenyl}$), 6.59 (d, J = 2.6 Hz, 1H, CH$_{phenyl}$), 6.39 (dd, J = 8.8 Hz, 1H, CH$_{phenyl}$), 3.84 – 3.79 (m, 2H, N3-CH$_2$), 3.76 (s, 3H, OCH$_3$), 3.26 – 3.20 (m, 4H, CH$_{piperazine}$), 3.01 – 2.97 (m, 4H, CH$_{piperazine}$), 1.61 – 1.53 (m, 2H, CH$_{2(propyl)}$), 0.87 (t, J = 7.4 Hz, 3H, CH$_{3(propyl)}$). ^{13}C NMR (126 MHz, DMSO-d_6) δ 156, 155.1 (C6$_{xanthine}$), 151.4, 151.1 (C2$_{xanthine}$), 135.7, 133.4, 132.8, 128.5, 127.2, 109.5 (C5$_{xanthine}$), 101.7, 100.4, 56.2, 48 (CH$_{piperazine}$), 45.9 (CH$_{piperazine}$), 41.7 (N3-CH$_2$), 21 (CH$_{2(propyl)}$), 11.3 (CH$_{3(propyl)}$). HPLC-UV (254 nm) ESI-MS, purity: 95.9%. LC-MS (m/z): 603.5 [M + H]$^+$. HRMS (ESI-TOF) m/z: [M - H]$^-$ calcd. for C$_{25}$H$_{27}$BrN$_6$O$_5$S 601.0947, found 601.0874.

8-(4-{[4-(4-Bromo-2-hydroxyphenyl)piperazin-1-yl]sulfonyl}phenyl)-1-propyl-2,3,6,7-tetrahydro-1*H*-purine-2,6-dione (35). To a flask containing (100 mg, 0.17 mmol) of **34a** dissolved in 5 mL of anhydrous DCM under an argon atmosphere and cooled to 0 °C, BBr$_3$ (1M in DCM, 2 mL) was added dropwise. The reaction was stirred under an argon atmosphere at rt for 24 h. When the reaction has finished, a mixture of ice and aqueous NaHCO$_3$ (20 mL) was added and then extracted with ethyl acetate (3 x 10 mL). The organic layers were dried with anhydrous Mg$_2$SO$_4$ and evaporated to give a precipitate that was further purified using column chromatography using the eluent system DCM/methanol (9.5:0.5). The desired product was obtained as a white solid in a yield of 26% (22 mg). M.p.: 336-338 °C. ^{1}H NMR (500 MHz, DMSO-*d$_6$*) δ 14.03 (s, 1H, NH$_{xanthine}$), 11.94 (s, 1H, NH$_{xanthine}$), 9.48 (s, 1H, OH), 8.35 (d, *J* = 8.5 Hz, 2H, CH$_{phenyl}$), 7.88 (d, *J* = 8.5 Hz, 2H, CH$_{phenyl}$), 6.95 – 6.87 (d, *J* = 2.3 Hz, 2H, CH$_{phenyl}$), 6.85 – 6.80 (dd, *J* = 8.4 Hz, 1H, CH$_{phenyl}$), 6.79 – 6.77 (dd, *J* = 8.5 Hz, 1H, CH$_{phenyl}$), 3.73 – 3.71 (m, 2H, N3-CH$_2$), 3.86 – 3.75 (s, 3H, OCH$_3$), 3.11 – 3.03 (m, 4H, CH$_{piperazine}$), 3.01 – 2.97 (m, 4H, CH$_{piperazine}$), 1.62 – 1.53 (m, 2H, CH$_{2(propyl)}$), 0.88 (t, *J* = 7.4 Hz, 3H, CH$_{3(propyl)}$). ^{13}C NMR (126 MHz, DMSO-*d$_6$*) δ 155.2 (C6$_{xanthine}$), 151.5, 151.1 (C2$_{xanthine}$), 148.2 (C8$_{xanthine}$), 138.7, 135.6, 133.4, 128.5, 127.1, 122, 120.9, 118.4, 114.8, 49.3 (CH$_{piperazine}$), 48.6, 46.2 (CH$_{piperazine}$), 41.7 (N3-CH$_2$), 30.2, 29.1, 21 (CH$_{2(propyl)}$), 17.4, 11.3 (CH$_{3(propyl)}$). HPLC-UV (254 nm) ESI-MS, purity: 99%. LC-MS (m/z): 589 [M + H]$^+$. HRMS (ESI-TOF) m/z: [M - H]$^-$ calcd. for C$_{24}$H$_{25}$BrN$_6$O$_5$S 587.0791, found 587.1301.

***tert*-Butyl 4-(2-hydroxyphenyl)piperazine-1-carboxylate (37).** To a solution of **36** (2.0 g, 11 mmol) and NaHCO$_3$ (1.6 g, 18.8 mmol) dissolved in 30 mL of THF/dioxane/H$_2$O solvent mixture (1:1:1), Boc$_2$O (2.88 g, 13.2 mmol) was added and the reaction was stirred at rt for 12 h. The solvents were evaporated, washed with 20 mL of water and the formed precipitate was collected by filtration. The desired product was obtained as a brown solid in a yield of 99% (3.17 g). *R$_f$* in DCM/methanol (9.5:0.5) = 0.7. ^{1}H NMR (600 MHz, DMSO-*d$_6$*) δ 6.89 – 6.80

(m, 2H, CH$_{phenyl}$), 6.78 (dd, J = 7.9, 1.5 Hz, 1H, CH$_{phenyl}$), 6.71 (td, J = 7.6, 1.5 Hz, 1H, CH$_{phenyl}$), 3.48 – 3.40 (m, 4H, CH$_{piperazine}$), 2.84 (dd, J = 11.3, 6.4 Hz, 4H, CH$_{piperazine}$), 1.41 (s, 9H). ^{13}C NMR (151 MHz, DMSO-d_6) δ 154, 150.5, 139.8, 123.4, 119.4, 119.1, 115.7, 78.9, 66.5, 50.3, 28.2. LC-MS positive mode (m/z): 278.9 [M + H]$^+$.

***tert*-Butyl 4-(2-(2-ethoxy-2-oxoethoxy)phenyl)piperazine-1-carboxylate (38a).** To a flask containing **37** (100 mg, 0.36 mmol) and K$_2$CO$_3$ (115 mg, 0.80 mmol) in 5 mL of DMF, ethyl bromoacetate (50 μl, 0.43 mmol) was added dropwise and the reaction was stirred at 40 °C for 4 h. Upon completion of the reaction, dist. water (10 mL) was added and the reaction mixture was extracted with ethyl acetate (3 x 10 mL). The organic layers were dried using MgSO$_4$ and concentrated. The desired product was obtained as a brown oil in a yield of 69% (91 mg). R_f in DCM/methanol (9.9:0.1) = 0.3. ^{1}H NMR (600 MHz, DMSO-d_6) δ 6.92 (dt, J = 11.3, 4.2 Hz, 3H, CH$_{phenyl}$), 6.84 (d, J = 7.3 Hz, 1H, CH$_{phenyl}$), 4.75 (s, 2H, CH$_2$), 4.20 – 4.14 (m, 2H, CH$_{2(ester)}$), 3.45 (s, 4H, CH$_{piperazine}$), 2.99 – 2.92 (m, 4H, CH$_{piperazine}$), 1.41 (s, 9H), 1.21 (t, J = 7.1 Hz, 3H, CH$_{3(ester)}$). ^{13}C NMR (151 MHz, DMSO-d_6) δ 168.9, 154.1, 150.3, 141.3, 122.7, 121.9, 118.7, 113.4, 79, 65.1, 60.8, 50.1, 28.2, 14.2. LC-MS positive mode (m/z): 364.7 [M + H]$^+$.

***tert*-Butyl 4-(2-(2-(2-hydroxyethoxy)ethoxy)cyclohexa-1,3-dien-1-yl)piperazine-1-carboxylate (38b).** To a flask containing **37** (250 mg, 0.9 mmol) and K$_2$CO$_3$ (250 mg, 1.8 mmol) in 5 mL DMF, 2-(2-chloroethoxy)ethanol (115 μl, 1.1 mmol) was added dropwise and the reaction was stirred at 100 °C for 24 h. Upon completion of the reaction, dist. water (10 mL) was added and the reaction mixture was extracted with ethyl acetate (3 x 10 mL). The organic layers were dried using MgSO$_4$ and concentrated. The desired product was obtained as a brown oil in a yield of 60% (200 mg). R_f in DCM/methanol (9.5:0.5) = 0.4. ^{1}H NMR (600 MHz, DMSO-d_6) δ 6.93 – 6.91 (m, 2H, CH$_{phenyl}$), 6.86 (dd, J = 3.6, 2.0 Hz, 2H, CH$_{phenyl}$), 4.58 – 4.54 (m, 1H,

OH), 4.09 – 4.04 (m, 1H, CH$_2$), 3.78 – 3.73 (m, 1H, CH$_2$), 3.53 – 3.49 (m, 4H, 2 CH$_2$), 3.43 (s, 4H, CH$_{piperazine}$), 2.94 – 2.90 (m, 4H, CH$_{piperazine}$), 1.41 (s, 9H). ^{13}C NMR (151 MHz, DMSO-d_6) δ 154.1, 151.2, 141.4, 122.7, 121.2, 118.3, 113.3, 79, 72.7, 69.3, 67.6, 60.4, 50.1, 28.2. LC-MS positive mode (m/z): 366.8 [M + H]$^+$.

tert-Butyl 4-(4-bromo-2-(2-ethoxy-2-oxoethoxy)phenyl)piperazine-1-carboxylate (39a).
This compound was synthesized using **38a** (250 mg, 0.69 mmol) dissolved in 10 mL DCM and cooled to 0 °C, bromine (40 µl, 0,76 mmol) was added dropwise and the reaction mixture was stirred for at rt for 1 h. Upon completion of the reaction, the reaction mixture was further treated with 10 mL NaHCO$_3$ and portioned between water and DCM. The organic layers were dried using anhydrous Mg$_2$SO$_4$ and evaporated obtaining an oily residue that was further purified using column chromatography using the eluent system DCM/methanol (9:1). A brownish oil was obtained in a yield of 90% (347 mg). ^{1}H NMR (600 MHz, DMSO-d_6) δ 7.14 (s, 1H, CH$_{phenyl}$), 7.09 (t, J = 2.3 Hz, 1H, CH$_{phenyl}$), 7.05 (d, J = 2.7 Hz, 1H, CH$_{phenyl}$), 4.22 – 4.14 (m, 2H, CH$_2$), 3.43 (s, 4H, CH$_{piperazine}$), 3.33 (s, 2H, CH$_{2(ester)}$), 2.96 – 2.90 (m, 4H, CH$_{piperazine}$), 1.40 (s, 9H), 1.25 – 1.18 (m, 3H, CH$_{3(ester)}$). ^{13}C NMR (151 MHz, DMSO-d_6) δ 170, 168.6, 154, 151.1, 139.6, 124.4, 120.3, 116.3, 114.7, 79.1, 65.3, 49.9, 43.3, 28.2. LC-MS positive mode (m/z): 443.1 [M + H]$^+$.

tert-Butyl 4-(4-bromo-2-(2-(2-hydroxyethoxy)ethoxy)phenyl)pipera-zine-1-carboxylate (39b).
This compound was synthesized using **38b** (500 mg, 1.37 mmol) dissolved in 20 mL DCM and cooled to 0 °C, bromine (77 µl, 1.50 mmol) was added dropwise and the reaction mixture was stirred for at rt for 1 h. Upon completion of the reaction, the reaction mixture was further treated with 20 mL NaHCO$_3$ and portioned between water and DCM. The organic layers were dried using anhydrous Mg$_2$SO$_4$ and evaporated obtaining an oily residue that was further purified using column chromatography using the eluent system DCM/methanol (9:1). A brownish oil

was obtained in a yield of 84% (510 mg). ^{1}H NMR (600 MHz, DMSO-d_6) δ 7.08 (d, J = 2.2 Hz, 1H, CH$_{phenyl}$), 7.03 (dd, J = 8.4, 2.2 Hz, 1H, CH$_{phenyl}$), 6.79 (d, J = 8.5 Hz, 1H, CH$_{phenyl}$), 4.12 – 4.08 (m, 1H, CH$_2$), 3.77 – 3.72 (m, 1H, CH$_2$), 3.52 – 3.48 (m, 1H, CH$_2$), 3.42 (s, 4H, CH$_{piperazine}$), 2.94 – 2.86 (m, 4H, CH$_{piperazine}$), 1.40 (s, 9H). ^{13}C NMR (151 MHz, DMSO-d_6) δ 154, 152.1, 140.7, 123.7, 119.9, 116, 114.1, 79, 72.6, 69.1, 68.1, 60.4, 49.9, 28.2. LC-MS positive mode (m/z): 445.1 [M + H]$^{+}$.

Ethyl 2-(5-bromo-2-(piperazin-1-yl)phenoxy)acetate (40a). To a solution of **39a** (500 mg, 1.12 mmol) in 5 mL DCM and cooled to 0 °C, TFA (2 mL) was added and the reaction was stirred at rt overnight. Upon completion of the reaction, aqueous solution of NaHCO$_3$ was added and the reaction mixture was subsequently extracted with ethyl acetate (3 x 10 mL). The organic layers were dried using MgSO$_4$, concentrated and the obtained oily residue was further purified using column chromatography using the eluent system DCM/methanol (8:2). A brownish oil was obtained in a yield of 73% (280 mg). LC-MS positive mode (m/z): 342.7 [M + H]$^{+}$.

2-(2-(5-Bromo-2-(piperazin-1-yl)phenoxy)ethoxy)ethan-1-ol (40b). This compound was synthesized using **39b** (1.28 g, 2.89 mmol) dissolved in 10 mL DCM and cooled to 0 °C, TFA (4 mL) was added and the reaction was stirred at rt overnight. Upon completion of the reaction, aqueous NaHCO$_3$ solution (20 mL) was added and the reaction mixture was extracted with ethyl acetate (3 x 10 mL). The organic layers were dried using MgSO$_4$, concentrated and the obtained oily residue was further purified using column chromatography using the eluent system DCM/methanol (8:2). A brownish oil was obtained in a yield of 40% (400 mg). ^{1}H NMR (600 MHz, DMSO-d_6) δ 7.10 (t, J = 4.6 Hz, 1H, CH$_{phenyl}$), 7.07 – 7.02 (m, 1H, CH$_{phenyl}$), 6.81 (t, J = 5.6 Hz, 1H, CH$_{phenyl}$), 4.13 – 4.07 (m, 2H, CH$_2$), 3.74 (dd, J = 12.0, 7.5 Hz, 2H, CH$_2$), 3.49 (dt, J = 8.3, 3.0 Hz, 4H, CH$_2$), 3.41 – 3.21 (m, 8H, CH$_{piperazine}$). ^{13}C NMR (151 MHz,

DMSO-d_6) δ 152, 140.5, 123.7, 119.8, 116.1, 114.3, 72.6, 69, 68.1, 60.4, 48.7, 44.4. LC-MS positive mode (m/z): 345.1 [M + H]$^+$.

Ethyl-2-(5-bromo-2-(4-((4-(2,6-dioxo-1-propyl-2,3,6,7-tetrahydro-1*H*-purin-8-yl)phenyl)sulfonyl) piperazin-1-yl)phenoxy)acetate (41a). This compound was synthesized according to the general procedure G using **32** (180 mg, 0.37 mmol) and **40a** (264 mg, 0.74 mmol) dissolved in 4 mL of anhydrous DMSO and the reaction mixture was stirred at 150 ^{o}C for 16 h. A white precipitate was obtained in a yield of 20% (40 mg). M.p.: 348-350 °C. ^{1}H NMR (500 MHz, DMSO-d_6) δ 13.99 (s, 1H, NH$_{xanthine}$), 11.93 (s, 1H, NH$_{xanthine}$), 8.35 (d, J = 8.4 Hz, 2H, CH$_{phenyl}$), 7.88 (d, J = 8.4 Hz, 2H, CH$_{phenyl}$), 7.08 – 7.04 (d, J = 8.5 Hz, 2H, CH$_{phenyl}$), 7.02 – 6.98 (d, J = 1.9 Hz, 1H, CH$_{phenyl}$), 6.87 – 6.80 (dd, J = 8.6 Hz, 1H, CH$_{phenyl}$), 4.73 (s, 2H, CH$_2$), 4.13 – 4.07 (m, 2H, CH$_2$), 3.84 – 3.81 (m, 2H, N3-CH$_2$), 3.06 (s, 8H, CH$_{piperazine}$), 1.60 – 1.54 (m, 2H, CH$_{2(propyl)}$), 1.13 (t, J = 7.1 Hz, 3H, CH$_3$), 0.87 (t, J = 7.4 Hz, 3H, CH$_{3(propyl)}$). ^{13}C NMR (126 MHz, DMSO-d_6) δ 168.5, 155.3 (C6$_{xanthine}$), 151.2 (C2$_{xanthine}$), 151, 140.1, 135.5, 128.5, 127.2, 124.4, 120.6, 116.2, 114.5, 65.3, 60.9, 49.3 (CH$_{piperazine}$), 46.3 (CH$_{piperazine}$), 41.7 (N3-CH$_2$), 21.1 (CH$_{2(propyl)}$), 14.2, 11.4 (CH$_{3(propyl)}$). HPLC-UV (254 nm) ESI-MS, purity: 97.4%. LC-MS (m/z): 675.3 [M + H]$^+$. HRMS (ESI-TOF) m/z: [M - H]$^-$ calcd. for C$_{28}$H$_{31}$BrN$_6$O$_7$S 673.1158, found 673.1091.

8-(4-((4-(4-bromo-2-(2-(2-hydroxyethoxy)ethoxy)phenyl)piperazin-1-yl)sulfonyl)phenyl)-1-propyl-3,7-dihydro-1*H*-purine-2,6-dione (41b). This compound was synthesized according to the general procedure G using **32** (150 mg, 0.32 mmol) and **40b** (264 mg, 0.74 mmol) dissolved in 5 mL of anhydrous DMSO and the reaction mixture was stirred at 150 ^{o}C for 18 h. A white precipitate was obtained in a yield of 28% (58 mg). M.p.: 352-354 °C. ^{1}H NMR (500 MHz, DMSO-d_6) δ 14.02 (s, 1H, NH$_{xanthine}$), 11.95 (s, 1H, NH$_{xanthine}$), 8.36 – 8.29 (d, J = 8.5 Hz, 2H, CH$_{phenyl}$), 7.90 – 7.85 (d, J = 8.5 Hz, 2H, CH$_{phenyl}$), 7.08 – 7.02 (d, J = 2.2 Hz, 1H, CH$_{phenyl}$), 7.02 – 6.98 (dd, J = 8.5, 2.2 Hz, 1H, CH$_{phenyl}$), 6.79 – 6.75 (d, J = 8.5 Hz, 1H,

CH$_{phenyl}$), 4.54 (s, 1H, OH), 4.05 – 3.99 (m, 2H, CH$_2$), 3.85 – 3.79 (m, 2H, N3-CH$_2$), 3.67 –

3.62 (d, 2H, CH$_2$), 3.44 – 3.41 (d, 2H, CH$_2$), 3.42 – 3.38 (d, 2H, CH$_2$), 3.05 (m, 8H, CH$_{piperazine}$),

1.61 – 1.54 (m, 2H, CH$_{2(propyl)}$), 0.87 (t, J = 7.4 Hz, 3H, CH$_{3(propyl)}$). ^{13}C NMR (126 MHz,

DMSO-d_6) δ 155.1 (C6$_{xanthine}$), 152, 151.1 (C2$_{xanthine}$), 148.2 (C8$_{xanthine}$), 147.8 (C4$_{xanthine}$),

140.1, 135.7, 133.3, 128.5, 127.2, 123.7, 120, 116, 114.4, 108.7(C5$_{xanthine}$), 72.6, 68.9, 68, 60.4,

49.2 (CH$_{piperazine}$), 46.3 (CH$_{piperazine}$), 41.7 (N3-CH$_2$), 21 (CH$_{2(propyl)}$), 11.3 (CH$_{3(propyl)}$). HPLC-

UV (254 nm) ESI-MS, purity: 96.1%. LC-MS (m/z): 679.3 [M + H]$^+$. HRMS (ESI-TOF) m/z:

[M - H]$^-$ calcd. for C$_{28}$H$_{33}$BrN$_6$O$_7$S 675.1315, found 675.1231.

8-(4-((4-(4-bromo-2-(2-hydroxyethoxy)phenyl)piperazin-1-yl)sulfonyl)phenyl)-1-propyl-3,7-dihydro-1*H*-purine-2,6-dione (42). To a solution of compound **41a** (26 mg, 0.04 mmol)

dissolved in 3 mL THF and cooled to 0 °C, LiBH$_4$ (2M in THF, 0.2 mL) was added under an

argon atmosphere and the reaction was stirred at rt for 90 h. Upon completion of the reaction,

sat. NH$_4$Cl solution (10 mL) was added at 0 °C and the reaction mixture was extracted with

ethyl acetate (3 x 10 mL). The organic layers were dried using anhydrous Mg$_2$SO$_4$ and

evaporated obtaining an oily residue that was further purified using column chromatography

using the eluent system DCM/methanol (9.5:0.5). A brown solid was obtained in a yield of

25% (6 mg). M.p.: 332-334 °C. ^{1}H NMR (500 MHz, DMSO-d_6) δ 11.54 (s, 1H, NH$_{xanthine}$),

8.32 – 8.29 (d, J = 8.2 Hz, 2H, CH$_{phenyl}$), 7.82 – 7.79 (d, J = 8.0 Hz, 2H, CH$_{phenyl}$), 7.08 – 7.03

(d, J = 2.2 Hz, 1H, CH$_{phenyl}$), 7.02 – 6.98 (dd, J = 8.5, 2.2 Hz, 1H, CH$_{phenyl}$), 6.80 – 6.77 (d, J =

8.5 Hz, 1H, CH$_{phenyl}$), 4.76 (s, 1H, OH), 3.96 – 3.90 (m, 2H, CH$_2$), 3.84 – 3.80 (m, 2H, N3-CH$_2$), 3.67 – 3.63 (s, 2H, CH$_2$), 3.05 (m, 8H, CH$_{piperazine}$), 1.61 – 1.50 (m, 2H, CH$_{2(propyl)}$), 0.85

(t, J = 7.4 Hz, 3H, CH$_{3(propyl)}$). ^{13}C NMR (126 MHz, DMSO-d_6) δ 155.1 (C6$_{xanthine}$), 152.3,

151.2 (C2$_{xanthine}$), 148.3 (C8$_{xanthine}$), 147.8 (C4$_{xanthine}$), 140.2, 136, 133.3, 128.5, 127.3, 123.7,

120.2, 116.2, 114.6, 108.7 (C5$_{xanthine}$), 70.5, 68.7, 59.8, 49.5 (CH$_{piperazine}$), 49.3, 46.3

(CH$_{piperazine}$), 41.7 (N3-CH$_2$), 32.3, 29.2, 21.1 (CH$_{2(propyl)}$), 11.4 (CH$_{3(propyl)}$). HPLC-UV (254

nm) ESI-MS, purity: 97.4%. LC-MS (m/z): 633.6 [M + H]$^+$. HRMS (ESI-TOF) m/z: [M - H]$^-$ calcd. for $C_{25}H_{27}N_6O_4S$ 631.1053, found 631.0954.

***tert*-Butyl 4-[(4-bromophenyl)amino]piperidine-1-carboxylate (45).** To a flask containing *N*-Boc piperidone (**43**, 250 mg, 1.26 mmol) and 4-bromoaniline (**44**, 216 mg, 1.26 mmol), 5 mL dichloroethane (DCE) and 0.15 mL of acetic acid were added. In 0 ℃, sodium acetoxyborohydride (400 mg, 1.90 mmol) was added and the reaction was stirred at room temperature for 6 h. Upon completion of the reaction, NaOH (2 N, 10 mL) was added at 0 ℃ and the reaction mixture was subsequently extracted with ethyl acetate (3 x 10 mL). The organic layers were dried using $MgSO_4$ and concentrated. The obtained brown oil was further purified using column chromatography DCM/methanol (9.9:0.1). The desired product was obtained as orange solid in a yield of 40% (175 mg). ^{1}H NMR (500 MHz, DMSO-*d$_6$*) δ 7.20 – 7.13 (d, *J* = 8.5 Hz, 2H, CH$_{phenyl}$), 6.52 (d, *J* = 8.3 Hz, 2H, CH$_{phenyl}$), 5.67 (d, *J* = 8.1 Hz, 1H, NH), 3.93 – 3.84 (m, 2H, CH$_{piperidyl}$), 2.94 – 2.85 (m, 2H, CH$_{piperidyl}$), 1.84 – 1.80 (m, 2H, CH$_{piperidyl}$), 1.44 – 1.37 (t, 9H, Boc), 1.11 – 1.26 (m, 2H, CH$_{piperidyl}$). ^{13}C NMR (126 MHz, DMSO) δ 154.1, 147.1, 131.6, 114.5, 106.1, 78.7, 48.7, 31.5, 28.2. LC-MS positive mode (m/z): 355.2 [M + H]$^+$.

Methyl 2-[(4-bromophenyl)(piperidin-4-yl)amino]acetate (46a). To a flask containing **45** (150 mg, 0.42 mmol) and methylbromoacetate (97 mg, 0.63 mmol), DIPEA (2 mL) was added and the reaction was heated at 90 ℃ for 24 h. Upon completion of the reaction, water (10 mL) was added and the reaction mixture was subsequently extracted with ethyl acetate (3 x 10 mL). The organic layers were dried using $MgSO_4$ and concentrated. In 0 ℃, the obtained solid was dissolved in HCl (4 M in dioxane, 3 mL) and stirred at rt for 12 h. Excess solvents were vaporized and the obtained solid was washed with diethyl ether. It was further purified using column chromatography DCM/methanol (9.9:0.1). The desired product was obtained as orange

solid in a yield of 60% (83 mg). ^{1}H NMR (600 MHz, DMSO-*d6*) δ 7.28 (d, *J* = 9.0 Hz, 2H, CH$_{phenyl}$), 6.67 (d, *J* = 9.1 Hz, 2H, CH$_{phenyl}$), 4.02 (s, 1H, CH$_{piperidyl}$), 3.65 (s, 3H, CH$_3$), 3.32 (s, 8H, CH$_{piperidyl}$), 2.95 (dt, *J* = 32.8, 16.3 Hz, 2H, CH$_2$). ^{13}C NMR (151 MHz, DMSO-*d6*) δ 171.8, 147.2, 131.6, 114.7, 108, 52.2, 46.5, 43.3, 31.1, 28.6, 27.4, 26.4. LC-MS positive mode (m/z): 327.0 [M + H]$^+$.

Ethyl 2-[(4-bromophenyl)(piperidin-4-yl)amino]acetate (46b). To a flask containing **45** (150 mg, 0.42 mmol) and ethyl bromoacetate (106 mg, 0.63 mmol), DIPEA (2 mL) was added and the reaction was heated at 90 °C for 24 h. Upon completion of the reaction, dist. water (10 mL) was added and the reaction mixture was subsequently extracted with ethyl acetate (3 x 10 mL). The organic layers were dried using MgSO$_4$ and concentrated. In 0 °C, the obtained solid was dissolved in HCl (4 M in dioxane, 3 mL) and stirred at rt for 12 h. Excess solvents were vaporized and the obtained solid was washed with diethyl ether. It was further purified with column chromatography using eluent DCM/methanol (9.9:0.1). The desired product was obtained as brown solid in a yield of 55% (79 mg). ^{1}H NMR (600 MHz, DMSO-*d6*) δ 7.27 (t, *J* = 6.2 Hz, 1H, CH$_{phenyl}$), 7.20 – 7.15 (m, 1H, CH$_{phenyl}$), 6.67 (d, *J* = 9.1 Hz, 1H, CH$_{phenyl}$), 6.56 (d, *J* = 8.8 Hz, 1H, CH$_{phenyl}$), 5.91 (d, *J* = 7.9 Hz, 1H, CH$_{piperidyl}$), 4.14 – 4.06 (m, 4H, CH$_2$), 3.37 – 3.23 (m, 4H, CH$_{piperidyl}$), 3.06 – 2.95 (m, 4H, CH$_{piperidyl}$), 1.81 (dd, *J* = 8.2, 5.5 Hz, 2H, CH$_{2(ester)}$), 1.19 – 1.16 (m, 3H, CH$_{3(ester)}$). ^{13}C NMR (151 MHz, DMSO-*d6*) δ 171.3, 158.6, 147.3, 131.7, 118.4, 114.7, 108.1, 60.8, 52.1, 46.7, 43.4, 28.7, 14.2. LC-MS positive mode (m/z): 341.0 [M + H]$^+$.

4-({4-[(4-Bromophenyl)-(2-methoxy-2-oxoethyl)amino]piperidin-1-yl}sulfonyl)benzoic acid (44). This compound was synthesized according to the general procedure A using **14** (133 mg, 0.61 mmol) and **46a** (220 mg, 0.61 mmol) in 20 mL DCM, DIPEA (0.13 mL) was added and the reaction mixture was stirred at rt for 72 h. The DCM was vaporized and then the obtained

residue was washed with water and neutralized with few drops of 1 N HCl. A white precipitate was formed **47** in a yield of 53% (162 mg). ^{1}H NMR (600 MHz, DMSO-d_6) δ 8.17 (s, 2H, CH$_{phenyl}$), 7.87 (s, 2H, CH$_{phenyl}$), 7.25 (d, J = 8.7 Hz, 2H, CH$_{phenyl}$), 6.70 (d, J = 9.0 Hz, 2H, CH$_{phenyl}$), 3.95 (s, 1H, CH$_{piperidyl}$), 3.70 (s, 3H, CH$_3$), 3.45 (m, 8H, CH$_{piperidyl}$), 2.95 (d, J = 16.8 Hz, 2H, CH$_2$). ^{13}C NMR (151 MHz, DMSO-d_6) δ 171.8, 166.3, 147.2, 139.5, 131.5, 130.4, 127.9, 114.5, 107.6, 53.5, 51.9, 45.8, 41.8, 28.2, 12.4. LC-MS positive mode (m/z): 513.0 [M + H]$^+$.

Methyl-2-[(1-{4-[(6-amino-2,4-dioxo-3-propyl-1,2,3,4-tetrahydropyrimidin-5-yl) carbamoyl]benzenesulfonyl}piperidin-4-yl)(4-bromophenyl)amino]acetate (48). This compound was synthesized according to general procedure E using **25** (75 mg, 0.40 mmol) and **47** (200 mg, 0.40 mmol) dissolved in 10 mL DMF, EDC (100 mg, 0.51 mmol) was added and the reaction mixture was stirred at rt for 8 h. A yellow precipitate was obtained in a yield of 78% (165 mg). LC-MS positive mode (m/z): 677.4 [M + H]$^+$.

Methyl 2-[(4-bromophenyl)({1-[4-(2,6-dioxo-1-propy l-2,3,6,7-tetrahydro-1H-purin-8-yl) benzenesulfonyl] piperidin-4-yl}) amino]acetate (49). To a flask containing **48** (90 mg, 0.13 mmol) dissolved in 5 mL DMF, (400 mg, 0.40 mmol) of P$_2$O$_5$. The reaction was refluxed at 120 ºC for 10 min. Upon completion of the reaction, dist. water (10 mL) was added yielding a white precipitate that was further purified using column chromatography using eluent DCM/methanol (9.5:0.5). The desired product was obtained as a brown solid in a yield of 56% (65 mg). M.p.: 330-334 °C. ^{1}H NMR (500 MHz, DMSO-d_6). δ 14.01 (s, 1H, NH$_{xanthine}$), 11.95 (s, 1H, NH$_{xanthine}$), 8.34 (d, J = 7.8 Hz, 2H, CH$_{phenyl}$), 7.87 (d, J = 8.4 Hz, 2H, CH$_{phenyl}$), 7.25 – 7.19 (d, J = 8.5 Hz, 2H, CH$_{phenyl}$), 6.61 – 6.53 (d, J = 8.3 Hz, 2H, CH$_{phenyl}$), 4.00 (s, 2H, CH$_2$), 3.86 – 3.79 (d, 2H, CH$_{piperidine}$), 3.80 – 3.74 (d, J = 11.7 Hz, 2H, CH$_{piperidine}$), 3.61 (t, 3H, OCH$_3$), 1.80 – 1.70 (d, J = 12.5 Hz, 2H, CH$_{piperidine}$), 1.65 – 1.60 (d, J = 12.5 Hz, 2H, CH$_{piperidine}$), 1.58

– 1.52 (m, 2H, CH$_{2(propyl)}$), 0.88 (t, 3H, CH$_{3(propyl)}$). ^{13}C NMR (126 MHz, DMSO) δ 171.8 (C=O), 155.1 (C6$_{xanthine}$), 151.1 (C2$_{xanthine}$), 148.2 (C8$_{xanthine}$), 147.8 (C4$_{xanthine}$), 147.2, 136.6, 133.1, 131.5, 128.3, 127.1, 114.5, 108.7 (C5$_{xanthine}$), 107.6, 53.4, 51.9, 46.4, 45.8, 41.6, 28.3, 21.0 (CH$_{2(propyl)}$), 11.3 (CH$_{3(propyl)}$). HPLC-UV (254 nm) ESI-MS, purity: 95.4%. LC-MS (m/z): 659.3 [M + H]$^+$. HRMS (ESI-TOF) m/z: [M - H]$^-$ calcd. for C$_{28}$H$_{31}$BrN$_6$O$_6$S 657.1209, found 657.1189.

8-[4-({4-[(4-Bromophenyl)(2-hydroxyethyl)amino]piperidin-1-yl}sulfonyl)phenyl]-1-propyl-2,3,6,7-tetrahydro-1H-purine-2,6-dione (50). To a solution of compound **49** (45 mg, 0.07 mmol) dissolved in 10 mL THF and cooled to 0 °C, LiBH$_4$ (2M in THF, 0.35 mL) was added dropwise under an argon atmosphere and the reaction was stirred at rt for 90 h. Upon completion of the reaction, sat. NH$_4$Cl solution (10 mL) was added at 0 °C and the reaction mixture was subsequently extracted with ethyl acetate (3 x 10 mL). The organic layers were dried using anhydrous Mg$_2$SO$_4$ and evaporated obtaining a residue that was further purified using column chromatography using the eluent system DCM/methanol (9.5:0.5). A white solid was obtained in a yield of 35% (15 mg). M.p.: 342-345 °C. ^{1}H NMR (500 MHz, DMSO-d_6) δ 14.01 (s, 1H, NH$_{xanthine}$), 11.95 (s, 1H, NH$_{xanthine}$), 8.34 (d, J = 8.4 Hz, 2H, CH$_{phenyl}$), 7.87 (d, J = 8.3 Hz, 2H, CH$_{phenyl}$), 7.21 – 7.14 (d, 2H, CH$_{phenyl}$), 6.69 (d, J = 9.1 Hz, 2H, CH$_{phenyl}$), 3.86 – 3.80 (d, 2H, CH$_{piperidine}$), 3.79 – 3.75 (d, J = 11.5 Hz, 2H, CH$_{piperidine}$), 3.39 (m, 2H, J = 5.2 Hz, 2H, CH$_2$ propyl), 3.17 (m, 2H, N-CH$_2$), 1.73 – 1.66 (d, 2H, CH$_{piperidine}$), 1.63 – 1.58 (d, J = 7.4 Hz, 2H, CH$_{piperidine}$), 1.25 – 1.20 (m, 2H, CH$_{2(propyl)}$), 0.86 (t, 3H, CH$_{3(propyl)}$). ^{13}C NMR (126 MHz, DMSO-d_6) δ 155.1 (C6$_{xanthine}$), 151.1 (C2$_{xanthine}$), 148.2 (C8$_{xanthine}$), 147.8 (C4$_{xanthine}$), 147.5, 136.6, 133, 131.5, 128.3, 127.1, 114.7, 108.7 (C5$_{xanthine}$), 107, 70, 59.4, 56.8, 53.2, 47, 45.9, 41.7, 30.5, 29.7, 29.1, 28.5, 22.2, 21 (CH$_{2(propyl)}$), 14.1, 11.3 (CH$_{3(propyl)}$). HPLC-UV (254 nm) ESI-MS, purity: 96.2%. LC-MS (m/z): 631.3 [M + H]$^+$. HRMS (ESI-TOF) m/z: [M - H]$^-$ calcd. for C$_{27}$H$_{31}$BrN$_6$O$_5$S 629.1813, found 629.1833.

Ethyl-*N*-(4-bromophenyl)-N-(1-((4-(2,6-dioxo-1-propyl-2,3,6,7-tetrahydro-1*H*-purin-8-yl) phenyl)sulfonyl)piperidin-4-yl)glycinate (51). This compound was synthesized according to the general procedure G using **32** (50 mg, 0.11 mmol) and **46b** (140 mg, 0.44 mmol) dissolved in 5 mL of anhydrous DMSO and the reaction mixture was stirred at 150 °C for 15 h. A white precipitate was obtained in a yield of 45% (32 mg). M.p.: 335-338 °C. ^{1}H NMR (500 MHz, DMSO-d_6) δ 14.01 (s, 1H, NH$_{xanthine}$), 11.95 (s, 1H, NH$_{xanthine}$), 8.34 (d, J = 8.6 Hz, 2H, CH$_{phenyl}$), 7.87 (d, J = 8.6 Hz, 2H, CH$_{phenyl}$), 7.19 (d, J = 9.1 Hz, 2H, CH$_{phenyl}$), 6.60 – 6.52 (m, 2H, CH$_{phenyl}$), 4.08 (q, J = 7.0 Hz, 2H, CH$_2$), 3.98 (m, 2H, CH$_{piperidine}$), 3.83 (m, 2H, CH$_{2(propyl)}$), 3.78 – 3.62 (m, 3H, CH$_{piperidine}$), 1.73 (d, J = 11.9 Hz, 2H, CH$_2$), 1.65 (dd, J = 4.0, 12.2 Hz, 2H, CH$_2$), 1.62 – 1.54 (m, 2H, CH$_{2(propyl)}$), 1.16 (t, J = 7.1 Hz, 3H, CH$_3$), 0.88 (t, J = 7.4 Hz, 3H, CH$_{3(propyl)}$). ^{13}C NMR (126 MHz, DMSO-d_6) δ 171.3 (C=O), 155.1 (C6$_{xanthine}$), 151.1 (C2$_{xanthine}$), 148.2 (C8$_{xanthine}$), 147.8 (C4$_{xanthine}$), 147.2, 136.6, 133.1, 131.5, 128.3, 127.1, 114.5, 108.7 (C5$_{xanthine}$), 107.6, 60.6, 53.4, 46.6, 45.8, 41.7, 28.3, 21.0 (CH$_{2(propyl)}$), 14.2, 11.3 (CH$_{3(propyl)}$). HPLC-UV (254 nm) ESI-MS, purity: 95.4%. LC-MS (m/z): 673.3 [M + H]$^+$. HRMS (ESI-TOF) m/z: [M - H]$^-$ calcd. for C$_{29}$H$_{33}$BrN$_6$O$_6$S 671.1366, found 671.1286.

{2-[8-(4-{[4-(4-Bromophenyl)piperazin-1-yl]sulfonyl}phenyl)-2,6-dioxo-1-propyl-2,3,6,7-tetrahydro-1*H*-purin-3-yl]ethoxy}phosphonic acid (52). This compound was synthesized according to the general procedure H using **30b** (30 mg, 0.05 mmol) dissolved in 2 mL of trimethyl phosphate, POCl$_3$ (24 µL, 0.25 mmol) was added dropwise and then the reaction was kept stirring at 0 °C for 6 h. The desired product was obtained as a white solid in a yield of 45% (15 mg). M.p.: 285-287 °C. ^{1}H NMR (600 MHz, D$_2$O) δ 8.06 (s, 2H, CH$_{phenyl}$), 7.57 (s, 2H, CH$_{phenyl}$), 6.75 (s, 2H, CH$_{phenyl}$), 6.07 (s, 2H, CH$_{phenyl}$), 4.25 – 4.20 (m, 2H, N1-CH$_2$), 3.95 – 3.85 (m, 2H, CH$_2$), 3.62 (m, 2H, N3-CH$_2$), 2.75 – 2.64 (m, 4H, CH$_{piperazine}$), 2.54 – 2.40 (m, 4H, CH$_{piperazine}$), 1.45 – 1.40 (m, 2H, CH$_{2(propyl)}$), 0.74 (t, J = 7.5 Hz, 3H, CH$_{3(propyl)}$). ^{13}C NMR (126 MHz, D$_2$O) δ 150.8 (C2$_{xanthine}$), 149.7, 135.8, 133.2, 131.7, 129, 128.5, 127.3, 121.9, 111,

61.7 (N1-CH$_2$), 49.3 (CH$_{piperazine}$), 47.8 (CH$_{piperazine}$), 45.9 (CH$_{2(propyl)}$), 20.9 (CH$_{2(propyl)}$), 11.4 (CH$_{3(propyl)}$). ^{31}P NMR (202 MHz, D$_2$O) δ 4.63. HPLC-UV (254 nm) ESI-MS, purity: 96.8%. LC-MS (m/z): 697.5 [M + H]$^+$. HRMS (ESI-TOF) m/z: [M - H]$^-$ calcd. for C$_{25}$H$_{27}$N$_6$O$_4$S 695.0767, found 695.0683.

2-(5-Bromo-2-(4-((4-(2,6-dioxo-1-propyl-2,3,6,7-tetrahydro-1*H*-purin-8-yl)phenyl)sulf-onyl)piperazin-1-yl)phenoxy)ethyldihydrogen phosphate (53). This compound was synthesized according to the general procedure H using **42** (40 mg, 0.06 mmol) dissolved in 3 mL of trimethyl phosphate, POCl$_3$ (28 µL, 0.30 mmol) was added dropwise and then the reaction was kept stirring at 0 °C for 8 h. The desired product was obtained as white solid in a yield of 60% (27 mg). M.p.: 305-307 °C. ^{1}H NMR (600 MHz, D$_2$O) δ 8.25 – 8.20 (d, *J* = 8.5 Hz, 2H, CH$_{phenyl}$), 7.79 – 7.75 (d, *J* = 8.6 Hz, 2H, CH$_{phenyl}$), 6.95 – 6.90 (d, *J* = 1.7 Hz, 1H, CH$_{phenyl}$), 6.67 – 6.62 (dd, *J* = 8.6, 2.2 Hz, 1H, CH$_{phenyl}$), 6.35 – 6.30 (d, *J* = 8.5 Hz, 1H, CH$_{phenyl}$), 4.03 – 3.98 (m, 2H, CH$_2$), 3.95 – 3.89 (m, 2H, N3-CH$_2$), 3.85 – 3.79 (s, 2H, CH$_{2(propyl)}$), 3.20 – 3.15 (m, 4H, CH$_{piperazine}$), 2.75 – 2.64 (m, 4H, CH$_{piperazine}$), 1.56 – 1.47 (m, 2H, CH$_{2(propyl)}$), 0.81 (t, *J* = 7.4 Hz, 3H, CH$_{3(propyl)}$). ^{13}C NMR (151 MHz, D$_2$O) δ 164.5, 163.7, 161.8, 158.7, 154.3 (C6$_{xanthine}$), 142.6, 141.3, 136.1, 130.8, 129.3, 126.6, 122.8, 121.8, 118.8, 118.5, 71.2, 65.1, 52, 48.1 (CH$_{piperazine}$), 45.5 (CH$_{piperazine}$), 24.3 (CH$_{2(propyl)}$), 13.5 (CH$_{3(propyl)}$). ^{31}P NMR (202 MHz, D$_2$O) δ 4.51. HPLC-UV (254 nm) ESI-MS, purity: 98.5%. LC-MS (m/z): 713.5 [M + H]$^+$. HRMS (ESI-TOF) m/z: [M - H]$^-$ calcd. for C$_{25}$H$_{27}$N$_6$O$_4$S 711.0716, found 711.0632.

2-((4-Bromophenyl)(1-((4-(2,6-dioxo-1-propyl-2,3,6,7-tetrahydro-1*H*-purin-8-yl) phenyl)sulfonyl)piperidin-4-yl)amino)ethyl dihydrogen phosphate (54). This compound was synthesized according to the general procedure H using **50** (50 mg, 0.08 mmol) dissolved in 3 mL of trimethyl phosphate under argon atmosphere at 0 °C, POCl$_3$ (38 µL, 0.4 mmol) was

added dropwise and then the reaction was kept stirring at 0 °C for 8 h. The desired product was obtained as yellowish solid in a yield of 50% (29 mg). M.p.: 235-237 °C. ^{1}H NMR (600 MHz, D$_2$O) δ 8.08 (d, J = 16.7 Hz, 2H, CH$_{phenyl}$), 7.87 (d, J = 8.3 Hz, 2H, CH$_{phenyl}$), 7.21 – 7.15 (d, J = 7.9 Hz, 2H, CH$_{phenyl}$), 6.69 (d, J = 7.9 Hz, 2H, CH$_{phenyl}$), 3.90 – 3.80 (m, 2H, CH$_{piperidine}$), 3.80 – 3.76 (d, J = 12.8 Hz, 2H, CH$_{piperidine}$), 3.36 – 3.22 (m, 2H, J = 5.0 Hz, 2H, CH$_{2(propyl)}$), 2.66 – 2.53 (m, 2H, NCH$_2$), 1.78 – 1.73 (d, 2H, CH$_{piperidine}$), 1.63 – 1.58 (d, J = 7.3 Hz, 2H, CH$_{piperidine}$), 1.54 – 1.50 (m, 2H, CH$_{2(propyl)}$), 0.91 (t, 3H, CH$_{3(propyl)}$). ^{13}C NMR (151 MHz, D$_2$O) δ 163.3, 162.2, 149.3, 138.6, 138, 134.6, 130.8, 129.4, 122.5, 114.4, 64.4, 59.5, 51.1, 50.8, 50.7, 49, 45.5, 30.3, 23.9, 19.7 (CH$_{2(propyl)}$), 13.4 (CH$_{3(propyl)}$). ^{31}P NMR (243 MHz, D$_2$O) δ 3.78. HPLC-UV (254 nm) ESI-MS, purity: 93%. LC-MS (m/z): 711.3 [M + H]$^+$. HRMS (ESI-TOF) m/z: [M - H]$^-$ calcd. for C$_{27}$H$_{32}$BrN$_6$O$_8$S 709.0923, found 709.0921.

4.1.6.2.   Biological Assays

Membrane preparation. The membrane preparations of recombinant CHO or HEK cells stably expressing human AR subtypes were conducted as previously described.[21,22] In some cases, membrane preparations were purchased from Perkin Elmer (Solingen, Germany).

Radioligand receptor binding assays. [^{3}H]2-chloro-N^6-cyclopentyladenosine ([^{3}H]CCPA, A$_1$), [^{3}H](E)-3-(3-hydroxypropyl)-8-(2-(3-methoxyphenyl)vinyl)-7-methyl-1-prop-2-ynyl-3,7-dihydropurine-2,6-dione ([^{3}H]MSX-2, A$_{2A}$), [^{3}H]8-(4-(4-(4-chlorophenyl) piperazine-1-sulfonyl)phenyl)-1-propyl-3,7-dihydropurine-2,6-dione ([^{3}H]PSB-603, A$_{2B}$), and [^{3}H]2-phenyl-8-ethyl-4-methyl-(8R)-4,5,7,8-tetrahydro-1H-imidazo[2.1-i]-purin-5-one ([^{3}H]PSB-11, A$_3$) were used as radioligands for human A$_1$, A$_{2A}$, A$_{2B}$, A$_3$ARs, respectively.

Competition binding experiments at human A$_1$, A$_{2A}$, and A$_3$ ARs were performed in a final volume of 400 μL containing 4 μL of test compound dissolved in DMSO, 196 μL buffer (50 mM Tris-HCl, pH 7.4, 10 mM MgCl$_2$, pH 7.4), 100 μL of radioligand solution in the same

buffer and 100 μL of membrane preparation (5-100 μg protein per vial, 2 U/mL adenosine deaminase (ADA) incubated for 15 min at rt). Competition binding experiments at human A$_{2B}$ARs were performed in a final volume of 1 mL containing 10 μL of test compound dissolved in DMSO, 790 μL of buffer (50 mM Tris-HCl, pH 7.4), 100 μL of radioligand solution in the same buffer, and 100 μL of membrane preparation (10-100 μg protein per vial, 2 U/mL ADA incubated for 15 min at rt). Non-specific binding was determined in the presence of 2-chloroadenosine (10 μM), 9-chloro-2-(2-furanyl)-[1,2,4]triazolo[1,5-c]quinazolin-5-amine (CGS-15943, 10 μM), dipropylcyclopentylxanthine (DPCPX, 10 μM), or N^6-(R-2-phenylisopropyl)adenosine (100 μM), respectively, for human A$_1$, A$_{2A}$, A$_{2B}$ and A$_3$AR binding assays.

The incubation time at rt was 90 min for the A$_1$AR, 30 min for the A$_{2A}$AR, 75 min for the A$_{2B}$AR, and 45 min for the A$_3$AR binding assay. After the incubation, the assay mixture was filtered through GF/B glass fiber filters using a Brandel harvester (Brandel, Gaithersburg, MD). Filters were washed three times (3-4 mL each) with ice-cold 50 mM Tris-HCl buffer, pH 7.4. For the A$_{2A}$AR binding assay the GF/B glass fiber filters were preincubated for 30 min in 0.3% aq. polyethylenemine solution before filtration. The GF/B glass fiber filters for the A$_{2B}$AR assays were washed four times (3-4 mL each) with ice-cold 50 mM Tris-HCl buffer, pH 7.4 containing 0.1% BSA in order to reduce non-specific binding. Then filters were transferred to scintillation vials, incubated for 9 h with 2.5 mL of scintillation cocktail (Luma Safe, Perkin Elmer), and counted in a liquid scintillation counter (Tri-Carb 2810 TR) with a counting efficiency of $\sim$52%. Three to four separate experiments were performed for the determination of K_i values. All data were analyzed with GraphPad Prism, Version 4.1 (GraphPad Inc., La Jolla, CA).

Author Information

Corresponding Author

*Christa E. Müller: Phone: +49-228-73-230; Fax: +49-228-73-2567; E-mail:

christa.mueller@uni-bonn.de

ORCID

Ahmed Temirak: 0000-0003-3862-5359

Christa E. Müller: 0000-0002-0013-6624

Notes

The authors declare no competing financial interest.

4.1.7. References

(1)   Attwood, T. K.; Findlay, J. B. Fingerprinting G-protein-coupled receptors. *Protein Eng.* **1994**, *7*, 195–203.

(2)   Kolakowski, L. F. GCRDb: a G-protein-coupled receptor database. *Receptors Channels* **1994**, *2*, 1–7.

(3)   Beukers, M. W.; den Dulk, H.; van Tilburg, E. W.; Brouwer, J.; Ijzerman, A. P. Why are A2B receptors low-affinity adenosine receptors? mutation of Asn273 to Tyr

increases affinity of human A2B Receptor for 2-(1-Hexynyl)adenosine. *Mol. Pharmacol.* **2000**, *58*, 1349–1356.

(4)   Pándy-Szekeres, G.; Munk, C.; Tsonkov, T. M.; Mordalski, S.; Harpsøe, K.; Hauser, A. S.; Bojarski, A. J.; Gloriam, D. E. GPCRdb in 2018: adding GPCR structure models and ligands. *Nucleic Acids Res.* **2018**, *46*, D440–D446.

(5)   Yaar, R.; Jones, M. R.; Chen, J.-F.; Ravid, K. Animal models for the study of adenosine receptor function. *J. Cell. Physiol.* **2005**, *202*, 9–20.

(6)   Aherne, C. M.; Kewley, E. M.; Eltzschig, H. K. The resurgence of A2B adenosine receptor signaling. *Biochim. Biophys. Acta - Biomembr.* **2011**, *1808*, 1329–1339.

(7)   Eisenstein, A.; Patterson, S.; Ravid, K. The many faces of the A2B adenosine receptor in cardiovascular and metabolic diseases. *J. Cell. Physiol.* **2015**, *230*, 2891–2897.

(8)   Eltzschig, H. K.; Bonney, S. K.; Eckle, T. Attenuating myocardial ischemia by targeting A2B adenosine receptors. *Trends Mol. Med.* **2013**, *19*, 345–354.

(9)   Antonioli, L.; Blandizzi, C.; Pacher, P.; Haskó, G. Immunity, inflammation and cancer: a leading role for adenosine. *Nat. Rev. Cancer* **2013**, *13*, 842–857.

(10)   Gao, Z.-G.; Jacobson, K. A. A2B adenosine receptor and cancer. *Int. J. Mol. Sci.* **2019**, *20*, 5139.

(11)   Müller, C. E.; Baqi, Y.; Hinz, S.; Namasivayam, V. Medicinal chemistry of A2B adenosine receptors. In *The Adenosine Receptors*; Springer International Publishing: Cham, 2018; pp 137–168.

(12)   Wei, Q.; Costanzi, S.; Balasubramanian, R.; Gao, Z.-G. G.; Jacobson, K. A. A2B adenosine receptor blockade inhibits growth of prostate cancer cells. *Purinergic Signal.* **2013**, *9*, 271–280.

(13) Abo-Salem, O. M.; Hayallah, A. M.; Bilkei-Gorzo, A.; Filipek, B.; Zimmer, A.; Müller, C. E. Antinociceptive effects of novel A2B adenosine receptor antagonists. *J. Pharmacol. Exp. Ther.* **2004**, *308*, 358–366.

(14) Müller, C. E.; Jacobson, K. A. Xanthines as adenosine receptor antagonists. *Handb. Exp. Pharmacol.* **2011**, *200*, 151–199.

(15) Cappelletti, S.; Daria, P.; Sani, G.; Aromatario, M. Caffeine: cognitive and physical performance enhancer or psychoactive drug? *Curr. Neuropharmacol.* **2015**, *13*, 71–88.

(16) Baratloo, A.; Rouhipour, A.; Forouzanfar, M. M.; Safari, S.; Amiri, M.; Negida, A. The role of caffeine in pain management: A brief literature review. *Anesthesiol. Pain Med.* **2016**, *6*, e33193.

(17) Wang, Z.; Gu, C.; Wang, X.; Lang, Y.; Wu, Y.; Wu, X.; Zhu, X.; Wang, K.; Yang, H. Caffeine enhances the anti-tumor effect of 5-fluorouracil via increasing the production of reactive oxygen species in hepatocellular carcinoma. *Med. Oncol.* **2019**, *36*, 97.

(18) Westcott, F. H.; Gillson, R. E. The treatment of bronchial asthma by inhalation therapy with vital capacity studies. *J. Allergy* **1943**, *14*, 420–427.

(19) Kim, Y.-C.; Ji, X.; Melman, N.; Linden, J.; Jacobson, K. A. Anilide derivatives of an 8-phenylxanthine carboxylic congener are highly potent and selective antagonists at human A2B adenosine receptors. *J. Med. Chem.* **2000**, *43*, 1165–1172.

(20) Hayallah, A. M.; Sandoval-Ramírez, J.; Reith, U.; Schobert, U.; Preiss, B.; Schumacher, B.; Daly, J. W.; Müller, C. E. 1,8-Disubstituted xanthine derivatives: synthesis of potent A2B-selective adenosine receptor antagonists. *J. Med. Chem.* **2002**, *45*, 1500–1510.

(21) Borrmann, T.; Hinz, S.; Bertarelli, D. C. G.; Li, W.; Florin, N. C.; Scheiff, A. B.; Müller, C. E. 1-Alkyl-8-(piperazine-1-sulfonyl)phenylxanthines: development and

characterization of adenosine A2B receptor antagonists and a new radioligand with subnanomolar affinity and subtype specificity. *J. Med. Chem.* **2009**, *52*, 3994–4006.

(22)   Jiang, J.; Seel, C. J.; Temirak, A.; Namasivayam, V.; Arridu, A.; Schabikowski, J.; Baqi, Y.; Hinz, S.; Hockemeyer, J.; Müller, C. E. A2B adenosine receptor antagonists with picomolar potency. *J. Med. Chem.* **2019**, *62*, 4032–4055.

(23)   Ma, D.-F. F.; Kondo, T.; Nakazawa, T.; Niu, D.-F. F.; Mochizuki, K.; Kawasaki, T.; Yamane, T.; Katoh, R. Hypoxia-inducible adenosine A2B receptor modulates proliferation of colon carcinoma cells. *Hum. Pathol.* **2010**, *41*, 1550–1557.

(24)   Du, X.; Ou, X.; Song, T.; Zhang, W.; Cong, F.; Zhang, S.; Xiong, Y. Adenosine A2B receptor stimulates angiogenesis by inducing VEGF and eNOS in human microvascular endothelial cells. *Exp. Biol. Med.* **2015**, *240*, 1472–1479.

(25)   Mølck, C.; Ryall, J.; Failla, L. M.; Coates, J. L.; Pascussi, J.-M. M.; Heath, J. K.; Stewart, G.; Hollande, F. The A2B adenosine receptor antagonist PSB-603 promotes oxidative phosphorylation and ROS production in colorectal cancer cells via adenosine receptor-independent mechanism. *Cancer Lett.* **2016**, *383*, 135–143.

(26)   Vecchio, E. A.; Tan, C. Y. R. R.; Gregory, K. J.; Christopoulos, A.; White, P. J.; May, L. T. Ligand-independent adenosine A2B receptor constitutive activity as a promoter of prostate cancer cell proliferation. *J. Pharmacol. Exp. Ther.* **2016**, *357*, 36–44.

(27)   Müller, C. E.; Baqi, Y.; Namasivayam, V. Agonists and antagonists for purinergic receptors. In *Methods in molecular biology (Clifton, N.J.)*; NLM (Medline), 2020; Vol. 2041, pp 45–64.

(28)   Kolachala, V. L.; Ruble, B. K.; Vijay-Kumar, M.; Wang, L.; Mwangi, S.; Figler, H. E.; Figler, R. A.; Srinivasan, S.; Gewirtz, A. T.; Linden, J.; et al. Blockade of adenosine

A2B receptors ameliorates murine colitis. *Br. J. Pharmacol.* **2008**, *155*, 127–137.

(29) Cekic, C.; Sag, D.; Li, Y.; Theodorescu, D.; Strieter, R. M.; Linden, J. Adenosine A 2B Receptor Blockade Slows Growth of Bladder and Breast Tumors. *J. Immunol.* **2012**, *188*, 198–205.

(30) Toldo, S.; Zhong, H.; Mezzaroma, E.; Van Tassell, B. W.; Kannan, H.; Zeng, D.; Belardinelli, L.; Voelkel, N. F.; Abbate, A. GS-6201, a selective blocker of the A2B adenosine receptor, attenuates cardiac remodeling after acute myocardial infarction in the mouse. *J. Pharmacol. Exp. Ther.* **2012**, *343*, 587–595.

(31) Karmouty-Quintana, H.; Zhong, H.; Acero, L.; Weng, T.; Melicoff, E.; West, J. D.; Hemnes, A.; Grenz, A.; Eltzschig, H. K.; Blackwell, T. S.; et al. The A2B adenosine receptor modulates pulmonary hypertension associated with interstitial lung disease. *FASEB J.* **2012**, *26*, 2546–2557.

(32) Zhang, H.; Zhong, H.; Everett, T. H.; Wilson, E.; Chang, R.; Zeng, D.; Belardinelli, L.; Olgin, J. E. Blockade of A2B adenosine receptor reduces left ventricular dysfunction and ventricular arrhythmias 1 week after myocardial infarction in the rat model. *Hear. Rhythm* **2014**, *11*, 101–109.

(33) Taliani, S.; Pugliesi, I.; Barresi, E.; Simorini, F.; Salerno, S.; La Motta, C.; Marini, A. M.; Cosimelli, B.; Cosconati, S.; Di Maro, S.; et al. 3-Aryl-[1,2,4]triazino[4,3-a]benzimidazol-4(10H)-one: A novel template for the design of highly selective A2B adenosine receptor antagonists. *J. Med. Chem.* **2012**, *55*, 1490–1499.

(34) Alnouri, M. W.; Jepards, S.; Casari, A.; Schiedel, A. C.; Hinz, S.; Müller, C. E. Selectivity is species-dependent: Characterization of standard agonists and antagonists at human, rat, and mouse adenosine receptors. *Purinergic Signal.* **2015**, *11*, 389–407.

(35)   Mustafa, S. J.; Nadeem, A.; Fan, M.; Zhong, H.; Belardinelli, L.; Zeng, D. Effect of a specific and selective A2B adenosine receptor antagonist on adenosine agonist AMP and allergen-induced airway responsiveness and cellular influx in a mouse model of asthma. *J. Pharmacol. Exp. Ther.* **2007**, *320*, 1246–1251.

(36)   El Maatougui, A.; Azuaje, J.; González-Gómez, M.; Miguez, G.; Crespo, A.; Carbajales, C.; Escalante, L.; García-Mera, X.; Gutiérrez-de-Terán, H.; Sotelo, E. Discovery of potent and highly selective A2B adenosine receptor antagonist chemotypes. *J. Med. Chem.* **2016**, *59*, 1967–1983.

(37)   Eastwood, P.; Esteve, C.; González, J.; Fonquerna, S.; Aiguadé, J.; Carranco, I.; Doménech, T.; Aparici, M.; Miralpeix, M.; Albertí, J.; et al. Discovery of LAS101057: a potent, selective, and orally efficacious A2B adenosine receptor antagonist. *ACS Med. Chem. Lett.* **2011**, *2*, 213–218.

(38)   Mallo-Abreu, A.; Rubén Prieto-Díaz, R.; Jespers, W.; Azuaje, J.; Majellaro, M.; Velando, C.; García-Mera, X.; Caamañ, O.; Josébrea, J.; Loza, M. I.; et al. Nitrogen-walk approach to explore bioisosteric replacements in a series of potent A2B adenosine receptor antagonists. *J. Med. Chem* **2020**, *63*, 7721–7739.

(39)   Antoniu, S. A. Discontinued drugs 2008: pulmonary and allergy. *Expert Opin. Investig. Drugs* **2009**, *18*, 1799–1805.

(40)   Pipeline - Palobiofarma https://www.palobiofarma.com/pipeline-2/ (accessed Nov 25, 2019).

(41)   PBF-1129 in patients with NSCLC - Full Text View - ClinicalTrials.gov https://clinicaltrials.gov/ct2/show/NCT03274479 (accessed Nov 25, 2019).

(42)   Evans, J.; Bobko, A.; Lewis, S.; Martin, C.; Rahman, M.; Cole, S.; Akhter, A.;

Antonucci, A.; Carbone, D.; Tchekneva, E.; et al. Targeting adenosine A2B receptor for modulation of tumor microenvironment, primary tumor growth, and lung metastasis. *J. Thorac. Oncol.* **2017**, *12*, S1013.

(43) Savjani, K. T.; Gajjar, A. K.; Savjani, J. K. Drug solubility: importance and enhancement techniques. *ISRN Pharm.* **2012**, *2012*, 1–10.

(44) Ettmayer, P.; Amidon, G. L.; Clement, B.; Testa, B. Lessons learned from marketed and investigational prodrugs. *J. Med. Chem.* **2004**, *47*, 2393–2404.

(45) Müller, C. E. Prodrug approaches for enhancing the bioavailability of drugs with low solubility. *Chem. Biodivers.* **2009**, *6*, 2071–2083.

(46) Rautio, J.; Meanwell, N. A.; Di, L.; Hageman, M. J. The expanding role of prodrugs in contemporary drug design and development. *Nat. Rev. Drug Discov.* **2018**, *17*, 559–587.

(47) Wang, T.; Ueda, Y.; Zhang, Z.; Yin, Z.; Matiskella, J.; Pearce, B. C.; Yang, Z.; Zheng, M.; Parker, D. D.; Yamanaka, G. A.; et al. Discovery of the human immunodeficiency virus type 1 (HIV-1) attachment inhibitor temsavir and its phosphonooxymethyl prodrug fostemsavir. *J. Med. Chem.* **2018**, *61*, 6308–6327.

(48) Sanches, B. M. A.; Ferreira, E. I. Is prodrug design an approach to increase water solubility? *Int. J. Pharm.* **2019**, *568*, 118498.

(49) Hauber, W.; Nagel, J.; Sauer, R.; Müller, C. E. Motor effects induced by a blockade of adenosine A_{2A} receptors in the caudate-putamen. *Neuroreport* **1998**, *9*, 1803–1806.

(50) Pereira, M.; Farrar, A. M.; Hockemeyer, J.; Müller, C. E.; Salamone, J. D.; Morrell, J. I. Effect of the adenosine A2A receptor antagonist MSX-3 on motivational disruptions of maternal behavior induced by dopamine antagonism in the early postpartum rat. *Psychopharmacol. Ser.* **2011**, *213*, 69–79.

(51) Díaz-Cabiale, Z.; Vivó, M.; Del Arco, A.; O'Connor, W. T.; Harte, M. K.; Müller, C. E.; Martínez, E.; Popoli, P.; Fuxe, K.; Ferré, S. Metabotropic glutamate mGlu5 receptor-mediated modulation of the ventral striopallidal GABA pathway in rats. Interactions with adenosine A2A and dopamine D2 receptors. *Neurosci. Lett.* **2002**, *324*, 154–158.

(52) Blum, D.; Galas, M.-C.; Pintor, A.; Brouillet, E.; Ledent, C.; Muller, C. E.; Bantubungi, K.; Galluzzo, M.; Gall, D.; Cuvelier, L.; et al. A dual role of adenosine A2A receptors in 3-nitropropionic acid-induced striatal lesions: Implications for the neuroprotective potential of A2A antagonists. *J. Neurosci.* **2003**, *23*, 5361–5369.

(53) Schindler, C. W.; Karcz-Kubicha, M.; Thorndike, E. B.; Müller, C. E.; Tella, S. R.; Ferré, S.; Goldberg, S. R. Role of central and peripheral adenosine receptors in the cardiovascular responses to intraperitoneal injections of adenosine A1 and A2A subtype receptor agonists. *Br. J. Pharmacol.* **2005**, *144*, 642–650.

(54) Worden, L. T.; Shahriari, M.; Farrar, A. M.; Sink, K. S.; Hockemeyer, J.; Müller, C. E.; Salamone, J. D. The adenosine A2A antagonist MSX-3 reverses the effort-related effects of dopamine blockade: differential interaction with D1 and D2 family antagonists. *Psychopharmacol. Ser.* **2009**, *203*, 489–499.

(55) Faivre, E.; Coelho, J. E.; Zornbach, K.; Malik, E.; Baqi, Y.; Schneider, M.; Cellai, L.; Carvalho, K.; Sebda, S.; Figeac, M.; et al. Beneficial effect of a selective adenosine A2A receptor antagonist in the APPswe/PS1dE9 mouse model of Alzheimer's disease. *Front. Mol. Neurosci.* **2018**, *11*.

(56) Agosto-Marlin, I. M.; Nichols, N. L.; Mitchell, G. S. Adenosine-dependent phrenic motor facilitation is inflammation resistant. *J. Neurophysiol.* **2017**, *117*, 836–845.

(57) Nunes, E. J.; Randall, P. A.; Hart, E. E.; Freeland, C.; Yohn, S. E.; Baqi, Y.; Müller, C. E.; López-Cruz, L.; Correa, M.; Salamone, J. D. Effort-related motivational effects of

the VMAT-2 inhibitor tetrabenazine: implications for animal models of the motivational symptoms of depression. *J. Neurosci.* **2013**, *33*, 19120–19130.

(58) Ishiwari, K.; Madson, L. J.; Farrar, A. M.; Mingote, S. M.; Valenta, J. P.; DiGianvittorio, M. D.; Frank, L. E.; Correa, M.; Hockemeyer, J.; Müller, C.; et al. Injections of the selective adenosine A2A antagonist MSX-3 into the nucleus accumbens core attenuate the locomotor suppression induced by haloperidol in rats. *Behav. Brain Res.* **2007**, *178*, 190–199.

(59) Boyd, B. J.; Bergström, C. A. S.; Vinarov, Z.; Kuentz, M.; Brouwers, J.; Augustijns, P.; Brandl, M.; Bernkop-Schnürch, A.; Shrestha, N.; Préat, V.; et al. Successful oral delivery of poorly water-soluble drugs both depends on the intraluminal behavior of drugs and of appropriate advanced drug delivery systems. *Eur. J. Pharm. Sci.* **2019**, *137*, 104967.

(60) Sherbiny, F. F.; Schiedel, A. C.; Maaß, A.; Müller, C. E. Homology modelling of the human adenosine A2B receptor based on X-ray structures of bovine rhodopsin, the β2-adrenergic receptor and the human adenosine A2A receptor. *J. Comput. Aided. Mol. Des.* **2009**, *23*, 807–828.

(61) Köse, M.; Gollos, S.; Karcz, T.; Fiene, A.; Heisig, F.; Behrenswerth, A.; Kieć-Kononowicz, K.; Namasivayam, V.; Müller, C. E. Fluorescent-labeled selective adenosine A2B receptor antagonist enables competition binding assay by flow cytometry. *J. Med. Chem.* **2018**, *61*, 4301–4316.

(62) Priego, E.-M.; Camarasa, M.-J.; Pérez-Pérez, M.-J. Efficient synthesis of N-3-substituted 6-aminouracil derivatives via N6-[(dimethylamino)methylene] protection. *Synthesis* **2001**, *2001*, 0478–0482.

(63) Müller, C. E. General synthesis and properties of 1-monosubstituted xanthines. *Synthesis* **1993**, *1993*, 125–128.

(64) Weyler, S.; Hayallah, A. M.; Müller, C. E. Versatile, convenient synthesis of pyrimido[1,2,3-cd]purinediones. *Tetrahedron* **2003**, *59*, 47–54.

(65) Modi, G.; Antonio, T.; Reith, M.; Dutta, A. Structural modifications of neuroprotective anti-parkinsonian (−)- N6-(2-(4-(biphenyl-4-yl)piperazin-1-yl)-ethyl)- N6-propyl-4,5,6,7tetrahydrobenzo[d]thiazole-2,6-diamine (D-264): an effort toward the improvement of in vivo efficacy of the parent mol. *J. Med. Chem.* **2014**, *57*, 1557–1572.

(66) Yan, L.; Müller, C. E. Preparation, properties, reactions, and adenosine receptor affinities of sulfophenylxanthine nitrophenyl esters: toward the development of sulfonic acid prodrugs with peroral bioavailability. *J. Med. Chem.* **2004**, *47*, 1031–1043.

(67) Yan, L.; Bertarelli, D. C. G.; Hayallah, A. M.; Meyer, H.; Klotz, K.-N.; Müller, C. E. A new synthesis of sulfonamides by aminolysis of p -nitrophenylsulfonates yielding potent and selective adenosine A 2b receptor antagonists. *J. Med. Chem.* **2006**, *49*, 4384–4391.

(68) Skerlj, R.; Bridger, G.; Zhou, Y.; Bourque, E.; McEachern, E.; Langille, J.; Harwig, C.; Veale, D.; Yang, W.; Li, T.; et al. Design and synthesis of pyridin-2-ylmethyl-aminopiperidin-1-ylbutyl amide CCR5 antagonists that are potent inhibitors of M-tropic (R5) HIV-1 replication. *Bioorg. Med. Chem. Lett.* **2011**, *21*, 6950–6954.

(69) Brown, G. A.; Congreve, M. S.; Pickworth, M.; Tehan, B. G. Muscarinic agonists. 2017, WO2017021730.

(70) chemaxon https://www.chemaxon.com.

(71) Klotz, K. N.; Lohse, M. J.; Schwabe, U.; Cristalli, G.; Vittori, S.; Grifantini, M. 2-Chloro-N6-[3H]cyclopentyladenosine ([3HCCPA) —a high affinity agonist radioligand

for A1 adenosine receptors. *N-S Arch. Pharmacol.* **1989**, *340*, 679–683.

(72) Müller, C. E.; Maurinsh, J.; Sauer, R. Binding of [3H]MSX-2 (3-(3-hydroxypropyl)-7-methyl-8-(m-methoxystyryl)-1-propargylxanthine) to rat striatal membranes—A new, selective antagonist radioligand for A2A adenosine receptors. *Eur. J. Pharm. Sci.* **2000**, *10*, 259–265.

(73) Müller, C. E.; Diekmann, M.; Thorand, M.; Ozola, V. [3H]8-Ethyl-4-methyl-2-phenyl-(8R)-4,5,7,8-tetrahydro-1H-imidazo[2,1-i]-purin-5-one ([3H]PSB-11), a novel high-affinity antagonist radioligand for human A3 adenosine receptors. *Bioorg. Med. Chem. Lett.* **2002**, *12*, 501–503.

(74) A. Haile, P.; N. Casillas, L.; J. Votta, B.; Z. Wang, G.; K. Charnley, A.; Dong, X.; J. Bury, M.; J. Romano, J.; F. Mehlmann, J.; W. King, B.; et al. Discovery of a first-in-class receptor interacting protein 2 (RIP2) kinase specific clinical candidate, 2-((4-(benzo[d]thiazol-5-ylamino)-6-(tert   -butylsulfonyl)quinazolin-7-yl)oxy)ethyl dihydrogen phosphate, for the treatment of inflammatory diseases. *J. Med. Chem.* **2019**, *62*, 6482–6494.

(75) Yoshikawa, M.; Kato, T.; Takenishi, T. A novel method for phosphorylation of nucleosides to 5′-nucleotides. *Tetrahedron Lett.* **1967**, *8*, 5065–5068.

(76) Pharmacelsus Contract Research Organisation CRO https://www.pharmacelsus.com/ (accessed Sep 26, 2019).

(77) Meanwell, N. A.; Krystal, M. R.; Nowicka-Sans, B.; Langley, D. R.; Conlon, D. A.; Eastgate, M. D.; Grasela, D. M.; Timmins, P.; Wang, T.; Kadow, J. F. Inhibitors of HIV-1 attachment: The discovery and development of Temsavir and its prodrug Fostemsavir. *J. Med. Chem.* **2018**, *61*, 62–80.

(78) Buscher, B.; Laakso, S.; Mascher, H.; Pusecker, K.; Doig, M.; Dillen, L.; Wagner-Redeker, W.; Pfeifer, T.; Delrat, P.; Timmerman, P. Bioanalysis for plasma protein binding studies in drug discovery and drug development: views and recommendations of the european bioanalysis forum. *Bioanalysis* **2014**, *6*, 673–682.

(79) Dow, N. Determination of compound binding to plasma proteins. *Curr. Protoc. Pharmacol.* **2006**, *34*, 7.5.1-7.5.15.

4.1.8. Supporting information

Water-soluble prodrugs of A$_{2B}$ adenosine receptor antagonists

Ahmed Temirak, Jörg Hockemeyer, Christin Vielmuth, Sonja Hinz, and Christa E. Müller*

PharmaCenter Bonn, Pharmaceutical Institute, Department of Pharmaceutical & Medicinal Chemistry, University of Bonn, An der Immenburg 4, D-53121 Bonn, Germany

Table of contents
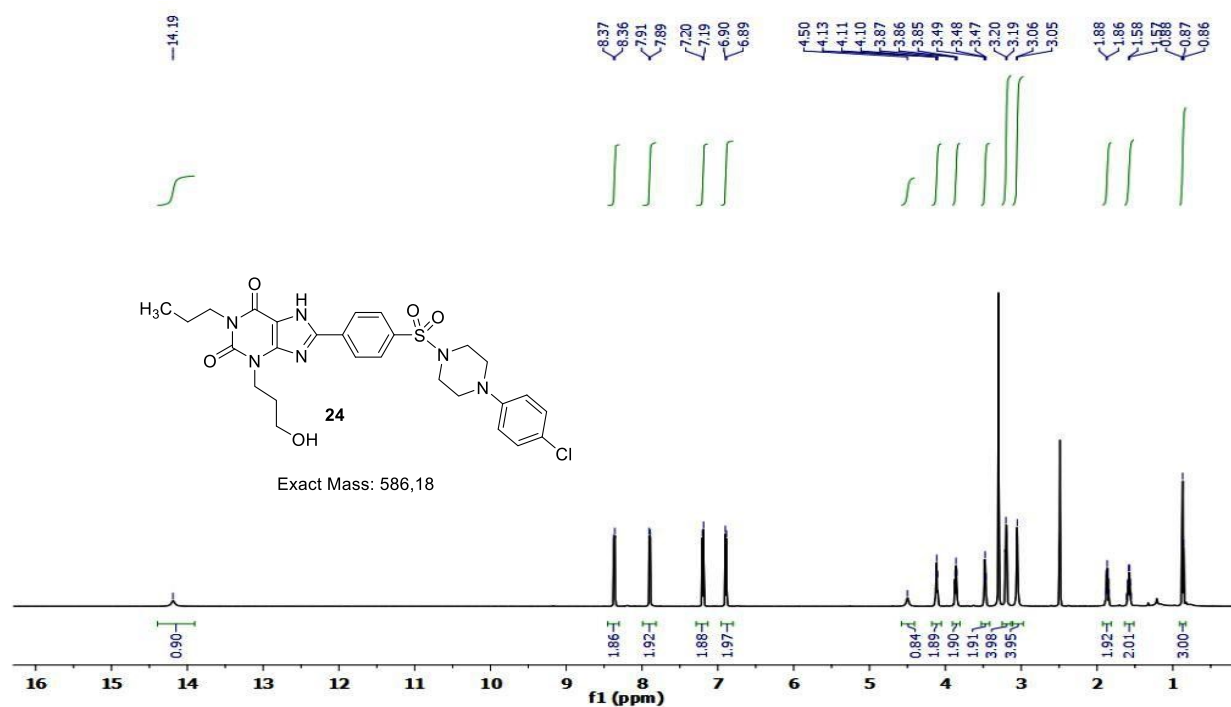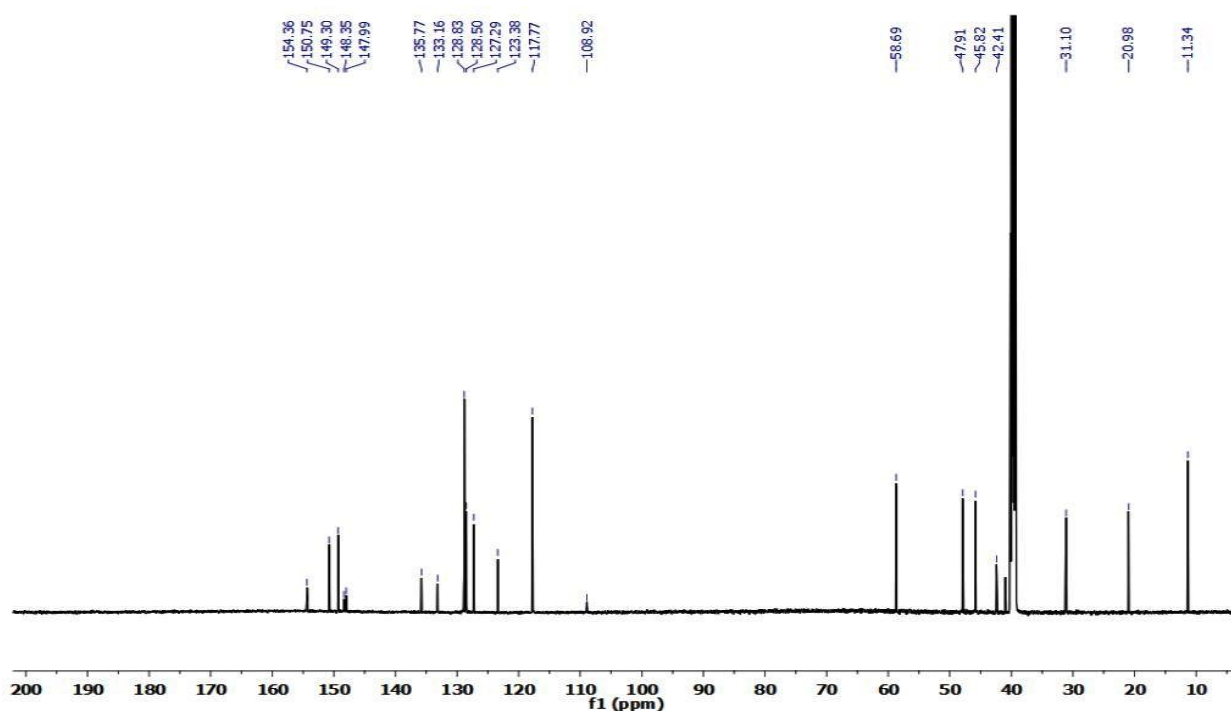
¹HNMR

¹³CNMR

Figure S1. ¹H (600 MHz) and ¹³C (151 MHz) spectra (DMSO-d_6) of 8-(4-((4-(4-chlorophenyl)piperazin-1-yl)sulfonyl)phenyl)-3-(3-hydroxypropyl)-1-propyl-3,7-dihydro-1*H*-purine-2,6-dione (**24**)

¹H NMR
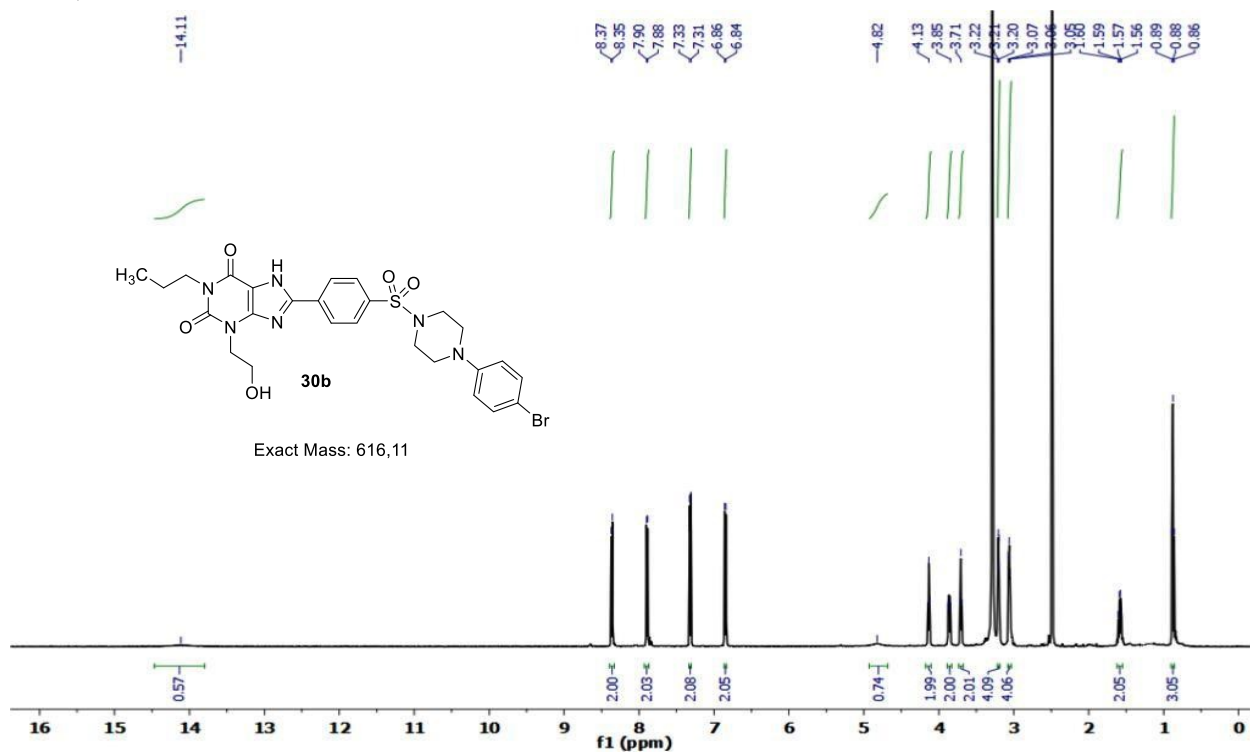
¹³C NMR
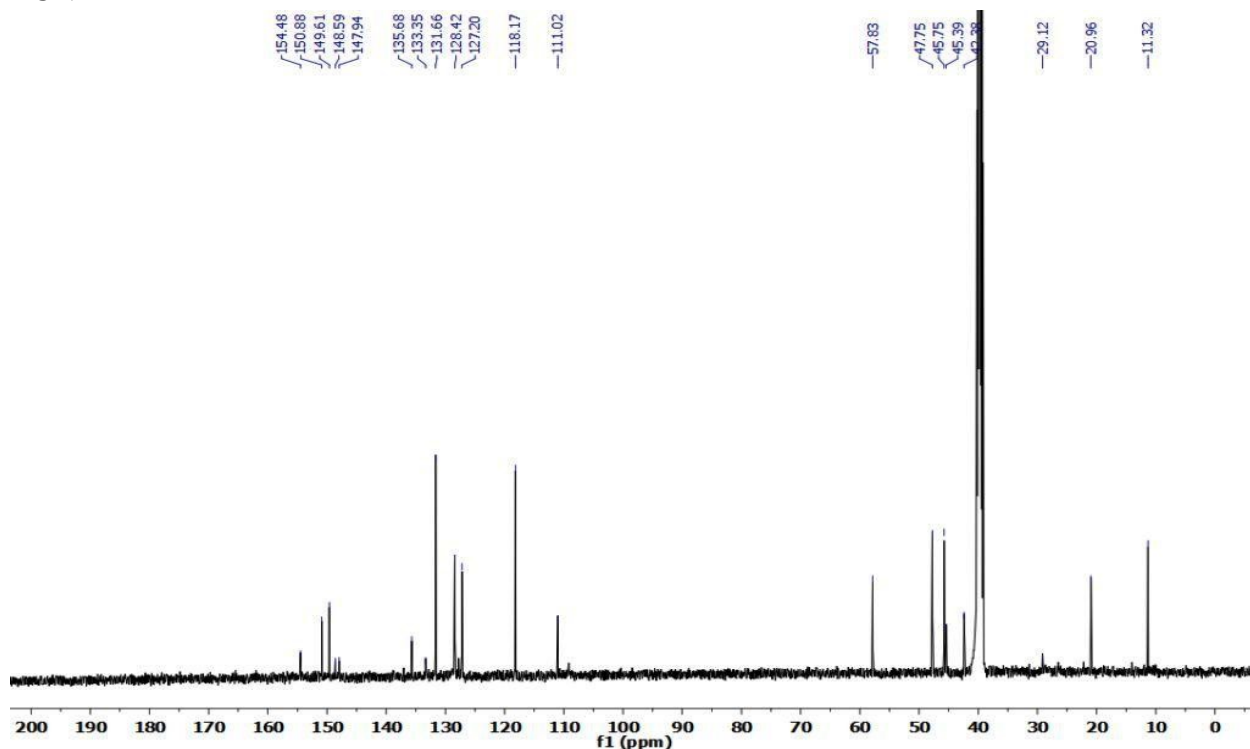
Figure S2. ¹H (500 MHz) and ¹³C (126 MHz) spectra (DMSO-d_6) of 8-(4-((4-(4-bromophenyl)piperazin-1-yl)sulfonyl)phenyl)-3-(2-hydroxyethyl)-1-propyl-3,7-dihydro-1*H*-purine-2,6-dione (**30b**)
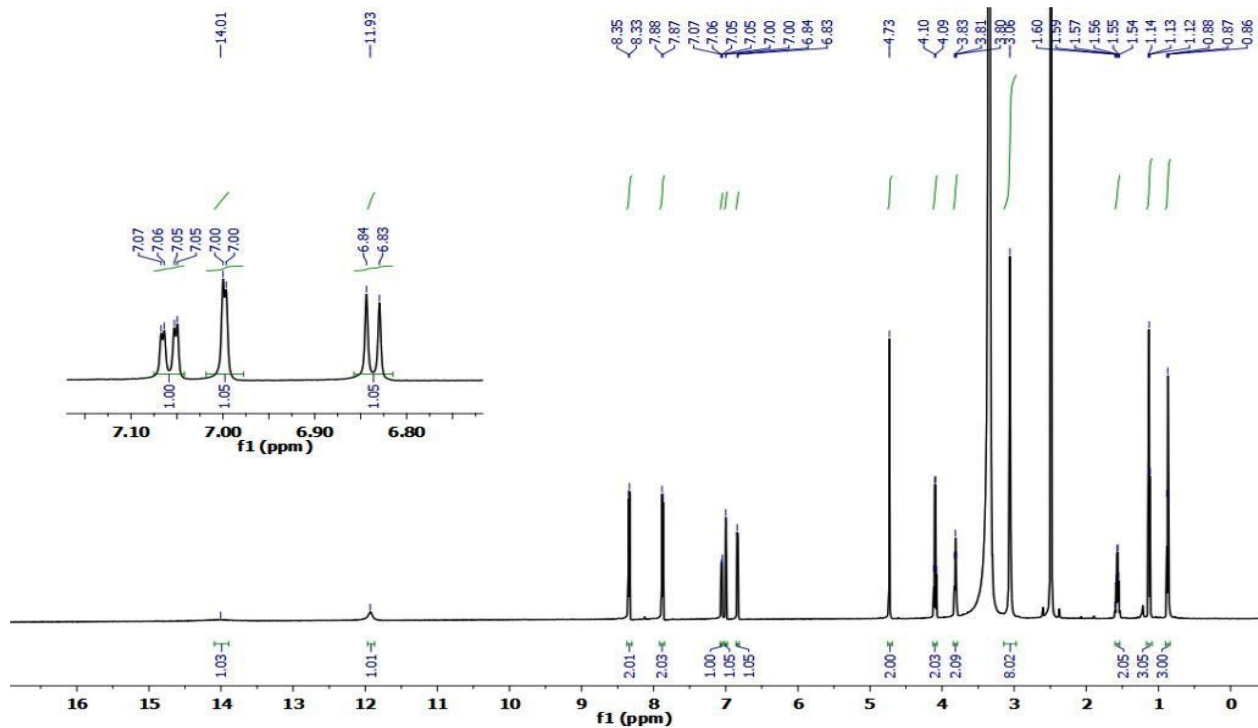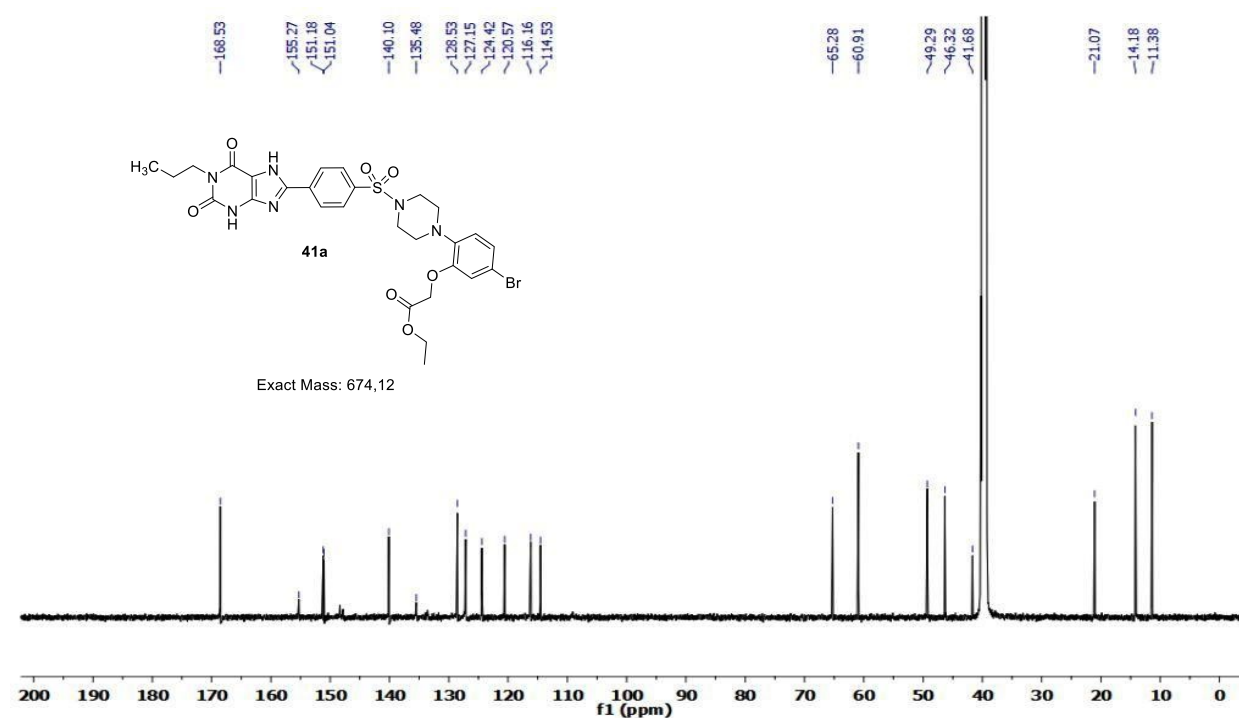
¹HNMR

¹³CNMR

Figure S3. ¹H (500 MHz) and ¹³C (126 MHz) spectra (DMSO-*d*₆) of ethyl 2-(5-bromo-2-(4-((4-(2,6-dioxo-1-propyl-2,3,6,7-tetrahydro-1*H*-purin-8-yl)phenyl)sulfonyl)piperazin-1-yl)phenoxy) acetate (**41a**)
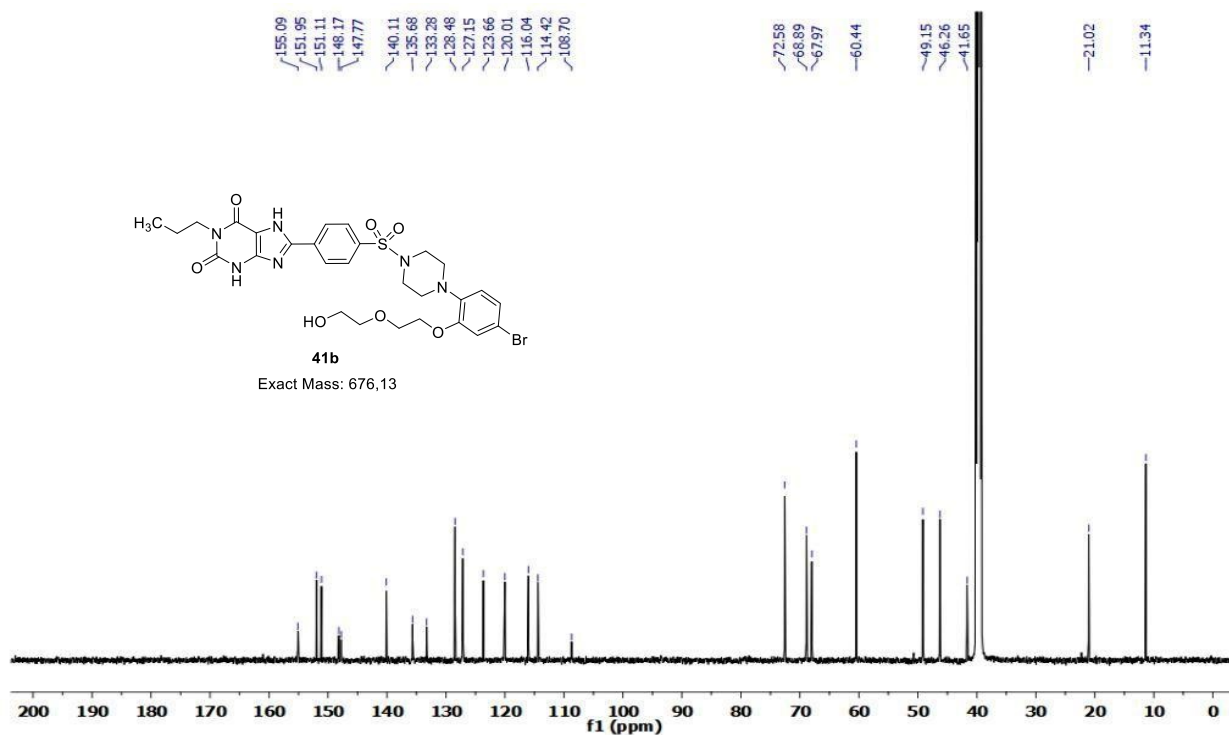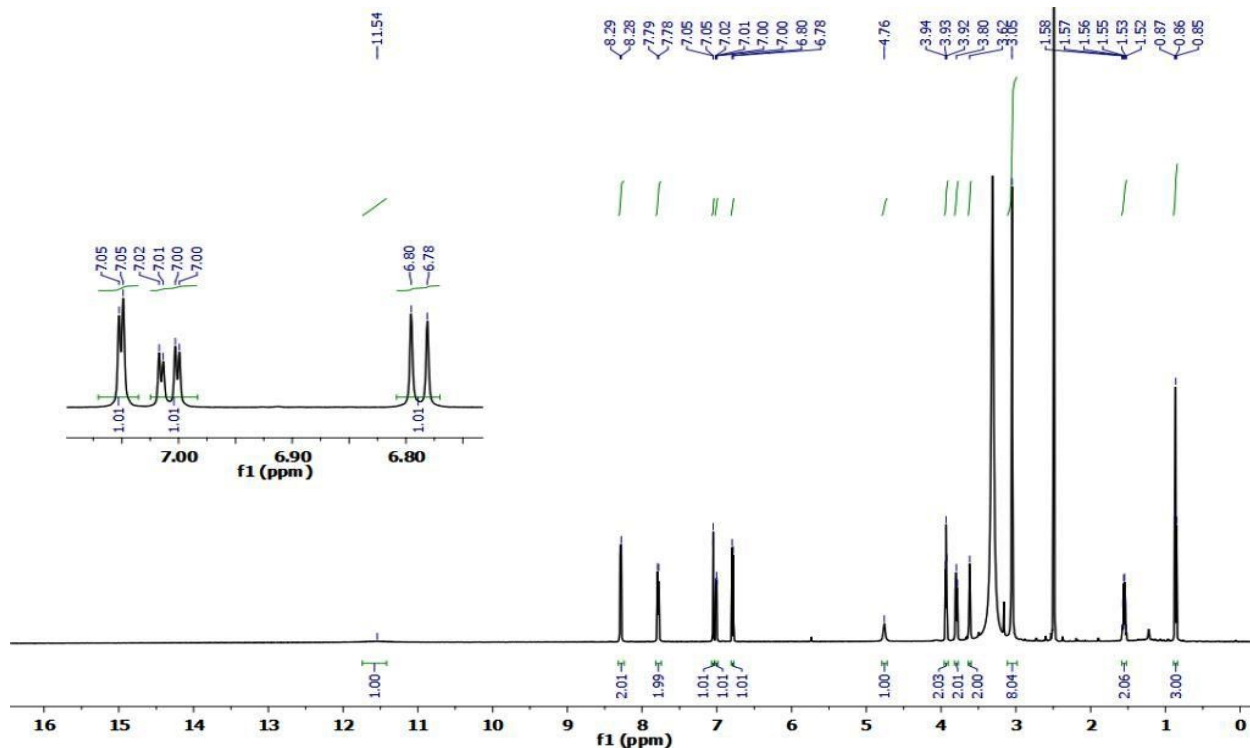
¹HNMR
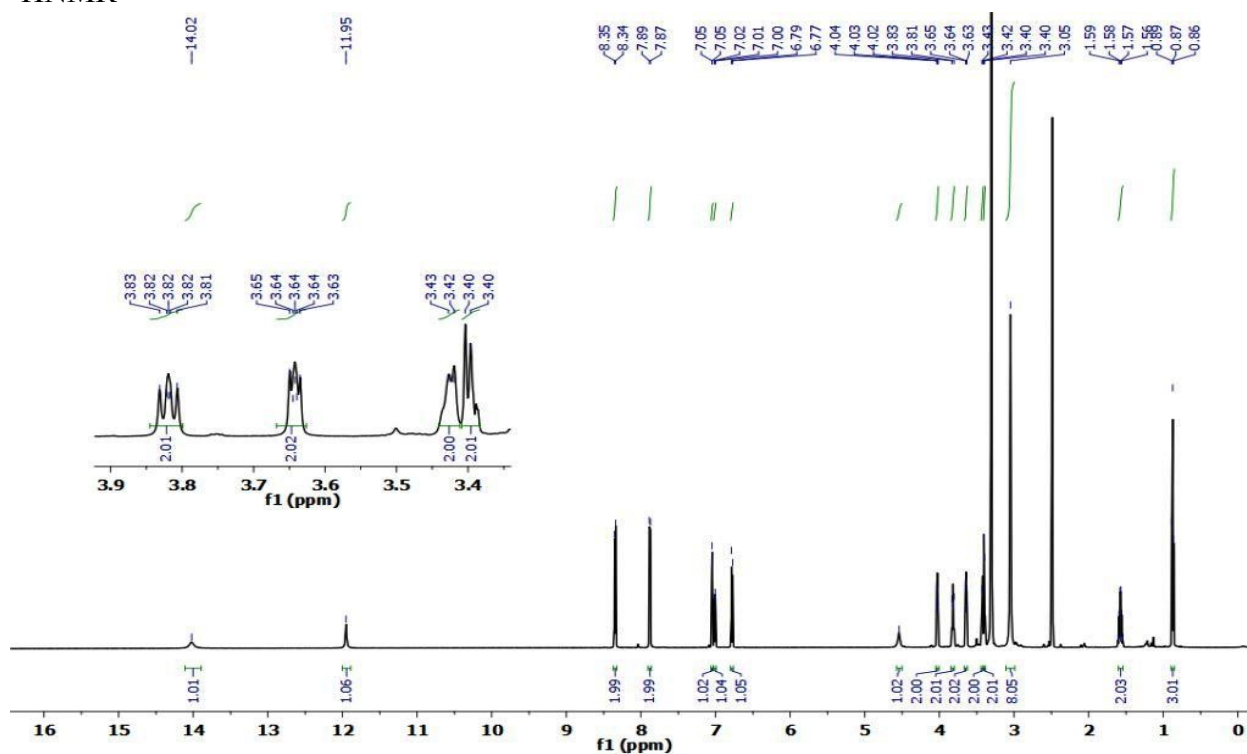
¹³CNMR

Figure S4. ¹H (500 MHz) and ¹³C (126 MHz) spectra (DMSO-d_6) of 8-(4-((4-(4-bromo-2-(2-(2-hydroxyethoxy)ethoxy)phenyl)piperazin-1-yl)sulfonyl)phenyl)-1-propyl-3,7-dihydro-1*H*-purine-2,6-dione (**41b**)
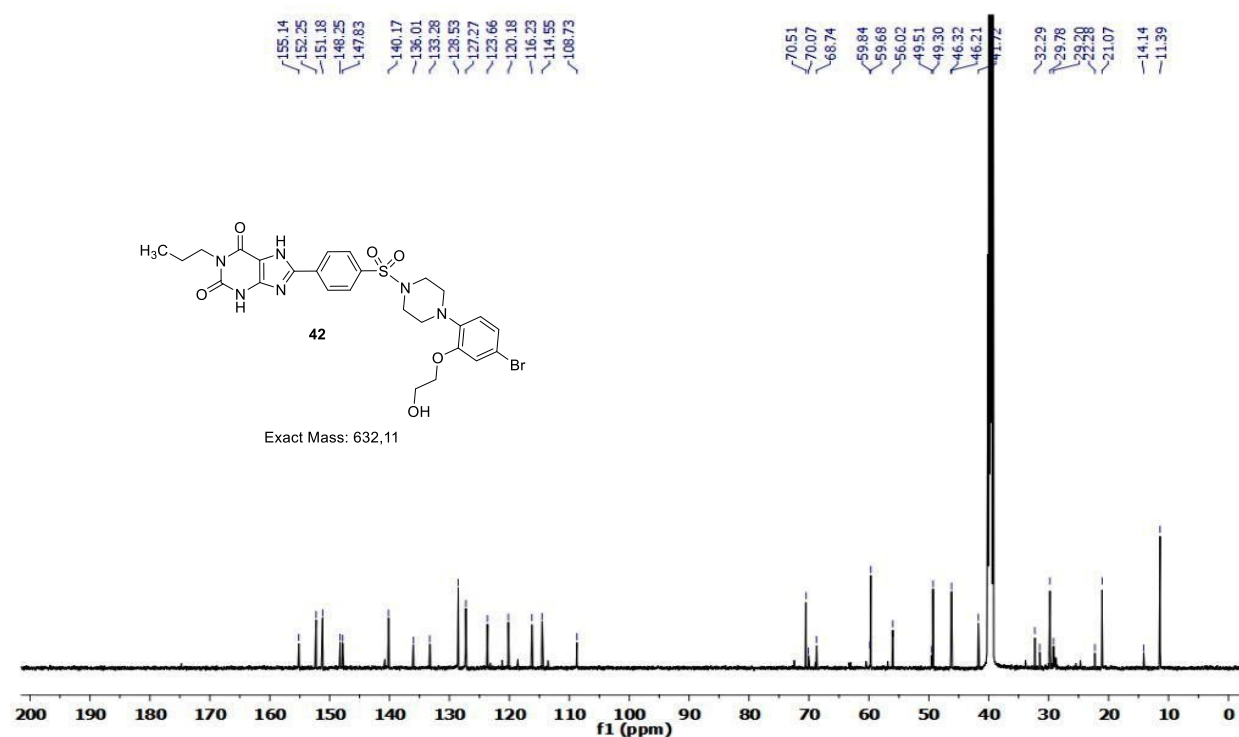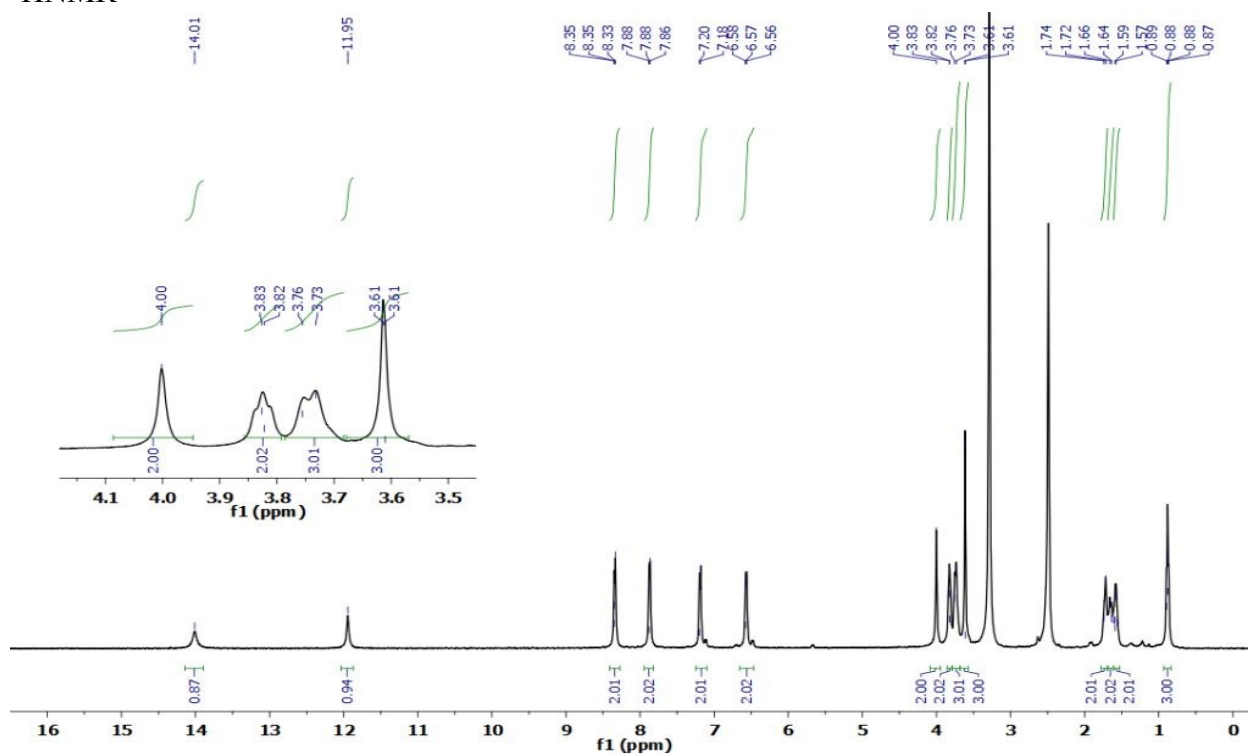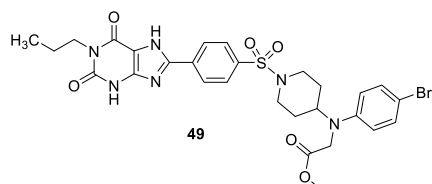
¹HNMR

¹³CNMR

Figure S5. ¹H (500 MHz) and ¹³C (126 MHz) spectra (DMSO-*d*₆) of 8-(4-((4-(4-bromo-2-(2-hydroxyethoxy)phenyl)piperazin-1-yl)sulfonyl)phenyl)-1-propyl-3,7-dihydro-1*H*-purine-2,6-dione **(42)**

¹HNMR

¹³CNMR
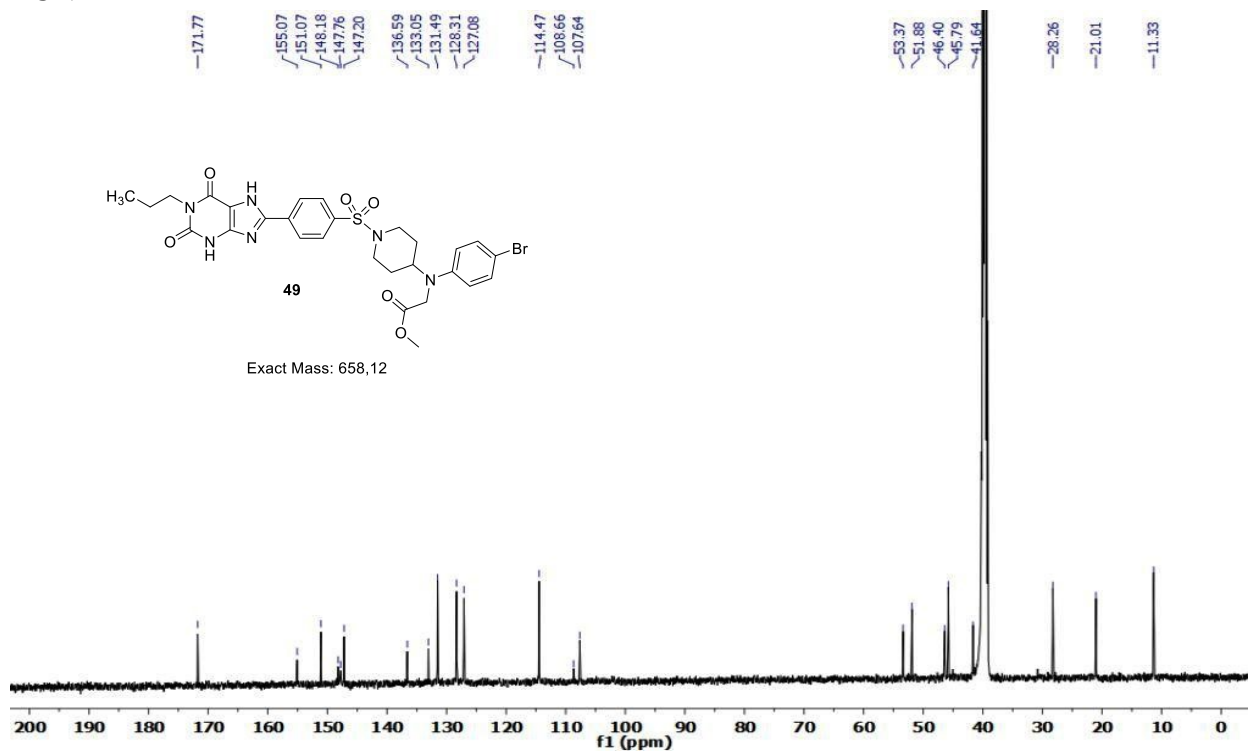
Figure S6. ¹H (500 MHz) and ¹³C (126 MHz) spectra (DMSO-d_6) of methyl N-(4-bromophenyl)-*N*-(1-((4-(2,6-dioxo-1-propyl-2,3,6,7-tetrahydro-1*H*-purin-8-yl)phenyl)sulfonyl)piperidin-4-yl)glycinate (**49**)
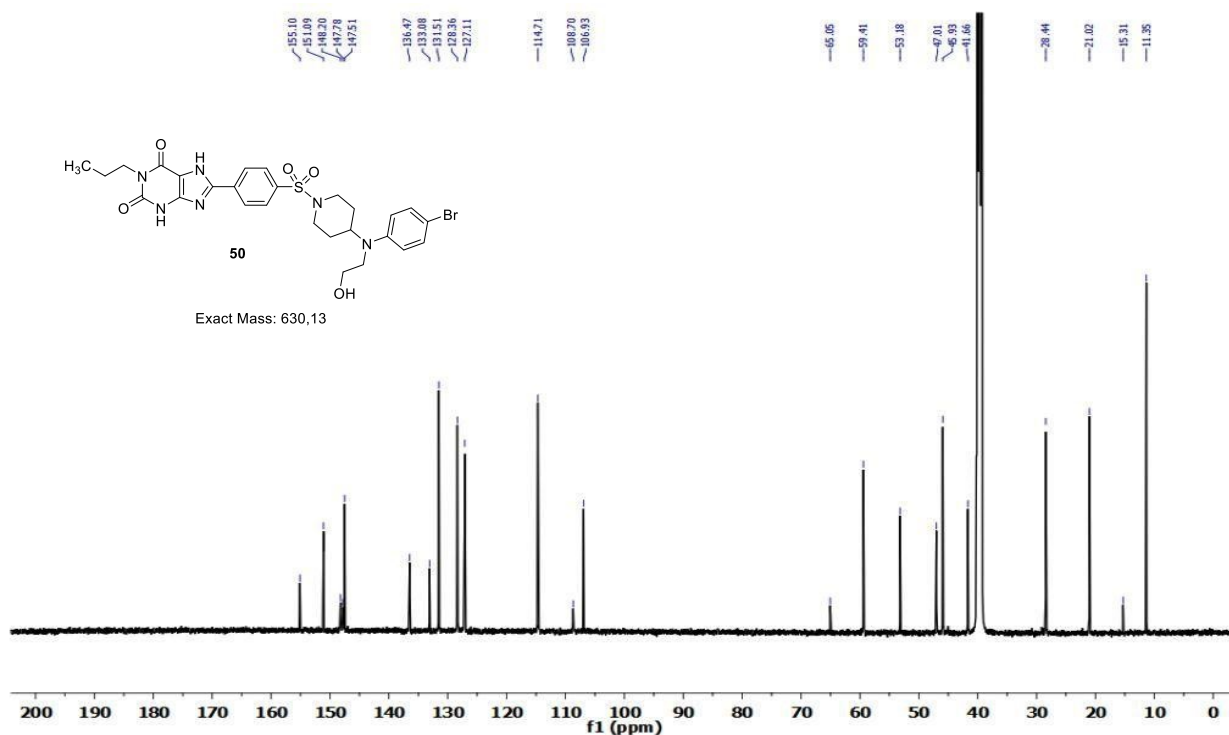
^{1}HNMR

^{13}CNMR

Figure S7. ^{1}H (500 MHz) and ^{13}C (126 MHz) spectra (DMSO-d_6) of 8-(4-((4-((4-bromophenyl)(2-hydroxyethyl)amino)piperidin-1-yl)sulfonyl)phenyl)-1-propyl-3,7-dihydro-1*H*-purine-2,6-dione (**50**)
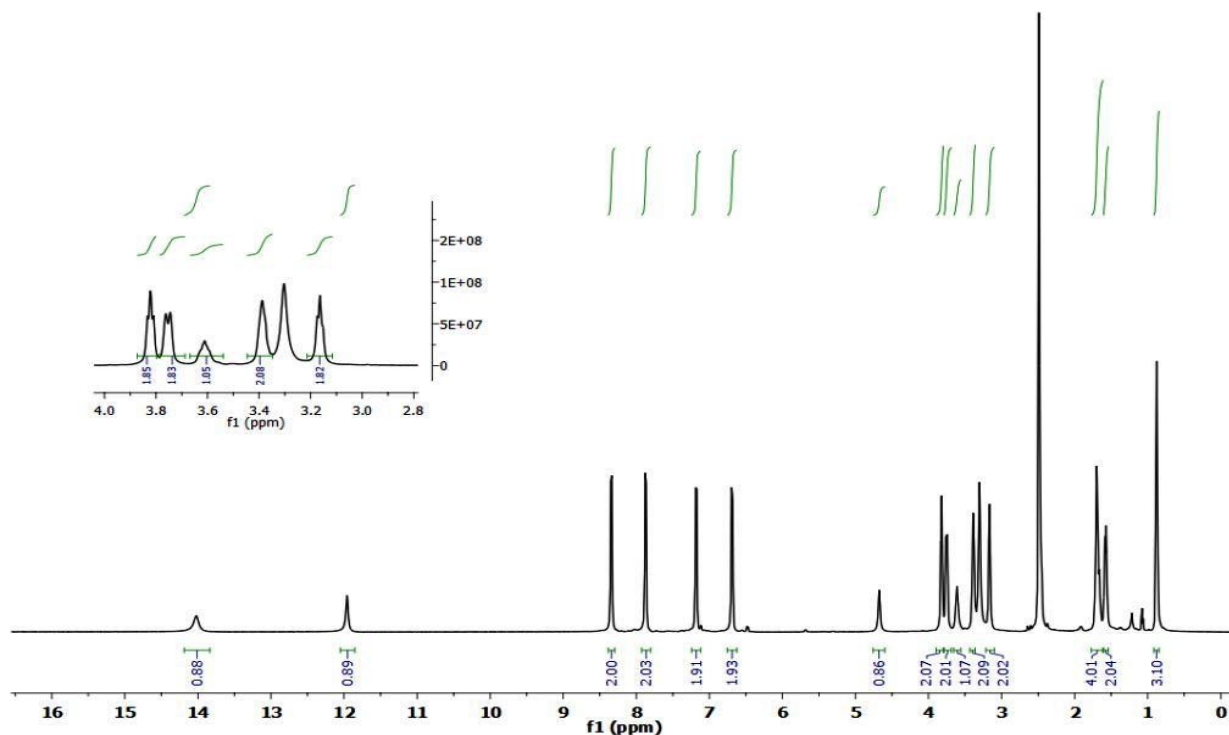
¹HNMR
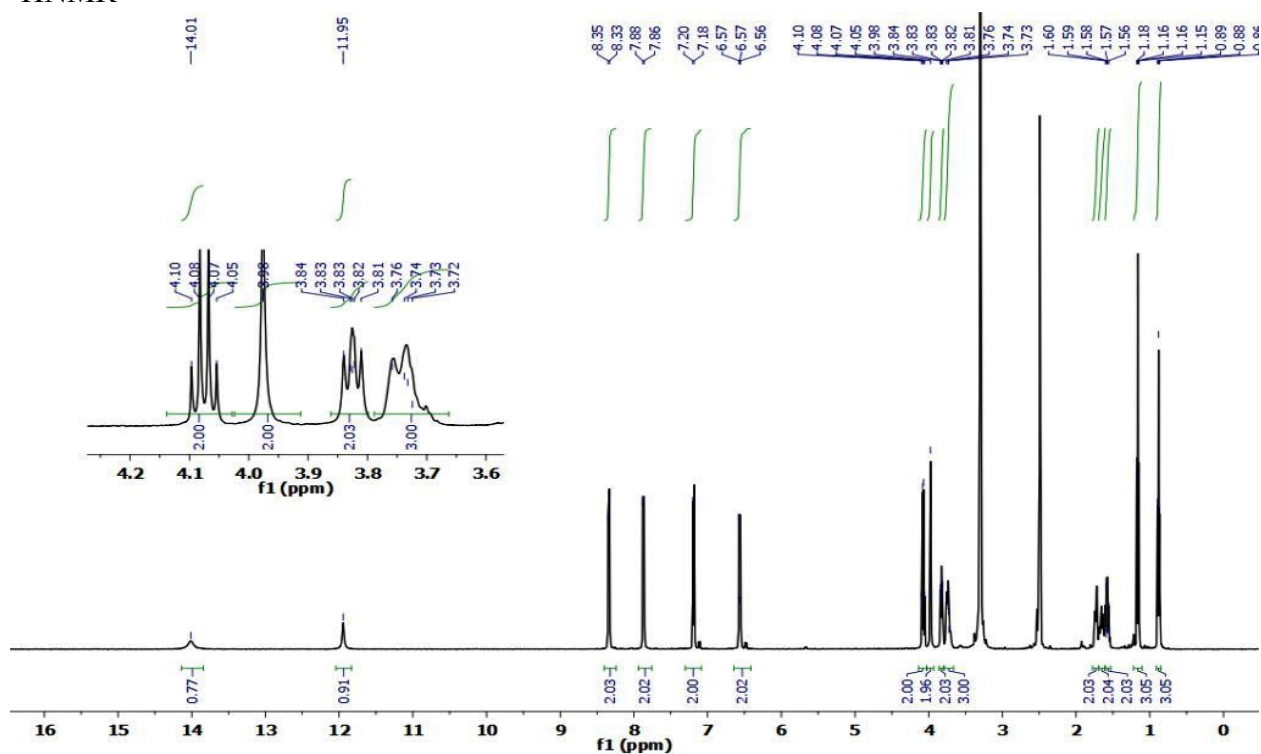
¹³CNMR
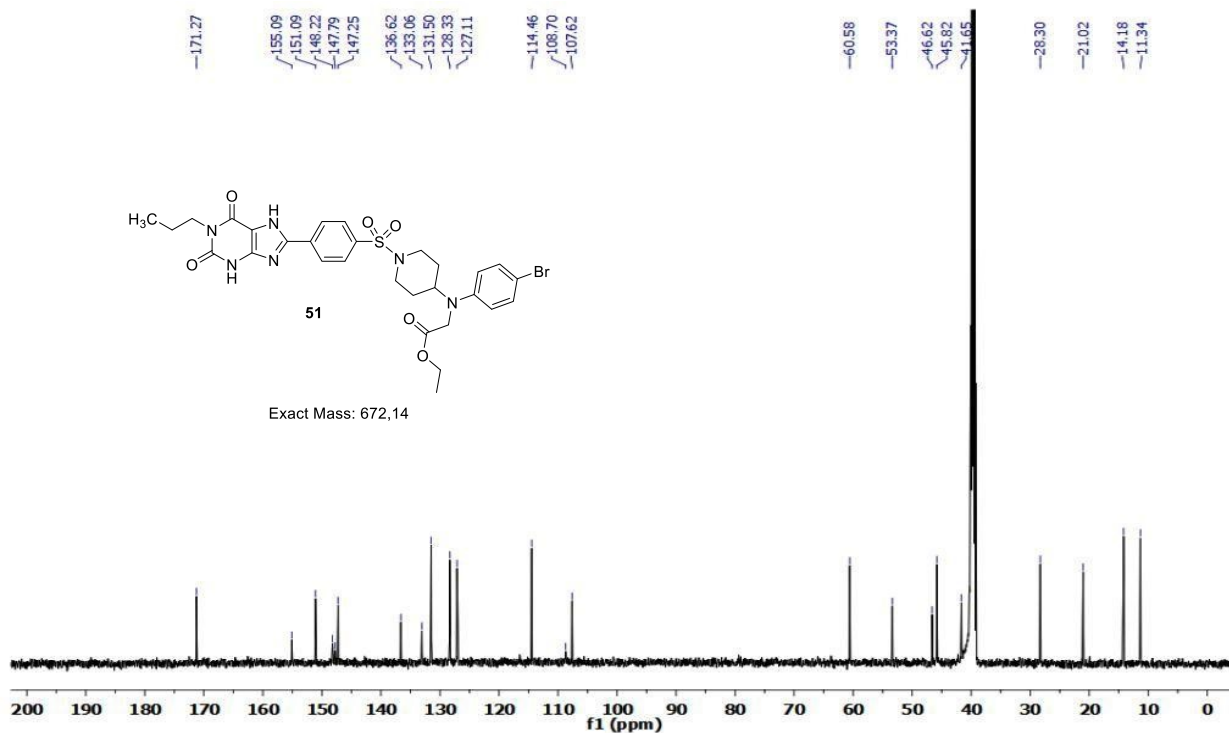
Figure S8. ¹H (500 MHz) and ¹³C (126 MHz) spectra (DMSO-d_6) of ethyl *N*-(4-bromophenyl)-N-(1-((4-(2,6-dioxo-1-propyl-2,3,6,7-tetrahydro-1*H*-purin-8-yl)phenyl)sulfonyl)piperidin-4-yl)glycinate (**51**)
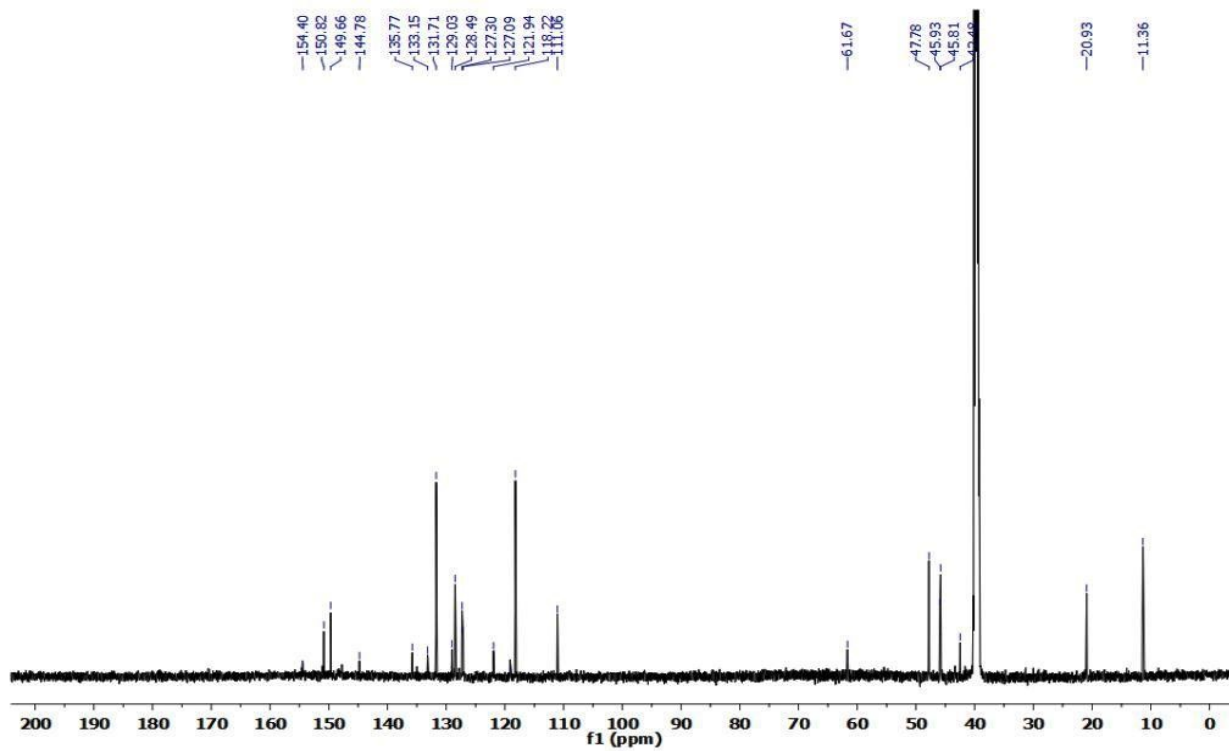
¹HNMR
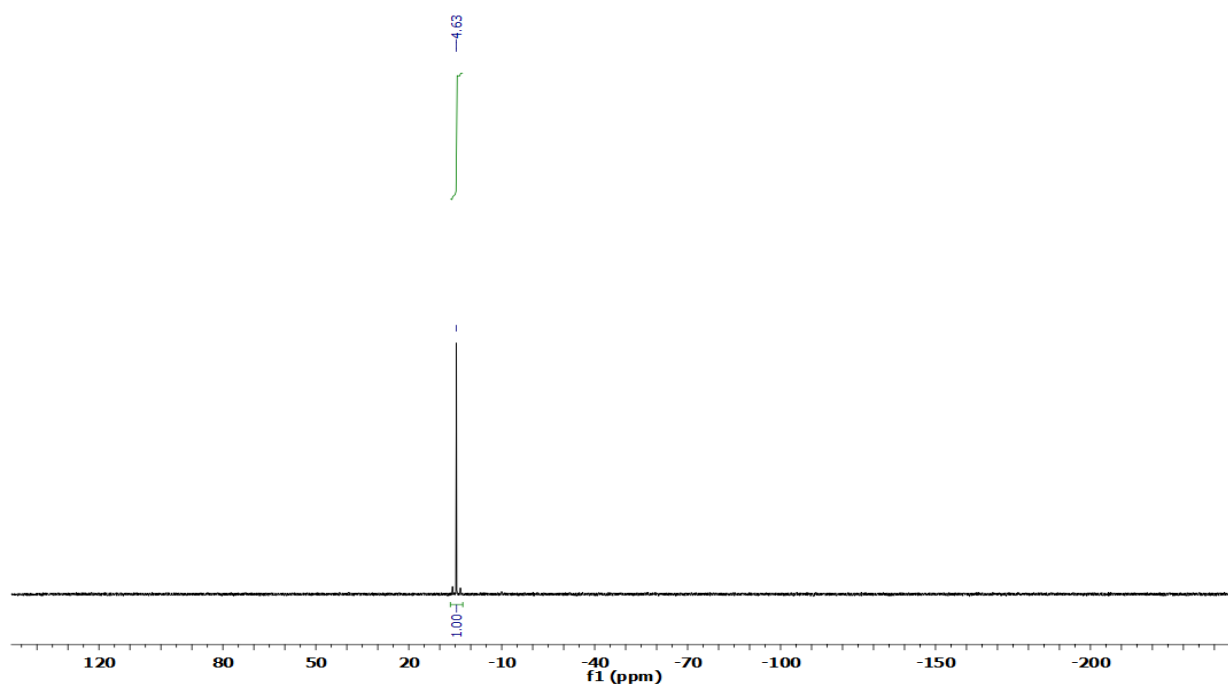
¹³CNMR

^{31}PNMR

Figure S9. ^{1}H (600 MHz), ^{13}C (151 MHz) and ^{31}P (243 MHz) NMR spectra (D$_2$O) of 2-(8-(4-((4-(4-bromophenyl)piperazin-1-yl)sulfonyl)phenyl)-2,6-dioxo-1-propyl-1,2,6,7-tetrahydro-3*H*-purin-3-yl)ethyl dihydrogenphosphate (**52**).

¹HNMR

Exact Mass: 712,07

53
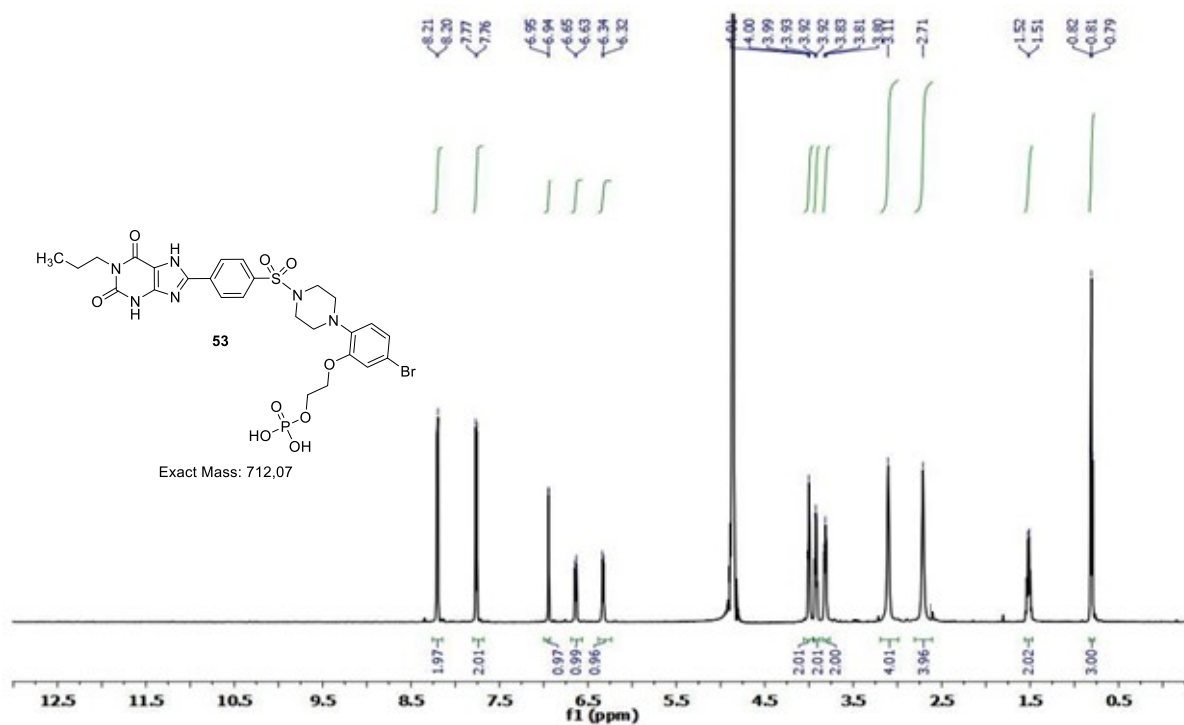
¹³CNMR
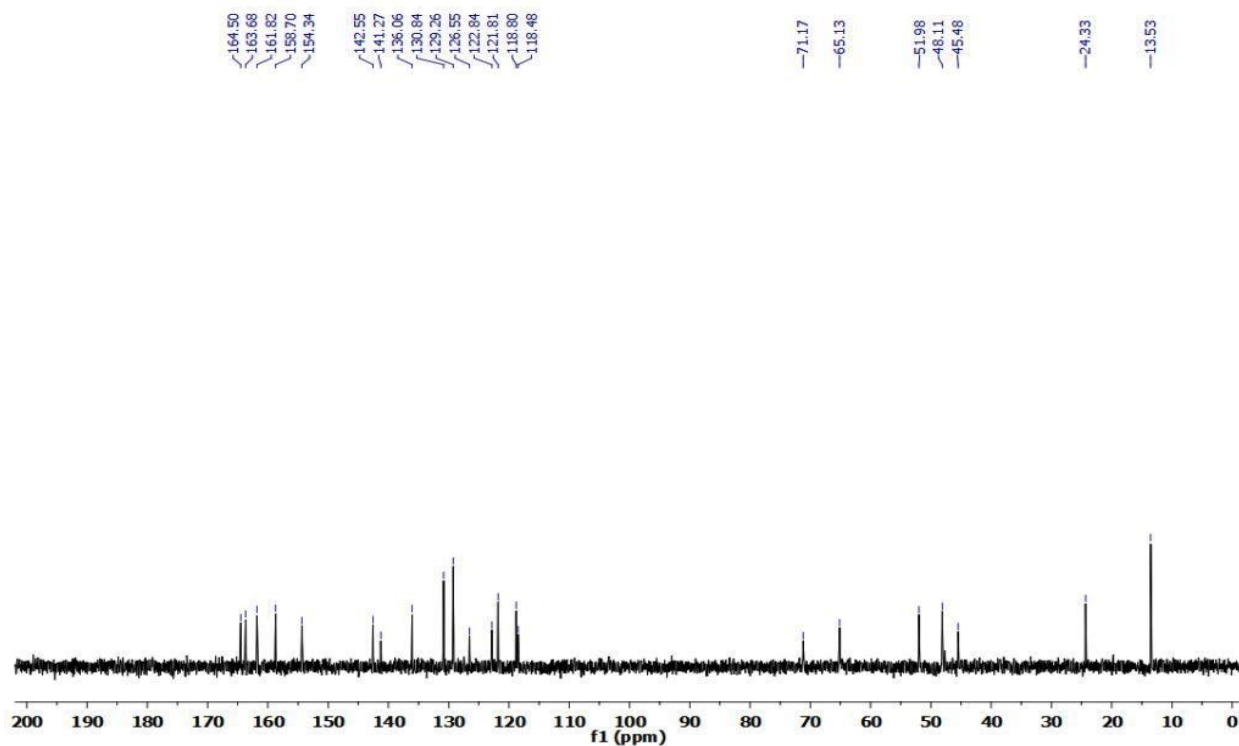
^{31}PNMR
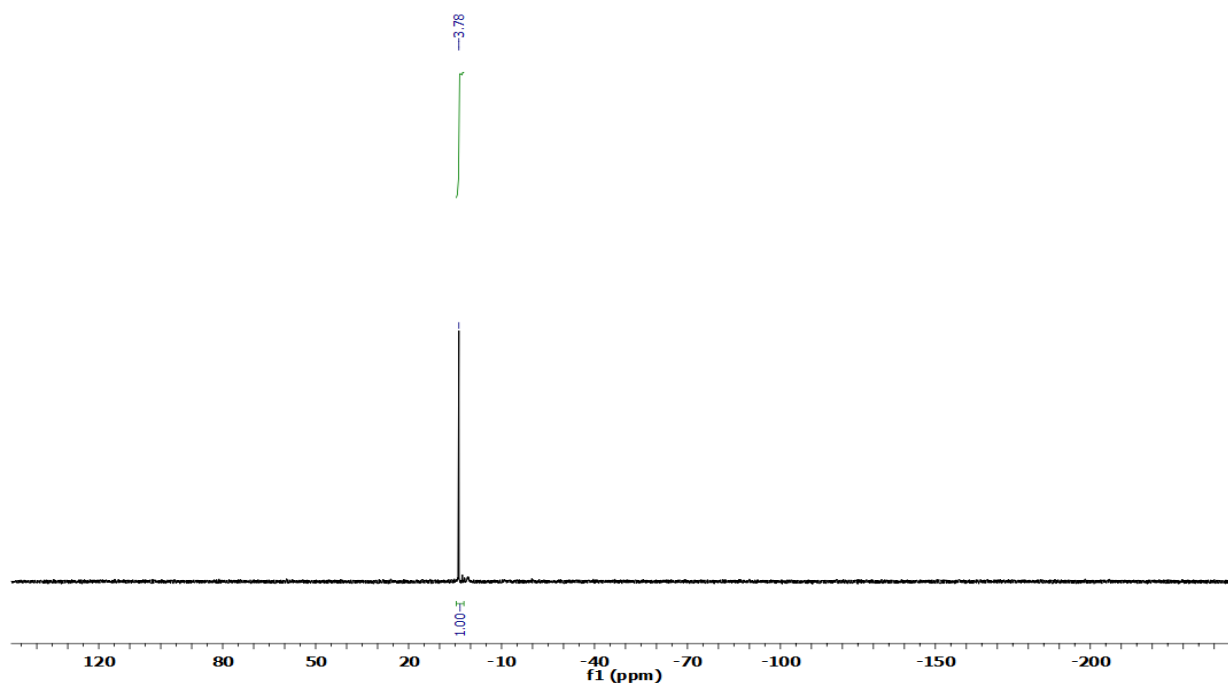
Figure S10. ^{1}H (600 MHz), ^{13}C (151 MHz) and ^{31}P (243 MHz) NMR spectra (D$_2$O) of 2-(5-bromo-2-(4-((4-(2,6-dioxo-1-propyl-2,3,6,7-tetrahydro-1*H*-purin-8-yl)phenyl)sulfonyl)piperazin-1-yl)-phenoxy)ethyl dihydrogenphosphate (**53**)

¹HNMR
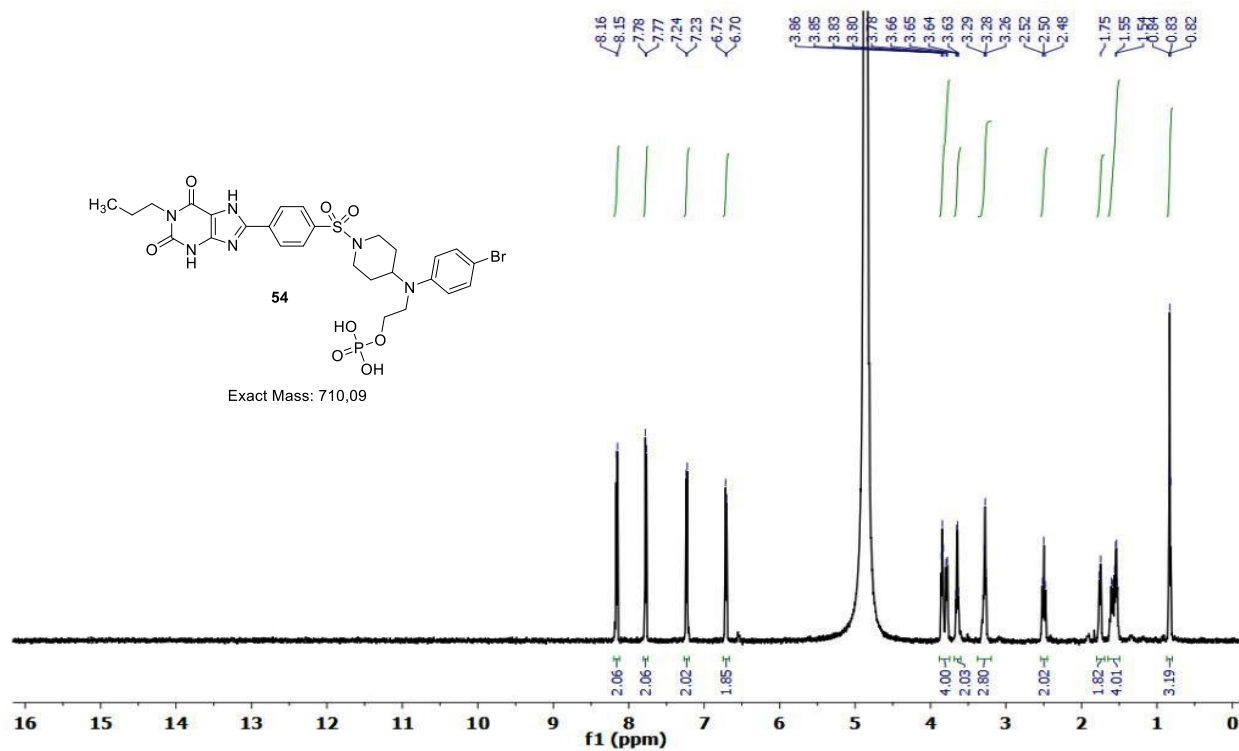
¹³CNMR
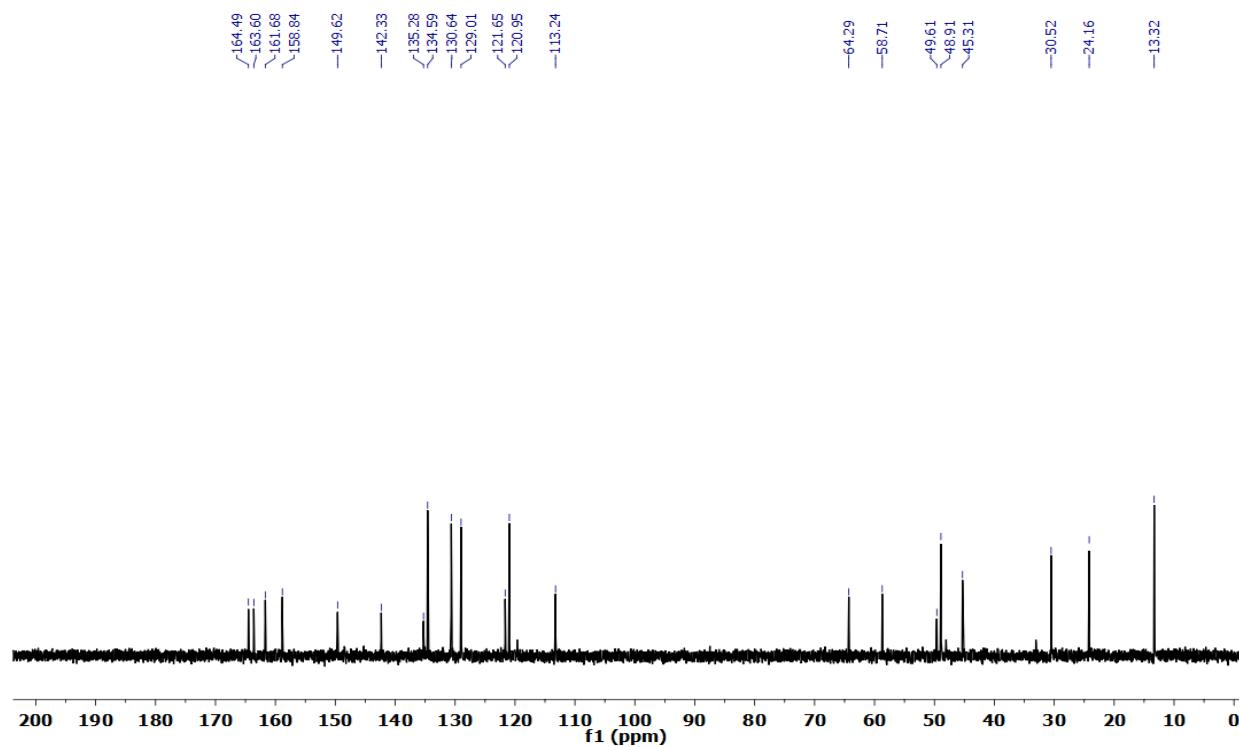
^{31}PNMR
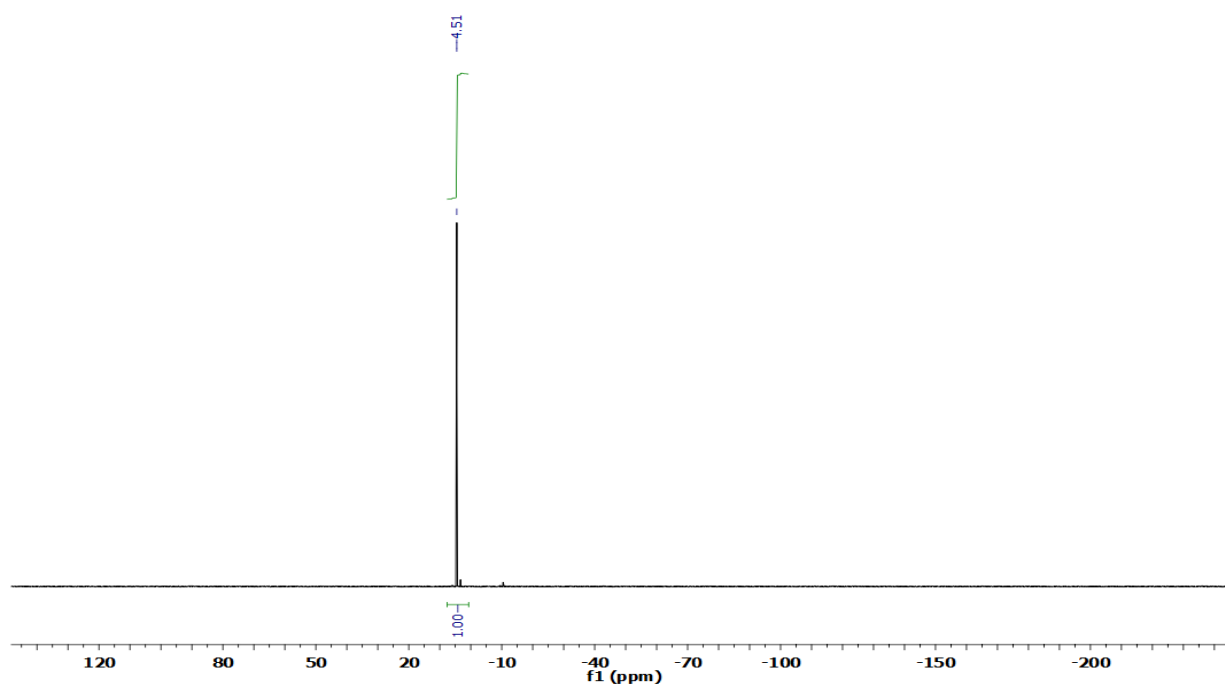
Figure S11. ^{1}H (600 MHz), ^{13}C (151 MHz) and ^{31}P (243 MHz) NMR spectra (D$_2$O) of 2-((4-bromophenyl)(1-((4-(2,6-dioxo-1-propyl-2,3,6,7-tetrahydro-1*H*-purin-8-yl)phenyl)sulfonyl)-piperidin-4-yl)amino) ethyl dihydrogenphosphate (**54**)
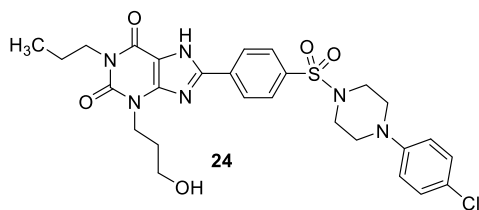
Exact Mass: 586,18
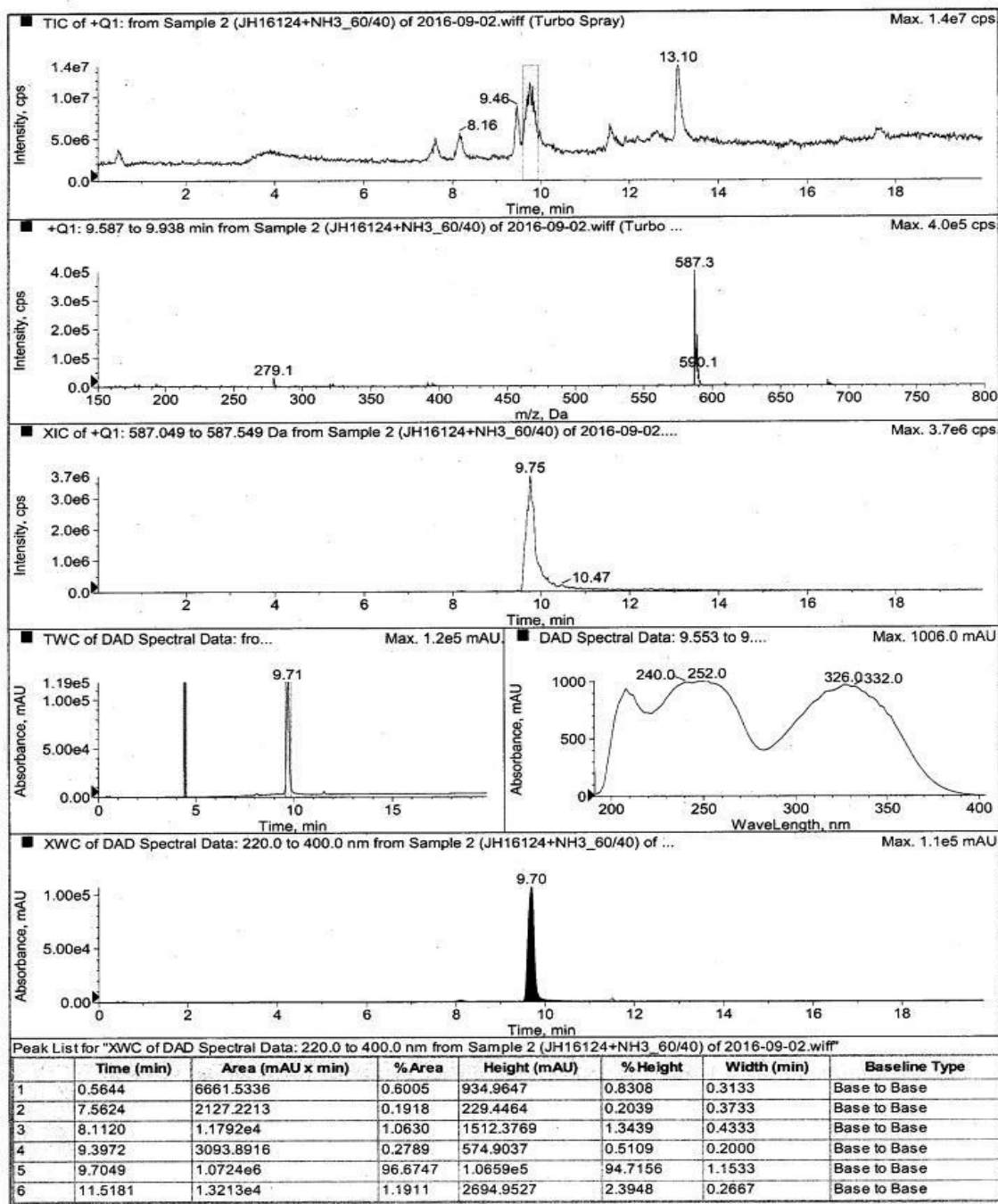
Figure S12. LC-MS spectrum of compound **24***

*The purity of the compound **24** is 96.67% (retention time: 9.70 min belongs to the desired compound **24**; also see NMR spectra, **Figure S1**)

30b

Exact Mass: 616,11

	Time (min)	Area (mAU x min)	%Area	Height (mAU)	%Height	Width (min)	Baseline Type
1	0.5413	2930.5087	0.3401	796.1333	0.5836	0.1467	Base to Base
2	10.7007	2.9204e4	3.3888	5239.9840	3.8409	0.3933	Base to Base
3	11.2950	3490.0045	0.4050	923.0333	0.6766	0.1400	Base to Base
4	11.5008	8.2072e5	95.2365	1.2824e5	93.9999	0.4733	Base to Base
5	11.8900	5425.8315	0.6296	1226.6584	0.8991	0.2133	Base to Base

Figure S13. LC-MS spectrum of compound **30b***

*The purity of the compound **30b** is 95.24% (retention time: 11.50 min belongs to the desired compound **30b**; also see NMR spectra, **Figure S2**).

Exact Mass: 674,12
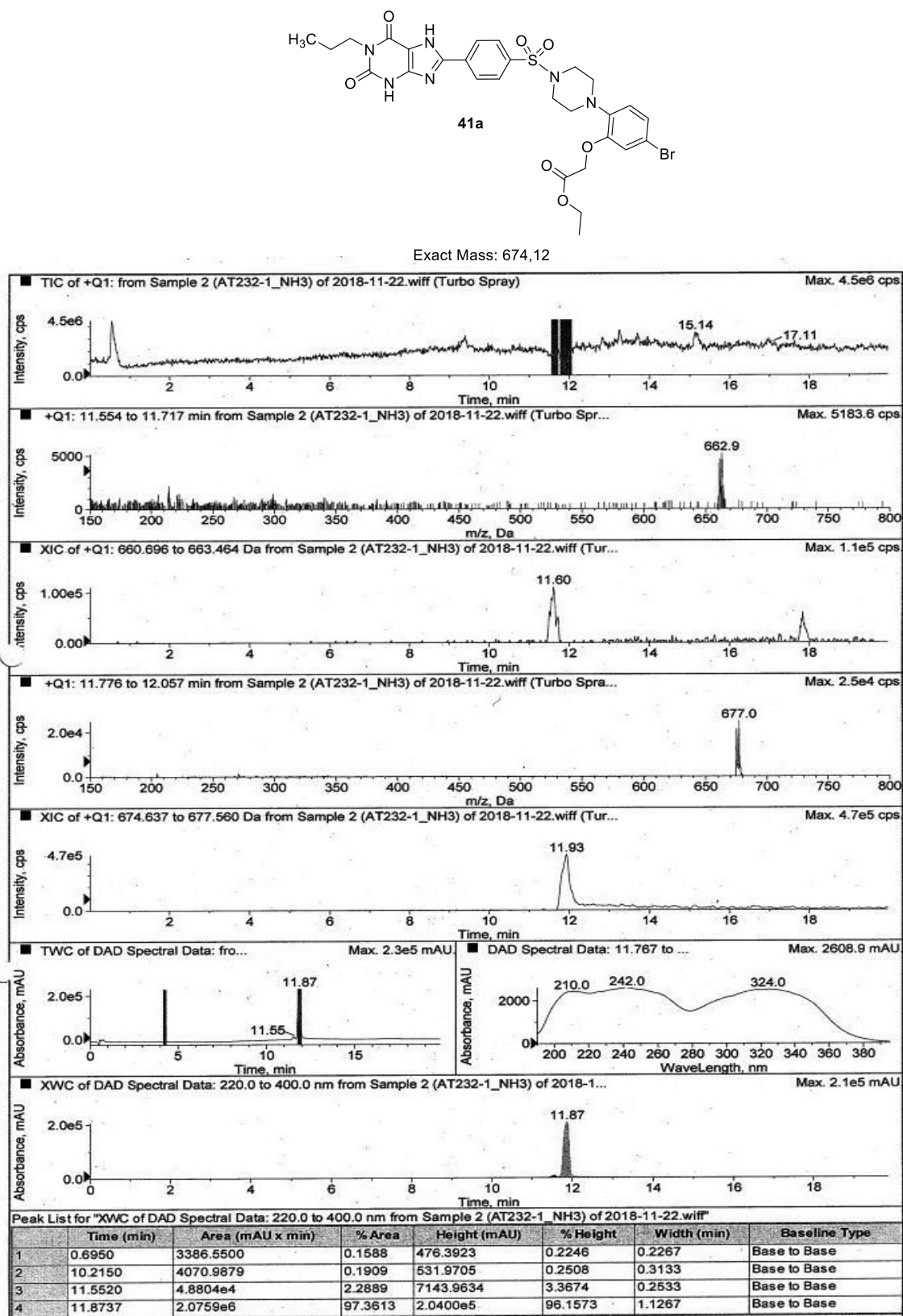
Figure S14. LC-MS spectrum of compound **41a***

*The purity of the compound **41a** is 97.36% (retention time: 11.87 min belongs to the desired compound **41a**; also see NMR spectra, **Figure S3**).

41b
Exact Mass: 676,13

Figure S15. LC-MS spectrum of compound **41b***
*The purity of the compound **41b** is 96.1% (retention time: 11.39 min belongs to the desired compound **41b** and the peak at 0.54 min belongs to the injection peak; also see NMR spectra, **Figure S4**).

Exact Mass: 632,11

Figure S16. LC-MS spectrum of compound **42***
*The purity of the compound **42** is 97.42% (retention time: 11.32 min belongs to the desired compound **42**; also see NMR spectra, **Figure S5**).

Exact Mass: 658,12

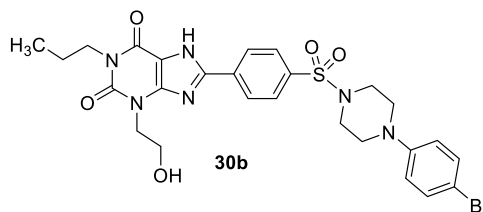|	Time (min)	Area (mAU x min)	%Area	Height (mAU)	%Height	Width (min)	Baseline Type
1	0.3838	1147.6267	0.1246	246.6084	0.2512	0.1600	Base to Base
2	0.4518	1080.4429	0.1173	557.3879	0.5678	0.0667	Base to Base
3	0.5343	4359.9142	0.4734	1032.0273	1.0513	0.1533	Base to Base
4	0.6778	1041.3417	0.1131	205.4949	0.2093	0.1467	Base to Base
5	9.6483	2534.1480	0.2751	485.7243	0.4948	0.2133	Base to Base
6	9.8309	3275.9532	0.3557	609.2024	0.6206	0.2133	Base to Base
7	10.5170	1897.1911	0.2060	318.6986	0.3246	0.3333	Base to Base
8	11.0824	3523.3622	0.3825	1106.1184	1.1267	0.0867	Base to Base
9	11.2804	8.7898e5	95.4357	8.9717e4	91.3879	0.3933	Base to Base
10	11.5960	2.3179e4	2.5166	3893.3679	3.9659	0.2867	Base to Base

Figure S17. LC-MS spectrum of compound **49***

*The purity of the compound **49** is 95.43% (retention time: 11.28 min belongs to the desired compound **49**; also see NMR spectra, **Figure S6**).

Exact Mass: 630,13

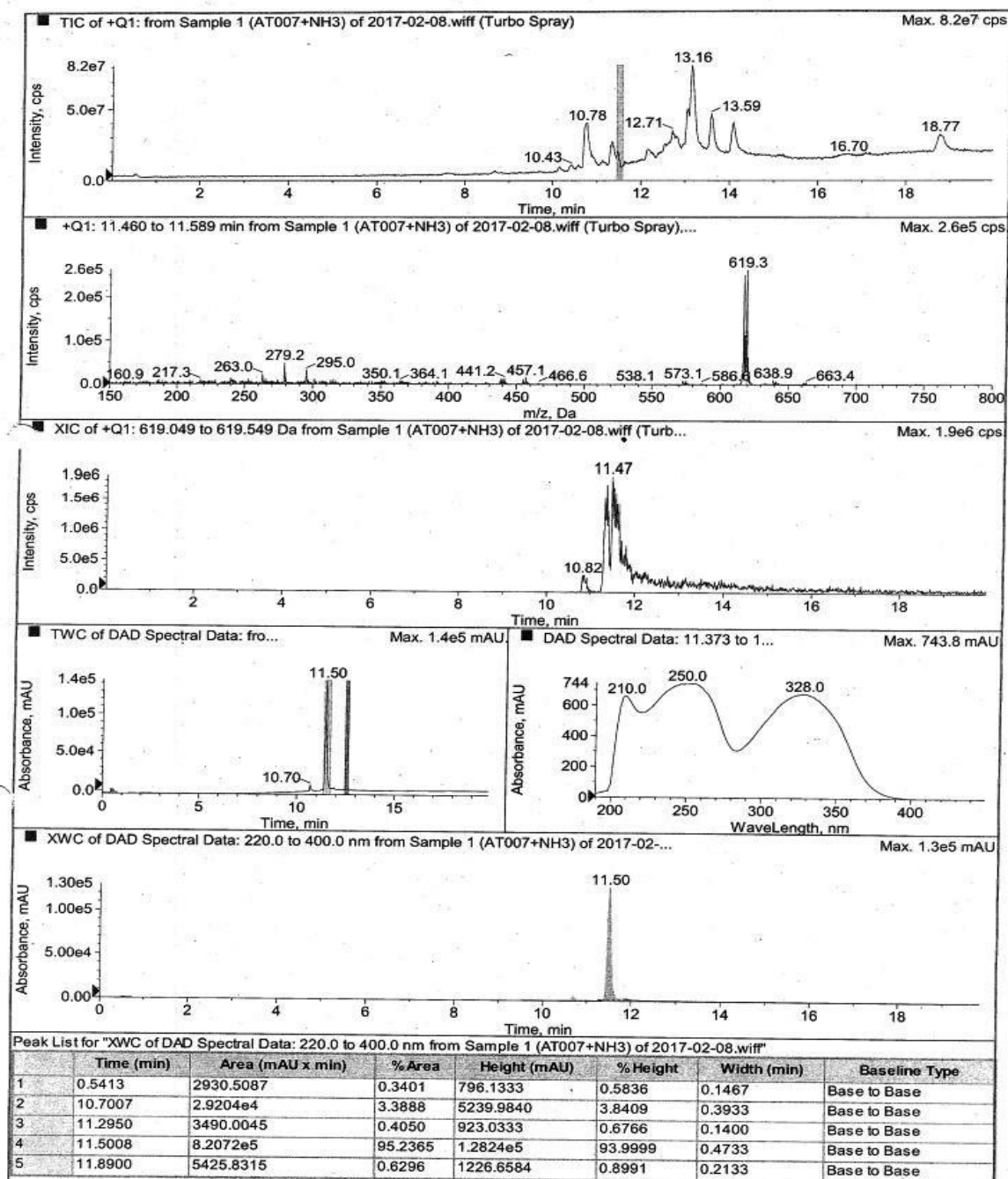|	Time (min)	Area (mAU x min)	% Area	Height (mAU)	% Height	Width (min)	Baseline Type
1	0.3570	5223.1479	0.3304	665.1192	0.3297	0.2600	Base to Base
2	0.4712	9135.4700	0.5779	1612.2915	0.7992	0.1467	Valley
3	0.6120	6706.4083	0.4242	952.9060	0.4724	0.2133	Valley
4	1.3482	3401.6636	0.2152	738.6347	0.3661	0.8200	Base to Base
5	8.3429	1798.9644	0.1138	304.0101	0.1507	0.2133	Base to Base
6	9.0539	5343.0896	0.3380	410.8541	0.2037	0.5467	Base to Base
7	9.4763	2994.0772	0.1894	418.1051	0.2073	0.2933	Base to Base
8	10.4159	950.0856	0.0601	243.3088	0.1206	0.1400	Base to Base
9	10.7031	1.5440e4	0.9767	2653.8502	1.3155	0.3333	Base to Base
10	10.9225	5668.6595	0.3586	676.5504	0.3354	0.2467	Base to Base
11	11.1946	2199.6875	0.1391	496.5595	0.2461	0.1600	Base to Base
12	11.4776	1.5208e6	96.1985	1.9228e5	95.3155	0.9067	Base to Base
13	12.2367	1236.7672	0.0782	277.9533	0.1378	0.1600	Base to Base

Figure S18. LC-MS spectrum of compound **50***

*The purity of the compound **50** is 96.20% (retention time: 11.48 min belongs to the desired compound **50**; also see NMR spectra, **Figure S7**).
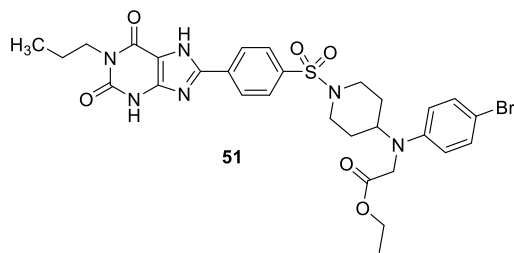
Exact Mass: 672,14
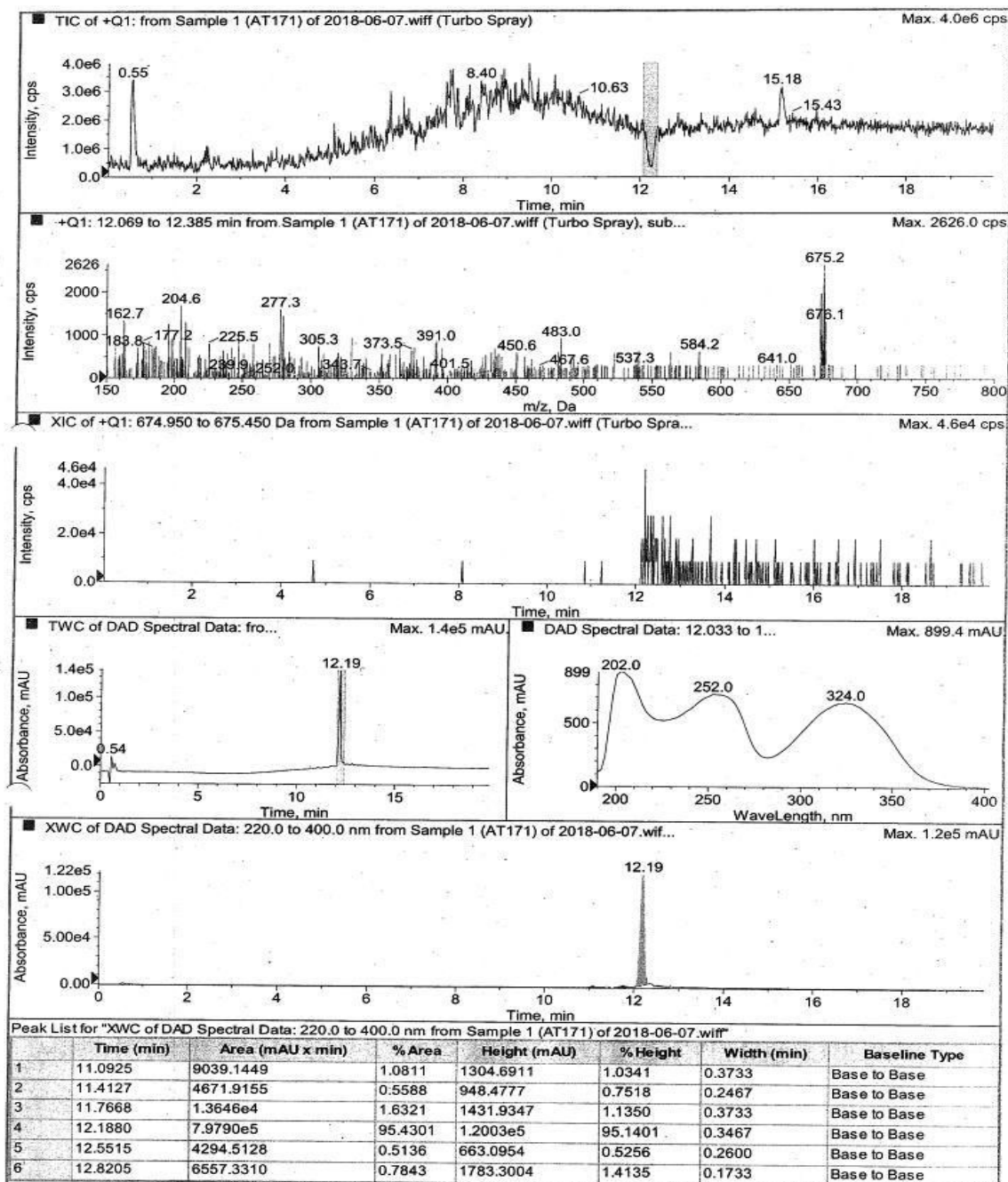
Figure S19. LC-MS spectrum of compound **51***
*The purity of the compound **51** is 95.43% (retention time: 12.19 min belongs to the desired compound **51**; also see NMR spectra, **Figure S8**).
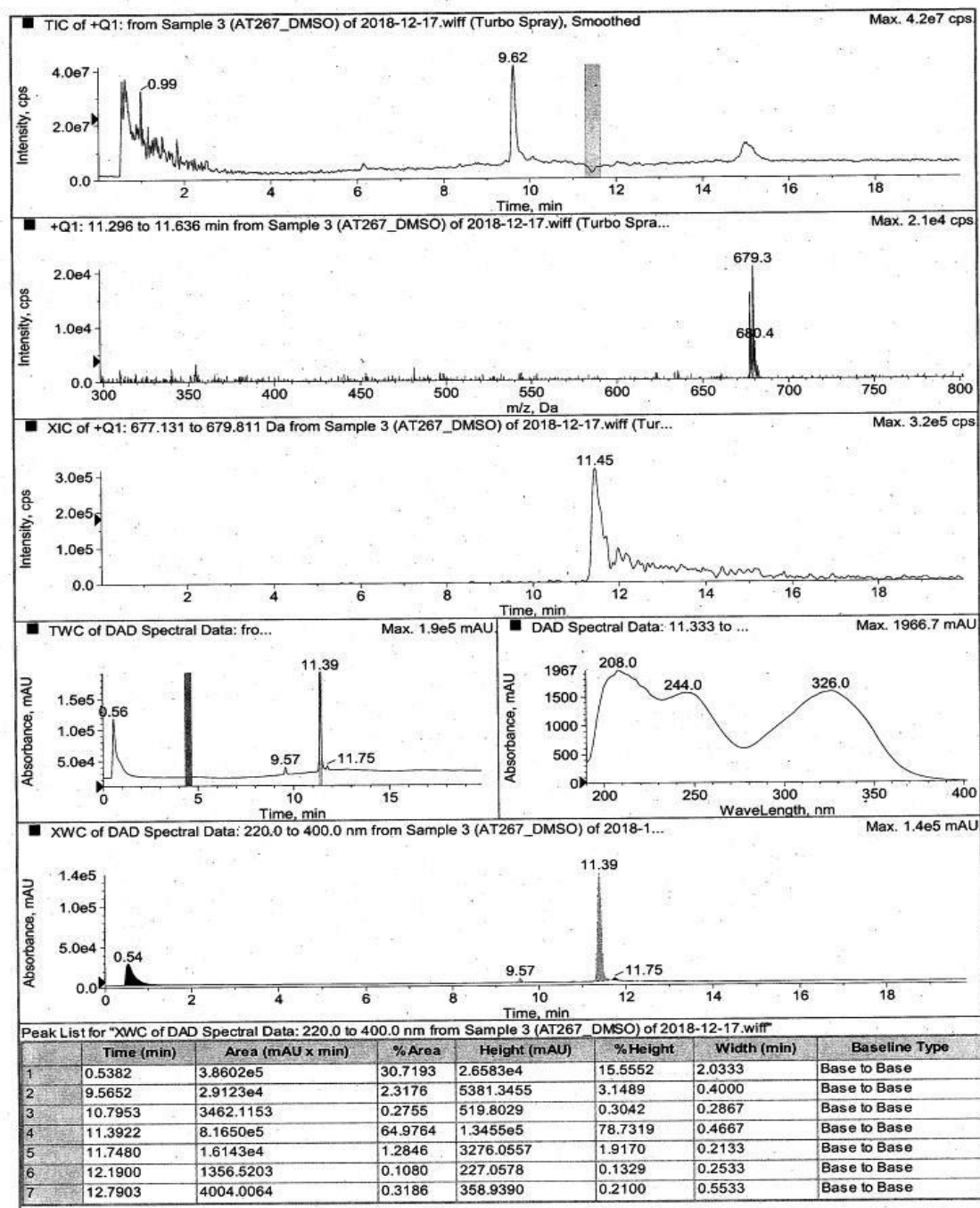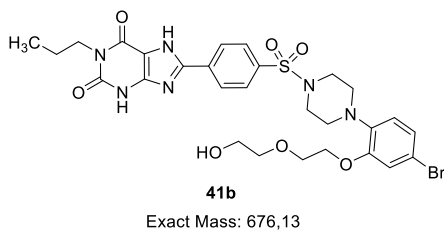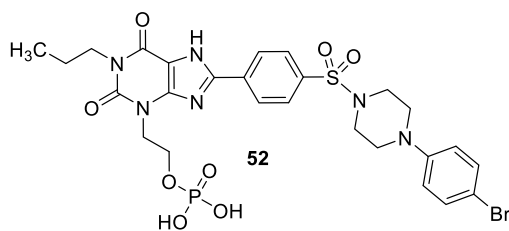
Exact Mass: 696,08
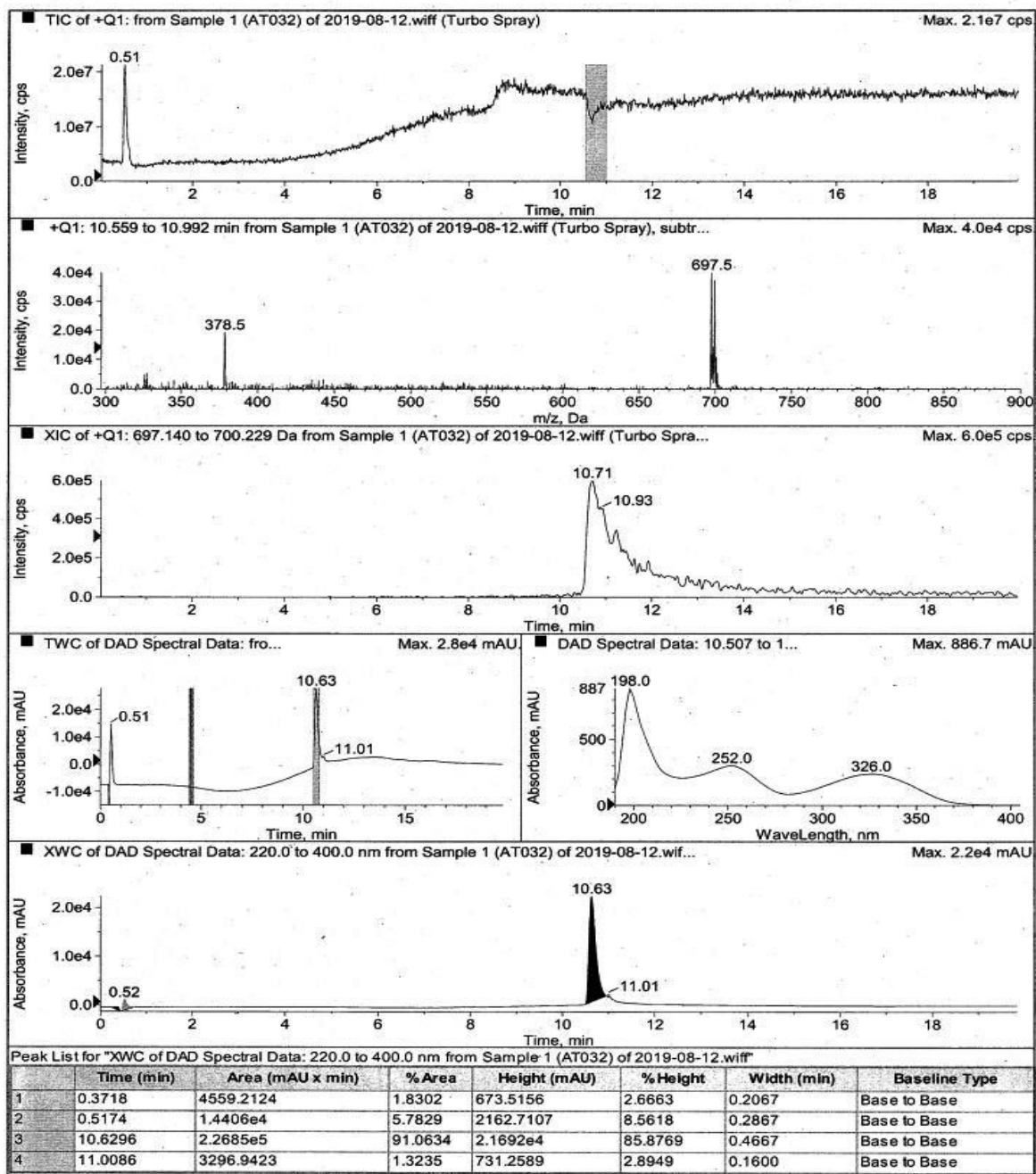
Figure S20. LC-MS spectrum of compound **52***

*The purity of the compound **52** is 96.84% (retention time: 10.63 min belongs to the desired compound **52** and the peak at 0.52 min belongs to the injection peak; also see NMR spectra, **Figure S9**).
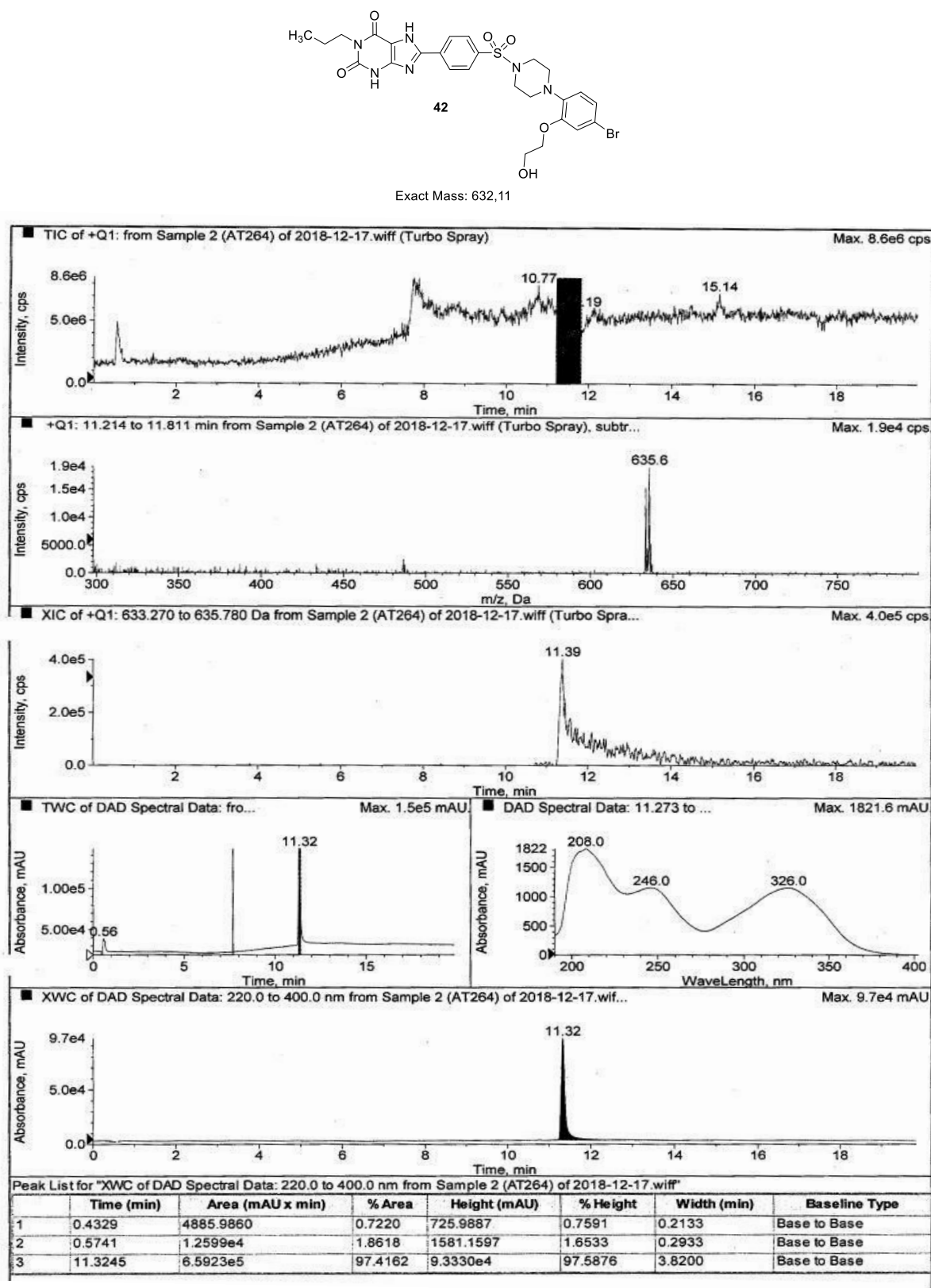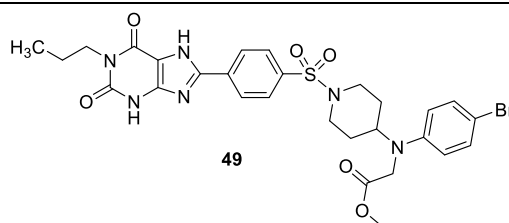
Exact Mass: 712,07

Figure S21. LC-MS spectrum of compound **53***

*The purity of the compound **53** is 95.97% (retention time: 10.04 min belongs to the desired compound **53**; also see NMR spectra, **Figure S10**.

Exact Mass: 710,09

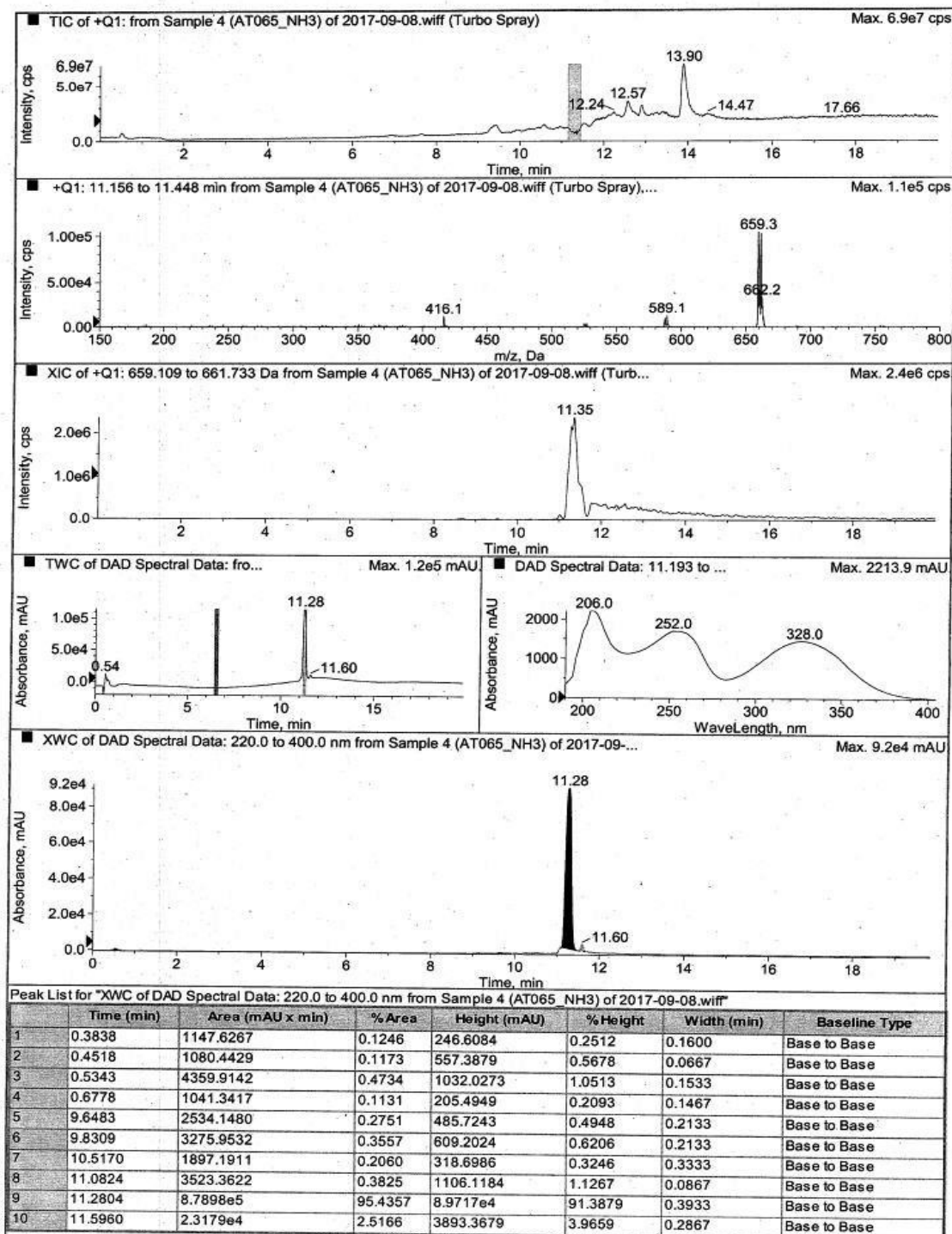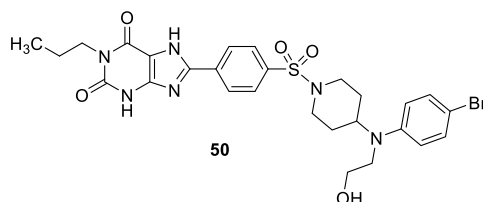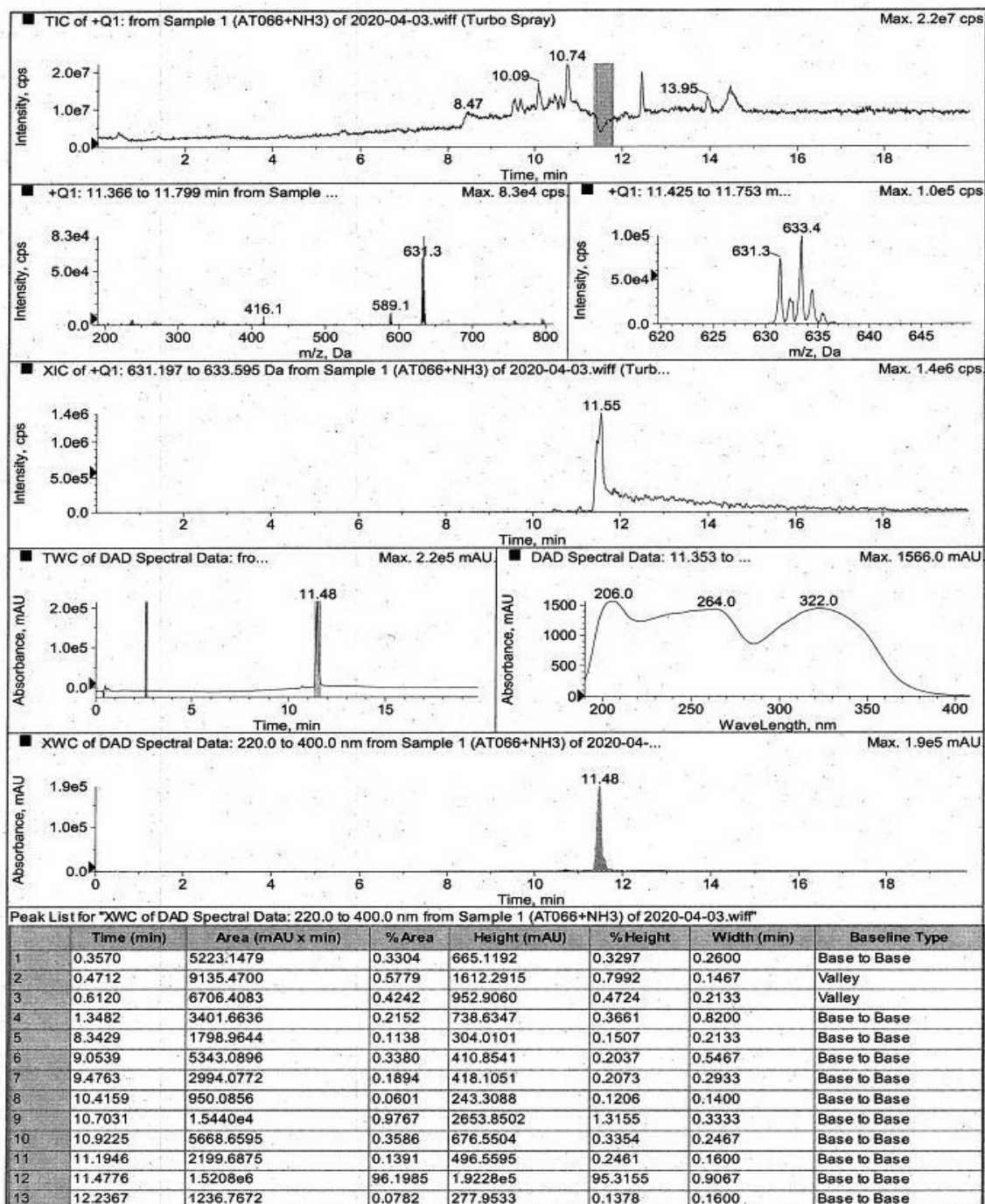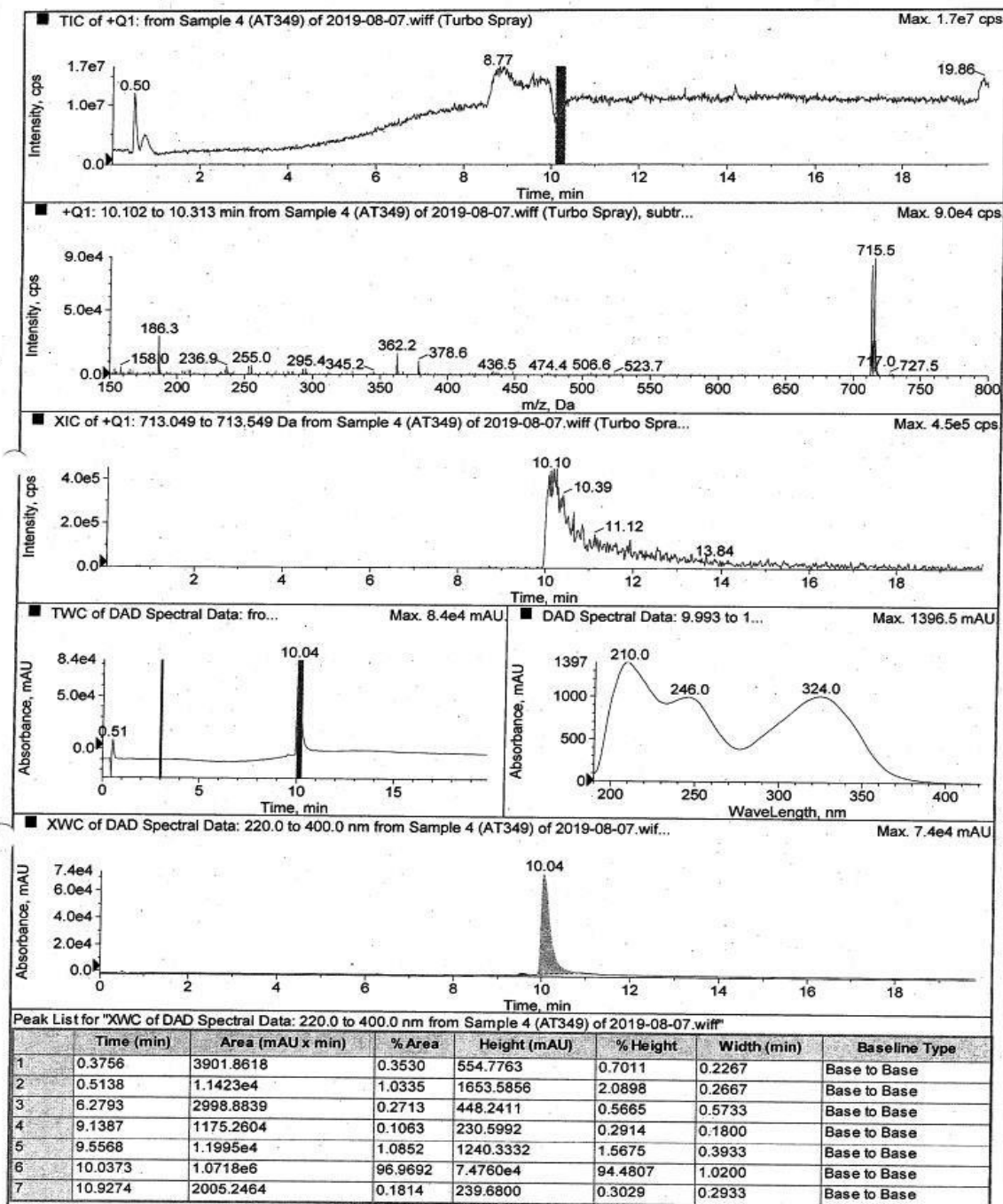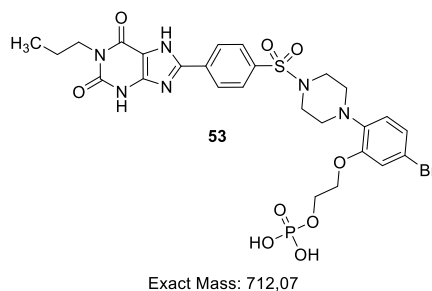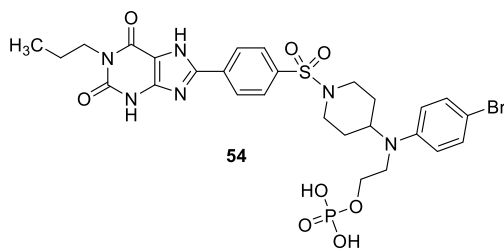|	Time (min)	Area (mAU x min)	% Area	Height (mAU)	% Height	Width (min)	Baseline Type
1	0.3774	954.8289	0.0408	154.4440	0.1122	0.2467	Valley
2	0.5785	1.1795e4	0.5040	1813.7377	1.3173	0.2533	Base to Base
3	6.7996	1551.2998	0.0663	215.6751	0.1566	0.4133	Base to Base
4	7.7159	1435.8278	0.0614	233.5633	0.1696	0.2800	Base to Base
5	9.2523	469.8711	0.0201	71.4675	0.0519	0.2667	Base to Base
6	9.4774	606.7288	0.0259	134.2279	0.0975	0.1600	Base to Base
7	9.6234	400.8780	0.0171	86.2979	0.0627	0.1667	Base to Base
8	9.9077	927.3660	0.0396	166.3563	0.1208	0.2200	Base to Base
9	10.4026	2.3184e6	99.0614	1.3400e5	97.3243	0.8467	Base to Base
10	11.1884	1639.0649	0.0700	341.5399	0.2481	0.1933	Base to Base
11	11.7066	2186.2887	0.0934	466.8026	0.3390	0.2533	Base to Base

Figure S22. LC-MS spectrum of compound **54***
*The purity of the compound **54** is 99.07% (retention time: 10.40 min belongs to the desired compound **54**; also see NMR spectra, **Figure S11**)

4.2. Part II: Development of dual A_{2A}/A_{2B} adenosine receptor antagonists

Development of dual A_{2A}/A_{2B} adenosine receptor antagonists

Ahmed Temirak, Christin Vielmuth, and Christa E. Müller*

PharmaCenter Bonn, Pharmaceutical Institute, Department of Pharmaceutical & Medicinal Chemistry, University of Bonn, An der Immenburg 4, D-53121 Bonn, Germany

4.2.1. Keywords

Adenosine, adenosine receptor, dual antagonists, cancer, immunotherapy, ADME, structure-activity relationships, xanthine

4.2.2. Abstract

The immunosuppressive effects of adenosine resulting in immune escape of cancer and infectious agents are mediated via A_{2A}- and A_{2B} adenosine receptors (ARs) expressed in a variety of immune cells. Therefore, dual A_{2A}/A_{2B}AR antagonists are promising drugs for the immunotherapy of cancer and infections. In addition, many cancer cells express both AR subtypes, and antagonists may exert direct antiproliferative effect. So far, only a few dual antagonists have been reported. Here, we present the development of a series of xanthine-based dual A_{2A}/A_{2B}AR antagonists which show high selectivity versus the other AR subtypes, A_1 and A_3. We modified the structure of the potent A_{2B}AR antagonist 8-(4-((4-(4-bromophenyl)piperazin-1-yl)sulfonyl)phenyl)-1-propyl-3,7-dihydro-1*H*-purine-2,6-dione (PSB-1901), by introducing various substituents that are expected to increase binding affinity for A_{2A}ARs without impeding blockade of A_{2B}ARs. Compounds with a terminal 4-pyridyl or thiazole moiety displayed high dual affinity for A_{2A}- and A_{2B}ARs with high selectivity versus A_1- and A_3ARs. Additionally, **46** and **48** expressed suitable physicochemical, i.e. aqueous solubility, metabolic stability and predicted blood brain barrier (BBB) permeability. The developed dual A_{2A}/A_{2B}AR antagonists may become drug candidates for cancer (immuno)therapy.

4.2.3. Introduction

Adenosine receptors (ARs) are purinergic receptors that are activated by their cognate ligand, the nucleoside adenosine. They belong to class A, rhodopsin-like G protein-coupled receptors (GPCRs) and comprise four subtypes, A_1, A_{2A}, A_{2B} and A_3ARs.[1] A_1-, A_{2A}- and A_3ARs show high affinity for adenosine in the nanomolar range, while $A_{2B}ARs$ require micromolar adenosine concentrations for their activation.[2,3] A_1- and $A_{2A}ARs$ are often activated under normal physiological conditions due to their frequent high expression levels, however, $A_{2B}ARs$ are typically activated under pathological conditions, when adenosine levels increase up to 100-fold, for example after hypoxia or tissue injury.[4–7] A_{2A}- and $A_{2B}ARs$ couple to the heterotrimeric G-protein $G\alpha_s$, which activates adenylate cyclase (AC), thus stimulating cAMP production, while A_1- and A_3ARs couple to $G\alpha_{i/o}$, inhibiting cAMP production by AC.[8,9] The $A_{2B}ARs$ couple additionally to Gq proteins, leading to the activation of phospholipase C (PLC) and subsequent increase in intracellular calcium levels.[10]

$A_{2A}ARs$ are densely expressed in the basal ganglia, which regulate motor control functions in the body.[11] The $A_{2A}AR$ antagonist istradefylline is used for treating Parkinson's disease and $A_{2A}AR$ antagonists may have potential for other neurodegenerative diseases, including Alzheimer's.[12,13] $A_{2A}ARs$ are also expressed on various immune cells, e.g. on T-lymphocytes, natural killer (NK) cells and dendritic cells.[14,15] The activation of $A_{2A}ARs$ on T-lymphocytes and NK cells minimizes cytokine production and tumor killing activity thus causing immunosuppression.[16,17] Therefore, $A_{2A}AR$ antagonists may be effective for cancer immunotherapy, since they can enhance anti-tumoral responses.[18,19] $A_{2B}ARs$ the most closely related subtype to $A_{2A}ARs$, are expressed in the gastrointestinal tract, in lung and mast cells, and have been shown to induce tumor proliferation, metastasis, angiogenesis and immune suppression.[20] Blocking of $A_{2B}ARs$ could reduce tumor growth, metastasis and enhance the tumor antigen presentation.[21,22] Additionally, potent $A_{2B}AR$ antagonists could provide a

therapeutic advantage in cancer therapy since they reduce inflammatory pain.[23,24] Hence, the two ARs are involved in the suppression of the antitumor immune responses, therefore there is a wide interest in developing potent dual A_{2A}/A_{2B}ARs antagonists as cancer (immuno)therapy.[25,26]

Various non-selective AR antagonists and selective A_{2A} or A_{2B}AR antagonists have been reported, however, reports on dual A_{2A}/A_{2B}AR antagonists are still rare.[27,28] Caffeine is a weak non-selective AR antagonist, commonly used as a central stimulant and painkiller in combination with paracetamol and nonsteroidal anti-inflammatory drugs (NSAIDs).[27,29] It is also synergistic with opioids.[24,30] Recent animal studies reported anticancer effects of caffeine likely due to its blockade of A_{2A}- and A_{2B}ARs, also it significantly reduced the risk of developing liver cancer.[22,31–33] Istradefylline is a xanthine-based selective A_{2A}AR antagonist approved in Japan as Nouriast® and recently in US for the treatment of Parkinson's disease in combination with levodopa/carbidopa.[34] Various selective A_{2A}AR antagonists are currently in clinical trials for cancer (immuno)therapy, e.g. Preladenant (SCH 420814), PBF-509 and CPI-444.[35] PSB-603 is a potent and selective A_{2B}AR antagonist that decreased the proliferation of various cancer cells, e.g. prostate and colorectal cancer cell lines.[36,37] Also, PBF-1129, developed by Palobiofarm is currently in phase I clinical trials for the treatment of non-small cell lung carcinoma (NSCLC). Many non-xanthine-based compounds were also reported as potent A_{2B}AR antagonists, e.g. ISAM 140.[38,39]

Recently, the dual A_{2A}/A_{2B}AR antagonists **1-8** were reported (Figures 1 and 2). AB928 (**1**), developed by Arcus Biosciences, reduced the immune suppression in tumor microenvironment through targeting various immune cells expressing the A_{2A}ARs, such as T-lymphocytes and NK cells, and by targeting myeloid cells expressing both A_{2A}- and A_{2B}ARs.[40–42] Currently, **1** is being investigated in several Phase 1b/2 studies as a mono- or combination therapy for the treatment of malignancies including triple-negative breast cancer (TNBC), colorectal cancer (CRC), non-small cell lung cancer (NSCLC), castration-resistant prostate

cancer (CRPC) and renal cell carcinoma (RCC).[43–46] Although **1** displays high affinity for A_{2A}- and A_{2B}ARs, it is only about (32-43)-fold selective versus the A_1AR, which is considered as an anti-target for this indication, due to its opposite effect on cAMP production. In this article, we also present the binding affinity studies we carried for compound **1**, it showed high affinity (< 10 nM) for A_1-, A_{2A}- and A_3ARs (Table 2).

1 AB928
K_i hA_1 64 nM
K_i hA_{2A} 1.5 nM
K_i hA_{2B} 2 nM
K_i hA_3 489 nM

2
K_i hA_{2A} ≤ 10 nM
EC_{50} hA_{2B} ≤ 10 nM

3 E-3210

4
IC_{50} hA_{2A} ≤ 100 nM
IC_{50} hA_{2B} ≤ 100 nM
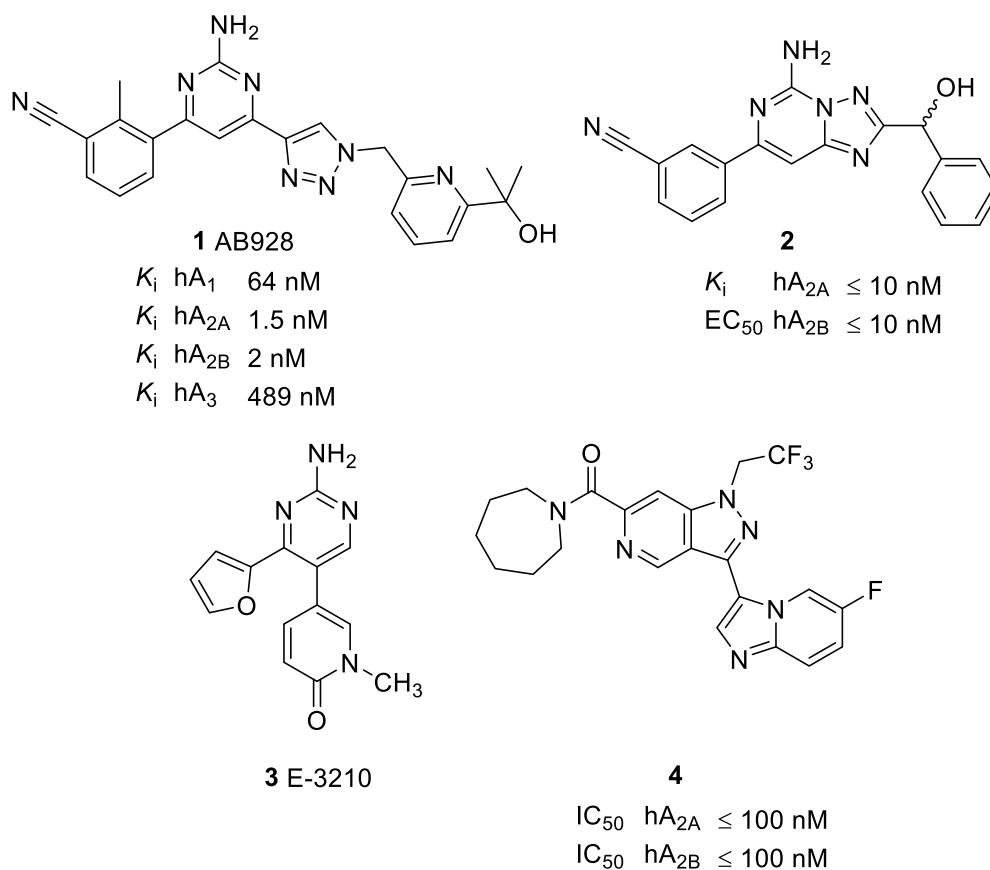
Figure 1. Chemical structures of non-xanthine dual A_{2A}/A_{2B}AR antagonists.[47–51]

Incyte Corporation reported three different classes of potent and efficacious dual A_{2A}/A_{2B}AR antagonists with K_i values of ≤ 10 nM for human A_{2A}ARs determined in binding assays and EC_{50} values of ≤ 10 nM at human A_{2B}ARs determined in cAMP assays.[48,52,53] Compound **2** representing a triazolopyrimidine derivative, is sharing some structural features with **1** including, the benzonitrile and the 2-aminopyrimidine moieties which may contribute to their dual A_{2A}/A_{2B}AR antagonistic activity.[48] Another amino-pyrimidine derivative, E-3210 (**3**) was reported by Eisai (Japan) as AR antagonist that displayed high affinity for A_1, A_{2A} and

$A_{2B}ARs.$[49,54] In other publications, it was described as a dual $A_{2A}/A_{2B}AR$ antagonist.[55,56] The compound which improves the parkinsonian symptoms and constipation, is currently under clinical investigation for the treatment of irritable bowel syndrome (IBS).[50,56] Recently, a new series of dual $A_{2A}/A_{2B}AR$ antagonists having the 5-azaindazole moiety was reported by Merck (Germany) for the treatment of hyperproliferative or infectious diseases. Compound **4** displayed high selectivity for A_{2A}- and $A_{2B}ARs$ in cAMP assays performed in HEK293 cells stably expressing both ARs with IC_{50} values < 100 nM.[51,57]

Dual $A_{2A}/A_{2B}AR$ antagonists with a pyrrolopyrimidine moiety based on a previous study by our group[58,59] were described by Almirall Prodesfarma, such as **5** (Figure 2).[60] However, most of the compounds reported in this patent displayed high fold of selectivity for $A_{2B}ARs$.[60] The xanthine-based compound **6**, previously developed in our group, displayed high dual antagonistic affinity for A_{2A}- and $A_{2B}AR$ in humans, however in rat, it showed significantly lower affinity for $A_{2A}ARs$.[61] Impetis Biosciences reported two more dual $A_{2A}/A_{2B}AR$ antagonists having either a pyrrole tricyclic ring, such as **7** or a tricyclic imidazo[2,1-*b*]purin-4(5*H*)-one moiety, such as **8**. Both compounds displayed high affinity for both AR subtypes with affinity values ≤ 10 nM and are proposed to be useful in the treatment of cancer, inflammatory disorders and neurodegenerative diseases (Figure 2).[52,53]

Few other examples for dual $A_{2A}/A_{2B}AR$ antagonists were reported, however their chemical structures have not been disclosed. X-Chem (USA) developed the dual $A_{2A}/A_{2B}AR$ antagonist X6350,[62] which was reported to display superior activity over selective $A_{2A}AR$ antagonists in counteracting the immunosuppression of myeloid cells.[63] This compound displayed high affinity to the $A_{2B}AR$ ($K_i = 4.4$ nM) and lower affinity for the $A_{2A}AR$ ($K_i = 21.0$ nM).[62] Compounds SEL330-584 and SEL330-639 were reported by Selvita (Poland) claimed to display high affinity for A_{2A}- and $A_{2B}AR$ at low and high adenosine concentrations (tumor-

like environment).[64,65] By inhibiting $A_{2B}AR$, they restored the impaired functional activity of

molybdate-transporting ATPase (moDC) in cytokine release assays induced by adenosine.[66]
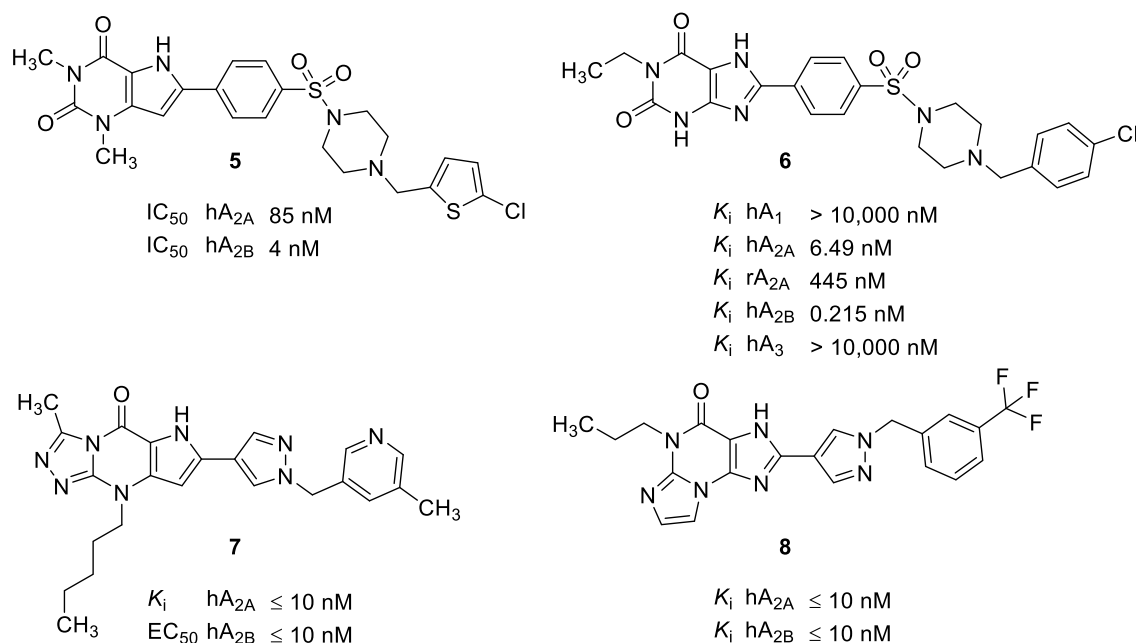
Figure 2. Chemical structures of xanthine or xanthine analogues as dual $A_{2A}/A_{2B}AR$ antagonists.[52,53,60,61]

Multi-target drugs that interact concurrently with two or more drug targets is a new

approach in drug development.[67] It has advantages, especially in complex diseases like

cancer.[68] Multi-targeting drugs often exhibit synergistic effects, display less side effects and

improve compliance.[69] Since effects of adenosine to A_{2A}- and $A_{2B}ARs$ are a control mechanism

for suppressing antitumor and anti-infectious immune responses, therefore developing dual

inhibitors that block both ARs can be envisaged as a new approach in cancer (immuno)therapy

and the treatment of infectious diseases in immune-compromised patients.[39] Many of the

reported dual $A_{2A}/A_{2B}AR$ antagonists lack selectivity versus A_1 and/or A_3 AR subtypes, so they

act as non-selective AR antagonists, or the selectivity data is missing for other compounds.

Also, some of them lack selectivity across different species. Therefore, we developed a series

of xanthine-based dual $A_{2A}/A_{2B}AR$ antagonists with high selectivity versus A_1 and A_3 AR subtypes.

4.2.4. Results and discussion

4.2.4.1. Design

Starting from our lead compound PSB-1901,[83] a potent and selective $A_{2B}AR$ antagonist, we will carry out modifications that are expected to restore $A_{2A}AR$ affinity without the loss of interaction with the $A_{2B}AR$ to obtain dual $A_{2A}/A_{2B}ARs$ antagonists (Figure 3). Starting with the substitution on the xanthine scaffold, we will study the effects of introducing different alkyl groups, such as methyl, ethyl, propyl and cyclopropyl, at $N1$- and $N3$-positions of xanthine for optimal dual $A_{2A}/A_{2B}AR$ antagonistic affinity.
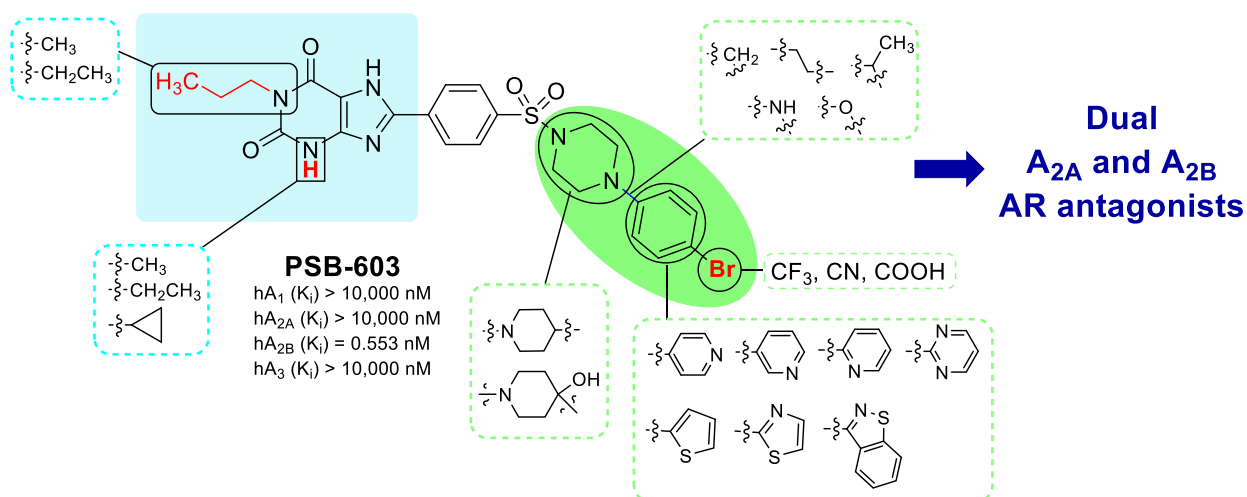
Figure 3. Schematic representation of the proposed structural modification of PSB-1901 structure to develop dual $A_{2A}/A_{2B}AR$ antagonists.

This will be carried out in combination with the replacement of the terminal 4-bromophenyl residue in PSB-1901, which is essential for $A_{2B}AR$ affinity, by various heterocyclic rings having different sizes including pyridyl, pyrimidyl, thienyl, thiazolyl and benzo[d]isothiazolyl. Different linkers connecting the terminal aromatic ring via piperazine or piperidine moieties will also be investigated (Figure 3).

4.2.4.2. Chemistry

The synthetic routes to obtain the target compounds are depicted in Schemes 1-3. The key starting compounds are the *p*-nitrophenoxy-sulfonylphenylxanthine derivatives **18-23**. Compound **18** was prepared as described in Scheme 1, while **19-23** were prepared as previously described.[61,70,71]

Scheme 1. Preparation of *p*-nitrophenoxysulfonylphenylxanthine derivative **18**.
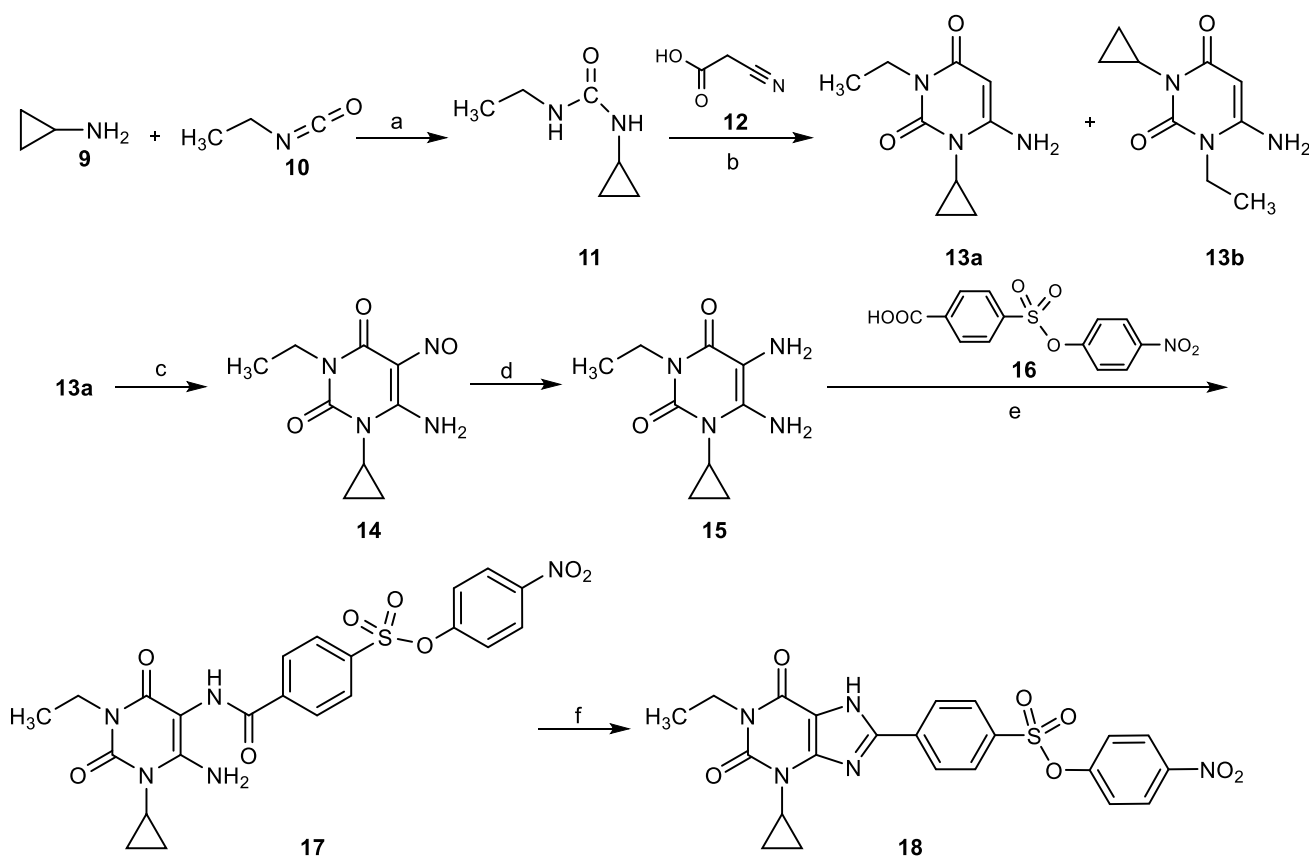
Reagents and conditions: (a) Toluene, 4 °C to rt, 4 h, 90%; (b) (i) Ac$_2$O, 60 °C, 15 W, 15 min, (ii) 5N NaOH, rt, 1 h, 48%; (c) NaNO$_2$, AcOH, H$_2$O, 65 °C, 10 min, 65%; (d) Na$_2$S$_2$O$_4$, NH$_4$OH (12.5%), 65 °C, 3 min, 95%; (e) COMU, DIPEA, DMF, rt, 10 min, 90%; (f) PPSE, 120 - 170 °C, 7 h, 94%.

Reaction of cyclopropylamine (**9**) with ethyl isocyanate (**10**) yielded 1-cyclopropyl-3-ethylurea (**11**). A mixture of **11** and cyanoacetic acid (**12**) dissolved in acetic anhydride was irradiated in a microwave instrument followed by cyclization using 5N sodium hydroxide

solution in water yielding a mixture of 1,3-disubstituted uracil derivatives, 6-amino-1-cyclopropyl-3-ethylpyrimidine-2,4(1*H*,3*H*)-dione (**13a**) and 6-amino-3-cyclopropyl-1-ethyl-pyrimidine-2,4(1*H*,3*H*)-dione (**13b**).[72]

Compound **13b** had previously been characterized by X-ray crystallography and NMR techniques.[72] We have now obtained an X-ray structure of the desired **13a** as well (Figure 4) unambiguously confirming the proposed structure. Compound **13a** was further nitrosated using sodium nitrite and reduced with sodium dithionite according to the published procedures,[73] yielding the diamino uracil **15**. Coupling of **15** with the benzoic acid derivative **16**[70] was achieved using (1-cyano-2-ethoxy-2-oxoethylidenaminooxy)dimethylamino-morpholino-carbenium hexafluoro phosphate (COMU).[74] Ring closure reaction of **17** using trimethylsilyl polyphosphate (PPSE), applying the previously described procedure, developed by Müller,[61,70] yielded the new *p*-nitrophenoxy-sulfonylphenylxanthine derivative **18** (Scheme 1).
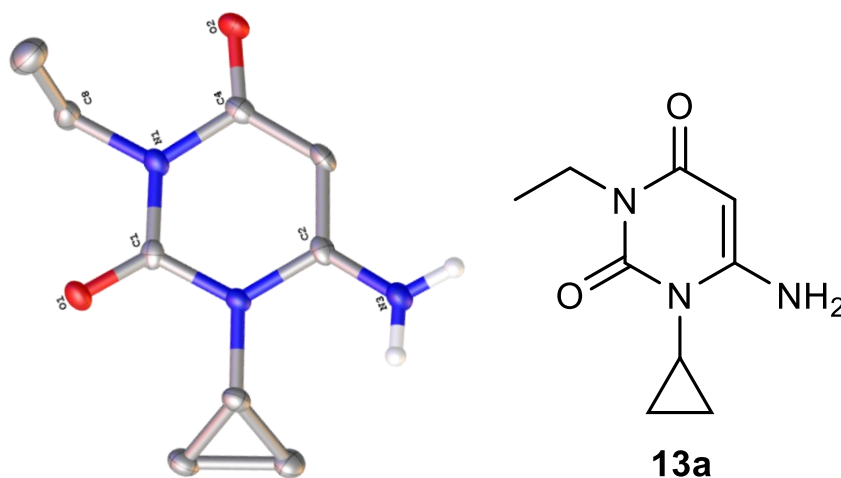
Figure 4. Crystal and chemical structures of 6-amino-1-cyclopropyl-3-ethylpyrimidine-2,4(1*H*,3*H*)-dione (**13a**).

Piperazines (**24**, **26**, **28**, **31**, **33** and **38**) were obtained from commercial sources, while piperazines (**25**, **27**, **29**, **30**, **32**, **34-37**) and piperidines (**39-43**) were prepared as described in literature (detailed synthesis in supporting information).[75–81] The previously described aminolysis

reaction[71,82,83] was employed for the synthesis of target compounds **44-88**. Compounds **18-23** were reacted with various piperazines (**24-38**) or with the piperidines (**39-43**) under reflux conditions in DMSO or sulfolane under an argon atmosphere producing the desired xanthine derivatives **44-88** (Schemes 2 and 3). The selection of the solvent for the aminolysis reaction was dependent on the piperazinyl or piperidinyl derivatives involved in the reaction.

Scheme 2. Preparation of piperazinylxanthine derivatives **44-80**.

18 (I), R$_1$ = ethyl, R$_2$ = cyclopropyl
19 (II), R$_1$ = propyl, R$_2$ = H
20 (III), R$_1$ = propyl, R$_2$ = methyl
21 (IV), R$_1$ = propyl, R$_2$ = ethyl
22 (V), R$_1$ = ethyl, R$_2$ = ethyl
23 (VI), R$_1$ = methyl, R$_2$ = methyl

R^3 =

44 (II), **45** (III), **46** (IV)
47 (VI), **48** (V), **49** (I)

50 (II), **51** (IV)

52 (II), **53** (III), **54** (IV), **55** (VI),
56 (V), **57** (I), X = H
58 (II), X = p-Br, **59** (V), X = p-CF$_3$
60 (II), X = p-CN, **61** (II), X = p-COOH
62 (II), X = o-CN

63 (II), **64** (III), **65** (IV), X = H
66 (II), X = Br

67 (II)

68 (II), **69** (IV), **70** (V)

71 (II), **72** (IV), **73** (V)

74 (II), **75** (V)

76 (II), **77** (IV), **78** (V)

79 (II), **80** (V)

R^3 =

24
34
25
35

26, X = H
27, X = p-Br
28, X = p-CF$_3$
29, X = p-CN
30, X = o-CN
26-30
36

31, X = H
32, X = Br
31, 32
37

33
38

Reagents and conditions: (a) DMSO, Ar, 140°C, 7-18 h, 29-58% (Method A); (b) Sulfolane, Ar, 130°C, 3-18 h, 30-51% (Method B).

Piperazines (**26-30** and **32**) and piperidines (**39-43**) substituted with chloro, bromo, trifluoromethane, hydroxy or cyano groups, DMSO was found to be the preferred solvent for the reaction resulting in few side products and higher conversion rates. Alternatively, for the

unsubstituted piperazines (**24**, **25**, **31**, **33-38**), higher yields and shorter reaction time for aminolysis

reaction was reported with the usage of sulfolane as a solvent (Schemes 2 and 3).

Scheme 3. Preparation of piperidinylxanthine derivatives **81-88**.
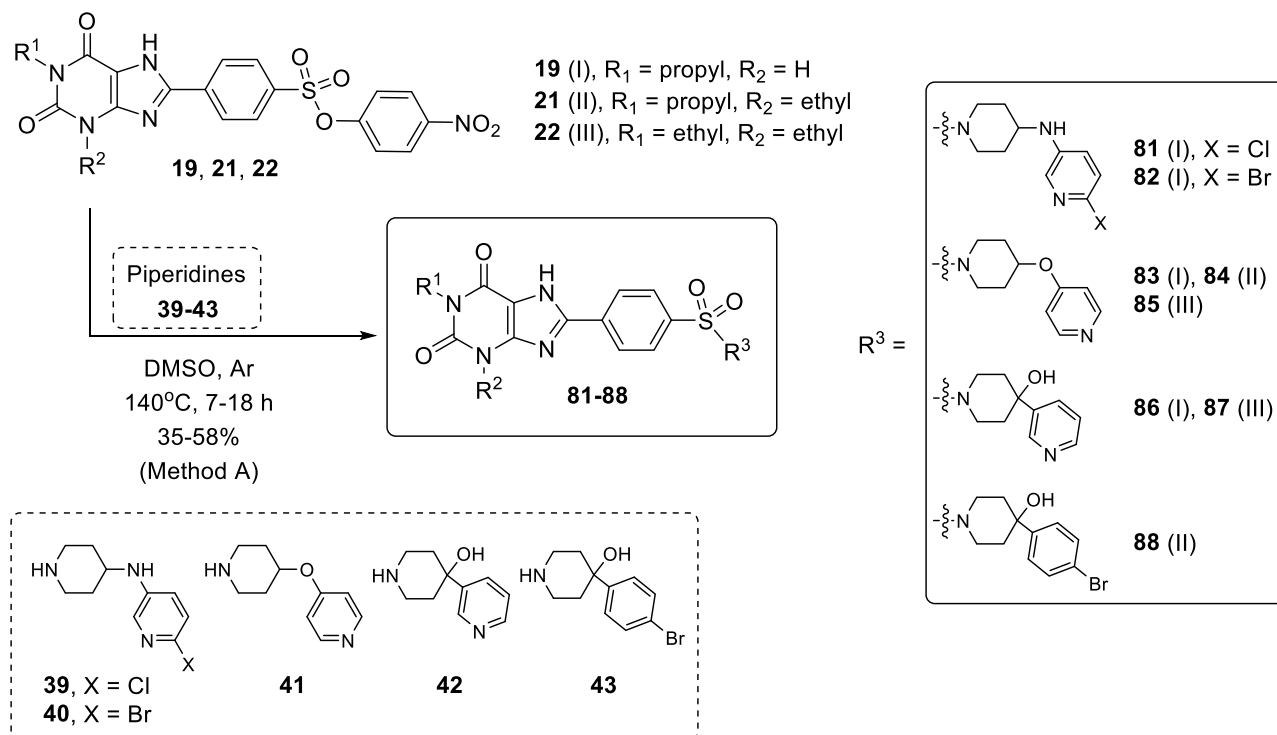
The synthesized compounds were purified using by flash chromatography on silica gel

or by reversed-phase high performance liquid chromatography (RP-HPLC), respectively.

Piperazinylxanthine derivatives **44-80** and piperidinylxanthine derivatives **81-88**, employed

synthetic methods, yields, and purities are collected in Table 1.

Table 1. Newly synthesized piperazinylxanthine derivatives **44-80** and piperidinylxanthine derivatives **81-88**.

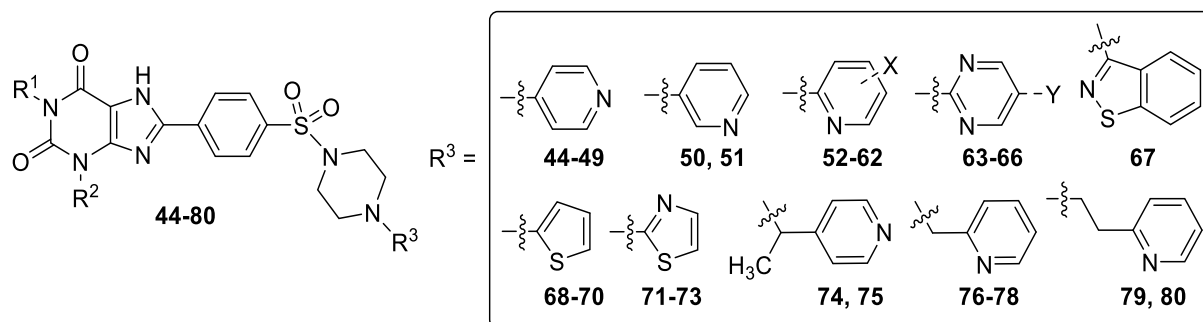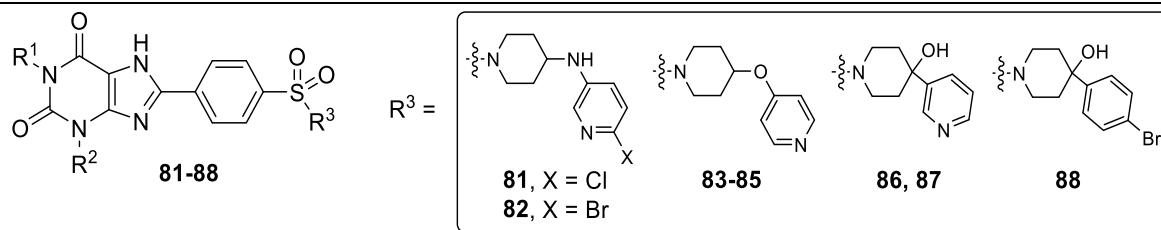| No.	R^1	R^2		Method	Purity (%)	Yield (%)	No.	R^1	R^2		Method	Purity (%)	Yield (%)
44	propyl	H		B	96.5	31	63	propyl	H	Y = H	B	97.4	35
45	propyl	methyl		B	97.7	46	64	propyl	methyl	Y = H	B	97.5	48
46	propyl	ethyl		B	96.7	39	65	propyl	ethyl	Y = H	B	98.2	35
47	methyl	methyl		B	98.7	41	66	propyl	H	Y = Br	A	95	38
48	ethyl	ethyl		B	95.5	58	67	propyl	H		B	97.5	45
49	ethyl	cyclo-propyl		B	99.5	41	68	propyl	H		B	97.8	54
50	propyl	H		B	100	48	69	propyl	ethyl		B	97.1	49
51	propyl	ethyl		B	97.8	50	70	ethyl	ethyl		B	95.6	48
52	propyl	H	X = H	B	98.7	38	71	propyl	H		B	98.2	53
53	propyl	methyl	X = H	B	98.3	29	72	propyl	ethyl		B	95	55
54	propyl	ethyl	X = H	B	99.4	37	73	ethyl	ethyl		B	96.3	51
55	methyl	methyl	X = H	B	97.6	48	74	propyl	H		B	98.2	55
56	ethyl	ethyl	X = H	B	98.7	50	75	ethyl	ethyl		B	98.5	52
57	ethyl	cyclo-propyl	X = H	B	96.5	54	76	propyl	H		B	99.1	47
58	propyl	H	X = p-Br	A	96.9	30	77	propyl	ethyl		B	97	56
59	ethyl	ethyl	X = p-CF3	A	100	47	78	ethyl	ethyl		B	98.4	55
60	propyl	H	X = p-CN	A	95	41	79	propyl	H		B	98.8	39
61	propyl	H	X = p-COOH	---	96.5	---	80	ethyl	ethyl		B	96.7	54
62	propyl	H	X = o-CN	A	97.8	51							

No.	R^1	R^2	Method	Purity (%)	Yield (%)	No.	R^1	R^2	Method	Purity (%)	Yield (%)
81	propyl	H	A	98.3	35	**85**	ethyl	ethyl	A	98.1	50
82	propyl	H	A	99.4	35	**86**	propyl	H	A	98.4	55
83	propyl	H	A	97.8	45	**87**	ethyl	ethyl	A	97.3	55
84	propyl	ethyl	A	97.3	52	**88**	propyl	ethyl	A	97.2	58

4.2.4.3. Radioligand Binding Assays

The affinity of the synthesized compounds towards all four human AR subtypes A$_1$, A$_{2A}$, A$_{2B}$, and A$_3$ were determined in radioligand binding assays (Table 3). The A$_1$AR-selective radioligand [^{3}H]CCPA,[84] the A$_{2A}$AR-selective radioligand [^{3}H]MSX-2,[85] the A$_{2B}$AR-selective radioligand [^{3}H]PSB-603,[61] and the A$_3$AR-selective radioligand [^{3}H]PSB-11[86] were used.

Exploring the terminal phenyl ring replacement with different heterocycles. The first series of compounds were those substituted with terminal 4-pyridyl moieties (Table 2). Compound **44** having a propyl substituent on *N*1 and a free *N*3 of the xanthine core, showed high A$_{2B}$AR affinity (K_i = 9.83 nM) combined with 15-fold selectivity versus the A$_{2A}$AR. Upon substitution of the *N*3 of the xanthine core with methyl or ethyl moieties resulting in compounds **45** and **46**, the affinity for the A$_{2A}$AR was increased by 2-7-fold, while the affinity for the A$_{2B}$AR was slightly decreased by 2-4-fold. Compound **46** having an ethyl substituent at the *N*3-position displayed higher affinity for both adenosine receptor subtypes than the 3-methyl substituted compound **45** (Table 2).

Compounds **48** and **49**, substituted at the *N*1-position of xanthine with an ethyl residue

and on *N*3 with an ethyl or cyclopropyl moieties respectively, showed high dual A$_{2A}$- and

A$_{2B}$AR affinity with K_i values at both AR subtypes ranging from 11.1 to 23.1 nM. While **48**

(1,3-diethyl-substituted derivative) showed slightly higher affinity for the A$_{2B}$AR, **49** (1-ethyl-

3-cyclopropyl-substituted derivative) was slightly more potent at the A$_{2B}$AR (Figure 8). 1,3-

dimethylxanthine derivative **47** displayed somewhat lower dual affinity in comparison to **48**

and **49** (Table 2). All of the dual A$_{2A}$/A$_{2B}$AR antagonists from this series **44-49** were highly

selective versus A$_1$ and A$_3$ARs.

Table 2. Human ARs affinities of substituted xanthine derivatives **44-88**.

No.	R^1	R^2	X	A$_1$AR^a	A$_{2A}$AR^b	A$_{2B}$AR^c	A$_3$AR^d	A$_{2B}^e$ selectivity
				$K_i \pm$ SEM (nM) (% inhibition of radioligand binding at indicated concentration)				
44	propyl	H	H	>1000 (16%)	149 ± 59	9.83 ± 0.62	>1000 (19%)	15.2
45	propyl	methyl	H	>1000 (13%)	72.7 ± 30.1	23.5 ± 4.4	>1000 (24%)	3.1
46	propyl	ethyl	H	>1000 (32%)	21.0 ± 1.7	39.8 ± 4.3	>1000 (22%)	0.5
47	methyl	methyl	H	>1000 (11%)	43.9 ± 0.50	56.6 ± 6.7	>1000 (21%)	0.8
48	ethyl	ethyl	H	>1000 (22%)	11.1 ± 1.5	21.0 ± 5.8	>1000 (28%)	0.5
49	ethyl	cyclopropyl	H	>1000 (23%)	23.1 ± 6.2	16.6 ± 3.6	>1000 (4%)	1.4
50	propyl	H	H	>1000 (31%)	68.3 ± 18.9	3.60 ± 0.74	>1000 (31%)	19
51	propyl	ethyl	H	218 ± 11	40.3 ± 19.1	14.9 ± 1.8	>1000 (37%)	2.7
52	propyl	H	H	>1000 (22%)	66.1 ± 13.8	1.39 ± 0.33	>1000 (29%)	47.6
53	propyl	methyl	H	>1000 (32%)	155 ± 56	5.09 ± 1.17	>1000 (28%)	30.5
54	propyl	ethyl	H	>1000 (29%)	68.3 ± 36.0	5.78 ± 1.19	>1000 (32%)	11.8
55	methyl	methyl	H	>1000 (25%)	88.6 ± 31.1	7.64 ± 2.15	>1000 (14%)	11.6

56	ethyl	ethyl	H	>1000 (28%)	55.2 ± 16.0	5.51 ± 0.92	>1000 (31%)	10
57	ethyl	cyclopropyl	H	>1000 (26%)	41.4 ± 15.0	2.48 ± 0.94	259 ± 42	16.7
58	propyl	H	*p*-Br	>1000 (29%)	311 ± 86	0.536 ± 0.063	1000 (30%)	580
59	ethyl	ethyl	*p*-CF$_3$	>1000 (-11%)	≈1000 (49%)	1.42 ± 0.09	>1000 (37%)	704
60	propyl	H	*p*-CN	2130 ± 1550	289 ± 113	5.02 ± 0.84	>1000 (28%)	57.4
61	propyl	H	*p*-COOH	>1000 (12%)	>1000 (13%)	not stable	>1000 (32%)	--
62	propyl	H	*o*-CN	>1000 (22%)	236 ± 46	1.81 ± 0.16	>1000 (34%)	130
63	propyl	H	H	>1000 (-16%)	231 ± 92	2.93 ± 0.60	>1000 (22%)	78.9
64	propyl	methyl	H	>1000 (17%)	1000 (45%)	14.4 ± 3.5	>1000 (15 %)	69.4
65	propyl	ethyl	H	>1000 (20%)	1000 (43%)	15.5 ± 1.8	>1000 (7%)	64.5
66	propyl	H	H	>1000 (23%)	>1000 (40%)	0.949 ± 0.117	>1000 (13%)	1053
67	propyl	H	H	<1000 (45%)	66.7 ± 12.8	0.318 ± 0.087	<1000 (47%)	209
68	propyl	H	H	>1000 (13%)	800 ± 299	1.20 ± 0.30	>1000 (30%)	667
69	propyl	methyl	H	608 ± 129	82.4 ± 11.0	2.53 ± 0.45	>1000 (40%)	33
70	ethyl	ethyl	H	1240 ± 108	42.3 ± 18.2	2.09 ± 0.52	>1000 (40%)	20.3
71	propyl	H	H	>1000 (3%)	205 ± 69	1.68 ± 0.13	>1000 (30%)	122
72	propyl	methyl	H	>1000 (36%)	46.4 ± 7.6	3.97 ± 0.52	>1000 (13%)	11.7
73	ethyl	ethyl	H	>1000 (28%)	28.5 ± 5.4	3.68 ± 0.32	>1000 (18%)	7.7
74	propyl	H	H	>1000 (20%)	344 ± 65	18.2 ± 1.9	>1000 (6%)	19
75	ethyl	ethyl	H	756 ± 104	66.1 ± 15.9	75.6 ± 14.1	>1000 (32%)	0.9
76	propyl	H	H	>1000 (-6%)	1500 ± 494	5.35 ± 0.85	>1000 (8%)	280
77	propyl	ethyl	H	632 ± 35	136 ± 26	9.81 ± 0.73	>1000 (35%)	14
78	ethyl	ethyl	H	>1000 (26%)	80.4 ± 11.2	14.0 ± 3.5	>1000 (17%)	5.7
79	propyl	H	H	387 ± 62	186 ± 31	11.6 ± 2.1	>1000 (27%)	16
80	ethyl	ethyl	H	423 ± 69	46.1 ± 5.7	50.1 ± 6.0	>1000 (29%)	0.9
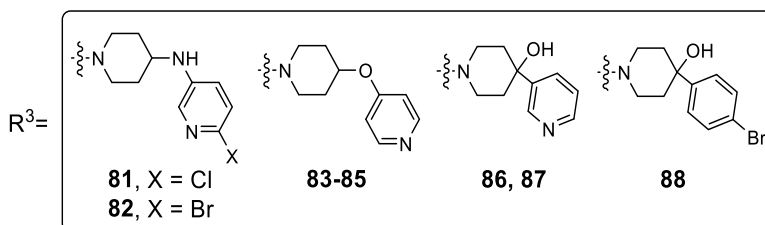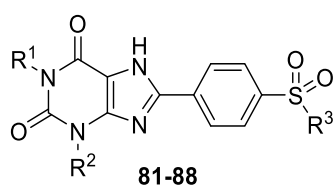
81	propyl	H	H	>1000 (43%)	182 ± 32	2.61 ± 0.75	>1000 (23%)	70
82	propyl	H	H	>1000 (44%)	112 ± 28	1.94 ± 0.49	>1000 (20%)	58
83	propyl	H	H	680 ± 117	91.6 ± 9.5	5.36 ± 0.77	>1000 (32%)	17
84	propyl	ethyl	H	498 ± 156	27.2 ± 7.7	21.2 ± 4.0	>1000 (36%)	1.3

85	ethyl	ethyl	H	1280 ± 306	15.7 ± 1.0	19.7 ± 2.9	>1000 (36%)	0.8
86	propyl	H	H	950 ± 311	180 ± 23	12.6 ± 2.3	>1000 (44%)	14.3
87	ethyl	ethyl	H	>1000 (28%)	33.8 ± 2.2	60.2 ± 1.5	>1000 (16%)	0.6
89[h]	propyl	H	H	> 1000 (19%)	45.5 ± 5.8	6.14 ± 0.51	> 1000 (10%)	7.4
90[h]	ethyl	ethyl	H	>1000 (25%)	20.5 ± 3.2	9.78 ± 3.07	>1000 (27%)	2.1
91[h]	propyl	H	H	754 ± 270	42.6 ± 16.4	1.57 ± 0.22	>1000 (33%)	27.1
88	propyl	ethyl	H	>1000 (13%)	36.0 ± 6.0	10.1 ± 2.5	>1000 (13%)	3.6
92[h]	methyl	methyl	H	>1000 (20%)	39.3 ± 5.9	4.06 ± 1.42	>1000 (28%)	9.7
93[h]	ethyl	ethyl	H	>1000 (24%)	20.7 ± 3.9	1.87 ± 0.34	>1000 (11%)	11.1
Caffeine[87]				$10,700^e$	9,560	10,400	$13,300^f$	0.9
Istradefylline[87]				841^e	26.4 ± 5.9	>10,000	4470^f	0.003
PSB-603[82]				>10,000 (10%)	>10,000 (7%)	0.553 ± 0.103	>10,000 (10%)	>18,000
AB928 (**1**)				5.74 ± 1.34^a 7.75 ± 1.28^e	0.960 ± 0.328	3.24 ± 0.50	354 ± 120	0.3

^{a} vs. [³H]CCPA (n = 3); ^{b} vs. [³H]MSX-2 (n = 3); ^{c} vs. [³H]PSB-603 (n = 3); ^{d} vs. [³H]PSB-11 (n = 3); ^{e} vs. [³H]DPCPX; ^{f} vs. [³H]NECA; ^{g} K_i A2A / K_i A2B; ^{h} unpublished data.

The second series of compounds were those substituted with a 2-pyridyl moiety **52-62** (Table 2). In general, this modification increased A2B-affinity and selectivity. Compound **52** displayed high A2BAR affinity (K_i = 1.39 nM) and ~50-fold selectivity versus the A2AAR. Compared to its *p*-pyridyl analogue **44**, the *o*-pyridyl derivative **52** was more potent at both receptor subtypes. Variations of different alkyl substituents (methyl, ethyl, propyl, cyclopropyl) at the xanthine *N*1- and *N*3-positions as in compounds **52-57**, had only minor effects on the A2BAR affinity and selectivity. Consistent with the SARs for the 4-pyridyl compound series (Table 2), **56** and **57**, having a 1-ethyl residue and an ethyl or cyclopropyl moieties at *N*3, displayed the best dual A2A- and A2BAR antagonistic affinity also in the 2-pyridyl series. Furthermore, substitution on the terminal 2-pyridyl ring with different groups including (CN, CF3, Br), as in compounds **58-62**, increased potency and selectivity for the A2BAR, with lower affinity for the A2AAR (Table 2).

Next, we investigated 3-pyrdiyl derivatives **50** and **51**. Their A$_{2B}$ affinity and selectivity was in between, i.e. they were less dual than the corresponding *p*-pyridyl analogs, and less potent and selective for the A$_{2B}$ARs than the *o*-pyridyl ones (Figure 5). Thus, *p*-pyridyl is the best for obtaining dual A$_{2A}$/A$_{2B}$AR antagonists, while *o*-pyridyl is optimal for obtaining potent A$_{2B}$AR-selective antagonists.
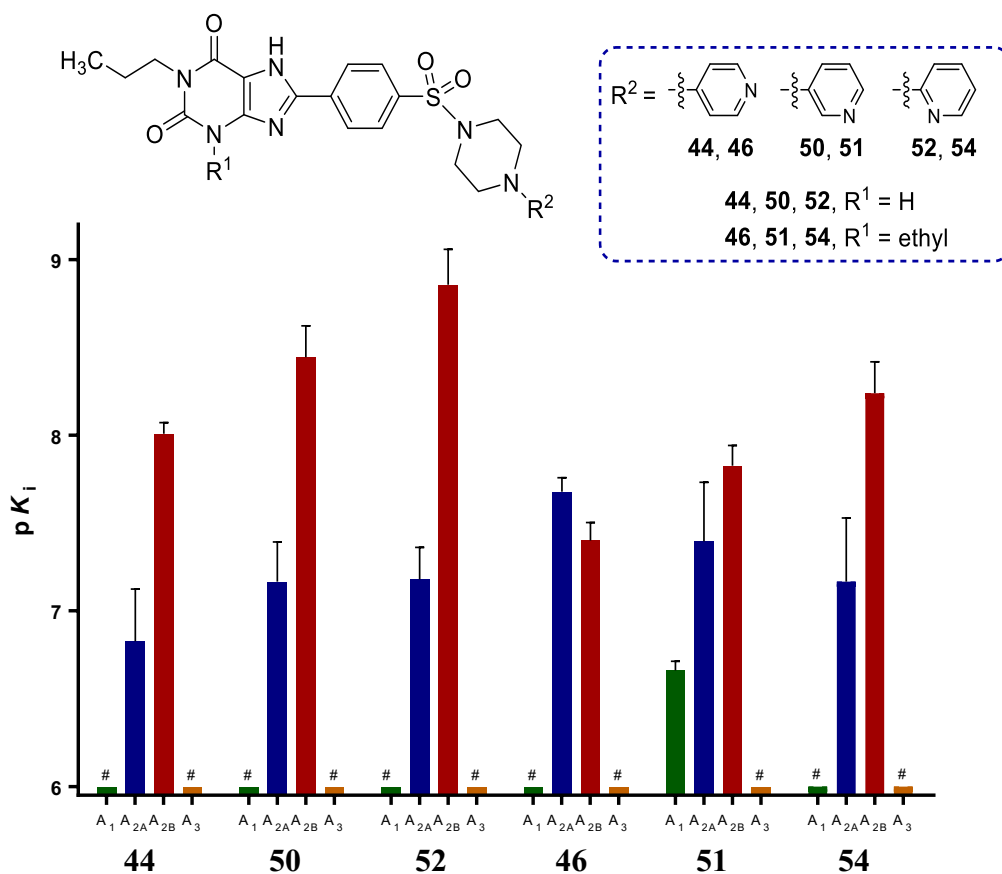

Figure 5. Affinities of pyridyl-substituted xanthine derivatives at the four human AR subtypes (A$_1$, A$_{2A}$, A$_{2B}$ and A$_3$) determined in radioligand binding assays; # pK_i < 6.

To study the effect of phenyl ring replacement with heterocyclic rings other than pyridine, we introduced a pyrimidine ring in compounds **63**-**66**, a benzo[d]isothiazole ring in (**67**), a thiophene ring in compounds **68**-**70**, and a thiazole ring in **71**-**73**. All of these ring systems led to high A$_{2B}$AR affinity, but in most cases A$_{2A}$AR affinity was reduced resulting in A$_{2B}$-selective antagonists. It could be again confirmed that having no substituent at *N*3

increased A_{2B} affinity and selectivity. The best dual $A_{2A}/A_{2B}AR$ antagonists of this sub-series were, thiazole derivative **73** (hA_{2A} (K_i) = 28.5 nM; hA_{2B} (K_i) = 3.68 nM) and thiophene derivative **70** (hA_{2A} (K_i) = 42.3 nM; hA_{2B} (K_i) = 2.09 nM) (Figure 6).

There are various variables that affect the design of the dual $A_{2A}/A_{2B}AR$ antagonists. Starting with the substitution on xanthine moiety, diethyl substituent on N1- and N3-positions was found to be one of the optimal options for high A_{2A}- and $A_{2B}ARs$ affinity. Different terminal heterocycles rings were introduced and their effects were investigated (Figure 6). Compound **48**, with the 4-pyridyl moiety, displayed high dual $A_{2A}/A_{2B}AR$ antagonistic affinity with almost similar affinity values for both ARs.
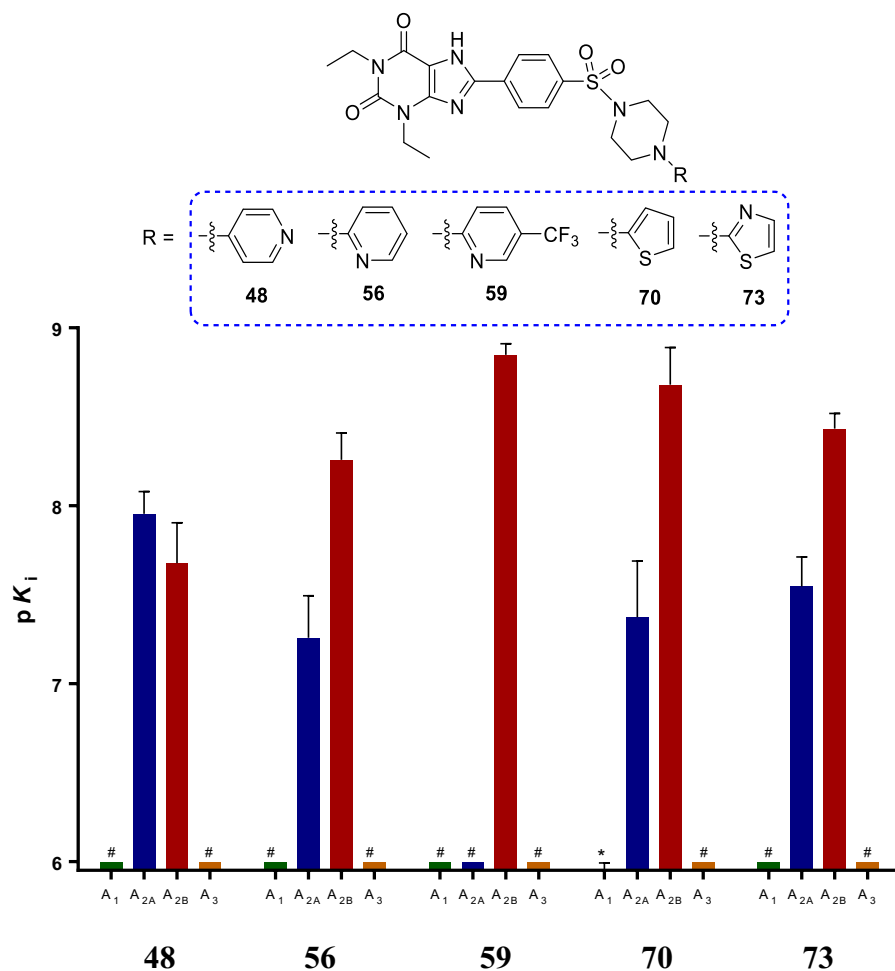

Figure 6. Affinities of compounds **48**, **56**, **59**, **70** and **73** at the four human AR subtypes (A_1, A_{2A}, A_{2B} and A_3) determined in radioligand binding assays; * pK_i < 5.5; # pK_i < 6.

On the other hand, compounds **56**, **70** and **73**, having terminal 2-pyridyl, thiophene or thiazole moieties respectively, displayed also dual $A_{2A}/A_{2B}AR$ antagonistic affinity but with higher preference for the $A_{2B}AR$. Substitution on the 5-position of 2-pyridyl ring with different halides, such as trifluoromethane in compound **59**, demolishes the affinity for the $A_{2A}AR$, resulting in a potent $A_{2B}AR$ antagonist (Figure 6).

Exploring different linkers. We studied the effect of introducing different linkers connecting terminal heterocyclic ring to the main xanthine-sulphonamide core. These linkers include alkyl linkers, for example compounds **74-80**, ether linker, for example compounds **83-85**, and amino linker, for example compounds **81** and **82** (Table 2). Compounds **74** and **75**, having the 4-pyridyl ring connected through an ethyl linker, displayed lower affinity for A_{2A}- and $A_{2B}ARs$ in comparison to the compounds having the directly attached 4-pyridyl ring, for example **44** and **48**. Methylene and ethylene linkers were also explored, for example compounds **76-78** and **79**, **80** respectively. Compounds having the methylene linker displayed slightly higher affinity for $A_{2B}AR$ in comparison for those having the ethylene linker. On the other hand, compounds having the ethylene linker showed higher affinity for $A_{2A}AR$. Compound **80** showed moderate dual antagonistic affinity for A_{2A}- and $A_{2B}ARs$ ($K_i \sim 50$ nM). In conclusion, three different alkyl linkers were explored, however they result in moderate dual antagonists (Table 2).

Amino linker was also explored. Compounds **81** and **82** having *p*-chloro and bromo groups respectively displayed slightly better affinity for $A_{2B}AR$ than the directly linked derivative, **50**. However, they showed lower affinity for the $A_{2A}AR$. The effect of introducing the amino linker in developing potent dual A_{2A}- and $A_{2B}AR$ antagonists is still not fully explored. Also, Compounds **84** and **85**, having an ether linker, displayed better affinity for A_{2A}- and $A_{2B}ARs$ as compared to the directly linked analogues, **44** and **48** (Table 2). Among the different explored linkers, the ether linker such as in **84** and **85** is the only preferential.

Exploring piperidin-4-ol derivatives. Compounds **89-93** having the terminal 4-phenylpiperidin-4-ol moiety were previously reported in our group to display dual antagonistic affinity for A_{2A}- and $A_{2B}ARs$ (unpublished data, Table 2). Compound **89** having a propyl substituent at $N1$ and free $N3$ of xanthine core, displayed high affinity for $A_{2B}AR$ ($K_i = 6.14$ nM) and moderate affinity for $A_{2A}AR$ ($K_i = 45.5$ nM). The substitution on the terminal phenyl ring with *p*-bromo group in compound **91** enhances the affinity for $A_{2B}AR$ ($K_i = 1.57$ nM) and with slight effect on the affinity for $A_{2A}AR$ ($K_i = 42.6$ nM). Introduction of ethyl group to the $N3$-position of xanthine in compound **88** decreased the affinity for $A_{2B}AR$ ($K_i = 10.1$ nM) and increased slightly the affinity for $A_{2A}AR$ ($K_i = 36.0$ nM). Compounds **90** and **93** having the ethyl substituent at $N1$- and $N3$-positions of xanthine displayed high dual antagonistic affinity for A_{2A}- and $A_{2B}ARs$ with affinities ≤ 20 nM, and compound **93** having the *p*-bromo substituent showed high affinity for $A_{2B}AR$ ($K_i = 1.87$ nM) in comparison to the un-substituted compound **90**. We also investigated the 4-(3-pyridyl)piperidin-4-ol moiety such as in compounds **86** and **87**, that combines the pyridyl and the 4-phenylpiperidin-4-ol moieties, that was previously reported from our work to increase the dual $A_{2A}/A_{2B}AR$ antagonistic affinity (Table 2). However, they showed moderate potency and selectivity (Table 2).

In summary, we have developed several dual $A_{2A}/A_{2B}AR$ antagonists. Substitution at the $N1$ with ethyl substituent and at $N3$-position of xanthine core with ethyl or cyclopropyl groups displayed the optimal affinity for both AR subtypes (Figure 7). Also, terminal heterocyclic rings, especially the 4-pyridyl moiety, for example compounds **48** and **49** enhanced the dual $A_{2A}/A_{2B}AR$ antagonistic affinity. Different linkers were investigated, compounds **84** and **85**, having the terminal 4-pyridyl ring connected through an ether linker, showed high dual antagonistic affinity, however alkyl linkers decreased the affinity (Table 2). Compounds **70**, **73** and **88** having the terminal thienyl, thiazolyl and 4-(4-bromophenyl)-

piperidin-4-ol moieties respectively showed good dual $A_{2A}/A_{2B}AR$ antagonistic affinity, but with higher preference for the $A_{2B}AR$ (Figure 7).
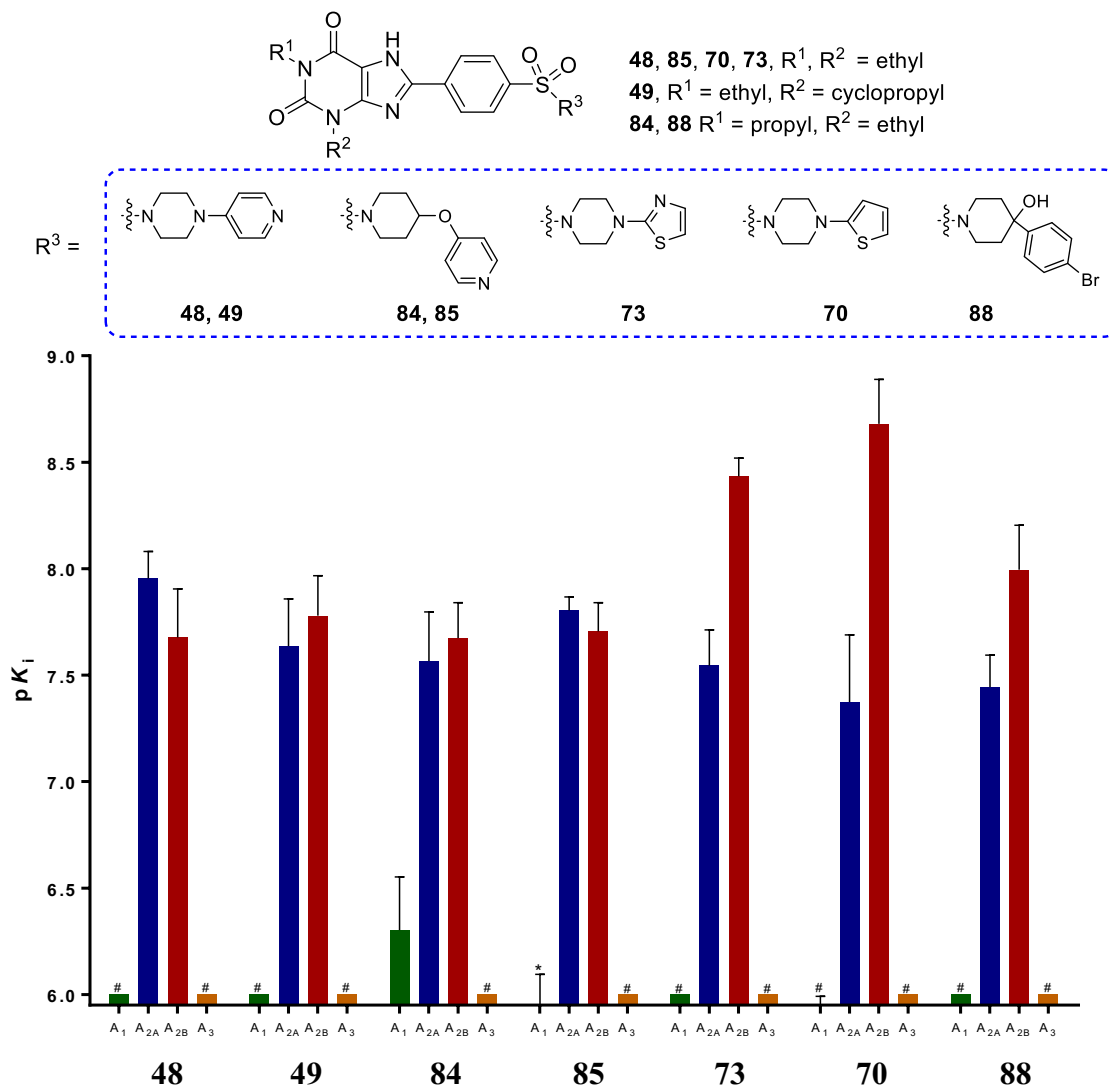

Figure 7. Comparison of the affinities of the best developed dual $A_{2A}/A_{2B}AR$ antagonists **48**, **49**, **84**, **85**, **73**, **70** and **88** at the four human AR subtypes (A_1, A_{2A}, A_{2B} and A_3) determined in radioligand binding assays; * $pK_i < 5.5$; # $pK_i < 6$.

Binding studies for AB928 (1). We selected the commercially available dual $A_{2A}/A_{2B}AR$ antagonist AB928 (**1**), which is currently investigated in clinical trials for the treatment of various malignancies,[40,43,44] as a standard compound for our assays. The reported functional assays in stably expressing CHO cells following stimulation by the AR agonist, 5′-(N-

ethylcarboxamido)adenosine (NECA), showed that the **1** displayed high affinity for A_{2A} and A_{2B}ARs with about (32-43)-fold selective versus A_1AR. Affinity studies showed that **1** exhibits high affinity for A_1, A_{2A} and A_{2B}ARs (Table 2, Figure 8).
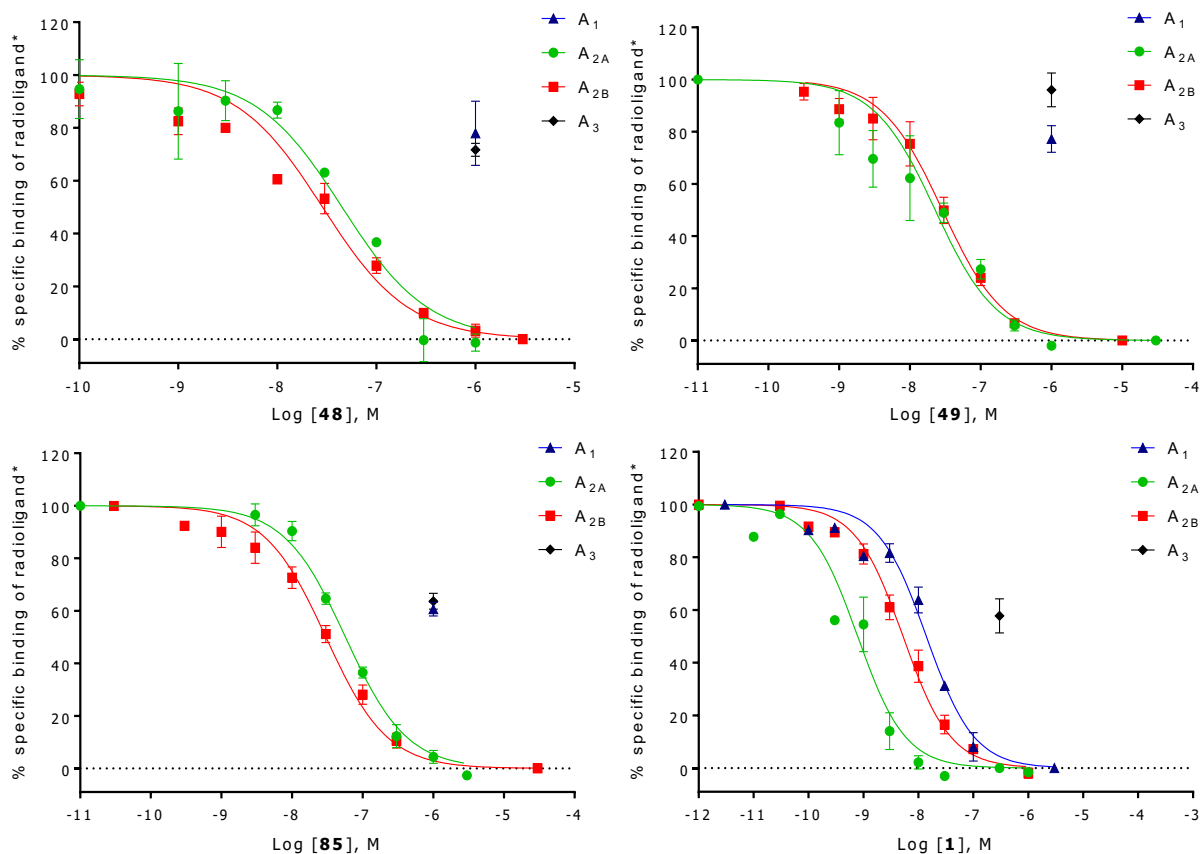

Figure 8. Concentration-dependent inhibition of radioligand binding by compounds **48**, **49**, **85** and AB928 (**1**) to the human AR subtypes. Data points are means (SEM of three experiments performed in duplicates. *A_1AR-selective radioligand [^{3}H]CCPA[69], A_{2A}AR- selective radioligand [^{3}H]MSX-2[70], the A_{2B}AR-selective radioligand [^{3}H]PSB-603[20], *A_3AR-selective radioligand [^{3}H]CCPA.[71] The curve for inhibition of radioligand binding by compound **1** to A_3AR was extrapolated to 100% specific binding.

4.2.4.4. Physicochemical and Pharmacokinetic Properties

The physicochemical properties of the developed compounds limits their further development as drug candidates, therefore these properties should be considered and optimized to have drug-

like compounds.[88] Selected compounds representing the different synthesized compounds were investigated for their physicochemical and pharmacokinetic properties by Pharmacelsus company (Table 3).[89]

Table 3. *In-vitro* ADME studies data of piperazinylxanthine derivatives **46-48**, **52**, **58**, **64**, **65** and **67** and piperidinylxanthine derivatives **82** and **88** in comparison to PSB-603.

Compd.	R^1	R^2	BBB	Aqueous Solubility (µM)^a	Microsomal Stability (µl/min/mg protein)	
46	propyl	ethyl	BBB+	12.2 ± 1.0	h: 17.6	m: 81.6
47	methyl	methyl	BBB+	n.d.	h: 4.8	m: 125.2
48	ethyl	ethyl	BBB+	4.6 ± 0.7	h: 2.8	m: 70.6
52	propyl	H	n.d.	4.7 ± 1.2	h: 32.6	m: 18.8
58	propyl	H	n.d.	0.2 ± 0.1	h: 14.0	m: 14.0
64	propyl	methyl	BBB-	0.4 ± 0.1	h: 8.4	m: 10.8
65	propyl	ethyl	BBB-	0.4 ± 0.1	h: 30.4	m: 33.0
67	propyl	H	n.d.	0.3 ± 0.1	h: 91.2	m: 79.4
82	propyl	H	n.d.	0.9 ± 0.1	h: 14.4	m: 38.6
88	propyl	ethyl	BBB-	0.2 ± 0.0	h: -11.6	m: 19.4
PSB-603	propyl	H	BBB-	0.2 ± 0.1	h: -3.8	m: 8.4
Verapamil					h: 217.3	m: 147.8
Testosterone			BBB+			

^{a} Measured using semi-thermodynamic approach in aqueous buffered solutions.

The blood–brain barrier (BBB) controls the entry of molecules and cells from the blood into the central nervous system (CNS). Compounds **46**-**48** containing the 4-pyridyl moiety can pass the BBB, therefore they could be further considered to target CNS. On the other hand, compounds **64** and **65** having the terminal pyrimidyl moiety and compounds **88** and **PSB-603** having the terminal phenyl moieties, failed to pass the BBB. We also measured the water solubility of some compounds, which is an important parameter that affects the oral bioavailability and the chemical stability of pharmaceutical compounds.[90] Compounds having terminal pyridyl moieties (4-pyridyl and 2-pyridyl) displayed good water solubility, especially compound **46** having propyl substituent at N3- of xanthine core and ethyl substituent at N1- position.

Substitution at the terminal pyridyl moiety with bromo substituent, for example compound **58**, demolishes the solubility. Compound **82** having the amino linker, displayed slightly better aqueous solubility (0.9 µM) than compound **58** (0.15 µM). Aromatic rings other than the pyridine, such as phenyl, pyrimidine and benzo[d]isothiazole, decrease greatly the aqueous solubility of the compounds. Compound **46** and **48**, having the terminal 4-pyridyl moiety, displayed good dual $A_{2A}/A_{2B}AR$ antagonistic affinity, also they showed good physicochemical properties (good aqueous solubility, can pass the BBB and are metabolically stable in humans). Therefore, they could be used as a pharmacological tool. Microsomal stability studies showed that our compounds are more stable in humans than in mouse, also there is a big variation in values between different species (Table 3).

4.2.5. Conclusion

Adenosine suppresses the antitumor immune responses mediated through A_{2A} adenosine receptors ($A_{2A}ARs$) expressed on the T-lymphocytes and $A_{2B}ARs$ expressed on myeloid cells. Therefore, developing a dual $A_{2A}/A_{2B}AR$ antagonist that can block the effects of adenosine on both AR subtypes could be synergistic in cancer (immuno)therapy. In this study, we optimized

the structure of the potent A$_{2B}$AR antagonist PSB-1901 to develop dual A$_{2A}$/A$_{2B}$AR antagonists. We carried out various structural modifications on the xanthine core and on the terminal phenyl substituent to restore the A$_{2A}$AR affinity while retaining A$_{2B}$AR affinity. Compounds **48**, **49**, **84** and **85** having a terminal 4-pyridyl moiety displayed high dual antagonistic affinity for A$_{2A}$- and A$_{2B}$ARs. Additionally, **46** and **48** expressed good aqueous solubility, they are predicted to pass the BBB and are metabolically stable in human liver microsomes. Compounds **70**, **73**, and **80** having terminal thienyl, thiazolyl or 4-(4-bromophenyl)piperidin-4-ol moieties showed good dual A$_{2A}$/A$_{2B}$AR antagonistic affinity with somewhat higher affinity for the A$_{2B}$AR. The developed dual A$_{2A}$/A$_{2B}$AR antagonists displayed drug-like properties and could be valuable tools and potentially become drugs in cancer (immnuo)therapy.

4.2.6. Experimental section

4.2.6.1.   Chemistry

General. All reagents used in this study were commercially obtained from various vendors (Sigma, Aldrich, Merck, Enamine and Acros) and used without further purification. Solvents were used without additional purification or drying, except dichloromethane which was freshly distilled. Reactions were monitored by thin-layer chromatography (TLC) using aluminum sheets coated with silica gel 60 F$_{254}$ (Merck). Column chromatography for the products was performed with a CombiFlash R_f Companion System using RediSep packed columns. Preparative HPLC was carried out on a Knauer HPLC system with a Wellchrome K-1800 pump, a WellChrome K-2600 spectrophotometer with a Eurospher 100 C18 column (250 mm × 20 mm, particle size 10 μm). A gradient of methanol or acetonitrile in water was used as indicated below with a flow rate of 15 mL/min. Lyophilization was performed with a CHRIST ALPHA 1-4 LSC freeze dryer.

The purity of all biologically evaluated compounds was determined by HPLC-UV using an LC-MS instrument (Applied Biosystems API 2000 LC-MS/MS, HPLC Agilent 1100)

according to the following procedure: Compounds were dissolved at a concentration of 0.5 mg/mL in methanol/H_2O (1:1). Then, 10 μL of the sample were injected into a Phenomenex Luna C18 HPLC column (50 mm × 2.00 mm, particle size 3 μm) and chromatographed using a gradient of water/methanol (containing 2 mM ammonium acetate) from 90:10 to 0:100 for 20 min at a flow rate of 250 μL/min. UV absorption was detected from 200 to 950 nm using a diode array detector. Mass spectra were recorded on an API 2000 mass spectrometer (electron spray ion source, Applied Biosystems, Darmstadt, Germany) coupled with an Agilent 1100 HPLC system. For all other intermediate compounds, the same method was employed, but the compounds were dissolved in methanol.

High-resolution mass spectra (HRMS) were recorded on a micrOTOF-Q mass spectrometer (Bruker) with ESI-source coupled with an HPLC Dionex Ultimate 3000 (Thermo Scientific) using an EC50/2 Nucleodur C18 Gravity 3 μm column (Macherey-Nagel). The column temperature was 25 °C. Ca. 1 μL of a 1 mg/mL solution of the sample in acetonitrile was injected and a flow rate of 0.3 mL/min was applied. HPLC was started with a solution of acetonitrile in water (10:90) containing 2 mM ammonium acetate. The gradient was started after 1 min reaching 100% acetonitrile within 9 min and then flushed at this concentration for another 5 min. ^{1}H- and ^{13}C-NMR data were collected on a Bruker Avance 500 MHz NMR spectrometer at 500 MHz (^{1}H), and 126 MHz (^{13}C), or on a 600 MHz NMR spectrometer at 600 MHz (^{1}H), and 151 MHz (^{13}C). DMSO-d_6 or Deuterium Oxide (D_2O) were used as solvents. Chemical shifts are reported in parts per million (ppm) relative to the deuterated solvent, i.e. DMSO, [1]H: 2.50 ppm; [13]C: 39.5 ppm; D_2O, δ [1]H: 4.80 ppm. Coupling constants J values were reported in Hertz and spin multiplicities are given as s (singlet), d (doublet), t (triplet), m (multiplet) and br (broad). Piperazines (**24**, **26**, **28**, **31**, **33** and **38**) were obtained from commercial sources. Detailed synthetic procedures for the required piperazines (**25**, **27**, **29**, **30**,

32, **34-37**) and piperidines (**39-43**) are described in the Supporting Information; they were obtained in analogy to previously described methods[75–81] with some modifications.

Synthesis of target compounds 44-88.

General procedure A. This procedure has been applied to the preparation of **58-60**, **62**, **66**, **81-88**. To a solution of *p*-nitrophenylsulfonate derivatives **19**, **21** or **22** (1 eq) dissolved in 3-5 mL of anhydrous DMSO, the appropriate amine (**27-30**, **32** or **39-43**, 4 eq) was added and the reaction mixture was stirred at 140ºC for 7-18 h under an argon atmosphere. Upon completion of the reaction, the reaction mixture was then poured into 30 mL of water and a precipitate was formed. The solid was filtered off and washed with water (3 × 10 mL) and methanol (3 × 5 mL). Samples were further purified using column chromatography using eluent system DCM/methanol (9:1) to DCM/methanol (9.8:0.2).

General procedure B. This procedure has been applied to the preparation of **44-57**, **61**, **63-65** and **67-80**. To a solution of *p*-nitrophenylsulfonate derivative **18-32** (1 eq) dissolved in 3-5 mL of sulfolane, the appropriate amine (**24-26**, **31**, **33-38**, 4 eq) was added and the reaction mixture was stirred at 130ºC for 3-18 h under an argon atmosphere. Upon completion of the reaction, the reaction mixture was then poured into 30 mL of water and a precipitate was formed. The solid was filtered off and washed with water (3 × 10 mL) and methanol (3 × 5 mL). Samples were further purified using column chromatography using eluent system DCM/methanol (9:1) to DCM/methanol (9.8:0.2).

1-Propyl-8-(4-{[4-(pyridin-4-yl)piperazin-1-yl]sulfonyl}phenyl)-2,3,6,7-tetrahydro-1*H*-purine-2,6-dione (44). This compound was synthesized according to the general procedure B using *p*-nitrophenylsulfonate derivative **19** (65 mg, 0.14 mmol) and piperazine **24** (70 mg, 0.43 mmol) dissolved in 3 mL of sulfolane and the reaction mixture was stirred at 130 ºC for 8 h. White solid; yield (31%, 21 mg). M.p.: 330-337 °C. ^{1}H NMR (500 MHz, DMSO-*d6*) δ 14.05 (s, 1H,

NH$_{xanthine}$), 11.95 (s, 1H, NH$_{xanthine}$), 8.35-8.30 (t, J = 8.2 Hz, 2H, CH$_{phenyl}$), 8.23-8.18 (d, J = 6.9 Hz, 2H, CH$_{pyridyl}$), 7.91-7.86 (dd, J = 8.2 Hz, 2H, CH$_{phenyl}$), 7.14-7.12 (dd, 2H, CH$_{pyridyl}$), 3.83-3.79 (m, 2H, CH$_{2(propyl)}$), 3.79-3.73 (m, 4H, CH$_{piperazinyl}$), 3.17-3.06 (m, 4H, CH$_{piperazinyl}$), 1.62-1.50 (m, 2H, CH$_{2(propyl)}$), 0.86 (t, J = 7.4 Hz, 3H, CH$_{3(propyl)}$). ^{13}C NMR (126 MHz, DMSO-d_6) δ 157, 155.4, 151.4, 140.6, 136.1, 133.7, 133.6, 128.8, 128.7, 127.6, 127.5, 108.3, 70.2, 45.5 (CH$_{piperazinyl}$), 45.3 (CH$_{piperazinyl}$), 21.3 (CH$_{2(propyl)}$), 11.7 (CH$_{3(propyl)}$). HPLC-UV (254 nm) ESI-MS, purity: 96.5%. LC-MS (m/z): 496.3 [M + H]$^+$. HRMS (ESI-TOF) m/z: [M - H]$^-$ calcd. for C$_{23}$H$_{25}$N$_7$O$_4$S 494.1689, found 494.1637.

3-Methyl-1-propyl-8-(4-{[4-(pyridin-4-yl)piperazin-1-yl]sulfonyl}phenyl)-2,3,6,7-tetrahydro-1*H*-purine-2,6-dione (45). This compound was synthesized according to the general procedure B using *p*-nitrophenylsulfonate derivative **20** (50 mg, 0.10 mmol) and piperazine **24** (55 mg, 0.34 mmol) dissolved in 4 mL of sulfolane and the reaction mixture was stirred at 130 °C for 12 h. White solid; yield (46%, 24 mg). M.p.: 340-344 °C. ^{1}H NMR (500 MHz, DMSO-d_6) δ 13.93 (s, 1H, NH$_{xanthine}$), 8.33-8.41 (t, J= 8.3 Hz, 2H, CH$_{phenyl}$), 8.16-8.25 (d, J = 7.0 Hz, 2H, CH$_{pyridyl}$), 7.85-7.94 (dd, J = 7.3 Hz, 2H, CH$_{phenyl}$), 7.11-7.14 (dd, 2H, CH$_{pyridyl}$), 3.82-3.89 (m, 2H, CH$_{2(propyl)}$), 3.72-3.80 (m, 4H, CH$_{piperazinyl}$), 3.45-3.54 (t, 3H, CH$_{3(methyl)}$), 3.06-3.17 (m, 4H, CH$_{piperazinyl}$), 1.51-1.65 (m, 2H, CH$_{2(propyl)}$), 0.87 (t, J = 7.4 Hz, 3H, CH$_{3(propyl)}$). ^{13}C NMR (126 MHz, DMSO-d_6) δ 156.7, 151, 140.3, 135.9, 133.2, 128.4, 127.3, 126.8, 126.1, 109, 108, 50.7, 45.3 (CH$_{piperazinyl}$), 42.4 (CH$_{piperazinyl}$), 22.2, 20.9 (CH$_{2\ (propyl)}$), 11.3 (CH$_{3(propyl)}$). HPLC-UV (254 nm) ESI-MS, purity: 97.7%. LC-MS (m/z): 510.0 [M + H]$^+$. HRMS (ESI-TOF) m/z: [M - H]$^-$ calcd. for C$_{24}$H$_{27}$N$_7$O$_4$S 508.1845, found 508.1764.

3-Ethyl-1-propyl-8-(4-{[4-(pyridin-4-yl)piperazin-1-yl]sulfonyl}phenyl)-2,3,6,7-tetrahydro-1*H*-purine-2,6-dione (46). This compound was synthesized according to the general procedure B using *p*-nitrophenylsulfonate derivative **21** (50 mg, 0.10 mmol) and piperazine **24** (55 mg, 0.34 mmol) dissolved in 4 mL of sulfolane and the reaction mixture was stirred at 130 °C for

15 h. White solid; yield (39%, 20 mg). M.p.: 342-347 °C. ^{1}H NMR (500 MHz, DMSO-d_6) δ 14.05 (s, 1H, NH$_{xanthine}$), 8.34-8.41 (t, J = 8.1 Hz, 2H, CH$_{phenyl}$), 8.15-8.25 (d, J = 6.8 Hz, 2H, CH$_{pyridyl}$), 7.85-7.94 (dd, J = 8.2 Hz, 2H, CH$_{phenyl}$), 7.07-7.15 (dd, 2H, CH$_{pyridyl}$), 4.03-4.13 (m, 2H, CH$_{2(ethyl)}$), 3.82-3.92 (m, 2H, CH$_{2(propyl)}$), 3.72-3.80 (m, 4H, CH$_{piperazinyl}$), 3.08-3.17 (m, 4H, CH$_{piperazinyl}$), 1.52-1.63 (m, 2H, CH$_{2(propyl)}$),1.18-1.31 (t, J= 7.0 Hz, 3H, CH$_{3(ethyl)}$), 0.87 (t, J = 7.4 Hz, 3H, CH$_{3(propyl)}$).^{13}C NMR (126 MHz, DMSO-d_6) δ 157.8, 156.6, 150.4, 148, 140.3, 135.9, 133.2, 128.4, 127.4, 107.9, 50.7, 45.3 (CH$_{piperazinyl}$), 42.4 (CH$_{piperazinyl}$), 22.23, 21 (CH$_{2(propyl)}$), 13.3, 11.3 (CH$_{3(propyl)}$). HPLC-UV (254 nm) ESI-MS, purity: 96.7%. LC-MS (m/z): 524.2 [M + H]$^+$. HRMS (ESI-TOF) m/z: [M - H]$^-$ calcd. for C$_{25}$H$_{29}$N$_7$O$_4$S 522.2002, found 522.1918.

1,3-Dimethyl-8-(4-{[4-(pyridin-4-yl)piperazin-1-yl]sulfonyl}phenyl)-2,3,6,7-tetrahydro-1*H*-purine-2,6-dione (47). This compound was synthesized according to the general procedure B using *p*-nitrophenylsulfonate derivative **23** (50 mg, 0.11 mmol) and piperazine **24** (55 mg, 0.34 mmol) dissolved in 3 mL of sulfolane and the reaction mixture was stirred at 130 °C for 10 h. White solid; yield (41%, 21 mg); ^{1}H NMR (500 MHz, DMSO-d_6) δ 13.92 (s, 1H, NH$_{xanthine}$), 8.44-8.30 (t, J = 7.9 Hz, 2H, CH$_{phenyl}$), 8.26-8.07 (d, J = 6.5 Hz, 2H, CH$_{pyridyl}$), 7.98-7.84 (dd, J = 7.7 Hz, 2H, CH$_{phenyl}$), 7.19-7.05 (dd, J = 6.7 Hz, 2H, CH$_{pyridyl}$), 3.84-3.70 (m, 4H, CH$_{piperazinyl}$), 3.55-3.40 (t, 3H, CH$_{3(methyl)}$), 3.27-3.23 (t, 3H, CH$_{3(methyl)}$), 3.12 (m, 4H, CH$_{piperazinyl}$). ^{13}C NMR (126 MHz, DMSO-d_6) δ 156.7, 154.5, 151.3, 148.5, 147.7, 140.2, 135.9, 133.2, 128.4, 127.3, 108.8, 108, 94.7, 45.3 (CH$_{piperazinyl}$), 42.4 (CH$_{piperazinyl}$), 30 (CH$_3$), 28 (CH$_3$). HPLC-UV (254 nm) ESI-MS, purity: 98.7%. LC-MS (m/z): 482.2 [M + H]$^+$. HRMS (ESI-TOF) m/z: [M - H]$^-$ calcd. for C$_{22}$H$_{23}$N$_7$O$_4$S 480.1532, found 480.1448.

1,3-Diethyl-8-(4-{[4-(pyridin-4-yl)piperazin-1-yl]sulfo-nyl}phenyl)-2,3,6,7-tetrahydro-1*H*-purine-2,6-dione (48). This compound was synthesized according to the general procedure

B using *p*-nitrophenylsulfonate derivative **22** (40 mg, 0.08 mmol) and piperazine **24** (45 mg, 0.28 mmol) dissolved in 3 mL of sulfolane and the reaction mixture was stirred at 130 °C for 10 h. White solid; yield (58%, 24 mg). M.p.: 346-349 °C. ^{1}H NMR (500 MHz, DMSO-*d$_6$*) δ 13.92 (s, 1H, NH$_{xanthine}$), 8.44-8.30 (t, *J* = 7.9 Hz, 2H, CH$_{phenyl}$), 8.26-8.07 (d, *J* = 6.5 Hz, 2H, CH$_{pyridyl}$), 7.98-7.84 (dd, *J* = 7.7 Hz, 2H, CH$_{phenyl}$), 6.84-6.68 (dd, 2H, CH$_{pyridyl}$), 4.24-4.01 (m, 2H, CH$_{2(ethyl)}$), 3.90-3.79 (m, 2H, CH$_{2(ethyl)}$), 3.59-3.34 (m, 4H, CH$_{piperazinyl}$), 3.14-2.98 (m, 4H, CH$_{piperazinyl}$), 1.33-1.21 (t, 3H, CH$_{3(ethyl)}$), 1.19-1.06 (t, 3H, CH$_{3(ethyl)}$). ^{13}C NMR (126 MHz, DMSO-*d$_6$*) δ 156.7, 154.5, 151.3, 148.5, 147.7, 140.2, 135.9, 133.2, 128.4, 127.3, 108.8, 108, 94.7, 45.3 (CH$_{piperazinyl}$), 42.4 (CH$_{piperazinyl}$), 30 (CH$_{3(ethyl)}$), 28 (CH$_{3(ethyl)}$). HPLC-UV (254 nm) ESI-MS, purity: 95.5%. LC-MS (m/z): 510.1 [M + H]$^+$. HRMS (ESI-TOF) m/z: [M - H]$^-$ calcd. for C$_{24}$H$_{27}$N$_7$O$_4$S 508.1845, found 510.1920.

3-Cyclopropyl-1-ethyl-8-(4-((4-(pyridin-4-yl)piperazin-1-yl)sulfonyl)phenyl)-3,7-dihydro-1*H*-purine-2,6-dione (49). This compound was synthesized according to the general procedure B using *p*-nitrophenylsulfonate derivative **18** (50 mg, 0.10 mmol) and piperazine **24** (50 mg, 0.31 mmol) dissolved in 5 mL of sulfolane and the reaction mixture was stirred at 130 °C for 14 h. White solid; yield (41%, 21 mg). M.p.: 346-349 °C. ^{1}H NMR (600 MHz, DMSO-*d$_6$*) δ 8.38-8.31 (d, *J* = 8.5 Hz, 2H, CH$_{phenyl}$), 8.17-8.09 (d, *J* = 3.9 Hz, 2H, CH$_{pyridyl}$), 7.91-7.85 (d, *J* = 8.5 Hz, 2H, CH$_{phenyl}$), 6.82-6.75 (d, *J* = 6.4 Hz, 2H, CH$_{pyridyl}$), 3.91 (q, *J* = 7.0 Hz, 2H, CH$_{2(ethyl)}$), 3.47-3.41 (m, 4H, CH$_{piperazinyl}$), 3.06-3.00 (m, 4H, CH$_{piperazinyl}$), 1.15-1.12 (t, 3H, CH$_{3(ethyl)}$), 1.10-1.03 (m, 2H, CH$_{2 (cyclopropyl)}$), 1.03-0.96 (m, 2H, CH$_{2(cyclopropyl)}$). ^{13}C NMR (151 MHz, DMSO-*d$_6$*) δ 154.5, 154.3, 151.3, 149.2, 149, 147.7, 135.4, 133.8, 128.4, 127.2, 125.9, 112.4, 109.8, 108.8, 56, 50.7, 45.5, 45.4, 45.1, 44.6, 36, 32.2, 29.8, 26.4, 13.3, 7.9. HPLC-UV (254 nm) ESI-MS, purity: 99.5%. LC-MS (m/z): 522.4 [M + H]$^+$. HRMS (ESI-TOF) m/z: [M - H]$^-$ calcd. for C$_{25}$H$_{27}$N$_7$O$_4$S 520.1845, found 520.1761.

1-Propyl-8-(4-((4-(pyridin-3-yl)piperazin-1-yl)sulfonyl)phenyl)-3,7-dihydro-1*H*-purine-2,6-dione (50). This compound was synthesized according to the general procedure B using *p*-nitrophenylsulfonate derivative **19** (60 mg, 0.13 mmol) and piperazine **25** (65 mg, 0.40 mmol) dissolved in 4 mL of sulfolane and the reaction mixture was stirred at 130 ºC for 15 h. White solid; yield (48%, 30 mg). M.p.: 330-337 °C. ^{1}H NMR (600 MHz, DMSO-*d₆*) δ 8.37-8.30 (d, *J* = 8.4 Hz, 2H, CH$_{phenyl}$), 8.24 (s, 1H, CH$_{pyridyl}$), 7.99-7.95 (d, *J* = 4.1 Hz, 1H, CH$_{pyridyl}$), 7.91-7.85 (d, *J* = 8.4 Hz, 2H, CH$_{phenyl}$), 7.29-7.23 (dd, *J* = 8.4 Hz, 1.7 Hz, 1H, CH$_{pyridyl}$), 7.20-7.16 (dd, *J* = 8.4 Hz, 4.5 Hz, 1H, CH$_{pyridyl}$), 3.84-3.78 (m, 2H, CH$_{2(propyl)}$), 3.29-3.24 (m, 4H, CH$_{piperazinyl}$), 3.11-3.03 (m, 4H, CH$_{piperazinyl}$), 1.61-1.52 (m, 2H, CH$_{2\ (propyl)}$), 0.90-0.83 (t, *J* = 7.4 Hz, 3H, CH$_{3(propyl)}$). ^{13}C NMR (151 MHz, DMSO-*d₆*) δ 155.2, 151.2, 148.1, 147.7, 146.2, 140.7, 138.5, 135.7, 133.4, 128.5, 127.2, 123.7, 122.8, 47.5, 45.8, 41.7, 21.1, 11.4. HPLC-UV (254 nm) ESI-MS, purity: 100%. LC-MS (m/z): 496.2 [M + H]$^+$. HRMS (ESI-TOF) m/z: [M - H]$^-$ calcd. for C$_{23}$H$_{25}$N$_7$O$_4$S 494.1689, found 494.1612.

3-Ethyl-1-propyl-8-(4-((4-(pyridin-3-yl)piperazin-1-yl)sulfonyl)phenyl)-3,7-dihydro-1*H*-purine-2,6-dione (51). This compound was synthesized according to the general procedure B using *p*-nitrophenylsulfonate derivative **21** (60 mg, 0.12 mmol) and piperazine **25** (65 mg, 0.40 mmol) dissolved in 3 mL of sulfolane and the reaction mixture was stirred at 130 ºC for 15 h. White solid; yield (50%, 31 mg). M.p.: 330-337 °C. ^{1}H NMR (500 MHz, DMSO-*d₆*) δ 14.18 (s, 1H, NH$_{xanthine}$), 8.40-8.35 (d, *J* = 8.5 Hz, 2H, CH$_{phenyl}$), 7.99-7.95 (d, *J* = 4.5 Hz, 1.2 Hz, 1H, CH$_{pyridyl}$), 7.91-7.86 (d, *J* = 8.5 Hz, 2H, CH$_{phenyl}$), 7.33-7.24 (m, 1H, CH$_{pyridyl}$), 7.20-7.16 (dd, *J* = 8.5, 4.6 Hz, 1H, CH$_{pyridyl}$), 4.15-4.05 (q, *J* = 7.0 Hz, 2H, CH$_{2(ethyl)}$), 3.84-3.78 (m, 2H, CH$_{2(propyl)}$), 3.29-3.23 (m, 4H, CH$_{piperazinyl}$), 3.12-3.05 (m, 4H, CH$_{piperazinyl}$), 1.61-1.56 (m, 2H, CH$_{2(propyl)}$), 1.27-1.23 (t, *J* = 7.1 Hz, 3H, CH$_{3\ (ethyl)}$), 0.90-0.83 (t, *J* = 7.4 Hz, 3H, CH$_{3(propyl)}$). ^{13}C NMR (126 MHz, DMSO-*d₆*) δ 154.3, 150.5, 148.1, 146.2, 140.6, 138.5, 135.8, 133.1, 128.5, 127.3, 123.6, 122.7, 108.9, 47.4, 45.8, 42.4, 38.3, 29.7, 21, 13.3, 11.3. HPLC-UV (254

nm) ESI-MS, purity: 97.8%. LC-MS (m/z): 524.3 $[M + H]^+$. HRMS (ESI-TOF) m/z: $[M - H]^-$ calcd. for $C_{25}H_{29}N_7O_4S$ 522.2002, found 522.1982.

1-Propyl-8-(4-{[4-(pyridin-2-yl)piperazin-1-yl]sulfo-nyl}phenyl)-2,3,6,7-tetrahydro-1*H*-purine-2,6-dione (52). This compound was synthesized according to the general procedure B using *p*-nitrophenylsulfonate derivative **19** (40 mg, 0.08 mmol) and piperazine **26** (40 mg, 0.25 mmol) dissolved in 4 mL of sulfolane and the reaction mixture was stirred at 130 ºC for 10 h. White solid; yield (37%, 16 mg). M.p.: 340-344 °C. ^{1}H NMR (500 MHz, DMSO-*d₆*) δ 14.00 (s, 1H, NH_xanthine), 11.94 (s, 1H, NH_xanthine), 8.37-8.27 (m, *J* = 4.9 Hz, 2H, CH_phenyl), 8.10-8.02 (m, *J* = 4.9 Hz, 1H, CH_pyridyl), 7.91-7.82 (m, *J* = 8.5 Hz, 1H, CH_pyridyl), 7.54-7.43 (m, *J* = 8.9 Hz, 2H, CH_phenyl), 6.84-6.75 (dd, *J* = 8.6 Hz, 1H, CH_pyridyl), 6.66-6.58 (dd, 1H, CH_pyridyl), 3.83-3.79 (m, 2H, CH_2(propyl)), 3.61-3.55 (m, 4H, CH_piperazinyl), 3.04-2.99 (m, 4H, CH_piperazinyl), 1.60-1.52 (m, 2H, CH_2(propyl)), 0.89-0.84 (t, 3H, CH_3(propyl)). ^{13}C NMR (126 MHz, DMSO-*d₆*) δ 158.4, 155.1, 151.1, 148.1, 147.8, 139.3, 137.9, 135.8, 133.2, 129.8, 128.5, 127.2, 124.2, 113.8, 108.7, 107.6, 45.7 (CH_piperazinyl), 44.2 (CH_piperazinyl), 41.7, 34.6, 30.5, 29.2, 22.2 (CH_3), 21, 11.4. HPLC-UV (254 nm) ESI-MS, purity: 98.7%. LC-MS (m/z): 496.3 $[M + H]^+$. HRMS (ESI-TOF) m/z: $[M - H]^-$ calcd. for $C_{23}H_{25}N_7O_4S$ 494.1689, found 494.1605.

3-Methyl-1-propyl-8-(4-((4-(pyridin-2-yl)piperazin-1-yl)sulfonyl)phenyl)-3,7-dihydro-1*H*-purine-2,6-dione (53). This compound was synthesized according to the general procedure B using *p*-nitrophenylsulfonate derivative **20** (70 mg, 0.14 mmol) and piperazine **26** (75 mg, 0.46 mmol) dissolved in 3 mL of sulfolane and the reaction mixture was stirred at 130 ºC for 15 h. White solid; yield (29%, 21 mg). M.p.: 330-337 °C. ^{1}H NMR (500 MHz, DMSO-*d₆*) δ 14.17 (s, 1H, NH_xanthine), 8.36 (d, *J* = 8.6 Hz, 2H, CH_phenyl), 8.06-8.01 (m, 2H, CH_pyridyl), 7.93-7.87 (m, 2H, CH_phenyl), 7.66 (d, *J* = 8.9 Hz, 1H, CH_pyridyl), 6.98 (d, *J* = 8.9 Hz, 1H, CH_pyridyl), 6.76-6.70 (t, *J* = 9.9 Hz, 1H, CH_pyridyl), 3.89-3.85 (q, *J* = 7.0 Hz, 2H, CH_2(propyl)), 3.09-3.05 (t, *J* =

5.1 Hz, 4H, CH$_{piperazinyl}$), 1.63-1.52 (m, 2H, CH$_{2(propyl)}$), 0.89-0.85 (t, J = 7.4 Hz, 3H, CH$_{3(propyl)}$). ^{13}C NMR (126 MHz, DMSO-d_6) δ 154.3, 151.1, 148.6, 147.8, 139.9, 136, 133.1, 128.4, 127.3, 113.6, 109.5, 108.8, 45.5, 44.6, 42.5, 29.9, 21, 11.3. HPLC-UV (254 nm) ESI-MS, purity: 98.3%. LC-MS (m/z): 510.1 [M + H]$^+$. HRMS (ESI-TOF) m/z: [M - H]$^-$ calcd. for C$_{24}$H$_{27}$N$_7$O$_4$S 508.1845, found 508.1811.

3-Ethyl-1-propyl-8-(4-((4-(pyridin-2-yl)piperazin-1-yl)sulfonyl)phenyl)-3,7-dihydro-1*H*-purine-2,6-dione (54). This compound was synthesized according to the general procedure B using *p*-nitrophenylsulfonate derivative **21** (70 mg, 0.14 mmol) and piperazine **26** (75 mg, 0.46 mmol) dissolved in 4 mL of sulfolane and the reaction mixture was stirred at 130 ºC for 15 h. White solid; yield (37%, 27 mg). M.p.: 330-337 °C. ^{1}H NMR (500 MHz, DMSO-d_6) δ 14.10 (s, 1H, NH$_{xanthine}$), 8.38-8.32 (d, J = 8.1 Hz, 2H, CH$_{phenyl}$), 8.10-8.02 (m, 2H, CH$_{pyridyl}$), 7.89-7.86 (d, J = 8.1 Hz, 2H, CH$_{phenyl}$), 7.55-7.43 (m, 1H, CH$_{pyridyl}$), 6.79-6.75 (d, J = 8.6 Hz, 1H, CH$_{pyridyl}$), 6.64-6.60 (dd, J = 7.1, 4.8 Hz, 1H, CH$_{pyridyl}$), 4.10-4.05 (q, J = 7.0 Hz, 2H, CH$_{2(ethyl)}$), 3.87-3.80 (dd, J = 8.6, 6.3 Hz, 2H, CH$_{2(propyl)}$), 3.67-3.53 (m, 4H, CH$_{piperazinyl}$), 3.05-3.00 (t, J = 4.9 Hz, 4H, CH$_{piperazinyl}$), 1.59-1.54 (q, J = 7.5 Hz, 2H, CH$_{2(propyl)}$), 1.27-1.24 (t, J = 7.0 Hz, 3H, CH$_{3(ethyl)}$), 0.89-0.85 (t, J = 7.4 Hz, 3H, CH$_{3(propyl)}$). ^{13}C NMR (126 MHz, DMSO-d_6) δ 158.4, 154.4, 150.5, 148.1, 148, 147.6, 137.8, 135.9, 133.2, 128.4, 127.3, 113.7, 107.6, 45.7, 44.2, 42.4, 21, 13.3, 11.3. HPLC-UV (254 nm) ESI-MS, purity: 99.4%. LC-MS (m/z): 524.1 [M + H]$^+$. HRMS (ESI-TOF) m/z: [M - H]$^-$ calcd. for C$_{25}$H$_{29}$N$_7$O$_4$S 522.2002, found 522.1931.

1,3-Dimethyl-8-(4-((4-(pyridin-2-yl)piperazin-1-yl)sulfonyl)phenyl)-3,7-dihydro-1*H*-purine-2,6-dione (55). This compound was synthesized according to the general procedure B using *p*-nitrophenylsulfonate derivative **23** (70 mg, 0.15 mmol) and piperazine **26** (75 mg, 0.46 mmol) dissolved in 5 mL of sulfolane and the reaction mixture was stirred at 130 ºC for 9 h. White solid; yield (48%, 35 mg). M.p.: 330-337 °C. ^{1}H NMR (500 MHz, DMSO-d_6) δ 14.15 (s, 1H, NH$_{xanthine}$), 8.38-8.32 (d, J = 8.1 Hz, 2H, CH$_{phenyl}$), 8.10-8.02 (m, 2H, CH$_{pyridyl}$), 7.92-

7.86 (d, J = 8.5 Hz, 2H, CH$_{phenyl}$), 7.52-7.46 (m, 1H, CH$_{pyridyl}$), 6.79-6.74 (d, J = 8.8, 1.0 Hz, 1H, CH$_{pyridyl}$), 6.64-6.60 (ddd, J = 7.1, 4.9, 0.9 Hz, 1H, CH$_{pyridyl}$), 3.58-3.50 (t, J = 5.0 Hz, 4H, CH$_{piperazinyl}$), 3.50-3.40 (t, J = 5.0 Hz, 4H, CH$_{piperazinyl}$), 3.25-3.20 (t, J = 0.9 Hz, 3H, CH$_{3(methyl)}$), 3.05-3.00 (t, J = 5.0 Hz, 3H, CH$_{3(methyl)}$). ^{13}C NMR (126 MHz, DMSO-d_6) δ 158.4, 154.5, 151.3, 148.5, 147.8, 147.6, 137.8, 135.9, 133.1, 128.4, 127.2, 113.7, 108.8, 107.6, 45.7, 44.2, 30.0, 28.0. HPLC-UV (254 nm) ESI-MS, purity: 97.6%. LC-MS (m/z): 482.0 [M + H]$^+$. HRMS (ESI-TOF) m/z: [M - H]$^-$ calcd. for C$_{22}$H$_{23}$N$_7$O$_4$S 480.1532, found 480.1474.

1,3-Diethyl-8-(4-((4-(pyridin-2-yl)piperazin-1-yl)sulfonyl)phenyl)-3,7-dihydro-1*H*-purine-2,6-dione (56). This compound was synthesized according to the general procedure B using *p*-nitrophenylsulfonate derivative **22** (60 mg, 0.12 mmol) and piperazine **26** (65 mg, 0.40 mmol) dissolved in 4 mL of sulfolane and the reaction mixture was stirred at 130 ºC for 12 h. White solid; yield (50%, 31 mg). M.p.: 330-337 °C. ^{1}H NMR (500 MHz, DMSO-d_6) δ 14.15 (s, 1H, NH$_{xanthine}$), 8.40-8.32 (m, 2H, CH$_{phenyl}$), 8.06 (ddd, J = 4.9, 2.0, 0.9 Hz, CH$_{pyridyl}$), 7.91-7.82 (m, 2H, CH$_{phenyl}$), 7.49 (ddd, J = 8.8, 7.1, 2.0 Hz, 1H, CH$_{pyridyl}$), 6.78 (dd, J = 8.7, 1.0 Hz, 1H, CH$_{pyridyl}$), 6.62 (dd, J = 7.2, 5.0 Hz, 1H, CH$_{pyridyl}$), 4.10-4.05 (q, J = 7.0 Hz, 4H, CH$_{2(ethyl)}$), 3.96-3.92 (q, J = 7.0 Hz, CH$_{2(ethyl)}$), 3.58-3.50 (dd, J = 6.1, 3.9 Hz, 4H, CH$_{piperazinyl}$), 3.05-3.02 (t, J = 5.1 Hz, 4H, CH$_{piperazinyl}$), 1.26 (t, J = 7.1 Hz, 3H, CH$_{3(ethyl)}$), 1.14 (t, J = 7.0 Hz, 3H, CH$_{3(ethyl)}$). ^{13}C NMR (126 MHz, DMSO-d_6) δ 158.4, 154.1, 150.3, 147.6, 137.8, 135.9, 133.1, 128.4, 127.2, 113.7, 107.6, 45.7, 44.2, 38.3, 36.0, 13.3. HPLC-UV (254 nm) ESI-MS, purity: 98.7%. LC-MS (m/z): 509.9 [M + H]$^+$. HRMS (ESI-TOF) m/z: [M - H]$^-$ calcd. for C$_{24}$H$_{27}$N$_7$O$_4$S 508.1845, found 508.1792.

3-Cyclopropyl-1-ethyl-8-(4-((4-(pyridin-2-yl)piperazin-1-yl)sulfonyl)phenyl)-3,7-dihydro-1*H*-purine-2,6-dione (57). This compound was synthesized according to the general procedure B using *p*-nitrophenylsulfonate derivative **18** (50 mg, 0.10 mmol) and piperazine **26** (50 mg,

0.31 mmol) dissolved in 4 mL of sulfolane and the reaction mixture was stirred at 130 °C for 12 h. White solid; yield (54%, 28 mg). M.p.: 346-349 °C.^{1}H NMR (600 MHz, DMSO-*d6*) δ 8.10-8.04 (m, 2H, CH$_{phenyl}$), 7.92-7.88 (d, *J* = 8.5 Hz, 2H, CH$_{phenyl}$), 7.52-7.46 (m, 2H, CH$_{pyridyl}$), 6.82-6.79 (t, *J* = 7.7 Hz, 2H, CH$_{pyridyl}$), 6.66-6.62 (dd, *J* = 7.0, 5.0 Hz, 2H, CH$_{pyridyl}$), 3.95-3.87 (m, 2H, CH$_{2(ethyl)}$), 3.61-3.54 (m, 4H, CH$_{piperazinyl}$), 3.05-2.97 (m, 4H, CH$_{piperazinyl}$), 2.10-2.05 (m, 1H, CH$_{(cyclopropyl)}$), 1.15-1.12 (t, 3H, CH$_{3(ethyl)}$), 1.13-1.09 (m, 2H, CH$_{2(cyclopropyl)}$), 1.03-0.98 (m, 2H, CH$_{2(cyclopropyl)}$). ^{13}C NMR (151 MHz, DMSO-*d6*) δ ^{13}C NMR (151 MHz, DMSO) δ 161.1, 158.8, 158.4, 154.3, 151.3, 149.0, 147.7, 147.7, 147.5, 137.8, 135.8, 133.3, 128.4, 127.2, 113.7, 113.5, 107.6, 55.0, 45.7, 44.4, 44.2, 36.0, 30.8, 26.4, 13.3, 7.9. HPLC-UV (254 nm) ESI-MS, purity: 96.5%. LC-MS (m/z): 522.4 [M + H]$^+$. HRMS (ESI-TOF) m/z: [M - H]$^-$ calcd. for C$_{25}$H$_{27}$N$_7$O$_4$S 520.1845, found 520.1761.

8-(4-{[4-(5-Bromopyridin-2-yl)piperazin-1-yl]sulfonyl}phenyl)-1-propyl-2,3,6,7-tetrahydro-1*H*-purine- 2,6-dione (58). This compound was synthesized according to the general procedure A using *p*-nitrophenylsulfonate derivative **19** (80 mg, 0.17 mmol) and piperazine **27** (135 mg, 0.56 mmol) dissolved in 4 mL of anhydrous DMSO and the reaction mixture was stirred at 140 °C for 9 h. Orange White solid; yield (60%, 29 mg). M.p.: 376-380 °C. ^{1}H NMR (500 MHz, DMSO-*d6*) δ 13.98 (s, 1H, NH$_{xanthine}$), 11.92 (s, 1H, NH$_{xanthine}$), 8.31 (dd, *J* = 8.5 Hz, 2H, CH$_{phenyl}$), 8.09 (t, *J* = 20.1 Hz, 1H, CH$_{pyridyl}$), 7.86 (d, *J* = 8.6, 2H, CH$_{phenyl}$), 7.65 (dd, *J* = 9.1 Hz, 1H, CH$_{pyridyl}$), 6.79 (dd, *J* = 9.2 Hz, 1H, CH$_{pyridyl}$), 3.81-3.77 (m, 2H, CH$_{2(propyl)}$), 3.60-3.55 (s, 4H, CH$_{piperazinyl}$), 3.07-2.98 (m, 4H, CH$_{piperazinyl}$), 1.64-1.52 (m, 2H, CH$_{2(propyl)}$), 0.86 (t, *J* = 7.4 Hz, 3H, CH$_{3(propyl)}$). ^{13}C NMR (126 MHz, DMSO-*d6*) δ 157.2, 155.1 (C4), 151.1 (C2), 147.8 (C5), 140, 135.9, 133.2, 128.4, 127.2, 109.6, 107.5, 45.6 (CH$_{piperazinyl}$), 45.3 (CH$_{piperazinyl}$), 44.2, 43.3, 41.6, 21 (CH$_{2(propyl)}$), 11.3 (CH$_{3(propyl)}$). HPLC-UV (254 nm) ESI-MS, purity: 96.9%. LC-MS (m/z): 574.2 [M + H]$^+$. HRMS (ESI-TOF) m/z: [M - H]$^-$ calcd. for C$_{23}$H$_{24}$BrN$_7$O$_4$S 572.0794, found 572.0710.

1,3-Diethyl-8-(4-((4-(5-(trifluoromethyl)pyridin-2-yl)piperazin-1-yl)sulfonyl)phenyl)-3,7-dihydro-1*H*-purine-2,6-dione (59). This compound was synthesized according to the general procedure A using *p*-nitrophenylsulfonate derivative **22** (50 mg, 0.10 mmol) and piperazine **28** (72 mg, 0.31 mmol) dissolved in 3 mL of anhydrous DMSO and the reaction mixture was stirred at 140 ºC for 7 h. White solid; yield (47%, 28 mg). M.p.: 330-337 °C. ^{1}H NMR (500 MHz, DMSO-*d₆*) δ 8.32 (d, *J* = 0.8 Hz, 1H, CH$_{pyridyl}$), 8.20-8.15 (d, *J* = 8.5 Hz, 2H, CH$_{phenyl}$), 7.69-7.76 (m, 1H, CH$_{pyridyl}$), 7.64 (d, *J* = 8.6 Hz, 2H, CH$_{phenyl}$), 6.89 (t, *J* = 9.9 Hz, 1H, CH$_{pyridyl}$), 4.02 (q, *J* = 7.0 Hz, 2H, CH$_{2(ethyl)}$), 3.88 (q, *J* = 7.0 Hz, 2H, CH$_{2(ethyl)}$), 3.74-3.65 (m, 4H, CH$_{piperazinyl}$), 3.01-2.93 (m, 4H, CH$_{piperazinyl}$), 1.20-1.14 (t, *J* = 7.0 Hz, 3H, CH$_{3(ethyl)}$), 1.07-1.02 (t, *J* = 7.0 Hz, 3H, CH$_{3(ethyl)}$). ^{13}C NMR (126 MHz, DMSO-*d₆*) δ 154.3, 151, 148.6, 147.8, 140, 136, 133.1, 128.4, 127.3, 113.6, 109.5, 108.8, 45.5 (CH$_{piperazinyl}$), 44.6 (CH$_{piperazinyl}$), 42.5, 30, 21 (CH$_{2(propyl)}$), 11.3(CH$_{3(propyl)}$). HPLC-UV (254 nm) ESI-MS, purity: 100%. LC-MS (m/z): 578.3 [M + H]$^+$. HRMS (ESI-TOF) m/z: [M - H]$^-$ calcd. for C$_{25}$H$_{26}$F$_3$N$_7$O$_4$S 576.1719, found 576.1635.

6-{4-[4-(2,6-Dioxo-1-propyl-2,3,6,7-tetrahydro-1*H*-purin-8-yl)benzenesulfonyl]piperazin-1-yl}pyridine-3-carbonitrile (60). This compound was synthesized according to the general procedure A using *p*-nitrophenylsulfonate derivative **19** (40 mg, 0.08 mmol) and piperazine **29** (50 mg, 0.27 mmol) dissolved in 5 mL of anhydrous DMSO and the reaction mixture was stirred at 140 ºC for 13 h. White solid (18 mg, 40%). M.p.: 336-341 °C. ^{1}H NMR (500 MHz, DMSO-*d₆*) δ 14.00 (s, 1H, NH$_{xanthine}$), 11.93 (s, 1H, NH$_{xanthine}$), 8.43 (dd, *J* = 2.0 Hz, 1H, CH$_{pyridyl}$), 8.29 (t, *J* = 12.7 Hz, 2H, CH$_{phenyl}$), 7.85 (d, *J* = 8.6, 2H, CH$_{phenyl}$), 7.81 (dd, *J* = 9.1 Hz, 1H, CH$_{pyridyl}$), 6.88 (dd, *J* = 9.4 Hz, 1H, CH$_{phenyl}$), 3.83-3.78 (m, 2H, CH$_{2(propyl)}$), 3.77-3.74 (s, 4H, CH$_{piperazinyl}$), 3.07-2.99 (m, 4H, CH$_{piperazinyl}$), 1.60-1.56 (m, 2H, CH$_{2(propyl)}$), 0.86 (t, *J* = 9.0 Hz, 3H, CH$_{3(propyl)}$). ^{13}C NMR (126 MHz, DMSO-*d₆*) δ 158.9, 155.1 (C4), 152.5, 152.2, 151.1 (C2), 148.1 (C5), 147.7, 140.3, 139.3, 135.8, 133.4, 128.4, 127.2, 126.1, 124.2, 118.6,

114.8, 106.9, 96, 46 (CH$_{piperazinyl}$), 45.6 (CH$_{piperazinyl}$), 43.6, 41.7, 30.5, 29.2, 26.7, 25.3, 21 (CH$_{2(propyl)}$), 14.1, 11.3 (CH$_{3(propyl)}$). HPLC-UV (254 nm) ESI-MS, purity: 95%. LC-MS (m/z): 521.2 [M + H]$^+$. HRMS (ESI-TOF) m/z: [M - H]$^-$ calcd. for C$_{24}$H$_{24}$N$_8$O$_4$S 519.1719, found 519.1551.

6-{4-[4-(2,6-Dioxo-1-propyl-2,3,6,7-tetrahydro-1*H*-purin-8-yl)benzenesulfonyl]piperazin-1-yl}pyridine-3-carbonitrile (61). To a flask containing **60** (15 mg, 0.03 mmol, 1 eq) dissolved in 2 mL dist. water, KOH (8 mg, 0.15 mmol, 5 eq) was added and the reaction was refluxed at 110 °C for 48 h. Upon completion of the reaction, the mixture was neutralized with few drops of 1N HCl and a white precipitate was formed. The formed solid was collected by filtration and purified using reverse-phase high performance liquid chromatography (RP-HPLC) to obtain **61**. White solid (9 mg, 60%). M.p.: 325-327 °C. ^{1}H NMR (600 MHz, DMSO-*d$_6$*) δ 10.82 (s, 1H, NH$_{xanthine}$), 8.48 (d, *J* = 2.2 Hz, 1H, CH$_{pyridyl}$), 8.16 (d, *J* = 8.5 Hz, 2H, CH$_{phenyl}$), 7.86 (dd, *J* = 8.7, 2.2 Hz, 1H, CH$_{phenyl}$), 7.62 (d, *J* = 8.5 Hz, 2H, CH$_{pyridyl}$), 6.63 (d, *J* = 8.7 Hz, 1H, CH$_{phenyl}$), 3.80-3.70 (m, 2H, CH$_{2(propyl)}$), 3.56 (d, *J* = 4.8 Hz, 4H, CH$_{piperazinyl}$), 2.99 (s, 4H, CH$_{piperazinyl}$), 1.52-1.46 (m, 2H, CH$_{2(propyl)}$), 0.84 (t, *J* = 7.4 Hz, 3H, CH$_{3(propyl)}$). ^{13}C NMR (126 MHz, DMSO-*d$_6$*) δ 158.9, 155.1 (C4), 152.5, 152.2, 151.1 (C2), 148.1 (C5), 147.7, 140.3, 139.3, 135.8, 133.4, 128.4, 127.2, 126.1, 124.2, 118.6, 114.8, 106.9, 96, 46 (CH$_{piperazinyl}$), 45.6 (CH$_{piperazinyl}$), 43.6, 41.7, 30.5, 29.2, 26.7, 25.3, 21 (CH$_{2(propyl)}$), 14.1, 11.3 (CH$_{3(propyl)}$). ^{13}C NMR (151 MHz, DMSO-*d$_6$*) δ 169.3, 159, 158.7, 153.7, 152.3, 149.9, 149.7, 141.5, 139.2, 131.7, 128.2, 125.9, 125.7, 118.6, 118.5, 116.7, 106.1, 46.2, 44.6, 41.5, 40.2, 21.7, 11.7. HPLC-UV (254 nm) ESI-MS, purity: 96.5%. LC-MS (m/z): 540.3 [M + H]$^+$. HRMS (ESI-TOF) m/z: [M - H]$^-$ calcd. for C$_{24}$H$_{25}$N$_7$O$_6$S 538.1587, found 538.1492.

6-{4-[4-(2,6-Dioxo-1-propyl-2,3,6,7-tetrahydro-1*H*-purin-8-yl)benzenesulfonyl]piperazin-1-yl}pyridine-3-carbonitrile (62). This compound was synthesized according to the general

procedure A using *p*-nitrophenylsulfonate derivative **19** (50 mg, 0.11 mmol) and piperazine **30** (100 mg, 0.53 mmol) dissolved in 5 mL of anhydrous DMSO and the reaction mixture was stirred at 140 ºC for 10 h. White solid; yield (51%, 28 mg). M.p.: 330-337 °C. ^{1}H NMR (600 MHz, DMSO-*d₆*) δ 14.03 (s, 1H, NH$_{xanthine}$), 11.97 (s, 1H, NH$_{xanthine}$), 8.36 (dd, *J* = 4.7, 1.3 Hz, 1H, CH$_{pyridyl}$), 8.33 (d, *J* = 8.3 Hz, 2H, CH$_{phenyl}$), 8.04 (dd, *J* = 7.6, 1.2 Hz, 1H, CH$_{pyridyl}$), 7.88 (d, *J* = 8.4 Hz, 2H, CH$_{phenyl}$), 6.93 (dd, *J* = 7.5, 4.9 Hz, 1H, CH$_{pyridyl}$), 3.83-3.78 (m, 2H, CH$_{2(propyl)}$), 3.66-3.62 (m, 4H, CH$_{piperazinyl}$), 3.11-3.03 (m, 4H, CH$_{piperazinyl}$), 1.60-1.52 (d, *J* = 7.4 Hz, 2H, CH$_{2(propyl)}$), 0.90-0.83 (t, *J*= 7.4 Hz, 3H, CH$_{3(propyl)}$). ^{13}C NMR (151 MHz, DMSO-*d₆*) δ 160.3, 155.1, 152.2, 151.1, 148.1, 147.8, 144.4, 135.8, 133.3, 128.5, 127.3, 117.6, 115.8, 108.7, 95.6, 47.5, 45.8, 41.7, 21.1, 11.4. HPLC-UV (254 nm) ESI-MS, purity: 97.8%. LC-MS (m/z): 521.3 [M + H]$^+$. HRMS (ESI-TOF) m/z: [M - H]$^-$ calcd. for C$_{24}$H$_{24}$N$_8$O$_4$S 519.1641, found 519.1560.

1-Propyl-8-(4-{[4-(pyrimidin-2-yl)piperazin-1-yl]sulfonyl}phenyl)-2,3,6,7-tetrahydro-1*H*-purine-2,6-dione (63). This compound was synthesized according to the general procedure B using *p*-nitrophenylsulfonate derivative **19** (50 mg, 0.11 mmol) and piperazine **31** (53 mg, 0.32 mmol) dissolved in 3 mL of sulfolane and the reaction mixture was stirred at 130 ºC for 15 h. White solid; yield (35%, 18 mg). M.p.: 356-358 °C. ^{1}H NMR (500 MHz, DMSO-*d₆*) δ 13.98 (s, 1H, NH$_{xanthine}$), 11.92 (s, 1H, NH$_{xanthine}$), 8.36-8.24 (m, *J* = 8.9, 3H, CH$_{phenyl}$), 7.91-7.78 (dd, *J* = 8.4 Hz, 2H, CH$_{phenyl}$), 6.66-6.55 (dd, 1H, CH$_{phenyl}$), 3.87-3.81 (m, 2H, CH$_{2(propyl)}$), 3.81-3.76 (m, 4H, CH$_{piperazinyl}$), 3.06-2.93 (m, 4H, CH$_{piperazinyl}$), 1.64-1.48 (m, 2H, CH$_{2(propyl)}$), 0.90-0.81 (t, 3H, CH$_{3(propyl)}$). ^{13}C NMR (126 MHz, DMSO-*d₆*) δ 160.9, 158.1, 155, 151.1, 148.1, 147.7, 135.9, 133.2, 128.4, 127.1, 110.8, 108.6, 45.8, 42.7 (CH$_{piperazinyl}$), 41.6 (CH$_{piperazinyl}$), 30.5 (CH$_3$), 21 (CH$_3$), 11.3. HPLC-UV (254 nm) ESI-MS, purity: 97.4%. LC-MS (m/z): 497.2 [M + H]$^+$. HRMS (ESI-TOF) m/z: [M - H]$^-$ calcd. for C$_{22}$H$_{24}$N$_8$O$_4$S 495.1641, found 495.1557.

3-Methyl-1-propyl-8-(4-{[4-(pyrimidin-2-yl)piperazin-1-yl]sulfonyl}phenyl)-2,3,6,7-tetrahydro-1*H*-purine-2,6-dione (64). This compound was synthesized according to the general procedure B using *p*-nitrophenylsulfonate derivative **20** (50 mg, 0.10 mmol) and piperazine **31** (51 mg, 0.31 mmol) dissolved in 4 mL of sulfolane and the reaction mixture was stirred at 130 ºC for 10 h. White solid; yield (48%, 25 mg). M.p.: 358-363 °C. ^{1}H NMR (500 MHz, DMSO-d_6) δ 14.13 (s, 1H, NH$_{xanthine}$), 8.36-8.32 (m, J = 8.5, 2H, CH$_{phenyl}$), 8.32-8.28 (m, J = 4.7, 2H, CH$_{phenyl}$), 7.88-7.83 (dd, J = 8.5 Hz, 2H, CH$_{phenyl}$), 6.62-6.59 (dd, 1H, CH$_{phenyl}$), 3.86-3.83 (m, 2H, CH$_{2(propyl)}$), 3.83-3.77 (m, 4H, CH$_{piperazinyl}$), 3.50-3.45 (t, 3H, CH$_3$ methyl), 3.04-2.97 (m, 4H, CH$_{piperazinyl}$), 1.61-1.52 (m, 2H, CH$_{2(propyl)}$), 0.94-0.70 (t, 3H, CH$_{3(propyl)}$). ^{13}C NMR (126 MHz, DMSO-d_6) δ 160.9, 158.1, 154.3, 151, 148.6, 147.9, 136, 133, 128.4, 127.2, 110.8, 45.8, 42.7 (CH$_{piperazinyl}$), 42.4 (CH$_{piperazinyl}$), 30.5 (CH$_3$), 29.9, 20.9 (CH$_3$), 11.3. HPLC-UV (254 nm) ESI-MS, purity: 97.5%. LC-MS (m/z): 511.1 [M + H]$^+$. HRMS (ESI-TOF) m/z: [M - H]$^-$ calcd. for C$_{23}$H$_{26}$N$_8$O$_4$S 509.1798, found 509.1714.

3-Ethyl-1-propyl-8-(4-{[4-(pyrimidin-2-yl)piperazin-1-yl]sulfonyl}phenyl)-2,3,6,7-tetrahydro-1*H*-purine-2,6-dione (65). This compound was synthesized according to the general procedure B using *p*-nitrophenylsulfonate derivative **21** (50 mg, 0.10 mmol) and piperazine **31** (49 mg, 0.30 mmol) dissolved in 3 mL of sulfolane and the reaction mixture was stirred at 130 ºC for 15 h. White solid; yield (35%, 18 mg). M.p.: 350-353 °C. ^{1}H NMR (500 MHz, DMSO-d_6) δ 14.14 (s, 1H, NH$_{xanthine}$), 8.36-8.32 (m, J = 8.5, 2H, CH$_{phenyl}$), 8.32-8.28 (m, J = 4.7, 2H, CH$_{phenyl}$), 7.88-7.83 (dd, J = 8.5 Hz, 2H, CH$_{phenyl}$), 6.62-6.59 (dd, 1H, CH$_{phenyl}$), 4.12-4.04 (m, 2H, CH$_{2(propyl)}$), 4.12-4.04 (m, 2H, CH$_{2(propyl)}$), 3.88-3.84 (m, 4H, CH$_{piperazinyl}$), 3.84-3.79 (m, 2H, CH$_{2(ethyl)}$), 3.03-2.98 (m, 4H, CH$_{piperazinyl}$), 1.62-1.53 (m, 2H, CH$_{2(propyl)}$), 1.27-1.23 (t, 3H, CH$_{3(ethyl)}$), 0.89-0.84 (t, 3H, CH$_{3(propyl)}$). ^{13}C NMR (126 MHz, DMSO-d_6) δ 161, 158.1, 154.3, 151, 150.5, 148.1, 136, 133.1, 128.4, 127.3, 110.9, 108.9, 45.8, 42.7 (CH$_{piperazinyl}$), 42.8 (CH$_{piperazinyl}$), 42.4, 30.5 (*C*H$_3$), 13.3 (*C*H$_3$), 11.3. HPLC-UV (254 nm) ESI-

MS, purity: 98.2%. LC-MS (m/z): 525.1 [M + H]$^+$. HRMS (ESI-TOF) m/z: [M - H]$^-$ calcd. for C$_{24}$H$_{28}$N$_8$O$_4$S 523.1954, found 523.1870.

8-(4-((4-(5-bromopyrimidin-2-yl)piperazin-1-yl)sulfonyl)phenyl)-1-propyl-3,7-dihydro-1H-purine-2,6- dione (66). This compound was synthesized according to the general procedure A using *p*-nitrophenylsulfonate derivative **19** (55 mg, 0.12 mmol) and piperazine **32** (100 mg, 0.41 mmol) dissolved in 5 mL of anhydrous DMSO and the reaction mixture was stirred at 140 °C for 14 h. White solid; yield (38%, 25 mg). M.p.: 351-353 °C. ^{1}H NMR (600 MHz, DMSO-*d$_6$*) δ 10.84 (s, 1H, NH$_{xanthine}$), 8.40 (s, 2H, CH pyrimidine), 8.16 (d, *J* = 8.2 Hz, 2H, CH$_{phenyl}$), 7.61 (d, *J* = 8.2 Hz, 2H, CH$_{phenyl}$), 3.87-3.82 (t, *J* = 8.8, 6.4 Hz, 4H, CH$_{piperazinyl}$), 3.81-3.76 (m, 2H, CH$_{2(propyl)}$), 3.00-2.93 (m, 4H, CH$_{piperazinyl}$), 1.53-1.49 (q, *J* = 7.5 Hz, 2H, CH$_{2(propyl)}$), 0.90-0.81 (t, *J* = 7.4 Hz, 3H, CH$_{3(propyl)}$). ^{13}C NMR (151 MHz, DMSO-*d$_6$*) δ ^{13}C NMR (151 MHz, DMSO) δ 159.4, 158.4, 158.2, 153.5, 151.9, 149.9, 141.9, 131.0, 127.7, 125.3, 118.5, 106.2, 63.3, 63.0, 45.7, 43.1, 41.0, 21.5, 11.5. HPLC-UV (254 nm) ESI-MS, purity: 95%. LC-MS (m/z): 574.8 [M + H]$^+$. HRMS (ESI-TOF) m/z: [M - H]$^-$ calcd. for C$_{22}$H$_{23}$BrN$_8$O$_4$S 573.0746, found 573.0744.

8-(4-{[4-(1,2-Benzothiazol-3-yl)piperazin-1-yl]sulfonyl}phenyl)-1-propyl-2,3,6,7-tetrahydro-1*H*-purine-2,6-dione (67). This compound was synthesized according to the general procedure B using *p*-nitrophenylsulfonate derivative **19** (50 mg, 0.11 mmol) and piperazine **33** (70 mg, 0.32 mmol) dissolved in 4 mL of sulfolane and the reaction mixture was stirred at 130 °C for 12 h. White solid; yield (45%, 26 mg). M.p.: 363-368 °C. ^{1}H NMR (500 MHz, DMSO-*d$_6$*) δ 14.02 (s, 1H, NH$_{xanthine}$), 11.94 (s, 1H, NH$_{xanthine}$), 8.44-8.28 (m, *J* = 8.3 Hz, 2H, CH$_{phenyl}$), 8.08-7.95 (m, *J* = 8.3 Hz, 2H, CH$_{phenyl}$), 7.93-7.80 (d, *J* = 8.4 Hz, 2H, CH$_{phenyl}$), 7.59-7.43 (dd, *J* = 7.5 Hz, 1H, CH$_{phenyl}$), 7.42-7.29 (dd, *J* = 7.6 Hz, 1H, CH$_{phenyl}$), 3.85-3.77 (m, 2H, CH$_{2(propyl)}$), 3.56-3.46 (m, 4H, CH$_{piperazinyl}$), 3.22-3.13 (m, 4H, CH$_{piperazinyl}$), 1.64-1.49 (m, 2H, CH$_{2(propyl)}$),

0.91-0.81 (t, 3H, CH$_{3(propyl)}$).^{13}C NMR (126 MHz, DMSO-d_6) δ 162.9, 155, 152.1, 151.1, 148.1, 147.8, 135.9, 133.3, 128.5, 128.1, 127.2, 124.6, 124.2, 121.2, 108.7, 49, 45.8 (CH$_{piperazinyl}$), 41.6 (CH$_{piperazinyl}$), 21, 11.3. HPLC-UV (254 nm) ESI-MS, purity: 97.5%. LC-MS (m/z): 552.0 [M + H]$^+$. HRMS (ESI-TOF) m/z: [M - H]$^-$ calcd. for C$_{25}$H$_{25}$N$_7$O$_4$S$_2$ 550.1409, found 550.1326.

1-Propyl-8-(4-((4-(thiophen-2-yl)piperazin-1-yl)sulfonyl)phenyl)-3,7-dihydro-1H-purine-2,6-dione (68). This compound was synthesized according to the general procedure B using *p*-nitrophenylsulfonate derivative **19** (70 mg, 0.15 mmol) and piperazine **34** (75 mg, 0.45 mmol) dissolved in 4 mL of sulfolane and the reaction mixture was stirred at 130 °C for 10 h. White solid; yield (54%, 40 mg). M.p.: 330-333 °C. ^{1}H NMR (600 MHz, DMSO-d_6) δ 14.02 (s, 1H, NH$_{xanthine}$), 11.95 (s, 1H, NH$_{xanthine}$), 8.44-8.20 (m, J = 8.3 Hz, 2H, CH$_{phenyl}$), 7.98-7.80 (m, 2H, CH$_{phenyl}$), 6.83-6.65 (m, 2H, CH$_{thiophene}$), 6.17 (dd, J = 3.7, 1.4 Hz, 1H, CH$_{thiophene}$), 3.85-3.72 (m, 2H, CH$_{2(propyl)}$), 3.15-3.11 (m, 4H, CH$_{piperazinyl}$), 3.11-3.07 (m, 4H, CH$_{piperazinyl}$), 1.60-1.53 (m, 2H, CH$_{2(propyl)}$), 0.87 (t, J = 7.4 Hz, 3H, CH$_{3(propyl)}$). ^{13}C NMR (151 MHz, DMSO-d_6) δ 158.0, 155.1, 148.2, 135.9, 133.4, 128.5, 127.2, 126.4, 113.4, 108.8, 106.8, 67.2, 59.3, 50.8, 49.7, 45.5, 41.7, 31.6, 21.1, 11.4. HPLC-UV (254 nm) ESI-MS, purity: 97.8%. LC-MS (m/z): 501.2 [M + H]$^+$. HRMS (ESI-TOF) m/z: [M - H]$^-$ calcd. for C$_{22}$H$_{24}$N$_6$O$_4$S$_2$ 499.1300, found 499.1234.

3-Ethyl-1-propyl-8-(4-((4-(thiophen-2-yl)piperazin-1-yl)sulfonyl)phenyl)-3,7-dihydro-1H-purine-2,6-dione (69). This compound was synthesized according to the general procedure B using *p*-nitrophenylsulfonate derivative **21** (70 mg, 0.14 mmol) and piperazine **34** (75 mg, 0.45 mmol) dissolved in 4 mL of sulfolane and the reaction mixture was stirred at 130 °C for 11 h. White solid; yield (49%, 36 mg). M.p.: 320-323 °C. ^{1}H NMR (600 MHz, DMSO-d_6) δ 14.19 (s, 1H, NH$_{xanthine}$), 7.89 (d, J = 8.2 Hz, 2H, CH$_{phenyl}$), 6.73 (s, 2H, CH$_{phenyl}$), 6.83-6.65 (m, 2H, CH$_{thiophene}$), 6.16 (d, J = 3.6 Hz, 1H, CH$_{thiophene}$), 4.09 (d, J = 7.1 Hz, 2H, CH$_{2(ethyl)}$), 3.94-3.76

(m, 2H, CH$_{2(propyl)}$), 3.13 (dd, J = 6.6, 3.8 Hz, 4H, CH$_{piperazinyl}$), 3.09 (dd, J = 7.1, 3.6 Hz, 4H, CH$_{piperazinyl}$), 2.07 (s, 1H), 1.58 (q, J = 7.5 Hz, 2H, CH$_{2(propyl)}$), 1.26 (t, J = 7.0 Hz, 3H, CH$_{3(ethyl)}$), 0.87 (t, J = 7.4 Hz, 3H, CH$_{3(propyl)}$). ^{13}C NMR (151 MHz, DMSO-d_6) δ 206.6, 157.9, 154.3, 150.5, 148.1, 136.0, 133.1, 128.4, 127.3, 126.4, 126.4, 113.3, 108.9, 106.7, 50.7, 50.7, 45.4, 42.4, 38.3, 30.8, 21.0, 21.0, 13.3, 13.3, 11.3. HPLC-UV (254 nm) ESI-MS, purity: 97.1%. LC-MS (m/z): 529.2 [M + H]$^+$. HRMS (ESI-TOF) m/z: [M - H]$^-$ calcd. for C$_{24}$H$_{28}$N$_6$O$_4$S$_2$ 527.1613, found 527.1530.

1,3-Diethyl-8-(4-((4-(thiophen-2-yl)piperazin-1-yl)sulfonyl)phenyl)-3,7-dihydro-1*H*-purine-2,6-dione (70). This compound was synthesized according to the general procedure B using *p*-nitrophenylsulfonate derivative **22** (70 mg, 0.14 mmol) and piperazine **34** (75 mg, 0.45 mmol) dissolved in 3 mL of sulfolane and the reaction mixture was stirred at 130 °C for 12 h. White solid; yield (48%, 35 mg). M.p.: 360-363 °C. ^{1}H NMR (600 MHz, DMSO-d_6) δ 14.20 (s, 1H, NH$_{xanthine}$), 8.38 (d, J = 8.3 Hz, 2H, CH$_{phenyl}$), 7.89 (d, J = 8.3 Hz, 2H, CH$_{phenyl}$), 6.75-6.69 (m, 2H, CH thiophene), 6.16 (dd, J = 3.6, 1.5 Hz, 1H, CH thiophene), 4.09 (q, J = 7.1 Hz, 2H, CH$_{2(ethyl)}$), 3.94 (q, J = 7.0 Hz, 2H, CH$_{2(ethyl)}$), 3.13 (dd, J = 6.6, 3.7 Hz, 4H, CH$_{piperazinyl}$), 3.09 (dd, J = 6.8, 3.5 Hz, 4H, CH$_{piperazinyl}$), 1.27 (t, J = 7.1 Hz, 3H, CH$_{3(ethyl)}$), 1.14 (t, J = 7.0 Hz, 3H, CH$_{3(ethyl)}$). ^{13}C NMR (151 MHz, DMSO-d_6) δ 157.9, 154.1, 150.3, 148.1, 136.0, 133.1, 128.5, 127.3, 126.4, 113.3, 108.9, 106.7, 50.7, 45.4, 38.3, 36.0, 13.3. HPLC-UV (254 nm) ESI-MS, purity: 95.6%. LC-MS (m/z): 515.2 [M + H]$^+$. HRMS (ESI-TOF) m/z: [M - H]$^-$ calcd. for C$_{23}$H$_{26}$N$_6$O$_4$S 513.1457, found 513.1373.

1-Propyl-8-(4-((4-(thiazol-2-yl)piperazin-1-yl)sulfonyl)phenyl)-3,7-dihydro-1*H*-purine-2,6-dione (71). This compound was synthesized according to the general procedure B using *p*-nitrophenylsulfonate derivative **19** (70 mg, 0.15 mmol) and piperazine **35** (75 mg, 0.44 mmol) dissolved in 4 mL of sulfolane and the reaction mixture was stirred at 130 °C for 12 h. White solid; yield (53%, 39 mg). M.p.: 322-325 °C. ^{1}H NMR (600 MHz, DMSO-d_6) δ 14.00 (s, 1H,

NH$_{xanthine}$), 11.95 (s, 1H, NH$_{xanthine}$), 8.32 (d, J = 8.1 Hz, 2H, CH$_{phenyl}$), 7.87 (d, J = 8.2 Hz, 2H, CH$_{phenyl}$), 7.11 (d, J = 3.6 Hz, 1H, CH$_{thiazole}$), 6.83 (d, J = 3.6 Hz, 1H, CH$_{thiazole}$), 3.85-3.78 (m, 2H, CH$_{2(propyl)}$), 3.49 (t, J = 5.1 Hz, 4H, CH$_{piperazinyl}$), 3.07 (t, J = 5.1 Hz, 4H, CH$_{piperazinyl}$), 1.56 (q, J = 7.5 Hz, 2H, CH$_{2(propyl)}$), 0.86 (t, J = 7.4 Hz, 3H, CH$_{3(propyl)}$). ^{13}C NMR (151 MHz, DMSO-d_6) δ 171.3, 171.0, 162.9, 155.1, 151.1, 148.1, 147.8, 139.6, 139.6, 135.9, 133.3, 131.7, 128.5, 127.3, 125.9, 113.1, 109.1, 109.0, 108.7, 50.8, 50.4, 48.7, 48.3, 47.9, 47.8, 45.3, 44.8, 41.7, 29.2, 29.1, 22.3, 22.3, 21.1, 14.1, 11.4. HPLC-UV (254 nm) ESI-MS, purity: 98.2%. LC-MS (m/z): 502.2 [M + H]$^+$. HRMS (ESI-TOF) m/z: [M - H]$^-$ calcd. for C$_{21}$H$_{23}$N$_7$O$_4$S$_2$ 500.1253, found 500.1169.

3-Ethyl-1-propyl-8-(4-((4-(thiazol-2-yl)piperazin-1-yl)sulfonyl)phenyl)-3,7-dihydro-1*H*-purine-2,6-dione (72). This compound was synthesized according to the general procedure B using *p*-nitrophenylsulfonate derivative **21** (70 mg, 0.15 mmol) and piperazine **35** (75 mg, 0.44 mmol) dissolved in 4 mL of sulfolane and the reaction mixture was stirred at 130 °C for 15 h. White solid; yield (55%, 41 mg). M.p.: 318-321 °C. ^{1}H NMR (600 MHz, DMSO-d_6) δ 14.00 (s, 1H, NH$_{xanthine}$), 11.95 (s, 1H, NH$_{xanthine}$), 8.36 (d, J = 8.5 Hz, 2H, CH$_{phenyl}$), 7.88 (d, J = 8.5 Hz, 2H, CH$_{phenyl}$), 7.11 (d, J = 3.6 Hz, 1H, CH$_{thiazole}$), 6.84 (d, J = 3.6 Hz, 1H, CH$_{thiazole}$), 4.09 (q, J = 7.0 Hz, 2H, CH$_{2(ethyl)}$), 3.89-3.82 (m, 2H, CH$_{2(propyl)}$), 3.52-3.47 (m, 4H, CH$_{piperazinyl}$), 3.08 (t, J = 5.1 Hz, 4H, CH$_{piperazinyl}$), 1.63-1.53 (m, 2H, CH$_{2(propyl)}$), 1.26 (t, J = 7.0 Hz, 3H, CH$_{3(ethyl)}$), 0.87 (t, J = 7.5 Hz, 3H, CH$_{3(propyl)}$). ^{13}C NMR (151 MHz, DMSO-d_6) δ 170.9, 154.4, 150.5, 148.1, 139.5, 136.0, 133.2, 128.4, 127.3, 109.0, 50.7, 47.7, 45.2, 42.4, 38.3, 30.8, 21.0, 13.3, 11.3. HPLC-UV (254 nm) ESI-MS, purity: 95%. LC-MS (m/z): 530.3 [M + H]$^+$. HRMS (ESI-TOF) m/z: [M - H]$^-$ calcd. for C$_{23}$H$_{27}$N$_7$O$_4$S$_2$ 528.1566, found 528.1563.

1,3-Diethyl-8-(4-((4-(thiazol-2-yl)piperazin-1-yl)sulfonyl)phenyl)-3,7-dihydro-1*H*-purine-2,6-dione (73). This compound was synthesized according to the general procedure B using *p*-

nitrophenylsulfonate derivative **22** (70 mg, 0.14 mmol) and piperazine **35** (75 mg, 0.44 mmol) dissolved in 4 mL of sulfolane and the reaction mixture was stirred at 130 $^{\circ}$C for 8 h. White solid; yield (51%, 38 mg). M.p.: 355-358 $^{\circ}$C. ^{1}H NMR (600 MHz, DMSO-d_6) δ 14.16 (s, 1H, NH$_{xanthine}$), 8.35 (d, J = 8.5 Hz, 2H, CH$_{phenyl}$), 7.88 (d, J = 8.5 Hz, 2H, CH$_{phenyl}$), 7.11 (d, J = 3.6 Hz, 1H, CH thiazole), 6.83 (d, J = 3.6 Hz, 1H, CH thiazole), 4.08 (d, J = 7.2 Hz, 2H, CH$_{2(ethyl)}$), 3.93 (d, J = 7.0 Hz, 2H, CH$_{2(ethyl)}$), 3.49 (dd, J = 6.5, 3.9 Hz, 4H, CH$_{piperazinyl}$), 3.08 (t, J = 5.1 Hz, 4H, CH$_{piperazinyl}$), 1.26 (t, J = 7.0 Hz, 3H, CH$_{3(ethyl)}$), 1.13 (t, J = 7.0 Hz, 3H, CH$_{3(ethyl)}$). ^{13}C NMR (151 MHz, DMSO-d_6) δ 171.0, 154.1, 150.3, 148.1, 139.5, 136.1, 133.2, 128.4, 127.4, 109.1, 109.0, 53.8, 50.7, 47.8, 45.3, 38.3, 36.0, 18.3, 16.9, 13.3. HPLC-UV (254 nm) ESI-MS, purity: 96.3%. LC-MS (m/z): 516.2 [M + H]$^+$. HRMS (ESI-TOF) m/z: [M - H]$^-$ calcd. for C$_{22}$H$_{25}$N$_7$O$_4$S$_2$ 514.1409, found 514.1355.

8-(4-((4-(Methyl(pyridin-4-yl)amino)piperidin-1-yl)sulfonyl)phenyl)-1-propyl-3,7-dihydro-1*H*-purine-2,6-dione (74). This compound was synthesized according to the general procedure B using *p*-nitrophenylsulfonate derivative **19** (60 mg, 0.13 mmol) and piperazine **36** (70 mg, 0.37 mmol) dissolved in 4 mL of sulfolane and the reaction mixture was stirred at 130 $^{\circ}$C for 16 h. White solid; yield (55%, 35 mg). M.p.: 348-351 $^{\circ}$C. ^{1}H NMR (600 MHz, DMSO-d_6) δ 14.02 (s, 1H, NH$_{xanthine}$), 11.96 (s, 1H, NH$_{xanthine}$), 8.44 (d, J = 6.0 Hz, 2H, CH$_{pyridyl}$), 8.32 (d, J = 8.5 Hz, 2H, CH$_{phenyl}$), 7.83 (d, J = 8.4 Hz, 2H, CH$_{phenyl}$), 7.23 (d, J = 6.1 Hz, 2H, CH$_{pyridyl}$), 3.86-3.78 (m, 2H, CH$_{2(propyl)}$), 3.48 (dd, J = 6.8 Hz, 1H, CH), 2.92 (s, 4H, CH$_{piperazinyl}$), 2.41-2.30 (m, 4H, CH$_{piperazinyl}$), 1.58 (q, J = 7.4 Hz, 2H, CH$_{2(propyl)}$), 1.21 (d, J = 6.7 Hz, 3H, CH$_3$ methyl), 0.88 (t, J = 7.4 Hz, 3H, CH$_{3(propyl)}$). ^{13}C NMR (151 MHz, DMSO-d_6) δ 155.4, 152.2, 151.4, 150.1, 148.5, 136.0, 133.5, 128.8, 127.4, 123.1, 62.3, 51.0, 49.0, 46.6, 42.0, 22.6, 21.3, 18.2, 11.7. HPLC-UV (254 nm) ESI-MS, purity: 98.2%. LC-MS (m/z): 524.3 [M + H]$^+$. HRMS (ESI-TOF) m/z: [M - H]$^-$ calcd. for C$_{25}$H$_{29}$N$_7$O$_4$S 522.2002, found 522.1918.

1,3-Diethyl-8-(4-((4-(methyl(pyridin-4-yl)amino)piperidin-1-yl)sulfonyl)phenyl)-3,7-dihydro-1*H*-purine-2,6-dione (75). This compound was synthesized according to the general procedure B using *p*-nitrophenylsulfonate derivative **22** (60 mg, 0.12 mmol) and piperazine **36** (80 mg, 0.42 mmol) dissolved in 3 mL of sulfolane and the reaction mixture was stirred at 130 °C for 12 h. White solid; yield (52%, 34 mg). M.p.: 328-332 °C. ^{1}H NMR (600 MHz, DMSO-*d₆*) δ 14.13 (s, 1H, NH$_{xanthine}$), 8.44 (d, *J* = 5.0 Hz, 2H, CH$_{pyridyl}$), 8.36 (d, *J* = 8.1 Hz, 2H, CH$_{phenyl}$), 7.84 (d, *J* = 8.2 Hz, 2H, CH$_{phenyl}$), 7.23 (d, *J* = 4.8 Hz, 2H, CH$_{pyridyl}$), 4.11 (q, *J* = 7.1 Hz, 2H, CH$_{2(ethyl)}$), 3.95 (q, *J* = 7.0 Hz, 2H, CH$_{2(ethyl)}$), 3.51-3.45 (m, 1H, CH), 2.94-2.88 (m, 4H, CH$_{piperazinyl}$), 2.46 (d, *J* = 7.5 Hz, 2H, CH$_{piperazinyl}$), 2.40-2.33 (m, 2H, CH$_{piperazinyl}$), 1.28 (t, *J* = 7.1 Hz, 3H, CH$_3$), 1.20 (d, *J* = 6.7 Hz, 3H, CH$_{3(ethyl)}$), 1.14 (dd, *J* = 13.4, 6.3 Hz, 3H, CH$_{3(ethyl)}$). ^{13}C NMR (151 MHz, DMSO-*d₆*) δ 154.2, 153.7, 151.9, 150.6, 150.3, 149.8, 148.1, 148.1, 145.3, 135.8, 133.1, 128.5, 127.3, 122.8, 121.6, 121.0, 109.1, 68.7, 62.0, 56.0, 48.7, 46.3, 42.3, 40.6, 38.3, 36.0, 32.2, 29.8, 22.2, 17.9, 13.3. HPLC-UV (254 nm) ESI-MS, purity: 98.5%. LC-MS (m/z): 538.5 [M + H]$^+$. HRMS (ESI-TOF) m/z: [M - H]$^-$ calcd. for $C_{26}H_{31}N_7O_4S$ 536.2185, found 536.2054.

8-(4-((4-(Methyl(pyridin-4-yl)amino)piperidin-1-yl)sulfonyl)phenyl)-1-propyl-3,7-dihydro-1*H*-purine-2,6-dione (76). This compound was synthesized according to the general procedure B using *p*-nitrophenylsulfonate derivative **19** (70 mg, 0.15 mmol) and piperazine **37** (80 mg, 0.45 mmol) dissolved in 4 mL of sulfolane and the reaction mixture was stirred at 130 °C for 12 h. White solid; yield (47%, 35 mg). M.p.: 339-342 °C. ^{1}H NMR (600 MHz, DMSO-*d₆*) δ 13.97 (s, 1H, NH$_{xanthine}$), 11.95 (s, 1H, NH$_{xanthine}$), 8.43 (d, *J* = 4.5 Hz, 1H, CH$_{pyridyl}$), 8.32 (d, *J* = 8.2 Hz, 2H, CH$_{phenyl}$), 7.84 (d, *J* = 8.1 Hz, 2H, CH$_{phenyl}$), 7.67 (t, *J* = 7.7 Hz, 1H, CH$_{pyridyl}$), 7.30 (d, *J* = 7.9 Hz, 1H, CH$_{pyridyl}$), 7.20 (t, *J* = 6.2 Hz, 1H, CH$_{pyridyl}$), 3.82 (t, *J* = 7.5 Hz, 2H, CH$_{2(propyl)}$), 3.57 (s, 2H, CH$_2$), 2.95 (m, 4H, CH$_{piperazinyl}$), 1.57 (q, *J* = 7.5 Hz, 2H, CH$_{2(propyl)}$), 0.87 (t, *J* = 7.5 Hz, 3H, CH$_{3(propyl)}$). ^{13}C NMR (151 MHz, DMSO-*d₆*) δ 165.0, 158.0, 155.2,

151.2, 149.0, 148.2, 147.8, 139.0, 137.1, 136.7, 135.8, 133.3, 128.5, 128.3, 127.8, 127.2, 122.9, 122.4, 108.8, 63.2, 55.1, 51.8, 46.2, 46.1, 41.7, 30.9, 29.2, 22.3, 21.1, 14.8, 11.4. HPLC-UV (254 nm) ESI-MS, purity: 99.1%. LC-MS (m/z): 510.1 [M + H]$^+$. HRMS (ESI-TOF) m/z: [M - H]$^-$ calcd. for $C_{24}H_{27}N_7O_4S$ 508.1845, found 508.1828.

3-Ethyl-1-propyl-8-(4-((4-(pyridin-2-ylmethyl)piperazin-1-yl)sulfonyl)phenyl)-3,7-dihydro-1*H*-purine-2,6-dione (77). This compound was synthesized according to the general procedure B using *p*-nitrophenylsulfonate derivative **21** (70 mg, 0.14 mmol) and piperazine **37** (80 mg, 0.45 mmol) dissolved in 4 mL of sulfolane and the reaction mixture was stirred at 130 °C for 17 h. White solid; yield (56%, 42 mg). M.p.: 325-329 °C. ^{1}H NMR (600 MHz, DMSO-d_6) δ 14.16 (s, 1H, NH$_{xanthine}$), 8.44 (d, J = 4.7 Hz,1H, CH$_{pyridyl}$), 8.37 (d, J = 8.5 Hz, 2H, CH$_{phenyl}$), 7.85 (d, J = 8.5 Hz, 2H, CH$_{phenyl}$), 7.67 (td, J = 7.7, 1.8 Hz, 1H, CH$_{pyridyl}$), 7.30 (d, J = 7.8 Hz, 1H, CH$_{pyridyl}$), 7.20 (ddd, J = 7.4, 4.8, 1.1 Hz, 1H, CH$_{pyridyl}$), 4.10 (q, J = 7.1 Hz, 2H, CH$_{2(ethyl)}$), 3.89-3.82 (m, 2H, CH$_{2(propyl)}$), 3.57 (s, 2H, CH$_2$), 2.96 (m, 4H, CH$_{piperazinyl}$), 1.59 (q, J = 7.5 Hz, 2H, CH$_{2(propyl)}$), 1.27 (t, J = 7.1 Hz, 3H, CH$_{3(ethyl)}$), 0.88 (t, J = 7.4 Hz, 3H, CH$_{3(propyl)}$). ^{13}C NMR (151 MHz, DMSO-d_6) δ 157.9, 154.3, 150.5, 148.9, 148.1, 148.0, 136.6, 135.9, 133.0, 128.4, 127.2, 122.8, 122.3, 63.2, 51.7, 46.1, 42.4, 38.3, 21.0, 13.3, 11.3. HPLC-UV (254 nm) ESI-MS, purity: 97%. LC-MS (m/z): 538.4 [M + H]$^+$. HRMS (ESI-TOF) m/z: [M - H]$^-$ calcd. for $C_{26}H_{31}N_7O_4S$ 536.2158, found 536.2090.

1,3-Diethyl-8-(4-((4-(pyridin-2-ylmethyl)piperazin-1-yl)sulfonyl)phenyl)-3,7-dihydro-1*H*-purine-2,6-dione (78). This compound was synthesized according to the general procedure B using *p*-nitrophenylsulfonate derivative **22** (70 mg, 0.14 mmol) and piperazine **37** (80 mg, 0.45 mmol) dissolved in 5 mL of sulfolane and the reaction mixture was stirred at 130 °C for 12 h. White solid; yield (55%, 41 mg). M.p.: 347-351 °C. ^{1}H NMR (600 MHz, DMSO-d_6) δ 14.16 (s, 1H, NH$_{xanthine}$), 8.43 (d, J = 4.5 Hz, 1H, CH$_{pyridyl}$), 8.36 (d, J = 8.4 Hz, 2H, CH$_{phenyl}$), 7.85

(d, *J* = 8.4 Hz, 2H, CH$_{phenyl}$), 7.66 (td, *J* = 7.7, 1.6 Hz, 1H, CH$_{pyridyl}$), 7.30 (d, *J* = 7.8 Hz, 1H, CH$_{pyridyl}$), 7.20 (dd, *J* = 7.0, 5.2 Hz, 1H, CH$_{pyridyl}$), 5.74 (s, 1H), 4.10 (q, *J* = 7.0 Hz, 2H, CH$_{2(ethyl)}$), 3.95 (q, *J* = 7.0 Hz, 2H, CH$_{2(ethyl)}$), 3.59 (d, *J* = 17.9 Hz, 2H, CH$_2$), 3.04-2.89 (m, 4H, CH$_{piperazinyl}$), 2.07 (d, *J* = 7.4 Hz, 1H), 1.28 (t, *J* = 7.1 Hz, 3H, CH$_{3(ethyl)}$), 1.15 (t, *J* = 7.0 Hz, 3H, CH$_{3(propyl)}$). ^{13}C NMR (151 MHz, DMSO-*d$_6$*) δ 157.9, 154.1, 150.3, 149.0, 148.9, 148.0, 136.6, 135.9, 133.0, 128.4, 127.2, 122.8, 122.3, 108.9, 63.1, 55.0, 51.7, 50.7, 46.1, 38.3, 36.0, 30.8, 13.3. HPLC-UV (254 nm) ESI-MS, purity: 98.4%. LC-MS (m/z): 524.2 [M + H]$^+$. HRMS (ESI-TOF) m/z: [M - H]$^-$ calcd. for C$_{25}$H$_{29}$N$_7$O$_4$S 522.2002, found 522.1953.

1,3-Diethyl-8-(4-((4-(pyridin-2-ylmethyl)piperazin-1-yl)sulfonyl)phenyl)-3,7-dihydro-1*H*-purine-2,6-dione (79). This compound was synthesized according to the general procedure B using *p*-nitrophenylsulfonate derivative **19** (70 mg, 0.15 mmol) and piperazine **38** (75 mg, 0.44 mmol) dissolved in 4 mL of sulfolane and the reaction mixture was stirred at 130 °C for 10 h. White solid; yield (43%, 28 mg). M.p.: 348-351 °C. ^{1}H NMR (600 MHz, DMSO-*d$_6$*) δ 13.99 (s, 1H, NH$_{xanthine}$), 11.95 (s, 1H, NH$_{xanthine}$), 8.41 (d, *J* = 4.6 Hz, 1H, CH$_{pyridyl}$), 8.32 (d, *J* = 8.3 Hz, 2H, CH$_{phenyl}$), 7.84 (d, *J* = 8.3 Hz, 2H, CH$_{phenyl}$), 7.62 (q, *J* = 8.0 Hz, 1H, CH$_{pyridyl}$), 7.20 (d, *J* = 7.8 Hz, 1H, CH$_{pyridyl}$), 7.13 (dd, *J* = 7.3, 5.0 Hz, 1H, CH$_{pyridyl}$), 3.85-3.76 (m, 2H, CH$_{2(propyl)}$), 2.89 (m, 4H, CH$_{piperazinyl}$), 2.82-2.77 (m, 2H, CH$_2$), 2.64 (t, *J* = 7.5 Hz, 2H, CH$_2$), 1.62-1.51 (m, 2H, CH$_{2(propyl)}$), 0.90-0.83 (m, 3H, CH$_{3(propyl)}$). ^{13}C NMR (151 MHz, DMSO-*d$_6$*) δ 159.9, 155.1, 151.1, 149.0, 136.5, 135.8, 133.2, 128.4, 127.1, 123.2, 121.4, 57.2, 51.6, 46.1, 41.6, 35.0, 21.0, 11.3. HPLC-UV (254 nm) ESI-MS, purity: 98.8%. LC-MS (m/z): 524.4 [M + H]$^+$. HRMS (ESI-TOF) m/z: [M - H]$^-$ calcd. for C$_{25}$H$_{29}$N$_7$O$_4$S 522.2002, found 522.1918.

1,3-Diethyl-8-(4-((4-(pyridin-2-ylmethyl)piperazin-1-yl)sulfonyl)phenyl)-3,7-dihydro-1*H*-purine-2,6-dione (80). This compound was synthesized according to the general procedure B using *p*-nitrophenylsulfonate derivative **22** (60 mg, 0.12 mmol) and piperazine **38** (72 mg,

0.38 mmol) dissolved in 3 mL of sulfolane and the reaction mixture was stirred at 130 °C for 15 h. White solid; yield (54%, 36 mg). M.p.: 344-348 °C. ^{1}H NMR (600 MHz, DMSO-d_6) δ 14.05 (s, 1H, NH$_{xanthine}$), 8.40 (d, J = 4.2 Hz, 1H, CH$_{pyridyl}$), 8.36 (d, J = 8.4 Hz, 2H, CH$_{phenyl}$), 7.85 (d, J = 8.4 Hz, 2H, CH$_{phenyl}$), 7.61 (td, J = 7.6, 1.5 Hz, 1H, CH$_{pyridyl}$), 7.20 (d, J = 7.8 Hz, 1H, CH$_{pyridyl}$), 7.13 (dd, J = 6.8, 5.3 Hz, 1H, CH$_{pyridyl}$), 4.09 (q, J = 6.9 Hz, 2H, CH$_{2(ethyl)}$), 3.94 (q, J = 6.9 Hz, 2H, CH$_{2(ethyl)}$), 3.31 (s, 4H, CH$_{piperazinyl}$), 2.97-2.86 (m, 4H, CH$_{piperazinyl}$), 2.79 (t, J = 7.5 Hz, 2H, CH$_2$), 2.68-2.57 (m, 2H, CH$_2$), 1.27 (t, J = 7.0 Hz, 3H, CH$_{3(ethyl)}$), 1.14 (t, J = 7.0 Hz, 3H, CH$_{3(ethyl)}$). ^{13}C NMR (151 MHz, DMSO-d_6) δ 159.9, 154.2, 150.3, 149.0, 148.1, 148.0, 136.5, 135.9, 133.1, 128.4, 127.2, 123.2, 121.4, 109.1, 57.2, 51.6, 50.7, 46.0, 38.3, 36.0, 35.0, 13.3. HPLC-UV (254 nm) ESI-MS, purity: 96.7%. LC-MS (m/z): 538.4 [M + H]$^+$. HRMS (ESI-TOF) m/z: [M - H]$^-$ calcd. for C$_{26}$H$_{31}$N$_7$O$_4$S 536.2158, found 536.2074.

8-(4-((4-((6-Chloropyridin-3-yl)amino)piperidin-1-yl)sulfonyl)phenyl)-1-propyl-3,7-dihydro-1*H*-purine-2,6-dione (81). This compound was synthesized according to the general procedure A using *p*-nitrophenylsulfonate derivative **19** (100 mg, 0.21 mmol) and piperazine **39** (120 mg, 0.56 mmol) dissolved in 5 mL of anhydrous DMSO and the reaction mixture was stirred at 140 °C for 8 h. White solid; yield (35%, 40 mg). M.p.: 328-331 °C. ^{1}H NMR (500 MHz, DMSO-d_6) δ 11.91 (s, 1H, NH$_{xanthine}$), 8.33 (d, J = 8.5 Hz, 2H, CH$_{phenyl}$), 7.91-7.81 (m, 2H, CH$_{phenyl}$), 7.68 (d, J = 3.0 Hz, 1H, CH$_{pyridyl}$), 7.07 (d, J = 8.7 Hz, 1H, CH$_{pyridyl}$), 6.97 (dd, J = 8.7, 3.1 Hz, 1H, CH$_{pyridyl}$), 5.93 (d, J = 8.0 Hz, 1H, CH$_{piperidyl}$), 3.87-3.78 (m, 2H, CH$_{2(propyl)}$), 3.58 (dd, J = 11.7, 4.9 Hz, 2H, CH$_{piperidyl}$), 2.62-2.52 (m, 2H, CH$_{piperidyl}$), 1.93 (dd, J = 13.3, 4.2 Hz, 2H, CH$_{piperidyl}$), 1.63-1.51 (m, 2H, CH$_{2(propyl)}$), 1.40 (dd, J = 12.3, 8.4 Hz, 2H, CH$_{piperidyl}$), 0.88 (t, J = 7.4 Hz, 3H, CH$_{3(propyl)}$). ^{13}C NMR (126 MHz, DMSO-d_6) δ 155.2, 151.1, 148.3, 147.7, 143.4, 136.5, 136.2, 134.2, 133.3, 128.3, 127.1, 124.0, 122.4, 47.5, 45.0, 41.6, 30.7, 21.0, 11.4. HPLC-UV (254 nm) ESI-MS, purity: 98.3%. LC-MS (m/z): 543.9 [M + H]$^+$. HRMS (ESI-TOF) m/z: [M - H]$^-$ calcd. for C$_{24}$H$_{26}$ClN$_7$O$_4$S 542.1456, found 542.1430.

8-(4-((4-((6-Bromopyridin-3-yl)amino)piperidin-1-yl)sulfonyl)phenyl)-1-propyl-3,7-dihydro-1*H*-purine-2,6-dione (82). This compound was synthesized according to the general procedure A using *p*-nitrophenylsulfonate derivative **19** (100 mg, 0.21 mmol) and piperazine **40** (140 mg, 0.55 mmol) dissolved in 4 mL of anhydrous DMSO and the reaction mixture was stirred at 140 °C for 8 h. White solid; yield (30%, 37 mg). M.p.: 318-322 °C. ^{1}H NMR (500 MHz, DMSO-d_6) δ 8.33 (d, J = 8.2 Hz, 2H, CH$_{phenyl}$), 7.86 (d, J = 8.2 Hz, 2H, CH$_{phenyl}$), 7.67 (d, J = 3.1 Hz, 1H, CH$_{pyridyl}$), 7.17 (d, J = 8.6 Hz, 1H, CH$_{pyridyl}$), 6.88 (dd, J = 8.7, 3.2 Hz,1H, CH$_{pyridyl}$), 5.94 (d, J = 8.1 Hz, 1H, CH$_{piperidyl}$), 3.82 (dd, J = 8.7, 6.3 Hz, 2H, CH$_{2(propyl)}$), 3.57 (d, J = 11.9 Hz, 2H, CH$_{piperidyl}$), 2.63-2.51 (m, 2H, CH$_{piperidyl}$), 2.01-1.84 (m, 2H, CH$_{piperidyl}$), 1.57 (q, J = 7.4 Hz, 2H, CH$_{2(propyl)}$), 1.48-1.33 (m, 2H, CH$_{piperidyl}$), 0.87 (t, J = 7.4 Hz, 3H, CH$_{3(propyl)}$). ^{13}C NMR (126 MHz, DMSO-d_6) δ 155.2, 151.2, 148.2, 147.8, 143.8, 136.6, 135.2, 135.1, 133.2, 128.3, 127.6, 127.6, 127.2, 125.8, 122.4, 108.9, 70.0, 68.7, 63.3, 56.0, 48.8, 47.5, 45.0, 41.7, 32.2, 30.7, 29.8, 21.1, 11.4. HPLC-UV (254 nm) ESI-MS, purity: 99.4%. LC-MS (m/z): 588.0 [M + H]$^+$. HRMS (ESI-TOF) m/z: [M - H]$^-$ calcd. for C$_{24}$H$_{26}$BrN$_7$O$_4$S 586.0950, found 586.0859.

1-Propyl-8-(4-((4-(pyridin-4-yloxy)piperidin-1-yl)sulfonyl)phenyl)-3,7-dihydro-1*H*-purine-2,6-dione (83). This compound was synthesized according to the general procedure A using *p*-nitrophenylsulfonate derivative **19** (50 mg, 0.11 mmol) and piperazine **41** (60 mg, 0.34 mmol) dissolved in 3 mL of anhydrous DMSO and the reaction mixture was stirred at 140 °C for 8 h. White solid; yield (45%, 24 mg). M.p.: 341-344 °C. ^{1}H NMR (500 MHz, DMSO-d_6) δ 14.01 (s, 1H, NH$_{xanthine}$), 11.95 (s, 1H, NH$_{xanthine}$), 8.34 (d, J = 8.5 Hz, 2H, CH$_{phenyl}$), 8.32-8.26 (m, J = 3.1 Hz, 2H, CH$_{pyridyl}$), 7.89 (d, J = 8.5 Hz, 2H, CH$_{phenyl}$), 6.90 (d, J = 6.5 Hz, 2H, CH$_{pyridyl}$), 4.64-4.50 (m, 1H, CH$_{piperidyl}$), 3.82 (t, 2H, CH$_{2(propyl)}$), 3.36-3.33 (m, 2H, CH$_{piperidyl}$), 2.88 (t, J = 12.4, 9.2, 3.4 Hz, 2H, CH$_{piperidyl}$), 2.05-1.84 (m, 2H, CH$_{piperidyl}$), 1.73-1.64 (m, 2H, CH$_{piperidyl}$), 1.62-1.52 (q, J = 7.4 Hz, 2H, CH$_{2(propyl)}$), 0.88 (t, J = 7.4 Hz, 3H, CH$_{3(propyl)}$). ^{13}C NMR (126 MHz, DMSO-d_6) δ 163.0, 155.1, 151.1, 151.1, 148.1, 147.7, 136.5, 133.1, 128.3, 127.2, 111.2,

108.8, 70.9, 56.0, 55.0, 43.5, 41.7, 30.8, 29.6, 21.0, 11.3. HPLC-UV (254 nm) ESI-MS, purity: 97.8%. LC-MS (m/z): 511.1 [M + H]$^+$. HRMS (ESI-TOF) m/z: [M - H]$^-$ calcd. for $C_{24}H_{26}N_6O_5S$ 509.1685, found 509.1642.

3-Ethyl-1-propyl-8-(4-((4-(pyridin-4-yloxy)piperidin-1-yl)sulfonyl)phenyl)-3,7-dihydro-1*H*-purine-2,6-dione (84). This compound was synthesized according to the general procedure A using *p*-nitrophenylsulfonate derivative **21** (50 mg, 0.10 mmol) and piperazine **41** (55 mg, 0.31 mmol) dissolved in 4 mL of anhydrous DMSO and the reaction mixture was stirred at 140 ºC for 12 h. White solid; yield (52%, 28 mg). M.p.: 327-330 °C. ^{1}H NMR (600 MHz, DMSO-*d$_6$*) δ 14.20 (s, 1H, NH$_{xanthine}$), 8.43-8.33 (m, 2H, CH$_{phenyl}$), 8.34-8.24 (m, 2H, CH$_{pyridyl}$), 7.94-7.86 (m, 2H, CH$_{phenyl}$), 6.95-6.86 (m, 2H, CH$_{pyridyl}$), 4.58 (dt, *J* = 8.2, 4.2 Hz, 1H, CH$_{piperidyl}$), 4.09 (t, *J* = 7.2 Hz, 2H, CH$_{2(propyl)}$), 3.91-3.83 (m, 2H, CH$_{2(ethyl)}$), 3.33 (dt, *J* = 11.6, 5.2 Hz, 2H, CH$_{piperidyl}$), 2.88 (ddd, *J* = 12.3, 9.2, 3.5 Hz, 2H, CH$_{piperidyl}$), 2.05-1.96 (m, 2H, CH$_{piperidyl}$), 1.68 (dd, *J* = 8.7, 4.3 Hz, 2H, CH$_{piperidyl}$), 1.58 (q, *J* = 7.5 Hz, 2H, CH$_{2(propyl)}$), 1.27 (t, *J* = 7.1 Hz, 3H, CH$_{3(ethyl)}$), 0.88 (t, *J* = 7.4 Hz, 3H, CH$_{3(propyl)}$). ^{13}C NMR (126 MHz, DMSO-*d$_6$*) δ 163.0, 154.3, 151.0, 150.5, 148.1, 148.0, 136.5, 133.2, 133.0, 130.7, 128.3, 127.3, 111.2, 108.9, 92.7, 70.8, 43.4, 42.4, 38.3, 29.6, 21.0, 13.3, 11.3. HPLC-UV (254 nm) ESI-MS, purity: 97.3%. LC-MS (m/z): 539.5 [M + H]$^+$. HRMS (ESI-TOF) m/z: [M - H]$^-$ calcd. for $C_{26}H_{30}N_6O_5S$ 537.1998, found 537.1925.

1,3-Diethyl-8-(4-((4-(pyridin-4-yloxy)piperidin-1-yl)sulfonyl)phenyl)-3,7-dihydro-1*H*-purine-2,6-dione (85). This compound was synthesized according to the general procedure A using *p*-nitrophenylsulfonate derivative **22** (50 mg, 0.10 mmol) and piperazine **41** (55 mg, 0.31 mmol) dissolved in 4 mL of anhydrous DMSO and the reaction mixture was stirred at 140 ºC for 12 h. White solid; yield (50%, 27 mg). M.p.: 350-354 °C. ^{1}H NMR (600 MHz, DMSO-*d$_6$*) δ 14.21 (s, 1H, NH$_{xanthine}$), 8.38 (d, *J* = 8.2 Hz, 2H, CH$_{phenyl}$), 8.30 (d, *J* = 5.5 Hz, 2H, CH$_{pyridyl}$),

7.90 (d, *J* = 8.2 Hz 2H, CH$_{phenyl}$), 6.90 (d, *J* = 5.3 Hz, 2H, CH$_{pyridyl}$), 4.58 (dt, *J* = 8.3, 4.4 Hz,1H, CH$_{piperidyl}$), 4.10 (q, *J* = 7.1 Hz, 2H, CH$_{2(ethyl)}$), 3.95 (q, *J* = 7.1 Hz, 2H, CH$_{2(ethyl)}$), 3.41-3.32 (m, 2H, CH$_{piperidyl}$), 2.92-2.85 (m, 2H, CH$_{piperidyl}$), 2.05-1.98 (m, 2H, CH$_{piperidyl}$), 1.71-1.63 (m, 2H, CH$_{piperidyl}$), 1.28 (t, *J* = 7.1 Hz, 3H, CH$_{3(ethyl)}$), 1.15 (t, *J* = 7.0 Hz, 3H, CH$_{3(ethyl)}$).^{13}C NMR (151 MHz, DMSO-*d$_6$*) δ 163.0, 154.2, 151.1, 150.3, 148.1, 148.0, 136.5, 133.0, 128.4, 127.3, 111.2, 109.0, 76.9, 76.0, 75.3, 74.4, 70.8, 68.6, 56.1, 56.0, 43.5, 40.2, 40.1, 40.0, 39.8, 39.7, 39.6, 39.4, 39.3, 38.3, 36.0, 29.7, 29.6, 13.3, 0.3. HPLC-UV (254 nm) ESI-MS, purity: 98.1%. LC-MS (m/z): 525.1 [M + H]$^+$. HRMS (ESI-TOF) m/z: [M - H]$^-$ calcd. for C$_{25}$H$_{28}$N$_6$O$_5$S 523.1842, found 523.1781.

8-(4-{[4-(4-Bromophenyl)-4-hydroxypiperidin-1-yl]sulfonyl}phenyl)-3-ethyl-1-propyl-2,3,6,7-tetrahydro-1*H*-purine-2,6-dione (86). This compound was synthesized according to the general procedure A using *p*-nitrophenylsulfonate derivative **19** (50 mg, 0.10 mmol) and piperazine **42** (76 mg, 0.42 mmol) dissolved in 3 mL of anhydrous DMSO and the reaction mixture was stirred at 140 °C for 15 h. White solid; The desired product was obtained as a White solid with a yield of 30% (29 mg). M.p.: 320-330 °C. ^{1}H NMR (500 MHz, DMSO-*d$_6$*) δ 0.84-0.91 (t, *J* = 7.5 Hz, 3H, CH$_{3(propyl)}$), 1.24-1.30 (t, *J* = 7.1 Hz, 3H, CH$_{3(ethyl)}$), 1.54-1.60 (dd, 2H, CH$_{2(propyl)}$), 1.90-2.00 (tt, *J* = 8.2 Hz, 2H, CH$_2$), 2.61-2.69 (m, 2H, CH$_2$), 3.54-3.63 (m, 2H, CH$_2$), 3.82-3.89 (m, 2H, CH$_{2(propyl)}$), 4.06-4.15 (m, 2H, CH$_{2(ethyl)}$), 7.34-7.39 (m, 2H, CH$_{phenyl}$), 7.44-7.48 (m, 2H, CH$_{phenyl}$), 7.88-7.93 (d, *J* = 8.6 Hz, 2H, CH$_{phenyl}$), 8.35-8.40 (d, *J* = 8.6 Hz, 2H, CH$_{phenyl}$). ^{13}C NMR (126 MHz, DMSO) δ 166, 154.4 (C4), 150.6, 148.3 (C2), 148.1, 136.5, 133, 131, 128.4, 127.3, 125.9, 119.9, 116.5, 109, 68.9, 48.4, 42.5, 38.4, 36.9, 36.5, 30.4, 21 (CH$_{2(propyl)}$), 13.3, 11.3 (CH$_{3(propyl)}$). HPLC-UV (254 nm) ESI-MS, purity: 98.4%. LC-MS (m/z): 616.2 [M + H]$^+$. HRMS (ESI-TOF) m/z: [M - H]$^-$ calcd. for C$_{27}$H$_{30}$BrN$_5$O$_5$S 614.1151, found 614.1111.

8-(4-((4-Hydroxy-4-(pyridin-3-yl)piperidin-1-yl)sulfonyl)phenyl)-1-propyl-3,7-dihydro-1*H*-purine-2,6-dione (87). This compound was synthesized according to the general procedure A using *p*-nitrophenylsulfonate derivative **22** (50 mg, 0.11 mmol) and piperazine **42** (60 mg, 0.34 mmol) dissolved in 3 mL of anhydrous DMSO and the reaction mixture was stirred at 140 ºC for 10 h. White solid; yield (55%, 30 mg). M.p.: 348-352 °C. ^{1}H NMR (600 MHz, DMSO-*d$_6$*) δ 14.03 (s, 1H, NH$_{xanthine}$), 11.97 (s, 1H, NH$_{xanthine}$), 8.65 (d, *J* = 2.5 Hz, 1H, CH$_{pyridyl}$), 8.45-8.40 (m, 1H, CH$_{pyridyl}$), 8.35 (d, *J* = 8.5 Hz, 2H, CH$_{phenyl}$), 7.91 (d, *J* = 8.6 Hz, 2H, CH$_{phenyl}$), 7.80 (d, *J* = 8.1 Hz, 1H, CH$_{pyridyl}$), 7.31 (dd, *J* = 8.0, 4.7 Hz, 1H, CH$_{pyridyl}$), 5.17 (s, 1H, OH), 3.86-3.79 (m, 2H, CH$_{2(propyl)}$), 3.61 (dd, *J* = 8.8, 2.8 Hz, 2H, CH$_{piperidyl}$), 2.72-2.62 (m, 2H, CH$_{piperidyl}$), 2.03 (td, *J* = 13.2, 4.7 Hz, 2H, CH$_{piperidyl}$), 1.73-1.66 (m, 2H, CH$_{piperidyl}$), 1.58 (q, *J* = 7.5 Hz, 2H, CH$_{2(propyl)}$), 0.88 (t, *J* = 7.4 Hz, 3H, CH$_{3(propyl)}$). ^{13}C NMR (151 MHz, DMSO-*d$_6$*) δ 172.1, 155.1, 151.1, 148.2, 148.0, 147.8, 146.7, 143.9, 136.3, 133.1, 132.8, 128.5, 128.3, 127.8, 127.2, 123.2, 108.7, 68.1, 42.3, 41.7, 36.8, 21.0, 14.8, 11.4. HPLC-UV (254 nm) ESI-MS, purity: 97.3%. LC-MS (m/z): 511.2 [M + H]$^+$. HRMS (ESI-TOF) m/z: [M - H]$^-$ calcd. for C$_{24}$H$_{26}$N$_6$O$_5$S 509.1685, found 509.1613.

1,3-Diethyl-8-(4-((4-hydroxy-4-(pyridin-3-yl)piperidin-1-yl)sulfonyl)phenyl)-3,7-dihydro-1*H*-purine-2,6-dione (88). This compound was synthesized according to the general procedure A using *p*-nitrophenylsulfonate derivative **21** (50 mg, 0.10 mmol) and piperazine **43** (70 mg, 0.39 mmol) dissolved in 4 mL of anhydrous DMSO and the reaction mixture was stirred at 140 ºC for 10 h. White solid; yield (55%, 30 mg). M.p.: 340-344 °C. ^{1}H NMR (600 MHz, DMSO-*d$_6$*) δ 14.20 (s, 1H, NH$_{xanthine}$), 8.65 (s, 1H, CH$_{pyridyl}$), 8.46-8.42 (m, 1H, CH$_{pyridyl}$), 8.40 (d, *J* = 8.3 Hz, 2H, CH$_{phenyl}$), 7.93 (d, *J* = 8.2 Hz, 2H, CH$_{phenyl}$), 7.81 (dt, *J* = 8.1, 2.0 Hz, 1H, CH$_{pyridyl}$), 7.32 (dd, *J* = 8.1, 4.7 Hz, 1H, CH$_{pyridyl}$), 5.16 (s, 1H, OH), 4.12 (q, *J* = 7.0 Hz, 2H, CH$_{2(ethyl)}$), 3.96 (q, *J* = 7.0 Hz, 2H, CH$_{2(ethyl)}$), 3.64-3.57 (m, 2H, CH$_{piperidyl}$), 2.66 (td, *J* = 11.9, 2.6 Hz, 2H, CH$_{piperidyl}$), 2.03 (td, *J* = 13.2, 4.7 Hz, 2H, CH$_{piperidyl}$), 1.73-1.66 (m, 2H, CH$_{piperidyl}$), 1.29 (t, *J*

= 7.1 Hz, 3H, CH$_{3(ethyl)}$), 1.15 (t, J = 7.0 Hz, 3H, CH$_{3(ethyl)}$). ^{13}C NMR (151 MHz, DMSO-d_6) δ 154.2, 150.3, 148.2, 148.1, 148.0, 146.7, 143.9, 136.4, 133.0, 132.7, 128.5, 127.3, 123.2, 109, 68.0, 42.2, 38.3, 36.8, 36.0, 13.3. HPLC-UV (254 nm) ESI-MS, purity: 97.2%. LC-MS (m/z): 525.2 [M + H]$^+$. HRMS (ESI-TOF) m/z: [M - H]$^-$ calcd. for C$_{25}$H$_{28}$N$_6$O$_4$S 523.1842, found 523.1758.

4.2.6.2. Biological assays

Membrane preparation. The membrane preparations of recombinant CHO or HEK cells stably expressing human AR subtypes were conducted as previously described[82,83] or purchased from Perkin Elmer (Solingen, Germany).

Radioligand receptor binding assays. [^{3}H]2-chloro-N^6-cyclopentyladenosine ([^{3}H]CCPA, A$_1$), [^{3}H](E)-3-(3-hydroxypropyl)-8-(2-(3-methoxyphenyl)vinyl)-7-methyl-1-prop-2-ynyl-3,7-dihydropurine-2,6-dione ([^{3}H]MSX-2, A$_{2A}$), [^{3}H]8-(4-(4-(4-chlorophenyl) piperazine-1-sulfonyl)phenyl)-1-propyl-3,7-dihydropurine-2,6-dione ([^{3}H]PSB-603, A$_{2B}$), and [^{3}H]2-phenyl-8-ethyl-4-methyl-(8R)-4,5,7,8-tetrahydro-1H-imidazo[2.1-i]-purin-5-one ([^{3}H]PSB-11, A$_3$) were used as radioligands for human A$_1$, A$_{2A}$, A$_{2B}$, A$_3$AR respectively.

Competition binding experiments at human A$_1$, A$_{2A}$, and A$_3$ ARs were performed in a final volume of 400 μL containing 4 μL of test compound dissolved in 100% DMSO, 196 μL buffer (50 mM Tris-HCl, pH 7.4, 10 mM MgCl$_2$, pH 7.4), 100 μL of radioligand solution in the same buffer and 100 μL of membrane preparation (5-100 μg protein per vial, 2 U/mL adenosine deaminase (ADA), incubation 15 min at rt). Competition binding experiments at human A$_{2B}$ARs were performed in a final volume of 1 mL containing 10 μL of test compound dissolved in 100% DMSO, 790 μL buffer (50 mM Tris-HCl, pH 7.4), 100 μL of radioligand solution in the same buffer, and 100 μL of membrane preparation (10-100 μg protein per vial, 2 U/mL ADA, incubation for 15 min at rt). Non-specific binding was determined in the

presence of 2-chloroadenosine (10 μM f. c.), CGS-15943 (10 μM f. c.), DPCPX (10 μM f. c.) and N^6-(L-2-phenylisopropyl)adenosine (100 μM f. c.) for human A_1, A_{2A}, A_{2B} and A_3AR respectively.

The incubation time at rt was 90 min for A_1ARs, 30 min for $A_{2A}ARs$, 75 min for $A_{2B}ARs$, 45 min for human A_3ARs with the radioligand [^{3}H]PSB-11. After the incubation, the assay mixture was filtered through GF/B glass fiber filters using a Brandel harvester (Brandel, Gaithersburg, MD). Filters were washed three times (3 - 4 mL each) with ice-cold 50 mM Tris-HCl buffer, pH 7.4. For the $A_{2A}AR$ assay the GF/B glass fiber filters were preincubated for 30 min in 0.3% aq. polyethylenemine solution. The GF/B glass fiber filters for the $A_{2B}AR$ assays were washed four times (3 - 4 mL each) with ice-cold 50 mM Tris-HCl buffer, pH 7.4 containing 0.1% BSA in order to reduce non-specific binding. Then filters were transferred to vials, incubated for 9 h with 2.5 mL of scintillation cocktail (Luma Safe, Perkin Elmer), and counted in a liquid scintillation counter (Tri-Carb 2810 TR) with a counting efficiency of $\sim$52%. Three to four separate experiments were performed for the determination of K_i values. All data were analyzed with GraphPad Prism, Version 4.1 (GraphPad Inc., La Jolla, CA).

Author Information

Corresponding Author

*Christa E. Müller: Phone: +49-228-73-230; Fax: +49-228-73-2567; E-mail: christa.mueller@uni-bonn.de

ORCID

Ahmed Temirak: 0000-0003-3862-5359
Christa E. Müller: 0000-0002-0013-6624

4.2.7. References

(1)   Fredholm, B. B.; IJzerman, A. P.; Jacobson, K. A.; Klotz, K.-N. N.; Linden, J. International Union of Pharmacology. XXV. Nomenclature and classification of adenosine receptors. *Pharmacol. Rev.* **2001**, *53*, 527–552.

(2)   Cieślak, M.; Komoszyński, M.; Wojtczak, A. Adenosine A_{2A} receptors in Parkinson's disease treatment. *Purinergic Signal.* **2008**, *4*, 305–312.

(3)   Fredholm, B. B. Adenosine, adenosine receptors and the actions of caffeine. *Pharmacol. Toxicol.* **1995**, *76*, 93–101.

(4)   Azambuja, J. H.; Ludwig, N.; Braganhol, E.; Whiteside, T. L. Inhibition of the adenosinergic pathway in cancer rejuvenates innate and adaptive immunity. *Int. J. Mol. Sci.* **2019**, *20*, 5698.

(5)   Gessi, S.; Merighi, S.; Varani, K.; Borea, P. A. Adenosine receptors in health and disease. In *Advances in Pharmacology*; Academic Press Inc., 2011; Vol. 61, pp 41–75.

(6)   Fredholm, B. B.; Irenius, E.; Kull, B.; Schulte, G. Comparison of the potency of adenosine as an agonist at human adenosine receptors expressed in chinese hamster ovary cells. *Biochem.*

Pharmacol. **2001**, *61*, 443–448.

(7)   Fredholm, B. B. Adenosine receptors as drug targets. *Experimental Cell Research*. Academic Press Inc. 2010, pp 1284–1288.

(8)   Sousa, J. B.; Fresco, P.; Diniz, C.; Goncalves, J. Adenosine receptor ligands on cancer therapy: A review of patent literature. *Recent Pat. Anticancer. Drug Discov.* **2018**, *13*.

(9)   Romanowska, M.; Komoszyński, M. [Adenosine--neurotransmitter and neuromodulator in the central nervous system]. *Postepy Biochem.* **2002**, *48*, 230–238.

(10)   Borea, P. A.; Gessi, S.; Merighi, S.; Vincenzi, F.; Varani, K. Pathological overproduction: the bad side of adenosine. *Br. J. Pharmacol.* **2017**, *174*, 1945–1960.

(11)   Franco, R.; Navarro, G. Adenosine A_{2A} receptor antagonists in neurodegenerative diseases: huge potential and huge challenges. *Front. Psychiatry* **2018**, *9*.

(12)   Schiffmann, S. N.; Fisone, G.; Moresco, R.; Cunha, R. A.; Ferré, S. Adenosine A2A receptors and basal ganglia physiology. *Prog. Neurobiol.* **2007**, *83*, 277–292.

(13)   Faivre, E.; Coelho, J. E.; Zornbach, K.; Malik, E.; Baqi, Y.; Schneider, M.; Cellai, L.; Carvalho, K.; Sebda, S.; Figeac, M.; et al. Beneficial effect of a selective adenosine A2A receptor antagonist in the APPswe/PS1dE9 mouse model of Alzheimer's disease. *Front. Mol. Neurosci.* **2018**, *11*.

(14)   Paul, S.; Lal, G. The molecular mechanism of natural killer cells function and its importance in cancer immunotherapy. *Front. Immunol.* **2017**, *8*.

(15)   Bassani, B.; Baci, D.; Gallazzi, M.; Poggi, A.; Bruno, A.; Mortara, L. Natural killer cells as key players of tumor progression and angiogenesis: old and novel tools to divert their pro-tumor activities into potent anti-tumor effects. *Cancers* **2019**, *11*, 461.

(16)   Hu, W.; Wang, G.; Huang, D.; Sui, M.; Xu, Y. Cancer immunotherapy based on natural killer cells: Current progress and new opportunities. *Front. Immunol.* **2019**, *10*.

(17) Melaiu, O.; Lucarini, V.; Cifaldi, L.; Fruci, D. Influence of the Tumor Microenvironment on NK Cell Function in Solid Tumors. *Front. Immunol.* **2020**, *10*.

(18) Gorain, B.; Choudhury, H.; Yee, G. S.; Bhattamisra, S. K. Adenosine receptors as novel targets for the treatment of various cancers. *Curr. Pharm. Des.* **2019**, *25*, 2828–2841.

(19) Fishman, P.; Bar-Yehuda, S.; Synowitz, M.; Powell, J. D.; Klotz, K. N.; Gessi, S.; Borea, P. A. *Adenosine receptors in health and disease*; Handbook of Experimental Pharmacology; Springer Berlin Heidelberg: Berlin, Heidelberg, 2009; Vol. 193.

(20) Gao, Z.-G.; Jacobson, K. A. A2B adenosine receptor and cancer. *Int. J. Mol. Sci.* **2019**, *20*, 5139.

(21) Chen, S.; Akdemir, I.; Fan, J.; Linden, J.; Zhang, B.; Cekic, C. The expression of adenosine A2B receptor on antigen-presenting cells suppresses CD8 + T-cell responses and promotes tumor growth. *Cancer Immunol. Res.* **2020**.

(22) Cekic, C.; Sag, D.; Li, Y.; Theodorescu, D.; Strieter, R. M.; Linden, J. Adenosine A 2B Receptor Blockade Slows Growth of Bladder and Breast Tumors. *J. Immunol.* **2012**, *188*, 198–205.

(23) Bilkei-Gorzo, A.; Abo-Salem, O. M.; Hayallah, A. M.; Michel, K.; Müller, C. E.; Zimmer, A. Adenosine receptor subtype-selective antagonists in inflammation and hyperalgesia. *Naunyn. Schmiedebergs. Arch. Pharmacol.* **2008**, *377*, 65–76.

(24) Abo-Salem, O. M.; Hayallah, A. M.; Bilkei-Gorzo, A.; Filipek, B.; Zimmer, A.; Müller, C. E. Antinociceptive effects of novel A2B adenosine receptor antagonists. *J. Pharmacol. Exp. Ther.* **2004**, *308*, 358–366.

(25) Allard, D.; Turcotte, M.; Stagg, J. Targeting A2 adenosine receptors in cancer. *Immunol. Cell Biol.* **2017**, *95*, 333–339.

(26) Allard, B.; Beavis, P. A.; Darcy, P. K.; Stagg, J. Immunosuppressive activities of adenosine in cancer. *Curr. Opin. Pharmacol.* **2016**, *29*, 7–16.

(27) Müller, C. E.; Jacobson, K. A. Recent developments in adenosine receptor ligands and their

potential as novel drugs. *Biochim. Biophys. Acta - Biomembr.* **2011**, *1808*, 1290–1308.

(28)   Müller, C. E.; Baqi, Y.; Namasivayam, V. Agonists and antagonists for purinergic receptors. In *Methods in molecular biology (Clifton, N.J.)*; NLM (Medline), 2020; Vol. 2041, pp 45–64.

(29)   Elmenhorst, D.; Elmenhorst, E. M.; Hennecke, E.; Kroll, T.; Matusch, A.; Aeschbach, D.; Bauer, A. Recovery sleep after extended wakefulness restores elevated A1 adenosine receptor availability in the human brain. *Proc. Natl. Acad. Sci. U. S. A.* **2017**, *114*, 4243–4248.

(30)   Baratloo, A.; Rouhipour, A.; Forouzanfar, M. M.; Safari, S.; Amiri, M.; Negida, A. The role of caffeine in pain management: A brief literature review. *Anesthesiol. Pain Med.* **2016**, *6*, e33193.

(31)   Eini, H.; Frishman, V.; Yulzari, R.; Kachko, L.; Lewis, E. C.; Chaimovitz, C.; Douvdevani, A. Caffeine promotes anti-tumor immune response during tumor initiation: Involvement of the adenosine A2A receptor. *Biochem. Pharmacol.* **2015**, *98*, 110–118.

(32)   Bai, K.; Cai, Q.; Jiang, Y.; Lv, L. Coffee consumption and risk of hepatocellular carcinoma: A meta-analysis of eleven epidemiological studies. *Onco. Targets. Ther.* **2016**, *9*, 4369–4375.

(33)   Edling, C. E.; Selvaggi, F.; Ghonaim, R.; Maffucci, T.; Falasca, M. Caffeine and the analog CGS 15943 inhibit cancer cell growth by targeting the phosphoinositide 3-kinase/Akt pathway. *Cancer Biol. Ther.* **2014**, *15*, 524–532.

(34)   Pinna, A. Adenosine A2A receptor antagonists in Parkinson's disease: Progress in clinical trials from the newly approved istradefylline to drugs in early development and those already discontinued. *CNS Drugs* **2014**, *28*, 455–474.

(35)   Gessi, S.; Merighi, S.; Varani, K. *The adenosine receptors*; The Receptors; Springer International Publishing: Cham, 2018; Vol. 34.

(36)   Mølck, C.; Ryall, J.; Failla, L. M.; Coates, J. L.; Pascussi, J.-M. M.; Heath, J. K.; Stewart, G.; Hollande, F. The A2B adenosine receptor antagonist PSB-603 promotes oxidative phosphorylation and ROS production in colorectal cancer cells via adenosine receptor-

independent mechanism. *Cancer Lett.* **2016**, *383*, 135–143.

(37) Vecchio, E. A.; Tan, C. Y. R. R.; Gregory, K. J.; Christopoulos, A.; White, P. J.; May, L. T. Ligand-independent adenosine A2B receptor constitutive activity as a promoter of prostate cancer cell proliferation. *J. Pharmacol. Exp. Ther.* **2016**, *357*, 36–44.

(38) El Maatougui, A.; Azuaje, J.; González-Gómez, M.; Miguez, G.; Crespo, A.; Carbajales, C.; Escalante, L.; García-Mera, X.; Gutiérrez-de-Terán, H.; Sotelo, E. Discovery of potent and highly selective A2B adenosine receptor antagonist chemotypes. *J. Med. Chem.* **2016**, *59*, 1967–1983.

(39) Müller, C. E.; Baqi, Y.; Hinz, S.; Namasivayam, V. Medicinal chemistry of A2B adenosine receptors. In *The Adenosine Receptors*; Springer International Publishing: Cham, 2018; pp 137–168.

(40) Seitz, L.; Jin, L.; Leleti, M.; Ashok, D.; Jeffrey, J.; Rieger, A.; Tiessen, R. G.; Arold, G.; Tan, J. B. L.; Powers, J. P.; et al. Safety, tolerability, and pharmacology of AB928, a novel dual adenosine receptor antagonist, in a randomized, phase 1 study in healthy volunteers. *Invest. New Drugs* **2019**, *37*, 711–721.

(41) Walters, M. J.; Tan, J. B.; Becker, A.; Yi, F.; Park, T.; Leleti, M. R.; Rosen, B.; Sharif, E.; Debien, L.; Young, S.; et al. Abstract 4572: Characterization of the potent and selective A2aR antagonist AB928 for the treatment of cancer. In *Clinical Research (Excluding Clinical Trials)*; American Association for Cancer Research, 2017; pp 4572–4572.

(42) 34th Annual meeting & amp; pre-conference programs of the Society for Immunotherapy of Cancer (SITC 2019): part 2. *J. Immunother. Cancer* **2019**, *7*, 283.

(43) A study to evaluate the safety and tolerability of immunotherapy combinations in participants with advanced malignancies - full text view - clinicaltrials.gov https://clinicaltrials.gov/ct2/show/NCT03629756 (accessed Oct 9, 2019).

(44)   A study to evaluate safety/tolerability of immunotherapy combinations in participants with triple-negative breast cancer and gynecologic malignancies - full text view - clinicaltrials.org https://clinicaltrials.gov/ct2/show/NCT03719326?term=NCT03719326&rank=1 (accessed May 4, 2020).

(45)   A study to evaluate immunotherapy combinations in participants with lung cancer - full text view   -   clinicaltrials.gov https://clinicaltrials.gov/ct2/show/NCT03846310?term=NCT03846310&draw=2&rank=1 (accessed May 4, 2020).

(46)   A study to evaluate immunotherapy combinations in participants with gastrointestinal malignancies   -   full   text   view   -   clinicaltrials.gov https://clinicaltrials.gov/ct2/show/NCT03720678?term=NCT03720678&rank=1 (accessed May 4, 2020).

(47)   Beatty, J.; Debien, L.; Jeffrey, J.; Leleti, M. R.; Mandal, D.; Miles, D.; Powers, J.; Rosen, B.; Thomas-Tran, R.; Sharif, E. Azolopyrimidine for the treatment of cancer-related disorders. July 26, 2018, WO2018136700.

(48)   Hoang, G.; Wang, X.; Carlsen, P. N.; Gan, P.; Li, Y.; Qi, C.; Wu, L.; Yao, W.; Yu, Z.; Zhu, W. Fused pyrazine derivatives as A2A/A2B inhibitors. 2020, WO2020010197.

(49)   Minamisono, T.; Sato, Y.; Ishihara, H.; Omae, T.; Hasebe, T.; Takiyama, H. Solid-state characterization of E3210 polymorphs. *J. Chem. Eng. Japan* **2012**, *45*, 233–238.

(50)   Eisai Co., Ltd. https://www.eisai.com/index.html (accessed Nov 19, 2019).

(51)   Blayo, A.-L.; Manteau, B.; Dorange, I.; Mayer, S.; Schann, S.; Catelain, T. 5-Azaindazole derivatives as adenosine receptor antagonists. 2020, WO/2020/083878.

(52)   Xiaozhao, W.; Niels, C. P.; Chunhong, H.; Taisheng, H. Pyrrole tricyclic compounds as A2A/A2B inhibitors. 2019, 20190337957.

(53)   Wang, X.; Han, H.; McCammant, M. S.; Wu, L.; Yao, W.; Yu, Z.; Zhao, L. Fused pyrimidine derivatives as A2A/A2B inhibitors. 2019, US20190375752.

(54)   Nakagawa, M.; Yasuda, M.; Nagakawa, J.; Ogura, H. 388 Novel adenosine receptor antagonist improves parkinsonian symptoms and constipation. In *10th Alzheimer's disease/Parkinson's disease (AD/PD) Conference*; 2011.

(55)   Pogacic Kramp, V. List of drugs in development for neurodegenerative diseases: update October 2011. *Neurodegener. Dis.* **2012**, *9*, 210–283.

(56)   Härter, M.; Kalthof, B.; Delbeck, M.; Lustig, K.; Gerisch, M.; Schulz, S.; Kast, R.; Meibom, D.; Lindner, N. Novel non-xanthine antagonist of the A2B adenosine receptor: from HTS hit to lead structure. *Eur. J. Med. Chem.* **2019**, *163*, 763–778.

(57)   Merck KGaA, Darmstadt, Germany https://www.merckgroup.com/en/research/science-space/patents/WO20083878A1.html (accessed May 4, 2020).

(58)   Hess, S.; Muller, C. E.; Frobenius, W.; Reith, U.; Klotz, K. N.; Eger, K. 7-Deazaadenines bearing polar substituents: Structure - Activity relationships of new A1 and A3 adenosine receptor antagonists. *J. Med. Chem.* **2000**, *43*, 4636–4646.

(59)   Grahner, B.; Winiwarter, S.; Lanzner, W.; Müller, C. E. Synthesis and structure-activity relationships of deazaxanthines: analogs of potent A1- and A2-adenosine receptor antagonists. *J. Med. Chem.* **1994**, *37*, 1526–1534.

(60)   Bernat, V. J.; Cristina, E. T. New-4-(pyrrolopyrimidin-6-yl)benzenesulphonamide derivatives. 2003, EP20030745198.

(61)   Borrmann, T.; Hinz, S.; Bertarelli, D. C. G.; Li, W.; Florin, N. C.; Scheiff, A. B.; Müller, C. E. 1-Alkyl-8-(piperazine-1-sulfonyl)phenylxanthines: development and characterization of adenosine A2B receptor antagonists and a new radioligand with subnanomolar affinity and subtype specificity. *J. Med. Chem.* **2009**, *52*, 3994–4006.

(62)   Mcriner, A. J. GPCR hit identification via DNA-encoded libraries and optimization towards therapeutic libraries and optimization towards therapeutic agents for inflammation and oncology. In *7th RSC/SCI symposium on GPCRs in Medicinal Chemistry*; Verona, Italy, 2018.

(63)   McRiner, A. J.; Andersen, J. N.; Fouser, L. A.; Zhang, J.; Certel, K.; Cuozzo, J.; Chan, B.; Chandran, R.; Clark, M.; Gikunju, D.; et al. Abstract 4453: Novel, potent, and selective small-molecule inhibitors modulating immuno-oncology targets CD73, A2A/A2B adenosine receptors and CSF1R discovered via DNA-encoded library screening. In *Cancer Research*; American Association for Cancer Research (AACR), 2019; pp 4453–4453.

(64)   Galezowski, M.; Wegrzyn, P.; Bobowska, A.; Commandeur, C.; Dziedzic, K.; Nowogrodzki, M.; Obara, A.; Szeremeta-Spisak, J.; Dzielak, A.; Lozinska, I.; et al. Abstract 3770: Characterization of novel dual A2A/A2B adenosine receptor antagonists for cancer immunotherapy. In *Immunology*; American Association for Cancer Research, 2018; pp 3770–3770.

(65)   Galezowski, M.; Węgrzyn, P.; Bobowska, A.; Dziedzic, K.; Szeremeta-Spisak, J.; Nowogrodzki, M.; Satala, G.; Obara, A.; Lozinska-Raj, I.; Dudek, M.; et al. Abstract 4135: Novel dual A2A/A2B adenosine receptor antagonists for cancer immunotherapy: in vitro and in vivo characterization. In *Immunology*; American Association for Cancer Research, 2019; pp 4135–4135.

(66)   33rd Annual meeting & pre-conference programs of the society for immunotherapy of cancer (SITC 2018). *J. Immunother. Cancer* **2018**, *6*, 114.

(67)   Simone Tranches Dias, K.; Viegas, C. Multi-target directed drugs: a modern approach for design of new drugs for the treatment of Alzheimer's disease. *Curr. Neuropharmacol.* **2014**, *12*, 239–255.

(68)   Sever, R.; Brugge, J. S. Signal transduction in cancer. *Cold Spring Harb. Perspect. Med.* **2015**, *5*, a006098–a006098.

(69)   Ramsay, R. R.; Popovic-Nikolic, M. R.; Nikolic, K.; Uliassi, E.; Bolognesi, M. L. A perspective on multi-target drug discovery and design for complex diseases. *Clin. Transl. Med.* **2018**, *7*, 3.

(70)   Yan, L.; Müller, C. E. Preparation, properties, reactions, and adenosine receptor affinities of sulfophenylxanthine nitrophenyl esters: toward the development of sulfonic acid prodrugs with peroral bioavailability. *J. Med. Chem.* **2004**, *47*, 1031–1043.

(71)   Yan, L.; Bertarelli, D. C. G.; Hayallah, A. M.; Meyer, H.; Klotz, K.-N.; Müller, C. E. A new synthesis of sulfonamides by aminolysis of p -nitrophenylsulfonates yielding potent and selective adenosine A 2b receptor antagonists. *J. Med. Chem.* **2006**, *49*, 4384–4391.

(72)   Euler, H.; Kirfel, A.; Zech, A.; Hockemeyer, J.; Müller, C. E. Crystal structure of 6-amino-3-cyclopropyl-1-ethyl-1Hpyrimidine- 2,4-dione hydrate, C9H13N3O2 · H2O. *Zeitschrift für Krist. - New Cryst. Struct.* **2010**, *225*, 595–596.

(73)   Müller, C. E. General synthesis and properties of 1-monosubstituted xanthines. *Synthesis* **1993**, *1993*, 125–128.

(74)   Marx, D.; Wingen, L. M.; Schnakenburg, G.; Müller, C. E.; Scholz, M. S. Fast, efficient, and versatile synthesis of 6-amino-5-carboxamidouracils as precursors for 8-substituted xanthines. *Front. Chem.* **2019**, *7*.

(75)   Wodtke, R.; Hauser, C.; Ruiz-Gómez, G.; Jäckel, E.; Bauer, D.; Lohse, M.; Wong, A.; Pufe, J.; Ludwig, F.-A.; Fischer, S.; et al. Nε-acryloyllysine piperazides as irreversible inhibitors of transglutaminase 2: synthesis, structure–activity relationships, and pharmacokinetic profiling. *J. Med. Chem.* **2018**, *61*, 4528–4560.

(76)   Yin, J.; Buchwald, S. L. Palladium-catalyzed intermolecular coupling of aryl halides and amides. *Org. Lett.* **2000**, *2*, 1101–1104.

(77)   Konze, K. D.; Ma, A.; Li, F.; Barsyte-Lovejoy, D.; Parton, T.; MacNevin, C. J.; Liu, F.; Gao, C.; Huang, X.-P.; Kuznetsova, E.; et al. An orally bioavailable chemical probe of the lysine

methyltransferases EZH2 and EZH1. *ACS Chem. Biol.* **2013**, *8*, 1324–1334.

(78)   Umar, T.; Shalini, S.; Raza, M. K.; Gusain, S.; Kumar, J.; Seth, P.; Tiwari, M.; Hoda, N. A multifunctional therapeutic approach: Synthesis, biological evaluation, crystal structure and molecular docking of diversified 1H-pyrazolo[3,4-b]pyridine derivatives against Alzheimer's disease. *Eur. J. Med. Chem.* **2019**, *175*, 2–19.

(79)   Guglielmo, S.; Bertinaria, M.; Rolando, B.; Crosetti, M.; Fruttero, R.; Yardley, V.; Croft, S. L.; Gasco, A. A new series of amodiaquine analogues modified in the basic side chain with in vitro antileishmanial and antiplasmodial activity. *Eur. J. Med. Chem.* **2009**, *44*, 5071–5079.

(80)   Morriello, Gregori, J.; Wendt, Harvey, R.; Edmondson, S. Novel pyrrolidine derived beta 3 adrenergic receptor agonists. 2012, WO/2012/012314.

(81)   Bailey, J.; Bruton, G.; Huxley, A.; Johnstone, V.; Milner, P.; Orlek, B.; Stemp, G. A practical synthesis of differentially protected 4,4′-dipiperidinyl ethers: novel ligands of pharmaceutical interest. *Synlett* **2009**, *2009*, 1051–1054.

(82)   Borrmann, T.; Hinz, S.; Bertarelli, D. C. G.; Li, W.; Florin, N. C.; Scheiff, A. B.; Müller, C. E. 1-Alkyl-8-(piperazine-1-sulfonyl)phenylxanthines: development and characterization of adenosine A2B receptor antagonists and a new radioligand with subnanomolar affinity and subtype specificity. *J. Med. Chem.* **2009**, *52*, 3994–4006.

(83)   Jiang, J.; Seel, C. J.; Temirak, A.; Namasivayam, V.; Arridu, A.; Schabikowski, J.; Baqi, Y.; Hinz, S.; Hockemeyer, J.; Müller, C. E. A2B adenosine receptor antagonists with picomolar potency. *J. Med. Chem.* **2019**, *62*, 4032–4055.

(84)   Klotz, K. N.; Lohse, M. J.; Schwabe, U.; Cristalli, G.; Vittori, S.; Grifantini, M. 2-Chloro-N6-[3H]cyclopentyladenosine ([3HCCPA) —a high affinity agonist radioligand for A1 adenosine receptors. *N-S Arch. Pharmacol.* **1989**, *340*, 679–683.

(85)   Müller, C. E.; Maurinsh, J.; Sauer, R. Binding of [3H]MSX-2 (3-(3-hydroxypropyl)-7-methyl-

8-(m-methoxystyryl)-1-propargylxanthine) to rat striatal membranes—A new, selective antagonist radioligand for A2A adenosine receptors. *Eur. J. Pharm. Sci.* **2000**, *10*, 259–265.

(86)   Müller, C. E.; Diekmann, M.; Thorand, M.; Ozola, V. [3H]8-Ethyl-4-methyl-2-phenyl-(8R)-4,5,7,8-tetrahydro-1H-imidazo[2,1-i]-purin-5-one ([3H]PSB-11), a novel high-affinity antagonist radioligand for human A3 adenosine receptors. *Bioorg. Med. Chem. Lett.* **2002**, *12*, 501–503.

(87)   Alnouri, M. W.; Jepards, S.; Casari, A.; Schiedel, A. C.; Hinz, S.; Müller, C. E. Selectivity is species-dependent: Characterization of standard agonists and antagonists at human, rat, and mouse adenosine receptors. *Purinergic Signal.* **2015**, *11*, 389–407.

(88)   Lipinski, C. a; Lombardo, F.; Dominy, B. W.; Feeney, P. J. Experimental and computational approaches to estimate solubility and permeability in drug discovery and development settings. *Adv. Drug Deliv. Rev.* **2001**, *46*, *(1-3)*, 3–26.

(89)   Pharmacelsus Contract Research Organisation CRO https://www.pharmacelsus.com/ (accessed Sep 26, 2019).

(90)   Sanches, B. M. A.; Ferreira, E. I. Is prodrug design an approach to increase water solubility? *Int. J. Pharm.* **2019**, *568*, 118498.

4.2.8. Supporting information

Development of dual A$_{2A}$/A$_{2B}$ adenosine receptor antagonists

Ahmed Temirak, Christin Vielmuth, and Christa E. Müller*

PharmaCenter Bonn, Pharmaceutical Institute, Department of Pharmaceutical & Medicinal Chemistry, University of Bonn, An der Immenburg 4, D-53121 Bonn, Germany

Table of contents

***tert*-Butyl 4-(pyridin-3-yl)piperazine-1-carboxylate (25a).**[1,2] To a solution of 1-*tert*-butoxy-carbonylpiperazine (500 mg, 2.68 mmol, 1 eq) in 10 mL dry THF under argon atmosphere was added Cs_2CO_3 (2.62 g, 8.04 mmol, 3 eq). The resulting suspension was stirred for 5 min followed by the addition of 3-bromopyridine (0.27 mL, 2.68 mmol, 1 eq), Xantphos (93.2 mg, 0.16 mmol, 0.06 eq), and $Pd_2(dba)_3$ (49.1 mg, 0.05 mmol, 0.02 eq) in the given order. The reaction mixture was stirred at 70 °C for 20 h under Ar atmosphere. Upon completion of the reaction, the solvents were removed in vacuo, and the residue was dissolved in(ethyl) acetate and washed with 0.03 M sodium diethyldithiocarbamate (5 × 15 mL) and brine (1 × 15 mL). The organic phases were filtered through celite, dried over $MgSO_4$, and evaporated. The obtained yellowish white precipitate was further purified using column chromatography using eluent DCM/Cyclohexane (9.7:0.3). The desired product was obtained with a yield of 86% (730 mg) as yellowish solid. ^{1}H NMR (600 MHz, DMSO-d_6) δ 8.30 (d, J = 2.6 Hz, 1H, CH$_{pyridyl}$), 8.00 (d, J = 4.5 Hz, 1H, CH$_{pyridyl}$), 7.36-7.28 (m, 1H, CH$_{pyridyl}$), 7.21 (dd, J = 8.4, 4.5 Hz, 1H, CH$_{pyridyl}$), 3.50-3.40 (m, 4H, CH$_{piperazinyl}$), 3.20-3.09 (m, 4H, CH$_{piperazinyl}$), 1.41 (s, 9H). ^{13}C NMR (151 MHz, DMSO-d_6) δ 154, 146.7, 140.3, 138.3, 123.7, 122.4, 79.2, 47.8, 28.2. LC-MS positive mode (m/z): 263.8 $[M + H]^+$.

1-(Pyridin-3-yl)piperazine (25). To a solution of **25a** (1,7 g, 6,4 mmol) in 10 mL ethyl acetate, HCl (13 mL, 1M in ethyl acetate) was added and the reaction was stirred at rt for 3 h and monitored using TLC. Upon completion of the reaction, the solvents were removed in vacuo, the residue was dissolved in water and the pH of the solution was neutralized using few drops of 1N NaOH. Extraction of the aqueous phase was done using ethyl acetate and the organic phases were combined, dried over $MgSO_4$, and evaporated to afford **25** with a yield of 47% (490 mg) as yellowish oil. ^{1}H NMR (600 MHz, DMSO-d_6) δ 8.28 (ddd, J = 30.8, 19.4, 13.0 Hz, CH$_{pyridyl}$), 8.03-7.96 (m, 1H, CH$_{pyridyl}$), 7.36-7.24 (m, 1H, CH$_{pyridyl}$), 7.19 (tt, J = 26.2, 11.2 Hz, 1H, CH$_{pyridyl}$), 4.04 (d, J = 82.5 Hz, 1H, NH), 3.54-3.45 (m, 4H, CH$_{piperazinyl}$), 3.24-3.16 (m,

4H, CH$_{piperazinyl}$), 1.41 (s, 9H). ^{13}C NMR (151 MHz, DMSO-d_6) δ 161.2, 147.2, 146.7, 140.5, 140, 138.6, 137.9, 123.8, 123.8, 122.9, 122, 48.9, 48, 47.7, 44.6. LC-MS positive mode (m/z): 163.9 [M + H]$^+$.

***tert*-Butyl 4-(6-bromopyridin-3-yl)piperazine-1-carboxylate (27a).**[3] A mixture of 5-Bromo-2-chloropyridine (2.0 g, 10.4 mmol, 1 eq), *tert*-butyl piperazine-1-carboxylate (5.8 g, 31.2 mmol, 3 eq) and potassium carbonate (4.3 g, 31.2 mmol, 3 eq) were mixed in 10 mL N-Methyl-2-pyrrolidon (NMP) and heated at 120°C overnight. The reaction mixture was cooled down to rt and diluted with 100 mL dist. water. The formed precipitate was collected by filtration, washed with water and dried in vacuo. The desired product was obtained with a yield of 85% (2.9 g) as yellowish solid. ^{1}H NMR (600 MHz, DMSO-d_6) δ 8.16 (d, *J* = 2.5 Hz, 1H, CH$_{pyridyl}$), 7.68 (dd, *J* = 9.1, 2.6 Hz, 1H, CH$_{pyridyl}$), 6.81 (d, *J* = 9.1 Hz, 1H, CH$_{pyridyl}$), 3.45 (dd, *J* = 6.6, 3.7 Hz, 4H, CH$_{piperazinyl}$), 3.41-3.35 (m, 4H, CH$_{piperazinyl}$), 1.40 (s, 9H, CH$_{3(Boc)}$). ^{13}C NMR (151 MHz, DMSO-d_6) δ 157.6, 154.1, 147.9, 139.9, 109.4, 107.1, 79.2, 44.5, 28.2. LC-MS positive mode (m/z): 342.1 [M + H]$^+$.

1-(6-Bromopyridin-3-yl)piperazine (27). To a flask containing **27a** (500 mg, 1.47 mmol) dissolved in 10 mL DCM and cooled to 0 °C, HCl (5 mL, 1M in ethyl acetate) was added and the reaction was stirred at rt overnight. Aqueous solution of NaHCO$_3$ was added and the reaction mixture was extracted with ethyl acetate (3 x 10 mL). The organic layers were dried using MgSO$_4$ and concentrated. The desired product was obtained as a brown oil with a yield of 60% (220 mg). ^{1}H NMR (600 MHz, DMSO-d_6) δ 8.12 (dd, *J* = 12.0, 2.4 Hz, 1H, CH$_{pyridyl}$), 7.68-7.60 (m, 1H, CH$_{pyridyl}$), 6.78 (dd, *J* = 18.9, 9.2 Hz, 1H, CH$_{pyridyl}$), 3.28 (s, 4H, CH$_{piperazinyl}$), 2.75 (s, 4H, CH$_{piperazinyl}$). ^{13}C NMR (151 MHz, DMSO-d_6) δ 158.1, 147.9, 139.7, 109.1, 106.5, 45.8, 45.3. LC-MS positive mode (m/z): 241.9 [M + H]$^+$.

3-(Piperazin-1-yl)isonicotinonitrile (29).[4] A mixture of 2-chloro-3-pyridinecarbonitrile (2.0 g, 14.4 mmol, 1 eq) and piperazine (8.8 g, 101 mmol, 7 eq) were mixed in 30 mL anhydrous methanol and heated to 70°C overnight. The solvents were vaporized in vacuo and the formed residue was dissolved in ethyl acetate and extracted twice with water then with brine. The organic phases were combined, dried over $MgSO_4$, evaporated and were further purified using column chromatography using eluent DCM/Methanol (9:1) to afford the desired product **29** with a yield of 95% (2.58 g) as a white solid. LC-MS positive mode (m/z): 188.8 $[M + H]^+$.

5-(Piperazin-1-yl)picolinonitrile (30).[4] A mixture of 5-chloropicolinonitrile (1.0 g, 7.2 mmol, 1 eq) and piperazine (4.4 g, 51 mmol, 7 eq) were mixed in 15 mL anhydrous methanol and heated to 70°C overnight. The solvents were vaporized in vacuo and the formed residue was dissolved in ethyl acetate and extracted twice with water then with brine. The organic phases were combined, dried over $MgSO_4$, evaporated and was further purified using column chromatography using eluent DCM/Methanol (9:1) to afford the desired product **30** with a yield of 89% (1.22 g) as a white solid. LC-MS positive mode (m/z): 188.8 $[M + H]^+$.

5-Bromo-2-(piperazin-1-yl)pyrimidine (32). To a solution of 2-(piperazin-1-yl)pyrimidine (2,0 g, 12.17 mmol, 1 eq) in 15 mL 1N HCl at 0 °C, 12.17 mmol (0.624 mL, 1 eq) of bromine was added dropwise using a dropping funnel over 15 min. The reaction was stirred for 30 min at 0 °C, then the mixture was heated to 100 °C until dissipation of the red color had occurred. The reaction mixture was filtered, cooled, made alkaline with 50% NaOH, and extracted three times with diethyl ether. The organic phases were combined, dried over $MgSO_4$, evaporated and was used in the next step without further purification. The desired product was obtained with a yield of 76% (2.21 g) as a white solid. ^1H NMR (600 MHz, DMSO-d_6) δ 8.40 (s, 2H, CH$_{pyrimidine}$), 3.78-3.49 (m, 4H, CH$_{piperazinyl}$), 2.83-2.59 (m, 4H, CH$_{piperazinyl}$), 1.53-1.49 (q, J = 7.5 Hz, 2H, CH$_{2(propyl)}$), 0.90-0.81 (t, J = 7.4 Hz, 3H, CH$_{3(propyl)}$). ^{13}C NMR (151 MHz, DMSO-

d₆) δ ¹³C NMR (151 MHz, DMSO) δ ¹³C NMR (151 MHz, DMSO) δ 159.8, 158, 157.9, 105.1, 45.5, 45. LC-MS positive mode (m/z): 242.8 [M + H]⁺.

Ethyl 4-(thiophen-2-yl)piperazine-1-carboxylate (34a).[5] To a flask containing 2-mercapto-thiophene (2.0 g, 17.2 mmol) in 15 mL anhydrous toluene, 1-ethoxycarbonylpiperazine-2-carboxylic acid (2.7 g, 17.2 mmol) were added and the reaction mixture was refluxed at 120°C for 2.5 h. The solvents were vaporized and the formed residue was further purified using flash chromatography eluting with PE/DCM (7:3) to 100% DCM yielding the product with a yield of 52% (2.40 g) as yellowish oil. ¹H NMR (600 MHz, DMSO-*d₆*) δ 6.75 (d, J = 2.3 Hz, 2H, CH $_{thiophene}$), 6.20 (t, J = 2.6 Hz, 1H, CH$_{thiophene}$), 4.07-4.03 (m, 2H, CH$_{2(ester)}$), 3.51-3.47 (m, 4H, CH$_{piperazinyl}$), 3.04-3.01 (m, 4H, CH$_{piperazinyl}$), 1.20-1.17 (m, 3H, CH$_{3(ester)}$). ¹³C NMR (151 MHz, DMSO-*d₆*) δ 161.2, 158.7, 154.7, 126.4, 112.9, 106.2, 61, 51.2, 42.9, 14.7. LC-MS positive mode (m/z): 240.8 [M + H]⁺.

1-(Thiophen-2-yl)piperazine (34). To a flask containing **34a** (2.3 g, 13.7 mmol, 1 eq) in 50 mL methanol/water (4:1) mixture, (8.0 g, 110 mmol, 8 eq) of KOH was added at 0 °C portionwise over 5 min. The reaction mixture was stirred at 80 °C for 12 h. The solvents were vaporized, water was added and then extracted three times with ethyl acetate. The organic phases were combined, dried over MgSO₄, evaporated and were further purified using flash chromatography eluting with DCM/methanol (9.5:0.5) yielding the product with a yield of 51% (1.47 g) as brown oil. ¹H NMR (600 MHz, DMSO-*d₆*) δ 6.68 (t, J = 7.0 Hz, 1H, CH$_{thiophene}$), 6.25-6.21 (m, 1H, CH$_{thiophene}$), 6.11 (d, J = 2.3 Hz, 1H, CH$_{thiophene}$), 3.49 (t, J = 28.1 Hz, 4H, CH$_{piperazinyl}$), 2.97-2.91 (m, 4H, CH$_{piperazinyl}$). ¹³C NMR (151 MHz, DMSO-*d₆*) δ 158.8, 126.4, 112.9, 111.7, 106.2, 52.2, 50.9, 45.1. LC-MS positive mode (m/z): 168.9 [M + H]⁺.

2-(Piperazin-1-yl)thiazole (35). To a flask containing piperazine (2.1 g, 24.4 mmol, 2 eq) of dissolved in 15 mL *n*-butanol, (2.0 g, 12.2 mmol, 1 eq) of 2-bromothiazole were added and the

reaction mixture was heated at 120°C for 16 h. The solvents were vaporized and the formed residue was further purified using flash chromatography eluting with PE/DCM (7:3) to 100% DCM yielding compound **35** with a yield of 52% (2.40 g) as yellowish oil. ^{1}H NMR (600 MHz, DMSO-d_6) δ 7.14 (d, J = 3.5 Hz, 1H, CH$_{thiazole}$), 6.80 (t, J = 6.5 Hz, 1H, CH$_{thiazole}$), 3.20 (s, 4H, CH$_{piperazinyl}$), 2.78 (d, J = 4.4 Hz, 4H, CH$_{piperazinyl}$). ^{13}C NMR (151 MHz, DMSO-d_6) δ 172, 139.6, 107.7, 49.5, 44.9. LC-MS positive mode (m/z): 169.8 [M + H]$^+$.

tert-Butyl 4-(1-(pyridin-4-yl)ethyl)piperidine-1-carboxylate (36a). To a flask containing *N*-Boc piperazine (3.8 g, 20.6 mmol) dissolved in 15 mL of 1,2-dichloroethane (DCE), 4-acetylpyridine (2.0 g, 16.5 mmol) were added and the reaction was stirred at rt for 10 min. Ti(OPr)$_4$ (5.9 g, 20.6 mmol) and three molecular sieves were added and the reaction mixture was further stirred at rt under argon atmosphere for 2 h and at 60 °C for another 2 h. The mixture was then cooled to room temperature and Na(OAc)$_3$BH (4.9 g, 21.4 mmol) and 85 mL of DCE were added. The reaction mixture was furtherly stirred at rt under argon for 72h. Dropwise addition of NaHCO$_3$ solution to the reaction at 0°C precipitates a solid that was filtered through celite and the filtrate was extracted three times with DCM, dried over MgSO$_4$, and concentrated in vacuo producing a yellowish residue. This residue was further purified using flash chromatography using eluent DCM/Methanol (9.5:0.5) to afford the desired product with a yield of 35% (1.66 g) as a yellowish oil. ^{1}H NMR (600 MHz, DMSO-d_6) δ 8.50 (d, J = 5.9 Hz, 2H, CH$_{pyridyl}$), 7.30 (d, J = 5.9 Hz, 2H, CH$_{pyridyl}$), 3.49 (q, J = 6.8 Hz, 1H, CH$_{piperazinyl}$), 3.28 (d, J = 4.4 Hz, 4H, CH$_{piperazinyl}$), 2.37-2.29 (m, 2H, CH$_{piperazinyl}$), 2.28-2.21 (m, 2H, CH$_{piperazinyl}$), 1.36 (s, 9H, CH$_{3(Boc)}$), 1.26 (d, J = 6.2 Hz, 3H, CH$_3$ methyl). ^{13}C NMR (151 MHz, DMSO-d_6) δ 153.9, 152, 149.7, 122.9, 78.9, 62.5, 49.6, 28.2, 18. LC-MS positive mode (m/z): 292.0 [M + H]$^+$.

4-(1-(Piperidin-4-yl)ethyl)pyridine (36). To a flask containing **35a** (1.0 g, 3.4 mmol, 1 eq) dissolved in 3 mL DCM and stirred at 0°C, HCl (4N in dioxane, 5.2 mL, 6 eq) was added and then the reaction mixture was stirred at rt overnight. Aqueous solution of NaHCO$_3$ (15 mL) was added dropwise and the reaction mixture was extracted with ethyl acetate. The organic layers were dried using MgSO$_4$ and concentrated. The desired product was obtained as a colorless oil with a yield of 41% (270 mg). ^{1}H NMR (600 MHz, DMSO-d_6) δ 8.82 (dd, J = 36.0, 30.1 Hz, 1H, NH), 8.64 (d, J = 6.1 Hz,2H, CH$_{pyridyl}$), 7.55 (d, J = 6.2 Hz, 2H, CH$_{pyridyl}$), 3.74 (q, J = 6.7 Hz, 1H, CH$_{piperazinyl}$), 3.09 (t, J = 5.0 Hz, 4H, CH$_{piperazinyl}$), 2.69-2.60 (m, 2H, CH$_{piperazinyl}$), 2.57-2.52 (m, 2H, CH$_{piperazinyl}$), 1.32 (d, J = 6.8 Hz, 3H, CH$_{3(methyl)}$). ^{13}C NMR (151 MHz, DMSO-d_6) δ 158.9, 147.6, 123.9, 118.2, 116.2, 62.2, 46.4, 43.1. LC-MS positive mode (m/z): 191.8 [M + H]$^+$.

***tert*-Butyl 4-(pyridin-4-ylmethyl)piperidine-1-carboxylate (37a).**[6] To a flask containing sodium hydride (60% dispersion in mineral oil) (250 mg, 5.9 mmol) in 15 mL DMF, *N*-Boc piperazine (1.0 g, 5.37 mmol) was added at 0°C and the suspension was stirred for 15 min under argon. The reaction was allowed to warm to rt followed by the addition of (1.0 g, 5.37 mmol) of 2-(bromomethyl)pyridine hydrobromide. After 6 h, the reaction was quenched with cold water and extracted three times with ethyl acetate (3 x 10 mL). The organic phases were combined, dried over MgSO$_4$, evaporated and was further purified using flash chromatography using eluent DCM/Methanol (9.5:0.5) to afford the desired product with a yield of 94% (1.90 g) as orange oil. ^{1}H NMR (600 MHz, DMSO-d_6) δ 8.52-8.42 (m, 1H, CH$_{pyridyl}$), 7.80-7.69 (m, 1H, CH$_{pyridyl}$), 7.42 (d, J = 7.8 Hz, 1H, CH$_{pyridyl}$), 7.67 (t, J = 7.7 Hz, 1H, CH$_{pyridyl}$), 7.24 (ddd, J = 7.4, 4.9, 0.9 Hz, 1H, CH$_{pyridyl}$), 3.58 (s, 2H, CH$_2$), 3.31 (m, 4H, CH$_{piperazinyl}$), 2.38-2.29 (m, 4H, CH$_{piperazinyl}$), 1.37 (s, 9H, CH$_{3(Boc)}$). ^{13}C NMR (151 MHz, DMSO-d_6) δ 158.2, 153.9, 148.9, 136.6, 122.9, 122.3, 78.8, 63.8, 52.7, 44.2, 28.2. LC-MS positive mode (m/z): 278.0 [M + H]$^+$.

4-(Piperidin-4-ylmethyl)pyridine (37). To a flask containing **37a** (2.5 g, 9.0 mmol) and cooled to 0 °C, iodotrimethylsilane (TMIS) (2.7 g, 18.0 mmol) dissolved in 8.3 mL DCM was added dropwise over 5 min. After 15 min, brownish precipitate was formed followed by the addition of 15 mL methanol to quench the reaction. The reaction mixture was basified using 2mL 1N NaOH and extracted three times with (3 x 10 mL). The organic phases were combined, dried over $MgSO_4$, evaporated and were used in the next step without further purification. The desired product was obtained with a yield of 65% (1.0 g) as a brownish oil. ^{1}H NMR (600 MHz, DMSO-d_6) δ 8.47 (d, J = 4.8 Hz, 1H, CH$_{pyridyl}$), 7.73 (tt, J = 5.9, 2.9 Hz, 1H, CH$_{pyridyl}$), 7.41 (d, J = 7.8 Hz, 1H, CH$_{pyridyl}$), 7.23 (dt, J = 8.4, 4.5 Hz, 1H, CH$_{pyridyl}$), 3.55 (s, 2H, CH$_2$), 2.78 (s, 4H, CH$_{piperazinyl}$), 2.37 (d, J = 18.9 Hz, 4H, CH$_{piperazinyl}$). ^{13}C NMR (151 MHz, DMSO-d_6) δ 158.4, 149, 148.9, 136.6, 122.9, 122.3, 64.3, 53, 52.9, 44.9. LC-MS positive mode (m/z): 178.0 [M + H]$^+$.

6-Chloro-N-(piperidin-4-yl)pyridin-3-amine (39). To a flask containing *N*-Boc piperidone (775 mg, 3.89 mmol) and 5-amino-2-chloropyridine (500 mg, 3.89 mmol), dichloroethane (7 mL) and acetic acid (0.35 mL) were added. In 0 °C, sodium acetoxyborohydride (1.65 g, 7.78 mmol) was added and the reaction was stirred at room temperature for 3.5 hours. Upon completion of the reaction, 2N NaOH (10 mL) were added and the organic phase was extracted three times with water. The organic layers were dried using $MgSO_4$ and concentrated. The obtained brown oil was further purified using column chromatography DCM/Methanol (9.8:0.2). The desired product was obtained as white solid with a yield of 80% (650 mg). ^{1}H NMR (500 MHz, DMSO-d_6) δ 7.74 (d, J = 3.0 Hz, 1H, CH$_{pyridyl}$), 7.12 (d, J = 8.7 Hz, 1H, CH$_{pyridyl}$), 7.02 (dd, J = 8.7, 3.1 Hz, 1H, CH$_{pyridyl}$), 5.93 (d, J = 8.2 Hz, 1H, CH$_{piperidyl}$), 3.84 (d, J = 13.3 Hz, 2H, CH$_{piperidyl}$), 3.47-3.33 (m, 1H, NH), 2.90 (s, 2H, CH$_{piperidyl}$), 1.90-1.78 (m, 2H, CH$_{piperidyl}$), 1.38 (d, J = 7.6 Hz, 9H, CH$_{3(Boc)}$), 1.28-1.14 (m, 2H, CH$_{piperidyl}$). ^{13}C NMR (126

MHz, DMSO-*d₆*) δ 154.1, 143.5, 136.1, 134.3, 124, 122.3, 78.8, 48.5, 31.3, 28.2. LC-MS positive mode (m/z): 312.0 [M + H]⁺.

6-Bromo-*N*-(piperidin-4-yl)pyridin-3-amine (40a). To a flask containing *N*-Boc piperidone (1.15 g, 5.78 mmol) of and 5-amino-2-bromopyridine (1.0 g, 5.78 mmol), dichloroethane (10 mL) and glacial acetic acid (0.52 mL) were added. In 0 ºC, sodium acetoxyborohydride (2.45 g, 11,56 mmol) was added and the reaction was stirred at room temperature for 5 hours. Upon completion of the reaction, NaOH (2N, 20 mL) was added and it was extracted three times with ethyl acetate (3 x 15 mL). The organic layers were dried using MgSO₄ and concentrated. The obtained brown oil was further purified using column chromatography DCM/Methanol (9.8:0.2). The desired product was obtained as white solid with a yield of 85% (2.0 g). ¹H NMR (500 MHz, DMSO-*d₆*) δ 7.74 (d, *J* = 3.1 Hz, 1H, CH_pyridyl), 7.23 (d, *J* = 8.7 Hz, 1H, CH_pyridyl), 6.94 (dd, *J* = 8.7, 3.1 Hz, 1H, CH_pyridyl), 5.95 (d, *J* = 8.1 Hz, 1H, CH_piperidyl), 3.84 (d, *J* = 13.3 Hz, 2H, CH_{2(propyl)}), 3.46-3.34 (m, 1H, NH), 2.90 (s, 2H, CH_piperidyl), 1.89-1.80 (m, 2H, CH_piperidyl), 1.39 (s, 9H, CH_{3(Boc)}), 1.26-1.13 (m, 2H, CH_piperidyl). ¹³C NMR (126 MHz, DMSO-*d₆*) δ 154.1, 143.8, 136.1, 135.1, 127.6, 127.5, 125.7, 123.9, 122.3, 78.8, 65.8, 48.5, 31.3, 28.2. LC-MS positive mode (m/z): 356.2 [M + H]⁺.

***tert*-Butyl 4-(pyridin-4-yloxy)piperidine-1-carboxylate (41a).**[7] To a flask containing sodium hydride (600 mg, 14.88 mmol, 3 eq) suspended in 15 mL anhydrous DMSO under argon atmosphere, 4-bromopyridine hydrochloride (1.16 g, 5.96 mmol, 1.18 eq) suspended in 5 mL DMSO, was added slowly over 45 min. The reaction was then stirred for 10 min, 1-boc-4-hydroxypiperidine (1.0 g, 4.96 mmol, 1 eq) dissolved in 5 mL DMSO was added over 15 min and the reaction mixture was stirred at r.t. overnight. Sat. NaHCO₃ solution (20 mL) was added slowly and the reaction was stirred for 20 min. The desired product was collected by filtration as brown solid with a yield of 90% (0.8 g). ¹H NMR (500 MHz, DMSO-*d₆*) δ 8.35 (d, *J* = 6.2

Hz, 2H, CH$_{pyridyl}$), 6.97 (d, J = 6.2 Hz, 2H, CH$_{pyridyl}$), 4.80-4.59 (m, 1H, CH$_{piperidyl}$), 3.66 (dt, J = 6.2 Hz, 2H, CH$_{piperidyl}$), 3.17 (s, 2H, CH$_{piperidyl}$), 1.97-1.85 (m, 2H, CH$_{piperidyl}$), 1.56-1.46 (m, 2H, CH$_{piperidyl}$), 1.38 (d, J = 11.9 Hz, 9H, CH$_{3(Boc)}$). ^{13}C NMR (126 MHz, DMSO-d_6) δ 163.1, 154.1, 151.2, 111.3, 79, 72.1, 30.2, 28.2. LC-MS positive mode (m/z): 278.9 [M + H]$^+$.

4-(Piperidin-4-yloxy)pyridine (41). To a flask containing **41a** (1.2 g, 3.60 mmol) dissolved in 5 ml DCM, TFA (2 mL) was added at 0 °C, then the reaction mixture was stirred at rt for 3 h. Aqueous solution of NaHCO$_3$ was added dropwise and the reaction mixture was extracted with ethyl acetate (3 x 10 mL). The organic layers were dried using MgSO$_4$ and concentrated. The desired product was obtained as a colorless oil with a yield of 68% (450 mg). ^{1}H NMR (500 MHz, DMSO-d_6) δ 8.40 (d, J = 5.9 Hz, 2H, CH$_{pyridyl}$), 7.03 (d, J = 6.0 Hz, 2H, CH$_{pyridyl}$), 4.74-4.69 (m, 1H, CH$_{piperidyl}$), 3.45 (m, 2H, CH$_{piperidyl}$), 2.85 (m, 2H, CH$_{piperidyl}$), 1.84-1.79 (m, 2H, CH$_{piperidyl}$), 1.52-1.45 (m, 2H, CH$_{piperidyl}$). ^{13}C NMR (126 MHz, DMSO-d_6) δ 162.8, 154, 151.4, 118, 111.3, 79.2, 72.2, 30.3. LC-MS positive mode (m/z): 179.0 [M + H]$^+$.

_t_ert-Butyl 4-(4-bromophenyl)-4-hydroxypiperidine-1-carboxylate (42a). To a flask containing 1,4-dibromobenzene (1.0 g, 4.24 mmol) in 20 mL anhydrous THF, (102 mg, 4.24 mmol) of magnesium and a catalytic amount of iodine crystals were added and the reaction was refluxed at 80 °C for 4 hours. *N*-Boc piperidone (704 mg, 3.54 mmol) was further added and the reaction mixture was refluxed at 80°C for 5 h. After the reaction has finished, we added 5 mL 1N HCl and the THF was vaporized. The formed residue was washed with water, collected with filtration yielding the desired product as a yellowish solid with a yield of 55% (680 mg). LC-MS positive mode (m/z): 356.2 [M + H]$^+$.

4-(4-Bromophenyl)piperidin-4-ol (42). To a flask containing **42a** (340 mg, 0.95 mmol) dissolved in 5 mL of DCM and cooled to 0 °C, HCl (1N in ethyl acetate, 2.5 mL) was added and the reaction was stirred at rt for 3h. Aqueous solution of NaHCO$_3$ was added and the

reaction mixture was extracted with ethyl acetate. The organic layers were dried using MgSO₄ and concentrated. The desired product was obtained as a white solid with a yield of 65% (150 mg). LC-MS positive mode (m/z): 256.3 [M + H]⁺.

tert-Butyl 4-hydroxy-4-(pyridin-3-yl)piperidine-1-carboxylate (43a). To a flask containing 3-bromopyridine (2.0 g, 12.65 mmol) in dry toluene (40 mL) at -78 °C, n-butyllithium (2.5M in hexane, 10.5 mL, 25.30 mmol) was added dropwise and the reaction was stirred for 1 h. A solution of *N*-Boc-piperidone (2.52 g, 12.65 mmol) in dry toluene (10 ml) was added dropwise and the mixture was stirred at -78 °C for 2 h. Upon reaction completion, sat. solution of ammonium chloride (20 mL) was added dropwise and the reaction mixture was warmed to rt and subsequently extracted with(ethyl) acetate (3 x 10 mL). The organic layers were dried using anhydrous Mg₂SO₄ and evaporated obtaining a brownish residue that was further purified with flash chromatography using the eluent system DCM/methanol (9.2:0.8). A yellowish precipitate was obtained in a yield of 40% (1.41 g). ¹H NMR (600 MHz, DMSO-*d₆*) δ 8.69 (d, *J* = 2.2 Hz, 1H, CH_pyridyl), 8.43 (dd, *J* = 4.7, 1.5 Hz, 1H, CH_pyridyl), 7.90-7.73 (m, 1H, CH_pyridyl), 7.32 (dd, *J* = 7.9, 4.7 Hz, 1H, CH_pyridyl), 5.25 (s, 1H, OH), 3.84 (s, 2H, 2H, CH_piperidyl), 3.13 (s, 2H, CH_piperidyl), 1.82 (td, *J* = 13.0, 4.8 Hz, 2H, CH_piperidyl), 1.61 (d, *J* = 12.2 Hz, 2H, CH_piperidyl), 1.41 (s, 9H, CH₃(Boc)). ¹³C NMR (151 MHz, DMSO-*d₆*) δ 153.9, 149.3, 148, 147.7, 140.3, 138.1, 134.6, 133.7, 124.3, 70.1, 41.3, 31.8, 18.6, 14. LC-MS positive mode (m/z): 278.9 [M + H]⁺.

4-(Pyridin-3-yl)piperidin-4-ol (43). To a flask containing **43a** (1.0 g, 3.59 mmol) and cooled to 0 °C, HCl (1M in ethyl acetate, 10.8 mL, 10.77 mmol) was added and the reaction was stirred at rt for 16 h. Upon completion of the reaction, aqueous solution of NaHCO₃ (10 mL) was added and the reaction mixture was subsequently extracted with ethyl acetate (3 x 10 mL). The organic layers were dried using MgSO₄, concentrated and the obtained oily residue was further

purified using column chromatography using the eluent system DCM/methanol (7:3). A brownish oil was obtained in a yield of 40% (250 mg). ^{1}H NMR (600 MHz, DMSO-*d$_6$*) δ 8.16-8.10 (m, 1H, CH$_{pyridyl}$), 8.03-7.98 (m, 1H, CH$_{pyridyl}$), 7.21-7.11 (m, 2H, CH$_{pyridyl}$), 5.23 (s, 1H, OH), 3.82 (s, 2H, 2H, CH$_{piperidyl}$), 3.20 (s, 2H, CH$_{piperidyl}$), 1.85 (d, *J* = 7.8 Hz, 2H, CH$_{piperidyl}$), 1.59 (d, *J* = 11.7 Hz, 2H, CH$_{piperidyl}$). ^{13}C NMR (151 MHz, DMSO-*d$_6$*) δ 153.9, 149.3, 148, 140.3, 138.1, 134.6, 133.7, 124.3, 122.3, 70.1, 41.3, 31.8. LC-MS positive mode (m/z): [M + H]$^+$. LC-MS positive mode (m/z): 179.1 [M + H]$^+$.

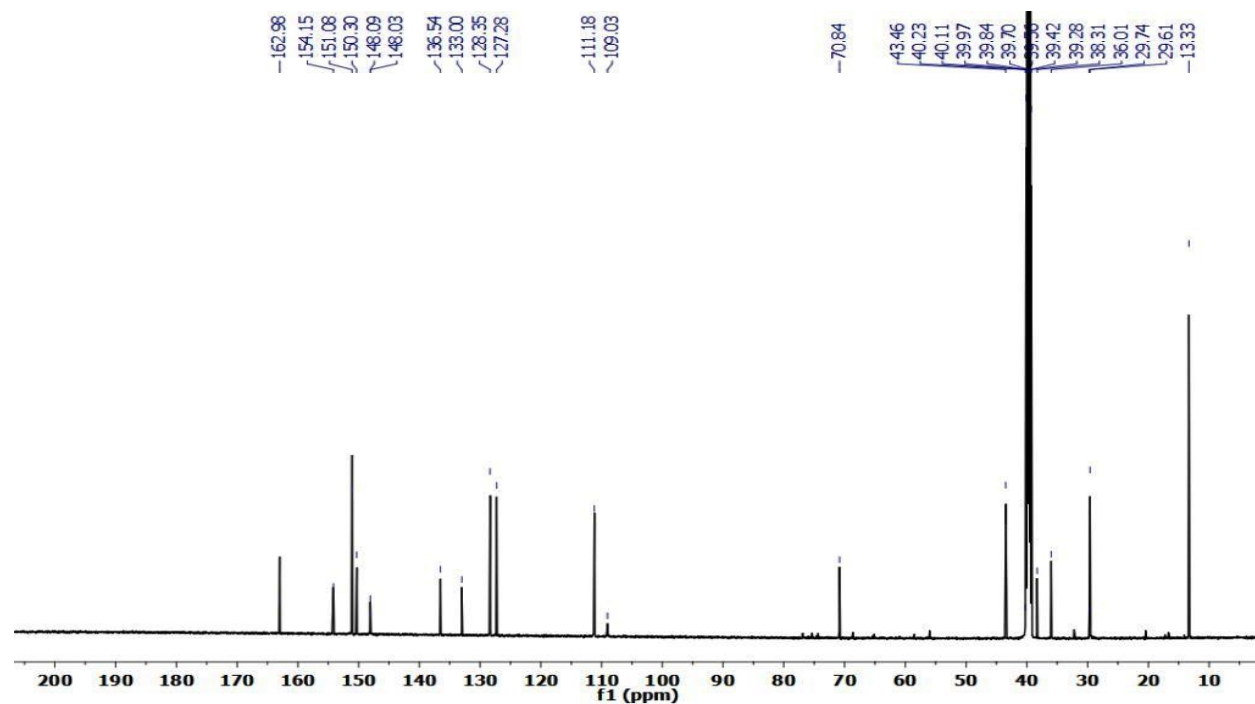¹HNMR
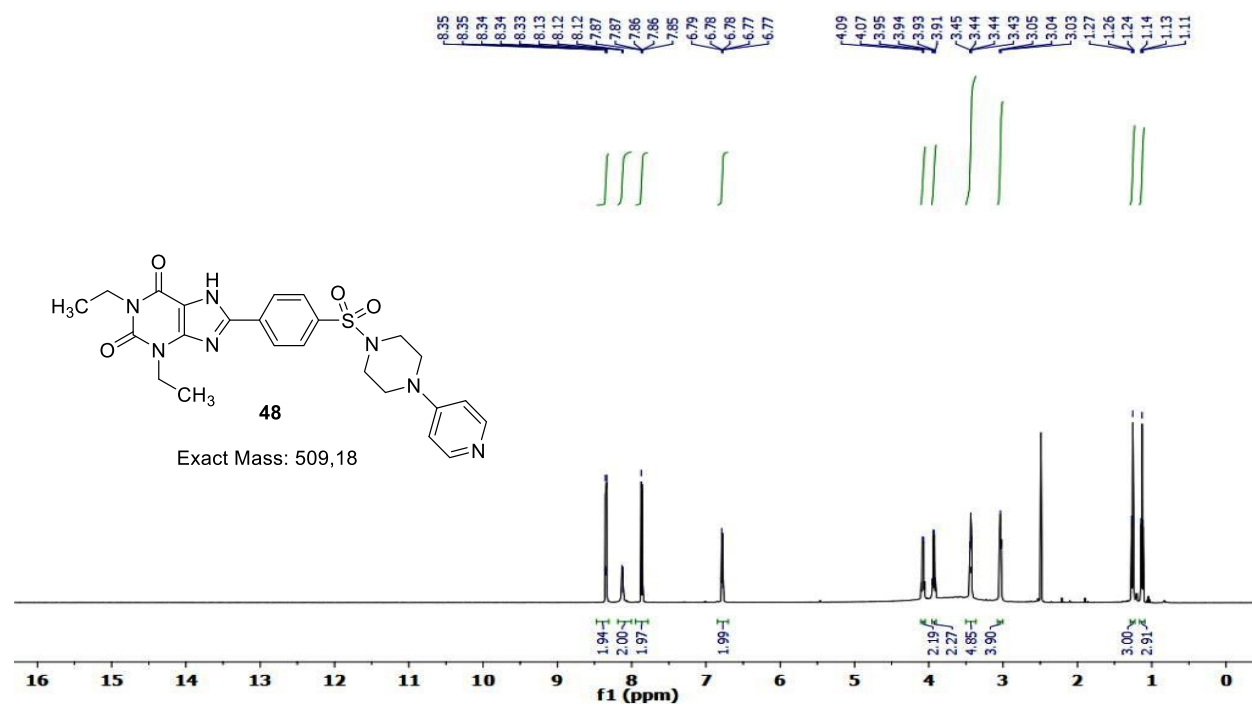
¹³CNMR
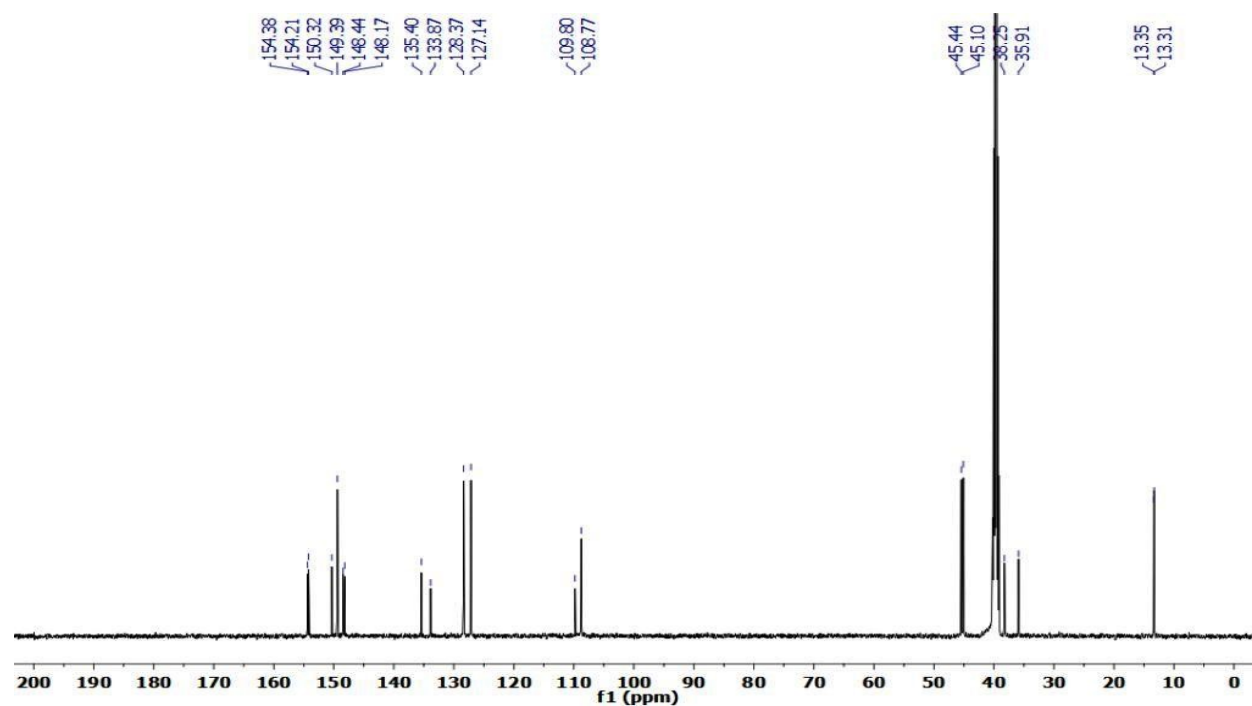
Figure S1. ¹H (600 MHz) and ¹³C (151 MHz) spectra (DMSO-d_6) of 1,3-diethyl-8-(4-((4-(pyridin-4-yl)piperazin-1-yl)sulfonyl)phenyl)-3,7-dihydro-1*H*-purine-2,6-dione (**48**)
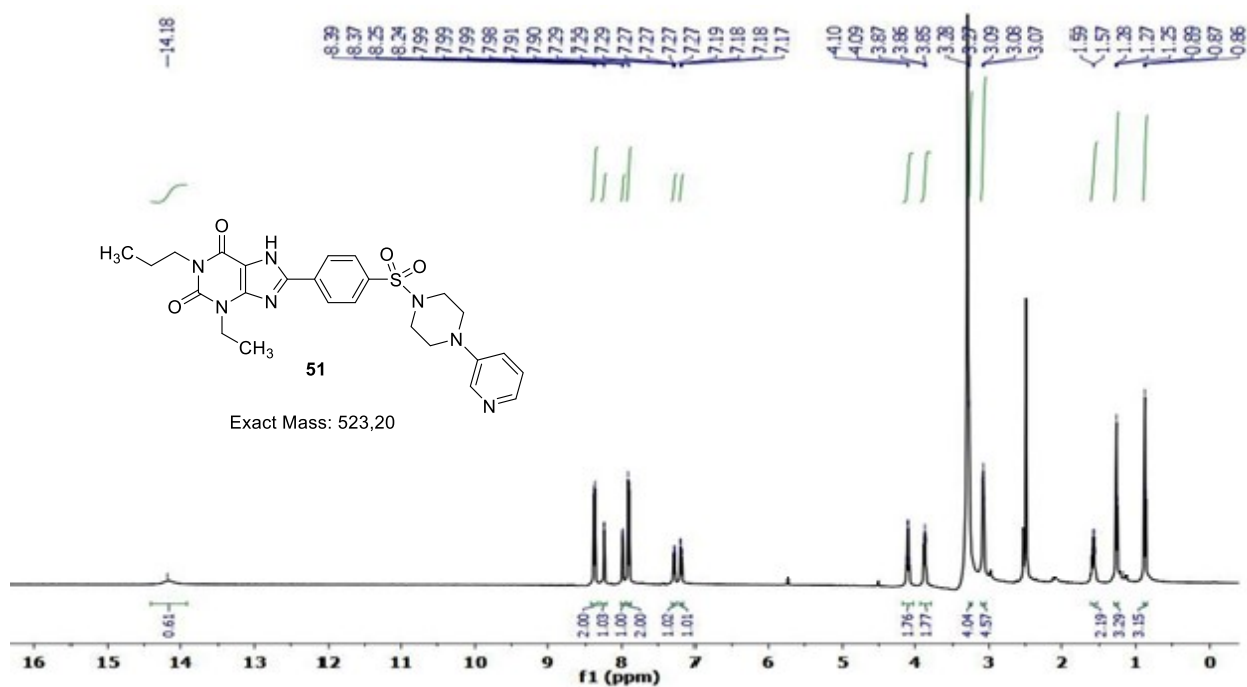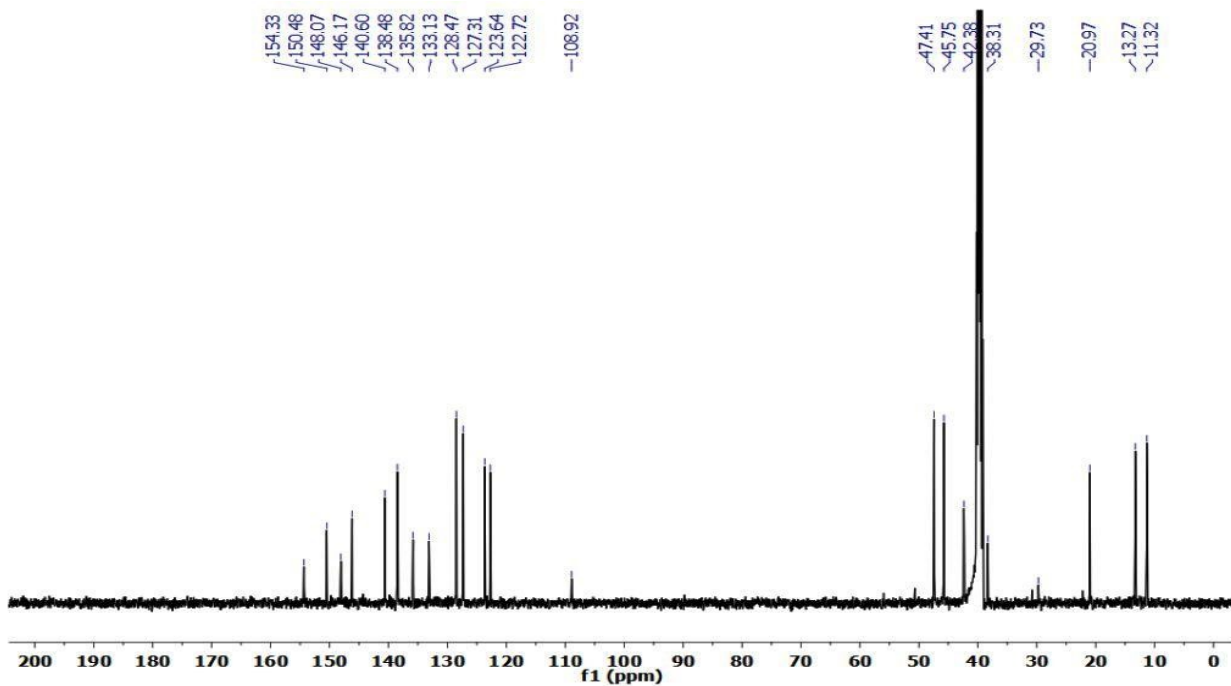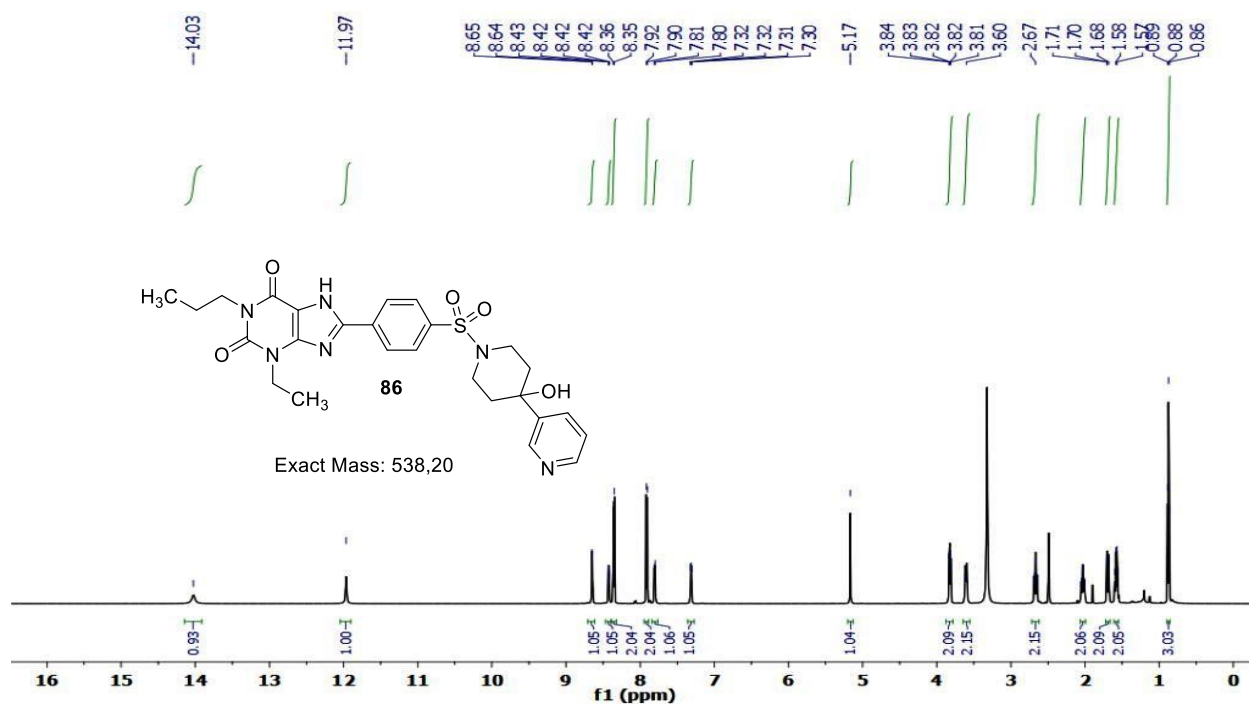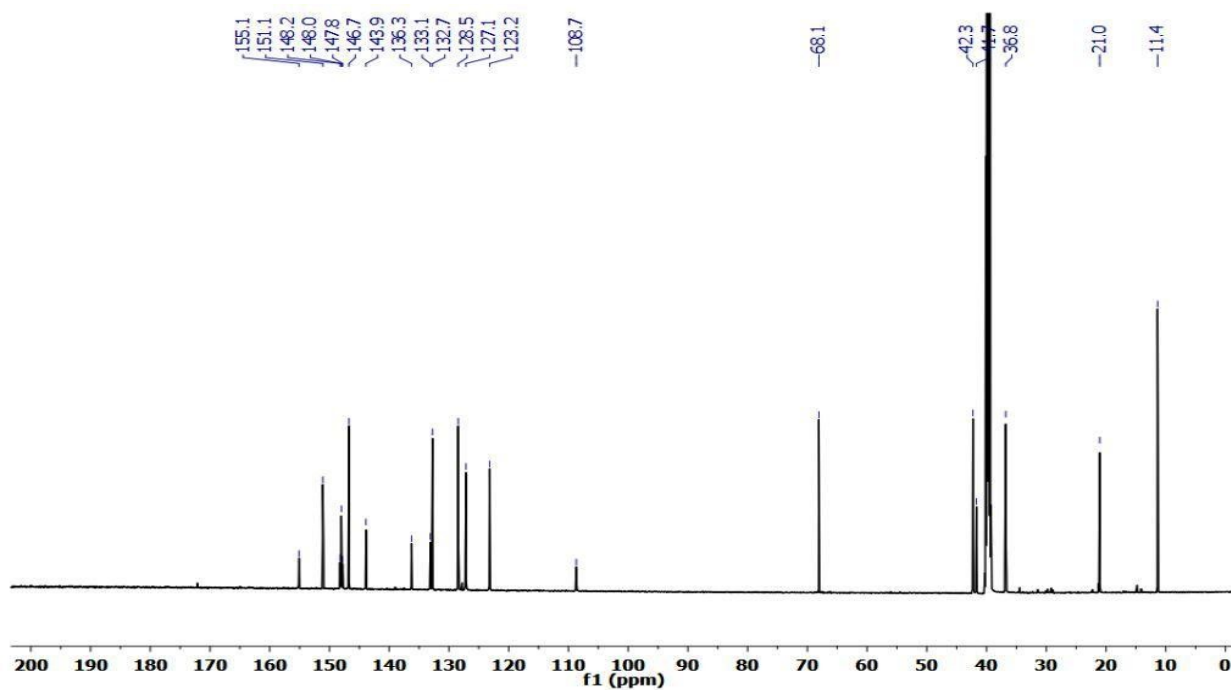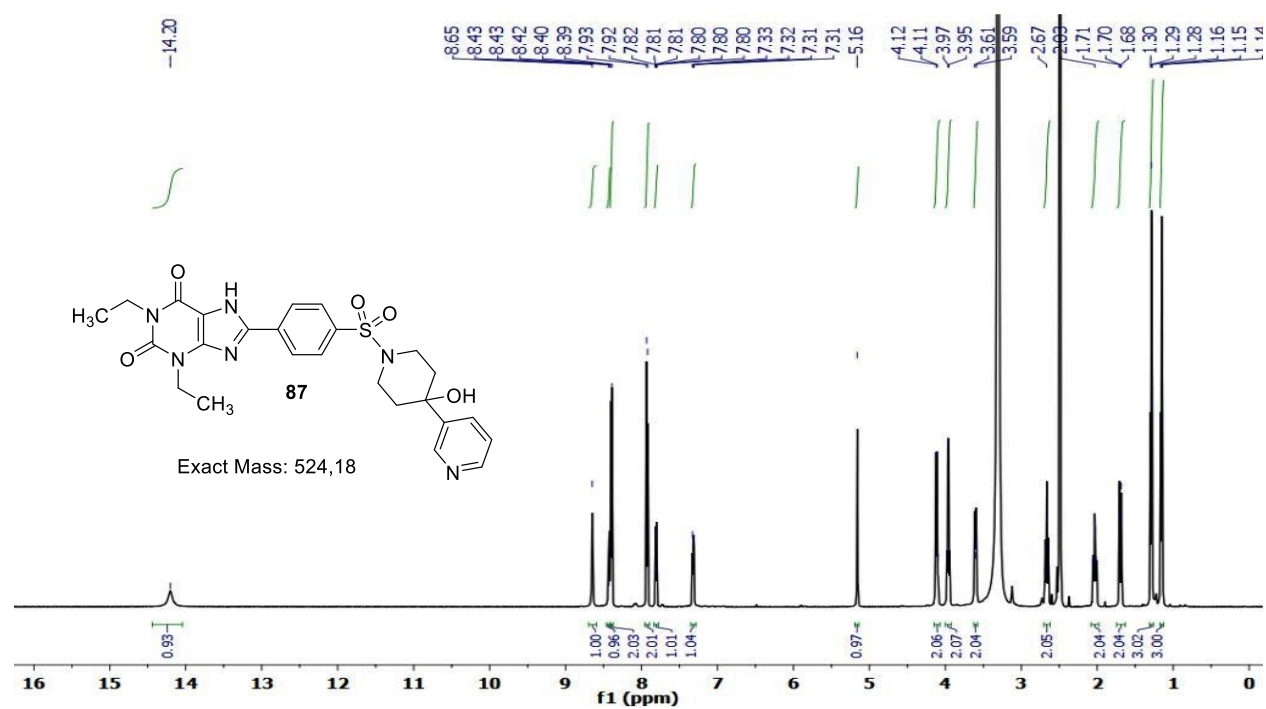
¹HNMR

¹³CNMR

Figure S2. ¹H (600 MHz) and ¹³C (151 MHz) spectra (DMSO-d_6) of 3-ethyl-1-propyl-8-(4-((4-(pyridin-3-yl)piperazin-1-yl)sulfonyl)phenyl)-3,7-dihydro-1*H*-purine-2,6-dione (**51**)

¹HNMR
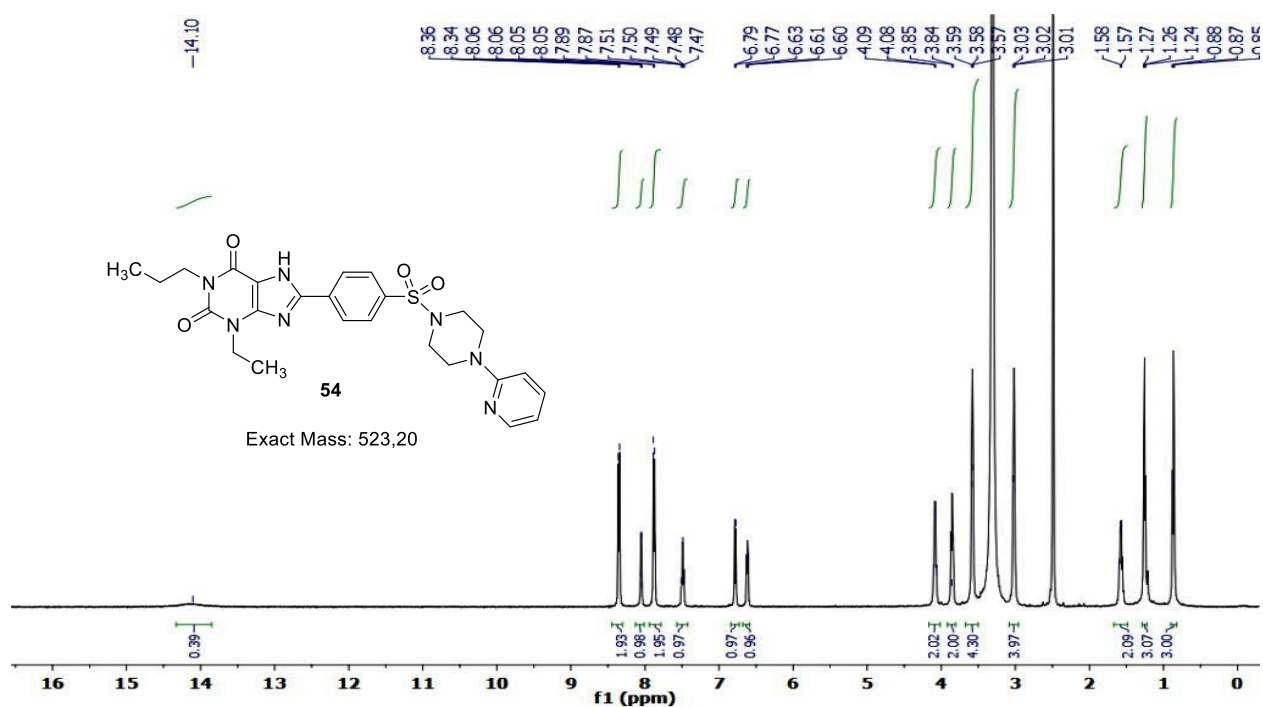
¹³CNMR
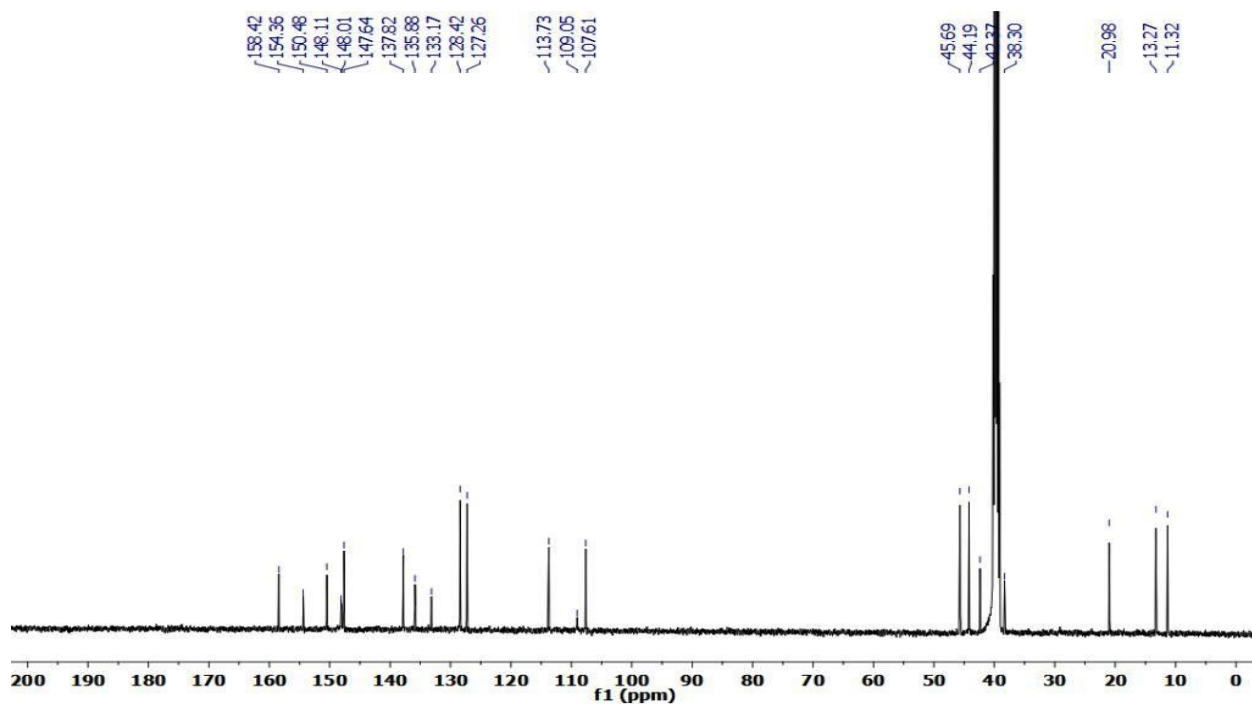
Figure S3. ¹H (600 MHz) and ¹³C (151 MHz) spectra (DMSO-d_6) of 3-ethyl-1-propyl-8-(4-((4-(pyridin-2-yl)piperazin-1-yl)sulfonyl)phenyl)-3,7-dihydro-1*H*-purine-2,6-dione (**54**)
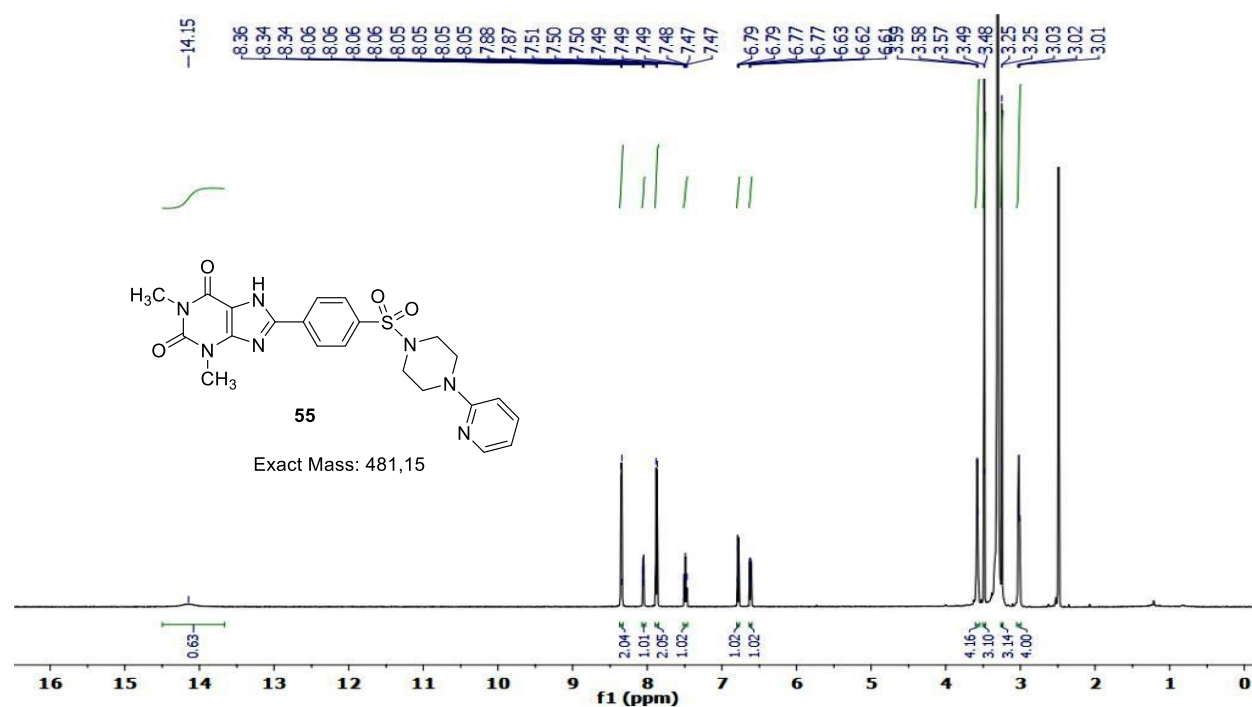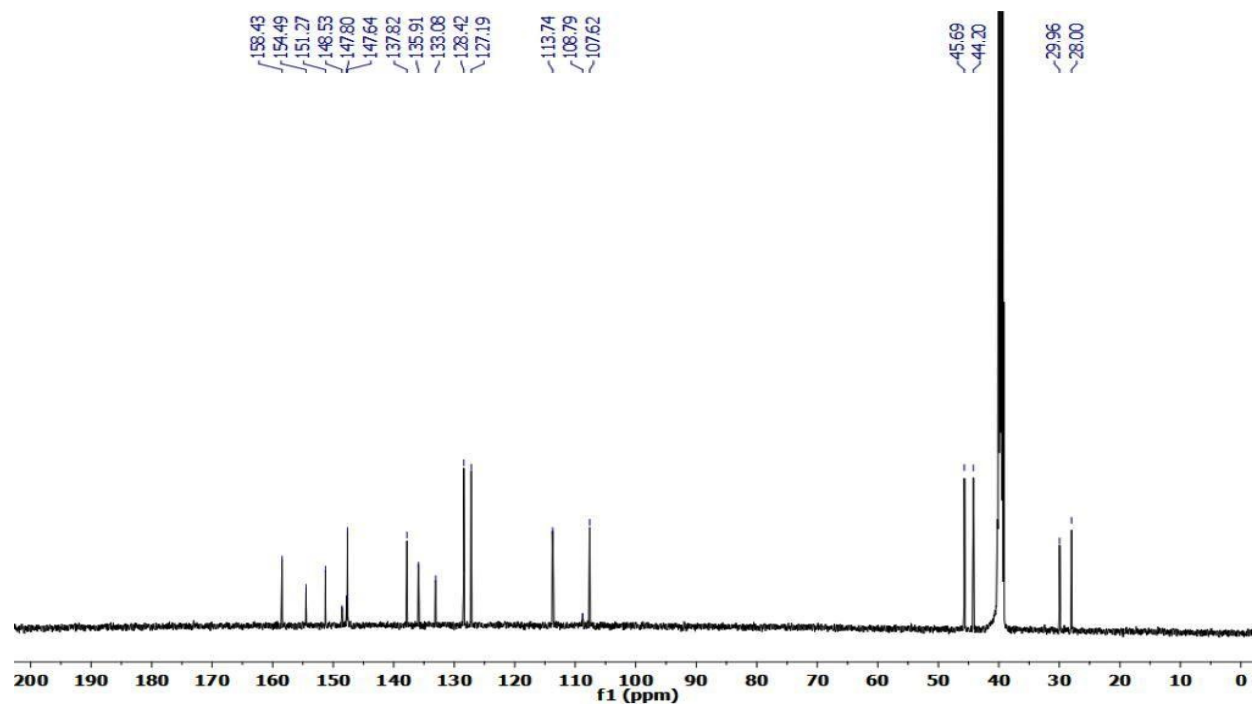
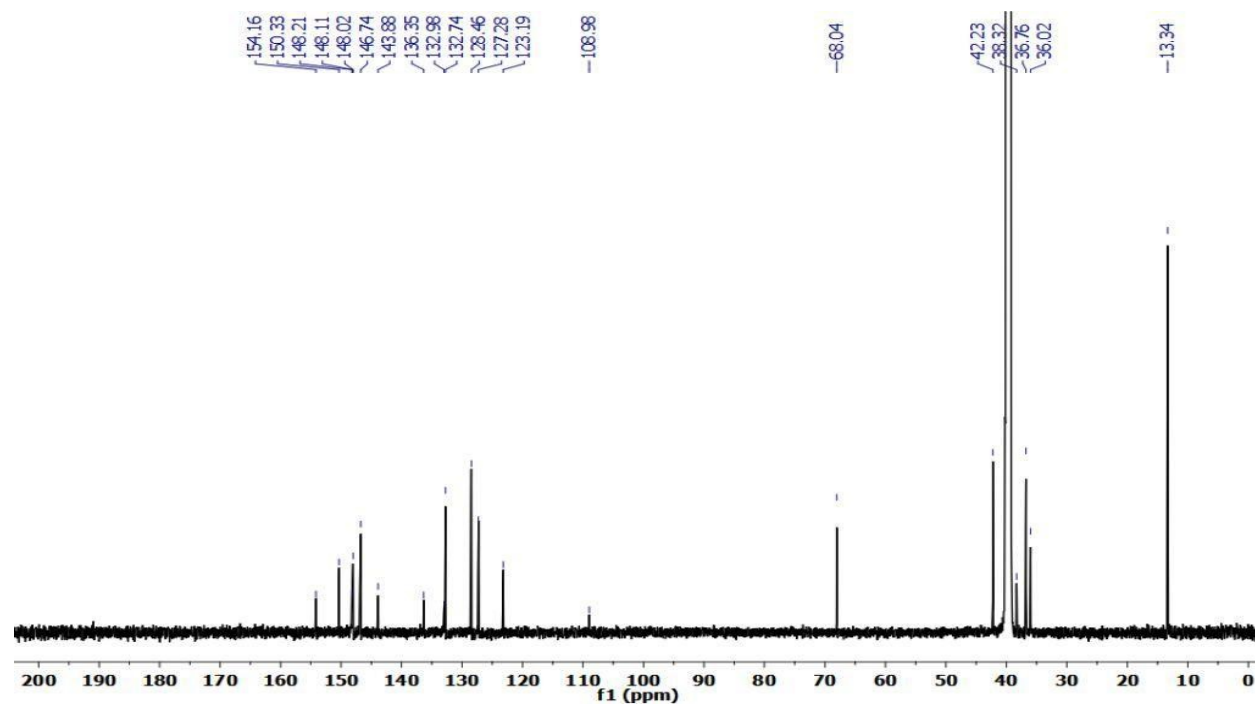¹HNMR

¹³CNMR

Figure S4. ¹H (600 MHz) and ¹³C (151 MHz) spectra (DMSO-*d*₆) of 1,3-dimethyl-8-(4-((4-(pyridin-2-yl)piperazin-1-yl)sulfonyl)phenyl)-3,7-dihydro-1*H*-purine-2,6-dione (**55**)

¹HNMR
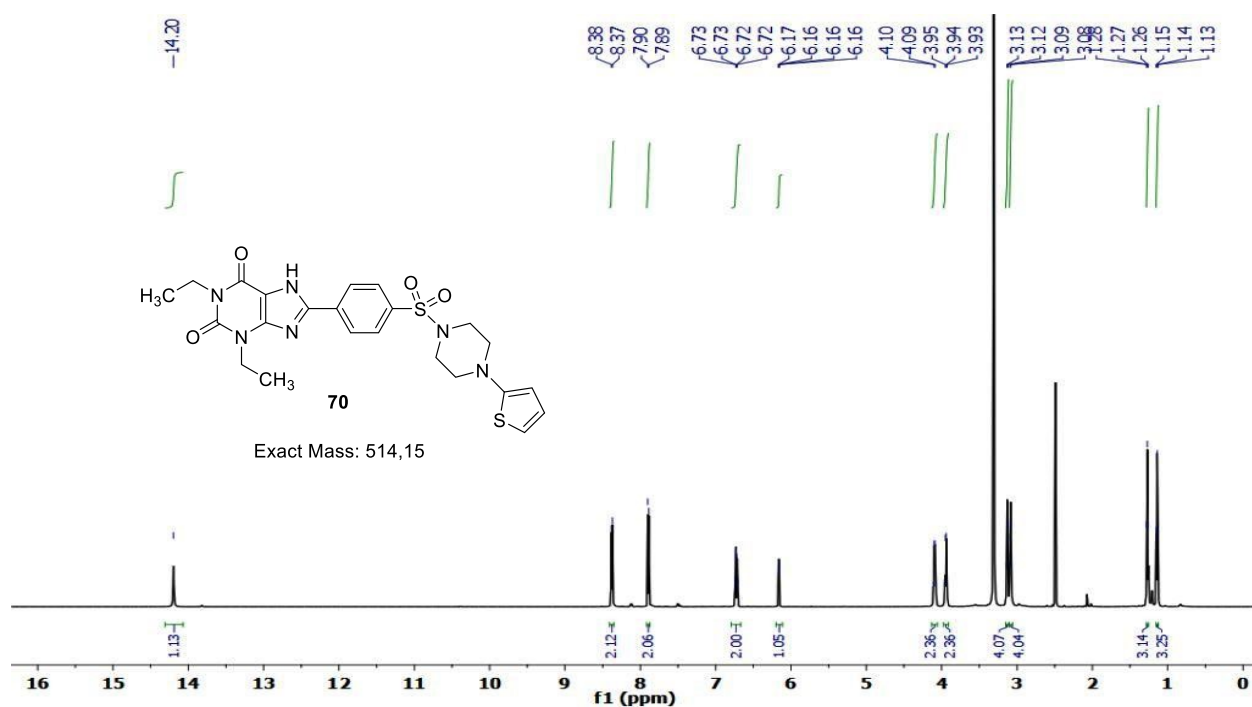
¹³CNMR
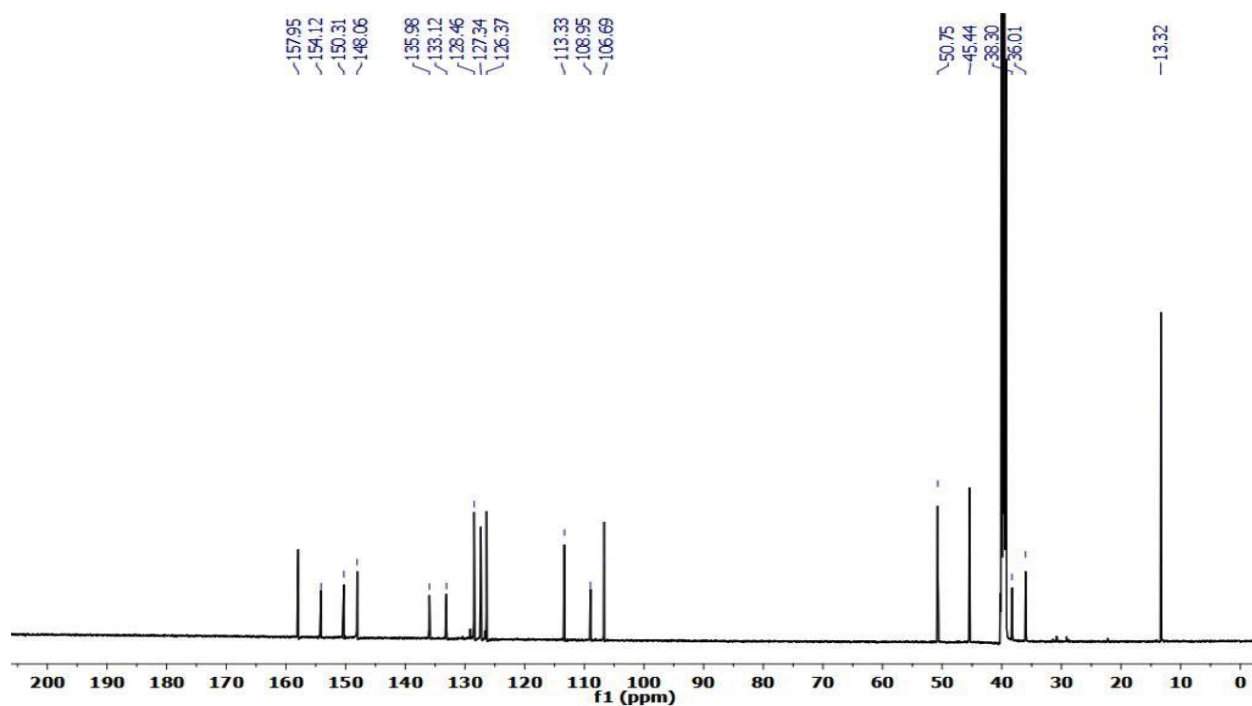
Figure S5. ¹H (600 MHz) and ¹³C (151 MHz) spectra (DMSO-d_6) of 1,3-diethyl-8-(4-((4-(thiophen-2-yl)piperazin-1-yl)sulfonyl)phenyl)-3,7-dihydro-1*H*-purine-2,6-dione (**70**)
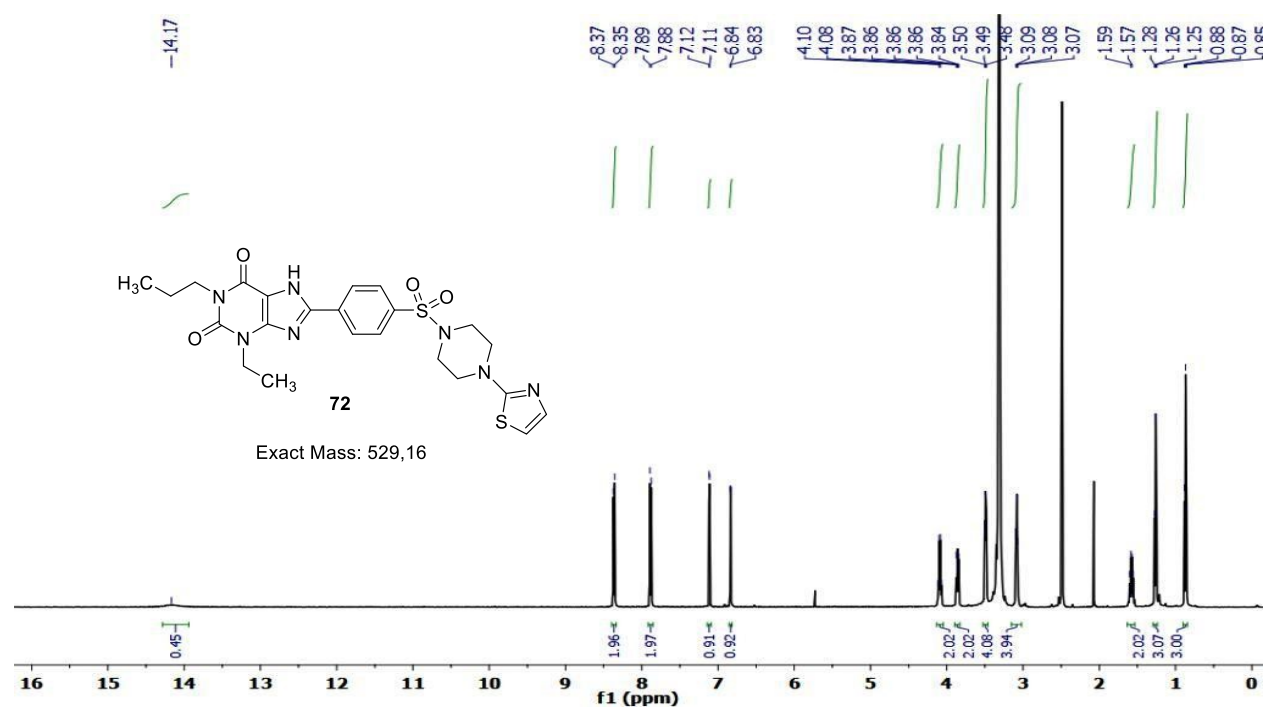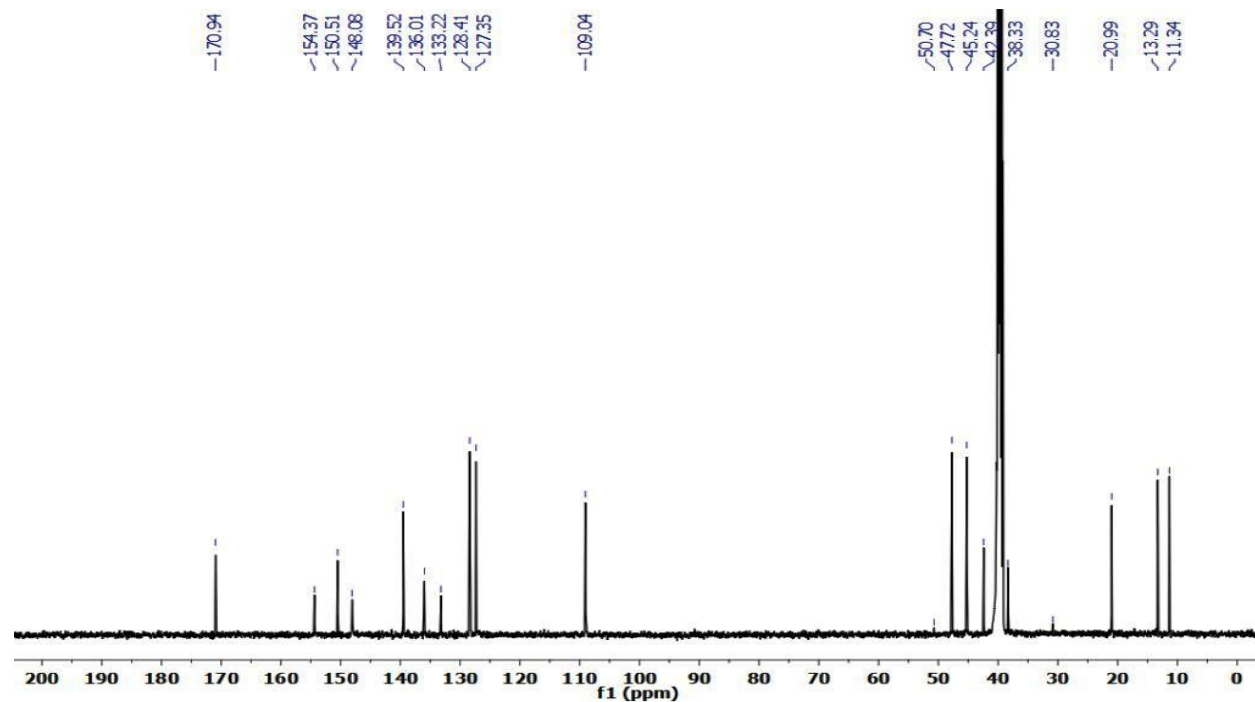
^{1}HNMR

^{13}CNMR

Figure S6. ^{1}H (600 MHz) and ^{13}C (151 MHz) spectra (DMSO-d_6) of 3-ethyl-1-propyl-8-(4-((4-(thiazol-2-yl)piperazin-1-yl)sulfonyl)phenyl)-3,7-dihydro-1H-purine-2,6-dione (**72**)

¹HNMR
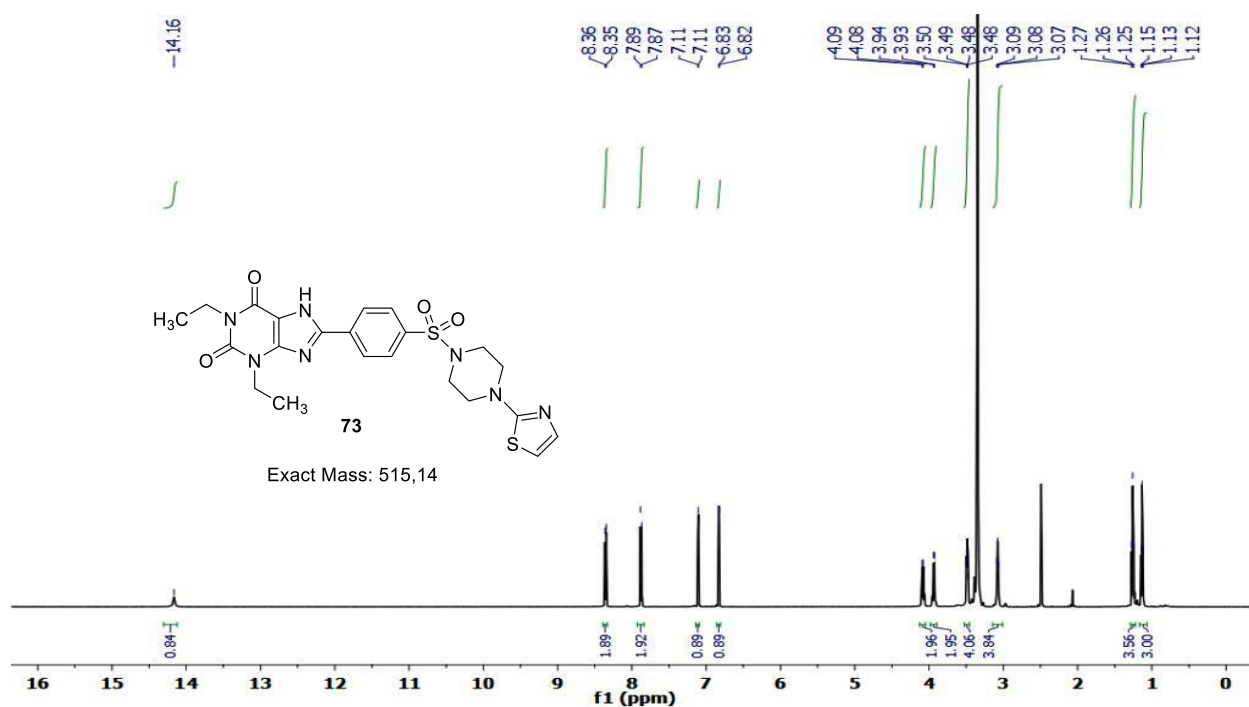
¹³CNMR
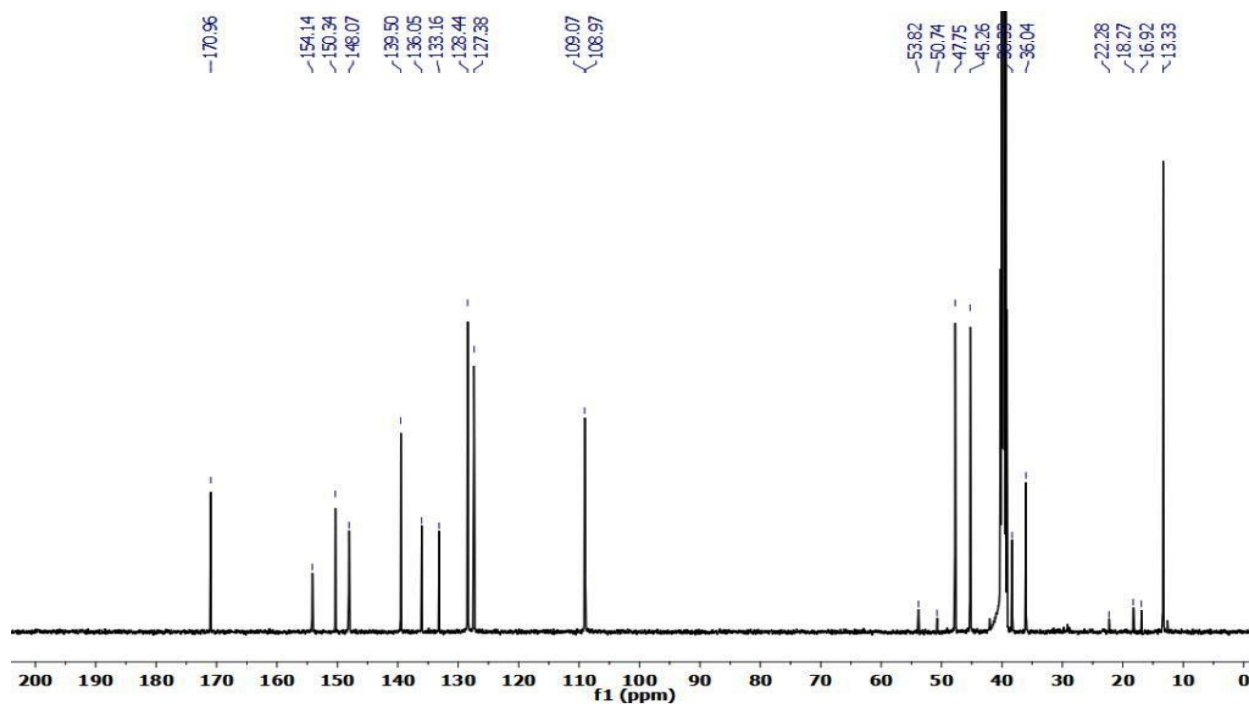
Figure S7. ¹H (600 MHz) and ¹³C (151 MHz) spectra (DMSO-d_6) of 1,3-diethyl-8-(4-((4-(thiazol-2-yl)piperazin-1-yl)sulfonyl)phenyl)-3,7-dihydro-1*H*-purine-2,6-dione (**73**)
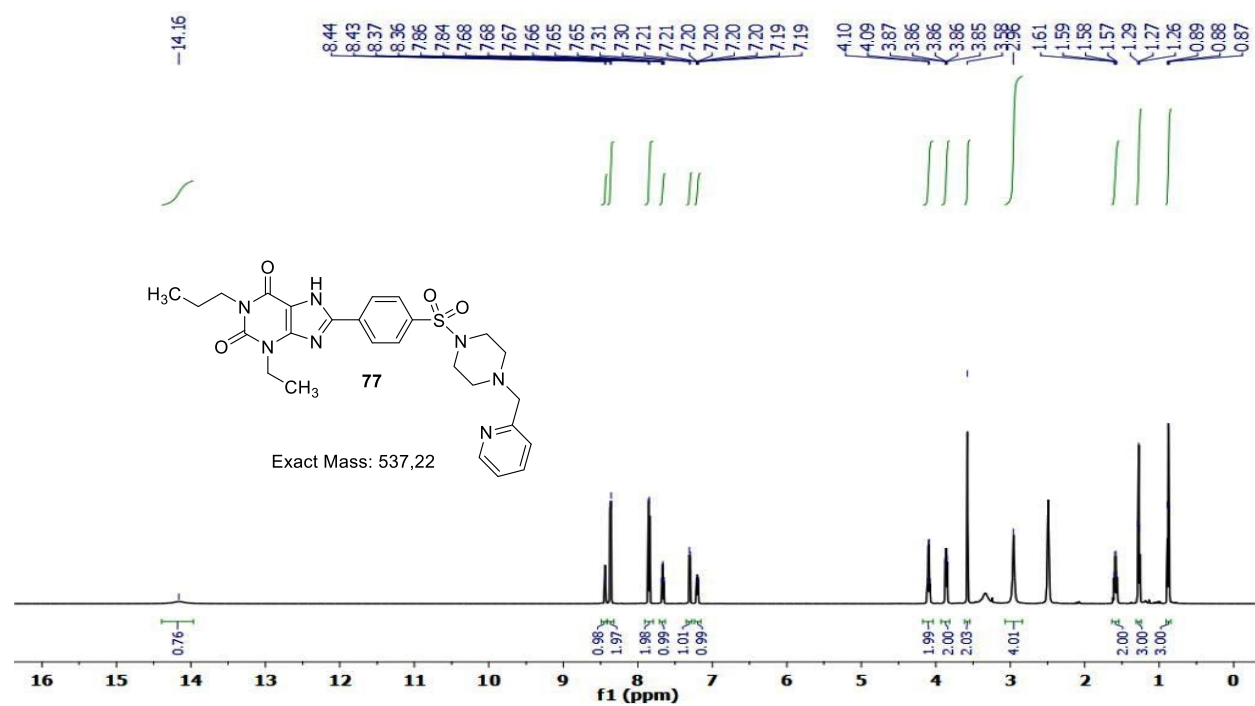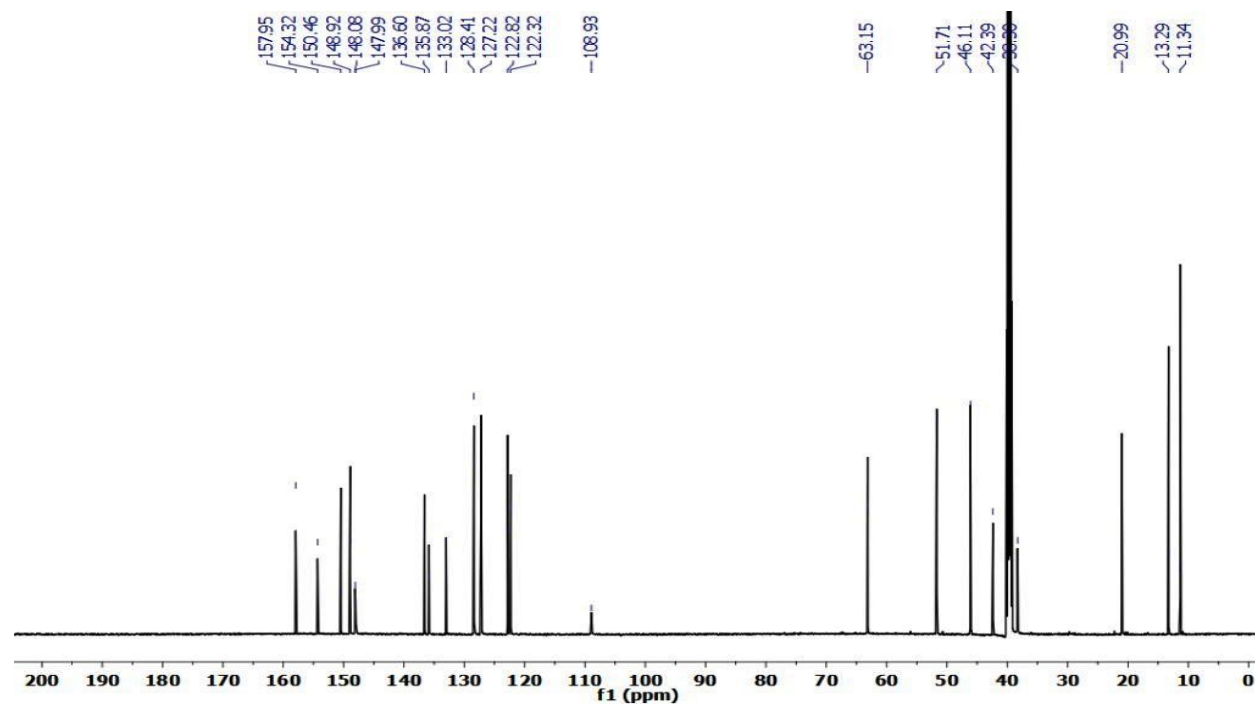
¹HNMR

¹³CNMR

Figure S8. ¹H (600 MHz) and ¹³C (151 MHz) spectra (DMSO-*d₆*) of 3-ethyl-1-propyl-8-(4-((4-(pyridin-4-ylmethyl)piperazin-1-yl)sulfonyl)phenyl)-3,7-dihydro-1*H*-purine-2,6-dione (**77**)

¹HNMR
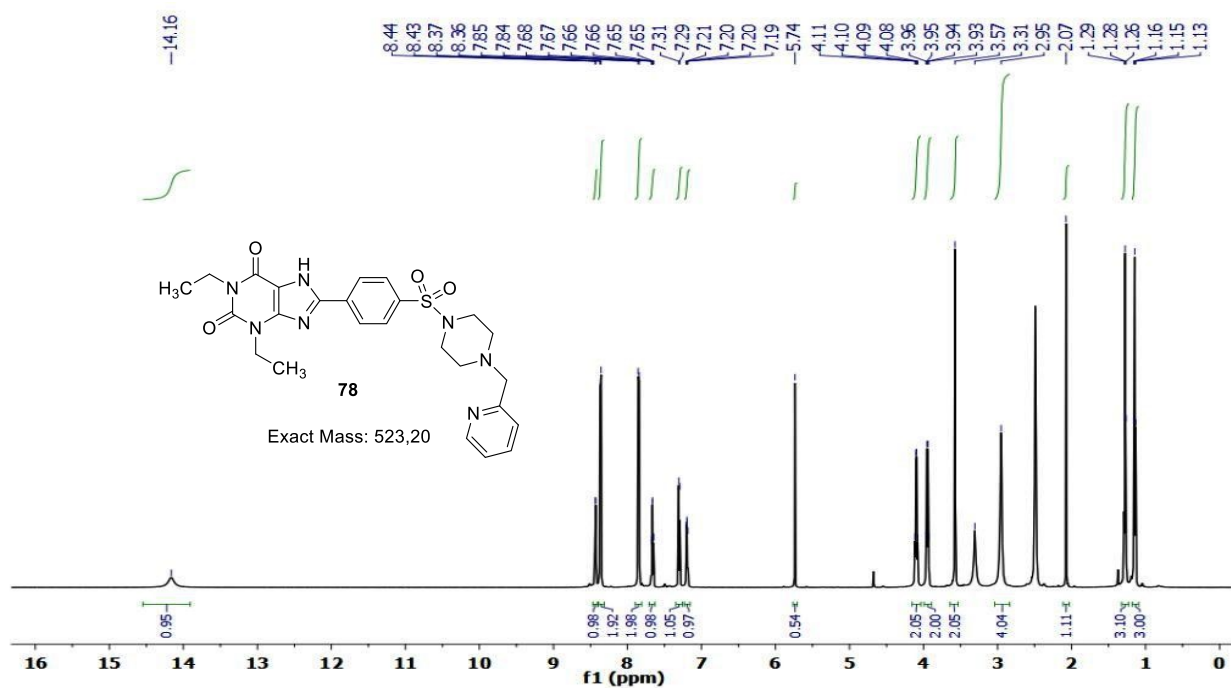
¹³CNMR
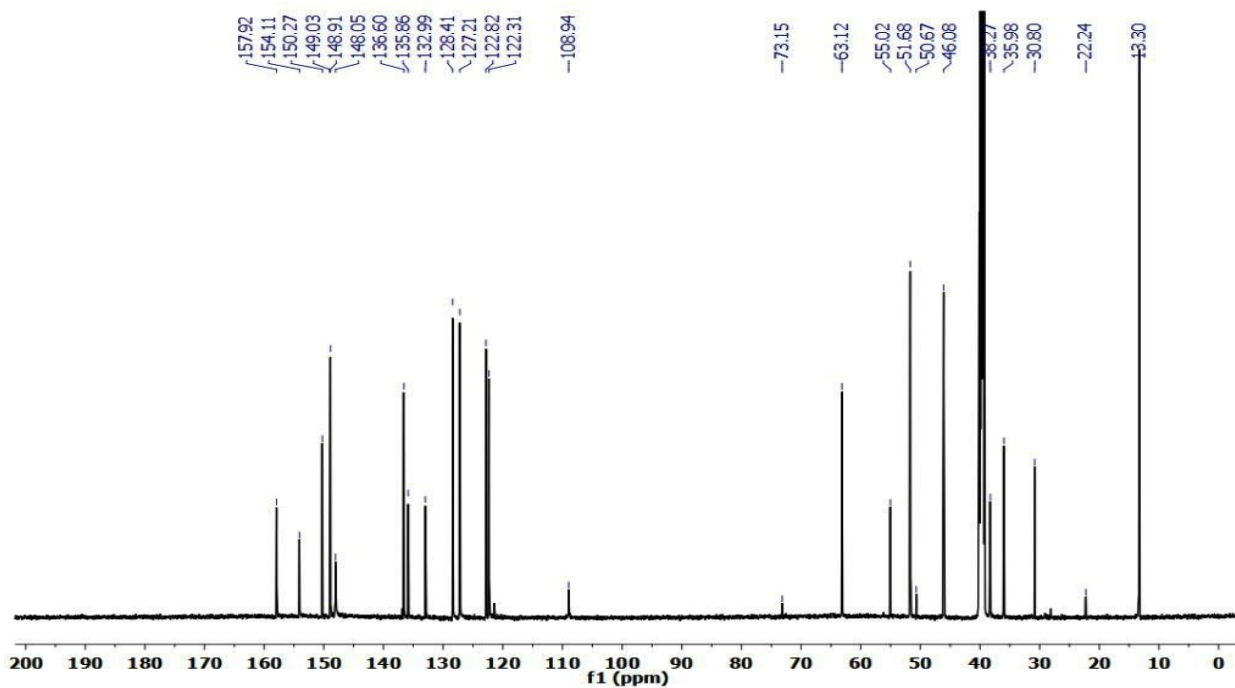
Figure S9. ¹H (600 MHz) and ¹³C (151 MHz) spectra (DMSO-d_6) of 1,3-diethyl-8-(4-((4-(pyridin-2-ylmethyl)piperazin-1-yl)sulfonyl)phenyl)-3,7-dihydro-1*H*-purine-2,6-dione (**78**).
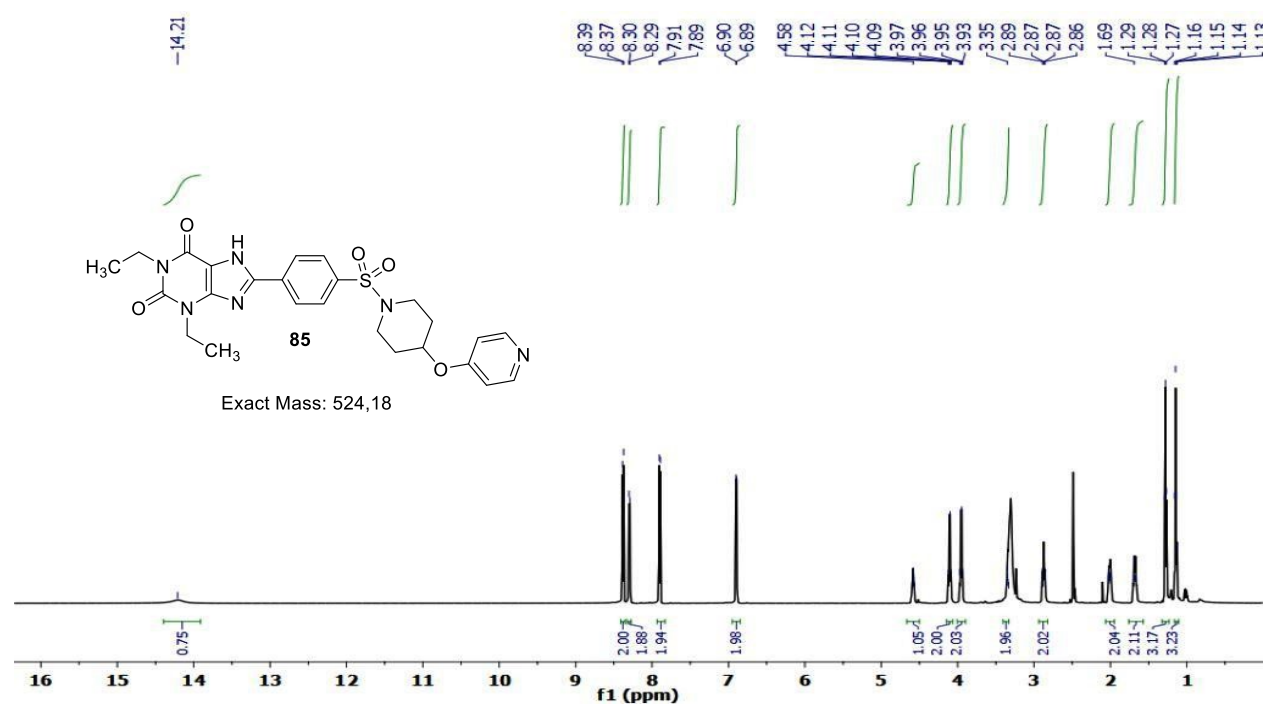
¹HNMR

¹³CNMR

Figure S10. ¹H (600 MHz) and ¹³C (151 MHz) spectra (DMSO-*d*₆) of 1,3-diethyl-8-(4-((4-(pyridin-4-yloxy)piperidin-1-yl)sulfonyl)phenyl)-3,7-dihydro-1*H*-purine-2,6-dione (**85**).

¹HNMR

¹³CNMR

Figure S11. ¹H (600 MHz) and ¹³C (151 MHz) spectra (DMSO-d_6) of 8-(4-((4-hydroxy-4-(pyridin-3-yl)piperidin-1-yl)sulfonyl)phenyl)-1-propyl-3,7-dihydro-1*H*-purine-2,6-dione (**86**).

^{1}HNMR

^{13}CNMR

Figure S12. ^{1}H (600 MHz) and ^{13}C (151 MHz) spectra (DMSO-d_6) of 1,3-diethyl-8-(4-((4-hydroxy-4-(pyridin-3-yl)piperidin-1-yl)sulfonyl)phenyl)-3,7-dihydro-1H-purine-2,6-dione (**87**)
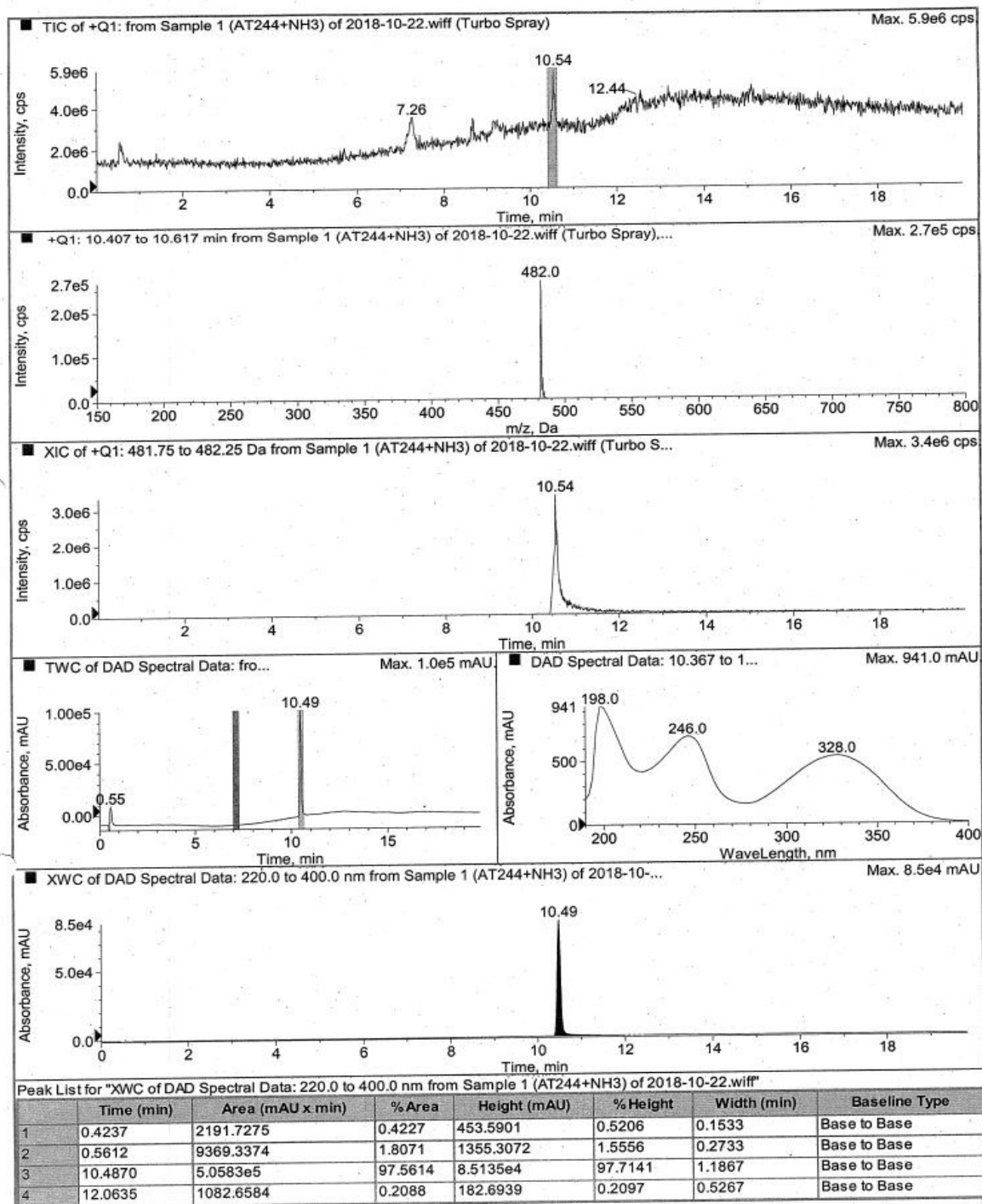
48
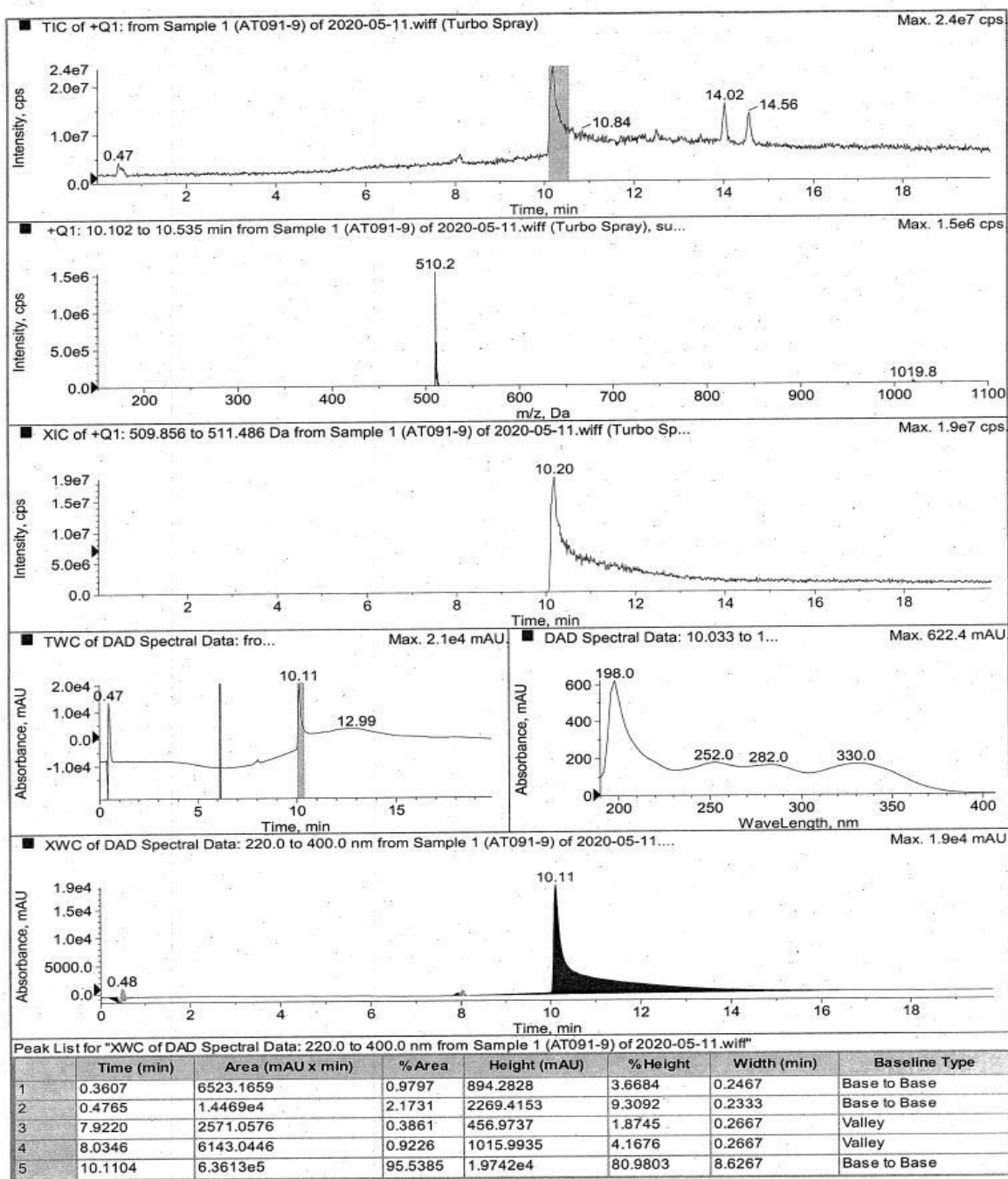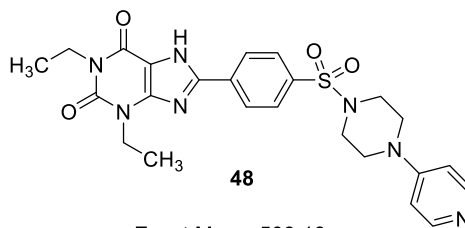
Exact Mass: 509,18

Figure S13. LC-MS spectrum of compound **48***

*The purity of the compound **48** is 95.5% (retention time: 10.11 min belongs to the desired compound **48**; also see NMR spectra, **Figure S1**)

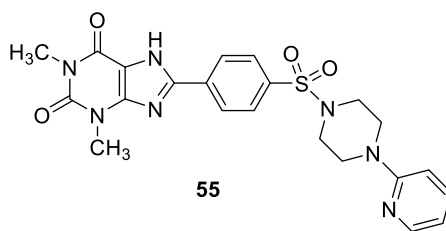**51**
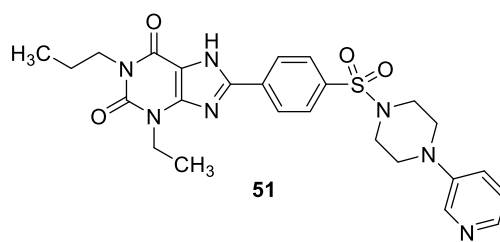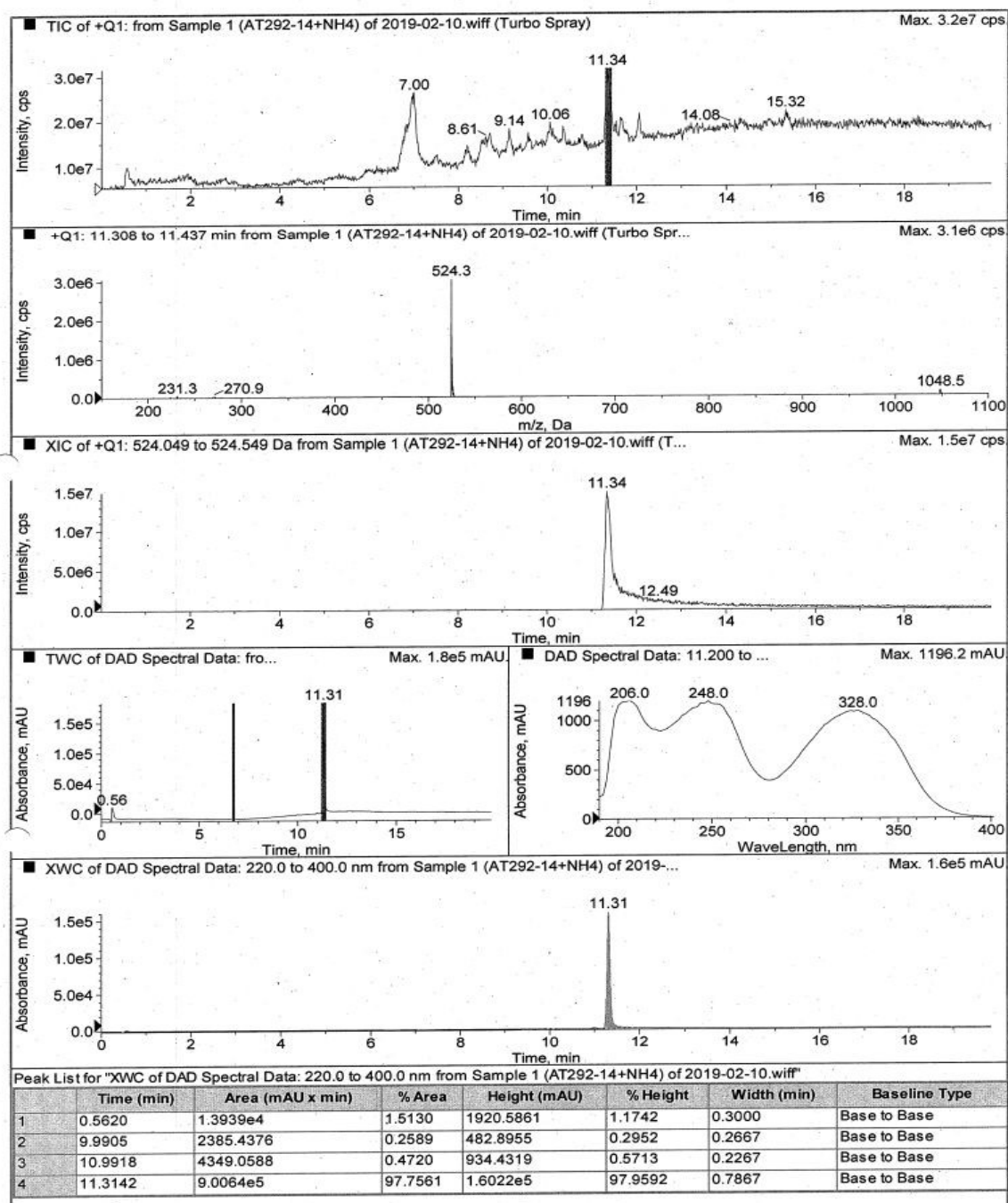
Exact Mass: 523,20

Figure S14. LC-MS spectrum of compound **51***

*The purity of the compound **51** is 97.76% (retention time: 11.31 min belongs to the desired compound **51**; also see NMR spectra, **Figure S2**)
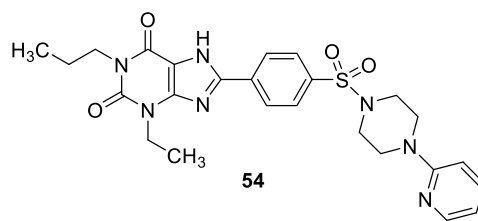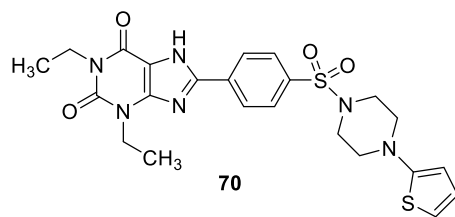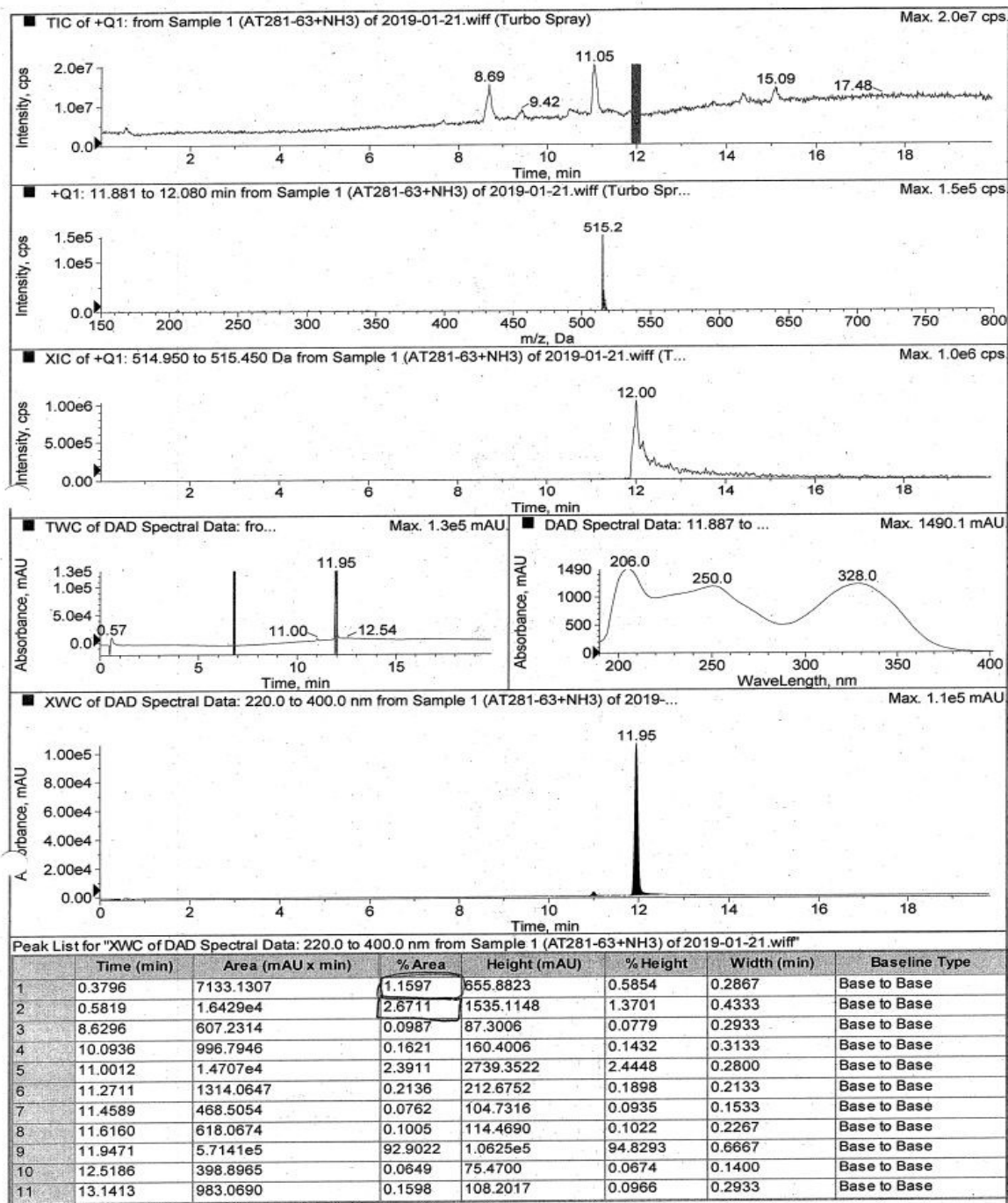
Exact Mass: 523,20
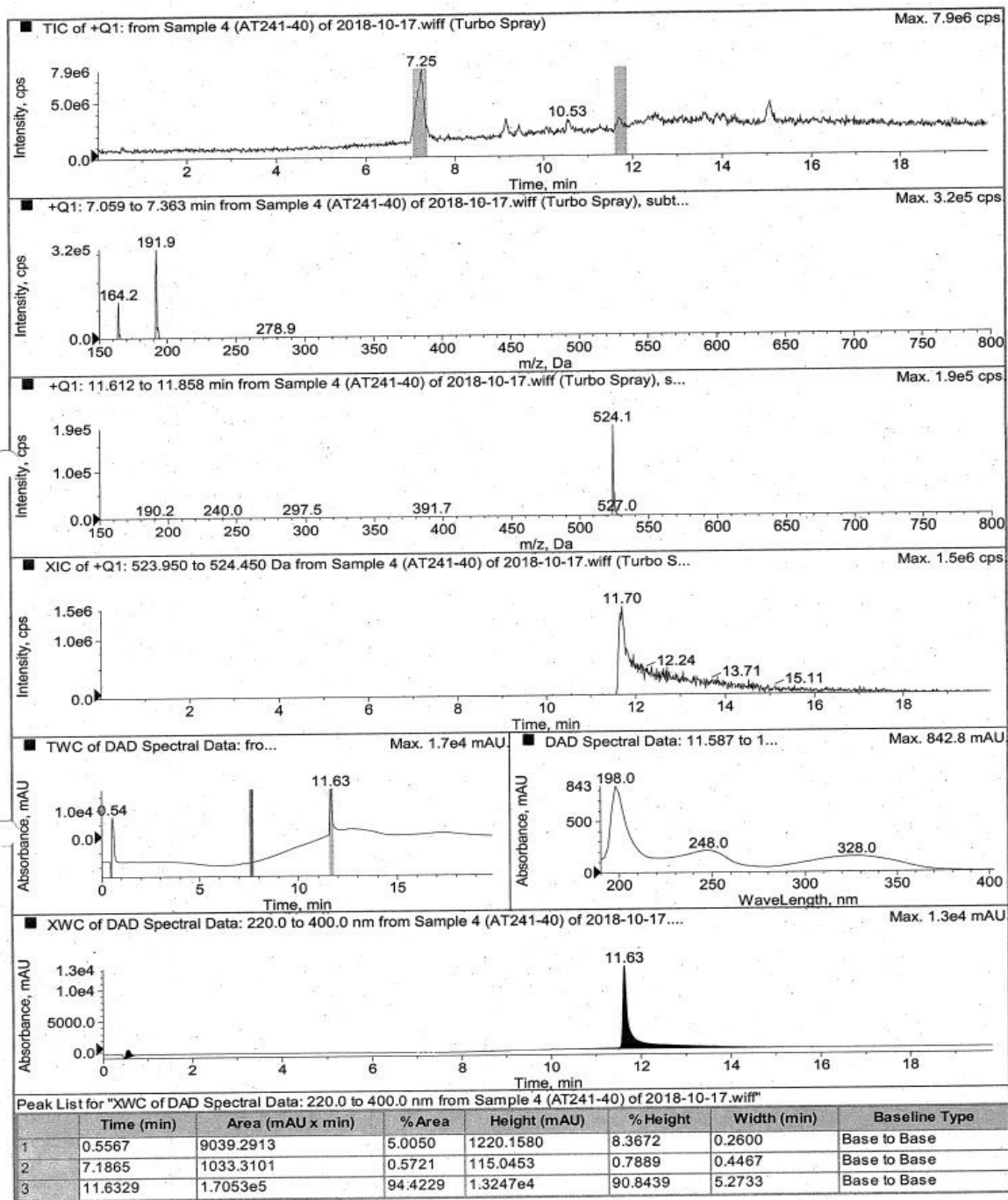
Figure S15. LC-MS spectrum of compound **54***

*The purity of the compound **54** is 99.4% (retention time: 11.63 min belongs to the desired compound **54** and the peak at 0.56 min belongs to the injection peak; also see NMR spectra, **Figure S3**)

55

Exact Mass: 481,15

	Time (min)	Area (mAU x min)	% Area	Height (mAU)	% Height	Width (min)	Baseline Type
1	0.4237	2191.7275	0.4227	453.5901	0.5206	0.1533	Base to Base
2	0.5612	9369.3374	1.8071	1355.3072	1.5556	0.2733	Base to Base
3	10.4870	5.0583e5	97.5614	8.5135e4	97.7141	1.1867	Base to Base
4	12.0635	1082.6584	0.2088	182.6939	0.2097	0.5267	Base to Base

Figure S16. LC-MS spectrum of compound **55***

*The purity of the compound **55** is 97.56% (retention time: 10.49 min belongs to the desired compound **55**; also see NMR spectra, **Figure S4**)
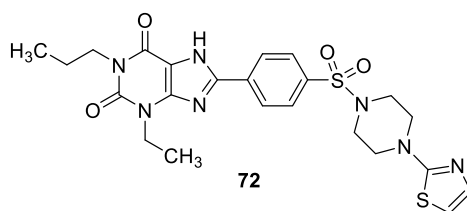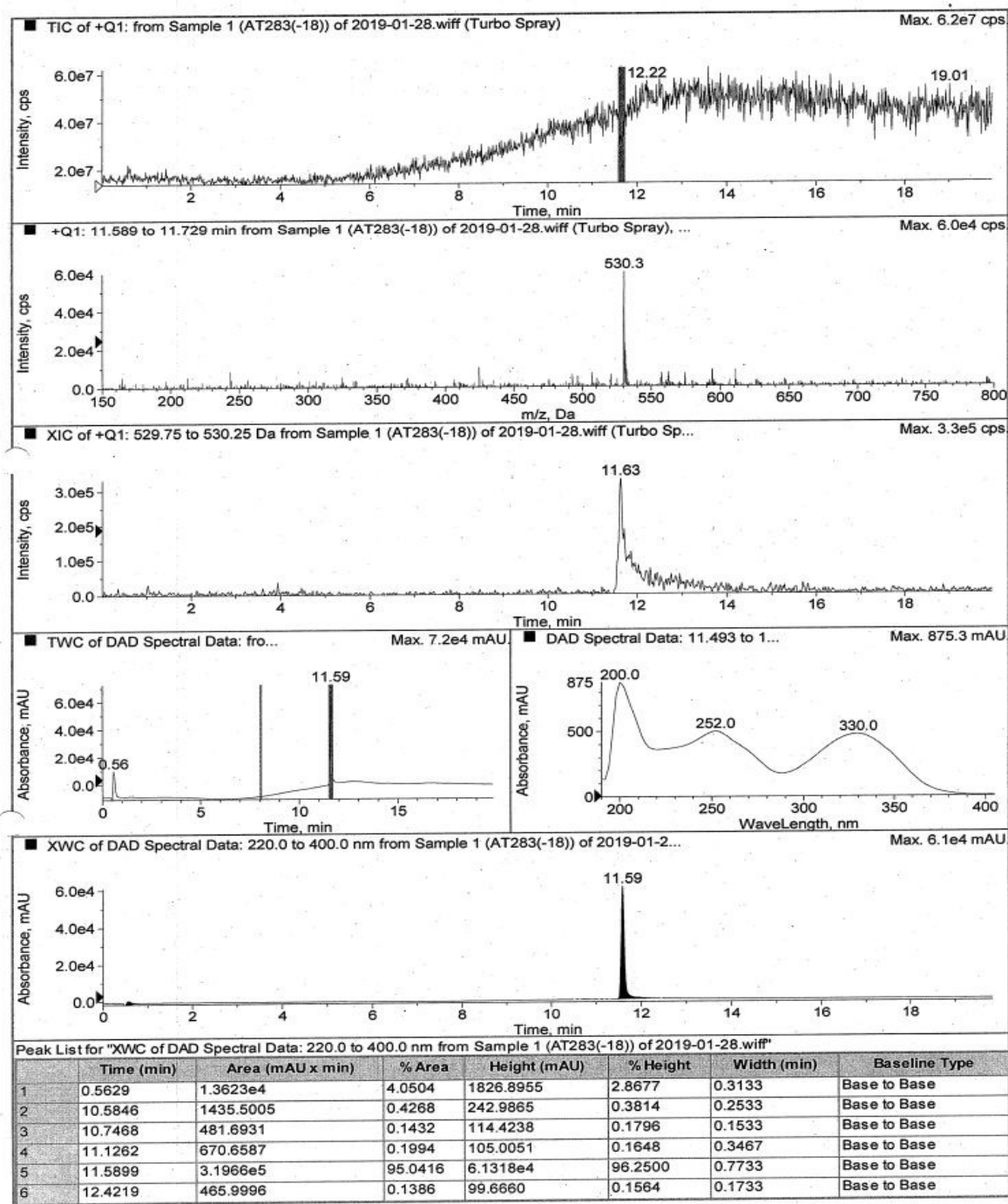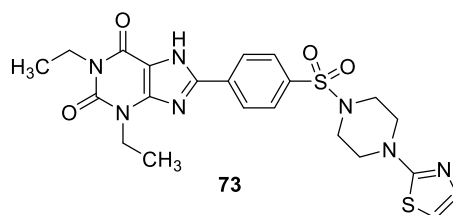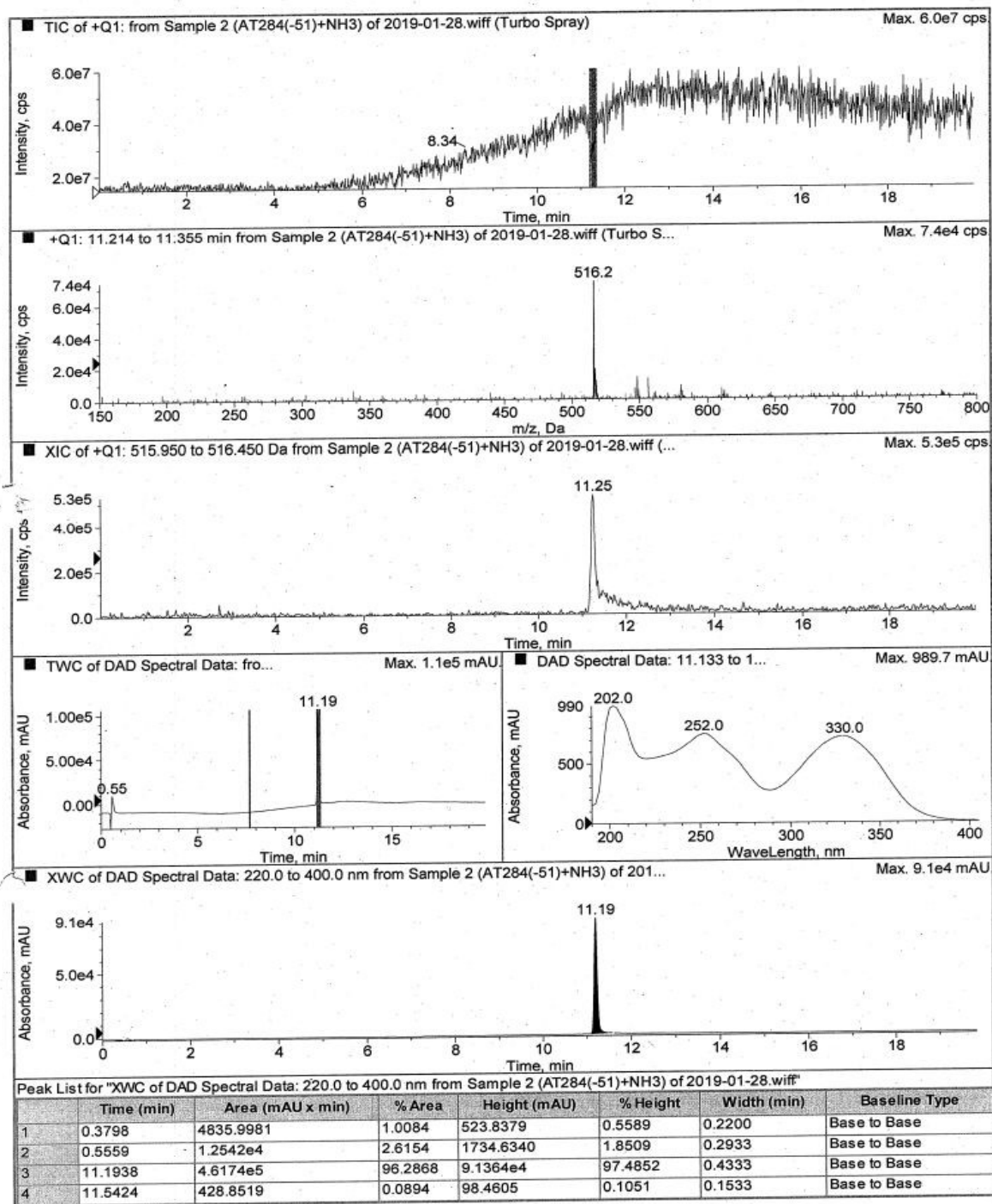
Exact Mass: 514,15

Figure S17. LC-MS spectrum of compound **70***

*The purity of the compound **70** is 95.57% (retention time: 9.70 min belongs to the desired compound **70** and the peak at 0.58 min belongs to the injection peak; also see NMR spectra, **Figure S5**)

Exact Mass: 529,16

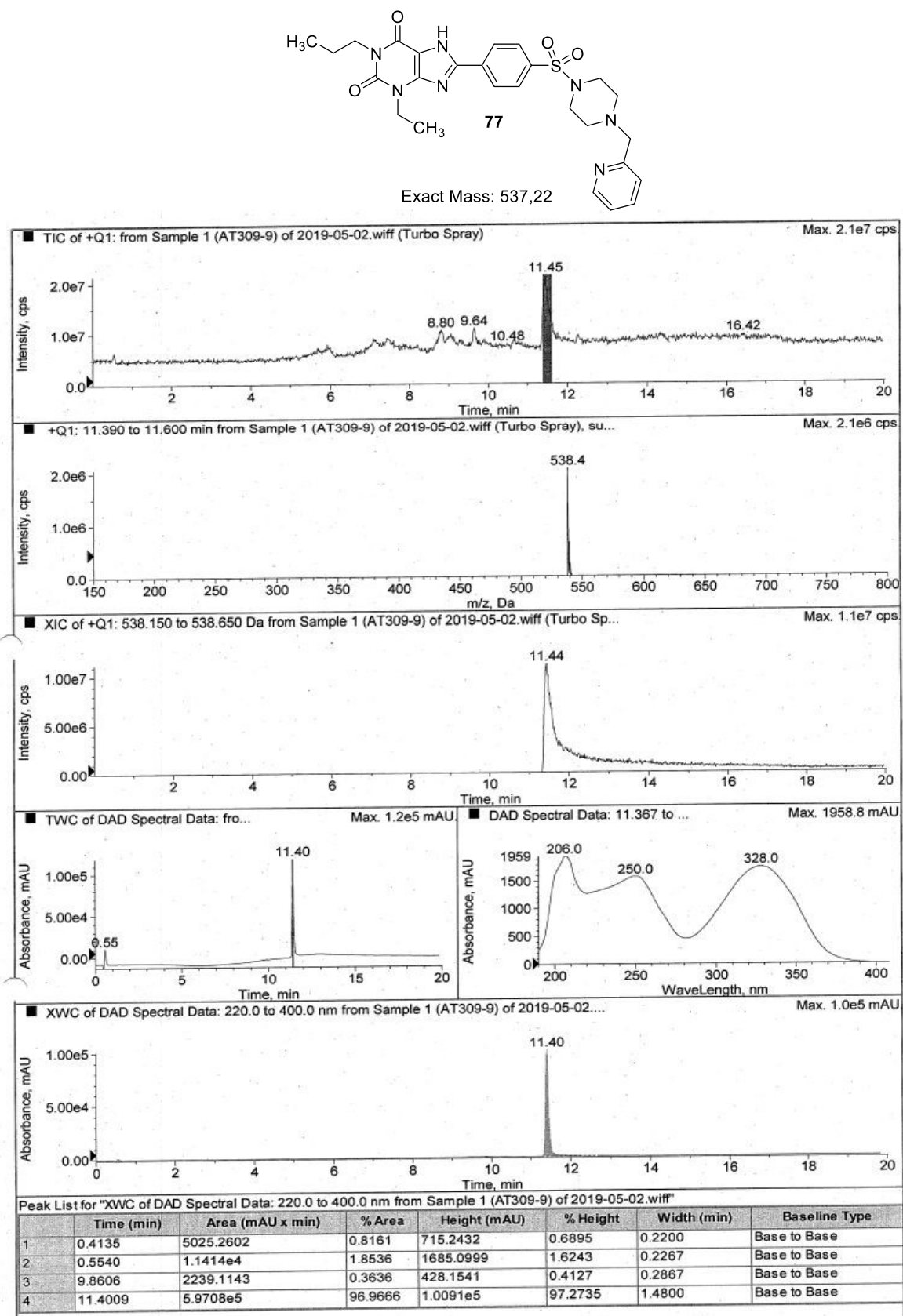|	Time (min)	Area (mAU x min)	% Area	Height (mAU)	% Height	Width (min)	Baseline Type
1	0.5629	1.3623e4	4.0504	1826.8955	2.8677	0.3133	Base to Base
2	10.5846	1435.5005	0.4268	242.9865	0.3814	0.2533	Base to Base
3	10.7468	481.6931	0.1432	114.4238	0.1796	0.1533	Base to Base
4	11.1262	670.6587	0.1994	105.0051	0.1648	0.3467	Base to Base
5	11.5899	3.1966e5	95.0416	6.1318e4	96.2500	0.7733	Base to Base
6	12.4219	465.9996	0.1386	99.6660	0.1564	0.1733	Base to Base

Figure S18. LC-MS spectrum of compound **72***

*The purity of the compound **72** is 95.04% (retention time: 11.59 min belongs to the desired compound **72**; also see NMR spectra, **Figure S6**)
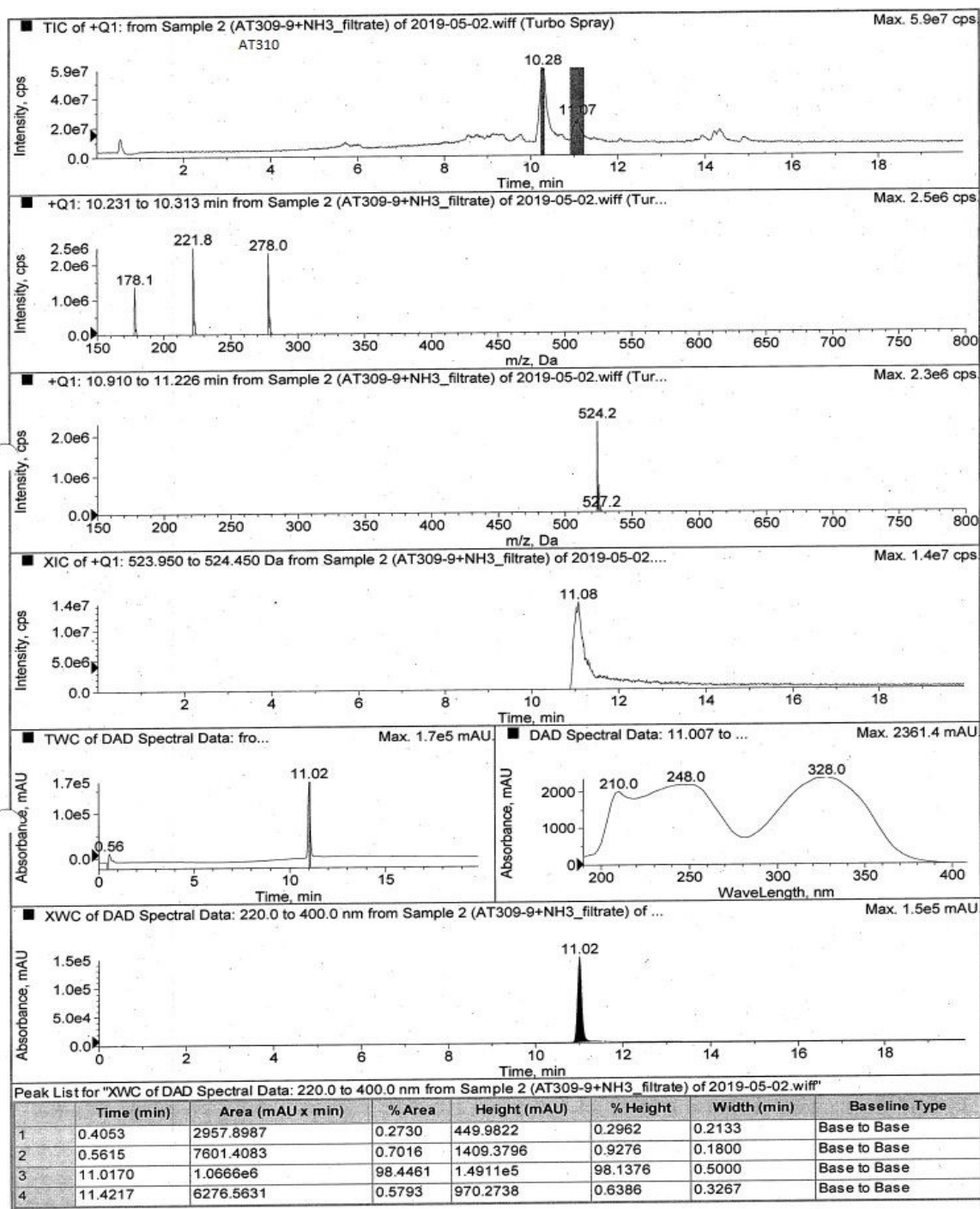
Exact Mass: 515,14

	Time (min)	Area (mAU x min)	% Area	Height (mAU)	% Height	Width (min)	Baseline Type
1	0.3798	4835.9981	1.0084	523.8379	0.5589	0.2200	Base to Base
2	0.5559	1.2542e4	2.6154	1734.6340	1.8509	0.2933	Base to Base
3	11.1938	4.6174e5	96.2868	9.1364e4	97.4852	0.4333	Base to Base
4	11.5424	428.8519	0.0894	98.4605	0.1051	0.1533	Base to Base

Figure S19. LC-MS spectrum of compound **73***

*The purity of the compound **73** is 96.29% (retention time: 9.70 min belongs to the desired compound **73**; also see NMR spectra, **Figure S7**)
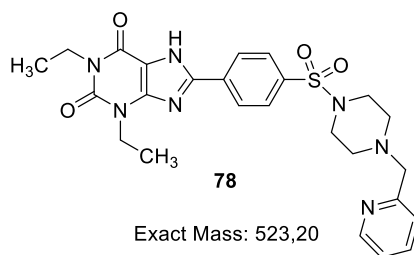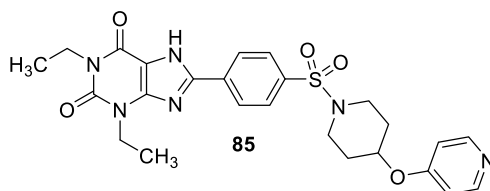
Exact Mass: 537,22

	Time (min)	Area (mAU x min)	% Area	Height (mAU)	% Height	Width (min)	Baseline Type
1	0.4135	5025.2602	0.8161	715.2432	0.6895	0.2200	Base to Base
2	0.5540	1.1414e4	1.8536	1685.0999	1.6243	0.2267	Base to Base
3	9.8606	2239.1143	0.3636	428.1541	0.4127	0.2867	Base to Base
4	11.4009	5.9708e5	96.9666	1.0091e5	97.2735	1.4800	Base to Base

Figure S20. LC-MS spectrum of compound **77***

*The purity of the compound **77** is 96.97% (retention time: 11.40 min belongs to the desired compound **77**; also see NMR spectra, **Figure S8**)

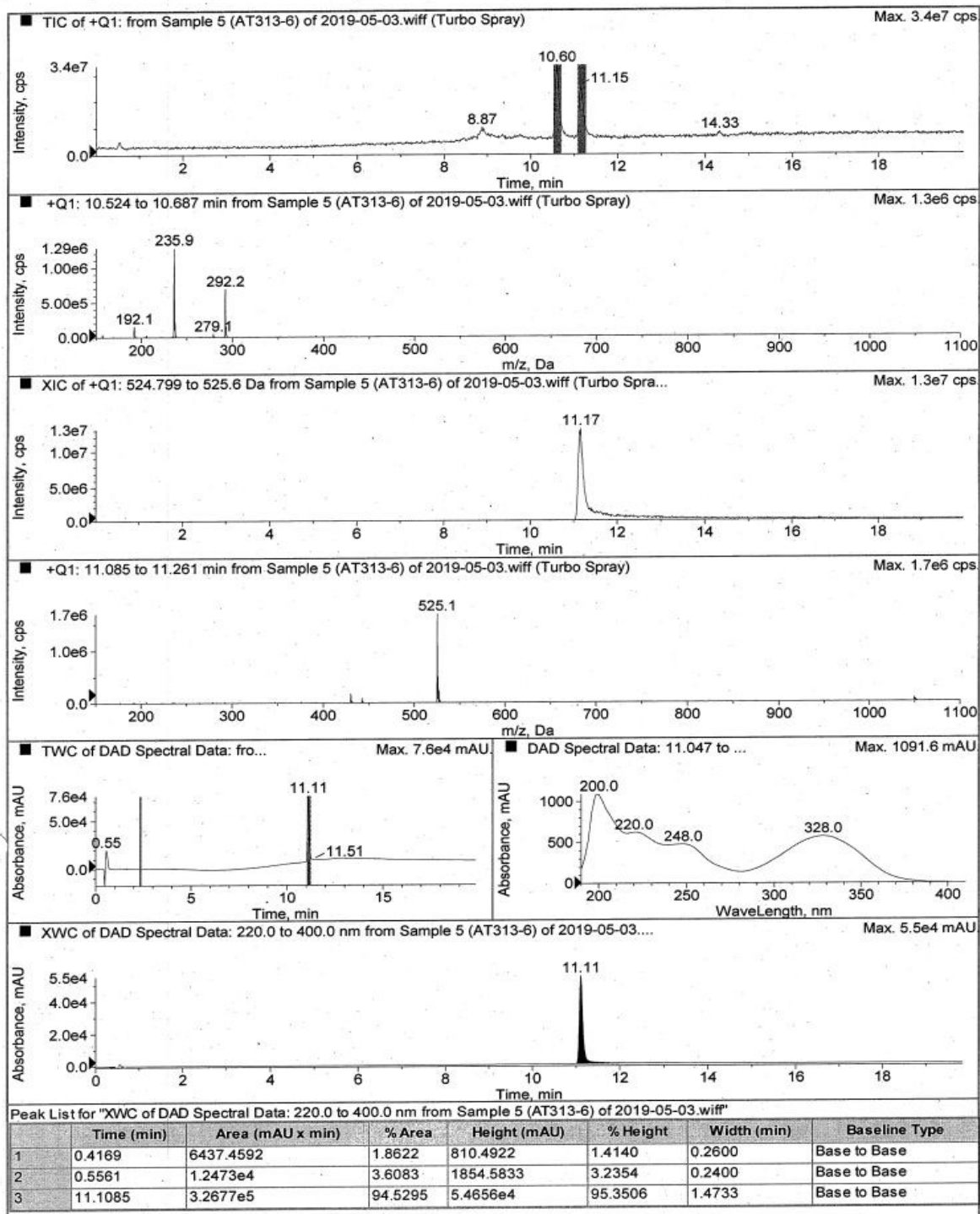**78**

Exact Mass: 523,20

Figure S21. LC-MS spectrum of compound **78***

*The purity of the compound **78** is 98.4% (retention time: 11.02 min belongs to the desired compound **78**; also see NMR spectra, **Figure S9**)

85

Exact Mass: 524,18

Figure S22. LC-MS spectrum of compound **85***

*The purity of the compound **85** is 98.13% (retention time: 11.11 min belongs to the desired compound **85** and the peak at 0.55 min belongs to the injection peak; also see NMR spectra, **Figure S10**)
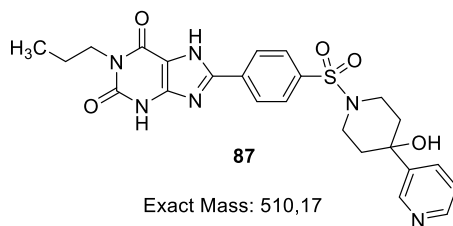
87

Exact Mass: 510,17
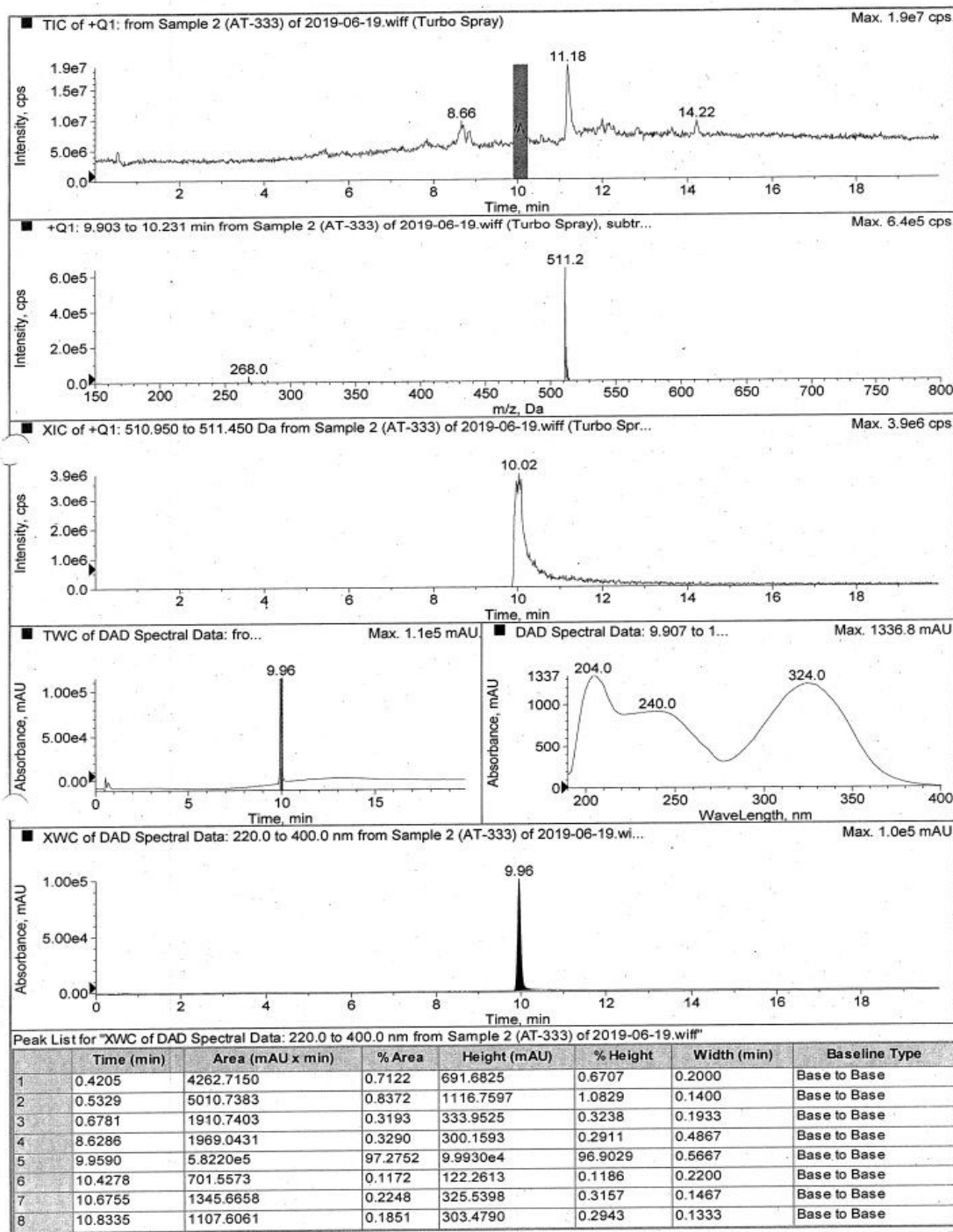
Figure S23. LC-MS spectrum of compound **86***

*The purity of the compound **86** is 97.3% (retention time: 9.96 min belongs to the desired compound **86**; also see NMR spectra, **Figure S11**)
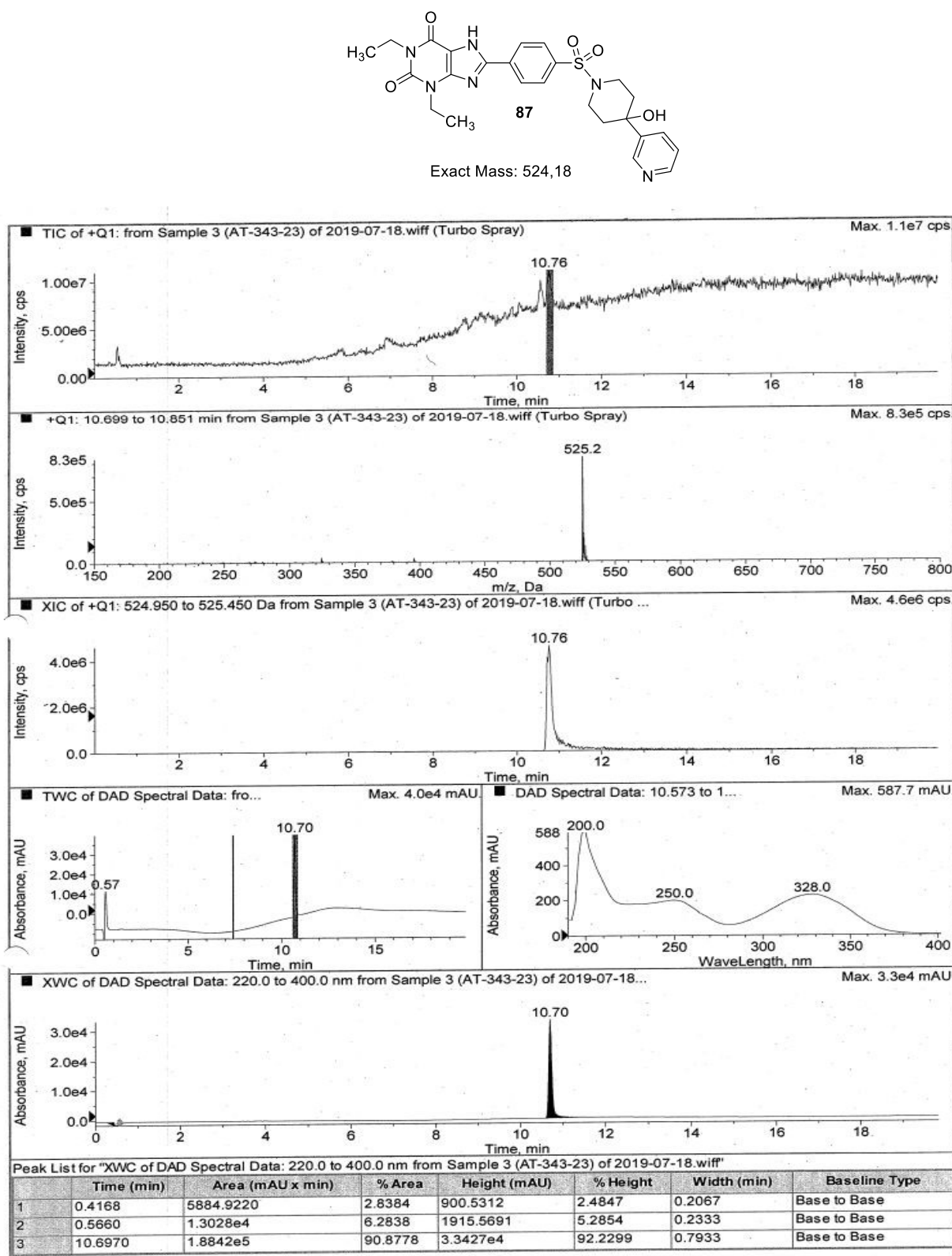
Exact Mass: 524,18

Figure S24. LC-MS spectrum of compound **87***

*The purity of the compound **87** is 97.16% (retention time: 10.70 min belongs to the desired compound **87** and the peak at 0.57 min belongs to the injection peak; also see NMR spectra, **Figure S12**)

References

(1)   Wodtke, R.; Hauser, C.; Ruiz-Gómez, G.; Jäckel, E.; Bauer, D.; Lohse, M.; Wong, A.; Pufe, J.; Ludwig, F.-A.; Fischer, S.; et al. Nε-acryloyllysine piperazides as irreversible inhibitors of transglutaminase 2: synthesis, structure–activity relationships, and pharmacokinetic profiling. *J. Med. Chem.* **2018**, *61*, 4528–4560.

(2)   Yin, J.; Buchwald, S. L. Palladium-catalyzed intermolecular coupling of aryl halides and amides. *Org. Lett.* **2000**, *2*, 1101–1104.

(3)   Konze, K. D.; Ma, A.; Li, F.; Barsyte-Lovejoy, D.; Parton, T.; MacNevin, C. J.; Liu, F.; Gao, C.; Huang, X.-P.; Kuznetsova, E.; et al. An orally bioavailable chemical probe of the lysine methyltransferases EZH2 and EZH1. *ACS Chem. Biol.* **2013**, *8*, 1324–1334.

(4)   Umar, T.; Shalini, S.; Raza, M. K.; Gusain, S.; Kumar, J.; Seth, P.; Tiwari, M.; Hoda, N. A multifunctional therapeutic approach: Synthesis, biological evaluation, crystal structure and molecular docking of diversified 1H-pyrazolo[3,4-b]pyridine derivatives against Alzheimer's disease. *Eur. J. Med. Chem.* **2019**, *175*, 2–19.

(5)   Guglielmo, S.; Bertinaria, M.; Rolando, B.; Crosetti, M.; Fruttero, R.; Yardley, V.; Croft, S. L.; Gasco, A. A new series of amodiaquine analogues modified in the basic side chain with in vitro antileishmanial and antiplasmodial activity. *Eur. J. Med. Chem.* **2009**, *44*, 5071–5079.

(6)   Morriello, Gregori, J.; Wendt, Harvey, R.; Edmondson, S. Novel pyrrolidine derived beta 3 adrenergic receptor agonists. 2012, WO/2012/012314.

(7)   Bailey, J.; Bruton, G.; Huxley, A.; Johnstone, V.; Milner, P.; Orlek, B.; Stemp, G. A practical synthesis of differentially protected 4,4′-dipiperidinyl ethers: novel ligands of pharmaceutical interest. *Synlett* **2009**, *2009*, 1051–1054.

5. Summary and outlook

A$_{2A}$ and A$_{2B}$ adenosine receptors (ARs) are novel drug targets in cancer (immuno)therapy. Activation of A$_{2A}$ARs expressed on the surface of many immune cells such as T-lymphocytes and natural killer (NK) cells decreases cytokine production causing immunosuppression. A$_{2B}$ARs promote tumor proliferation, angiogenesis, metastasis, and also mediate immunosuppression by acting on myeloid cells. Therefore, targeting both AR subtypes, A$_{2A}$ and A$_{2B}$, is highly promising for cancer (immuno)therapy. In the first project, we tackled the challenge of poorly water-soluble A$_{2B}$AR antagonists by developing water-soluble phosphate prodrugs. The second project involved the development of potent dual-acting A$_{2A}$/A$_{2B}$AR antagonists that block the activation of both AR subtypes, and which are therefore promising novel therapeutics for various tumors and potentially also for the immunotherapy of infectious diseases.

5.1. Water-soluble prodrugs of A$_{2B}$ adenosine receptor antagonists

Potent A$_{2B}$AR antagonists have been reported in literature, however many of them lack high water-solubility. Here, we present the development of several potent and selective A$_{2B}$AR antagonists substituted on various positions with phenolic or hydroxyalkyl residues. These compounds were phosphorylated to obtain the corresponding water-soluble phosphate prodrugs. The developed A$_{2B}$AR antagonist prodrugs will be useful as directly injectable tool compounds for pharmacological studies and may have potential as future drugs.

5.1.1. Target structures A: *N*3-hydroxyalkylxanthines

Various xanthine derivatives substituted at the 3-position of the xanthine core with hydroxyalkyl residues of different linker lengths combined with various substituents on the terminal phenyl ring in the 8-position of the xanthine nucleus were synthesized. SARs of the 3-substituted xanthines (target structures A) are summarized in Figure 32. Compound **30b** bearing a hydroxyethyl residue at the xanthine 3-position and a *p*-bromo-substituent on the terminal phenyl

ring showed the highest A₂ʙAR affinity and selectivity in this series. It was therefore selected for

subsequent phosphorylation to obtain its phosphate prodrug **52** (Figure 32).
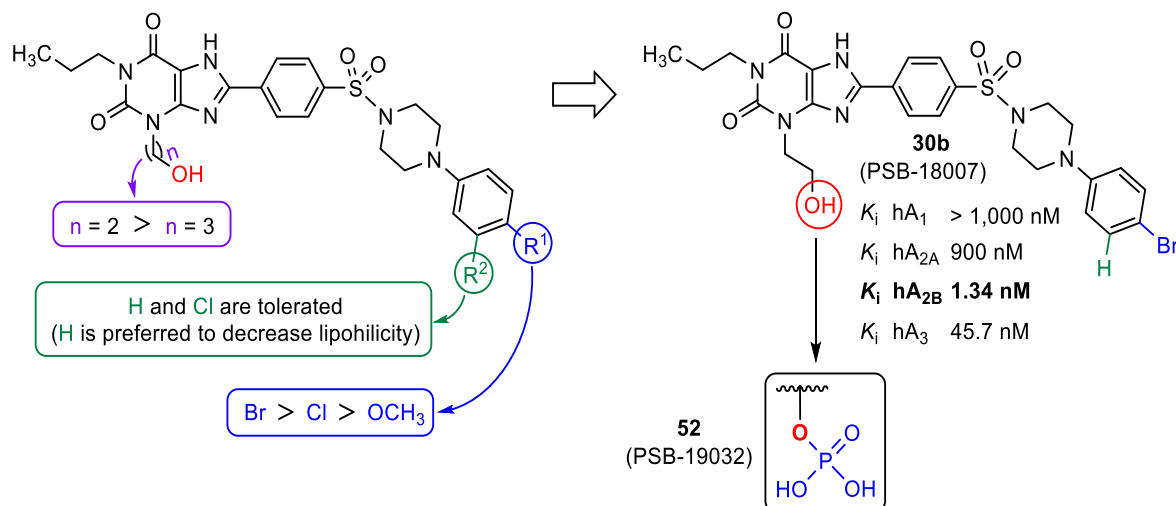

Figure 32. Structure-activity relationships of 3-substituted xanthines (target structures A).

5.1.2. Target structures B: substitution on the terminal phenyl ring

The second series of compounds were those substituted at the terminal phenyl ring with

a phenolic group or a hydroxyalkyl residue combined with halides, such as chloro or bromo,

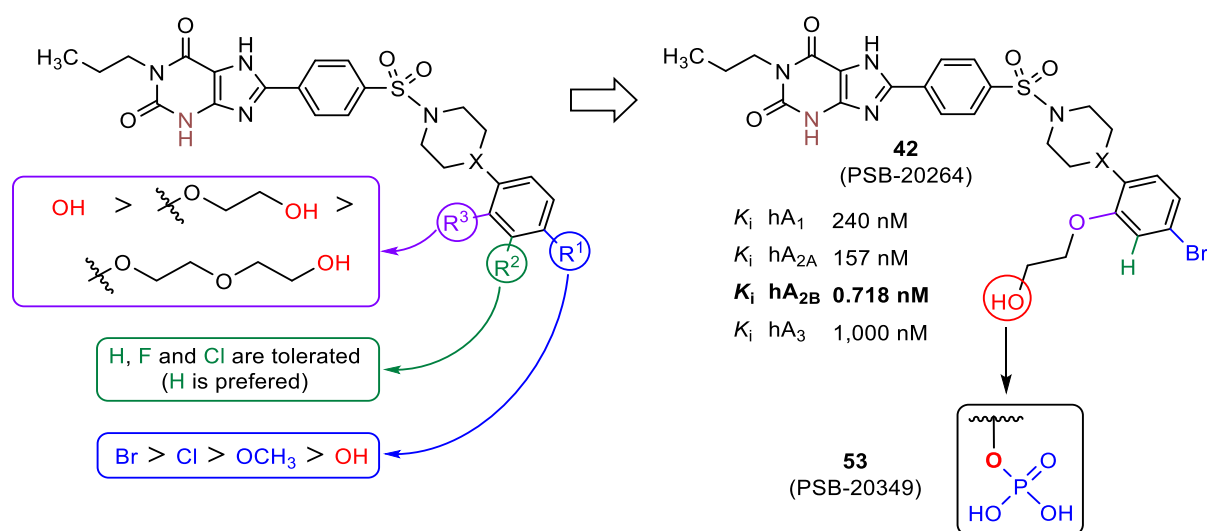which are important for high A₂ʙAR affinity (Figure 33).

Figure 33. Structure-activity relationships of hydroxyalkyl-substituted derivatives (target structures B).

Compounds with an *o*-hydroxyphenyl residue exhibited the highest affinity and selectivity in this series of A$_{2B}$AR antagonists. However, due to steric hindrance, phosphorylation of the phenolic group was not successful. Thus we developed compounds substituted on the phenyl ring with longer hydroxyalkyl chains. Compound **42** with a hydroxyethyl residue in the *ortho*-position of the terminal phenyl ring displayed excellent affinity and selectivity for the A$_{2B}$ARs and was therefore selected for phosphorylated yielding its phosphate prodrug **53** (Figure 33).

5.1.3. Target structures C substitution at the amino linker

The third series of compounds were those having a hydroxyalkyl chain attached to an amino linker connecting the terminal phenyl ring with the piperidinyl moiety (see Figure 34). *N*-substituted methyl or ethyl esters were reduced yielding compound **50**, which displayed high A$_{2B}$AR affinity and selectivity. The subsequently prepared phosphate prodrug **54** exhibited an 830-fold increase in water-solubility in comparison to its parent drug **50** (Figure 34).
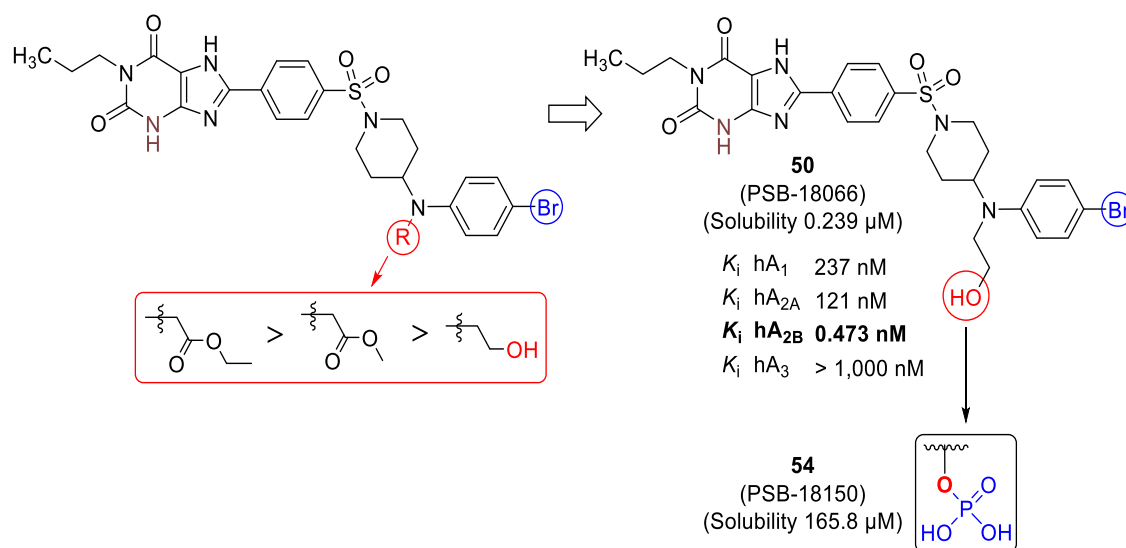

Figure 34. Structure-activity relationships of amino-linker substituted xanthines (target structures C).

In summary, we have reported the development of water-soluble phosphate prodrugs for potent and selective A$_{2B}$AR antagonists. These prodrugs could overcome the drawback of poor

water solubility which has limited the further development of many potent $A_{2B}AR$ antagonists. These compounds will be valuable tools that can be applied as injectables for in vivo studies, e.g. in animal models of cancer.

5.2. Development of dual A_{2A}/A_{2B} adenosine receptor antagonists

Activation of A_{2A}- and $A_{2B}ARs$ expressed on T-lymphocytes and myeloid cells, respectively, by adenosine was reported to suppress immune responses. Therefore, the development of potent dual A_{2A}/A_{2B} adenosine receptor antagonists could provide a novel effective treatment for cancer by activating anti-tumor immune responses, and for infections. In this project, we modified the structure of the potent $A_{2B}AR$ antagonist PSB-1901 through various ring replacements and substitutions that were expected to increase the potency at $A_{2A}ARs$ without significantly reducing $A_{2B}AR$ affinity. Structure-activity relationships of the developed dual A_{2A}/A_{2B} adenosine receptor antagonists are presented in Figure 35.
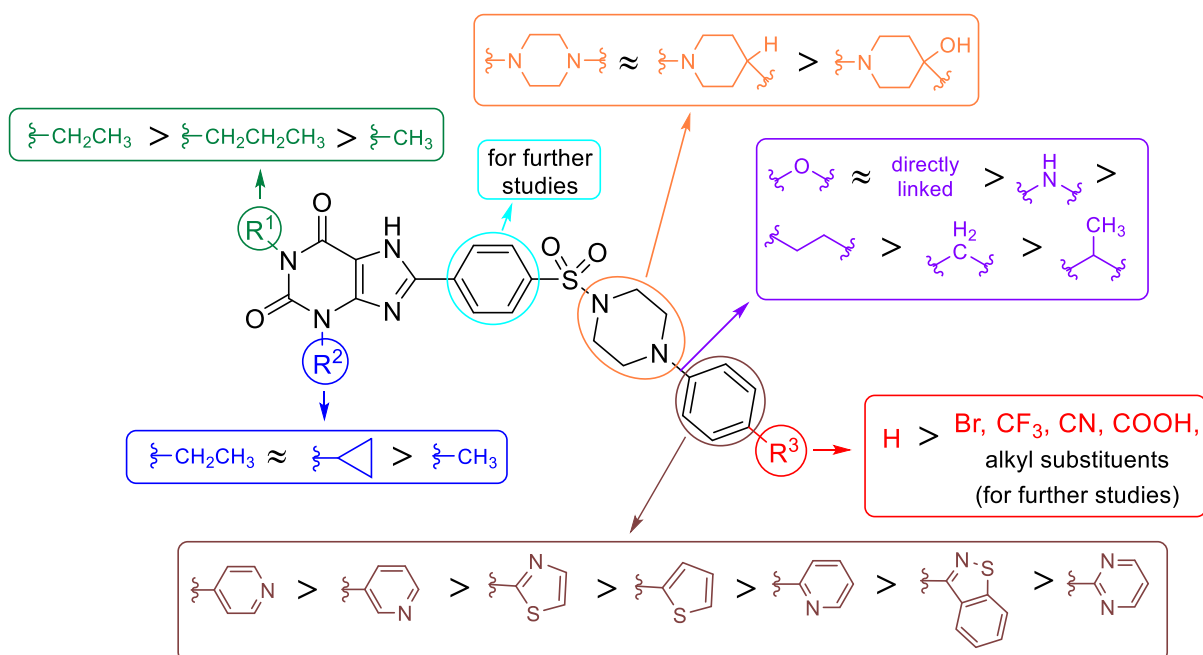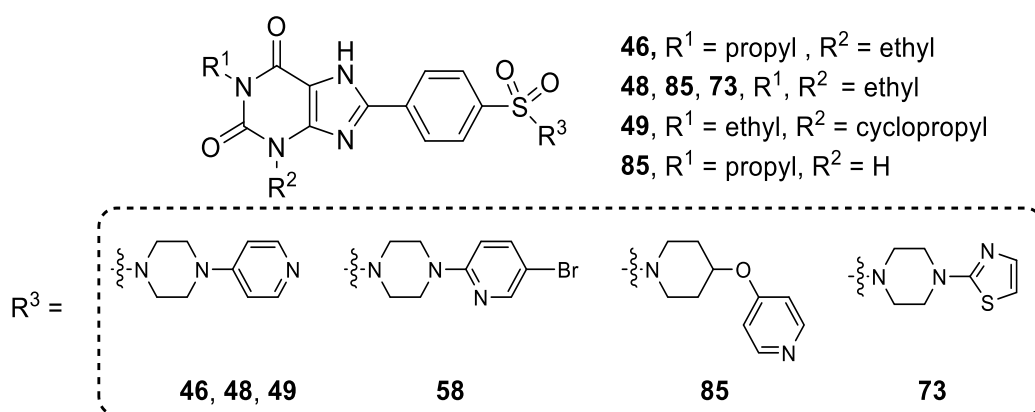

Figure 35. Structure-activity relationships of the developed dual A_{2A}/A_{2B} adenosine receptor antagonists which were designed based on lead structure PSB-1901.

Substitution at the 1-position of xanthine by ethyl combined with 3-substitution by an ethyl or cyclopropyl residue, as in compounds **48** and **49**, resulted in optimal affinity for both AR subtypes (Figure 36). Replacing the piperazine moiety with piperidine did neither affect affinity nor selectivity of the developed dual antagonists. Introducing an ether linker to connect the piperazine ring with the terminal phenyl residue, as in compound **85**, was found to increase affinity for both receptor subtypes as compared to other derivatives with amino or alkyl linkers.

46, R^1 = propyl , R^2 = ethyl
48, **85**, **73**, R^1, R^2 = ethyl
49, R^1 = ethyl, R^2 = cyclopropyl
85, R^1 = propyl, R^2 = H

R^3 =

Compound	46	48	49	58	85	73
K_i hA$_{2A}$ (nM)	21.0	11.1	23.1	311	15.7	28.5
K_i hA$_{2B}$ (nM)	39.8	21.0	16.6	0.536	19.7	3.68
Solubility (μM)	12.2	4.6	n.d.	0.2	n.d.	n.d.
BBB	BBB+	BBB+	n.d.	n.d.	n.d.	n.d.

Figure 36. Comparison of the affinities and selected physicochemical properties of the developed dual A$_{2A}$/A$_{2B}$AR antagonists **46**, **48**, **49**, **85** and **73** and the potent A$_{2B}$AR antagonist **58**.

Replacing the terminal phenyl ring with various heterocycles, especially 4-pyridyl, see compounds **48**, **49** and **85**, was found to be crucial for developing potent dual A$_{2A}$/A$_{2B}$AR antagonists. Compound **73** having a terminal thiazole ring also showed dual antagonistic potency, with somewhat higher affinity for the A$_{2B}$AR than the A$_{2A}$AR subtype. Substitution on the terminal heterocyclic ring with various residues, e.g. in compounds **58** and **59**, with a *p*-Br or a *p*-CF$_3$ substituent, respectively, decreased A$_{2A}$AR affinity resulting in potent and selective A$_{2B}$AR antagonists (Figures 35 and 36). Replacing the terminal phenyl ring with

heterocycles, especially 4-pyridyl rings, as in compounds **46** and **48**, did not only positively affect the affinities of the target compounds to the AR subtypes, but also improved their physicochemical properties, such as aqueous solubility and blood brain barrier (BBB) permeability. Introducing very lipophilic substituents, e.g. *p*-Br in compound **58**, resulted in potent $A_{2B}AR$ antagonists, however with only low aqueous solubility (Figure 36).

In conclusion, because the immunosuppressive effects of adenosine are mediated through the A_{2A}- and $A_{2B}ARs$ in immune cells, we developed potent xanthine-based dual $A_{2A}/A_{2B}AR$ antagonists with high selectivity versus A_1 and A_3 AR subtypes. This dual antagonists could become future drug candidates for the treatment of cancers and also for the immunotherapy of infectious diseases.

6. Acknowledgments

Firstly, I would like to express my sincere and deep gratitude to my supervisor **Prof. Dr. Christa E. Müller** for giving me the opportunity to join her research group. Also, I would like to thank her for the interesting projects and her inspiration, patience, mentorship and endless support throughout my PhD studies.

I would like to deeply thank **Prof. Dr. Finn Hansen** for his time and acceptance to act as a second supervisor.

Also, I would like to greatly thank **Prof. Dr. Günther Weindl** and **Prof. Dr. Rainer Manthey** for accepting to be co-examiners in my PhD examination committee.

I would like to thank Dr. Jörg Hockemeyer for introducing me to xanthine chemistry and for Dr. Sonja Hinz and Dr. Dr. Vigneshwaran Namasivayam for our active discussions and support.

Also, I would like to thank Christin Vielmuth for performing the radioligand binding assays, and Yulu Wang from Prof. Dr. med. Ingo Schmidt-Wolf group for performing cytotoxicity studies. I gratefully acknowledge Marion Schneider, Sabine Terhart-Krabbe and Annette Reiner for the LC-MS and NMR analyses.

To all my officemates: Dr. Aliaa, Conny, Vittoria, Riham, Jessica and Sophie, thanks for the wonderful and relaxing time in the office.

I wish to express my deep thanks and appreciation to the Ministry of Higher Education of Egypt (MOHE) for sponsoring my doctoral fellowship and providing me with all legal and financial support. I also wish to thank all my colleagues in the Division of Pharmaceutical Sciences, National Research Center, Cairo, Egypt.

I would like to thank BIGS Drugs and the international office for organizing important scientific workshops and personal support, and also to IPID4all, (DAAD) for the travel grant to attend a conference.

I extend my sincere thanks to my friends and colleagues Dr. Nader Boshta, Dr. Ahmed Elgokha, Andhika Mahardhika and Dr. Mahmoud Rashed, for their continuous inspiration and support.

Furthermore, I am especially grateful to my parents, my wife Noha, my son Adam and my family for their continuous encouragement and motivation throughout my PhD studies.

Finally, to all the present and past members in AK Müller group: thanks for the pleasant and cooperative working atmosphere which contributed to the accomplishment of this work.

Ahmed Temirak

Bonn July 2020